UNITED STATES DEPARTMENT OF COMMERCE • John T. Connor, *Secretary*

NATIONAL BUREAU OF STANDARDS • A. V. Astin, *Director*

CRITICAL PHENOMENA

Proceedings of a Conference Held in Washington, D.C., April 1965

Edited by

M. S. Green and J. V. Sengers

Institute for Basic Standards
National Bureau of Standards
Washington, D. C. 20234

Sponsored by

National Bureau of Standards
National Science Foundation
Office of Naval Research

National Bureau of Standards Miscellaneous Publication 273

Issued December 1, 1966

For sale by the Superintendent of Documents, U.S. Government Printing Office Washington, D.C., 20402 - Price $2.50

Library of Congress Catalog Card Number: 66-60040

Conference on
PHENOMENA IN THE NEIGHBORHOOD OF CRITICAL POINTS

Held at

The National Bureau of Standards

Washington, D.C.

April 5 to 8, 1965

Organizing Committee:

M. S. Green. *Chairman*	National Bureau of Standards
G. B. Benedek	Massachusetts Institute of Technology
M. E. Fisher	University of London King's College
E. W. Montroll	Institute for Defense Analysis and University of Maryland
C. J. Pings	California Institute of Technology

FOREWORD

One of the important responsibilities of the National Bureau of Standards is to help the Nation meet its needs for accurately measured, critically evaluated, and well-understood properties of materials. To aid in fulfilling this responsibility, the Bureau joined with the National Science Foundation and the Office of Naval Research in sponsoring a Conference on Phenomena in the Neighborhood of Critical Points, which was held at NBS in Washington, D.C., April 5 to 8, 1965. The Conference was attended by approximately 200 scientists from this country and abroad, representing many laboratories and disciplines. Most of the papers presented at the Conference, as well as the subsequent discussions, are included in this volume. Primary responsibility for their technical content must rest, of course, with the individual authors and their organizations.

A. V. Astin, *Director.*

PREFACE

In that system for defining, determining, communicating, and recording numerical descriptors of physical systems which has recently been called the National Measurement System, the National Bureau of Standards has had from its earliest beginnings a concern with the part having to do with properties of substances. Indeed, accurately determined values of key data on properties of substances are an essential means for the dissemination of measurement capability. The experimental determination, the critical evaluation and the theoretical understanding of well-defined properties of well-characterized substances is one of the major modes through which the scientific enterprise contributes to the technological enterprise and to the well-being of the nation. To facilitate and to contribute to this process and to bring it into close coupling with the national standards is one of the primary responsibilities of the Bureau and its component Institute for Basic Standards.

The program of the Conference on Phenomena in the Neighborhood of Critical Points, whose proceedings are recorded in the present volume, serves excellently to illustrate some of the ways in which this process takes place. An important part of the program of the conference was concerned with measurement techniques. New techniques were introduced. Advantages and limitations of traditional techniques were discussed. In many instances it became apparent that new techniques were necessary not only to provide more accurate data in new experimental ranges but to answer fundamental theoretical questions. The Institute for Basic Standards has a deep and perennial interest in techniques for measuring properties of substances.

The technological enterprise needs accurate data on the substances and materials from which the designs of our engineers are constructed, which constitute the ambience which they must take into account, or which enter into the various stages of the productive process. In meeting this need the task of the scientific enterprise does not end with the complete measurement of a property. Competent scientists must critically review and evaluate various measurements which inevitably conflict and contradict each other. Many of the papers at the conference were just such critical reviews and evaluation of experimental data. The literature was searched for relevant data. Factors affecting the accuracy and validity of the experimental approach were investigated. Patterns, meanings, and conclusions were drawn insofar as the data warranted. These reviews represent an essential step in the process by which primary experimental data become the reliable and easily accessible reference data which the technological enterprise requires.

Anyone who attempts even a rough estimate the dimensions of the need for data will realize that not even all the laboratories and data centers of the whole world are sufficient to provide an accurately measured and critically evaluated datum for every required property in every required condition. The scientific enterprise has, of course, another resource available to satisfy the data requirements of technology, the web of well-established theoretical relationships which relate properties in various substances and conditions among themselves and to the fundamental constants of nature. One of the purposes which has motivated the present conference was the expectation or hope that a common thread of explanation would be found among such diverse phenomena as liquid-vapor phase transitions, magnetism, superconductivity, order-disorder transitions. If these expectations are realized, a few theoretical concepts will provide knowledge of properties which is significant for a large number of very disparate fields of technology.

The task of providing adequate data on properties of substances is, of course, one which must be carried out by the scientists of the nation and indeed the world. The Bureau and Institute contribute to this task through services they provide to the scientific community as well as by the scientific work of its own laboratories. As I remarked in my address of welcome to the conference, the Bureau and Institute were happy and honored to serve as a place of congregation for the dis-

tinguished group of speakers and participants for the purpose of discussing a subject so germane to our function. We were happy also for the stimulus to our technical program which the conference provided through the activities of our staff as participants, speakers, and organizers. More than these, however, we were happy to have this important group of scientists in our midst so that we might learn from them about opportunities and needs to improve our services and they in turn might perhaps learn from us about those of our services and activities which might be of help to them.

R. D. Huntoon, *Director*
Institute for Basic Standards.

INTRODUCTION

As their temperature is raised, the properties of a liquid and of the vapor with which it is in equilibrium become more and more similar until, at a particular temperature, the difference disappears. The state of the fluid at this temperature is the critical point. At room temperature iron has the power to acquire a magnetic moment which remains even after the magnetic field is removed. As its temperature is raised this remanent magnetism diminishes until, at a temperature of some several hundred of degrees, it suddenly disappears. This state of iron is called the Curie point. Below the temperature of its critical point He^4 may exist in an ordinary liquid form which is qualitatively the same as liquids existing at room temperature. At a temperature several degrees below its critical point the ordinary liquid suddenly acquires new properties, especially those relating to flow, which are so extraordinary that the state has been called superfluid. The state at which this transition occurs is called the λ-point.

All these phenomena have in common that at a definite transition point a substance gains or loses all at once what another age would have called a *virtue*. In this they differ from first order phase transitions, melting, evaporation, sublimation, in which the physical change is not sudden, but takes place by a piecemeal transformation of small portions of the substance from one state to another. They differ also from first order phase transitions in that they seem to be the focus or source of anomalous behavior in a wide region of the surrounding thermodynamic phase plane. Critical points of liquid vapor transitions, consolute points in binary liquid mixtures, Curie and Néel points in magnetism, second order phase transition points in solids, λ-points in liquid helium together with the anomalous phenomena which occur in their neighborhood were the subject of the conference whose proceedings are reported in this volume.

That critical points in this general sense have much in common with each other is attested by the fact that they have been treated from the beginning by very similar models and theories. These models and theories are based on the idea that phase transitions and critical points are brought about through the mutual cooperative interaction of many particles. For this reason these phenomena are often called cooperative phenomena. The essential similarity of these early theories, the Van der Waals theory of the liquid-vapor critical point, Curie-Weiss theory of ferromagnetism, the Bragg-Williams and Bethe theory of order-disorder phenomena is emphasized in the introductory historical lecture of Uhlenbeck. They give, as Uhlenbeck pointed out, an excellent qualitative picture of critical phenomena, but fail more and more seriously in their quantitative predictions as the critical point is approached. Their ultimate inadequacy is demonstrated by their disagreement with Onsager's exact solution of the two-dimensional Ising model of ferromagnetism.

Several recent scientific developments, both experimental and theoretical, contributed to the feeling on the part of a number of scientists, and in particular, on the part of those who formed themselves into an *ad hoc* committee to organize it, that April 1965 was an appropriate moment for a conference on critical phenomena. Firstly, there was the theoretical prediction of nonclassical critical behavior for three dimensional lattice models of gases and magnets based on the numerical generation and summation of a large number of terms of exact low and high temperature series expansions. A second recent development, in this case experimental, was the discovery that the specific heat at constant volume of a simple fluid near the critical point is apparently singular and very similar in its behavior to the λ-singularity in the specific heat of liquid helium. A third development was the confirmation through measurement of the internal magnetic field by nuclear magnetic resonance that the shape of the magnetization versus temperature curve of a ferro- or antiferromagnet is similar if not identical to the shape of the coexistence curve of the liquid-vapor phase transition and similar to the shape predicted by the series summation method.

A fourth development was the critique of the Ornstein-Zernike theory of critical opalescence and the experimental confirmation of deviations from this theory.

A common feature of these developments and of others not listed is that they point up a relationship between phenomena which are normally investigated by different institutional groupings of scientists using different experimental techniques who perhaps normally do not meet each other at scientific conferences. It was the purpose of the conference to present these recent developments, to provide an opportunity to assess their significance both individually and as a total picture, to bring together for mutual enlightenment scientists working in different specialities and disciplines, to provide a forum for theoretical speculations.

The program of the conference consisted primarily of papers reviewing the experimental situation for various important critical phenomena. In addition to these, each session contained a selection of shorter papers presenting new data, a novel experimental method, or new theoretical ideas. These proceedings contain the text of the papers substantially as presented except for the paper of Passell which is represented only as an abstract. Also included is a "dictionary" of corresponding parameters in various critical systems together with a tabulation of results on critical exponents prepared by Fisher.

An attempt was made by the session chairmen to elicit as much discussion as time permitted and this is included almost *verbatim* in these proceedings. Certain discussion remarks were in effect short papers. In some of these cases a manuscript was available and was included in the text. In other cases it was possible to make references to a recent or shortly to appear publication.

It will be noted that the bulk of the papers at the conference were experimental. This does not represent a bias towards empiricism on the part of the conference organizers but rather their feeling that the most appropriate way to further an eventual theoretical understanding of critical phenomena was by a complete and critical presentation of the experimental situation. However, in addition to the theoretical papers of Domb, Fisher, Buckingham, and Marshall which were presented in the main program, the last session of the conference was almost entirely devoted to short theoretical presentations. Not all of these are published here. This supplementary session also included the experimental paper of Lorentzen. Although not actually presented at the conference, a review article by I. M. Firth, a participant, of certain techniques of low temperature calorimetry was felt to be relevant and is included in this volume.

The contribution of a conference such as this one is to be judged not only on the questions it answers but also for the issues which it brings to clear statement. I close this introduction with my own opinion of what some of these outstanding issues are.

It may perhaps be regarded as established that the thermodynamic properties of substances near critical points are singular functions in the mathematical sense. A primary issue then is *what is the nature of these singularities?*

One of the ways of expressing these singularities is through critical exponents as defined in the paper by Fisher. The fact, coming out of the papers by Rowlinson, Domb, Benedek, and Fisher, that values of critical exponents predicted by the series summation method are in very good agreement with experiments both in fluids and in magnets is an important success of theory. Nevertheless, several questions remain.

The summation theory predicts different results for different physical models such as the Heisenberg and Ising models of ferromagnetism. *Can we exhibit these differences experimentally?* The paper of Wolf describes an experimental realization of an Ising ferromagnet. *What is the significance of the quantum effects on critical exponents pointed out in the papers of Sherman and M. H. Edwards?*

Another aspect of the nature of the critical singularity is the behavior of the specific heat. *Is the logarithmic specific heat singularity, so convincingly demonstrated for the λ-transition in liquid helium in the paper of Fairbank, a paradigm for the behavior of specific heat on all critical systems?* The paper of Moldover and Little reports experiments on this question for the liquid vapor critical point of helium while Yamamoto reviews the situation for some solid-state second order transitions. Teaney discusses the specific heat of some ferromagnetic and antiferromagnetic transitions from

this point of view, while Kierstead presents results on the singular behavior of the pressure coefficient near the λ-point.

A question which was not represented in the program but which was touched upon in the discussion is *what is the relation of the superconducting transition point to the λ-point and to the liquid vapor critical point?*

The paper of Chu and the earlier work of McIntyre referred to in the discussion indicate deviations from the classical, Ornstein-Zernike theory of critical fluctuations within a few hundredths of a degree Kelvin from the critical consolute point of a liquid mixture. An obvious experimental problem is to *confirm these deviations, to correlate the results of light and x-ray scattering and to make precise the nature of the critical singularity in these phenomena.* The present status of results on elastic light and x-ray scattering was reviewed by Brumberger while Dietrich and Als-Nielsen presented their results obtained by elastic neutron scattering on β-brass. A related question brought up in the discussion is *why do deviations from the classical theory of critical opalescence occur only within hundredths of a degree of the critical point while deviations in thermodynamic quantities show nonclassical behavior much farther away?*

Phenomenological theory predicts that magnetic fluctuations become slower and slower near the Curie point, and therefore that critical magnetic scattering should be elastic, while the experiments of Passell and Jacrot show a definite and unexpected amount of inelastic scattering. Although Marshall's paper suggests a possible and even likely solution, the question still remains *why is critical magnetic neutron scattering inelastic?*

The review of transport phenomena by Sengers indicates that the thermal conductivity of simple fluids exhibits a large anomaly near the critical point while the viscosity exhibits no such anomaly or a very minor one. The opposite seems to be the case for binary liquid mixtures. The question arises, *which transport coefficients are anomalous near critical points and why?*

Several new techniques or techniques newly applied to critical phenomena were presented at the conference. One of these was the inelastic scattering of laser light, which was represented in the papers of Alpert and of Ford and Benedek. Another was nuclear magnetic resonance whose application to fluids was given in the paper by Bloom and in a discussion remark of Trappeniers. The application of this method to antiferromagnetism was presented in the talk of Heller.

Not a new method but one which has not perhaps been fully exploited is the diagnosis, using a light probe, of the density gradients produced by gravity in a fluid near its critical point. The papers of Schmidt and Lorentzen present results obtained by this method. A somewhat related method was brought up by Webb in the discussion in which the meniscus, which becomes more and more diffuse as the critical point is approached, is probed by its reflectivity to light.

Results on ultrasonic propagation in fluids near critical points were reviewed by Sette while the application of this method to a solid state second order transition is given in the paper of Garland and Renard and to helium near its critical point by Chase and Williamson.

Perhaps the foregoing questions can be subsumed under two fundamental questions: the first question is *are all the phenomena considered in the conference under the rubric of critical phenomena truly analogous?* This question can be perhaps answered quickly and affirmatively when, say, the liquid-vapor transition is compared to the phase separation of a binary liquid mixture or even to order-disorder phenomena in solids. The analogies become less clear when these are compared to magnetic phenomena, superfluidity, and superconductivity.

When available in any given case, the best experimental and theoretical evidence seems to show that the singular behavior of analogous properties in different systems is very similar. Of course, the series summation method indicates small but definite differences between different systems. Without prejudging the significance of these differences, the similarity of behavior already suggests a common explanation.

A second question is then, *what is the common reason for the singular behavior of analogous properties?*

MELVILLE S. GREEN.

ACKNOWLEDGEMENTS

The organizing committee wishes to express appreciation for the generous support of the National Science Foundation and the Office of Naval Research which enabled the conference to benefit from the participation of many scientists from western Europe, Japan, and Australia whose contribution otherwise would have been sorely missed. The committee also wishes to express its thanks to the many members of the NBS staff who contributed to making the conference arrangements pleasant and convenient. It wishes especially to thank Mr. Robert Cooke of the Office of Technical Information and Publications and Mrs. May J. Lum and Mrs. Hattie N. Brown of the Heat Division. It also wishes to thank Mrs. Vivian R. Green for her help in organizing the social program of the conference.

CONTENTS

CONTENTS – Continued

EQUILIBRIUM CRITICAL PHENOMENA IN FLUIDS

Chairman: A. M. J. F. Michels

The Classical Theories of the Critical Phenomena

G. E. Uhlenbeck

The Rockefeller University, New York, N.Y.

1. When the organizers of this conference on critical phenomena asked me to start the discussions with a review of the classical theories in order to provide the proper historical perspective, I had hoped that I would find the time to do this in a responsible way. However I soon found out that is not easy! The literature is large and very few (if any!) good historical studies have been made about the development of thermodynamics and statistical mechanics in the second half of the last century. I recommend it to the historian of science! There are many themes and questions which seem to me very worth while to study as for instance the penetration of the ideas of Gibbs and his methods (especially his graphical methods) into the Dutch school of thermodynamics of van der Waals, Bakhuis Roozeboom, Kamerlingh Onnes, and others: the relation of the Strassbourg school of Weiss on ferromagnetism with the ideas of van der Waals: the early controversies about the critical region versus the critical point which is now again so much in the center of attention: and so on!

I hope that you will take therefore the short historical remarks I will present with a grain of salt, and that you will consider my talk more as a kind of keynote address! I will try to mention some of the names and some of the notions which you will hear over and over again, and I will try to explain why I think the recent revival of the study of the critical phenomena is of such deep interest for the student of statistical mechanics.

2. Let me begin with some names and dates.

1869 Discovery of the critical temperature of CO_2 by Andrews. The general form of the set of isotherms for the liquid-vapor equilibrium can be found already in Andrews' paper plus the suggestion that this was a *general* phenomenon.

1873 Dissertation of J. D. van der Waals on the continuity of the gas and liquid state. You all know that the miraculous van der Waals equation:

$$p=\frac{kT}{v-b}-\frac{a}{v^2}$$

together with the Maxwell equal area rule (added by Maxwell in 1874 in a long review of the work of van der Waals) explains the vapor-liquid equilibrium and the existence of the critical point:

$$v_c=3b;\ p_c=\frac{1}{27}\frac{a}{b^2};\ kT_c=\frac{8}{27}\frac{a}{b}.$$

Of course this confirmed the idea that the critical point was a *general* phenomena and that there were no "permanent" gases. Made explicit by the

1880 law of corresponding states (van der Waals)

$$\frac{p}{p_c}=\pi=F(\omega,\ \vartheta)\quad \omega=\frac{v}{v_c}\quad \vartheta=\frac{T}{T_c}$$

with F a universal function. The role which this law played in the liquefaction of gases and especially of Helium (Kamerlingh Onnes, 1908)

209-493 O-66—2

was spectacular and I hope well known.

The discovery of the magnetic transition point came much later. So far as I know, it was only in:

1890 Hopkinson found that iron above a certain temperature ceased to be ferromagnetic. Confirmed and thoroughly investigated by Pierre Curie in a classical paper of 1895, and therefore now always called the Curie temperature.

1907 P. Weiss introduced the notion of the inner field and explained the existence of the Curie temperature T_c and of the spontaneous magnetization for $T < T_c$. The third critical transition phenomena is that of the order-disorder transformation in binary alloys or better substitutional solid solutions. Suspected in 1919 by Tammann, proved in 1925 by the x-ray work of Johanson and Linde, the theoretical explanation given in:

1934 by Bragg and Williams, was clearly patterned after the Weiss theory. One could still mention the discovery of the critical mixing temperature of two fluid phases for a binary mixture. Found by Alexejew around 1800. Explanation by van der Waals and a series of coworkers

1890–1905 (Kuenen, Kohnstamm, van Laar, Korteweg) 1890–1905, by generalizing the van der Waals equation for mixtures and applying for the thermodynamic discussion the graphical methods of Gibbs.

3. Leaving for a moment this sort of schoolbook history let me emphasize *the great similarity* of the three classical theories of van der Waals, Weiss, and Bragg-Williams although the derivations are often quite different. It is now clear and generally accepted that they are all based on the assumption that the attractive forces between the molecules which produce the cooperative effects have a *very long range*. As a result the type of singularity which the critical point represents is in all the theories exactly the same. To put this in evidence it is good to direct attention (following M. Fisher) to the following three theoretical predictions:

a. At the critical point *the specific heat makes a finite jump* and then decreases again. For a van der Waals gas at the critical density, one gets:

$$\Delta c_v \equiv c_v - \frac{3k}{2} = \begin{cases} 0 \text{ for } T > T_c \\ \frac{9}{2}k\left[1 - \frac{28}{25}\frac{T_c - T}{T_c} + \ldots\right] \end{cases}.$$

For a Weiss ferromagnet:

$$\Delta c_v = \begin{cases} 0 \text{ for } T > T_c \\ \frac{5}{2}k\left[1 - \frac{13}{5}\frac{T_c - T}{T_c} + \ldots\right] \end{cases}.$$

For a Bragg-Williams binary alloy:

$$\Delta c_v = \begin{cases} 0 \text{ for } T > T_c \\ \frac{3}{2}k\left[1 - \frac{8}{5}\frac{T_c - T}{T_c} + \ldots\right] \end{cases}.$$

b. At the critical point the coexistence curve is *parabolic*. For a van der Waals gas (with reduced quantities): $\omega_g - \omega_l = 4(1-\vartheta)^{1/2}$. For a Weiss ferromagnet:

$$I^* \equiv \frac{\mu W}{kT} M = \sqrt{15}\left(1 - \frac{T}{T_c}\right)^{1/2}$$

[also with reduced quantities: W = constant of Weiss inner field, M = magnetization; $T_c = \frac{N\mu^2 W}{3k}$ = Curie temperature. Putting $H^* = \frac{\mu}{kT} H$, then the magnetic equation of state becomes: $I^* = \frac{3}{\vartheta} L(H^* + I^*)$ where $L(x)$ is the Langevin Function].

c. At the critical point the compressibility or the susceptibility become infinite as $1/|T - T_c|$. For a van der Waals gas:

$$\left(\frac{\partial \pi}{\partial \omega}\right)_{\omega=1,\, T>T_c} = -6(\vartheta - 1)$$

$$\left(\frac{\partial \pi}{\partial \omega}\right)_{\text{coex},\, T<T_c} = -12(1-\vartheta).$$

For a Weiss ferromagnet: (χ is the susceptibility)

$$\chi^+ = \frac{1}{W}\frac{1}{\vartheta - 1} \qquad \chi^- = \frac{1}{2W}\cdot\frac{1}{1-\vartheta}$$

$$T > T_c \qquad T < T_c$$

For a Bragg-Williams alloy, properties b and c can be defined but they have less direct observational meaning.

4. At this point one may well already raise the question, *why* the classical theories represent so well, at least qualitatively, the observed critical phenomena. Of course, as long as little was known about the intermolecular forces, one could think that the attractive forces *had* a very long range. In fact van der Waals never doubted that, and probably Weiss also had always the long range dipole-dipole forces in mind. However the later development showed more and more clearly that the cooperative forces were *not* of a very long range, that each atom was influenced by at best a few shells of neighboring atoms. Of course, it took a long time before this was realized. It required the elucidation, of the nature of the van der Waals attractive forces by London and of the Weiss inner field by Heisenberg which came in the late twenties as a byproduct of the quantum mechanical revolution.

Partially because of this fact, the classical theories became more and more discredited in the thirties. This was also because it turned out that the classical theories although qualitatively correct could *not* be fixed up so as to give a precise quantitative description of the phenomena. For the van der Waals theory this became accepted already around 1900, and as a result Kamerlingh-Onnes started then to represent the experimental data by series expansions in the density, the so-called virial expansion, for which Ursell and Mayer then gave the theoretical analysis in the thirties. For the Weiss and the Bragg-Williams theory the attempts for improvement lasted a bit longer, but also here one soon began to turn more and more to series expansions. The reason is clear. The terms in the expansions can be calculated exactly (at least in principle) and related to the intermolecular forces. And since one began to learn more and more about these forces, this was of course of the greatest interest. However, one lost the general point of view which the classical theories provided, and perhaps because of this one also lost interest in these theories. They were considered to give "convenient interpolation formula" or "semiphenomenological descriptions." Remarkable for instance is the fact that in the great international congress in 1938 to celebrate van der Waals' 100th birthday, the van der Waals equation was mentioned only once, and all attention was centered on the so-called rigorous theories. I think one is now coming back from these theories because one has become dissillusioned about the series expansions since no general point of view emerges from them.

5. The first and unfortunately till now
1944 practically the only step forward beyond the classical theories was made in the famous paper by Onsager on the two-dimensional Ising model. I will not say much about it, because you will hear much more about it later. It has dominated the subject for the last 20 years. Let me remind you only that the Ising model (proposed by Ising in 1925) can be considered as a simplified version of the ferromagnetic, and of the order-disorder and even of the vapor-liquid problem (through the lattice gas). Each atom on a lattice site can be in two states (spin up or down) and the interaction is only between neighboring pairs and is $\pm J$ depending on whether the spins are parallel or antiparallel. It is therefore a model with *short range forces*. The most striking result of Onsager was that there *is* a critical point and that the specific heat is *logarithmically infinite* there in contrast to the classical result.

6. So far I have only talked about the critical point and its properties for the equation of state. A deeper question is the question what happens with the correlation function near a critical point. That the density fluctuations will get large near the critical point was pointed out by Smoluchowski, but that in addition the correlation of the density fluctuation at different points will become of very long range and that this is the cause of the critical opalescence was first clearly
1914 stated by Ornstein-Zernike in 1914, and then worked out in the Groningen dissertation of
1916 Zernike of 1916.

Angular distribution of the scattered radiation is related to the Fourier transform of the correlation function:

$$g(k, v, T)=\int d\vec{\mathbf{r}} e^{i(k\cdot r)}\left[n_2(r; v, T)-\frac{1}{v^2}\right]$$

$$k=\frac{2\pi}{\lambda}\sin\frac{\theta}{2}.$$

Ornstein and Zernike give specifically for

$T \gtrless T_c$ $v = v_c$:

$$g(k;\, v_c,\, T) = \frac{kT}{a} \frac{1}{k^2 R^2 - \frac{1}{3}(\partial \pi / \partial \omega)_{\omega=1}}$$

with

$$R^2 = \frac{1}{3} \frac{\int d\vec{\mathbf{r}} r^2 \varphi_{\text{attr}}(r)}{\int d\vec{\mathbf{r}} \varphi_{\text{attr}}(r)}$$

$\frac{1}{g(k)}$ versus k^2 (O-Z plot) should be a straight line whose intercept with the ordinate axis must go to zero if $T \to T_c$ as $(T - T_c)$.

There are many ways of justifying the O-Z theory. I think though that always one again has to assume that the forces *are of long range*, so that it can be considered a natural generalization of the van der Waals theory.

The corresponding theory for neutron scattering near the Curie point is so recent that it does not belong in a historical survey!

7. Outlook. What are the problems, and what can one hope from the present revival of interest? As always in statistical mechanics one must distinguish the equilibrium from the nonequilibrium properties.

A. I think it is wonderful that so much new experimental work is being done. For a long time experiment was too much dominated by the theory, and except in a few places (like in the van der Waals laboratorium in Amsterdam) experimental work on the properties of matter near the critical point nearly ceased. I am glad that it is different now. What can one hope to find? I hope that it will turn out that again there is a deep analogy between the various critical points, that there are similarities like in the classical theories. You will hear a lot about the new experimental work, so I will only mention a few points which seem to me very suggestive.

1. Near the critical point the coexistence curve seems much better represented by the empirical Guggenheim law: $\omega_g - \omega_l = \frac{7}{2}(1-\theta)^{1/3}$. Also the magnetization curve near T_c seems to show such a cubic behavior.

2. For Argon and O_2, and now also for He, it seems that c_v does *not* show a jump but becomes logarithmically infinite. For $T \gtrless T_c$

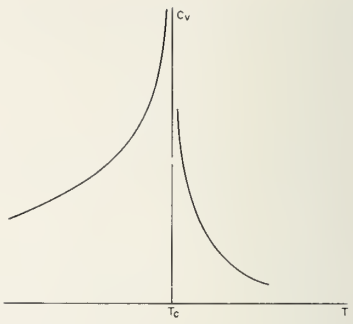

$$c_v = -B^{\pm} \ln \left| 1 - \frac{T}{T_c} \right| + C^{\pm}$$

with $B^+ \cong B^-$ and $C^- - C^+ \cong 10k$.

This surprising result by the Russians, is also found for $He^{II} - He^{I}$ transition and I believe also for some ferromagnetic transitions. You will hear more about it tomorrow.

If there is such an universal, but nonclassical behavior, then there must be an universal explanation which means that it should be largely independent of the nature of the forces. The only corner where this can come from is I think the fact that the forces are not long range. The Onsager solution gives I think a strong hint. It may well be so that away from the critical points the classical theories give a good enough description but that they fail close to the critical point where the substance remembers so to say Onsager. I think that to show something like this is the central theoretical problem. One can call it the reconciliation of Onsager with van der Waals.

With regard to the correlation function and the Ornstein-Zernike theory I hope that the new experimental work will show that there is a *critical region*, where already deviations from the classical van der Waals-Ornstein-Zernike theories begin to show up. I think there are indications (as the specific heat anomaly) that such a region exists. Of course there is *also* a singularity or a critical point.

B. Finally a remark about nonequilibrium phenomena. There are very surprising experimental results found about various transport coefficients, which clearly are worth pursuing. Till now there is no theory, not even a van der Waals like theory. The development of the proper transport theory with long range forces, van der Waals-like but probably with one more constant, seems to me not impossible and very worth while.

The Coexistence Curve of He^3*

Robert H. Sherman

Los Alamos Scientific Laboratory, Los Alamos, N. Mex.

In this report we wish to present the results of some recent *P-V-T* measurements on He^3 in the critical region. A significant departure was found in the shape of the coexistence curve from the behavior expected for classical systems such as Xe and CO_2.

The *P-V-T* surface of liquid He^3 was investigated by Sherman and Edeskuty [1][1] between 1.0 and 3.3 °K and for pressures from the vapor pressure to solidification. The measurements reported by these authors lacked detail in the region from 3.0 to 3.324 °K, the critical point, [2] and for pressures less than ~3 atm. In addition, there were no measurements reported on the fluid for $T > T_c$.

Recently 23 isochores of He^3 were measured with densities ranging from 0.015 to 0.066 g/cm³ using the apparatus of reference [1] with only slight modification. Along each isochore data were taken with temperature decreasing from 4 °K, a final observation being made along the liquid-vapor equilibrium curve (vapor pressure). Temperatures were reduced to the 1958 He^4 Scale of Temperatures [3]. Pressures were measured with a fused quartz bourdon tube gage having an accuracy of 0.05 mm Hg. While the cell has a vertical dimension of ~4.6 cm, measurements were not made very close to the critical point and as a result, density gradients within the cell were not of any significance.

P-V-T data taken by the isochoric method have the advantage of yielding *P-T* relations which are almost linear. Thus each isochore was extrapolated to the vapor pressure [4] to provide a ρ–T point on the coexistence curve. Values of ρ_l and ρ_g were read from a smooth ρ–T graph and $\rho_l - \rho_g$ was plotted as a function of $T_c - T$ using logarithmic coordinates as shown in figure 1. It is easily seen that the critical point exponent β [5, 6] in the relationship

$$\rho_l - \rho_g \propto (T_c - T)^{\beta}$$

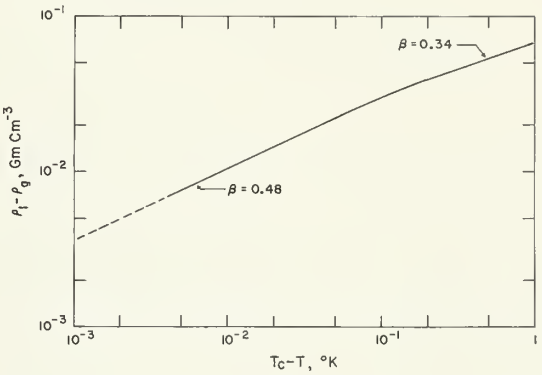

FIGURE 1. *A plot of* $\rho_l - \rho_g$ *versus* $T_c - T$ *along the coexistence curve for* He^3.

deviates from the "classical" value of ~⅓, and $\beta \rightarrow 0.48 \pm 0.02$ as $T \rightarrow T_c$. This slope appears to be constant up to $T_c - T = 0.07°$.

TABLE 1. *Densities of* He^3 *along the coexistence curve.*

T	ρ_g	ρ_l
°K	*gm cm*$^{-3}$	*gm cm*$^{-3}$
2.4	0.00801	0.07404
2.5	.00915	.07288
2.6	.01044	.07159
2.7	.01192	.07015
2.8	.01371	.06852
2.9	.01573	.06668
3.0	.01808	.06458
3.05	.01951	.06338
3.1	.02113	.06200
3.15	.02317	.06033
3.2	.02557	.05815
3.25	.02867	.05498
3.3	.03373	.04970
3.324	.04178	.04178

*Work performed under the auspices of the U.S. Atomic Energy Commission.

[1] Figures in brackets indicate the literature references at the end of each paper.

TABLE 2. *Properties of* He^3 *at the critical point*

$T_c = 3.324 \pm 0.0018$ °K [a]
$p_c = 873.0 \pm 1.5$ mm [a]
$\rho_c = 0.0418 \pm 0.001$ g/cm^{-3}

[a] Reference 2.

Kerr [7] has reported results of *P-V-T* measurements for He^3 along the coexistence curve. Above 3.0 °K, however, his results show increasing deviations from the present measurements probably due to the increasingly larger obnoxious volume corrections which must be made as the critical point is approached. Below 2.9 °K, Kerr's gas densities are in excellent agreement with those calculated using virial coefficients [8]. In table 1 values are given for the densities of He^3 liquid and vapor along the coexistence curve from the present series of experiments and in table 2 some of the properties of He^3 at the critical point are summarized.

References

[1] R. H. Sherman and F. J. Edeskuty, Annals of Physics **9,** 522 (1960). An error of +0.30 percent was made in the cell volume calibration. As a result all volumes and entropy changes reported should be reduced in magnitude by 0.30 percent. Expansion and compressibility coefficients are unaffected.

[2] S. G. Sydoriak and R. H. Sherman, J. Res. NBS **68A** (Phys. and Chem.) No. 6, 547 (1964).

[3] F. G. Brickwedde, H. Van Dijk, M. Durieux, J. R. Clement and J. K. Logan, NBS Mono. 10, (U.S. Govt. Printing Office, 1960).

[4] R. H. Sherman, S. G. Sydoriak, and T. R. Roberts, J. Res. NBS **68A** (Phys. and Chem.) No. 6, 579 (1964).

[5] For the critical point exponents the notation of Fisher [6] is used.

[6] M. E. Fisher, J. Math. Phys. **5,** 944 (1964).

[7] E. C. Kerr, Phys. Rev. **96,** 551 (1954).

[8] T. R. Roberts, R. H. Sherman, S. G. Sydoriak, J. Res. NBS **68A** (Phys. and Chem.) No. 6, 567 (1964).

Critical States of Simple Fluids and Fluid Mixtures; a Review of the Experimental Position

J. S. Rowlinson

Imperial College, London, Great Britain

At a critical point the intensive properties of two coexisting phases become identical. This review is a summary of our experimental knowledge of the rate of the approach to identity as $T-T_c$ approaches zero. Consider some property of the fluid $X(T, V)$ and define an index χ by

$$\chi^{\pm} = \lim_{T \to (T_c)^{\pm}} [\ln X(T, V)/\ln \pm (T-T_c)]. \qquad (1)$$

The limit is usually taken along the path $V=V_c$, and, in general, χ^+ and χ^- will be different.

The following indices are discussed below:

An elementary and ultimately erroneous analysis of the behavior of a system of one component may be based on the assumption that the Helmholtz free-energy is an analytic function of V and T at and near the critical point [1]. Let the first nonvanishing derivative of A with respect to volume be of the order $2n$. Thermodynamic stability requires that n be integral, and van der Waals's equation and all similar equations, require that $n=2$. This assumption leads to the following values of the indices above

$$\alpha^+ = \alpha_1^- = 0 \qquad \alpha_2^- = -(2-n)/(n-1) \qquad (2)$$

Property	Index	Conditions
C_v	$-\alpha$	α^+, limit along the critical isochore $V=V_c$. α_1^-, limit in the one-phase fluid along the outside of the coexisting curve. α_2^-, limit along the critical isochore in the two phase fluid.
$(V-V_c)_\sigma$	β	The subscript σ denotes the orthobaric phases, hence β^+ does not exist and the superscript may be omitted.
$(\partial p/\partial V)_T$	γ	γ^+ and γ_1^- are defined exactly as α^+ and α_1^-.
$(p-p^c)$ as a function of $(V-V_c)$ at $T=T_c$.	δ	δ^+ is apparently equal to δ^- and no distinction is made here.
$(\partial^2 p/\partial T^2)_\sigma$	$-\theta$	The derivative is the curvature of the vapor pressure line and so θ^+ does not exist.

$$\beta = 1/2(n-1) \tag{3}$$

$$\gamma^+ = \gamma_1^- = 1 \tag{4}$$

$$\delta = 2n - 1 \tag{5}$$

$$\theta = 0. \tag{6}$$

Thermodynamic stability requires that certain inequalities hold between the indices. Thus Rushbrooke [2] showed that for a magnetic critical point (and Fisher [3] extended the proof to the fluid of one component)

$$\alpha_2^- + 2\beta + \gamma_1^- \geq 2 \qquad R \tag{7}$$

Griffiths [4] has obtained the inequalities

$$\alpha_2^- + \beta(1+\delta) \geq 2 \qquad G1 \tag{8}$$

$$\alpha_2^- + \beta \qquad \geq \theta \qquad G2. \tag{9}$$

Widom [5] has shown that R becomes an equation if the conditions attached to α are that it represents the difference $(C_v)_2 - (C_v)_1$ across the orthobaric boundary. He has also made two conjectures [6, 7] for which there are no rigorous proofs; namely

$$\gamma^+ = 2(1-\beta) \qquad W1 \tag{10}$$

$$\gamma_1^- = \beta(\delta - 1) \qquad W2 \tag{11}$$

It is seen that $W2$, if correct, implies that R and $G1$ are the same inequality.

The classical equations (2) to (6) satisfy R, $G1$, $G2$, and $W2$ for all values of n.

The best experimental values do not fit (2) to (6) with any integral value of n, and certainly not with $n=2$. One concludes that A is nonanalytic.

The most probable values of the indices will now be reviewed in turn.

α.—The best measurements of C_v appear to be those of Voronel' and his colleagues for argon and oxygen [8]. Little experimental detail is given but the results are more consistent and extend to lower values of $(T-T_c)$ than any previous sets. However, they are restricted to the critical isochore. Fisher [9] has analyzed them in detail, and his analysis need not be repeated. The results of Michels and Strijland [10] for carbon dioxide are at densities above and below the critical, but no reliable value of α_1^- could be obtained from them.

Fisher [9] concludes that the singularity is a little sharper than logarithmic, both above and, probably, below. Hence

$$\alpha^+ \sim 0.1\text{–}0.2$$
$$\alpha_2^- \sim 0.0\text{–}0.1$$
$$\alpha_1^- \ ?$$

β.—Here there is substantial agreement of a large number of measurements. The most useful of these appear to be those of Michels, Blaisse, and Michels [11] (CO_2), those analyzed by Guggenheim [12] (inert gases), Cook [13] (N_2O), Weinberger and Schneider [14] (Xe) as analyzed by Fisher [3], Lorentzen [15] (CO_2), and Edwards and Woodbury [16] (He) as analyzed by Miller [17]. The conclusions are, as follows.

MBM	$\beta = 0.36$
G, C	$= 0.33$
WS(F)	$= 0.345 \pm 0.015$
L	$= 0.33 \pm 0.02$
EW(M)	$= 0.41$

Here, Lorentzen's value is that obtained with a freshly filled cell and includes points to within 10^{-3} °C of T_c. All figures except the last suggest that β is close to 1/3 but probably above it.

γ.—An analysis of the results of Michels, Blaisse, and Michels [11] (CO_2) and of Habgood and Schneider [18] (Xe) is shown in figure 1.

$\gamma^+ = 1.2$

γ^- is uncertain but probably exceeds unity.

σ.—Widom and Rice [19] have analyzed the results of Michels, Blaisse, and Michels [11] (CO_2), Habgood and Schneider [18] (Xe) and Johnston, Keller, and Friedman [20] (H_2). The results are

Xe, H_2	$\delta = 4.2$
CO_2	$\delta = 4.0$.

However more recent discussion [21, 22] of the optical determinations of density gradients near the critical point suggest that measurements of δ from *P-V-T* may not be as reliable as the analysis of Widom and Rice suggests. Because of the high value of δ the determination from *P-V-T* rests essentially on results at densities well-removed from the

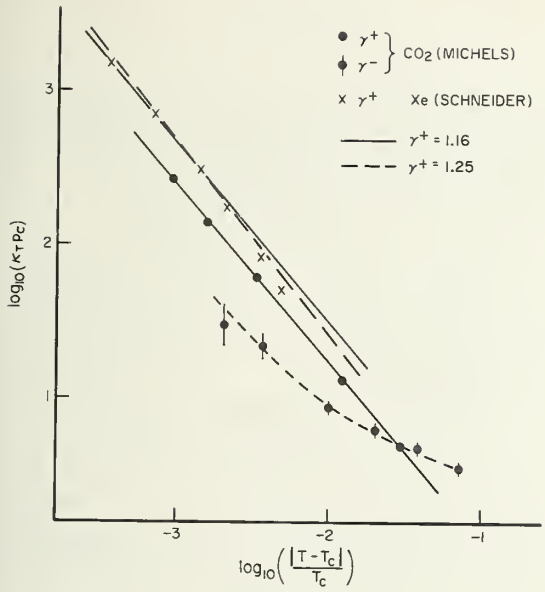

FIGURE 1

critical and hence possibly they are not a true guide to the limiting behavior.

θ.—Careful measurements of vapor pressure in the critical region [11, 23] suggest that θ may not be zero but might have a small positive value, since the fitting of a smooth curve through experimental points usually gives a deviation graph that shows a sharp rising upwards as T_c is reached.

In summary,

α^+	$0.1-0.2$
α_2^-	$0.0-0.1$
β	0.34 ± 0.02
γ^+	1.2 ± 0.1
γ_1^-	$1.0-1.3$
δ	apparently 4.2 ± 0.2
θ	>0 ?

β is the most certain of these, although δ is certainly of high apparent precision. If β and δ are taken as known within the limits shown then the incqualities above lead to the following results

$G1$	$\alpha_2^- \geqslant 0.06-0.40$
R	$\alpha_2^- \geqslant (0.08-0.16)\pm$ uncertainty in γ_1^-
$W1$	$\gamma^+ = 1.28-1.36$
$W2$	$\gamma_1^- = 0.96-1.22$.

Hence,

$G1$, the most useful inequality, probably requires $\alpha_2^- > 0$ and suggests that both β and δ are near to their upper limits, that is $\beta = 0.36$ and $\delta = 4.4$.

$G2$ is trivially satisfied. Possibly [5] $\theta = \alpha_2^-$.

R is too uncertain to be of practical value for fluids.

$W1$ is probably wrong.

$W2$ is probably correct but is subject to the same uncertainty as R. It also requires β and δ to be at their upper limits. A positive value of θ implies a "infinite asymmetry" in $(C_v)_2$ as T approaches $(T_c)^-$.

All these results can be extended to the critical point of a two-component system. Here there is no real distinction between a gas-liquid, a gas-gas, and a liquid-liquid point, but all precise work has been done on systems at which P is essentially zero and which are therefore called conventionally liquid-liquid critical points. The behavior of a two-component system can be obtained by analogy from that of a one-component system by replacing $A(V, T)$ by $G(x, T)$, where x is the mole fraction of one component and where the pressure of the system is fixed. Hence the indices above now refer to the following properties

α	C_p
β	x_σ
γ	$(\partial^2 G/x^2)_{P,T}$
δ	$(\mu_1-\mu)\lambda$ along $T=T_c$
θ	$(\partial C_p/\partial x)_T$ in the two-phase region.

Thus Fisher's proof [3] of Rushbrooke's inequality follows at once for a two-component system from an equation [24] for $(C_p)_2$.

The experimental results are now more fragmentary, although this probably reflects lack of effort rather than inherent difficulty. Precise calorimetry and measurement of vapor pressures should be easier than at the critical pressure of a one-component system since these critical points can be studied at negligible pressures.

α.—The best measurements of C_p are those of Schmidt, Jura, and Hildebrand [25] ($CCl_4 + C_6F_{11}CF_3$): Jura, Fraga, Maki, and Hildebrand [26] ($i-C_8H_{18}+n-C_7F_{16}$): Amirkhanow, Gurvich,

and Matizen [27] ($PhOH + H_2O$). These suggest either a weak infinity in C_p or possibly no infinity at all.

β.—The recent and precise results of Thompson and Rice [28] make it unnecessary to discuss earlier work, including their own. They studied $CCl_4 + n - C_7F_{16}$ to within 10^{-4} °C of T_c and obtain

$$\beta = 0.33 \pm 0.02.$$

γ, δ.—The results of Croll and Scott [29] for $CH_4 + CF_4$ suggest that γ^+ is about unity. The authors may have unpublished points on these systems to justify some attempt to determine γ and δ; no earlier work suffices.

If, by analogy with the more extensive work on systems with one component, it turns out that $\gamma^+ > 0$ then there are interesting consequences. Thus both $(\partial^2 H/\partial x^2)_{P,T}$ and $(\partial^2 S/\partial x^2)_{P,T}$ must be zero at the critical point. That is curves of the heat of mixing as a function of composition must have a point of inflexion. This is not inconsistent with, for example, the measurements of Copp and Everett [30] and of Matizen and Kushova [31] on the lower critical solution point of $Et_3N + H_2O$. There appear to be no other accurate measurements close to T_c.

A further consequence of $\gamma^+ > 1$ for which there is some experimental evidence is that coexistent curves calculated from excess Gibbs free-energies that have been extrapolated to T_c on the implicit assumption that $\gamma^+ = 1$ must always be too high at an upper critical solution temperature and too low at a lower critical solution temperature. It is common experience that this is so [32, 33]. A recent paper by Scatchard and Wilson [33] shows a closed solubility loop calculated by such extrapolations which shows simultaneously an upper critical point that is too high and a lower one that is too low. However more direct evidence of the magnitude of $(\gamma^+ - 1)$ would be welcome.

References

[1] J. S. Rowlinson, Liquids and Liquid Mixtures, ch. 3 (Butterworths, London, 1959).
[2] G. S. Rushbrooke, J. Chem. Phys. **39**, 842 (1963).
[3] M. E. Fisher, J. Math. Phys. **5**, 944 (1964).
[4] R. B. Griffiths, Phys. Rev. Letters **14**, 623 (1965).
[5] B. Widom, private communication.
[6] B. Widom, J. Chem. Phys. **37**, 2703 (1962).
[7] B. Widom, J. Chem. Phys. **41**, 1633 (1964).
[8] M. I. Bagatskii, A. V. Voronel, and B. G. Gusak, Soviet Phys. JETP **16**, 517 (1963); A. V. Voronel' Y. R. Chashkin, V. A. Popov, and V. G. Simkin, ibid. **18**, 568 (1964).
[9] M. E. Fisher, Phys. Rev. **136**, A1599 (1964).
[10] A. Michels and J. Strijland, Physica **18**, 613 (1952).
[11] A. Michels, B. Blaisse, and C. Michels, Proc. Roy. Soc. **A160**, 358, (1937).
[12] E. A. Guggenheim, J. Chem. Phys. **13**, 253 (1945).
[13] D. Cook, Trans. Faraday Soc. **49**, 716 (1953).
[14] A. M. Weinberger and W. G. Schneider, Canad. J. Chem. **30**, 422 (1952).
[15] H. L. Lorentzen, Paper read at conference on Statistical Mechanics at Aachen, 1964.
[16] M. M. Edwards and W. C. Woodbury, Phys. Rev. **129**, 1911 (1963).
[17] D. Miller, private communication.
[18] H. W. Habgood and W. G. Schneider, Canad. J. Chem. **32**, 98, 164 (1954).
[19] B. Widom and O. K. Rice, J. Chem. Phys. **23**, 1250 (1955).
[20] H. L. Johnston, K. E. Keller, and A. S. Friedman, J. Amer. Chem Soc. **76** (1954) 1482.
[21] S. A. Ulybin and S. P. Malyshenko, Third Symposium on Thermophysical Properties, Amer. Soc. Mech. Eng., Purdue, 1965, p. 68.
[22] S. Y. Larsen and J. M. H. Levelt Sengers, Third Symposium on Thermophysical Properties, Amer. Soc. Mech. Eng., Purdue, 1965, p. 74.
[23] A. Michels, J. M. H. Levelt and W. De Graaff, Physica **24**, 659 (1958); A. Michels, J. M. H. Levelt, and G. J. Wolkers, ibid. **24**, 769 (1958).
[24] Reference 1, p. 168.
[25] H. Schmidt, G. Jura and J. H. Hildebrand, J. Phys. Chem. **63**, 297 (1959).
[26] G. Jura, D. Fraga, G. Maki, and J. H. Hildebrand, Proc. Mat. Acad. Sci. **39**, 19 (1953).
[27] Kh. Amirkhanow, I. G. Gurvich and E. M. Matizen, Dokl. Akad. Nauk. SSSR **100**, 735 (1955).
[28] D. R. Thompson and O. K. Rice, J. Amer. Chem. Soc. **86**, 3547 (1964).
[29] I. M. Croll and R. L. Scott, J. Phys. Chem. **68**, 3853 (1964); see also N. Thorp and R. L. Scott, ibid. **60**, 670, 1441 (1956).
[30] J. L. Copp and D. H. Everett, Discuss. Faraday Soc. **15**, 174 (1953).
[31] E. M. Matizen and N. V. Kushova, Russ. J. Phys. Chem. **34**, 1056 (1960).
[32] G. E. Williamson and R. L. Scott, J. Phys. Chem. **65**, 275 (1961).
[33] G. Scatchard and G. Wilson, J. Amer. Chem. Soc. **86**, 133 (1964).

Optical Measurements of the Density Gradients Produced by Gravity in CO_2, N_2O, and $CClF_3$ Near the Critical Point

E. H. W. Schmidt

Technische Hochschule, München, Germany

1. Introduction

When Dr. Green asked me to read a paper dealing with my work on density gradients produced by gravity in fluids near their critical points, I hesitated to follow this invitation because I already presented some of such experiments with CO_2 at the Second Symposium on Thermophysical Properties held in Princeton University January 1962 [1]. However, meanwhile together with my collaborator J. Straub, we repeated these measurements with greater precision and extended them to N_2O and $CClF_3$ (Freon 13).

First I may remind you of the original purpose and the start of these experiments. The old conventional method for measuring the critical data of a substance by observing the disappearance of the meniscus i.e., the interface between the liquid and the vapor phase is not very exact because it needs a slow change of temperature or pressure and therefore the fluid is not in a state of equilibrium. Moreover it is difficult and depends upon the ability of the observer to state exactly when the meniscus has disappeared. This is the reason why the critical point of most substances is not very well known, and some observers even had the conception, that the critical point had to be extended to a critical region.

In order to avoid the difficulties of the conventional method I came to the idea of using the refractive index for the determination of the critical state data, which index depends in a simple way upon the density of the substance irrespective of its liquid or gaseous state.

As long as a meniscus is visible, the densities and the refractive indices are different in the liquid and in the vapor. However, when the critical state is attained, refractive index and density should be equal below and above the level where the meniscus disappeared.

2. The Pressure Chamber and Its Accessories

For our experiments we use now the installation shown in figure 1. The fluid is in a strong cylindrical chamber of stainless steel with horizontal axis closed on both ends by parallel windows of optical glass with 28 mm free diameter.

For equalizing the temperature of the pressure chamber it is placed in a big copper cylinder, which on its outer side is supplied with screw-shaped groves through which water from a thermostatic apparatus flows bifilarly. In order to minimize the fluctuations of the temperature produced by the switching in and out of the heating coil of the thermostat with the help of a mercury contact thermometer, three thermostats are used in series so that the first with its contact thermometer delivers warm water for heating the next one, and this again for the third, as shown in figure 2. In this way the temperature of the copper cylinder with the pressure chamber in it could be held constant for many hours and even for several days within deviations of less than ± 0.0015 °C.

The copper cylinder has on both ends conical holes for the optical observation. In these holes two more plates of thick optical glass are placed, which together with two outer thinner windows and electrically heated coils inside these windows prevent the cooling of the pressure chamber by the surrounding air.

The temperature of the room, in which the whole experimental arrangement has its place is also regulated by way of contact thermometers together with electric heaters and the fluctuations of the room temperature do not exceed ± 0.1 °C. Nevertheless, the copper cylinder is covered with a thick layer of polystyrol as heat insulation.

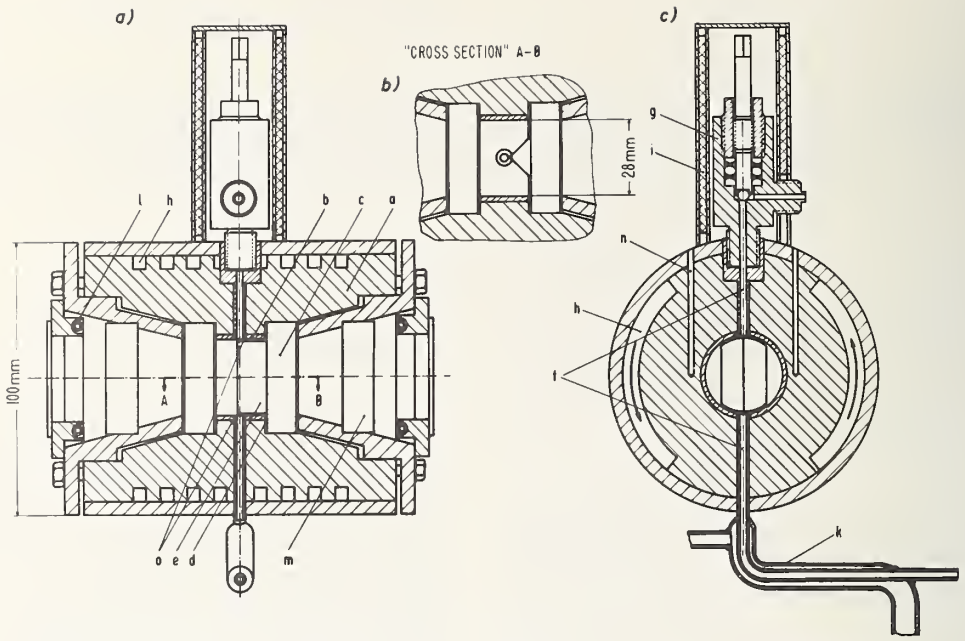

FIGURE 1. *The pressure chamber used for the experiments:*
(a) *Axial cross section*
(b) *Cross section A-B*
(c) *Cross section perpendicular to axis*

Dimensions in mm: a. Copper cylinder, b. Pressure chamber, c. Strong glass windows, d. Sealing foils, e. Glass prism, f. Tube, g. Filling valve, h. Screw shaped channels for water heating, i. Protective heating of the valve, k. Heating tube, l. Glass plate with protective heating coil behind it. m. Glass plates, n. Holes for thermocouples, o. Welded joints.

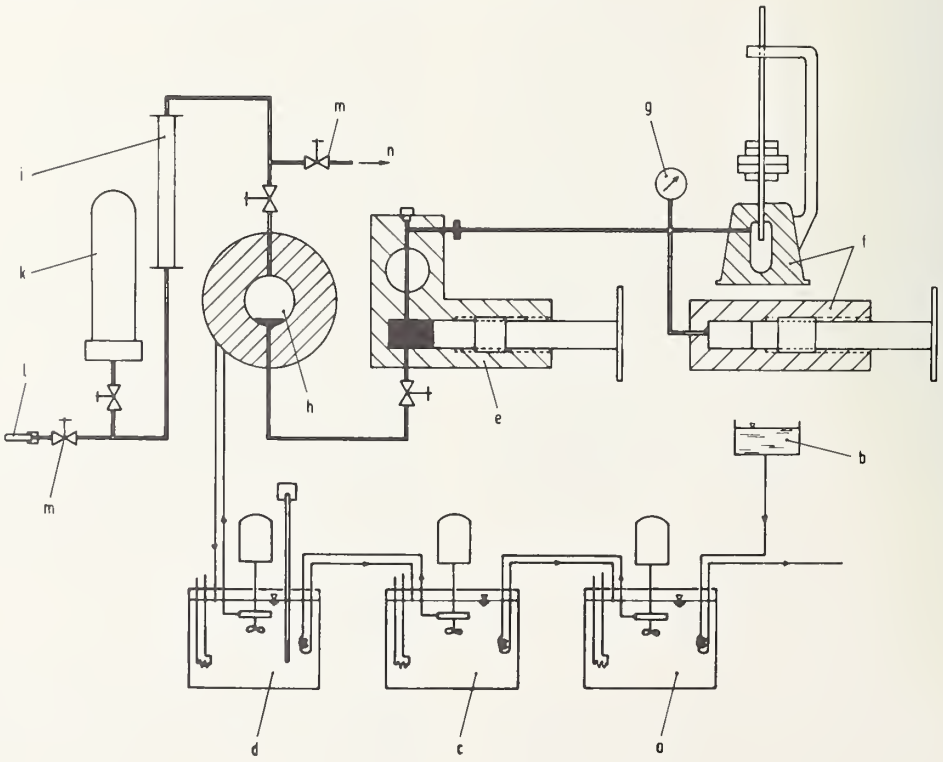

FIGURE 2. *Scheme of experimental arrangement:*
a. First thermostat, b. Water container, c. Second thermostat. d. Third thermostat. e. Screw pump for mercury. f. Pressure balance, g. Manometer. h. Pressure chamber. i. Dehydrator for gas, k. Container for pressurized gas, l. Glass tube for testing the vacuum, m. Valve, n. Joint to vacuum pump.

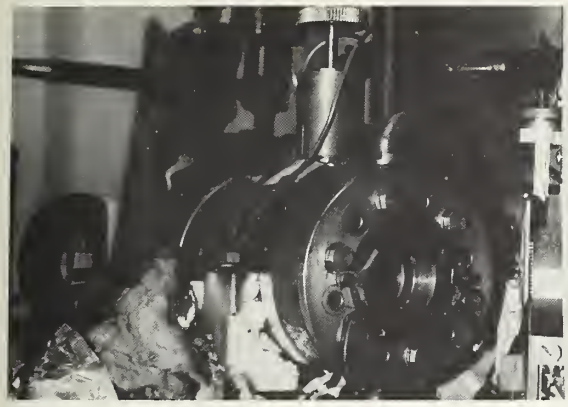

FIGURE 3. *Picture of the pressure chamber (heat insulation removed).*

A picture of the pressure chamber and the copper cylinder before surrounding it with the heat insulation is shown in figure 3. All tubes leaving the pressure chamber are provided with protective electrical heating in order to prevent any loss of heat which would cause local cooling. The purpose of all these arrangements is to improve the constancy of temperature in the pressure chamber and to avoid natural convection in the fluid, which disturbs the optical measurements.

The temperature of the fluid is measured with the help of manganin-constantan thermocouples placed in vertical holes drilled into the copper cylinder. The pressure of the fluid is measured with a piston manometer f shown in figure 2. This manometer is filled with oil which is separated from the fluid in the pressure chamber by mercury. With the help of a screw pump more or less mercury can be pumped into the pressure chamber changing the volume and the density of the fluid contained in it.

3. Optical Installation

The optical installation for measuring the refractive index and from it the density of the fluid is shown in figure 4. The pressure chamber a with the glass prism in it is placed in the middle of the disk c, around which two arms can be swung of which one supports the sodium lamp d, the condensor e, the vertical slit f, and the lens g; whilst the other arm bears the telescope h, the horizontal slit i, and a small concave mirror k. The sodium lamp with its monochromatic light illuminates with the help of the condensor the vertical slit which is placed in the focus of the lens g.

In this way a parallel beam of light enters the pressure chamber and is refracted by the glass prism and the prism-shaped fluid in the chamber. If the telescope is turned in the right direction, a vertical picture of the slit is to be seen in it, and from the angle of the position of the telescope the refractive index of the fluid in the pressure chamber can be calculated. This angle can be determined very exactly with the help of a small concave mirror placed above the middle of the pressure chamber and moving with the telescope, to which it is fixed. A light pointer reflected by the mirror throws a mark on a circular scale with 2.05 m radius. In this way the angle of the telescope can be determined with precision of better than 0.01°.

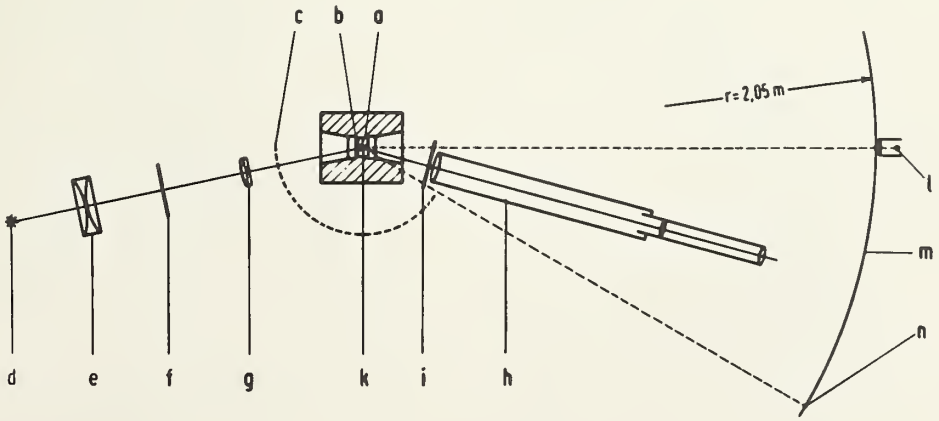

FIGURE 4. *Optical installation for measuring the refractive index.*

a. Pressure chamber, b. Glass prism, c. Circular disk, d. Sodium lamp, e. Condensor, f. Vertical slit, g. Lens, h. Telescope, i. Horizontal slit, movable up and down, k. Concave mirror, l. Lighting of the observation mark, m. Circular scale, n. Picture of the observation mark.

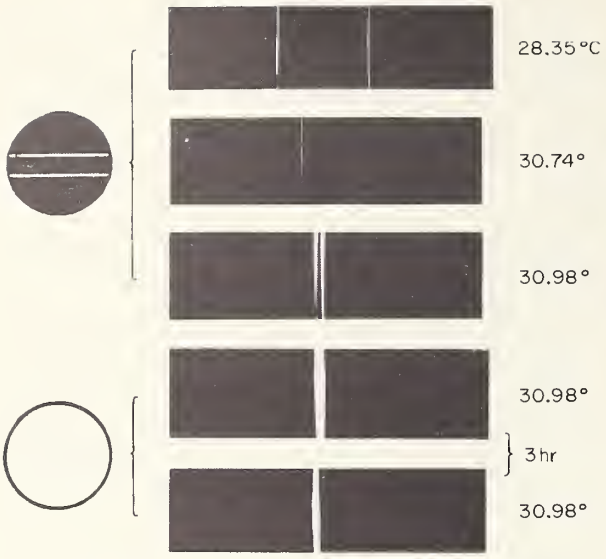

FIGURE 5 *Samples of photographs taken with the telescope.*

If the density of the fluid in the pressure chamber does not depend on height, the telescope shows a vertical picture of the slit. If there is a meniscus in the pressure chamber separating liquid and vapor, we get two different pictures in the telescope, one produced by the light passing the liquid phase, the other produced by the light passing the vapor phase, the distance of these lines being proportional to the difference in density of liquid and vapor.

One of the first photographs which I got in this way with CO_2 at its critical pressure is shown in figure 5. Here two horizontal slits are placed before the telescope so that the upper slit gets light having passed the vapor phase, the lower light having passed the liquid phase. On the right-hand side we see what the telescope shows. The distance of the two lines decreases if we approach the critical temperature, but they do not coincide when the meniscus has completely disappeared.

The last two pictures of figure 5 are taken without the horizontal slits. Here both lines are indistinct, showing that in the fluid there must be a change of density with height. A better picture of the same kind, also taken with two horizontal slits, is shown in figure 6; here even at the critical temperature of 31.01 °C the two lines have a substantial distance, as the third frame shows. The last frame was taken after stirring the fluid thoroughly with the help of a magnetic stirrer. However, if the stirrer is stopped the two lines of frame three reappear after some hours and we learn that in the field of gravity the stable state has gradients of density.

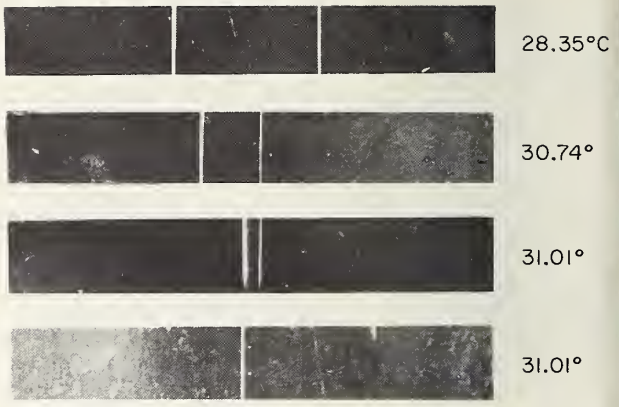

FIGURE 6 *Photographs taken below and at the critical temperature of* CO_2.

These experiences gave rise to use a horizontal slit before the objective of the telescope, which can be moved up and down, whereas the position of the slit can be measured with the help of a cathetometer. In this way the density of the fluid can be measured as a function of height.

4. Some Results of the Point by Point Measurements of the Density of CO_2 Near Its Critical Point as a Function of Height

As an example figure 7 shows the results of density measurements depending on height for CO_2 at its critical pressure and at a temperature

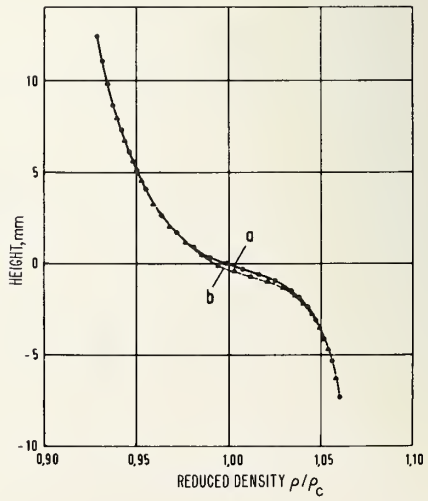

FIGURE 7. *Reduced density* ρ/ρ_c *of* CO_2 *at the critical pressure and* $\vartheta = 0.007$ *°C above the critical temperature.*
a. Curve with measured points. b. Corrected curve.

$\vartheta = 0.007$ °C above the critical temperature. We see how well the measured values lie on the curve *a* the scattering being less than the thickness of the line. All curves which we shall see later are determined by measurements with the same precision and thus it may be allowed to omit the measured points. The curve *b* is a slight correction of curve *a* due to the fact that in a field with a gradient of density the ray of light is slightly curved. In the figure the abscissa is the reduced density ρ/ρ_c where ρ_c is the density at the critical point. We see that for a change in height of only 10 mm (from +5 until −5) the change in density is about 10 percent.

Now already in 1892 Gouy [2] has emphasized that the critical pressure can only exist at a certain level of the fluid, because the pressure and thus the density decreases with height due to the weight of the fluid. However, the measured gradients of densities are 30 to 50 times larger than those produced by hydrostatic pressure if these are derived from a van der Waals equation.

Figure 7 is measured at a temperature $\vartheta = +0.007$ °C above the critical temperature and at a mean density very near the critical value. If we change the temperature at constant mean density of the fluid we get a set of curves as shown in figure 8, taken at a mean density of $\rho/\rho_c = 0.985$. The curve *a* corresponding to a temperature $\vartheta = -0.005°$ below the critical shows a jump in density corresponding to a visible meniscus, but nevertheless there is still a substantial gradient of density in the liquid and in the gaseous phase. The curve *b* is observed at a temperature very near the critical value, the curves *c*, *d*, *e*, and *f* are taken at temperatures from 0.003 until 0.095 °C above the critical. Here the jump in density has changed to an inflection point with a tangent growing steeper the more we surpass the critical temperature.

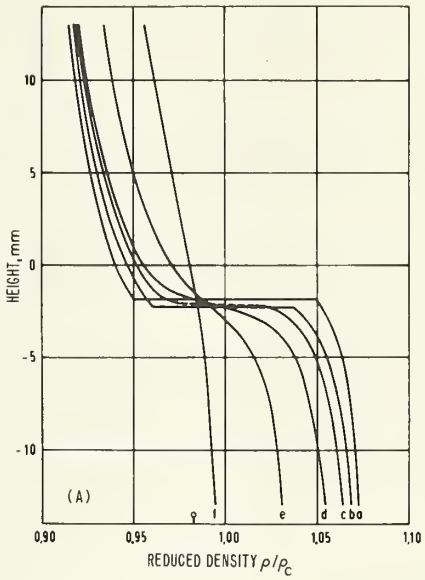

FIGURE 8. *Density ρ/ρ_c against height for CO_2 with a mean relative density 0.985 ρ_c and for the following temperatures ϑ relative to the critical value: a. −0.005 °C; b. 0.000 °C; c. 0.003 °C; d. 0.012 °C; e. 0.035 °C; f. 0.095 °C.*

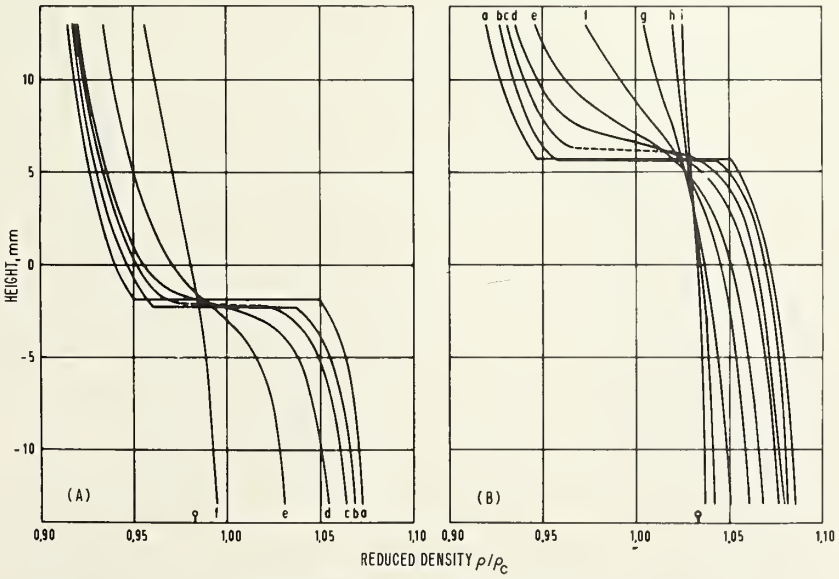

FIGURE 9. *Density ρ/ρ_c against height for CO_2.*
A. Same as figure 8. B. Mean relative density of 1.033 ρ_c and the following temperatures ϑ relative to the critical value: a. −0.008 °C; b. −0.003 °C; c. 0.002 °C; d. 0.005 °C; e. 0.015 °C; f. 0.035 °C; g. 0.065 °C; h. 0.125 °C; i. 0.232 °C.

The immediate neighborhood of the critical point is difficult to observe because here the gradient of density has its highest value, and the light is deflected down. Therefore, in what follows we will calculate the temperature difference ϑ using as the starting point the highest temperature at which the density versus height curve still shows a discontinuity.

If the mean density is increased by pumping more mercury into the pressure chamber the level where the meniscus disappears ascends as to be seen in figure 9, where the left-hand picture repeats figure 8 with the mean density $\rho/\rho_c = 0.985$, and the right-hand picture corresponds to a mean density $\rho/\rho_c = 1.033$. The different curves are isotherms from -0.008 up to 0.252 °C above critical temperature.

In figure 10 all curves are taken at the critical pressure and at the same temperature $\vartheta = -0.006$ °C below the critical value, only the mean densities differ from curve to curve and are denoted by the small circle in each curve.

Figure 11 shows the same very near the critical temperature. Figure 12 for $\vartheta = +0.007$ °C; figure 13 for $\vartheta = +0.03$ °C; figure 14 for $\vartheta = +0.06$ °C.

These figures show how difficult it is to determine the critical density without optical observation because the inflection point of the density curve (the level where the meniscus disappears) may have a higher or lower position. If it is high, more than half of the chamber is filled with fluid of larger density, if it is low, only a smaller part of volume has the higher density.

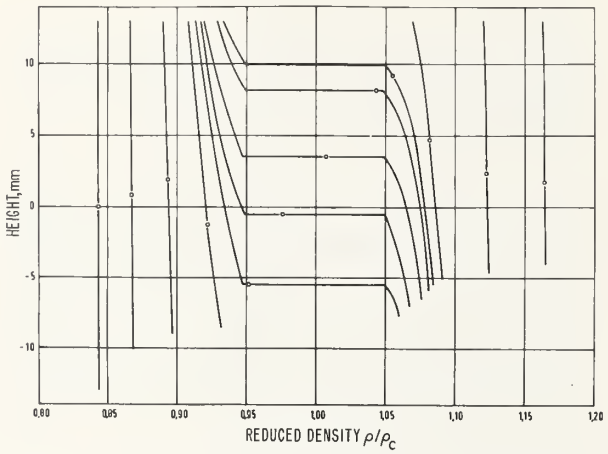

FIGURE 10. *Density against height for CO_2 at a relative temperature $\vartheta = -0.006$ °C and at different mean densities indicated by the small circle at each curve.*

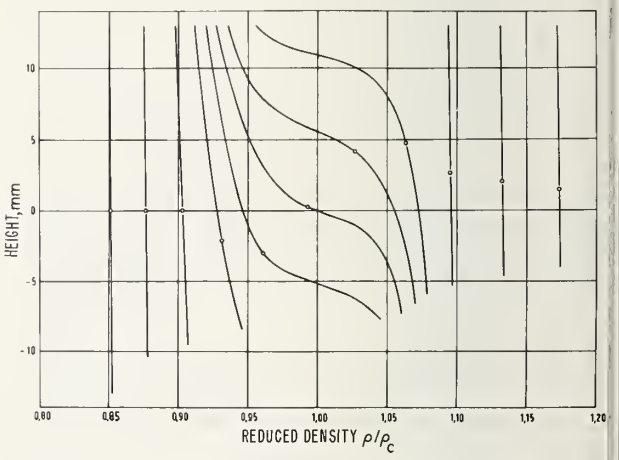

FIGURE 12. *The same as figure 10, but for a relative temperature $\vartheta = 0.007$ °C.*

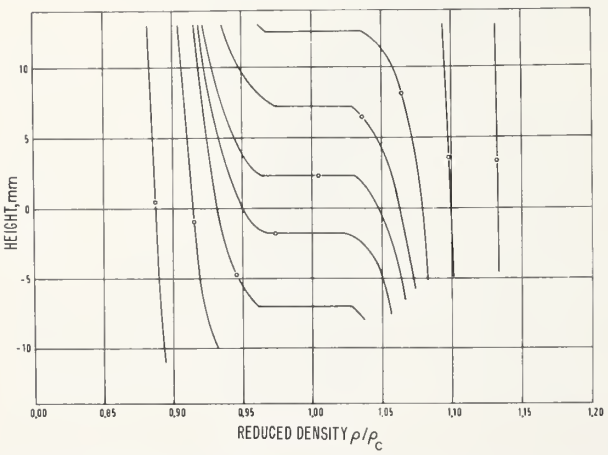

FIGURE 11. *The same as figure 10 but for a relative temperature $\vartheta = 0.000$ °C, that is at the critical temperature.*

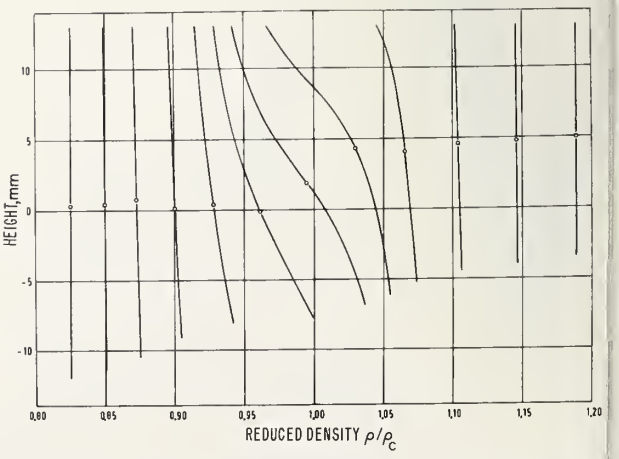

FIGURE 13. *The same as figure 10, but for a relative temperature $\vartheta = 0.030$ °C.*

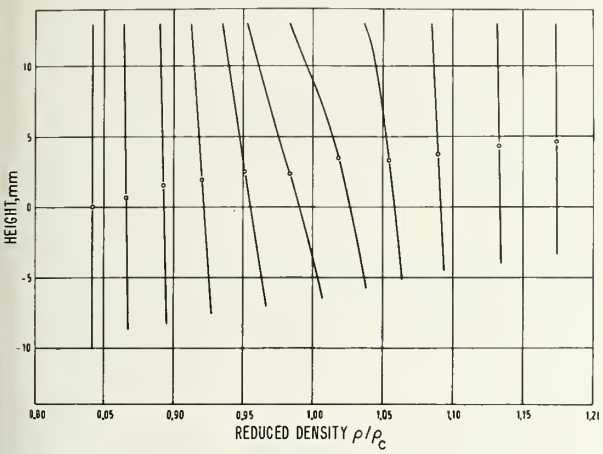

FIGURE 14. *The same as figure 10, but for a relative temperature* $\vartheta = 0.060$ °C.

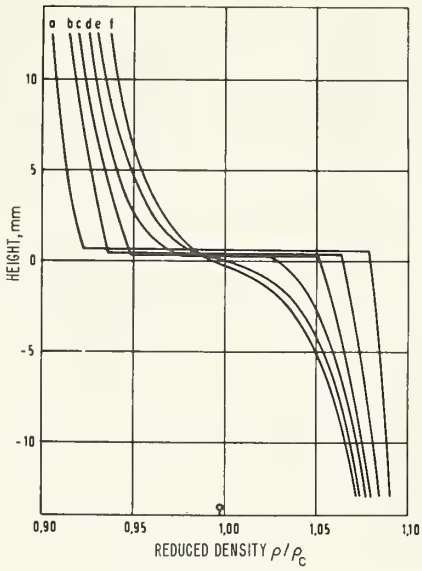

FIGURE 15. *Density against height for* N_2O *at a mean relative density 0.998* ρ_c *and for temperatures* ϑ *relative to the critical temperature* $t_c = 36.585$ °C:
a. -0.027 °C; *b.* -0.012 °C; *c.* -0.006 °C; *d. 0.000* °C; *e. 0.012* °C; *f. 0.021* °C.

5. Measurements With N_2O, $CClF_3$, and H_2O

All measurements up to here are made with CO_2. In order to show that not only this substance undergoes gradients of density in the field of gravity, experiments were also made with N_2O and with $CClF_3$.

Figure 15 shows isotherms of N_2O for temperatures $\vartheta = -0.027$ until $+0.021$ °C at a mean density $\rho/\rho_c = 0.998$. In figure 16 two sets of isotherms are placed side by side, the left with a mean density $\rho/\rho_c = 0.955$ and temperatures ϑ from 0.000 until $+0.056$ °C, the right with $\rho/\rho_c = 1.003$ and temperatures ϑ from -0.002 until $+0.218$ °C. The figure is very similar to figure 9. Figure 17 also relates to N_2O at a temperature $\vartheta = -0.004$ °C with different mean densities given by the small circles in the curves.

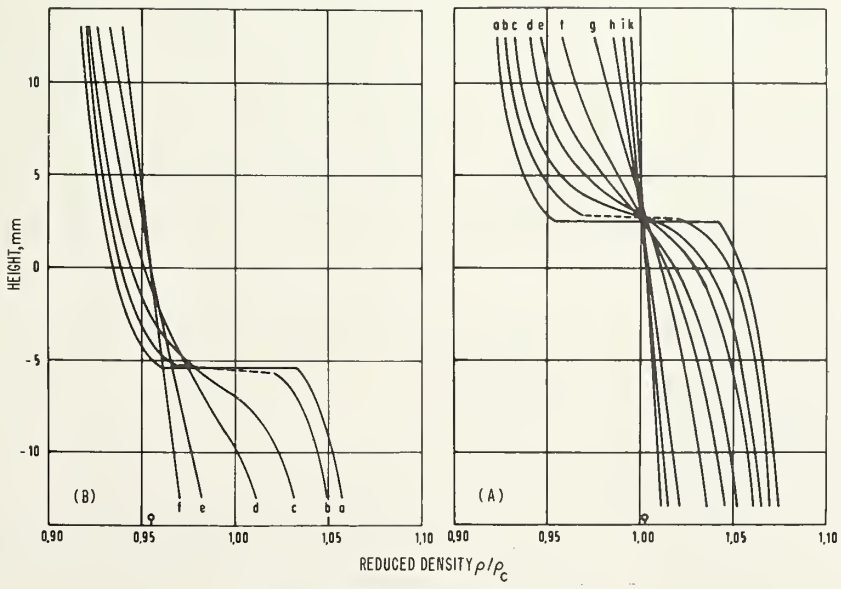

FIGURE 16. *Density against height for* N_2O.
A. Mean density 0.995 ρ_c *and for the following relative temperatures: a. 0.000* °C, *b. 0.004* °C, *c. 0.015* °C; *d. 0.020* °C; *e. 0.044* °C; *f. 0.056* °C. *B. Mean density 1.005* ρ_c *and for the following relative temperatures: a.* -0.002 °C; *b. 0.003* °C; *c. 0.010* °C; *d. 0.020* °C; *e. 0.032* °C; *f. 0.038* °C; *g. 0.063* °C; *h. 0.119* °C; *i. 0.167* °C; *k. 0.218* °C.

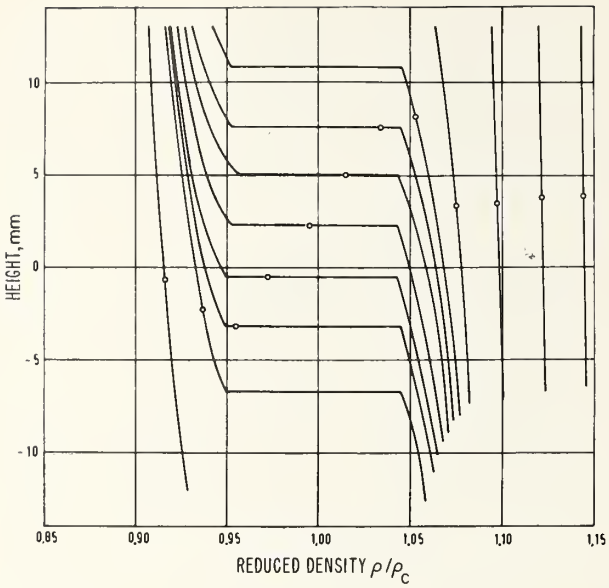

FIGURE 17. *Density against height for N_2O at a relative temperature $\vartheta = -0.004$ °C and at different mean densities given by the small circle at each curve.*

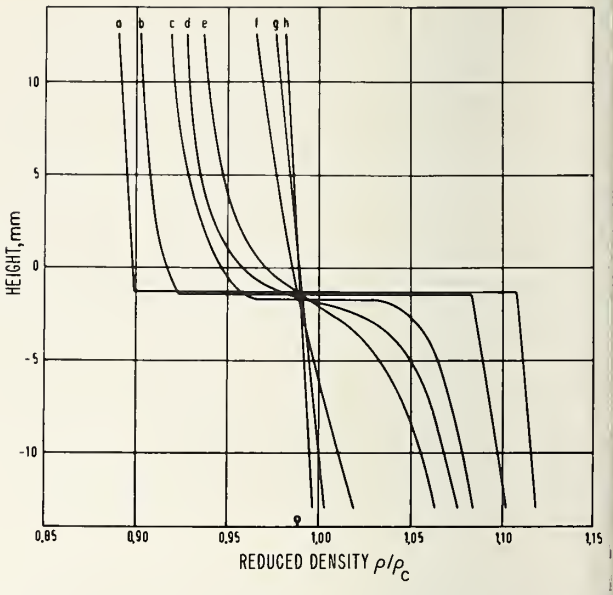

FIGURE 18. *Density against height for $CClF_3$ with the mean density 0.989 ρ_c and the following temperatures relative to the critical temperature $t_c = 28.715$ °C: a. −0.065 °C; b. −0.025 °C; c. 0.000 °C; d. 0.021 °C; e. 0.040 °C; f. 0.093 °C; g. 0.183 °C; h. 0.265 °C.*

Finally figure 18 is measured with $CClF_3$ at a mean density $\rho/\rho_c = 0.989$. and the different curves correspond to temperature differences with the critical value from $\vartheta = -0.065$ until $+0.265$ °C.

In the CO_2-molecule the two O-atoms are placed symmetrically on opposite sides of the C-atom. corresponding to the scheme O=C=O. The N_2O-molecule is asymmetric and therefore polarized following the scheme N≡N=O. The $CClF_3$ molecule has the shape of a tetraeder with the C-atom in the middle and the halogen atoms at the corners of the tetraeder. As these three molecules. differing in shape and chemical constitution show the same behavior in the neighborhood of the critical state. it is to be expected that this behavior is a general quality of all substances.

The critical data which we found are in good agreement with the results of other authors.

Measurements with H_2O are now being done. This molecule has the shape of a triangle and its behavior near the critical state seems to be the same as for the other substances. However. the measurements are much more difficult due to the higher temperature $t_c = 374.15$ °C and the higher pressure $p_c = 221.3$ bar. Windows of glass and even of quartz are impossible because these substances are corroded and lose their optical quality. Finally we found that sapphire windows withstand corrosion and these are used now.

6. Summary

The above experiments show undoubtedly that near the critical state of substances considerable gradients of density are produced by gravity. For the three substances encountered. the density at the critical pressure and near the critical temperature changes by about 10 percent over a height of about 10 mm. These distributions of density are stable and reproducible. After any changes of state of the fluid. they are restored by diffusion and some kind of sedimentation within times of about 2 hr for heights of some centimeters.

7. References

[1] Ernst H. W. Schmidt and K. Traube. Gradients of Density of Fluids Near their Critical States in the Field of Gravity. pp. 193-205. Progress in International Research on Thermodynamic and Transport Properties A.S.M.E. (Academic Press. New York and London 1962).

[2] R. Gouy. Effets de la pesanteur sur les fluides au point critique. Compt. Rend. Acad. Sci. Paris **115**, 720–22 (1892).

Notes, Definitions, and Formulas for Critical Point Singularities

M. E. Fisher

University of London, King's College, London, Great Britain*

1. Introduction

For the convenience of participants a set of definitions and notes concerning the various critical point singularities and a table of formulas relating the lattice gas and Ising ferromagnet models were distributed at the Conference. These are reproduced here with a few corrections and extensions.

Most of the results quoted are described and discussed in detail in references 1, 2, and 3 where further references to the literature are given. A few more recent results are contained in references 4 to 8 and, of course, in the work reported at this Conference particularly in connection with critical scattering by Chu, Passel, Nathans, Dietrich, and Als-Nielsen.

2. Critical Point Exponents

For theoretical discussions and in the analysis of experimental data it is useful to have a precise definition of a critical point exponent. This may be given as follows:

if $$\lim_{x \to 0+} \log f(x)/\log x = \lambda,$$

we say $$f(x) \sim x^{\lambda} \text{ as } x \to 0+.$$

Note that with this definition the statement $f(x) \sim x^{\lambda}$ does *not* exclude the possibility of a logarithmically divergent factor, i.e., $Ax^{\lambda}|\log x| \sim x^{\lambda}$. In particular if $\lambda = 0$ the function $f(x)$ might diverge as $|\log x|$ for example, or $f(0)$ might be finite, the function $f(x)$ then being either continuous or discontinuous as x passes through zero.

The definitions of the most important critical point exponents for gases and ferromagnets are set out in the following table together with certain relations between them. Analogous formulas hold for binary alloys and binary fluid systems. Note that the exponent η enters directly into the scattering of waves *at* the critical point through the formula

$$1/I_c(\mathbf{k}) \sim k^{2-\eta},$$

where $I(\mathbf{k})$ is the intensity of scattering at wave vector $\mathbf{k}$ with $k = (4\pi/\lambda) \sin \frac{1}{2}\theta$ (for $d = 3$).

The meanings of the symbols used in table 1 and below are

C_V, C_p, C_H, C_M	Specific heats at constant volume, pressure, field, and magnetization, respectively.
T, T_c	Temperature, critical temperature.
ρ, ρ_c; ρ_L, ρ_G	Density, critical density; densities of coexisting liquid and gaseous phases.
M, M_0	Magnetization, spontaneous magnetization.
K_T, K_S	Isothermal and adiabatic compressibilities.
χ_T, χ_S	Isothermal and adiabatic susceptibilities.
p, p_c, p_σ	Pressure, at the critical point and at coexistence (vapor pressure), respectively.
H	Magnetic field.
$g_2(\mathbf{r})$	Pair correlation function (in a fluid).

*Now at Cornell University, Ithaca, New York.

TABLE 1. *Critical point exponents*

Exponent	Fluid	Magnet
Below T_c	At coexistence as $T \to T_c$	At $H=0$ as $T \to T_c-$
α'	$C_V \sim (T_c - T)^{-\alpha'}$	$C_H \sim (T_c - T)^{-\alpha'}$
β	$(\rho_L - \rho_G) \sim (T_c - T)^{\beta}$	$M_0(T) \sim (T_c - T)^{\beta}$
γ'	$K_T \sim (T_c - T)^{-\gamma'}$	$\chi_T \sim (T_c - T)^{-\gamma'}$
α^*	$\lvert d^2 p_\sigma / dT^2 \rvert - (T_c - T)^{-\alpha^*}$	
At $T = T_c$	As $\rho \to \rho_c$	As $H \to 0$
δ	$\lvert p - p_c \rvert \sim \lvert \rho - \rho_c \rvert^{\delta}$ Note the exponents β, γ', and δ might differ on the gas and liquid sides.	$\lvert H \rvert \sim \lvert M \rvert^{\delta}$
η	At $\rho = \rho_c$ as $r \to \infty$ $\lvert g_2(\mathbf{r}) - 1 \rvert \sim 1/r^{d-2+\eta}$	At $H=0$ as $r \to \infty$ $\langle S_0^z S_{\mathbf{r}}^z \rangle \sim 1/r^{d-2+\eta}$
Above T_c	At $\rho = \rho_c$, as $T \to T_c+$	At $H=0$, as $T \to T_c+$
α	$C_V \sim (T - T_c)^{-\alpha}$	$C_H \sim (T - T_c)^{-\alpha}$
γ	$K_T \sim (T - T_c)^{-\gamma}$	$\chi_T \sim (T - T_c)^{-\gamma}$
ν	Inverse Range of Correlation	$\kappa(T) \sim (T - T_c)^{\nu}$
Rigorous inequalities	$\alpha' + (2\beta + \gamma')_{\min} \geq 2$ $\alpha' + \beta_{\max} + (\beta\delta)_{\min} \geq 2$ $\alpha^* \leq \alpha' + \beta_{\max}$	$\alpha' + 2\beta + \gamma' \geq 2$ $\alpha' + \beta(1+\delta) \geq 2$
Conjectured relations	$\alpha' + 2\beta + \gamma' = 2$, $\gamma' = \beta(\delta - 1)$, $\gamma = (2 - \eta)\nu$	

d	Dimensionality of the system.
$S_{\mathbf{r}}^z$	Spin variable at site $\mathbf{r}$.
$\mathscr{H}$	Hamiltonian.
z	Activity.
μ, μ_σ	Chemical potential, at coexistence.

In table 2 the exact, estimated and observed values of the critical exponents defined above are presented for various theoretical models and for real fluids and ferromagnets [1–6]. The queries indicate significant uncertainties or total ignorance! Notice that it is not clear that the existing experimental results for α', β, and δ satisfy the rigorous inequality recently derived by Griffiths [7] (see table 1).

For the standard three-dimensional ($d=3$) *spherical model* one may add the results: $\alpha' = \alpha = 0$ (continuous), $\beta = \frac{1}{2}$, γ' not defined, $\delta = 5$, $\eta = 0$, $\gamma = 2$, $\nu = 1$. For a spherical model with long range ferromagnetic forces decaying as $1/r^{d+\sigma}$ ($0 < \sigma < 2$) one has more generally [1]: $\alpha' = \alpha = 0$, $\beta = \frac{1}{2}$ as before, but (a) for $\sigma < \frac{1}{2}d$: $\gamma' = \gamma = 1$, $\delta = 3$, $\eta = 2 - \sigma$, ν undefined: while (b) for $\sigma \geq \frac{1}{2}d$: γ' undefined, $\delta = (d+\sigma)/(d-\sigma)$, $\eta = 2 - \sigma$, $\gamma = \sigma/(d-\sigma)$, ν undefined.

[1] These results have been obtained by G. S. Joyce.

TABLE 2. *Values of critical point exponents*

Exponent	"Classical" theory	Ising $d=2$	$d=3$	Heisenberg $d=3$	Observation	
					Fluids	Magnets
α'	0 (discon.)	0 (log)	$\gtrsim 0$?	?	$\gtrsim 0$ (log)	$\gtrsim 0$?
β	$\frac{1}{2}$	$1/8$	$0.312 \simeq 5/16$ 0.303 to 0.308	?	0.33 to 0.36	0.33 ± 0.015
γ'	1	$1\frac{3}{4}$	1.23 to 1.32	?	$\geqslant 1.2$?	?
α^*	0	0 (log)	$\gtrsim 0$	—	$\geqslant 0$?	—
δ	3	15	5.20 ± 0.15	?	4.2 ± 0.1	4.22 ± 0.05
η	0	$1/4$	$0.059 \simeq 1/18$ ± 0.006	0.08 ± 0.04	> 0 ?	> 0 ?
α	0 (discon.)	0 (log)	$\geqslant 0$ $\leqslant 0.2$	$\simeq 0$	$\geqslant 0$? $\leqslant 0.2$	> 0 ?
γ	1	$1\frac{3}{4}$	$1\frac{1}{4}$	$\simeq 1\frac{1}{3}$ 1.32 to 1.38	> 1.1 ?	1.35 ± 0.02
ν	$1/2$	1	0.644 ± 0.002	0.69 ± 0.02	> 0.55 ?	$\gtrsim 0.66$

3. Relation Between a Lattice Gas and an Ising Magnet

The mathematical equivalence of the lattice gas model of a fluid and the Ising model of a magnet, stressed originally by Yang and Lee, is well known but it was felt that a more complete account of the relation between the two models than normally given would be useful. Indeed some of the experimental results included in table 2 suggest that the fluid-magnet analogy might be deeper than the simplicity of the Ising model would indicate.

We consider a general d-dimensional lattice of N sites, each occupying a cell, of volume v_0. The pair interactions are not necessarily limited to nearest neighboring sites. Positive values of the exchange integral $J(\mathbf{r})$ correspond to ferromagnetic coupling but the formulas are valid for arbitrary coupling.

Lattice of N sites: d-dimensional volume v_0 per site. $(\beta = 1/k_B T)$

Total Potential Energy of n atoms	$U_n = \sum_{\substack{(ij) \\ \text{pairs}}} \phi(\mathbf{r}_{ij})$		$\mathcal{H}_N = -\sum_{(ij)} J(\mathbf{r}_{ij}) s_i s_j - H \sum_{i=1}^{N} s_i$	
Occupation Variables	$t_i = 1$ or 0	$t_i = \frac{1}{2}(1 - s_i)$	$s_i = 2S_i^z = \pm 1$	Spin Variables
Potentials	$\hat{\phi}(0) = \sum_j \phi(\mathbf{r}_{ij})$	$\phi(\mathbf{r}) = -4J(\mathbf{r})$		Exchange Integral
Density $\rho_{\max} = 1/v_0 = 2\rho_c$		$\rho/\rho_c = 1 - M$		Magnetization per Spin $M_{\max} = 1$
Chemical Potential μ $\beta\mu = \ln(z\Lambda^d)$ $\Lambda = (h^2/2\pi m k_B T)^{1/2}$ at condensation $\mu = \mu_\sigma = \frac{1}{2}\hat{\phi}(0) - kT \ln(v_0/\Lambda^d)$		$\mu - \mu_\sigma = -2H$		Magnetic Field, H units chosen so that magnetic moment per spin is unity.
Pressure $p(\mu, T)$		$p v_0 = -F^* - H - \frac{1}{8}\hat{\phi}(0) = \int_H^\infty [1 - M(H')] dH'$		Free Energy per Spin $F^*(H, T)$
Configurational Entropy Density		$\rho v_0 S^{\text{config}} = S^*$		Entropy per Spin
Isothermal Compressibility		$4 v_0 \rho^2 K_T = \chi_T$		Isothermal Susceptibility
Configurational Specific Heats		$\rho \nu_0 C_V^{\text{config}} = C_M = C_H - T\alpha_H^2/\chi_T$		Specific Heats
		$\rho \nu_0 C_p^{\text{config}} = T\left(\frac{S^*}{1-M}\right)^2 \chi_T + C_H + 2T\left(\frac{S^*}{1-M}\right)\alpha_H$		Note $1/\chi_T \equiv 0$ in the "two-phase" region. $\alpha_H = \left(\frac{\partial M}{\partial T}\right)_H$ $\alpha_H \equiv 0$ for $H = 0$, $T > T_c$.
Note		$C_p/C_V = K_T/K_S$	$C_H/C_M = \chi_T/\chi_S$	
Thermal Pressure Coefficient		$v_0 \gamma_V = v_0(\partial p/\partial T)_V = S^* + (1 - M)\alpha_H/\chi_T$		
Correlation Functions		$\rho v_0 G(\mathbf{r}) = \rho v_0[g_2(\mathbf{r}) - 1] = (\langle s_0 s_\mathbf{r}\rangle - \langle s_0\rangle^2)/(\langle s_0^2\rangle - \langle s_0\rangle^2) = \Gamma(\mathbf{r})$		
at $\rho = \rho_c$, $T > T_c$		$\frac{1}{2}G(\mathbf{r}) = \langle s_0 s_\mathbf{r}\rangle = \Gamma(\mathbf{r})$		at $H = 0$, $T > T_c$.

From the correlation functions $G(\mathbf{r})$ and $\Gamma(\mathbf{r})$ one may derive the critical scattering intensities through the formulas

$$I(\mathbf{k}) = \hat{\chi}(\mathbf{k}) I_0(\mathbf{k})$$

where $I_0(\mathbf{k})$ is the form factor for scattering from the noninteracting system and where

$$\chi(\mathbf{k}) = 1 + \rho \sum_{\mathbf{r} \neq \mathbf{0}} v_0 e^{i\mathbf{k}\cdot\mathbf{r}} G(\mathbf{r}) = 1 + \sum_{\mathbf{r} \neq \mathbf{0}} e^{i\mathbf{k}\cdot\mathbf{r}} \Gamma(\mathbf{r}).$$

The fluctuation relation may then be written

$$K_T/K_T^0 = \hat{\chi}(\mathbf{0}) = \chi_T/\chi_T^0$$

where the superscript zero refers to an ideal noninteracting system.

4. References

[1] M. E. Fisher, J. Math. Phys. **4**, 124 (1963).
[2] M. E. Fisher, J. Math. Phys. **5**, 944 (1964).
[3] M. E. Fisher, Proc. Int. Conf. on Magnetism. Nottingham 1964, 79 (The Physical Society, London, 1965).
[4] J. S. Kouvel and M. E. Fisher, Phys. Rev. **136**, A. 1626 (1964).
[5] M. E. Fisher, Phys. Rev. **136** A, 1599 (1964).
[6] D. S. Gaunt, M. E. Fisher, M. F. Sykes, and J. W. Essam. Phys. Rev. Letters **13**, 713 (1964).
[7] R. B. Griffiths, Phys. Rev. Letters, **14**, 623 (1965).
[8] R. J. Burford, and M. E. Fisher, to be published.

Discussion

R. L. Scott: Dr. Rowlinson made some reference to our work on mixtures of CF_4 with methane. Recently Croll and I published some rather old work on mixtures of CF_4 with ethane [1]. I did not actually consider the work good enough to apply this kind of consideration, but at the request of Dr. Widom, I looked at the results again. The data give the total pressure of CF_4 with ethane at about 150.6 °K, which is about 0.5° above the critical solution temperature. The curves are, in fact, nearly flat. If one ignores the fact that the only relevant data are considerably removed from the critical composition (just the point that Dr. Rowlinson made and that really vitiates the whole result), then the results are consistent with an exponent $\delta = 4$, but it would not be very difficult to make the data consistent with $\delta = 5$.

C. J. Pings: The one enigma in the data showed by Dr. Rowlinson for β was in the results obtained by Edwards and Woodbury for He^4. I believe those were deduced from refractive index measurements. We have some unpublished data on the Lorentz-Lorenz function for argon and methane which suggest a possible anomaly in the Lorentz-Lorenz function in the critical region [2]. Until this is resolved, we must be dubious about any conclusions of this type deduced from refractive index measurements.

J. S. Rowlinson: I mentioned the results of Edwards and Woodbury only in passing. I did not use them in any way in the analysis. They are clearly out of line with the results on gases at high temperatures. Whether this is a particular quantum effect or not, I do not know.

S. Y. Larsen: I would like to make a remark concerning the comment of Dr. Pings. Dr. Mountain, Dr. Zwanzig, and I have made a theoretical study of the behavior of the index of refraction [3]. We find no anomaly in the behavior of the real part of the index of refraction in the supercritical region when the critical point is approached.

O. K. Rice: I may mention that some years ago Rowden and I made vapor pressure measurements on the cyclohexane-aniline system [4]. We approached the critical point to within 0.1 or 0.2 °C and it looked like $\gamma = 1$.

J. S. Rowlinson: Did it?

O. K. Rice: We could not say definitely whether γ was either greater or smaller then 1, but it did look very much like $\gamma = 1$, as far as we could tell from the measurements.

J. S. Rowlinson: I am sorry that I omitted your results in my review. I did not try to deduce a value for γ from your results on the cyclohexane-aniline system.

M. E. Fisher: I would just like to emphasize one point, which Dr. Rowlinson made very well. There is an inconsistency with the rigorous inequalities if one takes the values of the exponents at their face value. Although one cannot be too sure that any of them are as good as they seem to be, the fact is that for δ to be consistent with the relationship (G1) a rather big change in its value is needed. It means that δ should be near 5 rather than 4.2, is not that right?

J. S. Rowlinson: It depends on what lower limit one puts on α_2^-. If one allows $\alpha_2^- = 0.06$, one can get away with $\beta = 0.36$ and $\delta = 4.4$.

M. E. Fisher: That is correct. However, since you multiply δ with 1/3 in relation (G1), the effect of a change in δ in order to satisfy the relation gets damped down. If you take the central values of β and δ, there really is quite a big discrepancy.

J. S. Rowlinson: I agree that the central values lead to a discrepancy, and if you prefer $\delta = 5$, I cannot say no.

E. Helfand: In a mixture there are many new thermodynamic variables because one has one extra variable and consequently many more derivatives. One of the interesting derivatives may be $\partial p/\partial \rho$. This property depends on the liquid correlation functions, that is density correlation function, whereas the second derivative of the free energy with respect to the concentration depends on the concentration correlation function. One might well expect these correlation functions to have the same range and the same analytic behavior. Thus perhaps $\partial p/\partial \rho$ would reflect the same γ behavior.

J. S. Rowlinson: It would be very difficult to measure the $\partial p/\partial \rho$ in a dense fluid with the precision that is needed to get these indices.

W. W. Webb presented measurements of the reflectivity of the interface between two phases in equilibrium just below the critical consolute temperature [5]. These measurements indicate that the effective equilibrium thickness of the transition region increases roughly as $(T_c - T)^{-0.7}$ as the critical temperature is approached, reaching $\sim 1{,}000$ Å at $(T_c - T)/T_c \approx 10^{-3}$.

S. Y. Larsen: Dr. J. M. H. Levelt-Sengers and I have looked at the disagreement between the optical data and the isotherms derived from *PVT* measurements [6]. This disagreement was first noticed by Dr. Schmidt and noted in the account of his optical work given at the 1962 Symposium of the A.S.M.E. on

Thermophysical Properties and also has been taken up by Ulybin and Malyshenko in a recent paper delivered at the Third Symposium on Thermophysical Properties [7].

Our conclusion is that the optical work may be in agreement with the *PVT* data. The disagreement lies between the optical results and the analytical forms for the isotherms which have been fitted to the *PVT* data. These include both the Taylor type expansions and the fit of Widom and Rice. We believe that one of the main reasons for the disagreement is that these expressions are really fitted to data somewhat outside the critical region. We find that the conventional way of effecting *PVT* measurements provides an exceedingly insensitive method of determining the pressure versus density relationship very close to the critical point and that optical methods are certainly to be preferred. Accordingly, we believe that the isotherms are very much flatter near the critical point, and the compressibilities very much larger, than has been inferred from *PVT* data.

C. B. Benedek: I wonder if those remarks could be translated into the following terms: What do you think is the proper value of δ, and what do you think is the proper value of γ?

S. Y. Larsen: At the present time we have not attempted to reevaluate the old data. The result that we have does not imply that the δ of Widom and Rice, for example, is not the correct one because one could still change the leading coefficient. I think that one would like to start with the beautiful new data of Dr. Schmidt and try again to look at these questions.

References

[1] I. M. Croll and R. L. Scott, J. Phys. Chem. **68,** 3853 (1964).
[2] C. P. Abbiss, C. M. Knobler, R. K. Teague, and C. J. Pings, J. Chem. Phys. **42,** 4145 (1965).
[3] S. Y. Larsen, R. D. Mountain, and R. Zwanzig, J. Chem. Phys. **42,** 2187 (1965).
[4] R. W. Rowden and O. K. Rice, J. Chem. Phys. **19,** 1423 (1951); Changements de Phases, Comptes rendus de la 2e Réunion Annuelle tenue en commun avec la Commission de Thermodynamique de l' Union Internationale de Physique, Paris, 1952, p. 78.
[5] G. H. Gilmer, W. Gilmore, J. Huang, and W. W. Webb, Phys. Rev. Letters **14,** 491 (1965).
[6] S. Y. Larsen and J. M. H. Levelt Sengers, Third Symposium on Thermophysical Properties, A.S.M.E., Purdue, 1965, p. 74.
[7] S. A. Ulybin and S. P. Malyshenko, Third Symposium on Thermophysical Properties, A.S.M.E., Purdue, 1965, p. 68.

CRITICAL PHENOMENA IN FERRO- AND ANTIFERROMAGNETS

Chairman: H. B. Callen

Critical Properties of Lattice Models

C. Domb

University of London King's College, London, Great Britain

Introductory Remarks

I shall assume that you all know what is meant by the Ising and Heisenberg models and are reasonably familiar with Onsager's exact solution of the two-dimensional Ising model [1][1]. My task is to discuss the three-dimensional model, and the effect of changing the spin and range of interaction, and for these problems exact methods have so far proved to be of no avail. Some people have no enthusiasm for methods which are not exact and consider that detailed investigation of higher order approximation terms is not the task of a theoretical physicist. I am reminded of a conversation which I had with Yvon about his own important contribution to this field (which I shall refer to later). He told me that he developed the method, tried it in lower order, and found that it gave the same result as other approximations. I asked if he had not been interested to go to higher orders to see whether it gave any improvement. He replied: "my task as a theoretical physicist is to develop methods, and see that they work and are correct: I then hand over to the engineers." By these standards, what I have to say to you this afternoon, is engineering, but at least I will spare you the technical details of the engineering methods and discuss only the results. Let us also remember that engineering methods led to the discovery of Fourier series, and I hope to terminate my talk with some remarks about the possibility of an engineering approach to an exact solution.

The methods I shall discuss depend on developing large numbers of terms of series expansions at high and low temperatures which are used to estimate critical behavior. Now any second-year mathematics student will tell you that nothing can be learned about the singularities of a function from a finite number of terms of a series expansion: for example, even if the first 15 terms of an expansion are positive and well-behaved, there is nothing to ensure that an effect which is small and unnoticed in the first few terms will not diminate asymptotically (and I shall later quote an example of such behavior for the Heisenberg model), but the following physical considerations enable one, nevertheless, in many cases, to make confident predictions about the singularities of functions from a finite number of terms of series expansions.

(a) The two-dimensional solution can act as a guide since we expect the three-dimensional solution to be similar to it in essential features.

(b) We have a few exact theorems which apply to three-dimensional solutions.

(c) Physical considerations of what is expected of the model can lead us to transformations of the series which reveal peculiarities of behavior.

We must be sure at the outset that we have enough terms of our series to get over small number effects. No general rule can be given since the number of terms needed varies from problem to problem. However, careful analysis of the data for each particular problem usually shows if the number of terms derived is adequate.

Before going into details of the behavior of the Ising and Heisenberg models, I should make the connection with this morning's lectures on liquids and gases. Fortunately, Professor Fisher has made my task very easy by circulating a sheet giving the detailed connection between the Ising model and the lattice gas. I should like, first, to point out that two quite different lattice models are used in connection with fluids. The first, with which we are concerned here, is a model of liquid vapor equilibrium, and it corresponds to the Ising model of a ferromagnet [2]. From the relations given by Professor Fisher, I shall draw attention to three which are of relevance to my talk. In critical behavior C_V for the fluid corresponds to C_H for the magnet in zero field at all temperatures: the density of one component of the fluid corresponds to minus the spontaneous magnetization: and the isothermal compressibility of the fluid corresponds to the isothermal susceptibility of the magnet. It is impor-

tant, also, to note that the chemical potential for the fluid is proportional to minus the magnetic field.

The second model applies to solid-fluid equilibrium and corresponds to the Ising model of an antiferromagnet [3]. This model has been extensively used as an analog of the condensation of a fluid of hard spheres [4], and will not be discussed further in the present talk.

Short range forces; Series expansions

May I start with a few elementary observations about power series expansions. If all the terms of a power series are positive, the dominant singularity is on the positive real axis [5]. If they alternate regularly the dominant singularity is on the negative real axis. If they manifest more complicated behavior, the dominant singularities are elsewhere in the complex plane. Physical interest centers largely on singularities on the real axis. For the Ising and Heisenberg models in zero field, we expect to find a positive singularity on the real axis corresponding to the Curie point, and possibly a singularity on the negative real axis corresponding to the Néel point.

It is convenient to divide the series expansions to be considered into three groups. Group I have all terms positive and from table 1 we select as an example the coefficients in the high tempera-

TABLE 1. *Coefficients* a_n *in the susceptibility expansion for a number of lattices*

n	Simple quadratic	Type of lattice		Face-centered cubic
		Triangular	Simple cubic	
0	1	1	1	1
1	4	6	6	12
2	12	30	30	132
3	36	138	150	1,404
4	100	606	726	14,652
5	276	2,586	3,510	151,116
6	740	10,818	16,710	1,546,332
7	1,972	44,574	79,494	15,734,460
8	5,172	181,542	375,174	139,425,580
9	13,492	732,678	1,769,686	.....
10	34,876	2,935,218	8,306,862	.....
11	89,764	11,687,202	38,975,286	.....
12	229,628	46,296,210	.....	.....
13	585,508	.....	.....	.....
14	1,486,308	.....	.....	.....
15	3,763,460	.....	.....	.....
16	9,497,380	.....	.....	.....

ture series for the susceptibility of the Ising model for triangular and F.C.C. lattices. These lattices are chosen because the absence of antiferromagnetic ordering leads one to expect a single clear and dominant singularity. The general behavior of the terms suggests comparison with a binomial expansion of the form

$$\chi_0 \sim A\left(1-\frac{w}{w_c}\right)^{-\gamma}. \tag{1}$$

and we therefore investigate the ratio of successive terms a_n/a_{n-1} as a function of $\frac{1}{n}$. For a binomial expansion (1) we should have

$$a_n/a_{n-1} \sim \left(\frac{1}{w_c}\right)\left[1+\frac{\gamma-1}{n}\right]. \tag{2}$$

Figure 1 shows that the terms converge rapidly and smoothly; for the triangular lattice the estimates of w_c and the slope are very close to the correct values [6] $2-\sqrt{3}$ and 3/4. For the F.C.C. lattice a good estimate can be obtained of w_c and one can conjecture that $\gamma=\frac{5}{4}$.

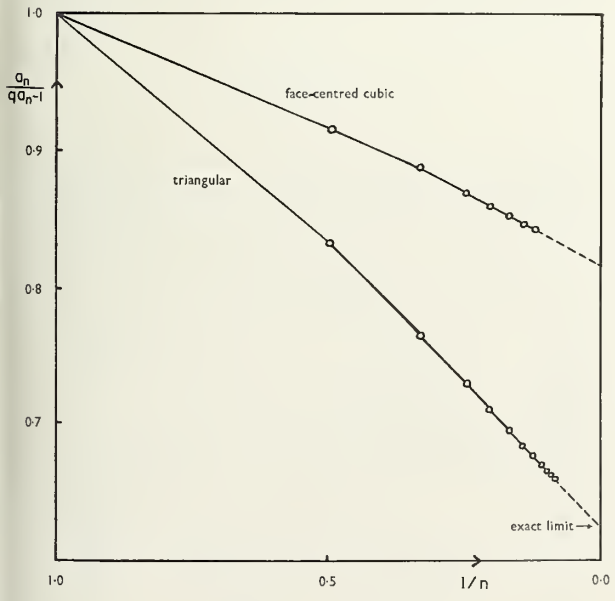

FIGURE 1. *Ising model.* [33]
Successive ratios in the susceptibility expansions of the triangular and face-centered cubic lattices as functions of $1/n$. (q=Coordination number of lattice=number of nearest neighbors of each atom.)

Passing now to "even" lattices like the S.C., B.C.C. and Diamond, we again find the same value for γ. However, now because of the symmetry between ferromagnetism and antiferromagnetism, we expect a corresponding singularity on the negative real axis which is much weaker and therefore masked by the positive singularity. We should therefore try to look for a function of the form

$$\chi_0 \sim B\left(1-\frac{w}{w_c}\right)^{-5/4} f\left(1+\frac{w}{w_c}\right) \tag{3}$$

where the second term represents the antiferromagnetic singularity. In order to focus attention on this second factor, Fisher and Sykes [7] took $\ln \chi_0$, subtracted $-\frac{5}{4}\ln\left(1-\frac{w}{w_c}\right)$, and obtained a well-behaved series with terms alternating in sign. After some ingenious manipulation they concluded that the second factor in (3) could be represented by

$$C+D\left(1+\frac{w}{w_c}\right)\ln\left(1+\frac{w}{w_c}\right). \tag{4}$$

The form of the susceptibility at the Néel point is shown in figure 2: it is characterized by a maximum above the Néel temperature and a logarithmically infinite slope at the Néel temperature.

The second example in this group is the high temperature expansions for the specific heat of the Ising model for the triangular and F.C.C. lattices [8]. The terms are again all positive but converge more slowly (eq. (5)).

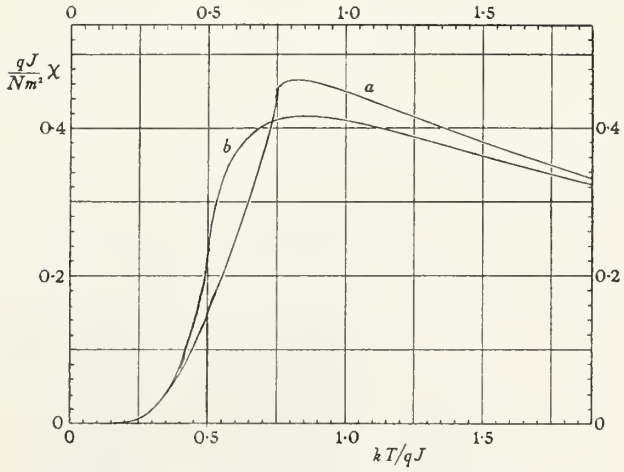

FIGURE 2. *Comparison of the antiferromagnetic susceptibility of (a) the simple cubic lattice* (q=6) *and (b) the plane honeycomb lattice* (q=3). [7]
The critical point is indicated by a small circle.

$$C_H/R = 0.06257t^2(1 + 0.8169t + 0.6778t^2 + 0.5680t^3 + 0.4818t^4 + 0.4190t^5 + 0.3725t^6 + 0.3364t^7 + \ldots) \quad \text{(F.C.C.)}$$

(5)

$$C_H/R = 0.2263t^2(1 + 1.0986t + 0.8298t^2 + 0.5525t^3 + 0.4021t^4 + 0.3384t^5 + 0.2971t^6 + 0.2614t^7 + \ldots) \quad \text{(Triangular).}$$

It is clear from the analysis shown in table 2 that not enough terms are yet available to draw definite conclusions; the slope for the three-dimensional lattice seems to be sharper than a logarithm corresponding to the two-dimensional lattice, and a figure of $\left(1-\frac{T_c}{T}\right)^{-1/5}$ could be regarded as reasonably consistent with the data. Table 2a shows an extension of the triangular lattice (calculated by D. L. Hunter) and it will be seen that for values of n greater than 11 the series settles down to steady behavior; a linear extrapolation would yield a value of α close to zero. The same steady behavior seems to set in earlier ($n=5$) in the three dimensional case, and this increases confidence in the above estimate of critical behavior.

It is interesting to ask why the convergence to the asymptotic value of the specific heat coefficients is so much slower than for the susceptibility. I think that this can best be understood by comparison with an analogous problem in the lattice model of polymer configurations. If c_n represents the number of simple chains of n links on a lattice and u_n the number of simple closed polygons, the series $\Sigma c_n x^n$ and $\Sigma u_n x^n$, both have the same radius of convergence: but the c_n reach their asymptotic value much more rapidly than the u_n, as can be seen from figure 3. The most important configurations contributing to the susceptibility are "chain-like," and those contributing to specific heat are "polygon-like."

Group II refers to series not consistent in sign in which the singularity of physical interest is masked by a spurious singularity. Examples of this group are given in table 3 of the coefficients in the low temperature expansion for the spontaneous magnetization. Only a real positive singularity is of physical significance here and it can be assumed that this singularity has been

Table 2a. *Triangular lattice*

n	h
8	0.117270
9	.122611
10	.122048
11	.113000
12	.104705
13	.098587
14	.093338
15	.088486
16	.084055
17	.080042
18	.076392
19	.073056
20	.069993
21	.067174
22	.064570
23	.062158
24	.059918
25	.057832
26	.055886
27	.054065
28	.052358
29	.050755
30	.049246

Table 2

n	h (triangular)	h (F.C.C.)
1	1.0986	0.8169
2	0.5106	.6594
3	−.0025	.5140
4	−.0887	.3930
5	.2079	.3483
6	.2676	.3341
7	.1599	.3215

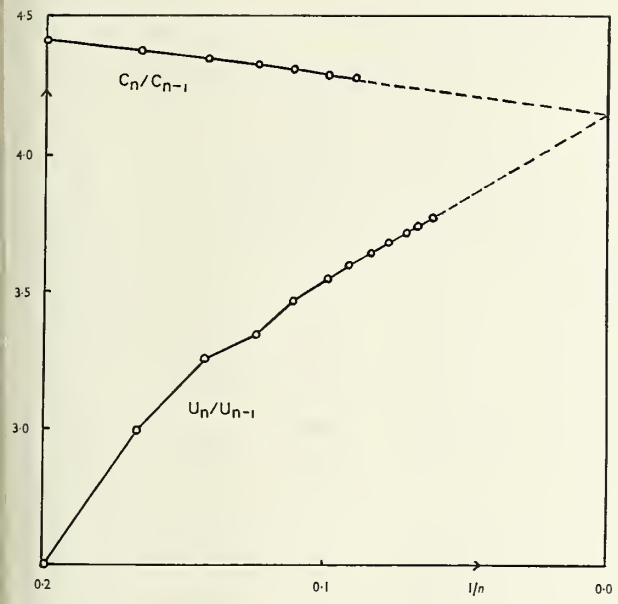

FIGURE 3. *Excluded volume problem.* [33]
Asymptotic limits of c_n and u_n for self-avoiding walks.

located by the high temperature susceptibility series. The triangular and S.C. lattices give rise to a regular alternation in sign, and the dominant singularity is therefore on the negative real axis: for the F.C.C. lattice a more complicated distribution in the complex plane is indicated. We know the exact solution for the triangular lattice [6], of the form

$$\frac{(1-3u)^{1/8}(1+u)^{3/8}}{(1+3u)^{1/8}(1-u)^{3/8}}. \tag{6}$$

We might therefore reasonably try for the spontaneous magnetization of three-dimensional lattices a function of the form

$$\Psi(u)=E(u-u_c)^{\beta}(u-u_1)^{\beta_1}(u-u_2)^{\beta_2} \ldots . \tag{7}$$

It is for this type of series that the Pade approximant, introduced into this field by G. A. Baker [9], is of prime importance. The $[N, M]$ approximant is defined by

$$f(u)=\frac{P(u)}{Q(u)}=\frac{\Sigma p_r u^r \text{ (degree } M)}{\Sigma q_r u^r \text{ (degree } N)}. \tag{8}$$

The $[N, N]$ approximant is the most useful since it is invariant under any homographic transformation of the type

$$u=A\omega/1+B\omega), \tag{9}$$

and we should expect it to be at least as useful in improving the convergence as the best such homographic transformation. Clearly, for a function of the type $\psi(u)$ it is best to approximate to $\frac{d}{du}\ln\psi(u)$, and the zeros of the denominator then locate the singularities $u_c, u_1, u_2 \ldots$. Our interest is focused on β, and it is best to assume the value of u_c from the high temperature susceptibility expansion and approximate to β by

$$[(u-u_c)\frac{d}{du}\ln\psi(u)]. \tag{10}$$

There are a number of devices which can be used to improve the estimate of β. After careful examination it has been conjectured that $\beta=\frac{5}{16}$ for three dimensional lattices.

For series of Group II we also find examples of slow convergence, and these are illustrated in table 4, which gives the low temperature susceptibility expansion for three-dimensional lattices [10]. The Pade approximant technique has again been applied assuming a function of the form (7), but even though a substantial number of terms are available, it will be seen from the analysis in table 5 that the limits of the index $\gamma'(\chi_0 \sim A'(u-u_c)^{\gamma'})$ are still between 1.27 and 1.37.

Similarly, the specific heat at low temperatures [11] converges slowly and present data are consistent with logarithmic behavior

$$C_H \sim B'\ell n\,(T_c-T), \tag{11}$$

but are not sufficiently convergent to draw reliable conclusions.

These last two quantities are of particular interest because of thermodynamic inequalities derived by Rushbrooke and Griffiths [12] which estimates of the indices fail to satisfy (this aspect will be discussed in more detail by Professor Fisher).

The best hope of obtaining more reliable information would seem to lie with the development of more terms for the diamond lattice [13] since they belong to Group I. Even with the powerful help of the Pade approximant, it is still true to say

TABLE 3. *Coefficients* b_n *in expansion of* $\{\partial\phi(t, \tau)/\partial\tau\}_0$ *for large* t

n	Type of lattice			Face-centered cubic
	Simple quadratic	Triangular	Simple cubic	
0	8	12	12	24
1	34	−2	−14	−26
2	152	78	90	0
3	714	−24	−192	0
4	3,472	548	792	48
5	17,318	−228	−2,148	252
6	88,048	4,050	7,716	−720
7	454,378	−2,030	−23,262	438
8	2,373,048	30,960	79,512	192
9	12,515,634	−17,670	−252,054	984
10	66,551,016	242,402	846,628	1,008
11	356,345,666	−152,520	−2,753,520	−12,924
12	.....	1,932,000	9,205,800	19,536
13	.....	−1,312,844	−30,371,124	−3,062
14	.....	15,612,150	.....	8,280
15	.....	−11,297,052	.....	−26,694
16	.....	.....	.....	−153,536
17	.....	.....	.....	507,948

that series of Group I provide the most reliable information. (Of course, the Pade approximants can be used to good effect on these series as well.) This program is being currently pursued.

Group III consists of series in which there is unexpected asymptotic behavior of the coefficients which does not manifest itself for many terms. Table 6 shows the coefficients in the high temperature susceptibility series for the Heisenberg model of the B.C.C. lattice [14]. If they are analyzed in the manner of Group I, they lead to a good estimate of Curie temperature and a susceptibility index of 4/3,[1]

$$[\chi_0 \sim C'(T_c - T)^{-4/3}] \tag{12}$$

(and this index is given more clearly by the F.C.C. lattice [15]).

However, physical considerations lead us to think that there is a corresponding antiferromagnetic singularity which is no longer symmetric with the ferromagnetic singularity. The position of this Néel point was located very strikingly by Rushbrooke and Wood recently [16], who used the staggered susceptibility, (i.e., susceptibility in a

[1] For subsequent work (spin ½) see Baker, Gilbert, Eve, and Rushbrooke, Phys. Letters **20**, 146 (1966).

TABLE 4

n	F.C.C.	B.C.C.	S.C.
	$q=12$	$q=8$	$q=6$
1	0	0	0
2	0	0	12
3	0	16	−14
4	0	−18	135
5	24	0	−276
6	−26	252	1 520
7	0	−576	−4 056
8	0	519	17 778
9	72	3 264	−54 392
10	378	−12 468	213 522
11	−1 080	20 568	−700 362
12	665	26 662	2 601 674
13	384	−215 568	−8 836 812
14	1 968	528 576	31 925 046
15	2 016	−164 616	−110 323 056
16	−25 698	−3 014 889	
17	39 552	10 894 920	
18	−3 872		
19	20 880		
20	−65 727		
21	−379 856		
22	1 277 646		

field which alternates in sign from one lattice point to the next). They found that the Néel temperature is 10 percent *higher* than the corresponding ferromagnetic Curie temperature. If we take off the ferromagnetic singularity (table 6) as for the Ising model, we find clear evidence of this dominant factor although insufficient terms are available to analyze the detailed critical behavior. Fisher has advanced general theoretical arguments [17] which lead us to expect a similar critical behavior to the Ising model, and if so, we can anticipate an asymptotic form for the coefficients of the type

$$\frac{4}{3}(2.537)^n+(-1)^n\,\frac{(2.791)^n}{n}. \tag{13}$$

The terms would then ultimately alternate in sign but the first negative coefficient would not occur until after about 60 terms.

209-493 O-66—4

TABLE 5. *Pade approximants for* γ'

N	F.C.C.			B.C.C.		
	$j=1$	$j=0$	$j=-1$	$j=1$	$j=0$	$j=-1$
6	1.207		1.254	1.241	1.246	1.264
7	1.259	1.251	1.254	1.280	1.402	1.374
8	1.287	1.244	1.247	1.375	1.405	1.285
9	1.249	1.262	1.236	1.295	1.273	1.268
10	1.240	1.360	1.332	1.269	1.272	1.276
11	1.332	1.353	1.350	1.277	1.274	1.273
12	1.350	1.353	1.270	1.274		
13	1.273	1.273				

TABLE 6

n	Heisenberg model	B.C.C. lattice		Magnetic susceptibility
	χ	$\frac{d \log \chi_0}{dK}$	$\frac{(4/3)}{(1-K/K_c)}$	Delta
1	4.00000	4	3.383236	+0.616764
2	12.00000	8	8.584714	−.584714
3	34.66666	24	21.783088	+2.216912
4	95.83333	52.6	55.272995	−2.606328
5	262.70000	154.16	140.251202	+13.915465
6	708.04166	350.11663	355.8773	−5.760670
7	1893.28968	943.01682	903.0126	+40.004
8	5012.10863	2189.44354	2291.329	−101.885
9	13235.59898	6111.4476	5814.018	+297.43

K_c taken as 0.3941, inverse 2.5374.

Summary of Critical Behavior of Nearest Neighbor Lattice Systems

We have already referred to the critical behavior of the magnetic susceptibility of ferro- and antiferromagnets in the previous section. Change in spin value from ½ to general s does not change this critical behavior either for the Ising or Heisenberg model [15].

Regarding the critical behavior of the spontaneous magnetization, accurate information is available only for the Ising model of spin ½ (see previous section). A Green's function interpolation method used by Tahir-Kheli [18] has suggested an index of ⅓ for β: this differs only slightly from the Ising value of 5/16.

Critical values of thermodynamic functions, particularly entropy, provide insight into the magnitude of the "tail" of the specific heat curve. For a model of spin ½ the total entropy change is $k\ln 2$ per system. With the Ising interaction in two-dimensions the tail is large and corresponds to more than 50 percent of the entropy; in three-dimensions the tail is very much reduced and corresponds to about 15 percent. For the three-dimensional Heisenberg model, the tail is increased by a factor of more than two and corresponds to about 35 percent of the entropy [19].

When we change from spin ½ to general s, the total entropy changes from $k\ln 2$ per system to $k\ln(2s+1)$. However, most of the change takes place below the Curie temperature and even in going from $s=½$ to $s=\infty$, the increase in entropy above the Curie temperature is less than 30 percent. This can readily be understood since the high temperature portion is derived from averages which are not likely to be very sensitive to change in spin value. However, the behavior at low temperatures is determined by the excitation spectrum which is extremely sensitive to the form of interaction.

We have referred to the critical behavior of the specific heat in the previous section. It is worth pointing out that this critical behavior is more dependent on the form of interaction than that of the magnetic susceptibility. Although only limited numbers of terms are available, they indicate an appreciable sharpening on the high temperature side as s changes from ½ to infinity; similarly, there are marked differences between the Ising and Heisenberg interactions [15].

Attention has recently been focused on the behavior of the magnetization as a function of field at the Curie point. For the Ising model the index δ ($H=M^{\delta}$) is about 15 in two dimensions and about 5.2 in three dimensions [20]. Data for the Heisenberg model are available but have not yet been put into a convenient form for detailed analysis.

Critical properties of the correlations are being discussed in detail by Professor Fisher.

Longer Range Forces

The precision of our knowledge of the effect of longer range forces has increased appreciably during the past few years. The idea had often been expressed intuitively that if the number of neighbors participating equally in the interaction tended to infinity the mean field or Bragg-Williams approximation would result exactly. This has now been established rigorously [21] by taking an interaction of the form $\epsilon Je^{-\epsilon R}$ and allowing ϵ to tend to zero; the result is valid even for a one-dimensional model.

A solution of Bethe type including a small residual specific heat above T_c results if the force is long range in one direction and short range in the other [22]. It is significant to observe this physical interpretation of the Bethe result which had previously been regarded as a first approximation to the solution for a nearest neighbor model, or the exact solution for an unphysical "pseudo-lattice" containing no closed circuits [23].

It is interesting to see how the mean field solution is approached as the range of force increases. For this purpose it has been found convenient to introduce an "equivalent neighbor (r shell)" model in which all interactions are equal up to the rth neighbor shell, and zero outside. The series expansion methods described in the previous section can be applied to this model, and Dalton and I have been able to take account of the second and third neighbor shells for a number of two and three dimensional lattices [24]. We find that the critical behavior (e.g., susceptibility index) is identical with that of a nearest neighbor model.

However, we noticed empirically that for large q simple asymptotic formulae fit the Curie temperature and thermodynamic functions. For example,

$$\frac{qJ}{kT_c}=1+H/q$$

and (14)

$$\frac{S_\infty-S_C}{k}=L/q.$$

Here H and L are constants which depend on the dimension and the type of interaction. Although this is the kind of asymptotic formula given by closed form approximations, the numerical values of H and L which we obtained were quite different from the closed form values.

We then tried to find a justification for this type of limiting form. Series expansions for an equivalent neighbor model can be expressed in terms of "lattice constants" which are the number of independent multiply connected graphs of various kinds which can be formed from the interacting bonds on the lattice. We realized that for a range of interaction which included many lattice points, these lattice constants could be regarded as lattice sum approximations to hard sphere cluster integrals, many of which have already been evaluated. The efficacy of this approximation can be judged from table 7 which gives typical estimates, and these are compared with the correct values based on exact enumerations.

We can thus readily see why the constants H, L differ for different dimensions since the cor

TABLE 7. *Asymptotic formula from cluster integrals*

Three Dimensions

$$p_{5a}=0.05903(q+1)^3-0.8360\sqrt{q+1}^2+3q+1.25$$

q	p_{5a}(calc.)	p_{5a}(exact)	$\frac{p_{5a}\text{(calc.)}}{p_{5a}\text{(exact)}}$
6	−0.46	0	.....
12	25.7	36	0.71
18	158.3	174,186	.88
26	637.8	630,690	.97
42	3274.8	3,318	.99

$$p_5=0.02381\sqrt{q+1}^4-0.3963\sqrt{q+1}^3+3.1719\sqrt{q+1}^2-8q-3.6$$

q	p_5(calc.)	p_5(exact)	$\frac{p_5\text{(calc.)}}{p_5\text{(exact)}}$
6	25.1	0	.....
12	245.8	168	1.5
18	1382.2	1212	1.14
26	6954.0	6852, 6276	1.06 (mean)
42	55418.3	54 564	1.02

responding cluster integrals will then have different values. The Bethe approximation gives the correct limiting value as the *dimension* becomes large, and not as the coordination number becomes large in a given dimension.

Using the above approximation based on cluster integrals, we find that the simple polygons dominate for the early terms, and these can be calculated to any order using the methods of Montroll and Mayer. The approximation must break down for higher order terms since it does not give correct critical behavior for magnetic susceptibility, specific heat, etc. However, it can give valid approximations for the Curie point and critical values of thermodynamic functions since higher order terms make only a small contribution to these. The approach to the mean field limit (linear inverse susceptibility, finite and discontinuous specific heat, etc.) occurs in a singular manner, and this is illustrated diagramatically for the specific heat in figure 4.

In the light of the above discussion, it is constructive to consider the effect of a $1/r^{l'}$ force for varying p and this is being currently investigated at King's College by one of my research students, G. S. Joyce. It is much more difficult to derive series expansions for such a law of force since all neighbors must be taken into account. A substantial simplification occurs for the Ising model of spin ½ if the method of Yvon (see next section) is used to eliminate all but multiply connected configurations. Joyce finds that a sufficiently small value of p can change critical behavior, and produce critical effects, even in one dimension.

FIGURE 4. *Diagrammatic illustration of the difference in specific heat curve between a finite range force and a force extending to infinity sufficiently slowly.*
For a finite cutoff the specific heat is always infinite although the residual entropy tends to zero as the range becomes large.

For example, taking the interaction between i-j pairs as J/r_{ij}^2 in one dimension (assuming unit lattice spacing), the series expansion of magnetic suceptibility is

$$\frac{kT\chi_0}{m^2} = 1 + 3.290\ \beta J + 8.659\ (\beta J)^2 + 20.686\ (\beta J)^3$$

$$+ 46.411\ (\beta J)^4 + 99.699\ (\beta J)^5 + 207.338\ (\beta J)^6. \quad (15)$$

This leads us to a Curie temperature

$$\frac{kT_c}{J} \simeq 0.51 \times \frac{\pi^2}{3}, \quad (16)$$

and a susceptibility index of about three. With an interaction J/r_{ij}^3 in two dimensions the corresponding susceptibility expansion is

$$\frac{kT\chi_0}{m^2} = 1 + 9.033622\ (\beta J) + 76.94741\ (\beta J)^2$$

$$+ 642.168\ (\beta J)^3 + 5302.1\ (\beta J)^4 + 43508\ (\beta J)^5 + \ldots, \quad (17)$$

and the susceptibility index is reduced from 7/4 for a short range force to about 1·13. This change in susceptibility index is demonstrated in figure 5.

Joyce has also investigated the properties of the spherical model in one dimension for long range forces. Whilst one must be cautious in drawing detailed conclusions about critical behavior from

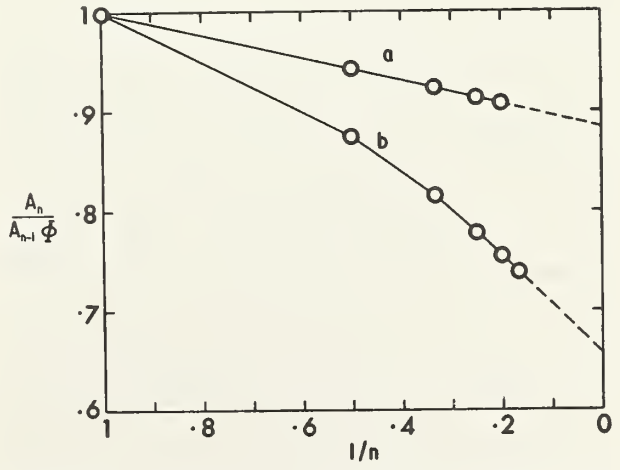

FIGURE 5. *Susceptibility of two-dimensional Ising model with a long range $1/R^3$ law of force: (a) long range interaction, (b) short range nearest and second neighbor interaction.* [14]
(The final slope represents the susceptibility index.)

the spherical model, I think it can act as a general guide to the influence of long range forces on critical behavior. Joyce finds that there is a critical point in one dimension when $1 < p < 2$. When $1 < p < \frac{3}{2}$ the susceptibility index is 1 and when $\frac{3}{2} < p < 2$ it is $\frac{p-1}{2-p}$, so that it is equal to 3 when $p = 1.75$. Corresponding results can be derived in two and three dimensions.

For the general spin s and for the Heisenberg model, the calculations are more complicated since all connected diagrams must be taken into account. However, if the spin is allowed to become infinite in the Heisenberg model (classical vector model), the conditions of applicability of the second Mayer theorem are satisfied, and only multiply connected clusters enter. The expansions can then be pushed much further, and this simplification is being currently exploited.

Diagram Expansions; Approach to the Exact Solution

Early work using closed form approximations provided no reliable information on detailed behavior near the critical point. One of the major defects of this work was the inability to develop a series of successive approximations which would tend in the limit to the exact solution. Even when the methods introduced could in principle produce such a series of approximations, the practical calculations were prohibitive.

The cluster integral development of Mayer can be adapted to the Ising model [25], and can be made to furnish a steady series of approximations based on all multiply connected graphs which can be constructed from bonds of the lattice. The kth stage of the approximation could correspond for example, to including all graphs of k lines where k is allowed to increase steadily. It was Yvon [26] who showed how to take all graphs into account, and not merely regular graphs in which vertices and bonds are equivalent. His method involved using the Mayer theory of multicomponent mixtures.

Hiley and I [27] investigated the critical behavior of such a series of approximations to see how they approached the exact solution as estimated from series expansions. To focus attention on the susceptibility index, for example, we calculated

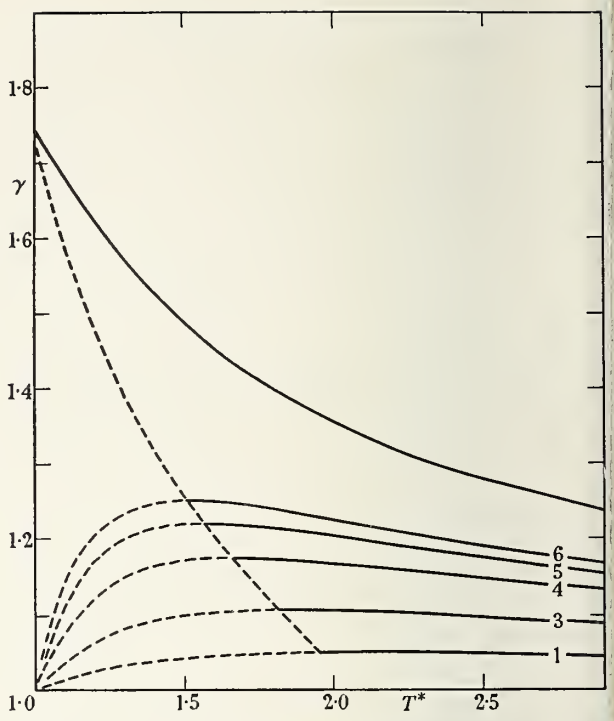

FIGURE 6. *Plot of* $\gamma(T^*)$ *against* $T^*(=T/T_c)$ *for the triangular lattice.* [27]

For each successive approximation γ passes through a maximum and then falls to unity. The locus of the maxima extrapolates to a value 1.75 for $T^* = 1$. The limiting curve is derived from series expansions.

$$\gamma(T) = (T - T_c) \frac{d}{dT} \ln \chi_0(T) \tag{18}$$

which should tend to 7/4 for a two dimensional and 5/4 for a three dimensional model as $T \to T_c$. Figure 6 shows the results for a two dimensional model. For each stage of the closed form approximation $\gamma(T)$ rises to a maximum and then falls to the mean field value of 1. For temperatures nearer to T_c than this maximum, the approximation cannot be regarded as reliable. The locus of maxima tends to 7/4, and we see that the approach of the closed form approximations to the exact solution is nonuniform.

We may follow an alternative approach classifying graphs into groups of increasing complexity and summing each group to infinity. Let us look at the high temperature partition function in zero field which can be written in the simple form [28]

$$\ln Z_N = N \ln 2 + \frac{qN}{2} \ln (\cosh K) + \sum p_{nx} f_{nx}(w) \tag{19}$$

$$K = J/kT \qquad w = \tanh K$$

where the p_{nx} are the "lattice constants" representing numbers of multiply connected graphs and the $f_{nx}(w)$ can be determined quite simply. Confining attention first to simple polygons which provide the dominant contribution, we obtain the function $\Sigma p_n \ln(1+\omega^n)$. Sykes [29] has suggested that for three dimensional lattices

$$p_n \simeq \frac{\mu^n}{n^k} (k \sim 1.75) \tag{20}$$

where μ is the self-avoiding walk limit. Hence, if we ignore all configurations other than simple polygons, we will obtain a specific heat singularity of the form $(T-T_c)^{-1/4}$, and an estimate of the Curie point which differs from the correct value by about 2½ percent (the close connection between μ and the Ising critical value was pointed out several years ago by Fisher and Sykes [30]).

To make further progress we must introduce a suitable topological classification of multiply connected graphs, and here Sykes [31] has suggested using the cyclomatic number c (number of bonds − number of vertices + 1); the types of graph corresponding to $c=1$, 2, 3, and 4 are shown in figure 7. Even here the number of types increases quite rapidly, but can be substantially reduced by ignoring in the first instance multiple connections between two vertices (thus p, θ, δ, and Q can also be considered basically as one type).

One must then consider the asymptotic numbers of each type of graph to understand how the asymptotic value of the coefficients in the high temperature series is constituted. The constant μ arises for a single self-avoiding walk: for more complex graphs the mutual interference of two or more self-avoiding walks must be considered. Even if this difficult empirical investigation is completely satisfactory the theory could only be considered respectable if the asymptotic estimates are established rigorously. But this at least is a far less formidable problem than the Ising problem itself, and Professor Edwards has taken an important step recently towards its solution [32].

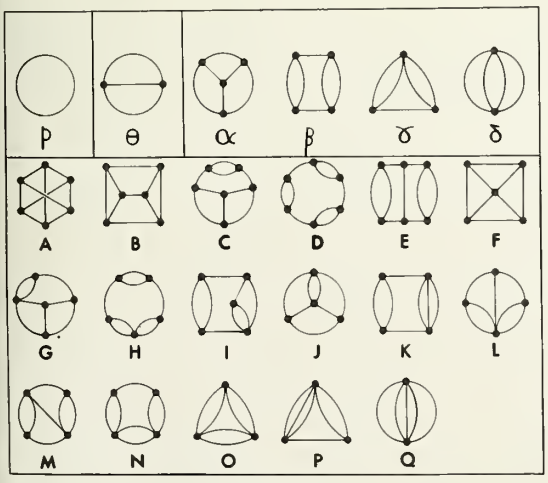

FIGURE 7.

Helpful discussion with colleagues and research students mentioned in the text is gratefully acknowledged. The remarks at the end of the final section were stimulated by a series of lectures given at King's College recently by Dr. R. Brout.

References

[1] L. Onsager, Phys. Rev. **65**, 117 (1944).
[2] C. N. Yang and T. D. Lee, Phys. Rev. **87**, 404, 410 (1952).
[3] C. Domb, Phil. Mag. **42**, 1316 (1951).
[4] C. Domb, Il Nuovo Cimento Supplement to Vol. **9**, 9 (1958); D. M. Burley, Proc. Phys. Soc. **77**, 262 (1960); D. M. Gaunt and M. E. Fisher, J. Chem. Phys. **43**, 2840 (1965).
[5] P. Dienes, The Taylor Series Oxford 1931, ch. 14.
[6] C. Domb, Advan. in Physics **9**, 149, 245 (1960).
[7] M. F. Sykes and M. E. Fisher, Physica **28**, 919, 939 (1962).
[8] C. Domb and M. F. Sykes, Phys. Rev. **108**, 1415 (1957).
[9] G. A. Baker, Phys. Rev. **124**, 768 (1961).
[10] J. W. Essam and M. E. Fisher, J. Chem. Phys. **38**, 802 (1963).
[11] D. S. Gaunt and J. W. Essam, Proc. International Conference on Magnetism, Nottingham 1964, p. 88.
[12] G. S. Rushbrooke, J. Chem. Phys. **39**, 842 (1963); R. B. Griffiths, Phys. Rev. Letters **14**, 623 (1965).
[13] J. W. Essam and M. F. Sykes, Physica **29**, 378 (1963).
[14] C. Domb and D. W. Wood, Proc. Phys. Soc. **86**, 1 (1965). C. Domb, N. W. Dalton, G. S. Joyce and D. W. Wood, Proc. International Conference on Magnetism, Nottingham 1964, p. 85.
[15] C. Domb and M. F. Sykes, Phys. Rev. **128**, 168 (1962); J. Gammel, W. Marshall and L. Morgan, Proc. Roy. Soc. **A275**, 257 (1963).
[16] G. S. Rushbrooke and P. J. Wood, Mol. Phys. **6**, 409 (1963).
[17] M. E. Fisher, Phil. Mag. **7**, 1731 (1962).
[18] R. A. Tahir Kheli, Phys. Rev. **132**, 689 (1963).
[19] C. Domb and A. R. Miedema, Progress in Low Temperature Physics, IV (1963), p. 296.
[20] D. S. Gaunt, M. E. Fisher, M. F. Sykes and J. W. Essam, Phys. Rev. Letters **13**, 713 (1964).
[21] G. A. Baker, Phys. Rev. **126**, 2071 (1962); M. Kac and E. Helfand, J. Math. Phys. **4**, 1078 (1963).
[22] G. A. Baker, Phys. Rev. **130**, 1406 (1963).
[23] M. Kurata, R. Kikuchi and T. Watari, J. Chem. Phys. **21**, 434 (1953); see also ref. 6, p. 284.
[24] N. W. Dalton, Thesis, London (1965); see also ref. 14.
[25] G. S. Rushbrooke and I. Scoins, Proc. Roy. Soc. **230**, 74 (1955).
[26] J. Yvon, Cah. Phys. No. 28 (1945), Nos. 31, 32 (1948).
[27] C. Domb and B. J. Hiley, Proc. Roy. Soc. **268**, 506 (1962).
[28] Reference 6, p. 322, eq (59).
[29] B. J. Hiley and M. F. Sykes, J. Chem. Phys. **34**, 1531 (1961).
[30] M. E. Fisher and M. F. Sykes, Phys. Rev. **114**, 45 (1959).
[31] M. F. Sykes, private communication. To be submitted to J. Math. Phys.
[32] S. F. Edwards, This Conference.
[33] C. Domb, J. Royal Stat. Soc. London **B26**, 373 (1964).

Equilibrium Properties of Ferromagnets and Antiferromagnets in the Vicinity of the Critical Point*

G. B. Benedek

Massachusetts Institute of Technology, Cambridge, Mass.

Within the past few years there has been a considerable advance both theoretically and experimentally in our knowledge of the behavior of magnetic systems in the vicinity of the critical temperature. The present paper consists of a presentation of some of the new experimental information and its connection with the new theoretical predictions.

Some of the equilibrium properties of magnetic systems which are important in the description of a ferromagnet in the critical region are the following:

1. The spontaneous magnetization versus temperature in zero external field,
2. the magnetic susceptibility $(\partial M/\partial H)_{H=0}=\chi$.
3. the magnetization versus field at the critical temperature T_c,
4. the specific heat at constant volume C_v, and
5. the thermal expansion coefficient.

In the discussion which follows, we shall present the experimental data and theoretical predictions now available on each of the properties listed above. In view of the fact that each of these properties has an analog in the liquid-gas system, as has been emphasized by Fisher [1] and his coworkers [2], we shall make the connection between each magnetic property and its fluid analog.

1. *The spontaneous magnetization.* In figure 1 we present a schematic drawing of the temperature dependence of the spontaneous magnetization $M(T)$ of a ferromagnet normalized to its value at $T=0$, $(M(0))$, in zero external field $(H=0)$. Along side this we present the fluid analog, namely the temperature dependence of the liquid-gas density along the coexistence curve. In the critical region the magnetization and orthobaric density data can be fit to equations of the form:

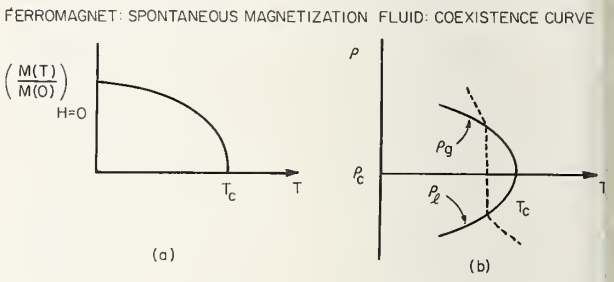

FIGURE 1. (a) *A schematic plot of the temperature dependence of the magnetization of a ferromagnet.* (b) *The fluid analog, the liquid and gas densities along the coexistence curve.*

$$\left(\frac{M(T)}{M(0)}\right)_{H=0} \rightleftharpoons D\left(1-\frac{T}{T_c}\right)^{\beta} \tag{1}$$

$$\left(\frac{\rho_l-\rho_g}{2\rho_c}\right) \rightleftharpoons D'\left(1-\frac{T}{T_c}\right)^{\beta'}. \tag{2}$$

The first experimental measurements of D and β were reported in 1962 by P. Heller and G. Benedek [3] through a study of the nuclear resonance of the F^{19} nucleus in the antiferromagnet MnF_2. In table 1 we show the temperature range $\Delta T/T_c$ over which (1) was found to fit the data, and the corresponding values of D and β. Equation (1) holds in MnF_2 over a temperature range $7\times10^{-5} \leqslant (\Delta T/T_c) < 0.1$. The closest point measured was about 3 mdeg from the critical point. This data shows that $\beta=0.333\pm0.003$. This result is in disagreement with molecular field theories which give $\beta=1/2$ in the limit $T\rightarrow T_c$. In view of the marked disparity between this result and that of the classical theories of magnetism, Heller and Benedek [4] later carried out a careful investigation of the insulating ferromagnet EuS. This crystal

*This research was supported by the Advanced Research Projects Agency under Contract SD 90.

Table 1. *Experimental and theoretical values for the parameters describing the temperature dependence of the spontaneous magnetization of a ferromagnet or antiferromagnet*

	$\left(\frac{\Delta T}{T_c}\right)$	D	β
MnF_2	$0.10 \leftrightarrow 7 \times 10^{-5}$	1.200 ± 0.004	0.333 ± 0.003
EuS	$0.08 \leftrightarrow 1 \times 10^{-2}$	1.145 ± 0.02	0.33 ± 0.015
$CrBr_3$	$0.04 \rightarrow 0.7 \times 10^{-2}$	1.32 ± 0.07	0.365 ± 0.015
Molecular field theory		1.48 (S = 5/2) 1.44 (S = 7/2)	0.500
Ising model		1.49	0.3125

is cubic, the magnetic europium spins are localized on the lattice sites and each magnetic ion has zero orbital angular momentum and S = 7/2. This crystal represents the closest known physical approximation to the ideal "Heisenberg" ferromagnet. The results of this investigation are summarized in table 1. The one-third power law was found to apply also to this system.

It is worth noting that the 1/3 power law starts to fit the data on EuS and MnF_2 when $\Delta T/T_c \sim 9$ percent. The magnetization at this point is about 1/2 the saturation value. Thus the 1/3 power law applies to the magnetization data over a rather wide range in M, namely $1/2 > (M(T)/M(0)) \geq 0$. In row 3 of table 1 we also present new measurements of D, β and $\Delta T/T_c$ made very recently by S. D. Senturia at MIT on the ferromagnetic insulator $CrBr_3$. This material is particularly interesting from the theoretical point of view because the ferromagnetic chromium spins are arranged in planes, and each plane is separated from the next plane by a plane of nonmagnetic Br ions. As a result, the coupling between the magnetic spins is very anisotropic. The exchange constant for coupling in the plane is 16 times stronger than the constant for coupling between the planes. Thus, this ferromagnet is almost two-dimensional, with only a small three-dimensional admixture. Nevertheless, this system behaves somewhat like the ideal three-dimensional Heisenberg ferromagnet EuS in that $\beta = 0.365$. The critical region for $CrBr_3$ sets in a $\Delta T/T_c \sim 5 \times 10^{-2}$ at which point $M(T)/M(0) \sim 0.41$.

In table 1 we also present the theoretical predictions of the Ising [5] and molecular field models. No theoretical prediction has yet appeared for the Heisenberg model. It should also be mentioned that H. Callen and E. Callen [6] have calculated $M(T)$ theoretically using a sophisticated cluster approximation, and report that $M(T)$ follows the 1/3 power law provided that T is not too near T_c. In the limit $T \rightarrow T_c$, of course, their cluster theory goes over to the $\beta = 1/2$ value.

As an example of the analogous behavior of a fluid we point out the work of Weinberger and Schneider [7, 1]. They found that eq (2) fits the data on xenon for $\Delta T/T_c$ as small as 3×10^{-5}, and that $\beta' = 0.345 \pm 0.015$ *and* $D' \simeq 1.61$. The van der Waals equation gives $\beta = 1/2$. In fact, Landau's theory [8] of the critical region shows that $\beta = 1/2$ follows from the very general assumption that the free energy can be expanded as a power series in density and temperature around the critical point.

Thus the breakdown of this law reflects a rather unusual mathematical and physical character of the critical point.

From an historical standpoint it should be noted that the departure of β from the classical value for magnetic systems was discovered at about the same time that important theoretical advances were being made. In 1961 and 1962 Domb and Sykes [9, 10] were able to show from a study of their high temperature expansions that the susceptability of a ferromagnet in the Ising and Heisenberg models did not diverge as slowly as was expected by the molecular field theories. Also, Baker [11, 12] introduced at this time the method of Pade approximants as an accurate and reliable means of extrapolating the high temperature expansions into the critical region. This extrapolation showed [13] that the susceptibility as calculated on the Heisenberg and Ising Hamiltonians diverged more rapidly than that predicted by the molecular field theories. These developments and the observation, which was stressed particularly by M. E. Fisher, of the close similarity in the behavior of systems as disparate as the ferromagnet and the fluid greatly contributed to the present expansion of work in this field.

2. *The susceptibility.* In figure 2 we show the temperature dependence of the isothermal susceptibility of a ferromagnet as $T \to T_c$. Along side it is shown the temperature dependence of the analogous property of the fluid, the isothermal bulk modulus along the critical isochore. The susceptibility of the ferromagnet is defined as

$$\chi = (\partial M(T, H)/\partial H)_{H=0}. \tag{3}$$

As one approaches T_c from the high temperature or paramagnetic side, χ diverges like

$$\chi \underset{(T_+ \to T_c)}{=} C/(1 - T/T_c)^{\gamma}. \tag{4}$$

As one approaches T_c from the ferromagnetic side, χ can be fit to an equation of the same form as (4) but one must leave the possibility that the coefficient D and exponent γ have different values for $T < T_c$. Thus, on this side of T_c we write

$$\chi \underset{(T_- \to T_c)}{=} C'/(1 - (T/T_c))^{\gamma'}. \tag{5}$$

In the fluid the analog is the isothermal compressibility β_T.

$$\beta_T = \frac{1}{\rho}\left(\frac{\partial \rho}{\partial P}\right)_T. \tag{6}$$

This can also be written in terms of the chemical potential μ using the thermodynamic identity that along an isotherm

$$\left(\frac{\partial P}{\partial \mu}\right)_T = \rho. \tag{7}$$

Thus

$$\beta_T = \frac{1}{\rho^2}\left(\frac{\partial \rho}{\partial \mu}\right)_T. \tag{8}$$

As $T \to T_c$ from above, the compressibility at $\rho = \rho_c$ diverges as follows:

$$\beta_{T, \rho_c} \underset{(T_+ \to T_c)}{=} d/(1 - (T/T_c))^{\Gamma}. \tag{9}$$

Below T_c the relevant compressibility is that evaluated right at the coexistence line for either the liquid or the gas

$$\beta_{T, \rho_c \text{ or } \rho_g} \underset{(T_- \to T_c)}{=} d'/(1 - (T/T_c))^{\Gamma'}. \tag{10}$$

We see that in the liquid case, the pressure, or the chemical potential plays the same role as does the magnetic field in the ferromagnetic case.

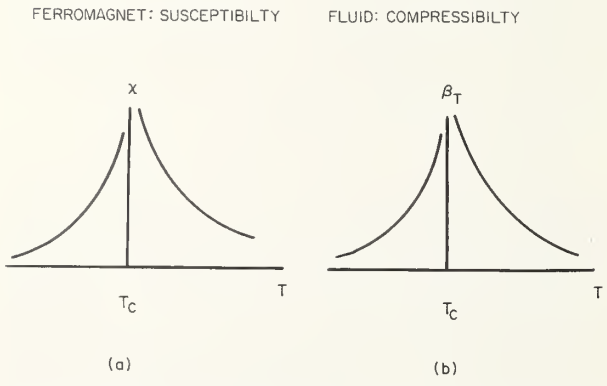

FIGURE 2. (a) *The temperature dependence of the isothermal susceptibility of a ferromagnet as* $T \to T_c$. (b) *The temperature dependence of the isothermal compressibility of a fluid evaluated at* $\rho = \rho_c$ *for* $T > T_c$ *and at* $\rho = \rho_l$ *or* $\rho = \rho_c$ *for* $T < T_c$.

The first comparison between the new theoretical predictions [9, 10, 13, 14] and experiments was provided by the work of Jacrot [15] who determined χ through a study of the scattering of neutrons from iron as $T \rightarrow T_c$ from above. His measurements indicated that $\gamma = 1.3$. Stimulated by the departure of γ from the classical value $\gamma = 1$. Noakes and Arrott [16] reexamined their older measurements of the susceptibility of iron for $T > T_c$, and they also carried out new measurements of this quantity. They found $\gamma = 1.37 \pm 0.04$. This result is tabulated in table 2 where we give γ for each ferromagnet which has been studied up till now. We also give in column 2 the maximum range over which eq (4) actually fits the experimental data. The range is $0 < \Delta T/T_c < \Delta T_M/T_c$, and $\Delta T_M/T_c$ represents the outer limit of the critical region insofar as the susceptibility is concerned. In their paper Noakes and Arrott pointed out that earlier data by S. Arajs [17], when analyzed in terms of eq (4) also gave a nonclassical value for γ. This observation was later confirmed by Arajs [18] who has measured γ from his studies on Fe, Co, and Ni. His important results on γ and $\Delta T_m/T_c$ are given in table 2. Kouvel and Fisher also examined the divergence in the susceptibility of nickel by going back to the very early careful work of P. Weiss and R. Forrer [20]. This gave $\gamma = 1.35 \pm 0.02$. Graham [21] has studied the susceptibility of Gd above the Curie point and concludes $\gamma = 1.3$ but does not give error limits for this estimate. Furthermore, his data indicates that γ depends on whether the magnetic field is applied along the c-axis or perpendicular to it.

In table 2 we also list in the last three rows the values of γ as obtained theoretically using the molecular field, Ising and Heisenberg models along with literature references to these calculation.

Table 2. *Experimental and theoretical values for the parameters describing the temperature dependence of the susceptibility of a ferromagnet as* $T \rightarrow T_c$ *from above*

Ferromagnet	$(\Delta T_M/T_c)$	γ	References
Fe	3×10^{-2}	1.3	15, 13
		1.37 ± 0.04	16
		1.33 ± 0.04	18
Co	1×10^{-2}	1.21 ± 0.04	18
Ni	2×10^{-2}	1.35 ± 0.02	19
		1.29 ± 0.03	18
Gd	4×10^{-2}	1.3	21
Theory			
Molecular field		1.00	
Ising		1.25	9, 11
Heisenberg		1.33 ± 0.01	13, 14

It is worth stressing that we do not know of data on γ' the parameter which describes the divergence of χ as $T \rightarrow T_c$ from the ferromagnetic side of the Curie point.

In the case of a fluid, the classical theories give $\Gamma = 1.0$. Because of the experimental difficulties, data on the isothermal compressibility appears to be scanty and insufficiently precise in the critical region. The measurements of Habgood and Schneider [22] indicate only that [1] $\Gamma > 1.1$. The Ising theory for the liquid predicts $\Gamma = 1.25$.

3. *The critical isotherm.* The next equilibrium property of a ferromagnet which is of particular interest in the critical region is the dependence of M on H at $T = T_c$. The divergence of the susceptibility as $T \rightarrow T_c$ shows that M is an extremely strong function of H at T_c. In figure 3 we show a schematic plot of M versus H at T_c. Along side it we present the fluid analog, namely the dependence of $(\rho - \rho_c)$ on the pressure for $T = T_c$, i.e., the shape of the critical $\rho - p$ isotherm. The data on both these systems may be fit to equations of the following form:

$$M(T_c, H) = AH^{1/\delta} \tag{11}$$

and

$$(\rho - \rho_c) \underset{T=T_c}{=} A'(p - p_c)^{1/\delta'} = A''(\mu - \mu_c)^{1/\delta'} \tag{12}$$

where μ is the chemical potential. The index δ or δ' is a measure of the verticality of the critical isotherms as sketched schematically in figure 3, as these indices are measures of the lowest nonvanish-

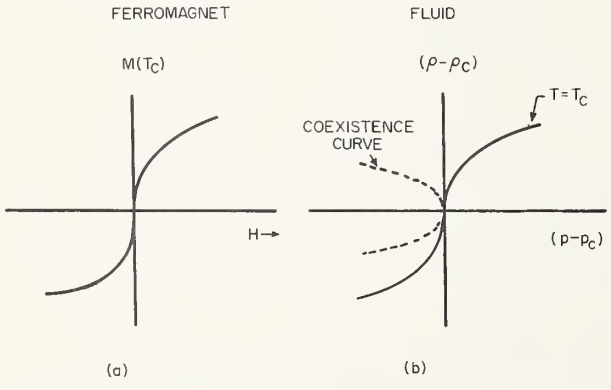

FIGURE 3. (a) *The dependence of the spontaneous magnetization* M *on the magnetic field* H *at the Curie point* (T = T_c). (b) *The shape of the critical isotherm of a fluid.*

ing derivative of H (or μ) relative to M (or ρ). In magnetic systems δ has been found for two materials, nickel and gadolinium. The information on nickel was obtained from Weiss and Forrer's 1926 measurements [20] by Kouvel and Fisher [19]. They found $\delta = 4.22 \pm 0.04$. Graham [21] reports that his studies of gadolinium give $\delta = 4$, without placing error limits on this figure. The molecular field theory predicts $\delta = 3$ while the best present analysis of the Ising model in three dimensions strongly indicates that the value $\delta = 5.2$ is the correct theoretical value for this Hamiltonian. There are as yet no calculations of δ using the Heisenberg Hamiltonian. These results are collected in table 3.

In the fluid there is considerably more data [23] on the shape of the critical isotherm. The data on Xe, Co_2, and H_2 indicates [2, 24] that for the fluid $\delta' = 4.2 \pm 0.1$. Once again we see the close similarity in behavior between the ferromagnet and the fluid. Theoretically the van der Waals theory, which is the analog of the molecular field theory of ferromagnetism, predicts a cubic equation for the $\rho - p$ critical isotherm, i.e., $\delta' = 3$. The Ising model as analyzed by Gaunt, Fisher, Sykes, and Essam [2] gives $\delta' = 5.2$. We tabulate these results in table 4.

4. *The specific heat.* Of all the physical quantities that vary rapidly near the critical point, the specific heat appears to diverge most delicately. Onsager's theoretical treatment [25] of the two-dimensional Ising system indicates that the specific heat diverges logarithmically as $T \rightarrow T_c$. Such a slow divergence requires very high precision in the measurement of the specific heat, and accurate temperature control very near to the critical point. A very careful study of the specific heat of a magnetic system has recently been carried out by Skalyo and Friedberg [26] on the antiferromagnet $CoCl \cdot 6H_2O$. These workers find that as one approaches T_c from above (+) or from below (−) that the specific heat appears to diverge like

$$\left(\frac{C_p(T)}{R}\right)^{\pm}_{H=0} = -a \ln \left| 1 - \frac{T}{T_c} \right| + \Delta_{\pm}. \tag{13}$$

This behavior begins when $(T - T_c)/T_c$ is of the order of a few percent. However, in the immediate vicinity of T_c ($(T - T_c)/T_c \sim -5 \times 10^{-3}$ and $+1 \times 10^{-3}$) this divergence does not continue. Presumably this is due to the presence of crystal strains and the resulting coexistence of the antiferromagnetic and paramagnetic phases.

TABLE 3. *Experimental and theoretical values of parameters describing the shape of the critical isotherm for a ferromagnet*

Ferromagnet	δ	Reference
Ni	4.22±0.04	19
Gd	4	21
Theory		
Molecular field	3.0	
Ising	5.2 ±0.15	2

TABLE 4. *Experimental and theoretical values of parameters describing the shape of the critical isotherm for a fluid*

Fluid	δ	References
CO_2, H_2, Xe	4.2±0.1	2, 23, 24
Theory		
van der Waals	3.0	
Ising	5.2±0.15	2

In addition, Yamomoto, et al. [27] have recently surveyed the literature for specific heat measurements on magnetic systems. They fit the experimental data to a logarithmic divergence of the form of eq (13), and present a table listing the resulting values of a and $(\Delta_+ - \Delta_-)$ for 28 ferromagnetic and antiferromagnetic elements and compounds.

It may be well to stress that while the data does show that C_p does get large very slowly as $T \to T_c$ the range over which the logarithmic dependence applies is $\sim 5 \times 10^{-3} < (T - T_c)/T_c \lesssim 5 \times 10^{-2}$. Measurements examining the question of continuance of the logarithmic divergence closer to the critical point are needed. Along these same lines it should be pointed out that what is measured experimentally is C_p and what is calculated theoretically is C_v. The difference is proportional to α^2/β_T where α is the thermal expansion and β_T

the isothermal compressibility. It is known that the thermal expansion increases markedly as $T \to T_c$, but accurate data is not now available giving the precise behavior of $\alpha(T)$ and $\beta(T)$. In view of the slow divergence of C_p it is particularly necessary to determine the importance of the $C_p - C_v$ correction term before reaching conclusions about the precise mathematical nature of the divergence of C_v.

In the case of the fluid, while the van der Waals theory predicts no divergence in C_v as $T \to T_c$, the experimental data has indicated [23] that C_v along the critical isochore grows very large as $T \to T_c$. Recently the work of Voronel and his coworkers [28, 29] has shown that the specific heat at constant volume in argon and oxygen apparently diverges logarithmically as $T \to T_c$. The data of these workers has recently been very carefully examined and discussed in the light of the best present theoretical information [30, 31].

Conclusions

Since 1961–1962 a considerable amount of experimental data on the equilibrium properties of magnetic systems has been obtained. The behavior of each of these properties in the critical region is in striking and clear-cut disagreement with the predictions of the "classical" molecular field theories of ferromagnetism. The development of the method of Pade approximants, in combination with the high temperature expansions of the partition functions have enabled calculations of the equilibrium properties of the ferromagnet using the Ising Hamiltonian. The results of such calculations are closer to the data than the "classical" theories, however, by and large the experimental results indicate that the Ising model is inadequate to describe a real ferromagnet. The Heisenberg Hamiltonian has been used successfully to calculate the divergence of the susceptibility and the results are in very good agreement with the experiment.

At this point in the development of the subject certain directions for the future work seem clear. On the experimental side there is a need for much more information particularly on the shape of the critical isotherm, the specific heat, the thermal expansion, and the susceptibility below T_c. Also, we have to have more data on the localized spin systems rather than the ferromagnetic metals. In the insulators we may expect that the Heisenberg Hamiltonian will apply, while the appropriate Hamiltonian for the metals is not known. Also, it would be most desirable to measure several equilibrium properties on a single ferromagnet.

On the theoretical side, the clear need is a calculation of the magnetization, the critical isotherm, the susceptibility below T_c and the specific heat using the Heisenberg Hamiltonian. And finally, the close analogy between the fluid and the ferromagnet, combined with the clear breakdown of the conventional expansions of the free energy in a power series around T_c suggest that the behavior of three-dimensional ferromagnets and fluids near the critical point may be a result of some very general property connected with the ordering and is relatively independent of the details of the Hamiltonian of the system.

References

[1] M. E. Fisher, J. Math. Phys. **5**, 944 (1964).
[2] D. Gaunt, M. E. Fisher, M. Sykes, and J. W. Essam, Phys. Rev. Letters **13**, 713 (1964).
[3] P. Heller and G. B. Benedek, Phys. Rev. Letters **8**, 428 (1962).
[4] P. Heller and G. B. Benedek, Phys. Rev. Letters **14**, 71 (1965).
[5] J. W. Essam and M. E. Fisher, J. Chem. Phys. **38**, 802 (1963).
[6] H. Callen and E. Callen, Conference on Magnetism, J. Appl. Phys. (1965), in press.
[7] M. A. Weinberger and Schneider, Can. J. Chem. **30**, 4222 (1952).
[8] L. D. Landau and Lifshitz, Statistical Physics (Addison-Wesley, 1958).
[9] C. Domb and M. F. Sykes, J. Math. Phys. **2**, 63 (1961).
[10] C. Domb and M. F. Sykes, Phys. Rev. **128**, 168 (1961).
[11] G. A. Baker, Jr., Phys. Rev. **124**, 168 (1961).
[12] G. A. Baker, Jr., Phys. Rev. **129**, 99 (1962).
[13] J. Gammel, W. Marshall and L. Morgan, Proc. Roy. Soc. (London), **A275** (1963).
[14] G. A. Baker, Jr., Phys. Rev. **136**, A1376 (1964).
[15] B. Jacrot, J. Konstantinovic, G. Parette, and D. Cribier, Symposium on Inelastic Scattering of Neutrons in Solids and Liquids, Chalk River (1962). (See also reference 13.)
[16] J. E. Noakes and A. Arrott, J. Appl. Phys. **35**, 931 (1964).
[17] S. Arajs and P. S. Miller, J. Appl. Phys. **31**, 986 (1960).
[18] S. Arajs, Conference on Magnetism and Magnetic Materials, J. Appl. Phys. (1965), in press.
[19] J. Kouvel and M. E. Fisher, Phys. Rev. **136**, A1626 (1964).
[20] P. Weiss and R. Forrer, Ann. Phys. (Paris), **5**, 153 (1926).
[21] G. D. Graham, Jr., Conference on Magnetism and Magnetic Materials, J. Appl. Phys. (1964), in press.
[22] H. Habgood and W. Schneider, Can. J. Chem. **32**, 98 (1954).
[23] J. S. Rowlinson, Liquids and Liquid Mixtures, ch. 3, pp. 93ff. (Butterworth's (London), 1959).
[24] B. Widom and O. K. Rice, J. Chem. Phys **23**, 1250 (1955).
[25] L. Onsager, Phys. Rev. **65**, 117 (1944).
[26] J. Skalyo, Jr. and S. A. Friedberg, Phys. Rev. Letters **13**, 133 (1964).
[27] T. Yamamoto, H. Matsuda, O. Tanimoto, and Y. Yasuda, Department of Chemistry, Kyoto University, Kyoto, Japan. (See Proceedings of Conference on Critical Phenomena, Washington, 1965.)
[28] M. Bagatskii, A. Voronel, and V. Gusak, Soviet Phys. JETP **43**, 728 (1962).
[29] A. Voronel, Y. Chashkin, V. Popov, and V. Sinkin, Soviet Phys. JETP **45**, 828 (1963).
[30] M. E. Fisher, Phys. Rev. **136**, A1599 (1964).
[31] C. N. Yang and C. P. Yang, Phys. Rev. Letters **13**, 303 (1964).

Experimental Studies of Magnetic Ising Systems Near the Critical Point*

W. P. Wolf

Yale University, New Haven, Conn.

The Ising model has long been used as a convenient approximation for the investigation of magnetic order-disorder transistions, but until recently no real magnetic substances were known in which the assumptions of the model coincided with reality. The advent of many new rare earth compounds has changed this position. There are now compounds in which it is an excellent approximation to treat the magnetic ions as effective spins $s'=1/2$, whose magnetic moments $\mu=g\cdot s'$ are constrained to one direction by an extremely anisotropic g tensor [1]. A simple material of this kind is dysprosium aluminum garnet (DAG) which orders antiferromagnetically at about 2.5 °K. The properties of DAG in the critical region have been investigated by a number of workers over the past three years [2–9].

The principal difference between such a material and the Ising model lies in the importance of long range magnetic dipole forces, which account for a major fraction of the total interactions. Dipolar forces lead to a shape dependence of all the magnetic properties (even the "zero field" susceptibility) and at present there is no theory better than the molecular field to allow for these effects. With a molecular field calculated from suitable lattice sums, it is possible to remove most of the long range effects, and to reduce measured magnetic properties to those corresponding approximately to a material with nearest neighbor forces only [7]. This has been done for the susceptibility of DAG in the region of the critical point. It was found that the results could be fitted to law of the form predicted by the Ising model theory [10]:

$$\chi T=\lambda[\xi_c-B_{\pm}\cdot(1-T/T_c)\log|1-T/T_c|],$$

with λ equal to the known Curie constant, 10.35/mol and ξ_c, B_+, and B_- respectively 0.565, 0.30, and 0.80. $T_c=2.493$ °K is critical (Néel) temperature in zero field. The values for ξ_c, B_+, and B_- are not strictly comparable with those given by any of the theoretical estimates since none of these have considered the garnet structure explicitly, but it is interesting to note that the ratio $B_-:B_+$ is close to the value 3 found for other three dimensional structures.

The "reduced" susceptibility measurements have also been used to compare Fisher's predicted relation for the specific heat [11], $C=A\frac{\partial}{\partial T}(\chi T)$, with the observed values [7]. (A is a slowly varying function of temperature whose value at T_c can be estimated from other measurements.) Excellent agreement was found over a range of temperatures $0.5\ T_c<T<1.5\ T_c$.

Critical effects at temperatures below T_c have also been investigated as a function of magnetic field [4]. The most striking result is that the transition from the antiferromagnetic state to the paramagnetic state seems to be first order for $T<\sim 0.6\ T_c$ and higher order for $\sim 0.6\ T_c<T<T_c$ [12]. A first order transition is not predicted by any of the simple Ising models at any finite temperature, and it is probably a result of the long range interactions.

Accompanying the change from antiferromagnetic to paramagnetic order in an applied field there are magneto-caloric effects and these have been studied by measuring adiabatic changes of temperature with field [13]. In contrast to the isothermal transitions, which are completely reversible, the adiabatic changes showed a large and as yet unexplained hysteresis.

Although most of the critical point measurements on Ising-like systems have so far been concentrated on dysprosium aluminum garnet, there is reason to believe that other rare earth compounds will be found which also approximate to an Ising model [14]. It seems rather certain that almost all materials of this kind will only order at low temperatures, where long-range magnetic dipole interactions are important, and it would therefore be very helpful

*This work was supported in part by the U.S. Atomic Energy Commission. A full account will be published at a later time.

if critical point theories could be extended to include these effects. Magnetic dipole forces are of course present also in all other materials, and as a matter of principle their effect should be considered even for materials in which exchange interactions are dominant.

It is a pleasure to acknowledge a number of stimulating discussions with Professor Michael E. Fisher. I should also like to thank Dr. A. F. G. Wyatt, Dr. B. Schneider, Dr. B. E. Keen and Mr. D. Landau for making available to me the results of their experiments prior to publication.

References

[1] See for example W. P. Wolf, M. Ball, M. T. Hutchings, M. J. M. Leask, and A. F. G. Wyatt, J. Phys. Soc. Japan **17**, Suppl. B–1, 443 (1962).
[2] M. Ball, M. T. Hutchings, M. J. M. Leask, and W. P. Wolf, Proc. 8th Int. Conf. on Low Temperature Physics, p. 248 (Butterworth, London, 1963).
[3] M. Ball, M. J M. Leask, W. P. Wolf, and A. F. G. Wyatt, J. Appl. Phys. **34**, 1104 (1963).
[4] M. Ball, W. P. Wolf, and A. F. G. Wyatt, Physics Letters **10**, 7 (1964).
[5] A. F. G. Wyatt, Thesis, Oxford University, 1963.
[6] A. Herpin and P. Mériel, C. R. Acad. Sc. Paris **259**, 2416 (1964).
[7] W. P. Wolf, and A. F. G. Wyatt, Phys. Rev. Letters **13**, 368 (1964).
[8] J. M. Hastings, L. M. Corliss, and C. G. Windsor, Phys. Rev. **138**, A176 (1965).
[9] A. H. Cooke, K. A. Gehring, M. J. M. Leask, D. Smith, and H. M. Thornley, Phys. Rev. Letters **14**, 685 (1965).
[10] See for example M. E. Fisher, and M. Sykes, Physica **28**, 939 (1962).
[11] M. E. Fisher, Phil. Mag. **7**, 1731 (1962).
[12] The temperature at which the transition changes from being first order has recently been determined with greater accuracy at $(0.65 \pm 0.02)T_c$ by B. Schneider and W. P. Wolf (to be published). Above $0.65T_c$ it is apparently higher than second order.
[13] B. E. Keen, D. Landau and W. P. Wolf (to be published).
[14] Substances already known to have Ising-like magnetic properties include several rare earth ethyl sulphates (A. H. Cooke, D. T. Edmonds, C. B. P. Finn, and W. P. Wolf, J. Phys. Soc. Japan **17**, Suppl. B–1, 481 (1962)) and a number of the anhydrous rare earth chlorides (J. C. Eisenstein, R. P. Hudson, and B. W. Mangum, Phys. Rev. **137**, A1886 (1965). However all these materials order at such low temperatures that it has not yet been possible to investigate their critical properties in any detail.

Specific Heats of Ferro- and Antiferromagnets in the Critical Region*

D. T. Teaney

IBM Watson Research Center, Yorktown Heights, N.Y.

1. Introduction

In this paper we shall describe for the first time the results of high resolution specific heat measurements of two classical magnetic systems: a ferromagnetic insulator, EuO, and an antiferromagnetic insulator, MnF_2. For completeness we shall also review the earlier results of Friedberg and Skalyo [1] on $CoCl_2 \cdot 6H_2O$, a rather different kind of antiferromagnet. A logarithmic form of the specific heat is found in all cases, the experimental results being the most clear in the case of MnF_2. The problem of separating lattice and magnetic specific heats will be discussed, and a number of other hazards will be described. The prospects of even more refined experiments are examined and found to be encouraging.

2. Choice of Material and the Lattice Subtraction Problem

The heat capacity of a typical magnetic system is shown in figure 1. The anomaly at the Curie point of EuO [2] (69 °K) is clearly displayed on top of the lattice specific heat, which is of about the same magnitude. From the figure it seems that EuS [3] would be a better case to study, but sufficiently large single crystals are not yet available. But the choice of material goes beyond the availability of crystals.

*Work supported in part by the USAFOSR of the Office of Aerospace Research under Contract AF 49(638)–1379 and Contract AF 49(638)–1230.

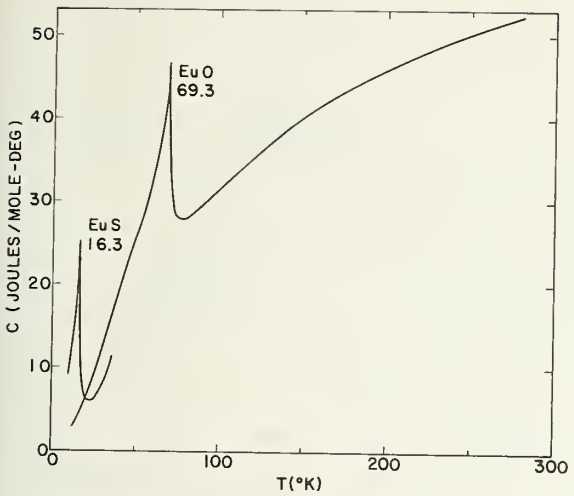

FIGURE 1. *The specific heat of* EuO *and* EuS.

At least for a start, it is desirable to study critical point phenomena in simple systems which are characterized by a clearly dominant strong interaction. In the case of a magnetic system this means we want an exchange interaction that is large compared to dipolar or crystal field effects. From this point of view the lattice becomes an inevitable complication and we now discuss briefly what can be done about it.

Fortunately the problem has been investigated in detail for the case of MnF_2 by Stout and Catalano [4] and by Hofman, Paskin, Tauer, and Weiss [5]. Stout and Catalano use a corresponding state method to deduce the lattice heat capacity of MnF_2 from that of isomorphous ZnF_2. Hofman et al., use a method of matching two Debye entropy functions to the experimental entropy of MnF_2 at high temperatures, having first subtracted an amount $R \ln (2S+1)$. That is, they find that for two Debye temperatures, $\theta = 220$ °K and $\theta' = 575$ °K.

$$S_{MnF2}(T) - R \ln 6 \cong S_D(\theta/T) + 2S_D(\theta'/T)$$

for temperatures above $\sim 2T_N$. This procedure when applied to ZnF_2 gives a two parameter Debye curve that fits the observed specific heat to within 1/2 percent in the temperature range 35 to 250 °K. The results obtained by the two methods are in excellent agreement.

It is important to stress that the apparent character of the singularity depends only weakly on the slope of the lattice background: changing this slope by a factor of two produces only faintly perceptible kinks in the highest $|\Delta T|$ data presented here. The apparent magnitude of the magnetic specific heat, that is, the value of B, is more directly influenced by the lattice subtraction, but in view of the extensive work by the above authors it seems unlikely that an error larger than 10 percent is introduced in the MnF_2 results by incorrect lattice subtraction.

In the case of EuO our results are only tentative. The diamagnetic isomorphs CaO and BaO are extremely hygroscopic, and we have not been able to make specific heat measurements on reliably dry samples, nor can we find reference to these measurements in the literature. The curve fitting method of Hofman et al., must then be relied upon, and it is here we wish to interject a word of caution.

In order to obtain the entropy from the measured specific heat the usual conversion

$$c_v = c_p(1 - Ac_pT)$$

is required, where the Nernst-Lindeman coefficient

$$A = \frac{\beta^2}{k\rho c_p^2}$$

is assumed to be temperature independent. The value of this coefficient strongly affects the estimate of lattice background since this estimate is based only on high temperature data. (Clearly, accurate specific heat data is also essential.) The choice of thetas is strongly influenced by the slope of the entropy curve because at high temperatures the Debye functions are becoming independent of the thetas. Since remarkably little expansivity or compressibility data exists for compounds it would be hazardous to guess a value for A, and we believe recourse to experiment is necessary. We are grateful to Professor R. Stevenson of McGill University for providing us with compressibility data prior to publication. We have obtained the expansivity from our own x-ray diffraction study [6]. The experimental value for A for EuO, accurate to about 20 percent, is found to be 7×10^{-6}. For comparison, the value for MgO is 1×10^{-6}. Tentative theta values of 175 and 560 give fair fits to the entropy above 150 °K, and the full scale numerical fitting program will be completed shortly. Again we emphasize that the uncertainties in lattice subtraction have very little effect on the apparent *form* of the specific heat in the critical region. The *magni-*

tude of the magnetic specific heat is, of course, very sensitive to the lattice subtraction, and we refrain from quoting a number for this magnitude until a detailed numerical analysis has been completed.

3. Experimental Technique

We use the standard discontinous heating method in these experiments. The sample is surrounded by a radiation shield the temperature of which could be held constant to about 1 mdeg by referencing a platinum thermometer against a Mueller bridge. Sample and shield are inside a vacuum jacket surrounded by double Dewars of liquid nitrogen. The temperature of the sample is monitored by a thermister of the type used to sense the level of liquid nitrogen [7]. The thermister comprises one arm of a constant amplitude 100 c/s resistance bridge stable to 1 part in 10^7. The overall sensitivity was limited to about 30×10^{-6} °K by Johnson noise of the bridge detector. The thermister is calibrated *in situ* against the platinum thermometer on the shield, equilibrium to within 5×10^{-4} °K being accomplished by condensing liquid nitrogen into the vacuum chamber. The platinum thermometer is calibrated against the vapor pressure of the condensed pure nitrogen, and the less than ideal arrangement for this part of the calibration is the cause of the relatively large systematic uncertainties quoted below. The function $Z_{63}^{77}(T)$ is used for interpolation [8]. Our apparatus records drift rate and heating interval data directly on punched cards, and all the data analysis including addendum corrections and lattice subtraction is done in a minute or two of computer time [9].

The importance of single crystal calorimetry is indicated in figure 2. The powder results are shown as the solid and dashed histograms, the width of the horizontal steps being equal to the heating interval. The single crystal results are shown by the circles. The rounding of the powder results is not a consequence of temperature gradients since the calorimeter is fairly small (25 cm^3), the monitoring power is only 10 μW, the drift rates are on the order of 1 mdeg per hour, and the calorimeter response time is about 3 min as compared with an overall discontinuous heating rate of 100 mdeg per hour. While a similar experiment with the same calorimeter loaded with a powder sample, the antiferromagnet $RbMnF_3$ ($T_N = 83$ °K), produced similar

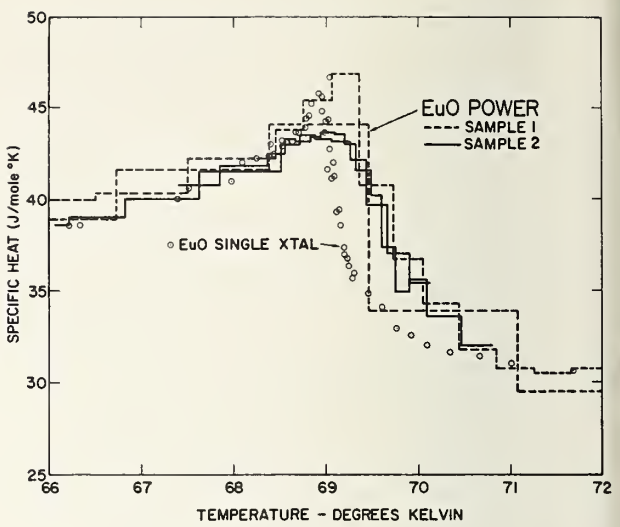

FIGURE 2. *Comparison of specific heat data of two powder samples (histograms) with the single crystal (circles) of* EuO.

results, we believe that this indicates a similarity in the rounding of the transition in two different powder samples and not the presence of some unaccountable systematic temperature gradient.

4. Transition Rounding

While it may not be surprising to find a smearing out of the critical point in a powder sample, we have two further remarks about transition rounding. (We feel that "transition truncation" is an expression to be avoided.) The first is an inference as to the effect of impurities on single crystals. The position of the transition in the EuO crystal is noticeably on the low side of the distribution indicated by the powder histogram. This crystal (1.7 g) contained filamentary inclusions of tantalum metal, amounting to as much as 2.0 percent by volume, which were observed by microscopic examination of the polished surfaces. The rounding of the transition which is suggested in figure 2 and is distressingly evident in figure 3 may well be correlated with this impurity. A new method of growing crystals has been found to avoid this problem, and hopefully we will have more to say on this point in the future.

The second remark on transition rounding is concerned with our results on MnF_2. These experiments were performed on two single crystals. One crystal (0.02 mole, closed circles in fig. 4) of Bell Telephone Laboratories origin, was obtained from Heller and Benedek and is the same one used by

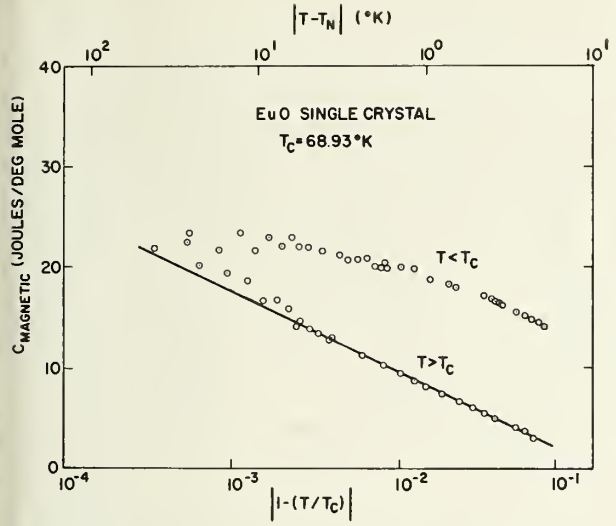

FIGURE 3. *Logarithmic plot of the magnetic specific heat of the* EuO *crystal.*

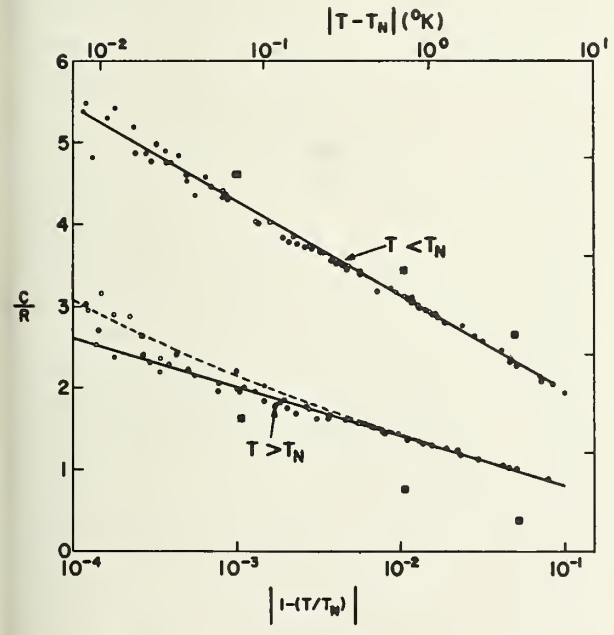

FIGURE 4. *Logarithmic plot of the magnetic specific heat of* MnF_2 *near the Néel temperature.*

Open circles, IBM crystal; closed circles, Heller and Benedek crystal. The closed squares are the specific heat density of argon. The dashed curve is for $\alpha=0.1$.

them in their classic NMR experiments [10]. The other crystal (0.06 mole, open circles) was "on the shelf" at our laboratory and is of lost commercial pedigree. The character of the singularity is seen to be identical in both crystals, but we found a significant difference in Néel temperatures. The Heller and Benedek crystal had $T_N=(67.33\pm0.01)$ °K in agreement with their result, while the IBM crystal had $T_N=(67.23\pm0.02)$ °K. (The error limits represent confidence in the absolute calibration of the thermometers in each of the two runs.) The difference is well outside experimental error and also well outside combined uncertainties in locating T_N. The discovery of such a large difference between two high quality crystals is remarkable. The transition in both crystals was sharper than our experimental resolution of about 10 mdeg K, and we are therefore unable to comment on the rounding which Heller found to amount to about 15 mdeg. The difference in Néel temperatures between the two crystals is not so large as the difference in Curie temperatures between the EuO crystal and the "best" powder, so that the suggestion made above about correlation between rounding and depression of the critical point need not be invalidated.

5. Results for EuO and MnF_2

We turn now to the results themselves. The EuO data is shown in figure 3. The rounding is much more pronounced on the low side of the transition (cf. fig. 6). The Curie temperature was taken as the apparent vertical tangent as seen on a linear plot of the data on the high temperature side. This tangent was apparent to an accuracy of 10 or 20 mdeg, so that the linearity of the high temperature data is not the result of choosing a fortuitous T_c within the range of the rounding. The slope of the logarithmic divergence for $T > T_c$ is given in table 1. We recall that EuO is a rock salt structure and that the dominant exchange interaction is between nearest neighbor Eu^{++} ions [11]. The appropriate coordination number is therefore 12. The coefficient A_+ for this crystal of EuO is seen to be noticeably larger than that for MnF_2 for which the coordination number is 8. Such a large difference is not expected theoretically; the somewhat disappointing character of this data may be, however, license for not taking it too seriously.

The experimental results for MnF_2 are shown by the open and closed circles in figure 4. A logarithmic form of divergence is clearly indicated over about three decades from 10^{-4} to 10^{-1} T_N. The striking resemblance to the configurational specific heat density of argon in the same region is shown by the closed squares which are taken from Fisher's analysis [12] of the results of Voronel' and coworkers [13]. Our data covers almost an additional decade in $|\Delta T/T_N|$ and has a rather better signal-to-noise

TABLE 1. *Logarithmic parameters for magnetic and configurational specific heats*

The specific heat is in units of R and the logarithm is to the base 10.

	EuO	MnF_2	Argon[2]	Lattice gas[2]	$CoCl_2 \cdot 6H_2O$[1]
A_-	1.	1.15	1.15	1.1	(0.27)
A_+		0.6	(0.5)	0.5	0.27
A_-/A_+		2.0	(2.3)	2.3	(1.0)
B_-		0.82	1.16	0.1	0.56
B_+		.14	(−0.3)	−.3	−.015

ratio than the argon results. The parameters that result from fitting the data with a logarithmic divergence of the form $C_\pm/R = A_\pm|\log_{10}|\Delta T/T_N| + B_\pm$ are summarized in table 1. Comparison is made with the argon experimental results and with the theoretical estimates for a lattice gas. In reference 12 the results of various approximations are listed along with detailed references to their origins. We have tabulated here only rounded values. It is clear that while the present experiments reveal the character of the singularity, the signal-to-noise ratio is not good enough to warrant a discussion of the theoretically rather small effects of lattice structure.

It is important to consider the possibility of a stronger than logarithmic singularity, particularly on the high temperature side. For purposes of comparison a divergence of the form $C_+ = A|\Delta T/T_N|^{-\alpha}$ with $\alpha = 0.1$ is plotted as the dashed curve in figure 4. Deviation of the experimental points from the logarithmic straight line, i.e., that for which $\alpha = 0$, is seen to be not inconsistent with a small positive α. Notice that shifting T_N down by 5 mdeg would improve the linear fit for $T < T_N$ but increase the upward trend of the points for $T > T_N$. The assignment of some definite value to α would place unjustified weight on the noisiest experimental points, those closest to T_N. We feel that these data can only be said to suggest that $0 \leq \alpha < 0.1$. Subject to the physical reservations expressed in sec. 7, a much better value of α is not inaccessible to experiment. Although complicated behavior and/or rounding of the transition might be expected in the next decade closer to T_N, improved precision in the present range would allow us to set improved limits on α.

6. Results for $CoCl_2 \cdot 6H_2O$

We turn now from our work on three dimensional Heisenberg-like systems to the work of Friedberg and coworkers on $CoCl_2 \cdot 6H_2O$, which has a transition temperature of 2.29 °K. Since detailed account of this work has been published elsewhere [1, 14] we mention here only the results of specific heat measurements, which are shown in figures 5 and 6 and in table 1. The principal point established is that this salt resembles a two-dimensional Ising antiferromagnet. Now that we have results on a three-dimensional antiferromagnet this resemblance becomes all the more impressive.

$CoCl_2 \cdot 6H_2O$ forms a layer lattice with the spins at Co^{++} arranged in planar tetragonal nets. The structure and exchange interactions in $CoCl_2 \cdot 6H_2O$ have been described by Shinoda et al., [15]. The Co^{++} form a tetragonal net, the plane of which also contains the Cl^-. The exchange interaction in the plane is $J/k = 2.03$ °K while that between planes, which are separated by waters, is found to be $J'/k = 0.39$ °K. Shinoda et al., obtained these results by careful theoretical analysis [16, 17] of the high temperature heat capacity tail as measured earlier [18]. (They have also analyzed their own results for $CoCl_2 \cdot 2H_2O$ ($T_N = 17.20$ °K) and find it to be a chain structure; the resolution of their experimental results is unfortunately such that they can only be said to indicate a logarithmic singularity.) In addition to the sheet-like structure of $CoCl_2 \cdot 6H_2O$, there are two other reasons to suggest its similarity to the Ising model. First, the effective spin of the Co^{++} is $S = 1/2$ at these temperatures and the moment is highly anisotropic. Sec-

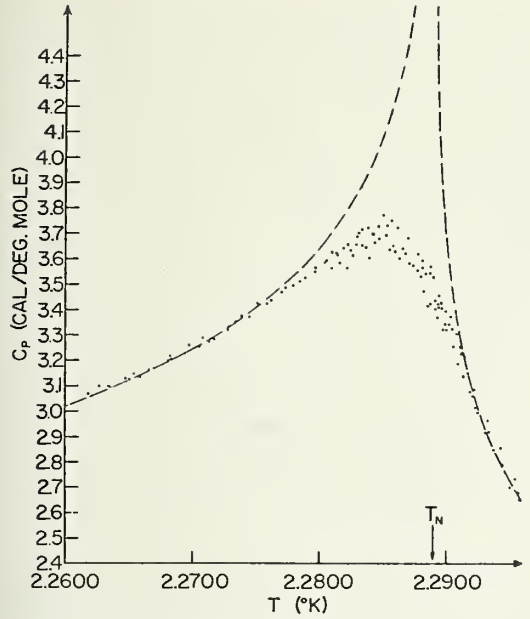

FIGURE 5. *The specific heat of* $CoCl_2 \cdot 6H_2O$ *after Skalyo and Friedberg.*

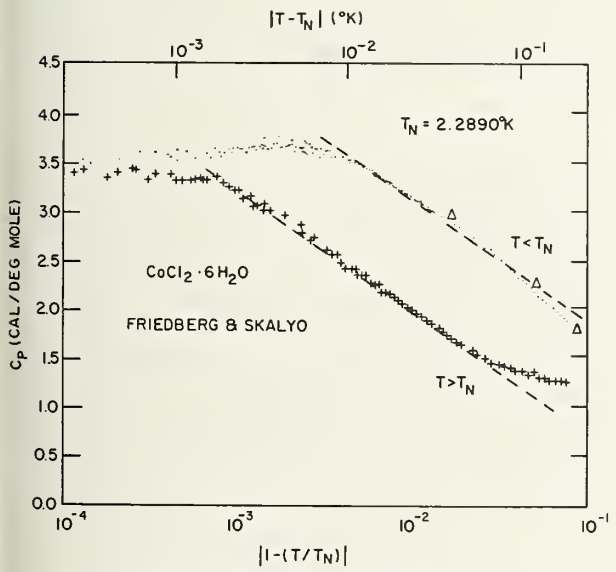

FIGURE 6. *Logarithmic plot of the specific heat of* $CoCl_2 \cdot 6H_2O$. Note that the horizontal scale is the same for all three logarithmic plots.

ond, the earlier c_p data [18] reveal a spin entropy gain of very nearly (1/2) R log $(2S+1)$ above the Néel temperature.

The critical point specific heat measurements, made on large aggregate specimens of single crystals, are difficult to interpret due to the fairly severe rounding. T_N is chosen in such a way as to produce a symmetric logarithmic singularity as is expected in two-dimensions [16, 19]. The magnitude of the logarithmic coefficient is comparable with the values calculated for the two-dimensional Ising model, and can even be gotten quantitatively by a suitable choice of anisotropy. While the data fall on a straight line above T_N for about 1.5 decades, not a great deal of confidence may be derived from the data below T_N. However, the specific heat results are strongly supported by their comparison with magnetic susceptibility measurements [14]. Good confirmation of the theoretical relation, [20] $C \simeq A\partial(\chi_{\|}T)/\partial T$, is found for experimental points in a range of $\pm 0.1\ T_N$. A good case is thus made for believing that outside of the complicated, rounded region, the actual specimens measured approximate rather well the behavior of an ideal crystal.

7. Lattice Stability

We have not mentioned in the discussion above the problem of lattice stability at the critical point, since there was no evidence of its being relevant to the experiments reported. Clearly, if the magnetic transition is accompanied by a crystallographic transition or even a lattice parameter anomaly the rigid lattice approximation no longer applies and the interpretation of experimental results becomes complicated. This problem has been considered in three dimensions by Bean and Rodbell [21] using the molecular field approximation, and more recently Garland and Renard [22] have studied the two-dimensional Ising model. It is not surprising that in the presence of a strain dependent exchange interaction the magnetic transition may become first-order unless the lattice is "clamped." Extensive experiments [23] on MnAs have demonstrated these effects, and Wangsness [24] pointed out the evidence for structure change in MnO on the basis of specific heat data. In the case of MnF_2, the c-axis undergoes a pronounced anomaly which has been carefully studied by Gibbon [25]. It has been pointed out [26] that this anomaly could lead to a first-order transition, and that, furthermore, the existence of this sort of incipient first-order transition could complicate the interpretation of a more rapid than logarithmic divergence, particularly for temperatures very close to T_N.

As an example of what can happen we would like to present some results of a perovskite antiferromagnet, $KMnF_3$. The temperature variation of the lattice parameters is shown in figure 7, and the specific heat [27] in the same range is shown in

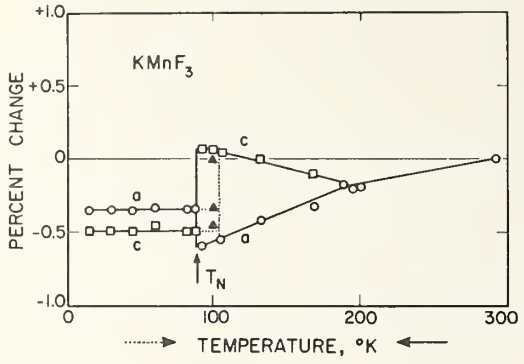

FIGURE 7. *Lattice parameters of* $KMnF_3$ *after O. Beckman and K. Knox, Phys. Rev.* **121**, *376 (1961).*

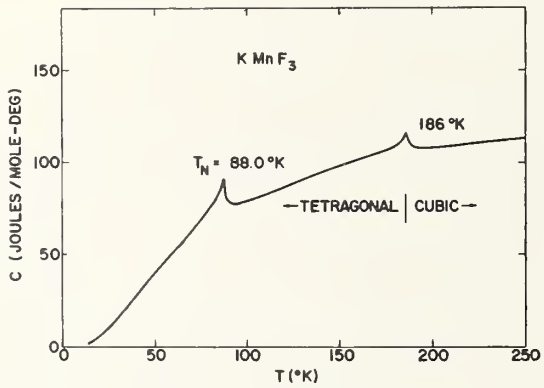

FIGURE 8. *The specific heat of* $KMnF_3$.

figure 8. The instability of this crystal is presumably due to a consequence of the low Goldschmit tolerance factor ($t = 0.94$). The situation may be described as follows: the pseudocubic unit cell is made up of Mn^{++} on the corners and F^- on the edges. The size of the cell is dominated by the Mn-F-Mn bonding, and the K^+ fits rather loosely in its position at the body center. This "looseness" has been invoked to explain the anomalously low thermal conductivity of $KMnF_3$ [28]. A qualitative investigation of the specific heat of a powder sample near the Néel temperature is shown in figure 9. It seems remarkable that the character of the nucleation on warming and cooling would be so clearly displayed in a powder sample. The much larger lattice parameter hysteresis was observed in the x-ray study of a tiny single crystal. In contrast to the x-ray and specific heat results, however, a careful study of the antiferromagnetic resonance near T_N produced no evidence of hysteresis larger than

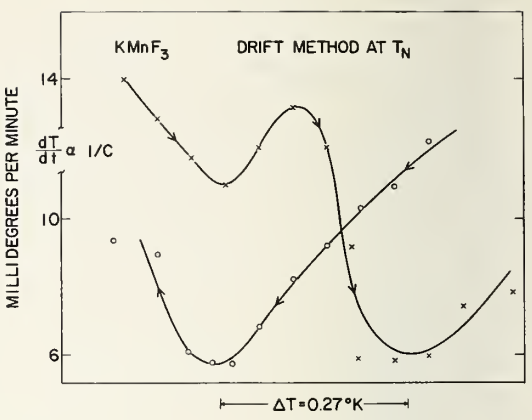

FIGURE 9. *Qualitative measurement of the specific heat of powder sample of* $KMnF_3$ *near* T_N.

about 0.05 °K [29]. Furthermore, no hysteresis was observed in neutron scattering experiments performed under conditions of even higher resolution [30]. Perhaps the fact that there is no anomaly in cell volume accounts for the apparent stability of the magnetic transition. It is tempting to identify the lower specific heat peak with the Néel temperature, but we lack the absolute accuracy necessary to make such an identification positively.

For EuO, the hardness of this material, especially in comparison with the fluorides, makes questions of stability less important. No structure change at low temperatures was found using standard powder x-ray techniques, [6] and Dillon [31] observes cubic anisotropy in ferromagnetic resonance. Since the rock salt structure is stable for the whole set of europium chalcogenides we would hardly expect any structure change; the hardness argument should therefore be adequate assurance that first-order effects will be small.

8. Conclusion

We have shown that an antiferromagnet makes a good gas—perhaps even better than argon. A logarithmic divergence of the specific heat is clearly found on both sides of the Néel temperature of MnF_2, while the possibility of a more rapid divergence on the high temperature side cannot be excluded. The specific heat of the ferromagnetic insulator EuO, though rounded from below, shows logarithmic divergence on the high side of the Curie temperature. We have reviewed the work of Friedberg and collaborators on $CoCl_2 \cdot 6H_2O$ which makes

a convincing case for the resemblance of the magnetic ordering of this crystal to the two-dimensional Ising model of antiferromagnetism. The experimental results reported are thus in substantial agreement with existing theory.

It is worthwhile to comment briefly on what is yet to be done experimentally on the specific heat of magnetic systems in the critical region. Clearly better results should be obtained on EuO because of the ideal nature of this material; these results should also be extended to include finite applied fields. A ferromagnetic metal should be studied. Nickel would be a good case because of the amount already known about it, but because the difficulties of specific heat measurements above about 20 °K increase with at least the third power of temperature, a more likely candidate may be found among the rare earth metals. As for antiferromagnets, MnF_2 should be measured more accurately and better limits put on α. Another ideal antiferromagnet is available for study, $RbMnF_3$. This perovskite structure remains simple cubic at low temperatures so that it is unlikely that lattice stability will be a problem. Good results for this system will give some insight into the problem of coordination number as well as contribute to the general validity of the experimental conclusions.

We are grateful for the stimulating and enlightening discussion with P. Heller, G. Benedek, M. Fisher, T. Yamamoto, and R. Nathans. The expert preparation of material by M. Shafer and C. Guerci have made it possible to study EuO. The encouragement of J. S. Smart and the collaboration of V. L. Moruzzi are greatly appreciated. The technical assistance of J. S. Leddy has made it possible to concentrate on these experiments, and the programming talents of Miss E. Bergonzi have been indispensible.

9. References

[1] J. Skalyo, Jr., and S. A. Friedberg, Phys. Rev. Letters **13**, 133 (1964).
[2] C. F. Guerci, V. L. Moruzzi and D. T. Teaney, Bull. Am. Phys. Soc. II, **9**, 225 (1964).
[3] V. L. Moruzzi and D. T. Teaney, Solid State Comm. **1**, 127 (1963).
[4] J. W. Stout and E. Catalano, J. Chem. Phys. **23**, 2013 (1955).
[5] J. A. Hofman. A. Paskin, K. J. Tauer and R. J. Weiss. J. Chem. Phys. Solids **1**, 45 (1956).
[6] D. T. Teaney, V. L. Moruzzi and J. E. Weidenborner, to be published.
[7] We are indebted to Dr. H. B. Sachse of the Keystone Carbon Company for samples of these thermisters and advice on their characteristics.
[8] J. M. Los and J. A. Morrison, Canadian J. Phys. **29**, 142 (1951).
[9] The computer program, expressly written to cover a wide range of laboratory circumstances, is available to interested experimenters.
[10] P. Heller and G. Benedek, Phys. Rev. Letters **8**, 428 (1962).
[11] B. A. Calhoun and J. Overmeyer, J. Appl. Phys. **35**, 989 (1964).
[12] M. E. Fisher, Phys. Rev. **136**, A1599 (1964).
[13] M. I. Bagatskii, A. V. Voronel, and B. G. Guzak, Zh Eksperim i Theor. Fiz. **43**, 728 (1962); English translation, Soviet Phys. JETP **16**, 517 (1963).
[14] J. Skalyo, A. F. Cohen and S. A. Friedberg, Proceedings of the Ninth International Conference on Low Temperature Physics, Columbus, Ohio, 1964.
[15] T. Shinoda, H. Chihara and S. Seki, J. Phys. Soc. Japan **19**, 1637 (1964).
[16] L. Onsager, Phys. Rev. **65**, 117 (1944).
[17] A. J. Wakefield, Proc. Cambridge Phil. Soc. **47**, 419, 799 (1951).
[18] W. K. Robinson and S. A. Friedberg, Phys. Rev. **117**, 402 (1960).
[19] See, for example: M. E. Fisher, J. Math. Phys. **4**, 278 (1963)
[20] M. E. Fisher, Phil. Mag. **7**, 1731 (1962).
[21] C. P. Bean and D. S. Rodbell, Phys. Rev. **126**, 104 (1962).
[22] C. W. Garland and R. Renard, to be published.
[23] R. W. De Blois and D. S. Rodbell, Phys. Rev. **130**, 1347 (1963).
[24] R. K. Wangsness, Science **116**, 537 (1952).
[25] D. F. Gibbons, Phys. Rev. **115**, 1194 (1959).
[26] P. Heller, G. Benedek, and T. Yamamoto, private communication.
[27] D. T. Teaney and V. L. Moruzzi, Bull. Am. Phys. Soc. II, **9**, 225 (1964).
[28] Y. Suemune and H. Ikawa, J. Phys. Soc. Japan **19**, 1686 (1964).
[29] D. T. Teaney, Thesis, University of California, 1960. (unpublished).
[30] R. Nathans, private communication.
[31] J. F. Dillon, Jr., and C. E. Olsen, Phys. Rev. **135**, A434 (1964).

Nuclear Resonance Studies of Magnetic Critical Fluctuations in MnF_2*

P. Heller

Brandeis University, Waltham, Mass.

Atomic nuclei with magnetic moments can serve to probe the local fields within magnetic materials. By studying the nuclear resonance frequency and line width in the critical temperature region near the magnetic transition, it is possible to obtain precise and detailed information [1, 2] on the establishment of magnetic order. Here we shall be concerned with the effect of the critical fluctuations on the NMR line width: associated with the approach to the critical temperature T_c the nuclear resonance lines in ferro- and antiferromagnets exhibit a remarkably rapid broadening. A very detailed study of this effect has been made for the case of the antiferromagnet MnF_2. ($T_c = 67.336$ °K, also denoted by T_N). These experiments shed light on the behavior of the electron spin correlation functions in the critical region. In this account we show that the experimental data implies a "slowing down" of the spin fluctuations in the critical region. A simple physical model for the time dependence of the correlation functions will then be presented. This model yields a theory which is in satisfactory accord with the observed broadening of the F^{19} resonance in MnF_2 as T approaches T_c from above.

The line width anomaly at the critical point for the F^{19} resonance in MnF_2 is shown in figure 1. We shall be largely concerned with the situation in the paramagnetic state $T > T_c$. The detailed behavior of the line width in the region $T_c + 0.006$ °K $< T < T_c + 10$ °K is shown by the experimental points in figure 2. (The drawn lines correspond to the theory to be outlined below.) The line-width is anisotropic with respect to the direction of the externally applied d-c field $\mathbf{H}_0$. For $\mathbf{H}_0$ along c (the antiferromagnetic axis), the line broadens by about a factor of ten as T_c is approached. In the region of severe broadening, the ratio of the line width for $\mathbf{H}_0$ along the c-axis to the line width for $\mathbf{H}_0$ along the a-axis is very nearly 2 to 1,

$$\delta\nu_c/\delta\nu_a = 2. \qquad (1)$$

* This work was supported by the Advanced Research Projects Agency under Contract SD-90 at the Massachusetts Institute of Technology. Also reported in part at the International Conference on Magnetism, Nottingham, England, 1964.

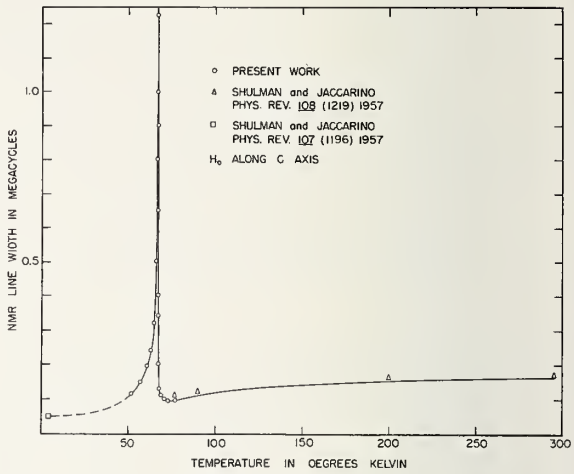

FIGURE 1. *Temperature dependence of* F^{19} *nuclear resonance line width in* MnF_2 *from 4 °K to 300 °K.*
Applied field along c-axis.

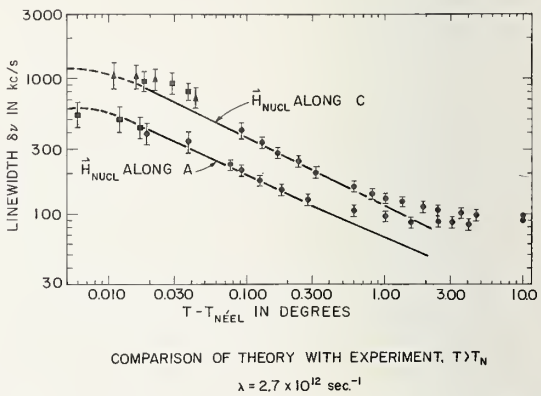

FIGURE 2. *Experimental* F^{19} *line widths in* MnF_2 *just above* T_c.
Drawn curves represent theoretical results with $\lambda = 2.7 \times 10^{12}$ sec^{-1}.

Just above T_c, the line widths level off at the values

$$\delta\nu_c(T_c) = 1100 \text{ kc/sec}$$

$$\delta\nu_a(T_c) = 550 \text{ kc/sec}. \qquad (2)$$

One observation, made at 200 mdeg above T_c, showed that the line width increases monotonically as $\mathbf{H}_0$ is turned from the a to the c direction. At

77 °K, where the line is relatively narrow, the line width is essentially isotropic.

We would like to understand these results. One possible mechanism for the line width broadening will now be stated and then shown to be incompatible with the experimental facts. Suppose that as T_c was neared, the electron spins in the sample became permanently ordered to a degree which varied from one region to another. This would result in a variation $\Delta\mathbf{H}$ in the time average local field seen by different nuclei. We assume the direction of antiferromagnetic spin alinement within each region to be along the c-axis, the direction of antiferromagnetic alinement below T_c. The direction of $\Delta\mathbf{H}$ will then also be along c. The nuclear resonance would then be inhomogeneously broadened. This broadening would be severe if the applied field $\mathbf{H}_0$ were colinear with $\Delta\mathbf{H}$. On the other hand, if $\mathbf{H}_0$ were perpendicular to $\Delta\mathbf{H}$, the observed broadening would be of the second order in $|\Delta H|$. A simple calculation shows that if this were the mechanism responsible for the line width, the anisotropy factor $\delta\nu_c/\delta\nu_a$ would be very much greater than 2, in contradiction with the experimental results.

The line width is therefore to be attributed to fluctuations in the local hyperfine fields seen by the nuclei; it can then be related to the electron spin correlation functions in a way that may be expressed quantitatively as follows. If the interaction between a nucleus and an electron spin has the form $\mathscr{H}=A\mathbf{I}\cdot\mathbf{S}$, where A is the hyperfine coupling constant, and if z is the direction of the average local field at the nucleus and furthermore if the correlation time for the spin fluctuations is short compared with the nuclear Larmor frequency, then [3, 4]

$$\delta\nu=\frac{1}{\pi\sqrt{3}}\left(\frac{A}{\hbar}\right)^2\int_0^\infty dt\Big[<\{\delta S_z(t)\delta S_z(0)\}>$$

$$+\frac{1}{2}<\{\delta S_x(t)\delta S_x(0)\}>+\frac{1}{2}<\{\delta S_y(t)\delta S_y(0)\}>\Big]. \quad (3)$$

Here $\delta S(t)=S(t)-<S>$ denotes the departure of the spin from its thermal average value and $\{AB\}=\frac{1}{2}(AB+BA)$.

We now show that in order to explain the line width anomaly within the framework of the formula (3), it must be assumed that the time dependence of the spin correlation functions becomes "slow" near T_c. Let

$$G_\mu(t)=\frac{<\{\delta S_\mu(t)\delta S_\mu(0)\}>}{<[\delta S_\mu(0)]^2>},$$

where $\mu=1, 2, 3$ denotes a Cartesian component, and define correlation times τ_μ by writing

$$\tau_\mu=\int_0^\infty G_\mu(t)dt.$$

Then (3) becomes

$$\delta\nu=\frac{1}{\pi\sqrt{3}}\left(\frac{A}{\hbar}\right)^2\Big[\tau_z<(\delta S_z)^2>$$

$$+\frac{1}{2}\tau_x<(\delta S_x)^2>+\frac{1}{2}\tau_y<(\delta S_y)^2>\Big]. \quad (4)$$

The experimental line width was found to be isotropic above T_c+10 °K. We then surmise that in this temperature range the spin fluctuations are isotropic and $\tau_x=\tau_y=\tau_z=\tau$. If the correlation times were constant as $T\to T_c$ we would have

$$\delta\nu=\frac{1}{\pi\sqrt{3}}\left(\frac{A}{\hbar}\right)^2\tau\Big[<(\delta S_z)^2>$$

$$+\frac{1}{2}<(\delta S_x)^2>+\frac{1}{2}<(\delta S_y)^2>\Big].$$

But for $T>T_c$, $<S>=0$, and the following identity holds

$$<(\delta S_x)^2>+<(\delta S_y)^2>+<(\delta S_z)^2>=S(S+1)=\frac{5}{2}\frac{7}{2}.$$

From this it may be seen that the temperature dependence of the time independent correlations $<(\delta S_\mu)^2>$ cannot be responsible for the tenfold increase in line width observed as $T\to T_c$. The correlation times evidently increase in the critical region.

The observed line width anisotropy is now interpreted as follows. Denoting the crystal axes by

c, a, and a', the line widths for the average local field along c and a are given respectively by

$$\delta\nu_c = \frac{1}{\pi\sqrt{3}}\left(\frac{A}{\hbar}\right)^2\left[\tau_c < (\delta S_c)^2 > + \frac{1}{2}\tau_a < (\delta S_a)^2 > + \frac{1}{2}\tau_{a'} < (\delta S_{a'})^2 >\right]$$

and

$$\delta\nu_a = \frac{1}{\pi\sqrt{3}}\left(\frac{A}{\hbar}\right)^2\left[\tau_a < (\delta S_a)^2 > + \frac{1}{2}\tau_c < (\delta S_c)^2 > + \frac{1}{2}\tau_{a'} < (\delta S_{a'})^2 >\right].$$

Therefore, the factor of 2 anisotropy actually observed just above T_c implies that at those temperatures

$$\tau_c < (\delta S_c)^2 > \gg \tau_a < (\delta S_a)^2 >. \tag{5}$$

A theory of the electron spin correlation functions in the critical region was given by Moriya [5]. The physical content of the theory may be expressed in the following terms. Just above T_c there exists a short range antiferromagnetic correlation between the spins. Roughly speaking, the spin arrangement at any instant of time consists of clusters of antiferromagnetically alined spins. The time average value of the spin at any site is zero, however, and so these clusters are constantly forming, dissolving and reforming. The average size *and lifetime* of the clusters increases as $T \to T_c$. This latter point, which corresponds to a "slowing" of the spin fluctuations is an essential part of the theory. The direction of antiferromagnetic alinement within the clusters is mainly along the c-axis; this is responsible for the inequality (5) and the consequent line width anisotropy.

On the basis of this picture it is clear that we should rewrite eq (3) in terms of the Fourier transform spin deviations $\delta\mathbf{S}_k(t)$. These are defined in terms of the ionic spin deviations $\delta\mathbf{S}_j(t)$ as follows

$$\delta\mathbf{S}_j(t) = \frac{1}{\sqrt{N}}\sum_k \delta\mathbf{S}_k(t)e^{-ik\cdot r_j}. \tag{6}$$

The theory is greatly simplified if we assume that the correlation functions for the Fourier transformed spin deviations decay exponentially with time, i.e.,

$$< \{\delta S_{k\mu}(t)\delta S^{\dagger}_{k\mu}(0)\} > = < |\delta S_{k\mu}(0)|^2 > e^{-\Gamma_\mu(k)t}. \tag{7}$$

Using eq (7) and (6) in eq (3) it follows that

$$\delta\nu_c = \frac{1}{\pi\sqrt{3}}\left(\frac{A}{\hbar}\right)^2\frac{1}{N}\sum_k\left[\frac{< |\delta S_{kc}(0)|^2 >}{\Gamma_c(k)} + \frac{1}{2}\frac{< |\delta S_{ka}(0)|^2 >}{\Gamma_a(k)} + \frac{1}{2}\frac{< |\delta S_{ka'}(0)|^2 >}{\Gamma_{a'}(k)}\right] \tag{8}$$

when the average local field is along the c-axis. If the average local field is along the a-axis one interchanges c and a.

The tenfold increase in the line width that is observed to occur as $T \to T_c$ from above can now be understood as follows. As $T \to T_c$, the quantities $< |\delta S_{kc}(0)|^2 >$ become very large while the corresponding decay rates $\Gamma_c(k)$ become very small for wave vectors k near the antiferromagnetic made k_0. This corresponds to the physical picture of increased correlation range and cluster lifetime near T_c.

To make a quantitative theory of these effects we thus need to know the temperature dependence of both the quantities $< |\delta S_{k\mu}|^2 >$ and $\Gamma_\mu(k)$. In his theory, Moriya used the fluctuation-dissipation theorem to relate $< |\delta S_{k\mu}|^2 >$ to the wavelength dependent d-c susceptibilities. The relation is

$$< |\delta S_{k\mu}|^2 > = \frac{k_B T}{g^2\mu_B^2}\chi_\mu(k), \tag{9}$$

where k_B is the Boltzman constant, μ_B the Bohr magneton, and $g = 2$. The susceptibilities $\chi_\mu(k)$ can be calculated on a molecular field model. The results are given by Moriya [5].

To calculate the decay rates $\Gamma_\mu(k)$, Moriya employed a technique developed by Mori and Kawasaki [6] for describing spin diffusion in ferromagnets. Here, however, we shall employ a very simple physical model. According to this view [7], the decay of a staggered spin configuration is inhibited by the staggered molecular field generated by that configuration, an effect which leads to a particularly slow decay near T_c. On this model the decay rates are related to the wavelength dependent d-c

susceptibilities as follows

$$\Gamma_\mu(k)=\lambda\frac{\chi_{\text{Curie}}(T)}{\chi_\mu(k,\,T)}, \tag{10}$$

where λ is a temperature independent parameter, and

$$\chi_{\text{Curie}}(T)=\frac{g^2\mu_B^2S(S+1)}{3k_BT} \tag{11}$$

is the Curie susceptibility.

The motivation behind eq (10) is as follows. Imagine that at some temperature $T>T_c$ we artificially produced a "staggered magnetization" M_s by applying a staggered field H_s. If H_s is turned off, M_s eventually relaxes to zero. Consider the situation at the instant that H_s is turned off. According to the viewpoint of the Weiss theory, where the coupling between the spins is replaced by an effective field, the spins would find themselves in a staggered "molecular field." We suppose this field to be strong enough to produce a staggered magnetization M_s^* at equilibrium. Evidently $M_s^*=f(T)M_s$ where $f(T)$ is a fraction which becomes equal to unity at T_c, that being the temperature at which the magnetization becomes self-sustaining. As a model to describe the decay of the staggered magnetization we now write the following differential equation

$$\frac{dM_s}{dt}=-\lambda(M_s-M_s^*)=-\lambda[1-f(T)]M_s.$$

This leads to an exponential decay $M_s=M_s(0)e^{-\Gamma_s t}$ where

$$\Gamma_s=\lambda[1-f(T)]. \tag{12}$$

Now let us calculate the staggered magnetization M_s produced at equilibrium by a staggered field H_s. In the absence of the molecular field we would have $M_s=H_s\chi_{\text{Curie}}$ where χ_{Curie} is given by (11). In the presence of the molecular field

$$M_s=H_s\chi_{\text{Curie}}+f(T)M_s$$

or

$$M_s=\frac{H_s\chi_{\text{Curie}}}{1-f(T)}.$$

Thus the "staggered susceptibility" is effectively

$$\chi_s=\frac{\chi_{\text{Curie}}}{1-f(T)}. \tag{13}$$

Comparing (13) with (12) we find

$$\Gamma_s=\lambda\frac{\chi_{\text{Curie}}}{\chi_s}.$$

The same argument may be applied to relate the relaxation of spin arrangements of arbitrary wavelength to the corresponding susceptibilities. We thus obtain eq (10). In applying this relation to a calculation of the time dependence of the correlation functions, we are assuming that the time decay in the kth Fourier component of the magnetization which occurs as a result of spontaneous fluctuations is similar to that which characterizes the return to equilibrium following an artificially produced nonequilibrium state.

The line width may now be expressed in terms of the wavelength dependent susceptibilities and the parameter λ. Using (9), (10), and (11) in (8) we find

$$\delta\nu_c=\frac{1}{\lambda}\frac{1}{\pi\sqrt{3}}\frac{A^2}{\hbar^2}\left(\frac{k_BT}{g^2\mu_B^2}\right)^2\frac{3}{S(S+1)}\frac{1}{N}\sum_k[\chi_\parallel^2(k)+\chi_\perp^2(k)] \tag{14}$$

$$\delta\nu_a=\frac{1}{\lambda}\frac{1}{\pi\sqrt{3}}\frac{A^2}{\hbar^2}\left(\frac{k_BT}{g^2\mu_B^2}\right)^2\frac{3}{S(S+1)}\frac{1}{N}\sum_k\left[\frac{1}{2}\chi_\parallel^2(k)+\frac{3}{2}\chi_\perp^2(k)\right],$$

where $\chi_{||}(k)$ and $\chi_\perp(k)$ denote the components of the wavelength dependent susceptibilities respectively parallel and perpendicular to the c-axis.

The discussion so far has assumed that each fluorine nucleus is coupled to a single manganese spin. In actual fact, there are three spins to which the coupling is important [8]. We denote these by **S**, **S′**, and **S″**, their positions in the lattice by r, r', and r'' and the corresponding hyperfine coupling tensors by **A**, **A′** and **A″**. We then replace the coupling $A\,\mathbf{I}\cdot\mathbf{S}$ in the preceding discussion by the coupling $\mathbf{I}\cdot(\mathbf{A}\cdot\mathbf{S}+\mathbf{A}'\cdot\mathbf{S}'+\mathbf{A}''\cdot\mathbf{S}'')$. The line width formulae (14) then become revised in a way which can be expressed compactly as follows. For each

wave-vector k construct the tensor

$$\mathbf{A}(k)=\mathbf{A}e^{ik\cdot r}+\mathbf{A}'e^{ik\cdot r'}+\mathbf{A}''e^{ik\cdot r''}. \tag{15}$$

For the present purposes, the principal axes can be taken to be along the $c=[100]$, $x=[110]$ and $y=[1\bar{1}0]$ directions. Then the line widths can be written

$$\delta\nu_c=\frac{1}{\lambda}\frac{\hbar^{-2}}{\pi\sqrt{3}}\left(\frac{k_BT}{g^2\mu_B^2}\right)\frac{3}{S(S+1)}\frac{1}{N}$$
$$\sum_k\left[|A_{cc}(k)|^2\chi_{\|}^2(k)+\frac{|A_{xx}(k)|^2+|A_{yy}(k)|^2}{2}\chi_{\perp}^2(k)\right] \tag{16}$$

$$\delta\nu_a=\frac{1}{\lambda}\frac{\hbar^{-2}}{\pi\sqrt{3}}\left(\frac{k_BT}{g^2\mu_B^2}\right)\frac{3}{S(S+1)}\frac{1}{N}\sum_k\left[\frac{1}{2}\right.$$
$$\left.|A_{cc}(k)|^2\chi_{\|}(k)+\frac{3}{2}\frac{|A_{xx}(k)|^2+|A_{yy}(k)|^2}{2}\chi_{\perp}^2(k)\right].$$

Since the modes $k\cong k_0$ make the most significant contribution near T_c, we can replace $\mathbf{A}(k)$ by $\mathbf{A}(k_0)$. The numerical values of the tensor components can be obtained from the electron spin resonance experiments [8] on Mn^{++} in ZnF_2 and may be expressed as follows

$$\frac{S}{\hbar}|A_{cc}(k_0)|=160\text{ Mc/s}$$

$$\left(\frac{S}{\hbar}\right)^2\frac{|A_{xx}(k_0)|^2+|A_{yy}(k_0)|^2}{2}=(68\text{ Mc/s})^2 \tag{17}$$

where $S=5/2$.

To obtain line width formulae which are asymptotically correct as $T\to T_c$, it will be sufficient to express the wavelength dependent susceptibilities $\chi(k)$ in a form valid near the antiferromagnetic mode k_0. Letting $k=k_0+q$ where $|q|\ll k_0$, the molecular field approximation yields the following results above T_c:

$$\chi_{\|}(k_0+q)=\frac{g^2\mu_B^2S(S+1)}{3k_BT_c}\frac{1}{\delta+\frac{1}{8}[a^2(q_a^2+q_{a'}^2)+c^2q_c^2]}. \tag{18}$$

Here a and c refer to the unit cell dimensions, and

$$\delta=\frac{T-T_c}{T_c}.$$

Also

$$\chi_{\perp}(k_0+q)=\frac{g^2\mu_B^2S(S+1)}{3k_BT_c}$$
$$\frac{1}{\delta+\delta_{\text{anis.}}+\frac{1}{8}[a^2(q_a^2+q_{a'}^2)+c^2q_c^2]}, \tag{19}$$

where $\delta_{\text{anis.}}=0.02$ is roughly the ratio of the dipolar anisotropy energy to the exchange energy. Note that $\chi_{\perp}(k_0)$ does not diverge at T_c, while $\chi_{\|}(k_0)$ does.

Using (17), (18), and (19) in (16), the temperature dependence of the line widths is found to be asymptotically

$$\delta\nu_c=\frac{1}{\lambda}\frac{4}{3}\sqrt{\frac{2}{3}}S(S+1)\frac{|A_{cc}(k_0)|^2}{h^2}$$
$$[\delta^{-1/2}+0.18(\delta+\delta_{\text{anis}})^{-1/2}]$$

$$\delta\nu_a=\frac{1}{\lambda}\frac{4}{3}\sqrt{\frac{2}{3}}S(S+1)\frac{|A_{cc}(k_0)|^2}{h^2}$$
$$[\frac{1}{2}\delta^{-1/2}+0.26(\delta+\delta_{\text{anis}})^{-1/2}]. \tag{20}$$

The quantity λ, which we regard as an adjustable parameter, is now chosen to fit the line width data for $T_c+0.015\text{ °K}<T<T_c+1\text{ °K}$. We find

$$\lambda=2.7\times10^{12}\text{ sec}^{-1}. \tag{21}$$

The fit is shown in figure 2, the solid lines corresponding to eq (20). Some deviation in the fit is apparent above T_c+1 °K. This is attributable to the use of the approximate expression (18) and (19) and the replacement of $\mathbf{A}(k)$ by $\mathbf{A}(k_0)$ in (16). Both approximations tend to underestimate the line width at temperatures where contributions from modes k not very close to k_0 become important.

A more serious defect in the theory occurs in the immediate vicinity of T_c where eq (20) predicts divergent line widths proportional to $\delta^{-1/2}$. This contrasts to the constant experimental values reported in eq (2). The infinity in the theory arises from the divergence at T_c of the staggered susceptibility $\chi_{\|}(k_0, T)$. We now suggest that in reality this quantity does not become infinite at T_c, but is merely very large over some narrow range of temperatures centered on T_c. In other words we suggest that the critical point is not perfectly sharp,

there being a distribution of critical temperatures of width δT_c. Such a situation might well arise when on account of crystalline strains, different parts of the sample have different Curie points. We do not wish to assert that this is really the source of the broadening, however. In any case, a distribution of Curie points should lead to two other experimentally observable effects near T_c:

(1) There should be a coexistence region in which nuclear resonances corresponding to both the paramagnetic and antiferromagnetic phases are simultaneously observable.

(2) The NMR lines observed in the antiferromagnetic state $T < T_c$ should be inhomogeneously broadened. The line width should be maximum when the average local field is along c and minimum when along a. Furthermore, the anisotropy factor $\delta\nu_{\max}/\delta\nu_{\min}$ should be greater than the 2:1 ratio associated with line broadening by fluctuating fields.

Both of these effects were observed and both were consistent with a Curie point distribution of width

$$\delta T_c \cong 17 \text{ millidegrees.} \tag{22}$$

We now show that such a distribution would result in a finite observed line width at the (average) Curie point $\overline{T}_c$, and we calculate this width. At that temperature, the observed line corresponding to the paramagnetic phase will be due to those members of the distribution which have Curie points T_c somewhat below $\overline{T}_c$. The larger the difference $\overline{T}_c - T_c$, the narrower and hence the stronger will be the contributed NMR line. Roughly speaking, the observed line should then be due to those members of the distribution for which $\overline{T}_c - T_c \cong \frac{1}{2}\delta T_c$. The observed line width should then be given by (20) by inserting the value

$$\delta = \frac{\frac{1}{2}\delta T_c}{T_c} = 1.3 \times 10^{-4}.$$

When this is done, using for λ the value given in (21) we find

$$\begin{aligned} \delta\nu_c &= 1200 \text{ kc/s} \\ \delta\nu_a &= 600 \text{ kc/s} \end{aligned} \tag{23}$$

in agreement with the experimental values reported in eq 2. The theoretical line width curves in figure 2 have been "leveled off" at the values (23) just calculated. Thus the divergent theoretical formulae, when modified for the experimentally observed Curie point distribution, yield a good account of the line width broadening above T_c.

Let us see whether our model eq (10) for the relaxation rates is still valid well above the critical point. For $T \gg T_c$, $\chi(k) = \chi_{\text{Curie}}$ and hence $\Gamma(k) = \lambda$ for all k. Then the decay rate for the single-ion correlation functions is also λ. This enables us to compute λ from the F^{19} line width observed at high temperatures [9],

$$\delta\nu_\infty = 170 \text{ kc/s}.$$

The result is

$$\lambda = 1.8 \times 10^{12} \text{ sec}^{-1}. \tag{24}$$

Comparing this with the result (21) deduced from the critical fluctuations, we see that the model eq (10) gives a satisfactory picture of the line width behavior above T_c.

We now turn briefly to the situation below T_c, where the line width data is shown by the experimental points in figure 3. In the antiferromagnetic state, the average local field at the nucleus $\mathbf{H}_{\text{NUCL}}$ is the resultant of the applied field and the field produced at the nucleus by the antiferromagnetically ordered Mn^{++} spins:

$$\mathbf{H}_{\text{NUCL}} = \mathbf{H}_0 + \mathbf{H}_{Mn^{++}}.$$

Most of the observations were made with $\mathbf{H}_0$ and hence $\mathbf{H}_{\text{NUCL}}$ along c. Some observations were made with $\mathbf{H}_0$ so oriented that $\mathbf{H}_{\text{NUCL}}$ was along a.

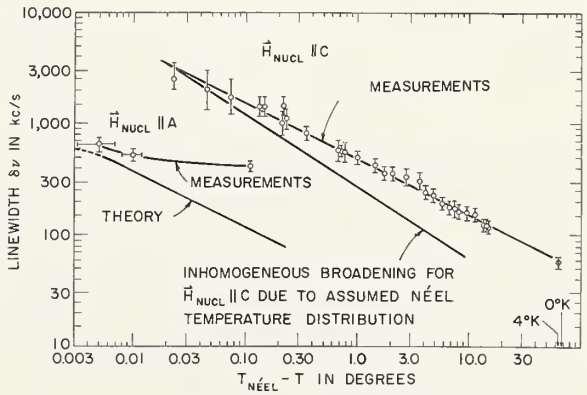

FIGURE 3. *Experimental* F^{19} *line widths below* T_c.
Curves drawn through experimental points represent smoothed data. Other drawn curves represent theoretically calculated line width for $\mathbf{H}_{\text{NUCL}}$ along a and inhomogeneous broadening with $\mathbf{H}_{\text{NUCL}}$ along c, calculated for a Curie point distribution of widht $\delta T_c = 17$ mdeg.

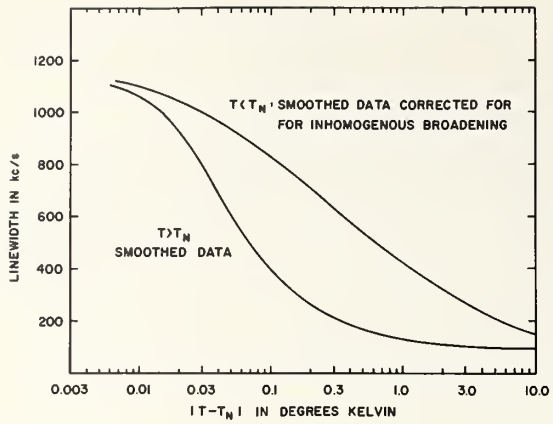

FIGURE 4. *Line widths for* $\mathbf{H}_{\mathrm{NUCL}}$ *along* c *above and below* T_c. Line widths for $T < T_c$ have been corrected for the inhomogeneous broadening due to the Curie point distribution.

When this condition was satisfied the NMR lines were quite narrow. This is because the inhomogeneous field $\Delta\mathbf{H}$ arising from the distribution of Curie points is along c; only a second order broadening results with $\mathbf{H}_{\mathrm{NUCL}}$ perpendicular to $\Delta\mathbf{H}$.

An upper bound on the second order inhomogeneous broadening for $\mathbf{H}_{\mathrm{NUCL}}$ along a was calculated by postulating that all of the observed broadening for $\mathbf{H}_{\mathrm{NUCL}}$ along c was inhomogeneous. This upper bound was considerably smaller than the line width $\delta\nu_a$ observed for $\mathbf{H}_{\mathrm{NUCL}}$ along a. We conclude that the $\delta\nu_a$ line widths shown in figure 3 do not reflect the inhomogeneous broadening. They are due presumably to fluctuations.

It was possible roughly to correct the data for $\mathbf{H}_{\mathrm{NUCL}}$ along c for the inhomogeneous broadening. This was done in two ways as follows:

(1) The corrected value of $\delta\nu_c$ was set equal to twice $\delta\nu_a$ at those temperatures where the $\delta\nu_a$ data was available.

(2) Assuming that the $\delta\nu_c$ line widths observed just below T_c were entirely inhomogeneous, the width of the Curie point distribution was found to be about 17 mdeg. Then the inhomogeneous part of the broadening was calculated as a function of temperature and "subtracted off" from the observed line width.

The estimated line width for $\mathbf{H}_{\mathrm{NUCL}}$ along c, corrected for the inhomogeneous broadening is shown as a function of $|T_c - T|$ in figure 4, together with the actual $\delta\nu_c$ line widths for $T > T_c$. Note that the corrected line width is continuous at T_c.

The theory described above, which gave a satisfactory account of the behavior above T_c, can be used to calculate the line widths for $T < T_c$. Using the molecular field model to calculate the wavelength dependent susceptibilities, the theoretically calculated line width is found to fall off much more rapidly with decreasing temperature than the experimentally observed width. This discrepancy is illustrated in figure 3, where the theoretical line width for $\mathbf{H}_{\mathrm{NUCL}}$ along a is compared with the data. At present, therefore, we do not understand the line width behavior below T_c.

The author is deeply grateful to Professor G. B. Benedek for many important comments and suggestions, to Professor T. Moriya for making available his theory prior to publication, and to Dr. Y. Obata, Dr. T. Izuyama, and Dr. K. Kawasaki for many helpful theoretical discussions.

References

[1] P. Heller and G. B. Benedek, Phys. Rev. Letters **8**, 428 (1962).
[2] P. Heller and G. B. Benedek, Phys. Rev. Letters **14**, 71 (1965).
[3] R. Kubo and K. Tomita, J. Phys. Soc. Japan **9**, 888 (1954).
[4] T. Moriya, Prog. Theor. Phys. **16**, 23, 641 (1956).
[5] T. Moriya, Prog. Theor. Phys. **28**, 371 (1962).
[6] H. Mori and K. Kawasaki, Prog. Theor. Phys. **25**, 723 (1962).
[7] P. Heller, Thesis, Harvard University 1963 (unpublished).
[8] A. M. Clogston, J. P. Gordon, V. Jaccarino, M. Peter, and L. R. Walker, Phys. Rev. **117**, 1222 (1960).
[9] R. G. Shulman and V. Jaccarino, Phys. Rev. **108**, 1219 (1956).

Discussion

G. S. Rushbrooke: May I ask Dr. Domb how summing over further graphs besides ring graphs differs fundamentally from applying say the Percus-Yevick equation to the Ising model, which one knows is not very good?

C. Domb: The approximation which I propose attempts to find an asymptotic representation of polygons and other graphs on the lattice. In terms of Mayer theory it corresponds to summing *all* cluster integrals which can be formed using all the bonds of these configurations on the lattice. Thus even in lowest order when it is concerned only with polygons it still takes into account a much more complex set of integrals than those of simple ring type. In this respect the lowest order approximation is the generalization to infinity of the ring approximation of Rushbrooke and Scoins. It seems to me that approximations like those of Percus-Yevick are derived by summing *Mayer* ring integrals, and make no serious attempt to estimate asymptotically the number of polygons on the lattice and the corresponding excluded volume effect.

M. E. Fisher: I would like to make a comment on the point that Dr. Rushbrooke raised. It is in the spirit of the Van der Waals equation to take into account the short range repulsion exactly. The short range repulsion with excluded volume effects is also a difficult problem, but the point is that it is possible to split the problem this way. This approach using the data from lattice models represents it, one hopes, in a better way.

C. N. Yang: Dr. Domb said he believed that for some three dimensional lattice models the specific heat singularities below

the critical temperature are logarithmic. What is the constant in front of the logarithm?

C. Domb: Unfortunately, I have not got the figures at this moment, but I can easily provide them at a later stage.

B. R. Livesay presented measurements of the magnetization of thin nickel films near the Curie temperature [1].

J. C. Eisenstein: I would like to report some measurements on $NdCl_3$, which have been carried out by Hudson and Mangum here at the National Bureau of Standards [2]. This substance has highly anomalous magnetic properties. It has two extremely sharp spikes in its susceptibility at approximately 1.0 and 1.7 °K. With regard to the dependence of the susceptibility on the temperature in the vicinity of the 1.7 °K peak, we found that the coefficients γ and γ' are approximately the same. However, they are not 1.3, but approximately 0.69. Also the susceptibility of $CeCl_3$ was measured [3]. It was found that the susceptibility of this substance has a very sharp spike at 0.345 °K. We think $CeCl_3$ has a second susceptibility peak at a lower temperature, but it has not been located yet. For $CeCl_3$ the value of γ on the high side of the transition is about 0.61. The measurements on $NdCl_3$ extended from about 5 to 55 mdeg on either side of the transition. For $CeCl_3$ the range was 10 to 100 mdeg.

E. Callen: There exists some theoretical analysis of the Heisenberg Hamiltonian. If one looks for the asymptotic behavior, any cluster theory or Green's function theories give the value $\beta = 1/2$. That is in

$$M = D(1 - T/T_c)^{\beta} \tag{1}$$

the behavior of M *asymptotically* at $T = T_c$ is given by $\beta = 1/2$. On the other hand, however, if one is content with some sort of a numerical procedure, it turns out that many results are already given by simple models. In particular, if one carries out the variational procedure as described by Dr. Livesay, in which one considers dM/dT as a function of β and takes the value of β which gives the best fit to the magnetization curve, the Green's function theories give $\beta = 1/3$ for a broad temperature range. Also the cluster theory including nearest-neighbor and next-nearest-neighbor interaction leads to the 1/3 power [4]. Furthermore, by taking the nearest and next-nearest exchange constant from experimental data without using any adjustable parameter, the cluster theory predicts the observed value of the coefficient D in (1) within 2 percent. Although these theories are not correct asymptotically at $T = T_c$, numerically one obtains rather good results from the present existing theory away from T_c. Perhaps only higher and higher sophistication will extend this range of validity to temperatures closer and closer to T_c.

H. B. Callen: I would like to amplify that. There has been a great deal of discussion, it seems to me, about rigorous theories. Nevertheless, the molecular field theory, the cluster theory and other phenomenological theories have historically turned out to be very convenient. These theories to my mind have not been considered sufficiently in the discussion so far. As my brother just observed, they are in fact considerably more successful than they have been given credit for. I would like to review very rapidly some of the successes these theories have had, choosing specifically a form of Green's function theory.

If one asks for the equation of motion of a spinwave, one has to take into account the interaction between two spinwaves. This interaction is described by the appearance of S_z in the Hamiltonian [5]. Now one can represent S_z in either of the following two forms [5]:

$$S_z = S - S^- S^+ \tag{2}$$

or

$$S_z = 1/2(S^+ S^- - S^- S^+) \tag{3}$$

As the averages are calculated by some kind of approximation the two methods do not lead to the same result. However it is possible to make a guess as to which of the two methods is better at low temperature and which one better at high temperature. One therefore introduces a parameter and says that the total S_z is a linear combination of (2) and (3), the ratio being $(1/2S)(S_z/S)^x$. This has been investigated for various values of the exponent x. At first we [5] had carried out the method for $x = 1$ but at the meeting in Kansas City in March 1965 Copeland and Gersch indicated that they had investigated the method for general x, and that for $x = 3$ the theory leads to excellent results [6]. For the shape of the critical isotherm, Copeland and Gersch reported $\delta = 4.22$, whereas various experiments that have been reported here give $\delta = 4.2 \pm 0.2$. For the coefficient of the susceptibility above the Curie temperature they reported $\gamma = 4/3$ quite accurately. As my brother told you, all Green's function theories give $\beta = 1/3$, but only at some distance below the Curie temperature (much further below than Dr. Benedek found). In fact, one finds that the value of β changes from 1/2 close to the Curie temperature to $\beta = 1/3$ some distance away from the critical temperature. Incidentally this is very reminiscent of the data in He^3 that Dr. Sherman presented, where they found experimentally a narrow region where the coexistence curve follows a 1/2-power law going over into a 1/3-power law beyond this region. Finally, I remind you that the coefficient D in (1) is correctly predicted to within 2 percent.

Anonymous: How is the value 3 chosen for the exponent x?

M. E. Fisher: By comparison with experiment?

H. B. Callen: Copeland and Gersch find the magnetization to be double valued if one takes x in the range $1 < x < 3$. The selection of $x = 3$, rather than $x > 3$, is on the ad-hoc basis of the results cited.

G. E. Uhlenbeck: I would like to make a comment with regard to the remarks of Dr. Callen. I am not in favor of saying that the theories you mentioned have not led to interesting results. However, I do not think it is right to treat them on the same level as the classical theory. The classical theory corresponds to a definite model namely long range forces, while the theories you mentioned contain what I would call uncontrolled approximations.

H. B. Callen: At the risk of a rebuttal which may call forth another rebuttal, I remark that the molecular field theory only became an exact model many years after it was phenomenological. That is, the model for which it is exact was not discovered until long after the theory has been presented. I imagine that for any so called phenomenological model, one can find, if one is clever enough, some obscure model for which it is a rigorous solution. In the case of the molecular field solution one contrives a model in which every spin interacts equally strongly with every other spin. It seems to me to be a technicality to call that a physical model, and to make a distinction between that theory and other phenomenological theories.

L. Tisza: The internal field theories can be discussed from two points of view and these are not in conflict if properly distinguished. We may search for models or types of interactions for which such a theory is more or less adequate, or else, we may consider the method as an approximation to the real state of matters and observe its point of breakdown. I wish to make a remark from the second point of view. It is possible to formulate the statistical thermodynamics of equilibrium in a fashion that a finite system appears to be coupled with its infinite environment. The system is specified by additive random variables the distribution of which contains the intensities of the environment as parameters. The theory is still valid for small systems, but it fails for critical points where an important Jacobian vanishes [7]. This argument justifies the use of an internal field as the intensity of the environment of a small open system, independently whether the interaction is of short or long range. However, the theory fails near the critical point and here more incisive methods have to take over.

O. K. Rice: I would like to say something about the accuracy with which one can measure β. As was mentioned by Dr. Rowlinson, Thompson, and I [8] measured the coexistence curve of the binary liquid system perfluoromethylcyclohexane-carbontetrachloride. We had a temperature control to about 0.0001 °C and we measured a curve which extended to about 0.02 °C from the critical temperature. We obtained data which looked as good as the magnetic data under discussion. However, we tried to distinguish between the value $\beta=1/3$ and the value $\beta=5/16$ that Fisher suggested. For this purpose we plotted our data both ways. We figured we did not know the critical temperature better than within 0.0001 °C, so that we had a small range in which the critical temperature could be adjusted. We found in doing this that one cannot distinguish between these two exponents. Therefore, I wonder whether in the case of the magnetic data the critical temperature is really definitely fixed. Perhaps with a slight shift of the critical temperature, one might get a fit of the data with exponents that are slightly different. In other words, I wonder whether even in the best cases, the data are really good enough to fix the exponent β to be 1/3.

P. Heller: In response to that last question, it should be remarked that there is no uncertainty about the value of β. If you plot the cube of the magnetization as a function of the temperature you get a straight line. If you plot the magnetization to a power slightly different from 3, you do not get a straight line. In this procedure of finding the exponent that rectifies the observed data, one does not need to know the temperature of the Curie point.

D. H. Douglass: I wish to point out, in addition to the magnetic and liquid-gas systems, that superfluid liquid helium is another system for which the exponent 1/3 probably appears. The quantity in liquid helium which corresponds, in the magnetic case, to the magnetization is $\rho_s^{1/2}$ (I get this from analogy with superconductivity). I have used the data of Dash and Taylor [Phys. Rev. **105**, 7 (1957)] to determine if, near the λ-point, the superfluid density follows the relation $\rho_s^{1/2}\alpha(T_\gamma-T)^\gamma$. I find that $\gamma=0.30\pm0.03$, which includes the value 1/3 (and 5/16, too).

C. Domb: With regard to the paper of Dr. Wolf, I would like to make two comments.

Firstly, I think the first order phase transition may be significant and is worthy of further investigation. The antiferromagnetic transition is the analog of an order-disorder transition with unequal ratios of the constituents. I believe the experimental data on the order-disorder transition of this kind in Cu_3Au are also thought to represent a first order transition. We might well expect something different to happen when the symmetry of equal ratios of constituents is removed in an order-disorder transition, and when the field is nonzero for an antiferromagnet. I would think this is a result worth following up.

Secondly, I do not think one can really say any one shape of specimen is better than another for testing the theory. I really think we just have to do more theory. In fact what has held us up with long range dipole forces is the terrifying nature of the calculations. However, if the dominating term is the short range interaction, and the dipole force, although it produces a shape dependent effect, is nevertheless a relatively small correction, I think the calculations may be manageable, and then we should be able to get a better comparison.

W. P. Wolf: Let me make that point quite clear. In our antiferromagnet the energy of three cells of nearest neighbors accounts for the major part of the energy. However, when you apply a magnetic field, the change in dipolar energy, the demagnetizing energy, that is, is comparable with the energy due to the applied magnetic field, and in a large field it can become rather comparable with all the other energies. I didn't give any numbers for this but for DAG, the effects are in fact all about comparable.

C. Domb: Well, perhaps you get cancellation in the higher order terms.

W. P. Wolf: Yes, when it is antiferromagnetic. However, not when you magnetize the system and polarize the spins.

C. Domb: Nevertheless, I think the susceptibility might possibly be manageable.

P. W. Kasteleyn: I have been asked to report some measurements which have been performed by Dr. W. J. Huiskamp, Dr. A. R. Miedema and Mr. R. F. Wielinga in the Kamerlingh Onnes laboratory in Leiden. Measurements were carried out on two groups of salts, one group representing the Ising system [9] and the other group representing the Heisenberg model [10]. The first group consists of cobalt potassium sulfate and cobalt cesium chloride, which have very anisotropic g-factors and which are neat Ising systems also in other respects. It was found, e.g., that for the first salt γ, the index for the susceptibility, is about 1.22, whereas the theoretical conjecture is $\gamma=1.25$ for Ising systems and $\gamma=1.33$ for Heisenberg systems. For $T>T_c$ the specific heat seems to diverge with a very high value of α in those cases. Namely, for the first salt $\alpha=0.57\pm0.06$ and for the second salt even $\alpha=0.68\pm0.05$ which is rather surprising. In most other salts measured up to now this coefficient of divergency was found to be much smaller. For $T>T_c$ it seems that the experiments can be fitted very reasonably by a logarithmic divergence. That these systems are Ising systems can also be seen from the difference in entropy S at infinite temperature and at the Curie temperature. This difference was found to be $(S_\infty-S_c)/R=0.14$ and 0.125 for the two salts mentioned, whereas for a simple cubic spin 1/2 Ising system one finds 0.133 and for a Heisenberg system 0.25.

In the second series of salts they took potassium chloride, rubidium chloride, ammonium chloride, and ammonium bromide. The structure is nearly body centered cubic. $(S_\infty-S_c)/R=0.222$, whereas for the Ising body centered cubic model this should be 0.107 and for the Heisenberg model about 0.25. The value of γ turned out to be 1.36, which is close to the value 1.33 expected for the Heisenberg system. It seems that the specific heat data can be fitted accurately by a logarithmic type of divergence both below and above the Curie temperature. Only above the Curie temperature the curve is much lower. The specific heat data plotted as a function of the reduced temperature T/T_c fit very closely the same curve for all four salts. This gave the authors reason to think that these salts are fairly ideal systems, because all deviations from ideality would be expected to be different for the various salts. As the data lie on the same curve, these deviations are apparently small. The data can be represented by a logarithmic curve over a broad temperature range from 0.1 to 0.001 °K from the Curie temperature. The authors also tried to fit the data to some power law, but it turns out that this can only be done for a much smaller temperature range, namely, between 0.01 and 0.001 °K from the Curie temperature. So it seems that the logarithmic shape is really the best one.

S. A. Friedberg presented experimental data for the specific heat and susceptibility of the antiferromagnet $CoCl_2\cdot6H_2O$ near its Néel point [11] drawing attention to the fact that these data satisfy Fisher's relation $C=Ad(\chi T)/dT$. It was further noted that the coefficient A yields a value for the curvature of the antiferro-paramagnetic phase boundary in the H–T plane at $H=0$ in good agreement with experiments.

E. Callen: I want to mention a quantity that one can measure and that gives essentially the same information as the specific heat. This is the magnetic contribution to the thermal expansion coefficient. This quantity is easier to obtain and in any case would allow an independent measurement of the same thing.

W. Marshall: Commenting on the paper of Dr. Heller, it is worth noting that the neutron scattering results of Turberfield [12] on manganese fluoride showed again explicitly the fact that the correlations in the a and b direction are more erratic than in the c direction as we would expect.

I have only one comment to make about the theory you described which, of course, pulls out all the essential physics but which is not actually strictly correct. This is because in the fluctuations which matter for you, there is a fluctuation near the superlattice vector and at the superlattice vector at high temperatures your response function does not follow an exponential decay. In fact you can show that its Fourier transform has a

Gaussian shape. Therefore, for example, the discrepancy between the λ you needed and the λ which was observed at high temperature may be due to a temperature dependence. However, a more important correction is probably due to the fact that the shape changes from Lorentzian to Gaussian as you go to high temperatures.

P. Martin: I am a little surprised that your theory agrees so well with experiment. We have been hearing that the molecular field theory is not adequate near T_c where it gives incorrect values for the temperature dependence of the susceptibility. Since the theory you have presented is basically a time dependent version of the same molecular field theory and the quantity you are calculating so closely related to the susceptibility, why does your theory work so well?

P. Heller: I agree that the molecular field theory should not be very accurate. In principle we could use the line width data to determine the actual temperature dependence of the susceptibilities in the critical region. I think that both the data and the theory are too crude for this purpose. The fact that theory and experiment agree as well as they do may be fortuitous. However, I feel that the qualitative nature of the line width anomaly has been correctly described by the theory.

References

[1] B. R. Livesay and E. J. Scheibner, J. Appl. Phys. **36**, 3240 (1965).
[2] J. C. Eisenstein, R. P. Hudson, and B. W. Mangum, Phys. Rev. **37**, A1886 (1965).
[3] J. C. Eisenstein, R. P. Hudson, and B. W. Mangum, Appl. Phys. Letters **5**, 231 (1964).
[4] E. Callen and H. Callen, J. Appl. Phys. **36**, 1140 (1965).
[5] H. B. Callen, Phys. Rev. **130**, 890 (1963).
[6] J. A. Copeland and H. A. Gersch, Bull. Am. Phys. Soc. **10**, 304 (1965).
[7] L. Tisza and P. M. Quay, Ann. Phys. (N.Y.) **25**, 48 (1963).
[8] D. R. Thompson and O. K. Rice, J. Amer. Chem. Soc. **86**, 3547 (1964).
[9] A. R. Miedema, R. F. Wielinga, and W. J. Huiskamp, Phys. Letters **17**, 87 (1965).
[10] A. R. Miedema, R. F. Wielinga, and W. J. Huiskamp, Physica **31**, 1234 (1965).
[11] J. Skalyo and S. A. Friedberg, Phys. Rev. Letters **13**, 133 (1964). J. Skalyo, A. F. Cohen and S. A. Friedberg, Proc. 9th Int. Conf. Low Temperature Physics, Columbus, Ohio, 1964.
[12] A. Okasaki, R. W. H. Stevenson and K. C. Turberfield, Proc. Intern. Conf. on Magnetism, Nottingham, 1964.

209-493 O-66—6

LOGARITHMIC SINGULARITIES

Chairman: C. N. Yang

The Lambda Transition in Liquid Helium*

W. M. Fairbank

Stanford University, Stanford, Calif.

and

C. F. Kellers

Wells College, Aurora, N.Y.

This talk is based on work done at Duke University several years ago by C. F. Kellers, M. J. Buckingham and myself [1]. A major part of the work constituted the Ph.D. thesis of Dr. Kellers [1b]. Much of what I will say has been previously reported [1]. Still, when Dr. Green asked me to give this talk I consented because I believed a review of the lambda transition in liquid helium is particularly pertinent to the present conference on critical phenomena. Not only were the Ehrenfest relationships for a second order transition enunciated first for the lambda transition in liquid helium, but liquid helium also served, through the experiments which I will describe, to first call attention to the logarithmic character of the lambda transition which is so much a part of the discussion of this conference.

The lambda transition in liquid helium is, of course, of particular interest because of the unique momentum ordering that takes place below the lambda point which makes it perhaps similar but certainly different from all other transitions. In addition, however, of all the cooperative transitions, it is the one which offers the best chance for experimental observations very close to the transition. Because liquid helium does not have any crystal structure, because it is a pure liquid changing at the lambda point only in its momentum ordering, it is apparently possible with sufficiently good thermal equilibrium to make measurements as close as experimental techniques permit to the lambda point without observing any of the broadening characteristics of other transitions.

Ever since London suggested that liquid helium represents in its superfluid phase a long-range order in momentum space, physicists have been puzzled by exactly what this means. London, Landau, Onsager, and Feynmann have suggested that liquid helium as a superfluid is required to be irrotational. If the helium rotates, it rotates according to the Onsager-Feynmann theory, with quantized vortex motion [2]. Helium rotating slowly enough is predicted to rotate in one single quantized state of rotation with each helium atom having angular momentum $\hbar$ regardless of the size of the bucket in which it is contained [2, 3]. The theoretical suggestion is then the following: If a bucket of helium no matter how large is cooled through the lambda transition into the superfluid state while rotating slowly enough, each superfluid helium atom will attain the same angular momentum. For the slowest stage the superfluid will stop rotating and the bucket, if suspended freely, will rotate faster [4]. This experiment has never been performed. Some physicists, including a graduate student George Hess at Stanford, are trying to perform this experiment [5]. This then is the type of order transition which is predicted for liquid helium, long-range order in momentum space of a very special kind.

Blatt, Butler, and Schafroth have taken another approach to the problem [6, 7, 8, 9]. They questioned whether a real liquid, as contrasted with an ideal Bose gas can exhibit arbitrarily long-range order or correlation in momentum space. They suggest that there may be a finite correlation length of approximately 10^{-5} cm over which helium atoms are correlated in momentum space, but beyond which there is no correlation at all. In particular, they developed a theory of a Bose liquid in which helium atoms are correlated over a distance of about 10^{-5} cm, the correlated atoms representing the superfluid. By calculating the amount of this correlated phase ρ, they calculate the ratio of uncorrelated to correlated phase (normal to superfluid, ρ_n/ρ_s) as a function of temperature, the correlation length being an adjustable parameter. With a cor-

*Supported in part by the National Science Foundation and the Army Research Office Durham.

relation length of 10^{-5} cm, they were able to accomplish something which to my knowledge had not been accomplished before. They were able to derive ρ_n/ρ_s as a function of temperature in agreement with experiment up through the lambda point and with the same theory, to derive the specific heat at the lambda point in quite good agreement with experiment both as to shape, magnitude, and temperature of the transition. Their theoretical curves are shown along with the then existing experimental data in figures 1 and 2. One characteristic new feature of this specific heat transition is that it is a quasi-transition. Instead of being a second-order transition with a discontinuity in the specific heat at the lambda point, the specific heat is rounded at the lambda point for a temperature interval of approximately 10^{-3} deg which is a direct result of a finite correlation length. This rounding could not have been observed in the then existing data. It also follows from their theory that curl $\mathbf{v}_s = 0$ is not an equilibrium property of superfluid helium II.

Feynmann [10] took issue with the premise that the correlation length in liquid helium could be cutoff at some finite distance, and suggested that the lambda point in liquid helium is not only sharp at one-thousandth of a degree from the lambda point but it is sharp at a hundred-thousandth of a degree. He believed that even though the correlation in liquid helium II gets weaker and weaker as the distance gets bigger, it still remains finite. Thus, no matter how large the bucket, liquid helium would still rotate in a single quantum state if the rotation were sufficiently slow.

At the expense of bringing you a free quote which was only told to me by Feynmann and therefore is not quoted from the literature, I am going to quote an exchange between Feynmann and Blatt because I think it illustrates the problem of long-range order very clearly for this conference. "Blatt, 'according to Feynmann', said to him, 'Feynmann, how is your intuition so good that you can say that there is a correlation between helium atoms separated by the size of the universe.' 'Feynmann said he replied', 'Blatt, how is your intuition so good that you can say a correlation which decreases as $1/r^2$ and is down by something like 10^{70} at the edge of the universe, doesn't exist'." That is just the point, this correlation falls off very rapidly. If the helium is to stop rotating in a rotating bucket when the bucket is cooled below the lambda point, then the rotational speed must decrease as $1/r^2$ as the size of the bucket becomes larger and larger.

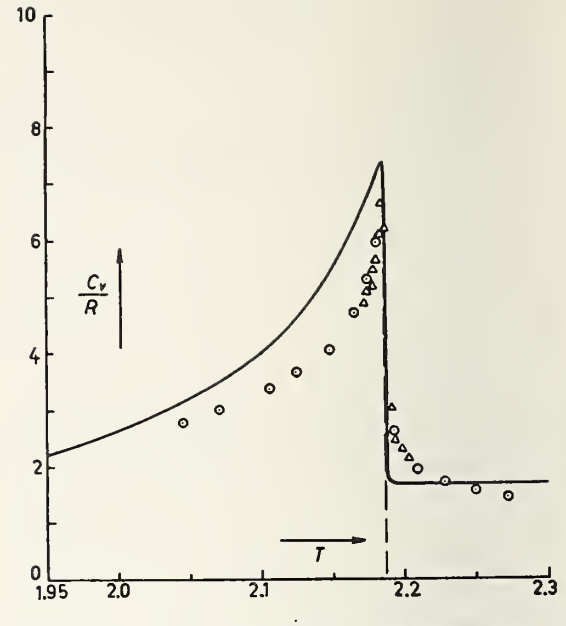

FIGURE 1. *The specific heat of liquid helium versus temperature in the neighborhood of the λ-point.*
The curve is theoretical, the experimental points are taken from Keesom: Helium (Amsterdam, 1942), Table 4.20. The theoretical curve is a continuous and differentiable function of temperature everywhere, represented by the same theoretical expression throughout the temperature region covered in ref. [8].

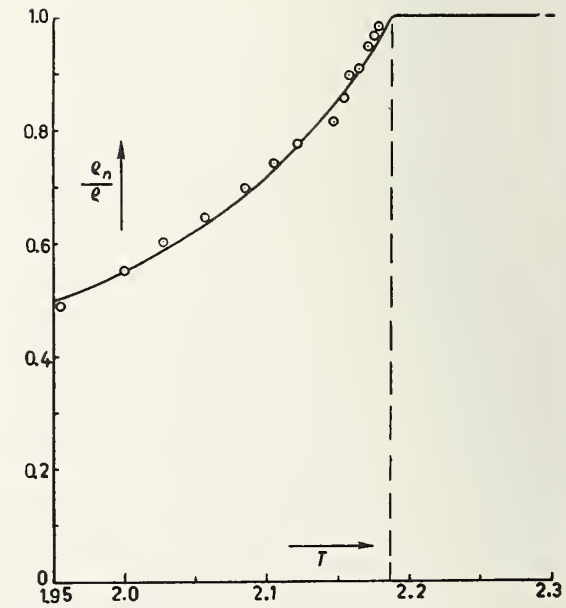

FIGURE 2. *The normal fluid concentration ρ_n/ρ in liquid helium versus temperature, in the neighborhood of the λ-point.*
The curve is theoretical, the experimental points are based on the second sound data of Pellam. The theoretical curve is a continuous and differentiable function of temperature everywhere, represented by the same theoretical expression throughout the temperature region covered in the ref. [9].

These conflicting theoretical predictions served as an incentive for us to perform a specific heat measurement to at least 10^{-5} deg of the lambda point. This experiment was performed by Buckingham, Kellers, and Fairbank, and has been reported in reference 1. Ultimately C_s was measured to within 10^{-6} deg of the lambda point T_λ, with equal precision both above and below T_λ. I would like to recall here just a few highlights of the experiment and comment on the possible significance of the data.

Many previous measurements have been made on the lambda point, including an unpublished master's degree thesis from our laboratory. The difficulty with all these earlier experiments was that reasonably large amounts of liquid helium was used in containers which were connected to the outside world.

To obtain the needed high temperature resolution it is essential that the attainment of equilibrium be unaffected by the drastic change of thermal conductivity of liquid helium at the lambda point, or by the onset of the creeping film. Both of these requirements were met by permanently sealing the helium (0.0587 g) in a cooper container (200 g), the inside of which was in the form of fins so placed that the helium was everywhere within 0.003 in. of the copper surface (fig. 3). With a heat input of 10 erg/s temperature equilibrium of greater than 10^{-6} deg could be obtained, even in the helium I region. In order to eliminate the need for removing exchange gas, the sealed container was suspended in a vacuum and a mechanical heat switch provided for contact with the bath when required.

Measurements were made by means of a carbon resistor with a minimal detectable change representing 2.10^{-7} deg. It was possible to make measurements both while increasing and decreasing the temperature.

Figure 4 shows the data. These of course are not new data just taken, but the reason I was asked to present them is that perhaps they are very similar to data which are now being obtained on other transitions. The specific heat, C_s, is plotted as ordinant versus $|T-T_\lambda|$. In order to show the nature of the transition very near the lambda point, the data are shown on successively expanded temperature scales. To aid in a visualization of the very large amount of expansion of each successive curve, a small vertical line has been drawn just above the origin. The width of the line indicating the fraction of the curve which is shown expanded in the curve directly to the right. The ratio of the expansion between

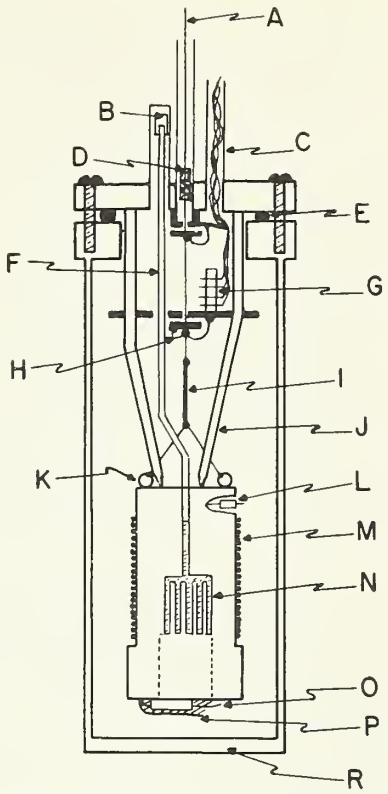

FIGURE 3. *Schematic diagram of adiabatic chamber for specific heat measurements [1c]: (A) stainless steel wire for closing heat switch; (B) brass cap on filling capillary; (C) wires connecting to heater and resistors on sample; (D) cotton plug dyed with carbon black as radiation trap; (E) indium "O" ring; (F) filling capillary; (G) Kovar seal used as thermal short for wires to sample; (H) radiation shield and thermal short for heat switch; (I) nylor cord; (J) three prongs of heat switch (copper); (K) indium coating and suspension for sample; (L) temperature-sensitive resistor; (M) heater; (N) sample cavity; (O) temperature-sensitive resistor; (P) copper shield over resistor; (R) calorimeter wall.*

Figure taken from ref. [1c].

the first and last curve is about 5×10^4. Thus if the projected slide of the first diagram is 10 ft, it would have to be expanded to 100 miles to obtain a 10 ft projection of the third figure.

It can be seen that as the specific heat is displayed on a more and more expanded scale, it maintains the same geometric shape. There is certainly no indication of a rounded quasi-transition as predicted by the theory of Blatt, Butler, and Schafroth.

Figure 5 shows the data in a form with which you are all now familiar. C_s has been plotted as ordinant against $T-T_\lambda$ in degrees Kelvin on a logarithmic scale. It is seen in this kind of a plot that near the lambda point on each side there is a factor of 10^4 in $T-T_\lambda$ over which the data fall in two

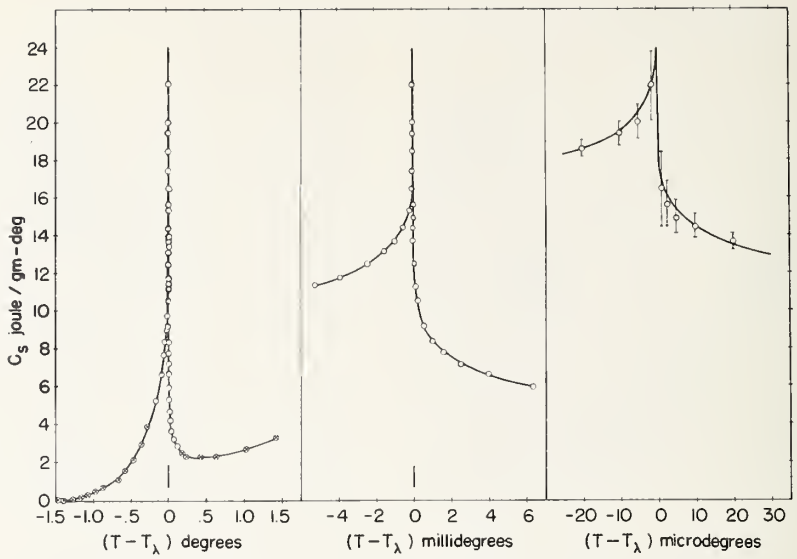

FIGURE 4. *Specific heat of liquid helium versus* $T-T_\lambda$ *in* °K [1].
0 represent data of Kellers, Fairbank and Buckingham [1]. ⊗ represent, above 1.5 °K, data of Hill and Lounasmaa [20] and Lounasmaa and Kojo [18] and, below 1.5 °K, data of Kramers, Wasscher, and Gorter [21]. Solid line near λ-point represents eq (1). Width of small vertical line just above origin indicates portion of diagram shown expanded (in width) in the curve directly to the right. Figure from ref. [1c].

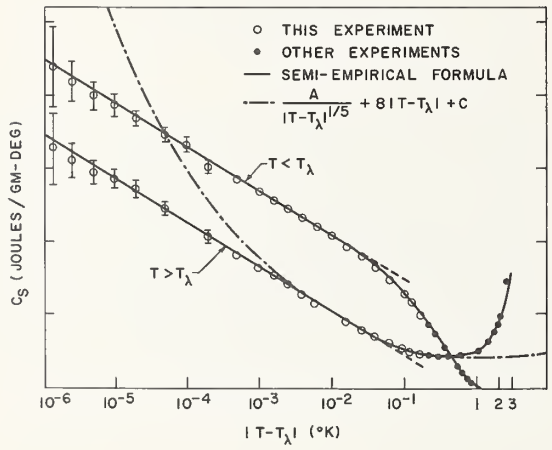

FIGURE 5. *The specific heat of liquid helium versus log* $|T-T_\lambda|$ [1].
0 represent data of Kellers, Fairbank and Buckingham [1]. ● represent, above 1.5 °K data of Hill and Lounasmaa [20] and Lounasmaa and Kojo [18] and, below 1.5 °K, data of Kramers, Wasscher, and Gorter [21]. Two parallel straight lines represent eq (1). The broken line represents formula shown in the figure. Figure from ref. [1c].

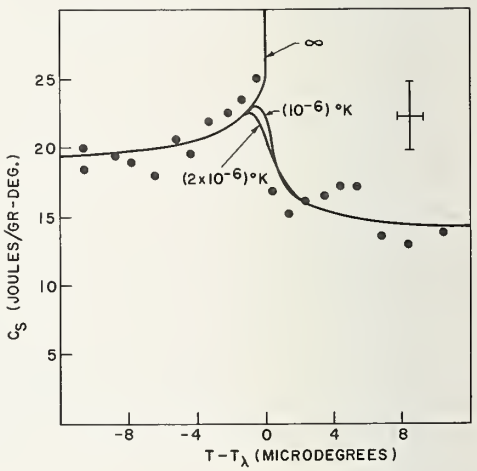

FIGURE 6. *Plot of* C_s *versus* $T-T_\lambda$ *very near* λ*-point.*
Data taken from one single run randomly selected from five runs where there were no disturbing influences. Figure from ref. [1b].

parallel straight lines which are branches of the expression

$$C_s = 4.55 - 3.00 \log_{10}|T - T_\lambda| - 5.20\Delta \qquad (1)$$

where $\Delta = 0$ for $T < T_\lambda$, and $\Delta = 1$ for $T > T_\lambda$. One reason that this was very interesting and exciting at the time, is that Onsager had published the exact solution of the two-dimensional Ising model [11]. The two-dimensional Ising model gives a logarithmic transition but only for an exact solution.

Figure 6 shows previously unpublished data from a single run taken from C. F. Keller's Ph.D. thesis [1b]. About 20 runs were taken back and forth through the lambda point over ±10 μdeg per minute. About half of the runs were discarded because the rate of cooling or heating at the beginning or end of the run was different. In about half of the remaining runs there was a big spike in the data due to someone opening the door and so forth. Of the remaining 5 runs, the one shown in figure 6 is typical and picked at random. The data is

averaged over 1 μdeg so the lambda point is still clearly observable. The three solid curves are placed in the diagram to show the effect of averaging over finite temperature intervals 10^{-6} deg Kelvin and 2×10^{-6} deg Kelvin. The curve labeled infinity is the curve given in eq (1) and represents infinite resolution. As stated above these data were averaged over 1 μdeg interval and should correspond to that curve labeled 10^{-6}.

Thus we see from the experimental data that the lambda point, instead of being a rounded quasi-transition as suggested by the theory of Blatt, Butler, and Schafroth assuming a finite correlation length, is in fact, sharp to at least 2 orders of magnitude closer in temperature to the lambda point than predicted by their theory. The simple logarithmic behavior of the data shown in figure 4 which extrapolates to a logarithmic singularity of the lambda point has stimulated more detailed experimental and theoretical investigation of the lambda point, as witnessed so completely by this conference. Although the two-dimensional Ising model has been solved exactly by Onsager giving such a logarithmic singularity, it is obvious from this conference that an exact solution to the three-dimensional Ising model will not be easily found.

In figure 5 the curve of the form

$$\frac{A}{|T-T_\lambda|^{1/5}}+B|T-T_\lambda|+C$$

which has been fitted to the data for $T-T_\lambda$ between 2×10^{-1} and 2×10^{-3} as shown. This is the fundamental form suggested by the Padé approximation of the three-dimensional Ising model. It is seen that although it fits the data rather well for $(T-T_\lambda)>2\times10^{-3}$°K, it departs very dramatically for temperatures closer to the lambda point. Unless data are obtained close enough to the lambda point one could not differentiate between this expression and the logarithmic singularity.

Much of this conference will be taken up with the exact nature of other kinds of lambda transitions. However, I wish to compare quickly two results by Robinson and Friedberg [12] and Skalyo and Friedberg [13] on the lambda transition in hydrated nickel and cobalt chloride with specific heat data on liquid helium.

Figure 7 shows the specific heat data of nickel chloride to within 0.07 °K of the lambda point from above, and within 0.2 °K from below the transition temperature. Figure 8 shows the same data with C_p plotted against $\log|T-T_\lambda|$. If one defines a reduced temperature by $t=|T-T_\lambda|/T_\lambda$ and compares the curve for nickel chloride with the helium curve, one sees for the same value of t both curves show nonparallel straight lines.

Figure 9 shows the data for cobalt chloride taken to smaller values of t. These data show two parallel straight lines and then a flattening out of the data.

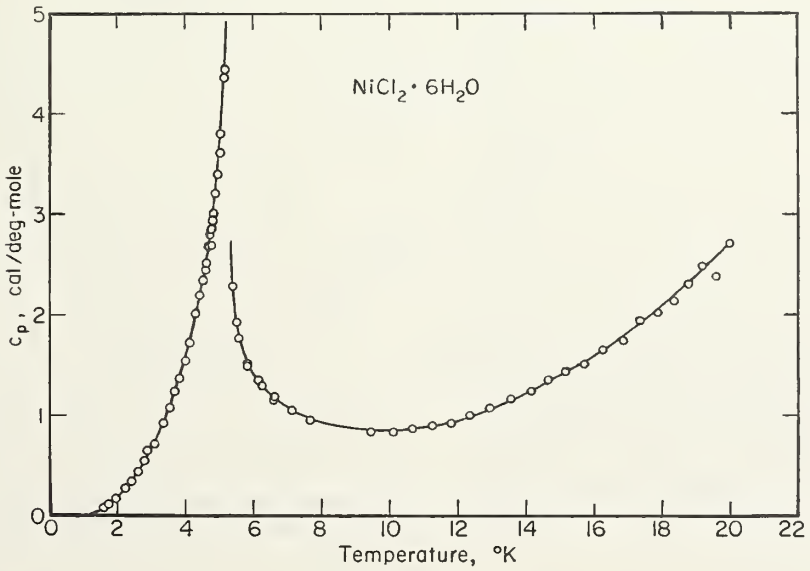

FIGURE 7. C_p *versus* $|T-T_N|$ *and* C_p *versus log* $|T-T_N|$ *for* $NiCl_2\cdot6H_2O$.
Data by Robinson and Friedberg taken from ref. [12].

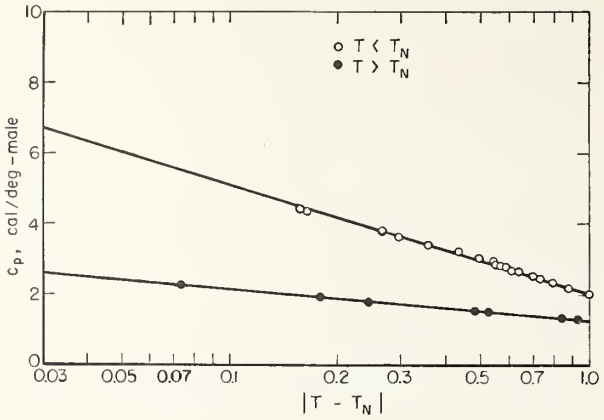

FIGURE 8. C_p *versus* $|T-T_N|$ *and* C_p *versus* $\log|T-T_N|$ *for* $NiCl_2 \cdot 6H_2O$.
Data by Robinson and Friedberg taken from ref. [12].

A comparison with helium indicate agreement as to the two parallel straight lines. The flattening out at values of t closer to the lambda point would be expected in either an experiment or theoretical model where long-range correlation is cutoff. These two sets of data are then seen to be consistent with the lambda transition for helium and indicates the possibility that other lambda points have the same form as the helium transition.

The suggestion that the specific heat of helium might become infinite at the lambda transition was first made by Tisza [14]. The first experimental evidence concerning the logarithmic nature of the lambda transition was obtained by Atkins and Edwards [15]. They suggested that a logarithmic term could be used to derive the result of their measurements of the thermal expansion coefficient below the lambda point. Figure 10 shows the data on the expansion coefficient of Atkins and Edwards, Chase and Maxwell, and Kerr and Taylor. It is seen that the data can be represented by two parallel straight lines from the plot of the expansion coefficient versus $\log(T-T_\lambda)$. This curve is reproduced from the paper by Kerr and Taylor [16]. Figure 11 shows the relative molar volume of helium in the vicinity of the lambda point as given by Kerr and Taylor. It is seen that the lambda point comes where the slope is infinite rather than at the point where the molar volume is minimum.

Buckingham [1c] has derived rigorously the thermodynamic consequences of lambda transitions characterized by the absence of a latent heat, but at which the specific heat at constant pressure becomes infinite. Pippard [17] had previously considered such a transition and worked out thermodynamic relationships based on the assumption that the entropy surface is cylindrical near the lambda point. The thermodynamic relationships worked out by Buckingham and Pippard can be

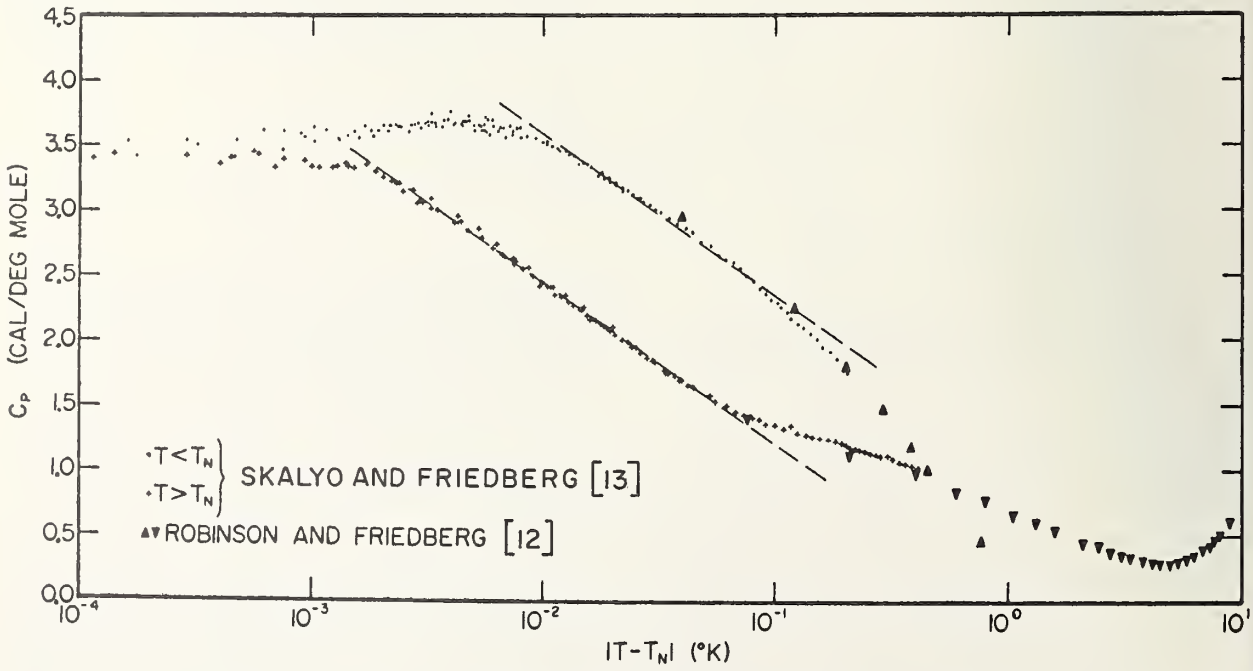

FIGURE 9. *The heat capacity,* C_p, *of* $CoCl_2 \cdot 6H_2O$ *as a function of* $\ln|T-T_N|$ *for* $T_N = 2.2890$ °K.
Figure taken from ref. [13].

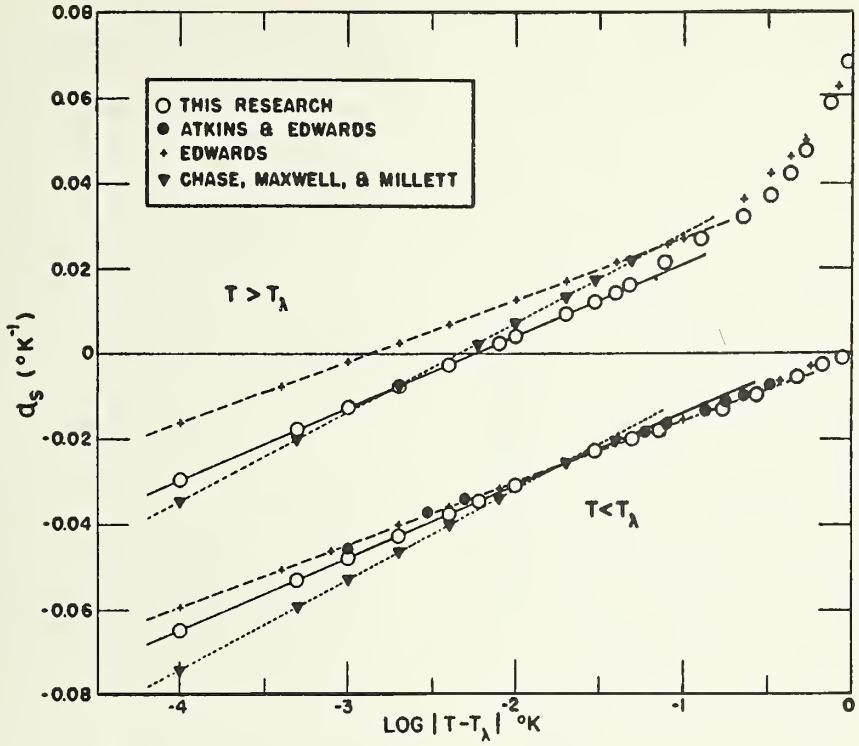

FIGURE 10. *The expansion coefficient, α_s, near the λ-point as a function of* $\log|T-T_\lambda|$.
Curve from Kerr and Taylor. Figure taken from ref. [16].

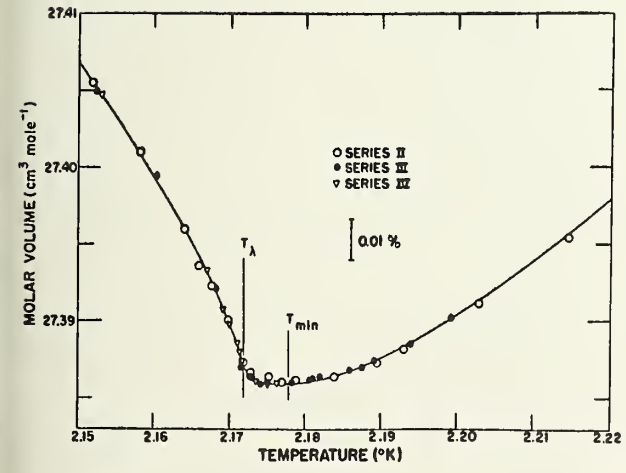

FIGURE 11. *The molar volume of He^4 in the vicinity of the λ-point.*
Data by Kerr and Taylor. Figure from ref. [16].

used to compare the behavior of various thermodynamic properties in the neighborhood of the lambda line [1c]. In reference 1c and 16 the specific heat and coefficient of expansion are compared using the Buckingham relationship. The slope of the lambda line $(\partial S/\partial T)_\lambda$ is taken from the data of Lounasmaa and Kojo [18] and Lounasmaa and Kaunisto [19]. The data can be plotted in a parametric plot which should give asymptotically a single straight line. Two parallel straight lines are obtained by Kerr and Taylor using the data shown in figures 4 and 10. This shows that the fundamental form of the data is correct but the details need to be refined. It is difficult to obtain exactly the same experimental conditions in different experiments very close to the lambda point. It seems worthwhile to make simultaneous specific heat and expansion coefficient measurements to within 10^{-6} °K of the lambda transition.

The behavior of the velocity of sound in the vicinity of the lambda point can also be predicted using specific heat and other thermodynamic data [1c]. Here again there is approximate but not exact agreement. Since there will be a separate talk on this subject I will not present further data here.

So in summary, the specific heat expansion coefficient and velocity of sound all give evidence to the logarithmic nature of the lambda transition in helium although refined details of comparison still need to be worked out. I would like to end by again mentioning that liquid helium presents the unique opportunity to obtain data close to the lambda point. The question naturally arises, is the transition in liquid

helium similar to lambda transition in other substances, and does liquid helium present an idealized experimental model for all lambda transitions? At first glance one might think that liquid helium doesn't. I would, however, like to point out a sense in which liquid helium does present such a model; a sense that has been emphasized by Buckingham in private discussions.

When one goes from the normal liquid to the superfluid in liquid helium, one gets a change from a normal system to something which is suddenly ordered throughout the whole container. In this particular case, it is an ordering in the superfluid. The superfluid atom in one part of the container knows what is happening to the superfluid atom in a different part of the container, and how long that order is depends only on the size of the container. One can disturb the system without destroying this order throughout the entire system provided the disturbances, for example rotational speeds, become smaller and smaller as the size of the system becomes larger and larger.

In the case of superconductors one has a quantized magnetic flux over supposedly the distance of the length of the wire in superconducting magnets that may be thousands of feet long. The length of the ordering depends only on the size of the superconducting loop and especially in the case of superconductors, exists in the presence of large quantities of impurities. Now there is different kind of order parameter in superconductors and that is the length of the correlation between electrons in a pair. This is only 10^{-4} cm, but the two electrons in a pair have equal and opposite momentum. The momentum of each pair is zero and therefore every pair throughout the whole superconductor has the same zero momentum. Thus there is a long-range order in momentum throughout the entire superconductor even though each pair is paired over 10^{-4} cm.

One doesn't have this momentum ordering in any other kinds of transition besides superconductors and liquid helium. But on the other hand, as Buckingham is going to point out at the end of the morning, one has a transition from a state where ordering exists within a small cluster in a particular part of a container, to a system where one has suddenly, for example in a liquid gas transition, order throughout the entire container. Part of the atoms have one special density and they are all together in the container, and all the rest of the atoms have a different density. This sudden transition is to a state of order which depends only on the size of the container.

I want to close with this question. Is the lambda transition in liquid helium, except for the fact that one has a lambda line, an exact model for other transitions when long-range correlations are not cutoff in other experiment systems or theoretical models?

References

[1] (a) W. M. Fairbank, M. J. Buckingham, and C. F. Kellers, Proc. 5th Int. Conf. Low Temp. Phys. (Madison, Wis., 1957), p. 50; (b) C. F. Kellers: Thesis (Duke University, 1960); (c) M. J. Buckingham and W. M. Fairbank, Progress in Low Temperature Physics, Vol. **3**, edited by C. J. Gorter (Amsterdam, 1961), ch. III; (d) W. M. Fairbank, Estratto da Rendiconti della Scuola Internazionale di Fisica (E. Fermi) XXI Corso.

[2] R. P. Feynmann, Progress in Low Temperature Physics, ch. 2.

[3] F. London, Superfluids, Vol. **II**, (John Wiley & Sons, New York, N.Y., 1954).

[4] H. London, Physical Society 1946 Cambridge Conference Report (London, 1947) p. 48.

[5] W. M. Fairbank and C. B. Hess, Angular Momentum of Helium II in a Rotating Cylinder (Proceedings of the IX International Conference on Low Temperature Physics, p. 188 (Plenum Press, New York, 1965).

[6] J. M. Blatt, S. T. Butler, and M. R. Schafroth, Phys. Rev. **100**, 481 (1955).

[7] S. T. Butler and J. M. Blatt, Phys. Rev. **100**, 495 (1955).

[8] S. T. Butler, J. M. Blatt, and M. R. Schafroth, Nuovo Cimento **4**, 674 (1956).

[9] J. M. Blatt, S. T. Butler, and M. R. Schafroth, Nuovo Cimento **4**, 676 (1956).

[10] R. P. Feynmann, private communication.

[11] L. Onsager: Phys. Rev. **65**, 117 (1944); G. G. Newell and E. W. Montroll: Rev. Mod. Phys. **25**, 353 (1953).

[12] W. K. Robinson and S. A. Friedberg, Phys. Rev. **117**, 402 (1960).

[13] J. Skalyo and S. A. Friedberg, Phys. Rev. Letters **13**, 133 (1964). See also the discussion remark of Dr. Friedberg on page 66.

[14] L. Tisza, Phase Transformations in Solids, edited by Smolychowski, Mayer, and Weyl (New York, 1951).

[15] K. R. Atkins and M. H. Edwards, Phys. Rev. **97**, 1429 (1955).

[16] E. C. Kerr and R. D. Taylor, Annals of Physics **26**, 292–306 (1964).

[17] A. B. Pippard: The Elements of Classical Thermodynamics (Cambridge, 1957), ch. IX.

[18] O. V. Lounasmaa and E. Kojo, Physica **36**, 3 (1959).

[19] O. V. Lounasmaa and L. Kaunisto, Ann. Acad. Sci. Fennicae **A6**, No. 59 (1960).

[20] R. W. Hill and O. V. Lounasmaa, Phil. Mag. **2**, 145 (1957).

[21] H. C. Kramers, J. D. Wasscher, and C. J. Gorter, Physica **18**, 329 (1952).

The Specific Heat of He^3 and He^4 in the Neighborhood of Their Critical Points*

M. R. Moldover and W. A. Little

Stanford University, Stanford, Calif.

Introduction

Recently Bagatskiĭ, Voronel', and Gusak [1] showed that the specific heat at constant volume of argon exhibited what appears to be a logarithmic singularity at the critical temperature (T_c) for measurements taken at a density near the critical density. This singular behavior is in sharp contrast to the predictions of the traditional view of this phase transition by Landau and Lifshitz [2]. However, the behavior is precisely that to be expected for the so-called "lattice gas" model for the liquid-gas transition. Lee and Yang [3] have shown that the partition function of a classical gas of particles moving on a discrete lattice with a repulsive force preventing double occupancy of any site, and a nearest neighbor attraction can be mapped precisely onto the partition function of an Ising model of a spin system in an external magnetic field. The specific heat for this Ising model in zero field exhibits a logarithmic singularity at the Curie point. The specific heat for the corresponding lattice gas on the critical isochore exhibits a logarithmic singularity at the critical point. The measurements on argon then indicate that for a *real* gas the specific heat behaves in a similar manner to that of a lattice gas. We have investigated this point further by studying the specific heat at constant volume (C_v) of both He^3 and He^4 at densities close to the critical density. We have done this for two main reasons. Firstly, to see whether the behavior observed for argon is also observed for helium, for which quantum effects should be important, and secondly, to investigate the detailed nature of the singularity in the pressure-density plane, not only *on* the critical density, but also in its immediate neighborhood. Yang and Yang [4] have conjectured that the quantum effects would reduce the magnitude of the singular contribution to the specific heat in helium. Our results confirm this view.

*Work supported in part by the National Science Foundation and the Office of Naval Research.

Experimental Procedure

There are several practical advantages to using helium rather than another noble gas for C_v measurements near the critical point. The low heat capacity of metals at liquid helium temperature permits one to use a massive calorimeter of large surface to volume ratio. Thus the path for heat transfer through the helium may be kept short. In addition, more nearly adiabatic conditions and high resolution thermometry are most easily attained at liquid helium temperatures.

Our calorimeter was built of two OFHC copper parts. The helium was contained in the lower part in 50 slots. Each slot was 0.01 cm wide to facilitate good thermal contact between the calorimeter and the helium. The slots were made only 0.3 cm deep in an effort to minimize possible gravitational effects. [In contrast a thin stainless steel shell 10 cm high and 4 cm in diameter containing a magnetic stirrer was used for the work on argon [1, 5]. This construction was necessary to obtain a low ratio of heat capacity of the calorimeter to its contents while maintaining constant volume at the high critical pressure of argon.] The lower part of our calorimeter was wound with a constantan heater and had a carbon resistor clamped and cemented to it. The calorimeter was supported on nylon threads in an evacuated chamber. Thermal contact to the bath was made with a mechanical heat switch. A stainless steel filling capillary 5 in. in length and 0.006 in. I.D. led from the calorimeter to a needle valve. The dead volume was about ½ percent of the total volume of the calorimeter. The helium was admitted to the calorimeter via a Toeppler pump which was used to measure the volume of gas to an accuracy of about 0.2 percent.

One of the precautions taken was the measurement of the stray heat input to the calorimeter before and after each data point. The approach to temperature equilibrium of the calorimeter was observed after each heating interval. As T_c was

approached, the equilibrium time increased from a few seconds to several minutes and became one of the limiting factors in this measurement.

A 1/10 W Ohmite carbon resistor of nominal resistance 560 Ω was used as a secondary thermometer. Its resistance was measured with a 100 c/s bridge using a lock-in amplifier. Temperature changes of about 2×10^{-6} °K at 5.2 °K and 1×10^{-6} °K at 3.3 °K could be observed. At the end of a run exchange gas was admitted to the vacuum space and the resistor was calibrated against the vapor pressure of the He^4 bath using the T_{58} scale either from 4.2 to 2.9 °K or from 5.15 to 4.2 °K depending on whether He^3 ($T_c=3.3$ °K) or He^4 ($T_c=5.2$ °K) was being studied. A smooth resistance-temperature relation was fitted. Hence relative specific heat measurements near the critical points are not sensitive to errors either in the calibration or in the vapor pressure-temperature scale near T_c. Calibration was always done as the bath temperature was reduced. A hydrostatic head correction was made. All residuals were less than 8×10^{-4} °K from a fit to the Clement-Quinnell [6] formula and less than 3×10^{-4} °K from a four constant formula. Each run, T_c was tentatively defined as the temperature at which C_v for a density near ρ_c fell most abruptly. The final value of T_c was then chosen to give the best fit to

$$\frac{C_v}{R}=-a\log_e\left(\frac{T_c-T}{T_c}\right)+b \qquad (1)$$

over the range 10^{-3} °K $<(T_c-T)<10^{-1}$ °K. The adjustment was less than 3×10^{-4} °K. This value of T_c was also used for analyzing data taken during the same run at densities far from ρ_c. On four separate runs with He^4, T_c was found to be 5.189 $\pm$0.001 °K. This is considerably below the value $T_c=5.1994$ °K defined on the T_{58} temperature scale. A single run with He^3 also yielded a value for T_c well below the accepted value.

Results

Figure 1 is a general view of the specific heats at the critical density of He^3 and He^4 at low temperatures [7]. We have indicated the temperature range covered by these measurements. In figure 2 we have plotted on both a linear and logarithmic scale measurements of C_v of He^4 at a density within 0.5 percent of the critical density. In the two

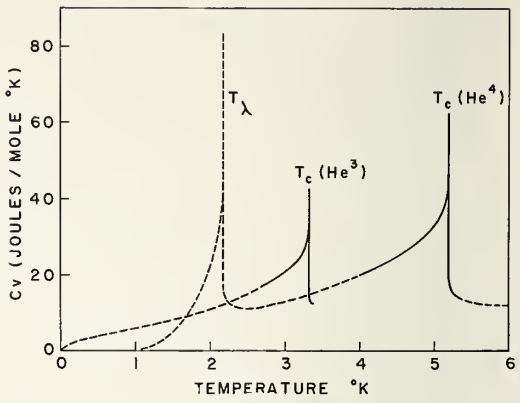

FIGURE 1. C_v *of* He^3 *and* He^4 *at their respective critical densities is plotted as a function of temperature.*
The solid curves are the present work.

phase region below T_c, C_v exhibits logarithmic behavior.

In the one phase region above T_c two alternatives have been suggested: First, $C_v\propto\log(T-T_c)$ has been suggested by an exact calculation on a two dimensional Ising model [9], by C_v measurements on argon [1] and oxygen [8], and by velocity of sound measurements on helium four [10]. Second, $C_v\propto(T-T_c)^{-\alpha}$ for some small positive α (such as 1/5) has been suggested by Fisher [11] on the basis of approximate calculations on a three dimensional Ising model and his analysis of the argon and oxygen data. We do not believe the present data permit one to distinguish between these two alternatives.

In figure 3 similar plots are given for He^3 for a density of $0.98^5\rho_c$. Logarithmic behavior is again observed for $T<T_c$. The data for argon, oxygen [8], and both isotopes of helium expressed in the dimensionless form (1) are summarized in table 1. We see that the coefficient a decreases from Ar to He^4 to He^3 in agreement with the conjecture of Yang and Yang [4]. We note that the coefficient 0.62 for He^4 is very close to that observed for the specific heat along the saturated vapor pressure curve near the λ-point of He^4 (0.64) by Buckingham and Fairbank [12] and may have particular significance in explaining the quantum transition.

Yang and Yang [4] have pointed out that one may write in the two phase region,

$$C_v=-NT\left(\frac{d^2\mu}{dT^2}\right)_v+VT\left(\frac{d^2P}{dT^2}\right)_v \qquad (2$$

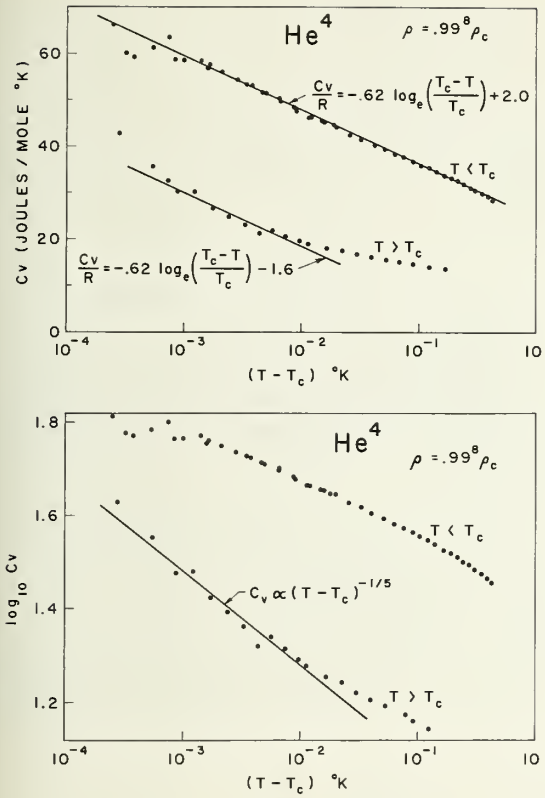

FIGURE 2. C_v *of* He^4 *is plotted against* $|T-T_c|$ *at a density of* $0.99_8\rho_c$.

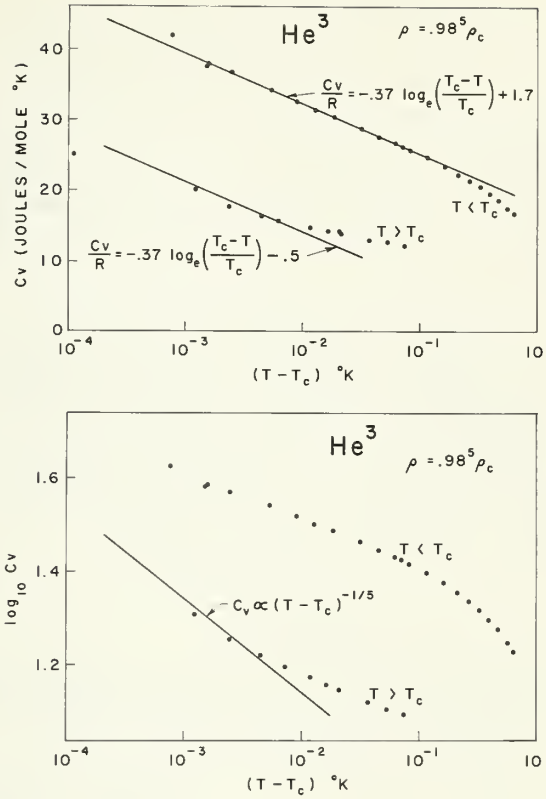

FIGURE 3. C_v *of* He^3 *is plotted against* $|T-T_c|$ *at a density of* $0.98\,\rho_c$.

TABLE 1. *Coefficients* a *and* b *of eq (1) for* O_2, Ar, He^4, *and* He^3

Element	a	b: $T<T_c$
O_2	2.4	10
Ar	1.8	8
He^4	0.62	2.0
He^3	.37	1.7

where μ is the chemical potential. They suggest that both $(d^2\mu/dT^2)_v$ and $(d^2P/dT^2)_v$ become infinite at T_c for a real gas, whereas $(d^2\mu/dT^2)_v=0$ for the two dimensional Ising model. Figure 4 shows data on He^4 taken at the densities 0.96 ρ_c and 1.07 ρ_c. T_c for these plots was chosen from data (not shown) taken during the same run at 0.99 ρ_c. The two phase region (lower temperatures) is the upper branch of each curve. The difference between the upper branches in this region is proportional to $(d^2P/dT^2)_v$. It is clear that $(d^2P/dT^2)_v$ does not approach zero as T approaches T_c. A similar plot with the ordinate heat capacity/volume rather than heat capacity/mole indicates that $(d^2\mu/dT^2)_v$ also does not approach zero as T approaches T_c. This is consistent with the suggestion of Yang and Yang.

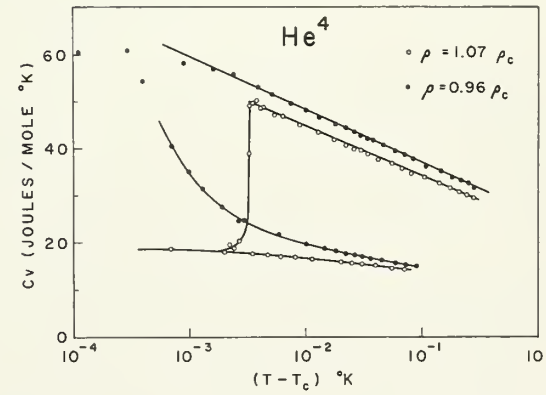

FIGURE 4. C_v *of* He^4 *is plotted against* $|T-T_c|$ *at densities of* 1.07 ρ_c *and* 0.96 ρ_c.

In the one phase region the two curves on figure 4 differ drastically. This suggests particular attention to density measurements will be required to determine behavior at the critical density. We also note the transition to the one phase region is particularly well marked in the case of $\rho = 1.07\ \rho_c$. This suggests specific heat measurements may be a sensitive method of determining the coexistence curve.

We thank Dr. Derek Griffiths, Dr. R. S. Safrata, Dr. C. F. Kellers, and Dr. M. H. Edwards for many useful discussions and Dr. Derek Griffiths and Donald Moldover for much help in analyzing data. We thank Professor C. N. Yang for his suggestions, interest and advice. Some of this data was presented at the LT9 Conference in 1964.

References

[1] M. I. Bagatskiĭ, A. V. Voronel', and V. G. Gusak, Zh. Eksperim. i Teor. Fiz. **43**, 728 (1962). [English Transl: Soviet Phys.—JETP **16**, 517 (1963)].

[2] L. D. Landau and E. M. Lifshitz, Statistical-Physics (Addison-Wesley Publishing Co., Inc., Reading, Mass., 1958).

[3] T. D. Lee and C. N. Yang, Phys. Rev. **87**, 410 (1952).

[4] C. N. Yang and C. P. Yang, Phys. Rev. Letters, **13**, 303 (1964).

[5] A. V. Voronel' and P. G. Strelkov, PTE **6**, 111 (1960). [English Transl: Cryogenics (G. B.), **2**, 91 (1961)].

[6] J. R. Clement and E. H. Quinnell, Rev. Sci. Instr. **23**, 213 (1952).

[7] The dashed curve for He^4 was calculated from data of ref. 12; R. W. Hill and O. V. Lounasmaa, Phil. Mag. **2**, Ser. 8, 145 (1957); O. V. Lounasmaa and E. Kojo, Series A., VI. Physica **36**, 3 (1959); H. C. Kramers, J. D. Wasscher and C. J. Gorter, Physica **18**, 329 (1952); M. H. Edwards, Canad. J. Phys. **36**, 884 (1958); H. van Dijk, M. Durieux, J. R. Clement, and J. K. Logan, J. Res. NBS **64A** (Phys. and Chem.) No. 1, 1 (1960). The dashed curve for He^3 was calculated from data of Henry Laquer, Stephen G. Sydoriak, and Thomas R. Roberts, Phys. Rev. **113**, 417 (1959); R. H. Sherman, S. G. Sydoriak, and T. R. Roberts, J. Res. NBS **68A** (Phys. and Chem.) No. 6, 579 (1964); and T. R. Roberts and S. G. Sydoriak, Phys. Rev. **98**, 1672 (1955).

[8] A. V. Voronel', Yu R. Chashkin, V. A. Popov, and V. G. Simkin, Zh. Eksperim. i Teor. Fiz. **45**, 828 (1963) [English Transl: Soviet Phys.—JETP **18**, 568 (1964)].

[9] L. Onsager, Phys. Rev. **65**, 117 (1944).

[10] C. E. Chase, R. C. Williamson, and Laszlo Tisza, Phys. Rev. Letters **13**, 467 (1964).

[11] Michael E. Fisher, Phys. Rev. **136**, A1599 (1964).

[12] M. J. Buckingham and W. M. Fairbank, The Nature of the λ-Transition, Progress in Low Temperature Physics, **III**. P. 86 (North Holland Publishing Co., Amsterdam, 1961).

The Coexistence Curve of He^4

M. H. Edwards*

Stanford University, Stanford, Calif.

During the years between 1956 and 1963 I measured the density of saturated He^4 liquid and vapor along the coexistence curve from 0.30 to 0.99 T_c, by refractive index measurements with a modified Jamin interferometer [1–3]. Between 0.95 and 0.993 T_c, 76 experimental points were taken. Advantages of this method of density measurement near the critical point are

1. High resolution of density to ~ 0.01 percent is possible.

2. There are *no* dead space corrections to the observed densities.

3. The density of a horizontal "slice" only 1 mm deep is measured and hydrostatic head effects were always less than 0.05 percent in density.

4. If temperature inhomogeneities of $\sim 10^{-4}$ °K appear in the optical cell the fringes disappear and *no* results are obtained.

We analyzed our data on the coexistence curve between 0.98 and 0.993 T_c by extending Landau and Lifshitz's theory using a fit to a power series expansion in volume and temperature [3]. If, as is now believed, the critical point is a singular point, this whole expansion procedure is questionable, since the coexistence curve cannot in principle be represented asymptotically by a Taylor series in the density about such a nonanalytic point. A reanalysis of this same data will now be presented, without the use of a Taylor series expansion.

The coexistence curve of saturated liquid and vapor densities ρ_l and ρ_g as a function of temperature, is symmetrical, not about the critical density, but about a "rectilinear diameter." This line of mean densities of vapor and liquid passes through ρ_c, the critical density, and for He^4 would extrapolate linearly to 1.1 ρ_c at $T = 0$. The symmetry of the coexistence curve is obscured on a plot of sat-

* On leave from Royal Military College, Kingston, Ontario, Canada.

urated molar volume V_l and V_g of liquid and vapor since the mean volume curves sharply away from the temperature axis at lower temperatures. In examinations of the shape of coexistence curves, it is customary to consider the quantity $(\rho_l-\rho_g)$ or $(\rho_l-\rho_g)/2\rho_c$ as a function of (T_c-T). If one attempts to write

$$\frac{\rho_l-\rho_g}{2\rho_c}=A(T_c-T)^{\beta}. \tag{1}$$

where A and β are constants, then classically (van der Waals), $\beta=1/2$, whereas a variety of experiments suggest that $\beta=1/3$ for a certain range of temperatures. Accurate values of T_c are needed for meaningful tests of such a relationship. Furthermore, the slope of the "rectilinear diameter," or line of mean densities, differs from substance to substance, so that the similarity of coexistence curves may be obscured by comparing experimental data in that manner. M. J. Buckingham has suggested that the shape of the coexistence curve should be analyzed using the natural variable

$$X\equiv\frac{\rho_l-\rho_g}{\rho_l+\rho_g}\equiv\frac{V_g-V_l}{V_g+V_l}\neq\frac{\rho_l-\rho_g}{2\rho_c}. \tag{2}$$

Advantages of this variable are

(1) X ranges from 1 to 0 as T ranges from 0 to T_c for any substance,

(2) there is equal symmetry using either density or molar volume, and the effect of the slope of the "rectilinear diameter" is entirely removed, and

(3) if we plot X^n, $\left(\text{where } n=\frac{1}{\beta}\right)$, against T, we need not know T_c or ρ_c or V_c and in fact may determine T_c by such plots.

Figure 1 shows how plots of X^2 (or $\beta=1/2$), and X^3 (or $\beta=1/3$), appear for He^4 over the whole range of measurements [1, 2, 3] from 0.3 to 0.99 T_c. Clearly, X^3 is nearly linear, (or $\beta=1/3$), above about 0.8 T_c (but not too near T_c, see later), in agreement with many other measurements for many fluids. Note that the classical X^2 is not linear over any extended range of temperature.

M. J. Buckingham has shown [4] that the simplest singular entropy surface which is consistent with a logarithmic infinity in C_v at the critical point, would imply a coexistence curve whose asymptotic form as $T\rightarrow T_c$ is given by

$$\frac{X^2}{1-\ln X}=at \tag{3}$$

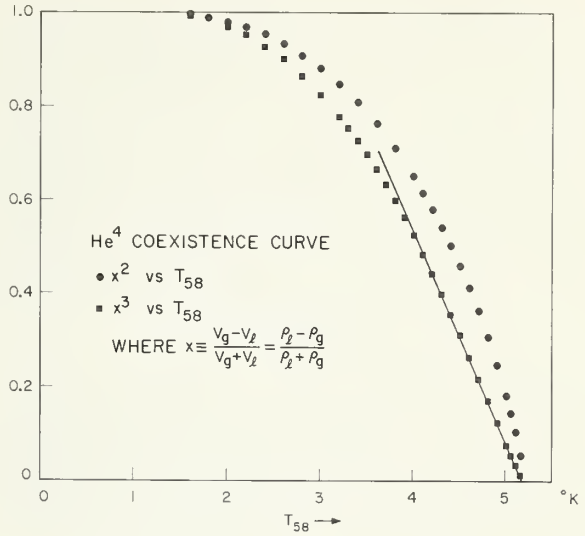

FIGURE 1. *Temperature dependence of* X^2 *and* X^3 *for* He^4. X^3 is linear above 0.8 T_c.

where a is a constant, and $t=T_c-T$. The quantity $X^2/(1-\ln X)$ lies between X^2 and X^3 for the whole temperature range.

The question of the asymptotic form of the coexistence curve of He^4 will now be examined using the 76 experimental points listed in table III of reference 3. All these points were taken within 250 mdeg of 5.1994 °K (the critical temperature of He^4 on the 1958 He^4 scale of temperatures [5]). The temperature of each data point was obtained directly from the measured saturated vapor pressure. Although both V_g and V_l were not often measured at precisely the same temperature, we may evaluate an X for each experimental point by writing

$$X=\frac{2V_g}{V_g+V_l}-1, \qquad \text{or } X=1-\frac{2V_l}{V_g+V_l}. \tag{4}$$

For each temperature at which either V_g or V_l was measured, the quantity (V_g+V_l), which varies rather slowly and smoothly with temperature, was read by interpolation, or, within 50 mdeg of T_c, by linear extrapolation. Thus 76 values of X are obtained within 250 mdeg of T_c. The added uncertainty in X produced by the uncertainty in the value of V_g+V_l falls from 0.6 percent at $t=35.9$ mdeg to below 0.3 percent above $t=50$ mdeg.

Figure 2 shows a graphical test of the three functional forms for the coexistence curve of He^4 for all points within 250 mdeg of 5.1994 °K. The straight line drawn on the plot of X^2 is a least-

209-493 O-66—7

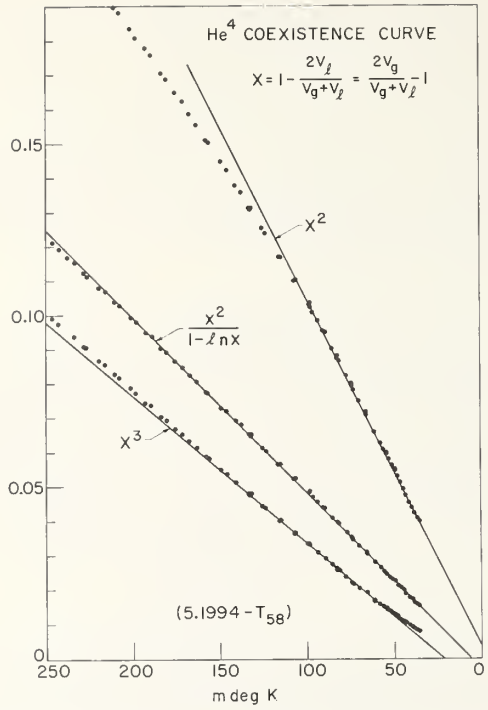

FIGURE 2. *Tests of the asymptotic form of the coexistence curve for* He^4 *above 0.95* T_c.

squares-fitted straight line for the 39 points within 100 mdeg of T_c. The lines shown on the plots of $X^2/(1-\ln X)$ and of X^3 are least-squares-fitted lines for the 65 points within 200 mdeg of T_c. Clearly over this temperature range the data are represented best by the function $X^2/(1-\ln X)$. Note particularly the marked curvature of X^3 as $T \to T_c$.

Table 1 shows the slopes and intercepts, with standard errors, computed by least squares fits of the data in the form

$$f(X_i) = at_i + a\Delta T_c \qquad (5$$

where $f(X)$ is X^2, $X^2/(1-\ln X)$, or X^3, and where $t = 5.1994 - T_{58}$, in millidegrees, and $\Delta T =$ the shift in critical point implied by a linear extrapolation of $f(X)$ to zero. None of these asymptotic fits extrapolates to the value $T_c = 5.1994$ °K assumed in the T_{58} scale of temperatures. Yang and Yang [6] have suggested that the T_{58} scale may be in error near T_c, and that the actual critical temperature should be lower.

As a more sensitive test of the experimental evidence in favor of any of these functional forms for the coexistence curve, we plot the residuals

$$\Delta t_i = t_i - \frac{1}{a} f(X_i) - \Delta T_c \qquad (6$$

for each of six fits with $f(X)$ equal to X^2, $X^2/(1-\ln X)$ and X^3, over the ranges $t < 100$ mdeg and

TABLE 1. *Linear fits of coexistence curve data to three functional forms*

	Range of data in fit			
	$t < 100$ mdeg (39 points)		$t < 200$ mdeg (65 points)	
$f(X)$	$10^3 a$ (mdeg K)$^{-1}$	ΔT_c mdeg K	$10^3 a$ (mdeg K)$^{-1}$	ΔT_c mdeg K
X^2	1.005 ± 0.004	$+4.2 \pm 0.3$	0.882 ± 0.007	$+14.2 \pm 0.9$
$\frac{X^2}{1-\ln X}$	0.527 ± 0.002	-7.5 ± 0.3	0.513 ± 0.001	-5.9 ± 0.3
X^3	0.404 ± 0.003	-18.1 ± 0.4	0.429 ± 0.002	-20.8 ± 0.4

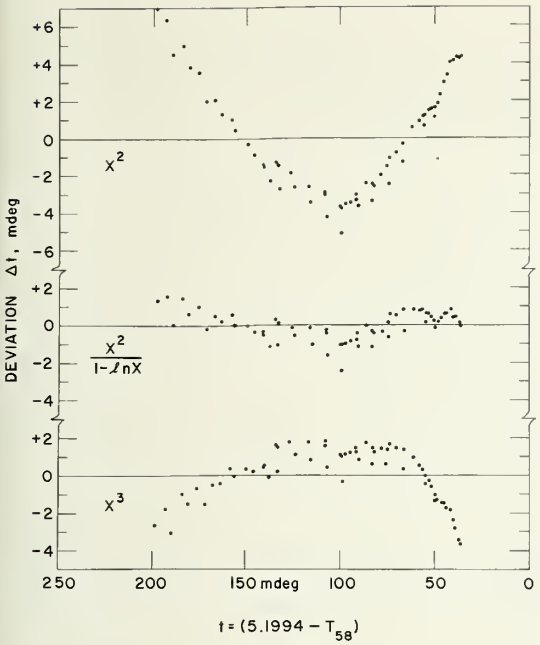

FIGURE 3. *Deviations from linearity, expressed in millidegrees, for linear fits of the data for* $t < 200$ *mdeg for the three functions* $f(X) = X^2$, $X^2/(1 - \ln X)$ *and* X^3.

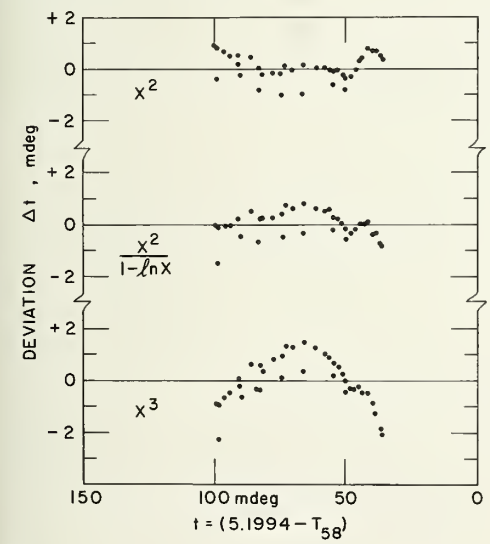

FIGURE 4. *Deviations from linearity, expressed in millidegrees, for linear fits of the data for* $t < 100$ *mdeg for the three functions* $f(x) = x^2$, $x^2/(1 - \ln x)$, *and* x^3.

$t < 200$ mdeg. Figures 3 and 4 are plots of these deviations from linearity, expressed in millidegrees. Figure 3 shows clearly that both X^2 and X^3 show systematic deviations fitted within 200 mdeg of T. Figure 4 shows that, using only the data points within 100 mdeg, both X^2 and $X^2/(1 - \ln X)$ appear to give almost equally good fits. However, $X^2/(1 - \ln X)$ gives much the best fit when all points within 200 mdeg of T_c are included.

Conclusions

The main conclusions of this analysis of the form of the He^4 coexistence curve are

1. X^3 is not asymptotically linear in T above about 0.98 T_c, despite its linearity from 0.8 to 0.98 T_c.

2. X^2 can be shown to be asymptotically linear only above 0.98 T_c, with the critical temperature 4 mdeg above the T_{58} value. Such a shift is in the opposite sense to that expected [6], and this functional form is inconsistent with the observed [7] logarithmic singularity in C_v below T_c.

3. $X^2/(1 - \ln X)$ is the best asymptotic form, with the critical point lowered 6 to 8 mdeg below the T_{58} value. This shift is in the sense expected [6], and the functional form is consistent [4] with the observed [7] logarithmic singularity in C_v below T_c.

I am grateful to M. J. Buckingham and M. R. Moldover for many discussions.

References

[1] M. H. Edwards, Can. J. Phys. **34**, 898 (1956); **36**, 884 (1958).
[2] M. H. Edwards, Phys. Rev. **108**, 1243 (1957).
[3] M. H. Edwards, and W. C. Woodbury, Phys. Rev. **129**, 1911 (1963).
[4] M. J. Buckingham, These proceedings.
[5] F. G. Brickwedde, H. van Dijk, M. Durieux, J. R. Clement, and J. K. Logan, J. Res. NBS **64A** (Phys. and Chem.) No. 1, 1 (1960).
[6] C. N. Yang and C. P. Yang, Phys. Rev. Letters **13**, 303 (1964).
[7] M. Moldover and W. A. Little, Proc. Ninth International Conference on Low Temperature Physics (Plenum Press, New York, 1965), to be published, and These proceedings.

Anomalous Specific Heats Associated With Phase Transitions of the Second Kind

T. Yamamoto, O. Tanimoto, Y. Yasuda, and K. Okada

Kyoto University, Kyoto, Japan

There are many reasons to expect a logarithmic singularity in the anomalous specific heat accompanied with the phase transition of the second kind. From the theoretical side one may refer to the classical work of Onsager [1] and the recent intensive investigations by Domb and Sykes, Fisher and others [2]. From the experimental side one may refer to at least three elaborate measurements of specific heat: the first is the experiment by Fairbank, Buckingham, and Kellers on the λ-transition of liquid He^4 [3], the second is that by Voronel' and his collaborators on the liquid-gas transition at the critical point [4], and the third is that by Skalyo and Friedberg on the antiferromagnetic transition of $CoCl_2 \cdot 6H_2O$ [5].

We have analyzed the experimental data available at present on the specific heat of many magnetic substances. The purpose is to disclose the analytical nature of the singularity which the specific heat has at the magnetic transition point of the second kind. We would like to report the results of our analyses. Our main conclusion is as follows: In the case of ferromagnetic transition in terbium and antiferromagnetic transition in $CoCl_2 \cdot 6H_2O$, if the system were ideally homogeneous, its anomalous specific heat, in the immediate neighborhood of the transition point, could be fitted by a "pinched" logarithmic function with a common coefficient above and below the transition point added to a step function with a step at the transition point. There are many other transitions in which the same conclusion seems to hold, but the experimental data now available in these cases are not sufficient to derive a conclusion as definitely as in the above two cases.

We start with the following assumptions:

I. Any real system is heterogeneous and composed of a large number of subsystems. Each subsystem is homogeneous and has its own transition temperature [5]. The observed specific heat is given by an average over those of the homogeneous subsystems:

$$C_p(T)=\int_0^\infty C_{\text{homog}}(T;\, T_\lambda) f(T_\lambda)\, dT_\lambda. \tag{1}$$

II. The distribution of the transition points of subsystems is Gaussian[1]:

$$f(T_\lambda)=\sqrt{\frac{\alpha}{\pi}}\exp\left[-\alpha(T_\lambda-T_0)^2\right]. \tag{2}$$

T_0 is identified with the Curie or Néel point of the real system.

III. The specific heat of the homogeneous system consists of two parts:

$$C_{\text{homog}}=C_{\text{sym}}+C_{\text{step}},$$

$$C_{\text{sym}}=\text{a function of } |T-T_\lambda|, \tag{3}$$

$$C_{\text{step}}=\begin{cases}0 & \text{for} \quad T>T_\lambda,\\ \Delta & \text{for} \quad T<T_\lambda.\end{cases}$$

IV. C_{sym} is a "pinched" logarithmic function:

$$C_{\text{sym}}=A\ln\left(|T-T_\lambda|+\delta\right)+\text{const.}, \tag{4}$$

$$A<0, \qquad \delta\geq 0.$$

From these assumptions one has

$$C_p(\tau)=A\cdot I(\tau;\, D)+\Delta\cdot F(\tau)+\text{const.}, \tag{5}$$

[1] This obvious assumption has already been adopted in, for example, Belov's book "Magnetic Transitions," Consultant Bureau, N.Y., 1961.

where

$$I(\tau;\, D) \equiv \frac{1}{\sqrt{\pi}} \int_{-\infty}^{\infty} e^{-x^2} \ln\left(|x-\tau|+D\right) dx, \qquad (6)$$

$$F(\tau) \equiv \frac{1}{\sqrt{\pi}} \int_{\tau}^{\infty} e^{-x^2} dx, \qquad (7)$$

$$\tau \equiv \sqrt{\alpha}\, t, \qquad t \equiv T - T_0, \text{ and } D \equiv \sqrt{\alpha}\, \delta. \qquad (8)$$

$I(\tau;\, D)$ is even with respect to τ so that one has from (5)

$$\frac{\Delta C_p(t)}{\Delta} \equiv \frac{1}{\Delta}\left\{C_p(-|t|) - C_p(|t|)\right\} = F(-|\tau|) - F(|\tau|). \qquad (9)$$

It should be noted here that (9) is independent of the assumption IV.

The values of $I(\tau;\, D)$ were machined—calculated and tabulated. τ runs from 0 to 1 with step of 0.1, from 1 to 2 with step of 0.2 and from 2 to 5 with step of 0.5. D runs from 0 to 0.2 with step of 0.02 and from 0.2 to 0.7 with step of 0.05. Figure 1 gives examples of the specific heat calculated from (5).

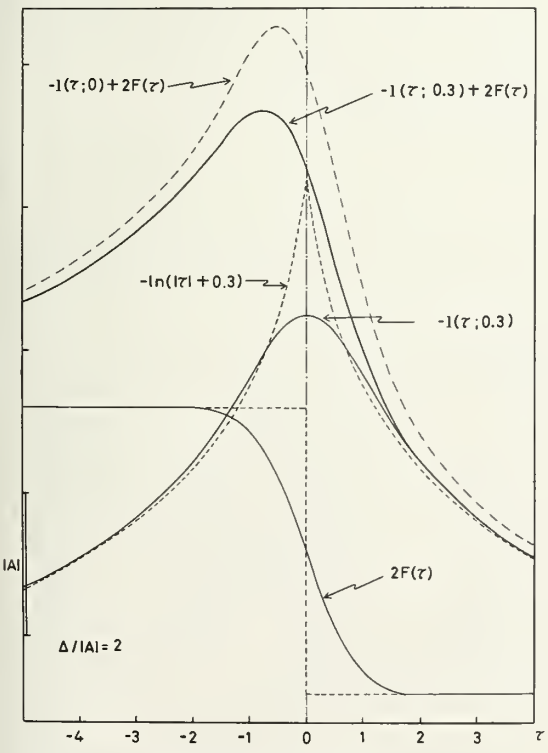

FIGURE 1. *Calculated curves for the specific heat:* $C_p = -I(\tau;\, D) + 2F(\tau)$.

The process of analysis consists of the following four steps. First the normal specific heat is subtracted from the observed values if it can be done without danger of introducing an appreciable error. When the transition temperature is in the region of liquid helium temperature, we omitted this step. In most cases we approximated the normal part by a linear equation of temperature, because we are interested in only a rather narrow interval of temperature. For our purpose we do not have to know the absolute values of the specific heat. This makes it considerably easier to find a linearized equation for the normal part with sufficient accuracy even by inspection. The second step of the analysis is to plot C_p or its anomalous part against log $|T-T_0|$. T_0 is chosen so that, except in the closest neighborhood of T_0, as many observed points as possible form two parallel straight lines, corresponding to the high- and low-temperature sides. Generally speaking, it is not always easy to carry through this procedure without any ambiguity. In several cases we have succeeded in locating the transition point quite definitely and in finding two parallel straight lines. Examples are shown in figures 2, 3, 4, and 5 [6, 7, 8]. When we could not get rid of some ambiguity, T_0 was found such that the plot resembles the characteristic shape as much as possible in the sense that the observed points begin to form two parallel straight lines after $|T-T_0|$ becomes less than several hundredths of T_0 (figs. 6 and 7) [9, 10]. Once T_0 is fixed in this way, the values of the step Δ and the slope A of the lines are read from the plot at once.

In not a small number of cases examined, the semilogarithmic plot gave a bill-shaped figure in the closest neighborhood of the transition point. We can proceed one step further in these cases and determine the value of α by making use of (9). Namely we plot $\Delta C_p(t)/\Delta$ against log $|t|$ and compare it with the plot $F(-|\tau|) - F(|\tau|)$ versus log $|\tau|$. The difference in the abscissae of the two figures is just equal to $\frac{1}{2}$ log α. If the figures coincide with each other through horizontal translation, this provides an empirical justification for the validity of our assumptions I, II, and III.[2] Figures 8 and 9 show examples of the third step. The

[2] The anomalous specific heat at the superconducting transition in Sn was measured very accurately by Kellers and Fairbank. Their data can almost exactly be reproduced by (5) with $T_c = 3.7230_6$ °K. $A = 0$ and $\left(\sqrt{2\alpha}T_c\right)^{-1} = 2.39 \times 10^{-4}$. This fact can be supposed as another support for the Gaussian distribution of the local transition temperatures.

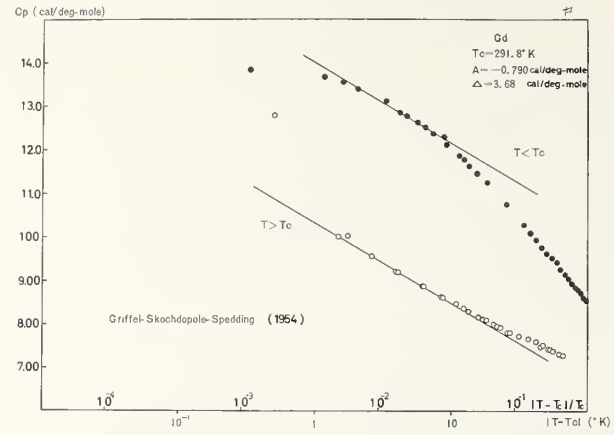

FIGURE 2. C_p *versus* $log|T-T_C|$ *plot of gadolinium.*

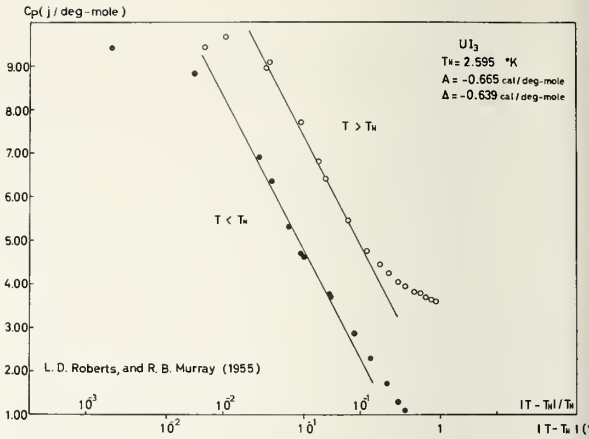

FIGURE 5. C_p *versus* $log|T-T_N|$ *plot of* UI_3.
This is an exceptional case in which Δ is negative.

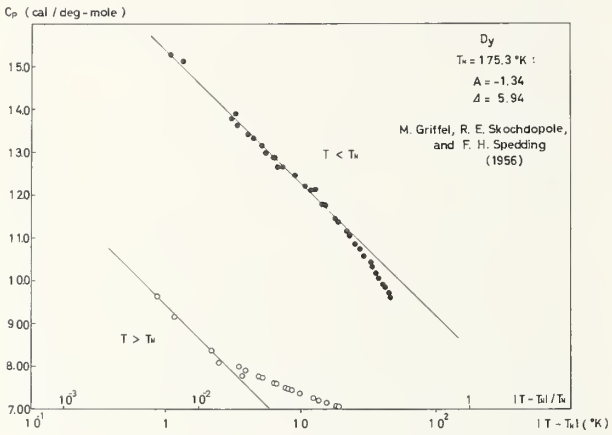

FIGURE 3. C_p *versus* $log|T-T_N|$ *plot of dysprosium.*

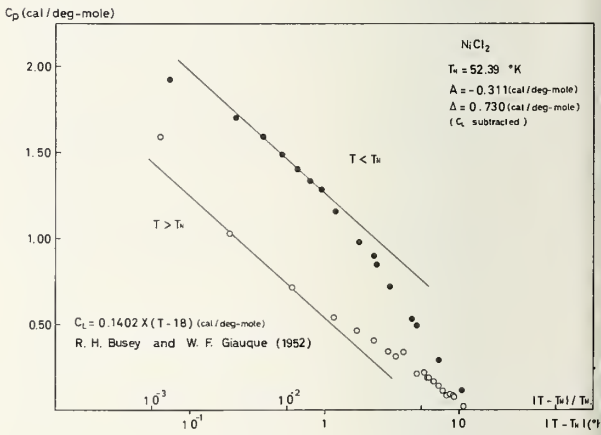

FIGURE 6. $C_p - C_L$ *versus* $log|T-T_N|$ *plot of* $NiCl_2$.

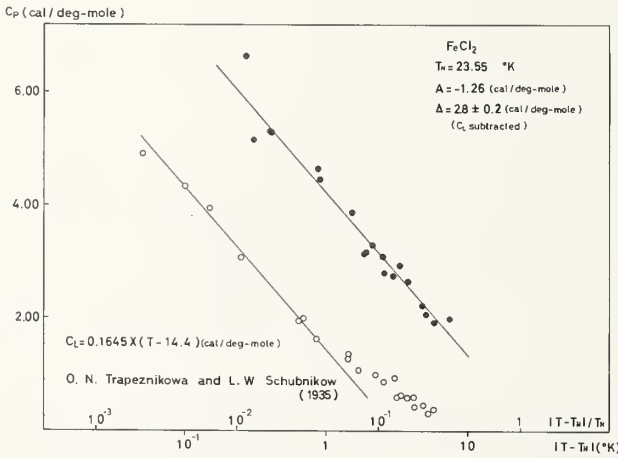

FIGURE 4. $C_p - C_L$ *versus* $log|T-T_N|$ *plot of* $FeCl_2$.

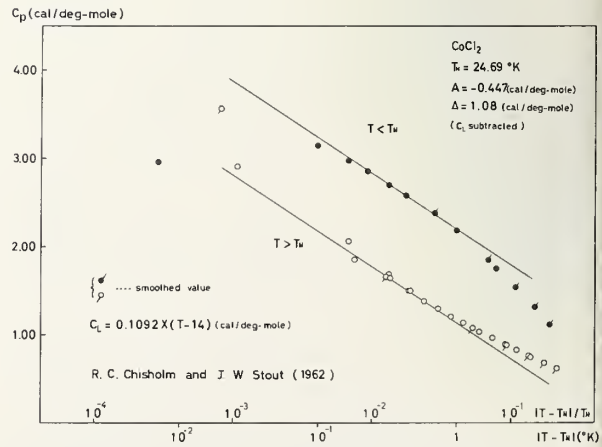

FIGURE 7. $C_p - C_L$ *versus* $log|T-T_N|$ *plot of* $CoCl_2$.

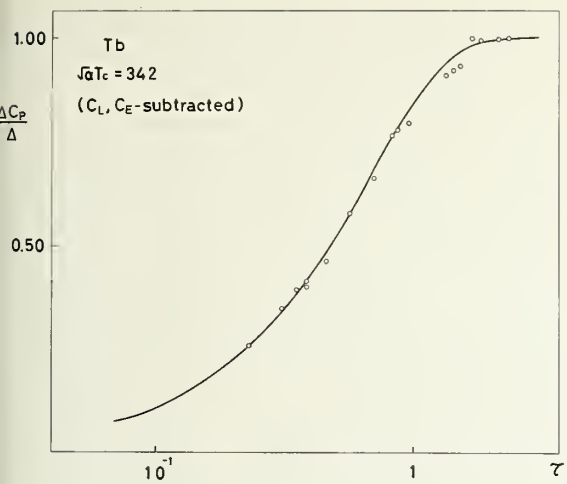

FIGURE 8. *Determination of α in terbium.*

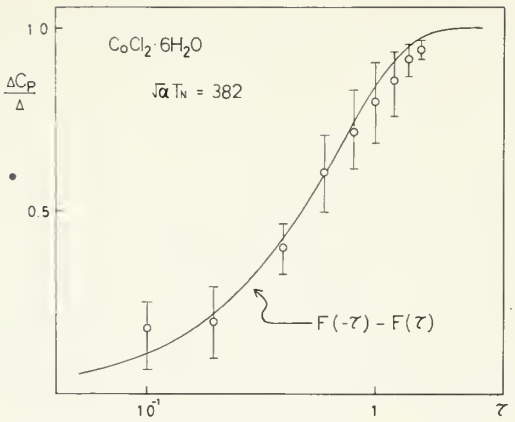

FIGURE 9. *Determination of α in* $CoCl_2 \cdot 6H_2O$.

value of δ is adjusted in the last step to reproduce the bill shape as truly as possible.

We have examined about 30 phase transitions of the second kind, mainly magnetic, and have succeeded to carry through the analysis up to the final step in about one fourth of these cases. Figures 10 [11], 11 [5], 12 [13], 13 [14], and 14 [15] show examples of the final results. The agreement between the observed and calculated values is satisfactory in at least two cases, terbium and $CoCl_2 \cdot 6H_2O$. In the other cases we can't say anything definite without reservation. Table 1 collects the numerical results of our analyses.

Now we would like to point out the following features common to all the magnetic transitions taken up in table 1. First, $|A|/\Delta$ is less than one half. This seems to be one of the characteristics of three-dimensionally coupled spin systems[3]

[3] Even when the spins substantially couple two-dimensionally, we observe that this ratio is less than one half. It becomes larger than unity only when the spins couple essentially one-dimensionally.

TABLE 1

Substance	T_0	$-A\left(\frac{\text{cal}}{\text{deg}-\text{mol}}\right)$	$\Delta\left(\frac{\text{cal}}{\text{deg}-\text{mol}}\right)$	$\frac{1}{\sqrt{2\alpha}T_0} \times 10^3$	$\frac{\delta}{T_0} \times 10^3$	Reference No.
	(°K)					
Samarium	105.8 (T_C)	0.471	3.04	3.01	0.85	[12]
Terbium	228.3 (T_C)	1.97	5.20	2.06	.88	[11]
$CoCl_2 \cdot 6H_2O$	2.2890 (T_N)	.538	1.14	1.85	.79	[5]
MnF_2	67.05 (T_N)	.530	2.73	4.86	3.4	[16]
NiF_2	73.33 (T_N)	.643	2.08	2.51	.71	[13]
Cr_2O_3	306.5 (T_N)	1.25	2.64	4.45	1.9	[14]
$\beta - UH_3$	172.0 (T_C)	.469	1.81	6.55	2.8	[15]

Secondly, the half-width of the Gaussian distribution, divided by T_0, is always of the order of magnitude of 10^{-3}. Thirdly, the degree of pinching, δ/T_0, also has the same order of magnitude, 10^{-3}, and is almost always less than $(\sqrt{2\alpha}\ T_0)^{-1}$. This fact has been preventing us from directly observing the pinched logarithmic anomaly.

As regards the origin of pinching in the logarithmic anomaly in an ideally homogeneous system, we would like to propose the following explanation. As is well known, a transition of the second kind is accompanied with an anomalous expansion. Now the transition temperature T_λ is a "temperature dependent quantity," as Heller and Benedek put it in their Phys. Rev. Letters [17]. To make the discussion more specific, let us assume that, when we approach the transition point from the high temperature side, the sample contracts and the value of the exchange coupling increases. This means that, if we stay at a distance from the transition point, we overestimate the distance therefrom. When we are in the low temperature side, we again overestimate it for the same reason. Since the anomalous expansion is really large only in the closest neighborhood of the transition point, the shift of the estimated transition point from the real transition point is almost constant, so long as we stay outside this narrow region. We identify this constant shift with our δ. Then the thermal expansion effect may be separated off by neglecting δ in the expression for the symmetric part of specific heat at constant pressure to get that of specific heat at constant volume. This interpretation leads us to the important conclusion that, if the system is ideally homogeneous, the specific heat at constant volume has a symmetrical nonpinched logarithmic singularity in addition to a discontinuity describable by a step function.

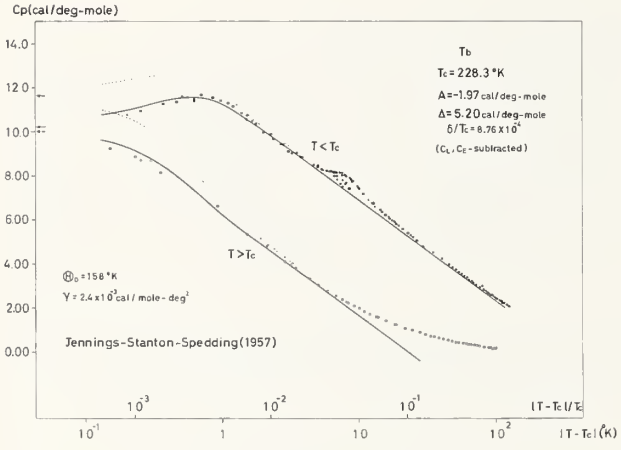

FIGURE 10. $C_p - C_L - C_E$ *versus* $log|T - T_C|$ *plot of terbium.*
The solid and dotted lines correspond to $\delta/T_C = 8.76 \times 10^{-4}$ and zero, respectively.

Before closing our report, we would like to add a few words: The conclusion of the present analysis is tentative and the possibility of some other kind of singularity still remains in the cases other than terbium and $CoCl_2 \cdot 6H_2O$. To establish our conclusion more definitely, we have to make further investigations from both the experimental and theoretical sides.

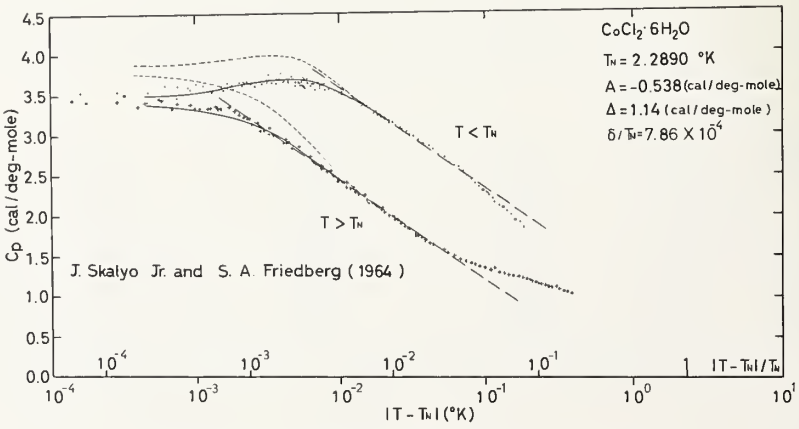

FIGURE 11. C_p *versus* $log|T - T_N|$ *plot of* $CoCl_2 \cdot 6H_2O$.
The solid and dotted lines correspond to $\delta/T_N = 7.86 \times 10^{-4}$ and zero, respectively.

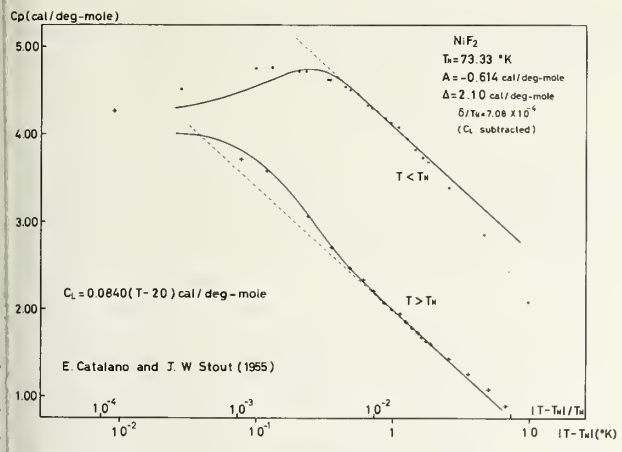

FIGURE 12. $C_p - C_L$ *versus* $log|T-T_N|$ *plot of* NiF_2.
The solid lines correspond to $\delta/T_N = 7.08 \times 10^{-4}$.

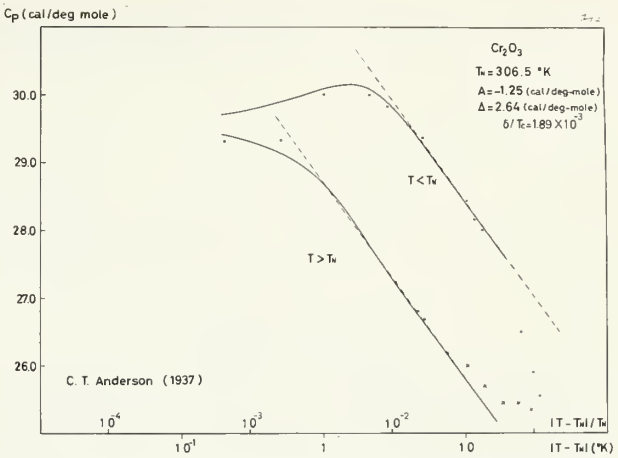

FIGURE 13. C_p *versus* $log|T-T_N|$ *plot of* Cr_2O_3.
The dotted lines correspond to $\delta/T_N = 1.89 \times 10^{-3}$.

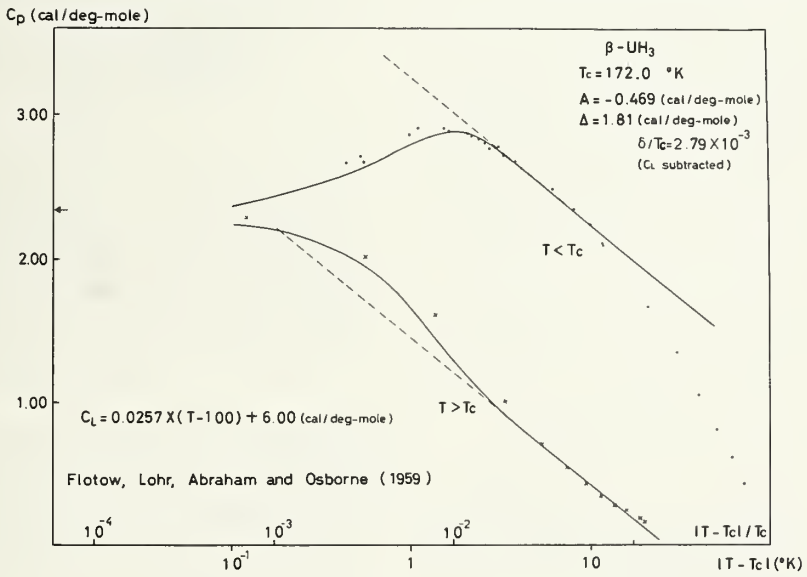

FIGURE 14. $C_p - C_L$ *versus* $log|T-T_C|$ *plot of* $\beta - UH_3$.
The dotted lines correspond to $\delta/T_C = 2.79 \times 10^{-3}$.

References

[1] L. Onsager, Phys. Rev. **65,** 117 (1944).

[2] A. J. Wakefield, Proc. Cambridge Phil. Soc. **47,** 419, 799 (1951); C. Domb and M. F. Sykes, Phys. Rev. **128,** 168 (1962); J. W. Essam and M. E. Fisher, J. Chem. Phys. **38,** 1802 (1963); J. Gammel, W. Marshall, and L. Morgan, Proc. Roy. Soc. (London) **A275,** 257 (1963). G. S. Rushbrooke, J. Chem. Phys. **39,** 842 (1963); G. A. Baker, Jr., Phys. Rev. **129,** 99 (1963); M. E. Fisher, J. Math. Phys. **4,** 278 (1963).

[3] W. M. Fairbank, M. J. Buckingham and C. F. Kellers, Proc. 5th Int. Conf. Low Temp. Phys., Madison, Wisconsin (1957), p. 50.

[4] M. I. Bagatskii, A. V. Voronel', and B. G. Gusak, Zh. Eksperim. i Teor. Fiz. **43,** 728 (1962) [Translation: Soviet Phys. —JETP **16,** 517 (1963)]; A. V. Voronel', Yu. R. Chashkin, V. A. Popov, and V. G. Simkin, Zh. Eksperim. i Teor. Fiz. **45,** 828 (1963) [Translation: Soviet Phys. —JETP **18,** 568 (1964)].

[5] J. Skalyo, Jr. and S. A. Friedberg, Phys. Rev. Letters **13,** 133 (1964). See also J. Skalyo, Jr., A. F. Cohen and S. A. Friedberg, Proc. 9th Int. Conf. Low Temp. Phys., Columbus, Ohio 1964. (To be published.)

[6] M. Griffel, R. E. Skochdopole. and F. H. Spedding, Phys. Rev. **93,** 657 (1954); J. Chem. Phys. **25,** 75 (1956).

[7] O. N. Trapeznikowa and L. W. Schubnikow, Phys. Z. Soviet. **7,** 66 (1935).

[8] L. D. Roberts and R. B. Murray, Phys. Rev. **100,** 650 (1955).

[9] R. H. Busey and W. F. Giauque, J. Am. Chem. Soc. **74,** 4443 (1952).

[10] R. C. Chisholm and J. W. Stout, J. Chem. Phys. **36,** 972 (1962).

[11] L. D. Jennings, R. M. Stanton, and F. H. Spedding, ibid. **27,** 909 (1957).

[12] L. D. Jennings, E. Hill and F. H. Spedding, ibid. **31,** 1240 (1959).

[13] E. Catalano and J. W. Stout, ibid. **23,** 1284 (1955).

[14] C. T. Anderson, J. Am. Chem. Soc. **59,** 488 (1937).

[15] H. E. Flotow, H. R. Lohr, B. M. Abraham, and D. W. Osborne, ibid. **81,** 3529 (1959).

[16] J. W. Stout and H. E. Adams, ibid. **64,** 1535 (1942).

[17] P. Heller and G. B. Benedek, Phys. Rev. Letters **11,** 428 (1962).

The Logarithmic Anomaly in the Pressure Coefficient of Helium Close to the Lambda Line*

H. A. Kierstead

Argonne National Laboratory, Argonne, Ill.

Introduction

Several investigators have reported logarithmic anomalies in the heat capacity [1], thermal expansion [2–6], and pressure coefficient [7–8] of liquid helium in the neighborhood of the lambda transition. Unfortunately, all of these experiments except those of Lounasmaa [7] and of Lounasmaa and Kaunisto [8] were done on the vapor pressure curve, where the anomalous behavior is confined to a very narrow temperature interval. The experiments of Lounasmaa and Kaunisto [8] at various pressures along the lambda curve show that the anomalous behavior is spread out over a larger temperature interval at higher pressures. Consequently, we have measured the pressure coefficient, $\beta_v=(\partial P/\partial T)_v$, of liquid helium along the isochore which crosses the lambda line at the melting curve. This intersection is called the upper lambda point ($T_{\lambda'}$, $P_{\lambda'}$).

Experimental Procedure

The apparatus used in these experiments is essentially the same as that used by Lounasmaa [7]. Therefore, it will be described only briefly here. It is shown schematically in figure 1.

Helium gas was purified in a trap (not shown) immersed in liquid helium, and was condensed into the piezometer G through the low-temperature valve A, which was kept closed during measurements. G was isolated from the liquid helium bath by the vacuum case B. Its temperature was controlled by the heater F and by pumping on liquid helium in E.

Changes in the pressure on the sample were measured by the oil manometer K and read with a cathetometer to 0.01 mm, which corresponded to about a millionth of an atmosphere. The absolute pressure was read to 0.01 atm on the Bourdon gage P, which was calibrated against a dead weight tester.

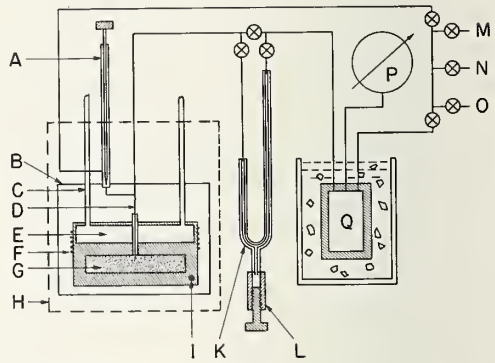

FIGURE 1. *Schematic drawing of the apparatus.*
(A) needle valve; (B) vacuum case; (C) pumping and vapor pressure tubes (2) f
(E); (D) 30 percent Cu-Ni capillary tubing, 0.1 mm ID; (E) temperature and vap
pressure compartment; (F) heater; (G) piezometer packed with fine copper wire f
rapid equilibrium (volume 39.83 cm³ at 1.76 °K, height 10 mm to keep hydrostat
pressure differences small); (H) dashed lines enclose space immersed in liquid heliu
bath; (I) germanium thermometer; (K) differential oil manometer, 0.060 in. ID consta
bore glass capillary (left arm 40 cm long, right arm 90 cm long); (L) oil reservoir ar
leveling device filled with Apiezon B oil; (M) to He⁴ supply tank and purifier; (N)
pump; (O) to atmosphere; (P) 25-cm dial test gauge calibrated against a dead weig
tester; (Q) ballast volume (1461 cm³) for balancing the right-hand side of K, held
constant temperature by an ice bath; ⊗ needle valves.

Small changes in the sample density could be mad
by raising the oil in the left limb of the manometer
forcing gas to condense into G. A change of 0.0
mm in the oil level caused a change of $2\times10^{-}$
g/cm³ in the density.

Temperatures were measured with a germaniun
resistance thermometer in a potentiometer circui
using a double potentiometer. At the uppe
lambda point the thermometer resistance wa
1483 Ω, and its sensitivity was 636 microdegree
per ohm. With 50 μA of measuring current, th
resistance could be measured with a precision o
0.002 Ω. The measuring current heated the the
mometer above the cell temperature; but this effec
was reproducible, and the same measuring curren
was used in calibrating the thermometer. It wa
calibrated against the vapor pressure of helium in I
on the T_{58} scale [9], using a tube separate from th
pumping tube. The change in the thermomete
resistance at the upper lambda point after warmin
to room temperature and recooling correspondec
to a temperature change of less than 10^{-4} °K. Al

*Based on work performed under the auspices of the U.S. Atomic Energy Commission.

temperatures were referred to the upper lambda point in order to correct for small changes in the thermometer or the measuring circuit.

Points on the lambda curve were found by warming the sample slowly at constant volume. Because of the large change in thermal conductivity at the lambda transition, the heating curve showed a sharp break, which could be located to within a microdegree. The sample was held at this temperature until equilibrium was established before reading the manometer. Then the density was changed slightly by raising the oil in the left limb of the manometer, and the new lambda point was found. The break in the heating curve was especially sharp with solid present in the cell, because the heat of melting increased the apparent heat capacity. Thus the upper lambda point could be determined directly, rather than as the intersection of two independently measured curves.

The pressure coefficient $\beta_v=(\partial P/\partial T)_v$ was determined by keeping the oil level in the left limb of the manometer constant and measuring the height of oil in the right limb at successively lower temperatures. After the lambda point was passed, as judged by the thermal response, the temperature was raised slowly in order to determine the lambda point exactly.

Results

The pressure coefficient $\beta_v=(\partial P/\partial T)_v$ was measured along an isochore which crossed the lambda line very close to $T_{\lambda'}$. Results are shown in figure 2, plotted against $\log_{10}(T-T_\lambda)$. The equation of the line is

$$\beta_v=9.39+7.69\log_{10}(T-T_\lambda)\ \text{atm/°K}, \qquad (1)$$

where T_λ is the lambda transition temperature for the isochore. This graph contains points taken on two different cooling runs. The lambda point for one run was 15 μdeg below $T_{\lambda'}$, and for the other it was 5 μdeg above. These small differences are not regarded as significant, but the observed lambda point was used in each run in plotting $T-T_\lambda$. Since this isochore meets the melting curve at the lambda point, the measurements in figure 2 refer to He *I*. One point was measured in supercooled He *II*, where β_v was found to be -27.6 at $T-T_\lambda=-1.08\times10^{-5}$. This point is not plotted in figure 2, but it is approximately the value to be expected for $T-T_\lambda=1.08\times10^{-5}$.

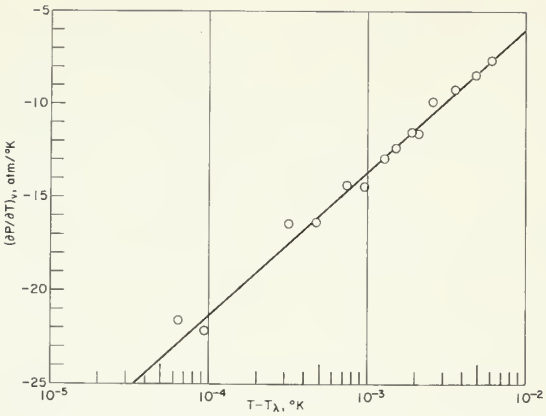

FIGURE 2. *Pressure coefficient* $\beta_V=(\partial P/\partial T)_V$ *of* He I *along the isochore* $V=V(T_\lambda')$.
Equation of line: $\beta_v=9.39+7.69\log_{10}(T-T_\lambda)$ atm/°K.

In connection with these experiments we have measured the change of pressure and density with temperature along the lambda line. These experiments, which are reported in detail elsewhere [10], can be summarized by the equations

$$\left(\frac{dP}{dT}\right)_\lambda=-55.54-96(T_\lambda-T_{\lambda'})\ \text{atm/°K} \qquad (2)$$

$$\left(\frac{d\rho}{dT}\right)_\lambda=-43.7-230(T_\lambda-T_{\lambda'})\ \text{mg/cm}^3\,\text{°K} \qquad (3)$$

$$\left(\frac{d\rho}{dP}\right)_\lambda=0.7868+2.8(T_\lambda-T_{\lambda'})\ \text{mg/cm}^3\ \text{atm}, \qquad (4)$$

where T_λ is the lambda temperature for the pressure P and density ρ, and $T_{\lambda'}$ is the temperature of the upper lambda point, 1.7633 °K.

Discussion

The logarithmic dependence of β_v on $T-T_\lambda$ is similar to that found by Lounasmaa [7] and by Lounasmaa and Kaunisto [8] at lower densities, and is consistent with their observation that the two constants in eq (1) both increase with increasing density. The measurements of Lounasmaa at 13 atm pressure ($T_\lambda=2.023$ °K) are of particular interest since he found that β_v fitted an equation of the same form as (1) to within 2×10^{-5} °K of the lambda point for both He I and He II, the constants being different for the two cases. In the same paper Lounasmaa presents measurements of the compressibility $\kappa_T=\rho^{-1}(\partial\rho/\partial P)_T$ along an isotherm

passing through the same lambda point. He finds no evidence for anything but a slow linear variation of κ_T with $P-P_\lambda$ to within 10^{-3} atm from the lambda line (corresponding to 2×10^{-5} °K for $T-T_\lambda$) and a small discontinuity at the lambda point.

Since an isochore cannot cross the lambda line with a slope greater in magnitude than that of the lambda line, $(dP/dT)_\lambda$ is a lower bound for β_v (both are negative); so eq (1) must break down for some small value of $T-T_\lambda$. On the other hand, there is no such restriction on κ_T. In fact, Buckingham and Fairbank [11] have shown that if C_P becomes infinite at the lambda line, κ_T must also. The experiments seem to suggest that β_v becomes infinite and κ_T does not. This situation can be examined more closely with the help of the equation

$$\beta_v=(dP/dT)_\lambda-(\rho\kappa_T)^{-1}(d\rho/dT)_\lambda, \tag{5}$$

which should apply to any point close enough to the lambda line that β_v and κ_T depend only on the distance from the lambda line. Solving for κ_T we have

$$\kappa_T=\frac{(d\rho/dT)_\lambda}{(dP/dT)_\lambda-\beta_v}. \tag{6}$$

This equation shows that κ_T will not vary much until β_v becomes nearly equal to $(dP/dT)_\lambda$. If β_v becomes equal to $(dP/dT)_\lambda$, as must happen if C_P becomes infinite, then κ_T becomes infinite. If β_v were to exceed $(dP/dT)_\lambda$ in magnitude, κ_T would become negative and a first-order phase transformation would ensue. Equation (6) has been used to calculate κ_T along the isotherm studied by Lounasmaa, [7] using his equation for β_v and Lounasmaa and Kaunisto's [8] data for $(dP/dT)_\lambda$ and $(d\rho/dT)_\lambda$. These calculated values are plotted as the solid line in the lower part of figure 3. The circles are Lounasmaa's measured points and the dashed lines are the ones he drew through his data. Although the agreement is not very good, it is apparent that he could not have expected to see an anomaly at the pressure resolution he attained. A similar calculation using the data reported in this paper is shown in the upper part of figure 3. The much larger change in κ_T results from the larger magnitude of β_v and the smaller magnitude of $(dP/dT)_\lambda$ at the higher pressure.

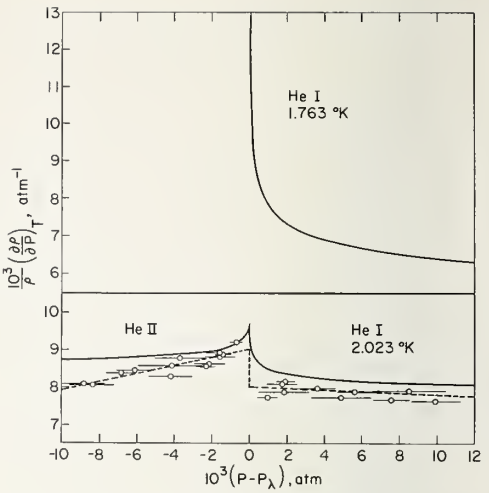

FIGURE 3. *Compressibility* $\kappa_T=\rho^{-1}(\partial\rho/\partial P)_T$ *of liquid helium.* Open circles: Points measured by Lounasmaa [7]. Dashed lines: lines drawn by Lounasmaa through his points. Solid lines: calculated from logarithmic relations for β_v.

We plan to measure κ_T near the upper lambda point in the near future.

To investigate the nature of the lambda transformation, it is very important to study how κ_T goes to infinity and how β_v approaches $(dP/dT)_\lambda$ (if indeed they do) at temperatures so close to T_λ that eq (1) breaks down. This is probably only possible near the upper lambda point. In Lounasmaa's experiment at 13 atm the logarithmic relation predicts that, for $T-T_\lambda=10^{-6}$, β_v will be less than a fourth of $(dP/dT)_\lambda$. In the present experiment, β_v was a fourth of $(dP/dT)_\lambda$ at $T-T_\lambda=10^{-3}$; and if eq (1) remains valid, β_v will be two-thirds of $(dP/dT)_\lambda$ at $T-T_\lambda=10^{-6}$. We are at present engaged in extending the measurements to smaller temperature intervals.

The author expresses his indebtedness to Professor O. V. Lounasmaa of the Institute of Technology, Helsinki, who originally constructed the apparatus and has contributed valuable advice; to Professor Dillon Mapother of the University of Illinois for fruitful discussions during the progress of the work; and to S. T. Picraux and Z. Sungaila for assistance in modifications to the apparatus.

References

[1] W. M. Fairbank, M. J. Buckingham, and C. F. Kellers, Proc. 5th Int. Conf. Low Temp. Phys., Madison, Wisconsin (1957), p. 50; C. F. Kellers, Thesis, Duke University (1960).
[2] K. R. Atkins and M. H. Edwards, Phys. Rev. **97**, 1429 (1955).
[3] M. H. Edwards, Can. J. Phys. **36**, 884 (1958).
[4] E. Maxwell, C. E. Chase, and W. E. Millet, Proc. 5th Int. Conf. Low Temp. Phys., Madison, Wisconsin (1957), p. 53.
[5] E. Maxwell and C. E. Chase, Physica **24**, 5139 (1958).
[6] E. C. Kerr and R. D. Taylor, Ann. Phys. (N.Y.) **26**, 292 (1965).
[7] O. V. Lounasmaa, Phys. Rev. **130**, 847 (1963).
[8] O. V. Lounasmaa and L. Kaunisto, Ann. Acad. Sci. Fenn. AVI, No. 59 (1960); Bull. Am. Phys. Soc. **5**, 290 (1960).
[9] H. van Dijk, M. Durieux, J. R. Clement, and J. K. Logan, National Bureau of Standards Monograph 10, 1960.
[10] H. A. Kierstead, **138**, A1594 (1965).
[11] M. J. Buckingham and W. M. Fairbank, Progress in Low Temperature Physics (C. J. Gorter, ed.) Vol. **III**, ch. III (North Holland Publishing Company, Amsterdam, 1961).

The Nature of the Cooperative Transition

M. J. Buckingham

University of Western Australia, Nedlands, Western Australia

1. Introduction

A thermodynamic singularity arises in statistical mechanics only in the limit $N \to \infty$, where N is the number of atoms in the system. By regarding an infinite system as made up of an infinite number of large but finite parts, called cells, with M atoms each, the singularity is seen to arise from the interactions between the cells—which for M large correspond to surface interactions, since the interatomic forces are short-ranged. For the same reason interactions between other than nearest neighbor cells are zero. Thus any thermodynamic singularity may be regarded as an example of a generalized near-neighbor lattice problem.

For very large M, one might expect the approximation of neglecting the surface interactions between cells to be a very good one since it corresponds to the neglect of only a fraction $1/M^{1/3}$ of all interactions. Indeed for a homogeneous stable thermodynamic system the approximation is extremely good. However it is not good near a singularity or in a two phase region, since the correct partition function for the system is then singular, whereas the exact solution of the zero-interaction-between-cells problem results in some power of the partition function for a finite system of M atoms, which is nonsingular.

It is easy to see the nature of the solutions in the two phase region. The correct solution describes a system with two phases separated in space by some minimum-area boundary. In the zero-interaction solution, each cell is properly described as a piece of one or other of the phases, but in the absence of the interaction these are mixed at random. The qualitative effect of the interactions between cells is thus the segregation or phase separation of the cells. The entropy associated with this separation is constant (depending on composition) in the two phase region and is, of course, zero in the one phase region—except for a very small temperature interval in the immediate neighborhood of the transition temperature.

At first sight the very small magnitude of the mixing entropy—associated with but one degree of freedom out of M, would suggest that it is entirely negligible. However the extreme smallness of the temperature interval ($\sim 1/M^{1/3}$ over which it can change means that, in some circumstances, it may be far from negligible—indeed accounting for the asymptotic form of the thermodynamic singularity. An example is the ordinary first order transition from gas to liquid phase, as mentioned below. The case of the critical transition is much more subtle, but by incorporating the assumption that the pair correlation function is just a function of r/r_0 where r_0 is the correlation length, we show below that a system, with finite range forces only, ostensibly possessing a "classical" van der Waals critical point would in fact have to have a logarithmic singularity in its specific heat. The discussion that follows is not intended as a "theory of the critical point" but as a preliminary account of the viewpoint that is being developed.

2. Division Into Cells

Consider a system with N atoms in a volume V, described by a Hamiltonian with finite range forces only, and with an exact partition function $Z(N, \beta)$. Imagine a division of the system into $\mathcal{N}$ "cells" each with M atoms ($N = M\mathcal{N}$) but with no restriction on the volume or energy of a cell (or of the magnetization in the case of a magnetic system). Number the cells with $i = 1, \ldots, \mathcal{N}$.

In any configuration contributing to the partition function, separate the interactions linking atoms in different cells. Imagine, for convenience, the latter all multiplied by a parameter λ say. Thus

$$H = \sum_{i=1}^{\mathcal{N}} H_i + \sum_{i,j} \langle H_{\text{int}} \rangle + \lambda \sum_{i,j} (H_{\text{int}} - \langle H_{\text{int}} \rangle)$$

where the first term contains all interactions linking atoms all of which are in the same cell; interactions between atoms in different cells contribute to the last term. $\langle 1 \rangle$ denotes mean value. Clearly for M large enough, interaction between atoms linking cells other than near neighbors can be neglected because of the finite range of the forces, so the sum of interaction terms can be written as a sum over near neighbors only. Note that the exact Hamiltonian is obtained with $\lambda = 1$.

Let $Z_\lambda(N, \beta)$ be the partition function for the system for some value of λ. Then $Z_1(N, \beta)$ is the exact $Z(N, \beta)$ while for $\lambda = 0$ we have a collection of noninteracting cells which can exchange energy, volume, etc. Thus

$$Z_0(N, \beta) = \{Z(M, \beta)\}^{\mathcal{N}}$$

This relation is exact, with $Z(M, \beta)$ the exact partition function for a system of M atoms. We use Z somewhat schematically for the appropriate partition function—the constant pressure one in the case of a gas liquid system for example. We will use the fact that, considering $\beta = 1/kT$ as a complex variable, $Z(N, \beta)$ is analytic[1] in the right half-plane for N finite, but not necessarily so in the limit $N \to \infty$.

Even when there is a singularity in $Z(N, \beta)$ as $N \to \infty$, the corresponding $Z_0(N, \beta)(\lambda = 0)$ is analytic. When Z_1 is at a normal, homogeneous stable thermodynamic point, then the operation of changing λ from 0 to 1 has a negligible effect for large M. However, near a point where say the specific heat at constant volume $C_V \to \infty$, for the $\lambda = 1$ system, C_V remains finite but dependent on M, for the $\lambda = 0$ system, see figure 1.

It is easy to show at a first-order transition for example that whereas $C_p(T)$ has a δ-function singularity, the corresponding $(C_p(T))_M$ reaches a value of order M with a width $\frac{1}{M}$ (all thermodynamic quantities being expressed per atom). Thus near enough (within $\frac{\delta T}{T_C} \sim \frac{1}{M}$, say) to a singularity the operation of putting $\lambda \to 1$, far from being negligible indeed produces the dominant effects and can be regarded as leading for example to the infinity in the specific heat.

Considering now the problem of obtaining the exact solution for the system from the solution $Z(M, \beta)$ we observe the following: The solution for $\lambda = 0$ represents an ensemble of cells with extensive parameters distributed according to the partition function $Z(M, \beta)$. Thus at a temperature a finite amount above a critical temperature, say at $T_C + \tau$, the density of cells is distributed about the mean value (say the critical density ρ_c) with a Gaussian distribution of width corresponding to the fluctua-

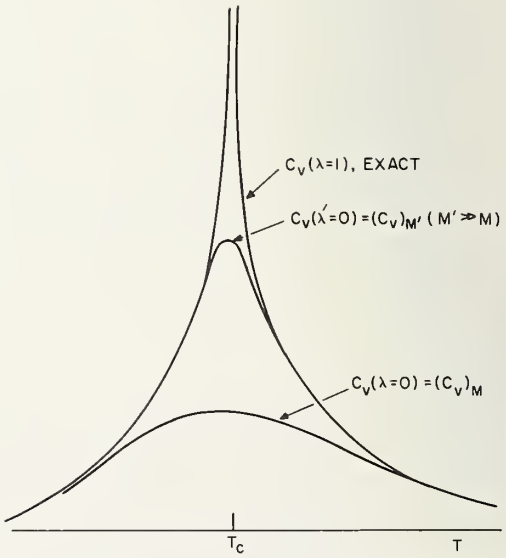

FIGURE 1. *Sketch of the qualitative temperature dependence of* C_V *near a singularity at* T_C *and that of* $C_V(\lambda=0)_M$ *for two values of* M.

[1] Z is the Laplace transform of the nonnegative degeneracy function $\omega(E, V, N)$, which is identically zero for E less than some finite (for N finite) ground state energy value and for V less than some finite value.

tions of the density for cells of size M.

$$\langle(\rho-\rho_c)^2\rangle \sim \frac{1}{M}\times(\text{compressibility}).$$

On the other hand, at a finite temperature below the critical temperature, $T_C-\tau$, (in a 2-phase coexistent region) the possible density values will be distributed in two Gaussians separated by the density difference of the two phases in equilibrium, figure 2.

We can regard the $\lambda\to 1$ problem as a generalized, near neighbor, lattice problem and we can estimate the magnitude of the effective interaction parameter. It is the total interaction energy due to interactions linking atoms across the boundary, say for the interaction between cells 1 and 2. This energy is proportional to the number of atoms within the interaction distance of the surface in cell 1 multiplied by the same number for cell 2.

$$\text{i.e., } \underset{1,2}{E_{\text{int}}} \sim M^{2/3}\epsilon_0 \frac{(\rho_1^s\rho_2^s)}{\rho^2}$$

where ϵ_0 is the strength of the interaction ($\epsilon_0 \sim kT_C$) and ρ_1^s is the density at the surface of cell 1. In the problem with $\lambda=0$, ρ_1^s is typical of the density anywhere in cell 1 so $\rho_1^s \sim \rho_1$. We now approximate E_{int}, by dropping the superscript on ρ_1^s. The effective interaction parameter of the lattice-interaction problem is the difference between the E_{int} in opposite configurations: i.e.,

$$E_{\text{int}}(\rho_1, \rho_1)+E_{\text{int}}(\rho_2, \rho_2)-2E_{\text{int}}(\rho_1, \rho_2).$$

Thus the effective interaction in the lattice problem is of order

$$E_{\text{int}}^{(1,2)} \sim M^{2/3}\epsilon_0 \frac{\Delta\rho_1\Delta\rho_2}{\bar{\rho}^2}.$$

The equivalent lattice variable is the ratio of the extreme values of E_{int} to kT

$$\frac{E_{\text{int}}}{kT} \sim \frac{M^{2/3}\epsilon_0}{kT}\frac{\langle\Delta\rho^2\rangle}{M\bar{\rho}^2} \to \frac{\epsilon_0}{kT}M^{2/3}\left(\frac{\kappa_T}{M}\right),\ T>T_C+\tau$$

$$\to \frac{\epsilon_0}{kT}M^{2/3}\times\frac{(\rho_l-\rho_g)^2}{\bar{\rho}^2},\ T<T_c-\tau$$

$$\text{i.e., } \frac{E_{\text{int}}}{kT} \underset{M\to\infty}{\to} 0\ T>T_C+\tau$$

$$\underset{M\to\infty}{\to} \infty\ T<T_C-\tau.$$

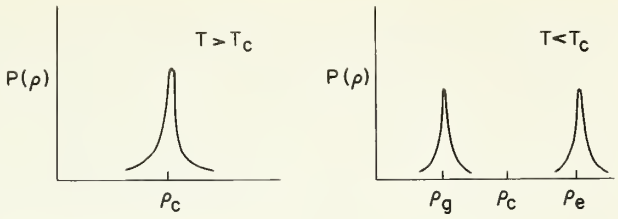

FIGURE 2. *Probability* P(ρ) *of finding a cell with density* ρ, *at temperatures above and below* T_C.

Thus "switching on" the interaction between cells does nothing to the distribution of the states of cells when $T>T_C+\tau$ since the effective temperature of the lattice problem is then $T_{\text{eff}} \sim \infty$ whereas for $T<T_C-\tau$ the effect is very great, $T_{\text{eff}} \sim 0$ in fact causing full "condensation" or "phase-separation" of the two types of cell—that is, those near the liquid density or the gas density, respectively; these are mixed at random for $\lambda=0$ but separated for $\lambda=1$. The entropy change involved is thus $\frac{\ln 2}{M}$ (per atom) and all this is lost in a very small temperature interval around the critical temperature.

$$\Delta S=\frac{\ln 2}{M}\text{ per atom.} \qquad (2.1)$$

3. Long Range Density Fluctuations

This entropy contribution, $M^{-1}\ln 2$, arising for $T<T_C$ as a result of the sorting of the previously ($\lambda=0$) randomly mixed "fluctuations of size M," might seem at first sight completely negligible. There are, after all, surface terms of order $M^{2/3}$ times greater. However we note that the contribution remains constant, $M^{-1}\ln 2$, throughout the temperature range $T<T_C-\tau$, and all its effect occurs in a small temperature interval, approaching zero as $M\to\infty$, about the critical temperature. (It may be noted that if the density had a value other than the critical one, say corresponding to a fraction f of the atoms in one component and $(1-f)$ in the other, then the entropy would be $-M^{-1}\{f\ln f+(1-f)\ln(1-f)\}$ and this can describe the smoothing, for a finite system, of the first order transition at temperatures and pressures below the critical values.)

This mixing entropy term corresponds, of course, to just one degree of freedom per cell of size M,

but it describes the relative configuration of the large size density fluctuations—and these are what ultimately become correlated near enough to the transition temperature. Thus if l_M is the linear dimension of a cell of size M, the number of Fourier components of the density with wavelength greater than l_M is just the same number, namely $1/M$ of all the degrees of freedom.

While it would seem quite possible for many more than one degree of freedom per cell to be involved in the cooperative transition—and indeed this is apparently the case for the two-dimensional Ising problem, we offer a tentative proof that, in fact, just this contribution is sufficient to make impossible the "classical" critical point—with properties typified by van der Waals equation. That is, a statistical system with finite range forces (in any number of dimensions) would not be self-consistent if it possessed a "Classical" critical point. In particular, we show that a system whose compressibility diverges as a simple pole as a function of temperature must have at least a logarithmic singularity in its specific heat.

4. Calculation of the Mixing Entropy

In order to obtain quantitative information concerning the interaction problem we shall invoke the fact that the nature of the problem is independent of the size, M, of the cells (provided M is sufficiently large); the size only determining the scale of the temperature interval in which the transition occurs. For this purpose we now define a sequence of cell divisions with ever increasing size of cell.

In the cell division defined above in section 2, let us replace M by M_0 and λ by λ_0, and introduce a new parameter λ_1 multiplying the interactions at the boundaries between cells of size $M_1 \gg M_0$. Thus λ_1 marks the interactions which would have been marked by λ before, had we chosen M_1 instead of M. For convenience let $M_1 = \nu M_0$ ($\nu \gg 1$). Similarly let us also introduce $\lambda_2, \lambda_3 \ldots \lambda_n \ldots$, dividing into cells of size $M_2, M_3, \ldots M_n \ldots$, respectively, with $M_n = \nu M_{n-1} = \nu^n M_0$.

Now by setting $\lambda_k = 1$, $k \neq n$ and $\lambda_n = 0$, we obtain a division of the system into cells of size M_n, which we call the nth order. The exact solution can now be regarded as that obtained in the nth order as $n \to \infty$, or as $\lambda_n \to 1$. We now determine the temperature interval required for the transition in the various orders. At some very small temperature $t = T/T_C - 1$, above the transition temperature, say, cells of sufficiently large size will be statistically independent of each other, whereas those of smaller size will not be. We can determine the number of statistically independent regions or elements by examining the fluctuations.

5. Number of Statistically Independent Elements

We are concerned with the development of correlations in a particular extensive property of our system—namely the one that is becoming long-range ordered and identifies the two components in the two phase region. The fluctuations of this quantity determine the number of statistically independent elements we require.

A number n of things each with an extensive property x, with mean square deviation δx^2, will, if they are statistically independent, have a mean square deviation $\langle (X - \bar{X})^2 \rangle = n \delta x^2$, where $X = \sum_{i=1}^{n} x_i$. In a gas-liquid system x_i is the number of atoms in a volume element δV i.e., $\rho \delta V$. This number is either 0 or 1, and has mean value $\bar{\rho} \delta V$. The number n of statistically independent fluctuating units in a large volume with mean number $\bar{N}$ of atoms is then

$$n = \frac{\bar{\rho}^2}{\langle (\rho - \bar{\rho})^2 \rangle}$$

which reduces, as it should, to $\bar{N}$ in the absence of any correlation, i.e., at infinite temperature. The mean number of atoms per independent element is then

$$M = \frac{\bar{N}}{n} = \frac{\langle (\rho - \bar{\rho})^2 \rangle}{\bar{\rho}^2} \bar{N} = kT \rho \kappa_T = \chi(t), \qquad (5.1)$$

say where κ_T is the isothermal compressibility. In the case of a magnetic system, the corresponding number of statistically independent magnetization elements is the magnetic susceptibility in units of the magnetic moment per particle.

6. Recurrence Relation

We have seen that the fluctuation of the natural extensive variable of the system determines the size $M(t)$ of the statistically independent regions. Returning to the cell division of our system, we assume that the temperature interval over which the nth order undergoes its transition is the tempera-

ture, t_n, such that $M_n \sim M(t_n) = \chi(t_n)$. That is, using the result (2.1) obtained in section 2, the nth order solution would lead to a change of entropy $\Delta S_n = \ln 2/M_n$, occurring in a temperature interval t_n.

We can now assert that for large enough cells the functional form of this entropy change is given by

$$\Delta S_n(t) = \frac{\ln 2}{M_n} f(t/tn) \tag{6.1}$$

where the function f is independent of n. This assertion enables us to write a recurrence relation which we solve for the function f. and is the main source of our argument—it depends on the fact that for large enough M (or small enough t) the interaction problem has ceased to depend on any detailed property of the interaction between atoms, or of any finite number of atoms and has taken an asymptotic form. We are effectively *assuming* the *existence* of an asymptotic "lattice problem" such that the description of the nth order in terms of the $(n-1)$th is the same as that of the $(n+1)$th in terms of the nth.

The function $f(x)$ is continuous monotonic increasing and satisfies the boundary conditions $f(x) \to 0$, $x > 1$ and $f(x) \to -1$, $x < -1$.

The partition function corresponding to the choice $\lambda_n = 0$, $\lambda_k = 1$, $k \neq n$, i.e., the nth order, is a valid approximation to the exact one for $t > t_n$, since regions of size M_n are then statistically independent. Similarly, except for the constant mixing entropy, it is valid for $t < -t_n$. The exact solution $\lambda_n = 1$, contains the additional contribution to the entropy given by (6.1).

7. Difference Equation for Specific Heat

Let $C_n(t)$ be the specific heat corresponding to the partition function with $\lambda_n = 0$. $C_n(t)$ will have the shape of the exact specific heat except that the singularity will be smoothed out over an interval $\sim t_n$, with $C_n(t)$ finite for all t. We can now write, using T_C as the unit of temperature,

$$C_\infty(t) - C_n(t) = \frac{\ln 2}{M_n} \frac{\partial}{\partial t} f(t/tn)$$

$$= \frac{\ln 2}{\chi(t_n) t_n} f'(t/tn) \tag{7.1}$$

using the result (5.1). The derivative of f has been written f'.

For a "Classical" critical point $\chi(t) \propto t^{-1}$, but for other suggested[2] singularities $\chi \propto t^{-\gamma}$ where $\gamma > 1$.

Let us write

$$\chi(t)^{-1} = a' t^\gamma \qquad \gamma \geq 1 \tag{7.2}$$

eq (7.1) becoming

$$C_\infty(t) - C_n(t) = a t_n^{\gamma - 1} f'(t/t_n), \tag{7.3}$$

where a is written for $a' \ln 2$. The cases $\gamma = 1$ and $\gamma > 1$ are different and we discuss first the case $\gamma = 1$.

8. The "Classical" Critical Point, $\gamma = 1$

The equation for the singularity becomes, for the case $\gamma = 1$,

$$C_\infty(t) - C_n(t) = a f'(t/t_n) \tag{8.1}$$

It is easy to see that the function $f'(x)$ cannot be finite at $x = 0$. For let such finite value of the right side of (8.1) be C_0. Then $C_m(0) - C_n(0) = 0$ for any m, n and yet $C_\infty(0) - C_n(0) = C_0 \neq 0$. We find below that the asymptotic solution requires $f'(x) \sim -\ln x$ as $x \to 0$.

Taking the difference of (8.1) for n and $n+r$, we obtain

$$C_{n+r}(t) - C_n(t) = a\{f'(t/t_n) - f'(\mathcal{N}^r t/t_n)\}$$

where $t_n/t_{n+1} = \mathcal{N}$. Setting $x = t/t_n$ we write this equation as

$$C_{n+r}(xt_n) - C_n(xt_n) = a\{f'(x) - f'(\mathcal{N}^r x)\} \tag{8.2}$$

where the right-hand side is independent of n and can be written $ag(\mathcal{N}^r, x)$ say. Now $C_n(t)$ is finite for all t and by putting $r = 1$ and, repeatedly, $n+1$ for n, we find

$$C_{n+r}(0) - C_n(0) = ar\, g(\mathcal{N}, 0) = ar\, g_0 \ln \mathcal{N}$$

where g_0 is a constant (independent of r, and n).

[2] See for example: M. E. Fisher, J. Math Phys. **5**, 944 (1964). The two dimensional Ising problem has $\gamma = 7/4$.

Thus

$$C_{n+1}(0)-C_n(0)=ag_0 \ln \mathcal{N}, \tag{8.3}$$

so that, increasing the order n by one increases $C_n(0)$ by a constant independent of n, and thus $C_n(0)$ increases linearly with n. Now $t_n=\mathcal{N}^{-1}t_{n-1}=\ldots=\mathcal{N}^{-n}\tau$ say, so that

$$n=\frac{-\ln (t_n/\tau)}{\ln \mathcal{N}}.$$

Thus

$$C_n(0)=C_0+nag_0 \ln \mathcal{N},$$

becomes

$$C_n(0)=C_0-a\ g_0 \ln (t_n/\tau).$$

Thus we see that the specific heat becomes infinite like the logarithm of the temperature. We can easily find the asymptotic form of the function $f'(x)$, since by (8.2) and (8.3) we can write

$$f'(x)-f'(\mathcal{N}x) \underset{x\to 0}{\to} g_0 \ln \mathcal{N}. \tag{8.4}$$

Now the equation

$$F(x)-F(bx)=C$$

has the solution

$$F(x)=\frac{-C \ln x}{\ln b}+F_0$$

where F_0 is an arbitrary constant. Hence the asymptotic solution of the eq (8.4) is

$$f'(x) \underset{x\to 0}{\to} -g_0 \ln x+f_0. \tag{8.5}$$

The eq (8.1) whose asymptotic solution we have found contains an arbitrary multiplicative constant which should be determined from the normalization condition given in section 6. We can see from (8.5) together with this condition that g_0 will be a number of order unity.

Summarizing the results of this section we assert that a system whose compressibility diverges like a simple pole as $T\to T_C$ cannot possess the "Classical" specific heat temperature dependence, but that it must have a logarithmic divergence and furthermore, the coefficient of the logarithm, a in eq (7.2), is proportional to the inverse of the coefficient of $(T-T_C)^{-1}$ in the compressibility (5.1). That is we expect

$$k^{-1}C_v \sim -a \ln \left(\frac{T-T_C}{T_C}\right)+C_0$$

where $$a \sim \ln 2\ \rho_c k(T-T_C)\kappa_T, \tag{8.6}$$

k being Boltzman's constant, κ_T the compressibility and ρ_c the critical density.

9. Nonclassical Critical Point, $\gamma > 1$

We do not give a detailed discussion of this case, since it is not hard to show that the solution of eq (7.3) for $\gamma > 1$ is not singular. This suggests, in terms of the discussion in section 3 above, that a singularity with $\gamma > 1$ involves more than just the one degree of freedom per cell which describes the spacial arrangement of the large scale fluctuations.

It is not a pleasing circumstance that the simplest possibility in the present theory appears inadequate to account for the behavior of the two dimensional Ising problem, but further discussion of these points must be left to another occasion.

10. Further Properties of the Transition

We have discussed at some length the nature of the singularity to be expected at the critical point of a system which could be said to have a "Classical" critical point in the "zeroth order" approximation. We have seen that the specific heat diverges logarithmically with a characteristic coefficient. The singularity is not necessarily symmetric however. Certainly the constant C_0 in (8.6) is not the same on the two sides of the transition temperature. In fact it differs by approximately the amount of the discontinuity in the original "Classical" specific heat. We have obtained a first approximation in which the coefficient, a, is different above and below the transition, but there are indications that this is not the final asymptotic form and that the latter may well be symmetric. The preliminary results of this approximation lead to a coexistence curve different from the classical one, which is a quadratic relationship between the

density difference of the two phases and the temperature difference from the critical temperature. This could also be described as a quadratic relation between the density and the *energy* difference from the critical energy—the energy being taken on the critical density line. This relation between the extensive parameters is preserved in our result, but the relation between energy difference and temperature is no longer linear—in fact $E-E_C \propto t \ln t$. This results in a coexistence curve which can be represented:

$$\Delta\rho = \rho_l - \rho_g \propto (-t \ln t)^{1/2}$$

or, equivalently,

$$\frac{\Delta\rho^2}{-\ln \Delta\rho} \propto t.$$

It is useful to express this in terms of the natural variable x, in this case $x=\rho_l-\rho_g/\rho_l+\rho_g$, and in the case of a magnetic system, $x=M/M_0$ where M is the spontaneous magnetization and M_0 the saturation magnetization. The natural variable ranges between 0 and 1 as $t=1-T/T_C$, ranges from 0 to 1. In this variable the expression for the asymptotic coexistence curve is

$$\frac{x^2}{-\ln x} \propto t,$$

but this is not very suitable for comparison with experiment because of the spurious singularity at $x=1$. An expression with the same asymptotic form, but with the correct limit at $T=0$ is

$$\frac{x^2}{1-\ln x} \propto t.$$

This expression (in which the coefficient unity multiplying $\ln x$ is quite arbitrary) has been compared with his measurements of the coexistence curve for liquid helium by Dr. M. Edwards who has presented the comparison to this conference. It is interesting that he obtains an agreement rather better than with the usually accepted cubic relation. Concerning the experimental test of the predicted relation (8.6) between the coefficient of the logarithm and the compressibility, we have unfortunately not been able to obtain data with which to make a useful comparison but it is to be hoped that some will soon be available. In passing we note that the van der Waals equation would yield for the value of a in (8.6) the number $\frac{9}{4} \ln 2$, (for $T > T_C$) which is near values that have been observed.

This work was carried out with the enthusiastic and able assistance of J. D. Gunton. Much of it was performed during the tenure of a National Science Foundation Senior Foreign Scientist Fellowship at Stanford University, which is gratefully acknowledged.

Discussion

C. N. Yang: We are very grateful to Dr. Fairbank for presenting his most interesting results. One cannot emphasize too much that one of the most important results of recent years is the verification that in some quantum mechanical systems there exists a new long range order which is macroscopic as is demonstrated by this experiment. In 1961 Dr. Fairbank was also involved in an experiment which demonstrated the existence of quantized flux in a superconductor showing the macroscopic effects of long range order [1]. These together with the recent discovery of the Josephson effect [2], have proved once and for all that quantum mechanical systems at very low temperatures often exhibit correlations which are different from crystalline correlations, but which also extend to infinite distances. Dr. Fairbank said that this experiment was brought about on a fifteen dollar bet from theoreticians. Let us hope that if we make a bet at the thirty dollar level, we will obtain more results.

W. M. Fairbank: I would like to point out that Fred Kellers carried out the experiment on the λ point I just described.

M. E. Fisher: It is perhaps worth pointing out that, although you do have a λ-line in liquid helium and not a λ-line in the ferromagnet, in the antiferromagnetic transition you do have a very close analog of the λ-line. In fact, in a spin flop antiferromagnet, I think, you have something rather closely analogous to the off-diagonal long range order which Dr. Yang was talking about [3].

L. Tisza: The λ-"point" in a ferromagnet is a point only in the same sense as the melting "point" is. Both refer to atmospheric pressure and a variation of this parameter yields $T_\lambda(P)$, a line in the P-T plane. This is in contrast with the critical point in fluids.

J. S. Rowlinson: Even at the liquid-vapor critical point of fluids you do have a λ-line if you have a two component system, where there is an extra degree of freedom.

L. Tisza: This is correct. The prediction of Gibbs' phase theory is that the dimensionality of critical states in the thermodynamic space of intensities is $\delta=c-1$ where c is the number of independent components. The difficulty in interpreting λ-lines as critical states is that this would mean $\delta=1$ for $c=1$, a contradiction to this rule. Ehrenfest [4] sought to remedy the situation by assimilating the λ-lines to lines of ordinary phase equilibrium. (I confine this remark to the case $c=1$.) His problem was then to explain the absence of discontinuities in the first derivatives of the Gibbs function that are characteristic, say of melting. He did this by postulating higher order transitions for which nth derivatives of the Gibbs function exhibit discontinuities along a line in the space of intensities, while the lower derivatives

are continuous. Shortly thereafter Landau showed that such transitions can be indeed expected to occur on the basis of the thermodynamic theory of stability. The seemingly satisfactory situation was upset by Onsager's discovery of the singularity of the Ising model, particularly since experiment showed that logarithmic singularities provide good descriptions also of real systems. These developments posed two problems for the student of Gibbsian thermodynamics: (i) identify the flaw in Landau's argument; (ii) generalize Gibbs' phase rule to account for λ-lines. It can be indeed shown that [5] (i) at critical states the discriminant of the so-called stiffness matrix vanishes and this invalidates Landau's power series expansion; (ii) at critical states there are two modifications that become identical to each other. In the classical case these modifications differ energetically (liquid and vapor). At λ-points we have, say, the two polarized states of the Ising model which are energetically equivalent and which transform into each other by a symmetry operation; in this case the dimensionality of singular points becomes $\delta = c$ and the above mentioned difficulty is removed. The nature of this symmetry is evident in all cases involving solids where the mechanism underlying the λ phenomenon is understood. A remarkable exception is the λ-line of liquid helium. I find myself incapable of refuting the argument that this system exhibits some elusive intrinsic symmetry. This is interesting also in view of the recently discovered singularity of C_v at fluid critical points which seems to point into a similar direction (see the contribution of Dr. Chase on Wednesday afternoon). A precise formulation of this symmetry may well be at present the most challenging problem of the theory of critical points.

P. W. Anderson: For a study of fluctuation phenomena in superconductors, perhaps the best direction there is not to go to increasingly pure systems but to increasingly impure systems, because the amount of the critical point fluctuations will increase when one shortens the correlation length. So one would hope to bring out the critical point fluctuation phenomena by decreasing the path, thus by making an increasingly impure system, which, however, should be as homogeneous as possible.

I. Rudnick reported measurements of the sound velocity near the λ-point [6] in liquid helium.

M. J. Buckingham: With regard to the paper of Dr. Rudnick, I would like to point out that if one would find a violation of the Pippard relations, this means either that the system is not in thermodynamic equilibrium or that the singularity is not qualitatively the same all along the λ-line. The latter property is used in deriving the Pippard relations [7].

E. Helfand: I want to mention something which surprisingly has not been mentioned yet. Perhaps, it may be important here. There has been some thought recently about whether some of these apparent second order phase transitions really should not be first order phase transitions. The analysis has been made mostly in magnetic systems, where one takes into account the volume dependence of the exchange coupling. An analogous effect may enter into fluids, namely, by introducing many body potentials one may get an effective density dependent potential which may destroy the second order nature of the phase transition except for one particular density. This would imply that you have to do constant volume measurements in order to get the proper second order phase transitions.

C. W. Garland: With respect to the comment of Dr. Helfand, I wish to point out that in the paper on an ultrasonic investigation of ammonium chloride, to be presented later at this conference, we shall show in some detail that for an Ising ferromagnet such a first order transition does occur across an instability region.

C. N. Yang: Could I ask Dr. Edwards what happens to the critical temperature if you make a plot of the variable $X^2/(1-\ln X)$ that Buckingham suggested?

M. H. Edwards: I forgot to point out that on this basis the best straight line goes through a temperature which is 0.006 °K below the critical temperature on the T_{58} scale. I would therefore suggest that one should treat the plots made to fractions of a millidegree from the critical temperature with reservation, if this is indeed that uncertain. In view of the thermometry involved and my inability to put a thermometer into the actual optical path, I do not know whether this difference is precisely 0.006 °K, but I think that there is a significant difference. It is conceivable that my whole curve is shifted somewhat. I should have said that for the X^3-plot this would require a shift of 0.020 °K, which is certainly beyond the realms of possibility. The X^2-plot leads to a critical temperature somewhat above the listed one depending on where you put the tangent.

M. J. Buckingham: I would like to make two remarks. The first is a plea for the use of the proper natural variable in studies of the coexistence curve of gas-liquid systems. This is the variable $X=(\rho_l-\rho_g)(\rho_l+\rho_g)=(v_g-v_l)(v_g+v_l)$, rather than the often used $(\rho_l-\rho_g)/2\rho_c$. The variable X ranges from 0 to I as $t=1-T/T_c$ ranges from 0 to 1 and is indifferent to the choice of number of atoms or volume as the basic extensive variable. The other variable and X are equal if the "rectilinear diameter" is not only straight but constant as in the case of the Ising cell model. It has other advantages for plotting experimental results as mentioned by Dr. Edwards.

Concerning the particular form of the suggested coexistence function, namely $X^2/(1-\ln X)$, I should say that the theoretical argument which I will mention in my talk later, merely indicates the asymptotic form $-X^2/\ln X$ for $X\to 0$. The factor $(-\ln X)^{-1}$ in this particular expression is not useful because of the spurious infinity at $X=1$. One is led therefore to consider the factors $(1-n\ln X)^{-1}$ which have the required asymptotic form and which for all n are zero at $X=0$ and unity at $X=1$ where the slope is n. These properties are shared with the set of functions X^n; indeed their general shape is remarkably similar to the corresponding simple power function.

We can now emphasize the great difficulty of obtaining reliably the correct asymptotic behavior of empirical results however accurate, over a limited range of the variable. As Dr. Edward's illustrations showed, the function $X^2/(1-\ln X)$ is over his range of parameters, numerically much closer to the function X^3 than X^2, although the corresponding value for Fisher's coefficient β would be $1/2$ as for X^2, rather than $1/3$.

L. Tisza: Even if the Buckingham variable X is "natural" for the analysis of the coexistence curve, it is not a substitute for ρ used with its conjugate intensity μ (see paper of Chase and Williamson). In fact, X is defined only on the coexistence curve and has no meaning for the homogeneous fluid.

J. S. Rowlinson: Dr. Moldover gave us some information on the variation of C_v with the density in the two phase region which he said implied $(d^2\mu/dT^2)_V \neq 0$. Does this imply that $-NT(d^2\mu/dT^2)_V$ becomes infinite? Or do your C_v data imply that the curvature of the vapor pressure line $(d^2p/dT^2)_V$ becomes infinite?

M. R. Moldover: So far as I can see in the region I showed both terms are at least not decreasing and one of them is surely increasing.

R. E. Barieau: Dr. Moldover, did you say that the quantity $-NT(d^2\mu/dT^2)_V$ is positive?

M. R. Moldover: Yes, the sign of this quantity does not change in the vicinity of the critical point.

R. E. Barieau: Recently, I have analyzed the data of Hill and Lounasmaa [8] for helium in this way to obtain the quantities $(d^2\mu/dT^2)_V$ and $(d^2p/dT^2)_V$. Now ordinarily below the critical point $(d^2\mu/dT^2)_V$ is negative, so that the two contributions to C_v namely $-NT(d^2\mu/dT^2)_V$ and $VT(d^2p/dT^2)_V$ are both positive down around the boiling point. Now when the critical point is approached, the data of Hill and Lounasmaa indicate that $-NT(d^2\mu/dT^2)_V$ is first positive and then becomes negative.

M. R. Moldover: I believe the data of Hill and Lounasmaa were taken at intervals of 0.050 °K or larger and were not taken particularly at the critical density.

R. E. Barieau: That is correct. They made the measurements at different densities and the measuring points were not chosen to get these two quantities with the maximum accuracy. However, it is possible to deduce some figures for these quantities and there are two series of experiments between 4.2 and 4.5 °K in which the densities are far apart so that one can obtain these quantities with considerable accuracy.

M. R. Moldover: Yes, there is a conflict between your conclusion from the Hill and Lounasmaa data and mine. With respect to the data of Hill and Lounasmaa in the vicinity of the critical point it should be remarked that they used a large chamber in which complete thermal equilibrium is difficult to realize.

M. H. Edwards: They also smoothed their data.

M. S. Green: I would like to ask Dr. Edwards and Dr. Moldover how much the density dependence on the height in the fluid would affect their experiments. I think Dr. Edwards had some control of this height. Is that correct?

M. H. Edwards: Yes. Of course, this effect is not important further away from the critical point. At least at 5 °K the correction due to the compressibility, which incidentally, I have measured in this range, is less than 0.05 percent in any of the individual density measurements. The liquid had only a helium liquid pressure between 1 mm and perhaps in the extreme case 4 mm above it. This correction was completely trivial even while the extrapolated compressibility is going to infinity.

M. R. Moldover: Most of the helium in my cell is in the slots which are 3 mm deep. There will be a distribution of densities in this helium column as you approach the critical point. Dr. Edwards measured the compressibility far from the critical point and also gave an equation of state, which he derived in the earlier days when one used a power series expansion. Using this I calculated that in my cell the distribution of densities is less than 2 percent at the temperatures closest to the critical point. So on the plot I presented this gives a contribution to the curvature.

M. S. Green: In computing this correction one should probably use the nonanalytic character of the density dependence as Dr. Larsen pointed out yesterday. It actually makes a significant difference. One cannot be satisfied to use an analytic expansion in computing this correction.

M. E. Fisher: I want to ask Dr. Edwards: what is the actual value of the parameter X in your experiments? In their experiments on xenon, Weinberger and Schneider [9] approached the critical point to within $\Delta T/T_c = 3\times 10^{-5}$, while you essentially approached the critical point only to within 2 percent. So Weinberger and Schneider approached the critical point a few decades closer, but even as close as that this parameter X was 0.07. In other words, the curve is so flat that the density difference $\rho_l - \rho_g$ is still very large. Dr. Rowlinson made the point, which I think is a relevant one, that you have to approach the critical point considerably closer.

M. H. Edwards: Yes, this is a curious feature. I went to within 2 percent from the critical temperature. My corresponding X values and consequently my density differences $\rho_l - \rho_g$, however, are smaller. In other words, their xenon data look flatter than my helium data. After studying the data of Weinberger and Schneider, I concluded that they did not adequately guard against the gravitational gradients effects. They had a sample that was 1 cm deep and the compressibility correction is 15 times what it would be for helium in the corresponding case.

M. E. Fisher: Well, I do not want to defend the measurements of Weinberger and Schneider either, but they did a series of experiments to make a special study of the density effect. (The experiments on xenon, hydrogen, He^4 and He^3 have since been analyzed systematically with a suggestion as to the nature of the quantum deviations [3].)

M. H. Edwards: Yes, but only down to 1 cm. They had a cell that was approximately 1.2 cm by approximately 10 cm, normally used in the vertical position. They rotated to the horizontal position to change the gradient from a height of 10 cm to a height of 1 cm, but not further. I claim that with a smaller slice of the fluid I got a different result.

G. B. Benedek: I wonder whether we could clear up the question not of the difference in flatness between your data and those of Schneider, but between your data and those of Moldover.

Dr. Moldover made the point that he had evidence that his density curve was flatter than a dotted curve of yours.

M. H. Edwards: Not entirely clarified. On the density versus temperature plot Woodbury and I had results that were extrapolated to go through a temperature which corresponded to the T_{58} value of the critical temperature. That is the temperature to which he is comparing it with. My evidence now suggests that the critical temperature should be reduced. If I now fit the data not with the power series but with the logarithmic function, which calculation I have not yet completed, and extrapolate, the curve becomes flatter.

However, the real answer is that our experimental data do not yet overlap so that the disagreement is between an extrapolation based on a misconception and a clear experiment. I would say that the weight of evidence is in favor of the direct measurements of Dr. Moldover with respect to this point. As he pointed out, he is measuring a very large quantity.

R. Renard: I would like to point out that Dr. Garland and I have developed a theory in which not only the spin contribution but also the lattice contribution to the specific heat of a crystal is taken into account. For an Ising model in two dimensions it can be shown that the system is mechanically unstable around the critical temperature, leading to a hysteresis. This must also be true for a three dimensional system if it is correct that C_v goes to infinity at the critical temperature for this model, where one has to replace dT_λ/dp by dT/dp along a line of instability points. It is predicted that C_p should go to infinity but that C_v would not.

References

[1] B. S. Deaver and W. M. Fairbank, Phys. Rev. Letters **7**, 43 (1961).
[2] B. D. Josephson, Phys. Rev. Letters **1**, 251 (1962).
[3] See, M. E. Fisher, Phys. Rev. Letters **16**, 11 (1966).
[4] P. Ehrenfest, Leiden Comm. Suppl. 75b (1933).
[5] L. Tisza, Ann. Physics (N.Y.) **13**, 1 (1961). See also L. Tisza "Phase Transformations in Solids," Smoluchowski, Mayer, and Weyl, eds., ch. 1 (John Wiley & Sons, Inc., New York, N.Y., 1951).
[6] I. Rudnick and K. A. Shapiro, Phys. Rev. Letters **15**, 386 (1965).
[7] M. J. Buckingham and W. M. Fairbank, Progress in Low Temperature Physics, ed. by C. Gorter (North Holland Publ. Comp. Amsterdam, 1961, Vol. III, p. 80).
[8] R. W. Hill and O. V. Lounasmaa, Phil. Trans. **A252**, 357 (1960).
[9] M. A. Weinberger and W. G. Schneider, Can. J. Chem. **30**, 422 (1952).

SCATTERING: ELASTIC

Chairman: P. Debye

Introductory Remarks

P. Debye

Cornell University, Ithaca, N.Y.

Since Dr. Montroll will not talk, I will take the opportunity to speak two minutes to give you my conception of what he would have said. I think he would have said that, if you want to look at what radiation is going to do when it falls on a medium with irregular fluctuations, you have to characterize these fluctuations first in a phenomenological way. He would have started (don't believe what I say; this is only my conception) by characterizing these fluctuations by a correlation function. Then he would have insisted that this correlation function has to be a correlation function in space as well as in time. Then he would have said that from this correlation function you can calculate the intensity of the scattered radiation directly by a simple Fourier transformation. Then he would have said that you have to look at two things in the intensity distribution. First, how is the intensity distributed over the angles? This geometrical feature of the intensity gives you an opportunity to characterize a length. Then he would have said that you can also make a spectral investigation of the scattered light, which would be characteristic for time correlations. Then he would have said that this is characterized by a correlation time or by a relaxation time, if you want to call it that way depending on the circumstances. This would be completely phenomenological.

I was prepared to tell him that this is a linear theory, which you generally call a Born approximation. If you come in the neighborhood of the critical point, the correlations become bigger and bigger and bigger, so that probably your linear theory will not work anymore. If you want to tell something about the angular distribution of the frequency distribution of the scattered radiation derived from actual observations, you have to introduce the right theory. The linear theory may not be correct at the critical point, because you get such big fluctuations. So I had hoped to induce him to say something about the second approximation and about what we are going to see there at least in a qualitative way.

Now, this is, of course, a phenomenological background. If you want to know anything about your correlation function, you have to build that upon a molecular theory. I hope that we will hear something about this molecular background. What about it, Dr. Fisher? From you?

Theory of Critical Fluctuations and Singularities

M. E. Fisher

King's College, London, Great Britain[1]

(1) In the previous lectures the behavior of the macroscopic thermodynamic functions of systems in equilibrium near critical points has been discussed. Notations for the various exponents describing the critical singularities have been introduced and the connections between them have been described [1]. In this talk we enter the microscopic domain by studying the correlation functions and their relation, on the one hand, to the thermodynamic properties and, on the other hand, to the phenomena of critical fluctuations as observed through critical opalescence and scattering experiments.

Perhaps the most important correlation function is the net pair correlation function, namely, in a fluid system

$$G(r)=g(r)-1=v^2n_2(r)-1 \tag{1}$$

and in a magnetic system in zero field

$$\Gamma(\mathbf{r})=\Gamma_{zz}(\mathbf{r})=\langle S_0^z S_{\mathbf{r}}^z\rangle/\frac{1}{3}S(S+1), \tag{2}$$

both of which reduce to $\langle s_0 s_{\mathbf{r}}\rangle$ in a simple Ising spin system ($s=\pm 1$) or a lattice gas at critical density. In terms of these functions the compressibility and magnetic susceptibility of the systems are given by

$$K_T=K_T^{\text{ideal}}\left[1+\rho\int G(\mathbf{r})d\mathbf{r}\right], \tag{3}$$

$$\chi_T=\chi_T^{\text{ideal}}\left[1+\sum_{r\neq 0}\Gamma(\mathbf{r})\right]. \tag{4}$$

Furthermore the internal energy can also be found since

$$U_{\text{config}}=\tfrac{1}{2}\rho\hat{\varphi}(0)+\tfrac{1}{2}\rho\int\varphi(\mathbf{r})G(\mathbf{r})d\mathbf{r} \tag{5}$$

and

$$U_{\text{magnetic}}\propto-\sum_{\mathbf{r}}J(\mathbf{r})\Gamma(\mathbf{r}), \tag{6}$$

where $\varphi(\mathbf{r})$ is the pair potential, with Fourier transform $\hat{\varphi}(\mathbf{k})$, and $J(\mathbf{r})$ is the exchange energy coupling the spins. The specific heat, in which we expect a critical point anomaly, can, of course, be derived by differentiating the energy with respect to temperature.

It is convenient to introduce the Fourier transforms

$$\hat{\chi}(\mathbf{k})=1+\rho\hat{G}(\mathbf{k}),\qquad \hat{G}(\mathbf{k})=\int e^{i\mathbf{k}\cdot\mathbf{r}}G(\mathbf{r})d\mathbf{r}, \tag{7}$$

$$=1+\sum_{r\neq 0}e^{i\mathbf{k}\cdot\mathbf{r}}\Gamma(\mathbf{r}), \tag{8}$$

which are directly related to the fluctuations of the Fourier coefficients of density and spin deviation through

$$\frac{\langle|\delta\rho_{\mathbf{k}}|^2\rangle}{V\rho}=\hat{\chi}(\mathbf{k})=\frac{\langle|\delta S_{\mathbf{k}}^2|^2\rangle}{N\langle|\delta S_0|^2\rangle}. \tag{9}$$

The thermodynamical formulas (3) to (6) may then be rewritten as

$$K_T|K_T^{\text{ideal}}|=\hat{\chi}(0)=\chi_T/\chi_T^{\text{ideal}}, \tag{10}$$

and

$$\int\hat{\varphi}(-\mathbf{k})\hat{\chi}(\mathbf{k})d\mathbf{k}\propto\Delta U\propto-\int\hat{J}(\mathbf{k})\hat{\chi}(\mathbf{k})d\mathbf{k}. \tag{11}$$

Furthermore the scattering intensity observed with light, x rays or neutrons at wave number $k=(4\pi/\lambda)\times\sin(\theta/2)$ is given (in first Born approximation) by

$$I(\mathbf{k})/I_0(\mathbf{k})=\hat{\chi}(\mathbf{k}), \tag{12}$$

where $I_0(\mathbf{k})$ is the intensity which would be observed from the ideal, noninteracting, system.

[1] Present address: Cornell University, Ithaca, New York.

These results show that $\chi(\mathbf{k})$ is the quantity of most fundamental and direct theoretical and experimental interest. In as much as a critical point is associated with an infinite divergence of K_T and χ_T we see from (3) and (4) that the correlations must become of increasingly long range near a critical point. This, in turn, implies some singularity in the behavior of $\hat{\chi}(\mathbf{k})$ for small k as T approaches T_c. Indeed a rapid increase of $\hat{\chi}(\mathbf{k})$ for small k is the mathematical expression of the observed critical opalescence.

(2) Let us review briefly the "classical" approximate theories of the behavior of the correlations near a critical point. The first theory was that due to Ornstein and Zernike [2] for a fluid; in many ways it is still to be preferred since its theoretical assumptions are clear and easy to appreciate. Firstly, the direct correlation function $C(\mathbf{r})$ is introduced via the relation for its Fourier transform.

$$\hat{\chi}(\mathbf{k}) = 1/[1-\rho\hat{C}(\mathbf{k})]. \tag{13}$$

It is then argued, or assumed [3], that $C(\mathbf{r})$ is of short range and *remains* so up to and *at* the critical point. If this is so one may expand its transform in a convergent Taylor series as

$$\hat{C}(\mathbf{k}) = \hat{C}(0) - r_0^2 k^2 + \ldots, \tag{14}$$

since $\hat{C}(\mathbf{k})$ is analytic in k^2 even at the critical point. The "interaction length" r_0 is constant (or slowly varying) and remains finite at the critical point. Truncation yields the well-known result

$$\hat{\chi}(\mathbf{k}) \simeq r_0^{-2}/(k^2+\kappa^2), \tag{15}$$

where κ is related to $\hat{C}(0)$ and turns out to be the inverse *range of correlation*. From (15) a plot of the experimentally observed inverse scattering intensity $I^{-1}(k)$ should be *linear* in k^2 at *all* temperatures approaching T_c as shown in figure 1. This Lorentzian line shape is a central prediction of the theory.

As k approaches zero we see from (10) that

$$K_T,\ \chi_T \sim \lim_{k\to 0} \hat{\chi}(\mathbf{k}) = \hat{\chi}(0) \sim 1/\kappa^2, \tag{16}$$

so that κ must vanish as the critical point is approached. We may assume, rather generally, that

$$\kappa(T) \sim (T-T_c)^{\nu} \text{ as } T \to T_c, \tag{17}$$

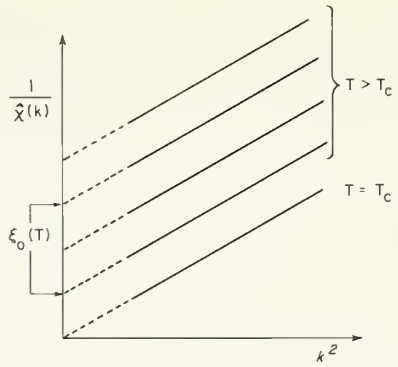

FIGURE 1. *Plot of inverse scattering intensity versus* k^2 *near the critical point to be expected on the basis of the Ornstein-Zernike and equivalent theories.*

along the critical isochore or in zero field. It follows that a plot of $I^{-1}(\mathbf{k})$ should intersect the origin when $T=T_c$ (see fig. 1).

Inverting the transform (15) for a d-dimensional system yields:

(a) for fixed $T > T_c$ and $r \to \infty$

$$G(r) \sim e^{-\kappa r}/r^{(d-1)/2}, \tag{18}$$

(b) for $T = T_c$ and $r \to \infty$

$$G(r) = G_c(r) \sim 1/r^{d-2}, \tag{19}$$

where $1/r^0$ corresponds to $\log r$ for $d=2$. In general these results can be combined into a formula of the form

$$G(r) \approx D(e^{-\kappa r}/r^{d-2})[1+Q(\kappa r)],\ (r\to\infty) \tag{20}$$

where

$$Q(x) \to 0 \text{ as } x \to 0, \tag{21}$$

and

$$1+Q(x) \sim x^{(d-3)/2} \text{ as } x \to \infty. \tag{22}$$

If we assume a van der Waals equation of state we have [1] from (16)

$$\gamma = 1 \text{ and } \nu = \tfrac{1}{2}, \tag{23}$$

but more generally according to Ornstein and Zernike we would have only the relation

$$\gamma = 2\nu. \tag{24}$$

We may cite briefly many later alternative treatments that are essentially equivalent as regards their consequences (but in which the nature of the basic assumptions are frequently somewhat obscure). For fluids there are the semithermodynamic or phenomenológical theories based on the introduction of gradient terms into the free energy due to Rocard, Klein and Tisza, Debye, Fixman, and Hart. Yvon has argued that $C(r)$ could be replaced by the Mayer function $f(r)$ i.e., by its leading term in a virial expansion. In a somewhat similar way the Pęrcus-Yevick equation always predicts a short range $C(r)$ if the potential $\varphi(r)$ is of short range. Brout's self-consistent field approach yields, with $\beta = 1/kT$,

$$\hat{\chi}(\mathbf{k}) \approx \hat{\chi}_{\text{H.C.}}(\mathbf{k})/[1-\beta\rho\hat{\varphi}'(\mathbf{k})\hat{\chi}_{\text{H.C.}}(\mathbf{k})], \qquad (25)$$

where H.C. denotes the corresponding pure hard core system and $\hat{\varphi}'(\mathbf{k})$ is the Fourier transform of $\varphi(\mathbf{r})g_{\text{H.C.}}(\mathbf{r})$. This is again equivalent near T_c. (Some of these theories have been reviewed in more detail recently [3].) For binary alloys one may mention work by Landau, Krivoglaz, Zernike, and Cowley amongst others. For magnetic systems the phenomenological theory of Van Hove was modeled on the Ornstein-Zernike and van der Waals theories and is quite analogous. The generalized mean field treatments of Brout, and Elliott and Marshall [4], etc., yield results of the form

$$\hat{\chi}(\mathbf{k}) \approx 1/[1-\beta\hat{J}(\mathbf{k})], \qquad (26)$$

which, for short range exchange potentials, are essentially equivalent. The more recent Green's functions treatments of Tyablikov and others, Mori and Kawasaki, and Kubo and Izuyama (for the itinerant electron model) lead again to virtually the same results: in particular the direct correlation function is always of short range. The spherical model of Berlin and Kac is also similar but with $\nu = 1$ rather than $\nu = \frac{1}{2}$ as in most of the other theories, since $\gamma = 2$ in that case.

(3) I would now like to point out a conclusion drawn from many of these theories [2] concerning the nature of the specific heat singularity (C_V or $C_{H=0}$). Firstly note that one can hope to justify most of these approximate expressions for $G(r)$ at *fixed* $T > T_c$ only as $r \to \infty$ [3]. If, however, we assume they are also valid for *small* r (specifically of order of the range of direct interaction) we may calculate the specific heat as $T \to T_c$. If, as is often fashionable, we perform the calculations entirely in terms of Fourier transforms it is quite easy to overlook this implicit assumption since the "derivation" runs roughly as follows: For example for a magnet, assuming (15) and using (11), we have

$$C_H = \frac{\partial U}{\partial T} \propto \left(\frac{\partial \kappa}{\partial T}\right) \int \frac{2\kappa\hat{J}(k)dk}{(\kappa^2+k^2)^2}. \qquad (27)$$

Thus putting $k = \kappa x$, we find as $\kappa \to 0$ (i.e., $T \to T_c$)

$$C_H \sim \kappa^{d-2}\left(\frac{\partial \log \kappa}{\partial T}\right) 2\hat{J}(0) \int \frac{d\mathbf{x}}{(1+x^2)^2}, \qquad (28)$$

so that from (17) the exponent for the specific heat [1] would be

$$\alpha = 1-(d-2)\nu. \qquad (29)$$

For $d = 3$ and the usual approximation, $\nu = \frac{1}{2}$, we thus find

$$C_H \sim 1/(T-T_c)^{1/2}, \qquad (30)$$

which is a surprizingly common prediction in the literature! The analysis, however, is quite unjustified as is rather easier to see if one works in real space using (18) or (20) and (5) or (6) and explicitly inserts the short range character of the potential by cutting off the integral or sum at some $r = r_1$ [5]. In fact the specific heat is determined by the variation of $G(r)$ or $\Gamma(\mathbf{r})$ *with* T as $T \to T_c$ for *small, fixed* r (i.e., by $Q(x)$ for *small* x in (20); see also below). Thus although in a general sort of way the long range behavior of $G(r)$ is a direct "indicator" of the transition it is not sufficient to determine the specific heat singularity.

(4) We have listed the "classical" approximate theories which concur with the predictions (15) to (20) of Ornstein and Zernike. Recently, however, other answers have been proposed, in the first place by M. S. Green [6] on the basis of the hypernetted chain integral equation. Green argued that certain irreducible diagrams might be neglected *at* the critical point and thereby obtained an equation for $\hat{\chi}_c(k)$. As observed by Stillinger and Frisch [7] his argument may be applied in d dimensions and yields [3]

$$G_c(r) \approx D/r^{d-2+\eta}, \qquad (T-T_c) \qquad (31)$$

[2] But not all! See the discussion comment by Marshall concerning an honorable exception [4].

with

$$\eta = 2 - (d/3). \tag{32}$$

Taking the Fourier transform of (31) with $\eta > 0$ leads to the important prediction, contrasting with that of the O–Z theory, that a plot of inverse scattering intensity versus k^2 at $T = T_c$ should be *curved upwards* according to

$$I_{\bar{0}}^{-1}(\mathbf{k}) \sim 1/\hat{\chi}_c(\mathbf{k}) \sim k^{2-\eta}, \tag{33}$$

(see fig. 2). This point will be returned to.

More recently another expression for $\hat{\chi}(\mathbf{k})$, namely

$$\hat{\chi}(\mathbf{k}) \sim 1/(A + k^{1/2d}), \qquad (k \to 0), \tag{34}$$

has been presented by Abe [8] who was inspired by the recent paper of Patashinskii and Pokrovskii [9] on the lambda anomaly in helium. This latter work has attracted a great deal of attention since it claimed to predict theoretically the logarithmic specific heat anomaly which is observed in the beautiful experiment described by Professor Fairbank this morning. Indeed the formula (34) is "designed" to predict a logarithmic specific heat by just the same false argument we outlined above! [In the analysis of Patashinskii and Pokrovskii and of Abe it is assumed that $A(T)$ varies as $(T - T_c)$ to the power unity. However some other power would not alter the logarithm but only its amplitude.] Even if (34) is correct, we cannot, therefore, believe in the "derivation" of the logarithmic specific heat. Actually, as we will see below, (34) is *not* correct for the Ising model and its analog for helium, in terms of the one-body density matrix, is equally to be doubted. From (34) we find

$$G_c(r) \approx D/r^{1/2d} \tag{35}$$

which is equivalent to (31) with

$$\eta = 2 - \tfrac{1}{2}d. \tag{36}$$

Note that in significant contrast with all other theories, $G(r)$ will *still* have a long-range tail ($1/r^{3/2}$ for $d = 3$) when T *exceeds* T_c according to (34) since $\hat{\chi}(\mathbf{k})$ is still singular at $k^2 = 0$. (Patashinskii and Pokrovskii were more circumspect on this point!)

(5) Now I will turn to some more rigorous results on the behavior of the correlation functions which will enable us to judge the approximate theories. Firstly, as to the question of the exponential decay of the correlation functions away from the critical point (in the case envisaged of short range interactions). With fair generality one may define the inverse range of correlation through [3]

$$\kappa(T) = -\limsup_{r \to \infty} (1/r) \log |G(r)|, \qquad (T > T_c). \tag{37}$$

The existence of this limit with $\kappa > 0$ implies the asymptotic exponential decay of $G(r)$. For the Ising model the matrix method provides expressions for the correlation functions from which (37) is an immediate consequence in a system of finite cross-section (but infinite length). Onsager's [10] explicit solution for $d = 2$ shows this remains true for a system of infinite width above T_c. For a continuum classical gas one may construct a generalized integral kernel for which one similarly finds an exponential decay, the parameter κ being determined, as in the matrix case, by the ratio of the two largest eigenvalues.

The convergence of the activity and virial expansions for gases recently established rigorously by Penrose, Lebowitz, and Ruelle implies a similar result for $G(r)$ in the domain of convergence—and, by continuation along the physical axis, up to some singularity which would have a physical significance (probably the critical or condensation point). We can thus expect rather generally that $\hat{\chi}(\mathbf{k})$ should be analytic for small k^2 *above* T_c (in disagreement with Abe's result but in agreement with the O–Z theories).

The vanishing of κ as T approaches T_c according to (17) is confirmed rigorously by Onsager's result,

$$\exp(-\kappa a) = v(1+v)/(1-v), \qquad v = \tanh(J/kT), \tag{38}$$

for the $d = 2$ Ising model. This yields the nonclassical value $\nu = 1$ for the exponent defined in (17).

Further details of the decay of correlation *above* T_c for the simple Ising model follow from an analysis of the matrix method [3, 11] which confirms the O–Z result (18). For the more general integral kernels an appropriate form of perturbation theory reveals a spectrum of eigenvalues from which a similar conclusion will follow. The analyses of nonuniform fluids by Lebowitz and Percus in terms of the direct correlation function also serve to justify the asymptotic validity of the O–Z theory *away* from the critical point [3].

The most important rigorous result for our present purpose, however, follows [3, 7] from the work of Onsager and Kaufman [12] on the pair correlation functions of the $d=2$ Ising model at the critical point. Their result shows that

$$G_c(r) \approx D/r^{1/4}, \qquad \text{i.e., } \eta = 1/4, \qquad (d=2). \quad (39)$$

This is in clear contradiction with the predictions of Ornstein and Zernike ($\eta=0$) and all other theories! [See eqs (32) and (36).]

To summarize these considerations, we can still hope generally to describe the correlations near the critical point in terms of two lengths, the "range of correlation" $1/\kappa(T)$ which diverges as $T \to T_c$ and a "range of direct interaction" $r_0(T)$ which remains finite. However, generalizing (20), we must expect for all small κ that

$$G(r) \approx D(e^{-\kappa r}/r^{d-2+\eta})[1+Q(\kappa r)], \qquad (r \to \infty) \quad (40)$$

where $D = d_0/\rho r_0^{2+\eta}$ and $Q(x)$ satisfies (21) and, in place of (22),

$$1 + Q(x) \approx x^{(d-3)/2+\eta}, \qquad \text{as } x \to \infty. \quad (41)$$

If we neglect Q (which is valid near T_c) the Fourier transform of (40) is well approximated by

$$\hat{\chi}(\mathbf{k}) \approx D/(\kappa^2 + k^2)^{1-\eta/2}, \quad (42)$$

which extends (33) to temperatures above T_c. (See also fig. 2.) In view of (39) we might expect the exponent η to have a relatively small but positive value. Letting k approach zero and using (10) and (17) shows that the divergence of the susceptibility and compressibility (along the isochore) [1] is now given by

$$\gamma = (2-\eta)\nu \quad (43)$$

in place of the Ornstein-Zernike formula (24). As observed some time ago [13] this result applied to the $d=2$ Ising model using (38) and (39) yields $\gamma = 7/4$ which is just what is found by careful extrapolation of the series expansion [14, 15] as explained yesterday by Professor Domb.

(6) In view of my remarks on the impossibility of determining the specific heat singularity from the long-range part of the pair potential[3] it is worth pausing to ask how Onsager's famous result that the specific heat of the $d=2$ Ising model diverges as $\log |T-T_c|$ fits into the picture. Accepting the form (40) as the leading contribution to $G(r)$ for all r and using (6) and (38) one can easily see that the logarithmic singularity in the specific heat means that

$$Q(x) \approx Bx \log x, \qquad \text{as } x \to 0. \quad (44)$$

As explained, it is only the behavior for small x which is relevant. More generally if $\alpha + 2\nu > 1$ (as is probably always the case) a specific heat exponent $\alpha > 0$ would follow from (40) if

$$Q(x) = x - bx^{(1-\alpha)/\nu} + \ldots \qquad \text{as } x \to 0. \quad (45)$$

(7) In the absence of exact results for the three-dimensional Ising model (or for the Heisenberg model) one must return to approximate methods of calculation. However, by developing systematic successive approximations, notably sufficiently long series expansions, one may hope, as in the case of the thermodynamic functions, to draw reliable conclusions about the critical behavior. I will report on progress along these lines in work undertaken in collaboration with Mr. R. J. Burford.

Firstly, for the $d=3$ Ising model one may develop a series expansion for the range of correlation κ in powers of $v = \tanh(J/kT)$. In the standard Ising problem the partition function can be expanded in terms of configurations of (closed) polygons on the lattice (each bond being associated with a factor v) subject to the condition that an even number of bonds meet at each vertex. To calculate $e^{-\kappa a}$ (where a is the lattice spacing) one needs in addition to the polygons a single chain of bonds that stretches right across the lattice (in the direction of interest). By enumerating these configurations one finds for the propagation of correlation parallel to a principal axis of the simple cubic lattice

$$e^{-\kappa a} = v + 4v^2 + 12v^3 + 36v^4 + 108v^5 + 356v^6 + 1204v^7 + 4420v^8 + 16124v^9 + \ldots . \quad (46)$$

[3] The specific heat divergence can, however, be found from the long range part of the *fourth* order correlation functions. See remarks in the discussion following this talk.

Evaluation of this series with the aid of Padé approximants enables accurate plots of $\kappa(T)$ to be drawn which reveal clear deviations from the predictions of the simpler approximate theories [16]. The series is not, however, sufficiently regular to yield a firm estimate of the exponent ν although one may conclude that it lies in the range 0.60 to 0.7. Since $\gamma = 1.25$ for the simple cubic this is consistent with some small value of η in (43) but evidently cannot decide for or against the Ornstein-Zernike prediction $\eta = 0$.

A more fruitful approach has been to calculate the series expansions for the correlation function $G(\mathbf{r})$ at all values of $\mathbf{r}$ on the lattice. The relevant configurations consist again of polygons plus a chain but the chain is now of finite length and simply runs from the origin to the lattice point at $\mathbf{r}$ (these being the only points at which an odd number of bonds may now meet). Appreciable assistance in the calculations may be gained from the known series for the susceptibility and from available numerical data on self-avoiding lattice walks. From the series for $G(\mathbf{r})$ one may form the moments

$$\mu_s(T) = \rho \int r^3 G(\mathbf{r}) d\mathbf{r},$$

or

$$= \sum_{\mathbf{r}} r^s \Gamma(\mathbf{r}) = \sum_{\mathbf{r}} r^s \langle s_0 s_{\mathbf{r}} \rangle. \qquad (47)$$

Of course the zeroth moment is just proportional to the susceptibility itself while the second moment is directly related to the initial *slopes* of plots of the inverse scattering versus k^2 (and to the so-called Debye "persistence length," see ref. 3). By using (40) and (43) we find immediately that

$$\mu_2(T) \approx M_2/\kappa^{4-\eta} \sim 1/(T - T_c)^{2\nu+\gamma}. \qquad (48)$$

Consequently estimates of the critical behavior of $\mu_2(T)$ will yield estimates of ν and η. For the simple cubic the following terms have been obtained (while one more is available for the plane square lattice)

$$\mu_2 = 6v + 72v^2 + 582v^3 + 4032v^4 + 25542v^5$$
$$+ 153000v^6 + 880422v^7 + 4920576v^8 + 26879670v^9$$
$$+ 144230088v^{10} + \ldots . \qquad (49)$$

This series and the corresponding ones for the plane square lattice and other three-dimensional lattices are very regular and may be extrapolated by the ratio and Padé approximant techniques. As a check on the consistency of our analysis let us first look at the two-dimensional series for μ_2. Using the exactly known critical point and the result $\gamma = 7/4$ the Padé approximants to $(v - v_c)(d/dv) \log \mu_2$ yield the successive estimates:

$$\eta \simeq 0.2495,\ 0.2532,\ 0.2485,\ 0.2511,\ 0.2507, \quad (d = 2).$$

These are evidently approaching the exact limit $\eta = 1/4$ rather rapidly which confirms the validity of our approach. For the simple cubic a corresponding sequence of estimates (taking $\gamma = 1.250$ and using the accurately known critical point) is:

$$\eta \simeq 0.0696,\ 0.0684,\ 0.0621,\ 0.0583,\ 0.0580, \quad (d = 3).$$

These values seem to be converging to a limit in the vicinity of 0.058 to 0.060 and studies of related series lead to a similar result. We may conclude with fair confidence that

$$\eta = 0.059 \pm 0.006, \qquad \nu = 0.644 \pm 0.002, \qquad (d = 3). \quad (50)$$

The results for the B.C.C. and F.C.C. lattice are quite similar although less precise as the series are shorter. The value (50) for η is consistent with the rather natural conjecture $\eta = 1/16 = 0.06250$ (implying $\nu = 20/31 = 0.64516\ldots$) but the true value might well be lower, say, $\eta = 1/18 = 0.05555$ (implying $\nu = 9/14 = 0.64285\ldots$). (It is interesting to note that the values of the analogous exponent for the self-avoiding walk or excluded volume problem are $\eta' = 2/9$ and $1/18$ in two and three dimensions, respectively.)

One may also use the series for $G(\mathbf{r})$ to estimate $G_c(\mathbf{r}) = G_c(x, y, z)$ directly for small values of r although this cannot be very accurate owing to the singularity of $G(\mathbf{r})$ as a function of T which is similar to that in the energy i.e., *roughly* $(T - T_c)$ log $(T - T_c)$. For the nearest lattice points to the origin we estimate:

$$(0, 0, 1)\ 0.328,\ (0, 0, 2)\ 0.160,\ (0, 0, 3)\ 0.11;$$

$$(0, 1, 1)\ 0.206,\ (0, 1, 2)\ 0.137;\ (1, 1, 1)\ 0.163.$$

These values are quite consistent with (31) and (50) i.e., with $G_c(\mathbf{r}) \sim 1/r^{1.06}$, but they do not yield an independent estimate of η.

For the Heisenberg model fewer terms can be calculated and their behavior is less regular especially for low spin values. The most favorable case is the F.C.C. lattice for $S=\infty$ where we obtain the sequence of estimates:

$$\nu \simeq 0.786,\ 0.760,\ 0.724,\ 0.710,\ 0.702.$$

From this and other sequences we feel able to estimate

$$\eta = 0.075 \pm 0.035,\ \nu = 0.692 \pm 0.012. \qquad (51)$$

The values of η and ν (as those of γ) do not appear to depend significantly, if at all, on the value of the spin (or on the lattice structure).[4]

(8) It seems clear from these calculations that η has a positive value for three-dimensional Ising models and for the Heisenberg models. The value of η is, however, rather small although it is interesting to note that it is apparently slightly larger for the Heisenberg model. (This is in accord with the larger deviation of the exponent γ from its classical value of unity.) I feel η *might* be somewhat larger still in a continuum fluid with molecules of a nonsimple shape where "excluded volume effects" would be expected to play a larger part.

In as much as η is positive we must expect a plot of the inverse scattering intensity versus k^2 to be curved *at* and (by continuity) *near* T_c for small k as shown by (33) and (42). Since the expected value of η is so small, however, this curvature (even if present) might not be very evident. In fact, the main effect (as may be verified by plotting curves according to (42) for small values of η) is to cause the scattering plots "to hang up" so that the intercepts appear not to approach zero as $T \to T_c$, and even at T_c the curve appears to extrapolate linearly with k^2 to a nonzero value. These effects are indicated in figure 2 where, however, a relatively large value of η has been assumed for the sake of clarity.

What do the experiments say? Well, we will hear the latest situation from some of the following speakers but perhaps I should finish by reviewing very briefly a few relevant experiments which, I think, give some indications of small deviations from the Ornstein-Zernike theory. These deviations are in the expected direction although, I should stress, the problem is still very much "in the air"!

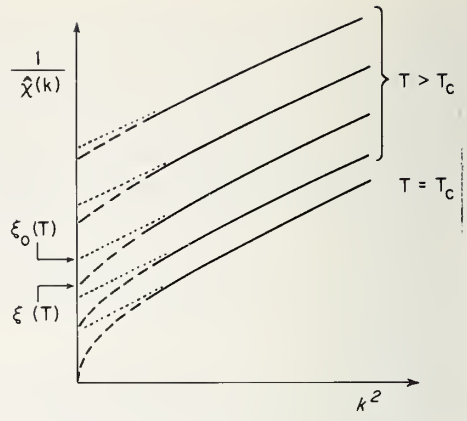

FIGURE 2. *Plot if inverse scattering to be expected with a positive value of η (larger than that estimated for the three-dimensional Ising or Heisenberg models) illustrating the difference between the apparent linear intercept $\xi_0(T)$ and the true intercept $\xi(T) = 1/\hat{\chi}(0)$.*

Walker and Keating in their recent neutron scattering experiments on the binary alloy β-brass [17] observed that when T approached T_c the intensity of the superlattice line (which is analogous to K_T in a fluid system) increased more rapidly than expected on the classical theories. Their observations were, in fact, consistent with $\gamma = 1.25$. They also observed a slight *narrowing* of the line relative to a Lorentzian line shape near T_c which would be expected from (42) with a small positive value of η. More recent experiments on β-brass by Dr. Als-Nielson and Dr. Dietrich will be reported tomorrow.

Jacrot's original neutron scattering experiments on iron yielded, on reanalysis, the estimates $\gamma = 1.30$ to 1.33 for the behavior of $1/\hat{\chi}(0)$ near T_c. This is in agreement with direct measurements of the susceptibility as has already been reported (and with the Heisenberg model predictions). Passell and coworkers have also found a value of $\gamma \simeq 1.33$ from their more recent experiments on iron. They seem, in addition, to find evidence that the intercepts of the scattering curve are "hung up" in a way consistent with a small value of η; but this is very tentative and I will leave Dr. Passell himself to describe his very careful and difficult experiments.

[4]Note added in Proof. However, recent work on the susceptibility for $S = \frac{1}{2}$ indicates that the value of γ is probably appreciably larger than the $S=\infty$ value $\gamma = 1.33$ (although η may not change much); see G. A. Baker, H. E. Gilbert, J. Eve, and G. S. Rushbrooke, Physics Letters, **20**, 146 (1966).

Thomas and Schmidt [18] have made x-ray experiments on argon in the critical region; they observed *no* deviations from Ornstein-Zernike theory! However, they did not measure along an isochore nor did they go very close to the critical point. It is to be hoped that these experiments will be extended both with x rays and with light, since the behavior of (presumably) simple fluids like xenon and argon is obviously of cardinal interest.

The most extensive critical scattering measurements have been made on binary fluid systems where in most cases one or both species are comparatively complicated organic molecules. This makes me, as a theoretician, somewhat apprehensive when it comes to applying the (relatively) simple theories we have been discussing! Professor Brumberger will review this field in detail later this afternoon so let me just sketch some of the recent work. Professor Debye and his collaborators working in particular with polystyrene-cyclohexane solutions have found little or no evidence of deviations from the classical theories—*even* as regards the value of γ for $\hat{\chi}(0)$ which appears to be quite close to unity. However, the experiments are quite difficult to perform, especially near T_c, and McIntyre, Wims, and Green, in experiments on the same system, have indeed found deviations from the classical expectations close to T_c roughly of the sort to be expected with a positive value of η. Brady and Frisch [19] have also observed somewhat similar nonclassical anomalies in the system perfluoroheptane in iso-octane.

More recently Dr. Chu in a series of very careful experiments on *n*-dodecane in dichloroethyl ether has found significant deviations from linearity in the inverse scattering plots at temperatures very close to critical. I do not want to anticipate Dr. Chu's lecture later this afternoon but let me say that the value of η that seems to fit his excellent data, namely $\eta \simeq 0.35$, is much larger than our simple theoretical models would suggest. Maybe this is an effect of steric hindrance due to the shape of his molecules—I do not know! Whatever the answer, it is clear that there remains much scope for experimental and theoretical work before our understanding of these subtle but fundamental questions will be complete.

References

[1] See the associated notes on "Critical Point Singularities," these Proceedings page 21.
[2] L. S. Ornstein and F. Zernike, Proc. Acad. Sci. Amsterdam **17**, 793 (1914); Physik. Z. **19**, 134 (1918).
[3] M. E. Fisher, J. Math. Phys. **5**, 944 (1964); reprinted in The Equilibrium Theory of Classical Fluids, eds. H. L. Frisch and J. L. Lebowitz (W. A. Benjamin, Inc. 1964).
[4] R. J. Elliott and W. Marshall, Rev. Mod. Phys. **30**, 75 (1958).
[5] This has been pointed out by others, e.g., in M. Fixman, Adv. in Chemical Phys. **4**, 175 (1964), although it seems not to be generally appreciated.
[6] M. S. Green, J. Chem. Phys. **33**, 1403 (1960).
[7] F. H. Stillinger and H. L. Frisch, Physica **27**, 751 (1961).
[8] R. Abe, Progr. Theoret. Phys. **33**, 600 (1965).
[9] A. Z. Patashinskii and V. L. Pokrovskii, Soviet Phys. JETP **19**, 677 (1964).
[10] L. Onsager, Phys. Rev. **65**, 117 (1944).
[11] L. P. Kadanoff, to be published.
[12] B. Kaufman and L. Onsager, Phys. Rev. **76**, 1244 (1949).
[13] M. E. Fisher, Physica **25**, 521 (1959).
[14] C. Domb and M. F. Sykes, J. Math. Phys. **2**, 63 (1961).
[15] G. A. Baker, Jr., Phys. Rev. **124**, 768 (1961).
[16] See the figure due to R. J. Burford and M. E. Fisher in Proc. Inc. Conf. on Magnetism, Nottingham, Sept. 1964 (Phys. Soc. London) page 81.
[17] C. B. Walker and D. T. Keating, Phys. Rev. **130**, 1726 (1963).
[18] J. E. Thomas and P. W. Schmidt, J. Chem. Phys. **39**, 2506 (1963).
[19] G. W. Brady and H. L. Frisch, J. Chem. Phys. **35**, 2234 (1961); **37**, 1514 (1962).

209-493 O-66—9

Scattering of Light and X-rays from Critically Opalescent Systems

H. Brumberger

Syracuse University, Syracuse, N.Y.

Introduction

The experimental investigation of critical phenomena has become an actively pursued area of research in recent years for two major reasons—a renewal of interest in the statistical-mechanical theory of these phenomena (for reviews see, for instance, references 1–5), and a considerable increase of experimental sophistication coupled with a better understanding of the experimentally significant variables.

The review will attempt to survey, briefly, the experimental literature dealing with light and x-ray scattering from one- and two-component systems near critical points, beginning in 1950 and concluding in March 1965. Magnetic phenomena will not be considered, but attention confined to gas-liquid, liquid-liquid, and solid-solid critical points. The review will not be completely exhaustive, but attempt to compare the most important results critically, and to extract any common observational features. Some criteria for comparison will be discussed below. The systems reported on are summarized in tables 1–3.

TABLE 1. *One-component fluid systems*

System	Technique	References	l [a] (Å)
Argon	X ray	6 (1942) 7 (1951) 8 (1963)	5.4 near transition.
Neon	X ray	9 (1962)	
Nitrogen	X ray	10 (1950) 11 (1964)	6.0 near transition.
Ethylene	Light	12 (1950)	
Carbon dioxide	Light	13 (1960)	
Methane	X ray	14 (1957)	
Ethane	X ray	14 (1957)	
	Light	15 (1950)	
Propane	X ray	14 (1957)	
Butane	X ray	14 (1957)	
Ether	X ray	16 (1960)	
Benzene	X ray	16 (1960)	

[a] Debye "range of intermolecular forces."

System	Technique	References	l^a(Å)
Perfluoromethyl-cyclohexane-carbon tetrachloride	Light	17 (1950)	14.7
Carbon disulfide-methanol	X ray	18 (1958)	
	Light	20 (1954)	
Phenol-water	X ray	19 (1956)	
	Light	20 (1954)	
Isobutyric acid-water	Light	20 (1954)	
Phenol-heptane	Light	20 (1954)	
Methanol-cyclohexane	Light	20 (1954)	
	Light	21 (1962)	12.7
	Light	22 (1963)	
Methanol-hexane	Light	20 (1954)	
Nitrobenzene-isopentane	Light	20 (1954)	
Aniline-cyclohexane	Light	20 (1954)	
	Light	21 (1962)	~ 0
	Light	23 (1963–1964)	
Triethylamine-water	Light	20 (1954)	
β, β'-Dichloroethyl-ether-n-decane	Light	24 (1964)	~ 13
i-Octane-perfluoro-heptane	X ray	25 (1961)	
	X ray	26 (1961)	
	X ray	27 (1962)	
	X ray	28 (1964)	
2, 6-Dimethylpyridine-water	Light	29 (1964)	8.7
Nitrobenzene-n-heptane	X ray	30 (1963)	3.5
	Light	31 (1964)	9.4
Perfluorotributyl-amine-isopentane	Light	32 (1964)	12.5
	X ray	32 (1964)	14.0
Polystyrene-cyclohexane	Light	33 (1960)	
		34 (1960)	From 27–66 depending on average molecular weight
		35 (1962)	
		36 (1962)	
		37 (1962)	
		38 (1960)	
	X ray and Light	39 (1965)	27($M_n = 14700$)
β, β'-Dichloroethyl-ether-*n*-dodecane	Light	40 (1965)	

[a] Debye "range of intermolecular forces."

System	Technique	References
α-β Quartz.....	Light	41 (1957)
Aluminum-zinc.....	X ray	42 (1958)

General Criteria

The observations reported in the tabulated publications must be subjected to critical examination from two viewpoints: (1) Are the reported data reliable—i.e., were proper precautions taken to insure purity of materials, precise temperature control, etc., and were other experimental factors kept to a minimum or corrected for? These might include interfacial reflections, dust, inconstancy of light source, cell geometry, multiple scattering, refraction corrections, beam divergence, monochromaticity, etc., for light-scattering experiments; and collimation errors, background corrections, absorption corrections, monochromaticity, etc. for x-ray experiments. (2) Are the data sufficiently extensive (i.e., do they extend over a sufficient range of angles and temperatures), do they confirm theoretically predicted behavior, and does the collective body of observations indicate some trends of sufficiently general nature to rule out the possibility that they are experimental artifacts? This is a particularly important point for critical phenomena, which apparently are subject to a variety of experimental effects not usually observed under noncritical conditions (for instance, gravitational effects).

Most of the recent theoretical treatments of critical opalescence have been based on an extended, and sometimes reformulated, Ornstein-Zernike (O-Z) Theory, and on various lattice gas calculations [3, 4, 5]. Direct experimental tests of the scattering behavior predicted by classical O-Z theory as reformulated by Debye are

1. The inverse of the relative scattered intensity should vary linearly with s^2, where $s=4\pi\lambda^{-1}\sin(\theta/2)$, λ is the wavelength in the medium, θ the scattering angle.

2. $i^{-1}(s)$ *versus* s^2 curves obtained at different temperature distances $\Delta T(\Delta T=T-T_c)$ from the critical temperature should be essentially parallel.

3. The extrapolated zero-angle intercepts of these curves should vary linearly with ΔT and go to zero at T_c.

Further analysis of the approximations in the O.-Z. theory [4] indicates the possibility that the $i^{-1}(s)$ *versus* s^2 plot might show downward curvature near $T\rightarrow T_c$ for small values of s^2, and that the $i^{-1}(0)$ *versus* ΔT plot might no longer be linear.

Münster and coworkers [43, 44] have recently shown that a more rigorous result for i^{-1}, on the basis of a modernized version of the O.-Z. theory, is

$$i^{-1}(s)\propto \frac{1}{4\pi\rho A}\,\frac{k^2+s^2}{1-\dfrac{s^2}{4\pi\rho A}} \qquad (1)$$

where $k\rightarrow 0$ as $T\rightarrow T_c$, ρ is an "effective density," A is a constant. (1) yields the O.-Z. relation as an asymptotic approximation for small s, and would predict long-range curvature in the $i^{-1}(s)$ *versus* s^2 plot.

Debye, in recent publications [32], has also stressed the fact that his original theory [1] is an approximation taking only the average square of the local gradient of density or composition fluctuations into account, and that inclusion of higher-order terms in the series expansion for the inverse intensity would introduce curvature into O.-Z. plots when carried over a sufficient range of s^2. Nevertheless, the approximate Debye theory is useful in correlating experimental observations, and yields the characteristic parameters l and L, defined by

$$L^2=(\text{persistence length})^2=\frac{\int 4\pi r^2 G(r) r^2 dr}{\int 4\pi r^2 G(r) dr} \qquad (2)$$

and $$L^2=\frac{l^2}{\tau-1} \qquad (3)$$

where $\tau=T/T_c$. l. the "range of intermolecular forces," is predicted to be constant for O.-Z. behavior; where this parameter has been reported. its value is given in tables 1–3.

One-Component Systems

One observation which turns out to be generally true is that a differential of about 10 years between publications dealing with the same system is frequently good reason to discard the earlier work.

For argon and nitrogen, several x-ray studies are available in the 1950–1965 period. For argon, the 1951 paper by Graham and Lund [7] is based on much earlier data obtained by Eisenstein and Gingrich [6] which were taken to a minimum scattering angle of 2° only. A correlation function is obtained by direct Fourier inversion of the extrapolated scattering curves and used to calculate

$$\langle r^2\rangle = L^2 = \int_0^\infty 4\pi r^2 G(r) r^2 dr \Big/ \int_0^\infty 4\pi r^2 G(r) dr$$

yielding values of 6–8.5 Å, which would indicate that measurements were not extended to sufficiently small angles. In view of this situation, only the recent work on argon by Schmidt and Thomas [8] can be used to test the O.-Z. predictions.

For the x-ray investigations of nitrogen [10], paraffins [14], ether [16], benzene [16], and neon [9] somewhat similar remarks apply. In the Russian paper on ether and benzene [16], insufficient experimental information is given; it is difficult to credit the observation of several x-ray diffraction maxima within 2 deg θ for benzene, and to accept the authors' analysis of their data as indicating density fluctuations of certain discrete sizes only. For the other systems, the measurements were not extended to sufficiently small angles or ΔT's. nor were collimation corrections applied. Interpretation of these data was generally attempted by means of a Guinier approximation (assuming spherical inhomogeneities) and invariably yielded very small radii (3–14 Å) for the inhomogeneities.

The recent nitrogen work of Schmidt and Thomas [11] must remain the major source of useful data for this system. Schmidt and Thomas' observations on argon and nitrogen are in general agreement with the classical O.-Z. theory. The zero-angle inverse intensity is linear with ΔT for both vapor and liquid over several degrees near the critical temperature T_c. A meaningful l-value —~5 Å near T_c—is obtained in both cases. No deviations from the Ornstein-Zernike plot—$i^{-1}(s)$ *versus* s^2—are observed at small angles: this may be because the smallest ΔT was 0.05 °K and the smallest scattering angle about 2×10^{-3} radians (MoKα radiation for argon, CuKα for nitrogen).

All three of the light-scattering measurements—carbon dioxide [13], ethane [15], and ethylene [12]—were made at scattering angles of 90° only. In the case of carbon dioxide, the critical temperature was only approached to within ~0.2°, and the authors report generally good agreement with Rayleigh's equation except nearest T_c, where the exponent of λ is 3.2 instead of 4. The experiments on ethane and ethylene which were very precise as far as temperature was concerned (±0.001 °C) but much less precise with respect to pressure control (±1 psi), indicated four regions: (1) $T \gg T_c$, λ^{-4} law holds, (2) a region where intensity increased, λ-dependence decreased, within about a degree above T_c. (3) a reversal in intensity with close approach to T_c (ascribed to multiple scattering and absorption). (4) and a rapid, erratic increase (ascribed to condensation droplets) which showed hysteresis phenomena on temperature reversal. The authors conclude that the O.-Z. theory, which predicts a change in wavelength dependence proportional to λ^{-2}, does not apply at temperatures below the temperature of maximum scattering, i.e., very near T_c. Nevertheless, they calculate "cluster diameters" from the O.-Z. intensity expression (for the region where this applies) to be of the order of 1000 molecular diameters closest to T_c. While it is not possible to translate these observations directly into the language of this paper, it appears that the O.-Z. theory yields meaningful parameters—comparable to values for L found from the Debye treatment—within a 1-deg region of T_c. but *not* in the immediate neighborhood of the critical point.

The general conclusion for the one-component systems evaluated is that the x-ray observations show good agreement with O.-Z. theory, the light-scattering observations reasonable agreement except very near T_c, where results are seriously afflicted by multiple-scattering and turbidity problems.

The possibility of gravitational effects was examined by Mason and coworkers [45–49], who report definite effects in one-component but not in two-component systems. These are probably not serious for the above cases.

Fluid Two-Component Systems

Because of considerable difficulties in controlling pressures precisely for one-component systems near the critical point, more experiments have been done with two-component systems, which show analogous behavior near the extrema of the consolute curve. The temperature variable is more easily controllable, but purification of the samples becomes harder.

Most of the work on two-component systems has been done by light-scattering, and for several systems a series of recent publications is available.

The x-ray observations by Kirsh and Mokhov on the carbon disulfide-methanol and phenol-water systems [18, 19] neither approach T_c sufficiently closely nor extend to sufficiently small scattering angles. It is difficult to understand the series of five small-angle maxima reported within a scattering angle of one degree at temperatures 22.5 and 28.5 °C from T_c for the CS_2-MeOH system.

An extensive series of binaries was investigated by Chow Quantie [20] using light-scattering. Results fell generally into two categories—systems showing strong opalescence, a wavelength exponent between 3.2 and 4.3, and a maximum scattered intensity at about $\frac{\pi}{2}$ (CS_2-MeOH, ΦOH-H_2O, ΦNO_2-isopentane, ΦNH_2-cyclohexane); and systems showing weak opalescence, a wavelength exponent between 2.2 and 2.5, strong dissymmetry, but no maxima (MeOH-cyclohexane, isobutyric acid-H_2O, MeOH-C_6H_{14}, Et_3N-H_2O). It is likely that the angular intensity distributions for the strongly opalescent systems are distorted in the forward direction by multiple scattering effects; this is borne out by Quantie's observation that even the weakly opalescent systems showed a forward drop-off (and corresponding development of a maximum) as the wavelength was shortened. Similar observations, and a shift of the intensity maximum to larger scattering angles with smaller λ are reported for the aniline-cyclohexane system. Attempts to account for multiple scattering were made by Quantie.

Replotting of the Quantie data for the aniline-cyclohexane (strong) and isobutyric acid-water (weak) systems shows the following: for isobutyric acid-water runs at 0.02 and 0.07 °C from T_c, nearly parallel O.-Z. lines are obtained, both showing a slight downward curvature at small angles. For aniline-cyclohexane (at 0.04 and 0.10 °C), parallel but curved O.-Z. lines result, with upward curvature at both smallest and largest angles. The high-angle behavior seems fairly typical for strongly opalescent systems and is also observed for nitrobenzene-heptane, etc.

It is interesting to compare these results to the light-scattering observations of Debye and coworkers [21, 22] for cyclohexane-aniline and methanol-cyclohexane. The latter system, according to Quantie, exhibits weak opalescence and similar light-scattering behavior to isobutyric acid-water. Slightly different concentrations and critical temperatures are reported by the two investigators; it is probable that the purity of Debye's samples is better. In the methanol-cyclohexane case, a "normal" O.-Z. plot is found within 0.68 °C from T_c. There are no obvious deviations from linearity except a slight upward drift at small and large angles. O.-Z. curves are nearly parallel. These measurements were only extended to a scattering angle of 30°, however. The zero angle intercepts somewhat doubtful because of the limited low angle range, are linear with ΔT. For cyclohexane-aniline, the Debye group reports nearly horizontal O.-Z. curves bending upward substantially at high scattering angles and slightly at small ones, and becoming more erratic at larger ΔT's. Intercepts are no longer linear in ΔT. The similarity between Debye's and Chow Quantie's data close to T_c is striking.

More recent and very careful light-scattering experiments by McIntyre and Wims [23] have brought several new and interesting discrepancies to light for the cyclohexane-aniline system. A definite downward curvature of the O.-Z. plots is observed at $\Delta T < 0.01$ °C and at small scattering angles, using sample cells of thickness down to 0.5 mm. For smaller cells (~ 0.1 mm), new phenomena appear—for instance, a change in separation temperature by as much as 0.5 °C. Whether this is due to surface or other effects is not known; nevertheless it is a graphic illustration that attempts to reduce one difficulty (multiple scattering in this instance) may introduce a host of new ones in the neighborhood of the critical point.

Among the remaining fluid binary systems investigated by means of light-scattering alone are perfluoromethylcyclohexane-carbon tetrachloride [Zimm, 17], 2, 6-dimethylpyridine-water [Pancirov and Brumberger, 29], *n*-decane-β, β'-dichloroethyl ether and *n*-dodecane-β, β'-dichloroethylether [Chu, 24, 40]. Of these, two [17 and 24] apparently show "normal" O.-Z. behavior, the latter to within 0.04 °C of T_c. The 2, 6-dimethylpyridine-water system can largely be described by the Ornstein-Zernike-Debye theory, but shows typical upward deviations from O.-Z. linearity at high scattering angles and the beginnings of a downward deviation at small angles and near T_c ($\Delta T = 0.02$ °C). The dodecane-dichloroethyl ether system, on which particularly careful measurements were made by Chu very near T_c ($\Delta T \sim 0.002$ °C), and at several wavelengths, shows a gentle concave-downward curvature of the O.-Z. lines over the entire range of s. It is significant that these results cover a considerable range of s and that multiple scattering effects were minimized by choosing a system of small Δn and superimposing scattering curves for several wavelengths. It is not, of course, unexpected that a large-angle deviation of the O.-Z. plot from linearity appears, since the O.-Z. correlation function is an asymptotic approximation for large r and should therefore hold best at small s.

An x-ray investigation exclusively has been made by Brady and coworkers on the perfluoroheptane-*i*-octane system [25–28]. Here also, a downward deviation of O.-Z. curves is found at the smallest scattering angles, the O.-Z. curves typically showing an inverted S-shape; it must, however, be noted that the curves were obtained no closer than 0.16 °C from the separation temperature at the composition used, which was not the critical composition. More recent precision experiments on this system are reported to be in progress [50].

The remaining fluid binaries to be discussed probably represent the most important experimental set, since composite light and x-ray scattering data are available for them, and they thus extend over a very much greater range of s-values. Included are nitrobenzene-*n*-heptane [Pancirov, Farrar, and Brumberger, 30, 31], perfluorotributylamine-isopentane [Debye, Caulfield, and Bashaw, 32], and polystyrene-cyclohexane [Debye et al., McIntyre et al., Eskin, Chu, 33–39]. Experimental difficulties are considerable in trying to overlap the two regions. This must primarily be done by extending the x-ray measurements to extremely small angles, which necessitates particularly accurate intensity measurements and collimation corrections.

In the case of nitrobenzene-*n*-heptane, while an overlap has still not been achieved, the change in slope with ΔT for the O.-Z. curves based on x-ray intensities is several times greater than for light-scattering curves in the same temperature interval; further, an l-value nearly three times as large is obtained from the light-scattering results. These observations imply that there is long-range curvature in the O.-Z. plot and that zero-angle x-ray intensity extrapolations are likely to be most unreliable unless the light-scattering range is substantially overlapped.

The perfluorotributylamine-isopentane measurements reported show just adjacent curves which are not, however, taken at exactly the same temperatures. The x-ray results alone show a distinct curvature in i^{-1} *versus* s^2; a downward curvature at large s^2 and no curvature at small s^2 are indicated, $\Delta T = 0.08$ °C. Light and x-ray data yield a consistent picture in terms of the Debye parameter l. Here also, the high-angle behavior is not unexpected.

Where the use of critical opalescence data of polymeric systems is concerned, the author feels that some caution is indicated because interpretation of the observations is rendered highly complex by the considerable range of molecular weights in even the most carefully fractionated polymer sample, and by the anisotropy of the molecules themselves. Nevertheless, Debye and coworkers have found that the light-scattering observations agree well with the Ornstein-Zernike-Debye theory. McIntyre, Wims, and Green, on the other hand, report that the extension of measurements to small angles reveals a severe drop-off of O.-Z. curves near T_c; extrapolated i^{-1} (0) values *versus* ΔT deviate upward from linearity. Chu has achieved a composite light- and x-ray scattering O.-Z. curve which apparently shows no small-angle deviations but does drop below the O.-Z. line at large s. Here, again, each curve is a composite of data taken over a range of temperatures as large as 0.32 °C. All of the polystyrene observations are strongly dependent on the average molecular weight of the dissolved fraction.

Solid Systems

Phenomena analogous to those observed in fluid systems appear in the neighborhood of certain phase-transitions in the solid state.

The aluminum-zinc system exhibits greatly enhanced small-angle x-ray scattering at temperatures above the separation temperature of the solid solution phase, 351.5 ± 0.4 °C. A careful study by Műnster et al. [42, 43, 44], indicates that a treatment of the data is feasible by means of an extension of the Ornstein-Zernike theory to eq (1). Here, again, curvature in the i^{-1} (s) *versus* s^2 plot is observed.

The available light-scattering evidence for the α-β transition of quartz [41] is limited to measurements at $\frac{\pi}{2}$ and was found to obey the λ^{-4} law. Partial depolarization (about 6%) of the scattered light is reported. The presence of an opalescent strip of finite width between the two phases is taken as evidence that the transition is not first-order.

General Conclusions

It is clear that a search for deviations from the predictions of the classical Ornstein-Zernike-Debye theory must for the moment center on observations dealing with binary systems. There is no clear deviation apparent in any of the one-component studies so far undertaken. This is unfortunate, since our theoretical understanding is greater for the simpler systems. Conversely, it is not unexpected that deviations from classical behavior occur in systems of greater complexity, where the scattering involves not just the intermolecular potential $\epsilon(r)$, but ϵ_{11}, ϵ_{22}, and ϵ_{12} [1].

For binary systems investigated by one technique only, the results on the whole are inconclusive. Nearly all the light-scattering observations have certain features in common: reasonably good fit to the O.-Z. curves is found, but deviations appear at largest and smallest scattering angles. Those at large angles are usually upward, the others are sometimes downward for temperatures quite near T_c, but do not appear regularly; this may be a function of the minimum scattering angle accessible in each experiment. Extrapolated zero-angle intercepts are proportional to ΔT for some systems but not for others and in any case rather suspect since few small-angle light-scattering data exist. The observed anomalies unfortunately often occur at the limits of experimental accessibility, and undoubtedly are at least to some extent rendered uncertain by multiple scattering effects. Perhaps the best light-scattering results are those for the *n*-dodecany$-\beta,\beta'$dichloroethyl ether system, for which long-range O.-Z. curvature is reported for $\Delta T \approx 0.002$ °C [40] and where multiple scattering is apparently negligible, and those for cyclohexane-aniline [23] indicating downward small-angle curvature of the O.-Z. plots for $\Delta T < 0.01$ °C.

Small-angle x-ray measurements alone are less conclusive; the small-angle drop-off reported for isooctane-perfluoroheptane is in the range where collimation corrections become very significant. In any case only one or two experimental points are shown lying below the O.-Z. curves. Zero-angle extrapolations are almost certainly misleading here.

Additional evidence that the theoretical predictions of the O.-Z. theory are inadequate comes from the combined light-scattering and x-ray scattering data of references 30–39. All of these report curvature over a large range of s, but the observations are not sufficient to permit general conclusions to be drawn.

The total weight of evidence indicates that there are real deviations from the Ornstein-Zernike picture, and that these are in the direction suggested by newer theories. What is uncertain is the precise nature of the deviations. This suggests quite clearly what needs to be done:

1. Future experiments should be a composite of light- and x-ray scattering to cover the maximum possible range in s. To this end, small-angle light-scattering studies should be included, and a range of wavelengths should be used. With the availability of laser sources, much greater control over the monochromaticity of the radiation and the scattering geometry can be exercised.

2. The critical point must be approached more closely ($\Delta T \sim 0.001°$) though this may introduce new difficulties which are not now apparent.

3. A serious attempt (theoretical and experimental) needs to be made to account for multiple scattering, since this problem will be aggravated as the critical point is approached more closely.

4. It is likely that, at least for some time, the most precise experiments will be done with binary systems. It would be of great value to concentrate on relatively few of these which display deviations and also are good experimental systems, and to test them with a much greater variety of experimental approaches—scattering, transport properties, etc. It is quite apparent that many of the phenomena occurring near critical points are poorly understood and others still unknown. In spite of the concentration on binary systems, precision

experiments on one-component systems of spherical molecules are still desirable. It is to be expected, however, that deviations from classical behavior will be harder to find, and will occur in regions where the experimental difficulties are very great.

Bibliography

[1] Debye, P., J. Chem. Phys. **31**, 680 (1959).
[2] Kac, M., Uhlenbeck, G. E., and Hemmer, P. C., J. Math. Phys. **4**, 216 (1963).
[3] Fixman, M., Adv. in Chem. Phys. **VI**, (1964).
[4] Fisher, M. E., J. Math. Phys. **5**, 944 (1964).
[5] Münster, A., article on "Critical Fluctuations," Fluctuation Phenomena in Solids, p. 180, R. E. Burgess, ed., (Academic Press, N.Y. 1965).
[6] Eisenstein, A., and Gingrich, N. S., Phys. Rev. **62**, 261 (1942).
[7] Graham, W., and Lund, L. H., J. Chem. Phys. **19**, 1380 (1951).
[8] Thomas, J. E., and Schmidt, P. W., ibid. **39**, 2506 (1963).
[9] Stirpe, D., and Tompson, C. W., ibid. **36**, 392 (1962).
[10] Wild, R. L., ibid, **18**, 1627 (1950).
[11] Thomas, J. E., and Schmidt, P. W., in press.
[12] Cataldi, H. A., and Drickamer, H. G., J. Chem. Phys. **18**, 650 (1950).
[13] Skripov, V. P., and Kolpakov, Yu. D., Kriticheskiye Yavleniya i Flyuktuatsii v Rastvorakh, Moskov. Gosudarst. Univ., Trudy Soveshchaniya, Moscow, 1960; p. 126.
[14] Buttrey, J. W., J. Chem. Phys. **26**, 1378 (1957).
[15] Babb, A. L., and Drickamer, H. G., ibid. **18**, 655 (1950).
[16] Mokhov, N. V., and Labkovskii, Ya. M., ref. 13, p. 81.
[17] Zimm, B. H., J. Phys. and Coll. Chem. **54**, 1306 (1950).
[18] Kirsh, T. V., Zh. Khim. Fiz. **32**, 1116 (1958).
[19] Mokhov, N. V., and Kirsh, T. V., ibid. **30**, 1319 (1956).
[20] Chow, Quantie, Proc. Roy. Soc. **224A**, 90 (1954).
[21] Debye, P., Chu, B., and Kaufmann, H., J. Chem. Phys. **36**, 3378 (1962).
[22] Chu, B., J. Phys. Chem. **67**, 1969 (1963).
[23] McIntyre, D., Wims, A., private communication.
[24] Chu, B., J. Chem. Phys. **41**, 226 (1964).
[25] Brady, G. W., and Petz, J. I., ibid. **34**, 332 (1961).
[26] Brady, G. W., and Frisch, H. L., ibid. **35**, 2234 (1961).
[27] Frisch, H. L., and Brady, G. W., ibid. **37**, 1514 (1962).
[28] Brady, G. W., ibid. **40**, 2747 (1964).
[29] Pancirov, R., and Brumberger, H., J. Am. Chem. Soc. **86**, 3562 (1964).
[30] Brumberger, H., and Farrar, W. C., Proc. Interdisciplinary Conf. Electromag. Scatt. p. 403 (Pergamon Press, New York, 1963).
[31] Brumberger, H., and Pancirov, R., J. Phys. Chem. **69**, 4312 (1965).
[32] Debye, P., Caulfield, D., and Bashaw, J., J. Chem. Phys. **41**, 3051 (1964).
[33] Debye, P., Coll, H., and Woermann, D., ibid. **32**, 939 (1960).
[34] Debye, P., Coll, H., and Woermann, D., ibid. **33**, 1746 (1960).
[35] Debye, P., Woermann, D., and Chu, B., ibid. **36**, 851 (1962).
[36] Debye, P., Chu, B., and Woermann, D., ibid. **36**, 1803 (1962).
[37] McIntyre, D., Wims, A., and Green, M. S., ibid. **37**, 3019 (1962).
[38] Eskin, V. E., Vysokomolekul. Soedin. **2**, 1049 (1960).
[39] Chu, B., J. Chem. Phys. **42**, 426 (1965).
[40] Chu, B., Paper presented at APS Meeting, Kansas City, March 1965.
[41] Yakovlev, I. A., and Velichkina, T. S., Uspekhi Fiz. Nauk. **63**, 411 (1957).
[42] Münster, A., and Sagel, K., Mol. Phys. **1**, 23 (1958).
[43] Münster, A., and Schneeweiss, ch., Z. physik. Chem. (NF) **37**, 353 (1963).
[44] Münster, A., and Schneeweiss, ch., ibid. **37**, 369 (1963).
[45] Murray, F. E., and Mason, S. G., Can. J. Chem. **30**, 550 (1952).
[46] Whiteway, S. G., and Mason, S. G., ibid. **31**, 569 (1953).
[47] Murray, F. E., and Mason, S. G., ibid. **33**, 1399 (1955).
[48] Murray, F. E., and Mason, S. G., ibid. **33**, 1408 (1955).
[49] Murray, F. E., and Mason, S. G., ibid. **36**, 415 (1958).
[50] McIntyre, D., Wims, A., and Brady, G. W., Proc. Conf. Small-Angle X-Ray Scatt. Syracuse, 1965; to be published.

Experiments on the Critical Opalescence of Binary Liquid Mixtures: Elastic Scattering*

B. Chu

University of Kansas, Lawrence, Kans.

The purpose of this paper is two-fold. Firstly, it tries to provide a careful review of many of the pertinent experimental studies on the elastic scattering of visible light as well as on the small-angle x-ray scattering of critical binary liquid mixtures. It is hoped that the review portion of the article, although in the main argumentative in character, will clear up some of the confusion which many readers inevitably get in trying to interpret scattering data on critical opalescence without investigating the experimental details. Secondly, preliminary work on visible light scattering of a binary fluid mixture, *n*-dodecane-β,β' dichloroethyl ether, at small values of s/λ ($s=2$ sin $\theta/2$, $\lambda=$ wavelength in the medium) and very close to its critical mixing point does demonstrate a breakdown of the Ornstein-Zernike [1] and the Debye [2] theories. Further theoretical work becomes necessary.

*Elastic scattering here refers to the unresolved scattered intensity in the absence of a spectrometer or an interferometer. This differs from inelastic scattering where the frequency spectrum of the scattered light has been resolved into central, Brillouin, and Raman components by means of optical beat frequency technique, interferometry and spectrometry.

Experimental Validity of Elastic Scattering Measurements

Accurate experiments are not easy to perform near the critical point and the interpretation can be confused by many experimental effects, such as multiple scattering, impurities, and temperature fluctuations. Qualitatively, the observed data on binary fluid mixtures seem to confirm the classical theories [1, 2]. On closer examination, one finds numerous "anomalies," especially from data published in the past 10 years or so. Perhaps, one of the reasons for us to find so many "anomalies" is because we expect to see deviations from the classical theory on the basis of simple analysis in terms of its theoretical limitations and approximations. Needless to say, the reported deviations tend to coincide with some of the theoretical expectations and vice versa. However, I am reasonably certain that many observed data are tinged with experimental effects [3]. It would be desirable to have more accurate and extensive data to substantiate my suspicions. Indeed, several systems have been and others are being reinvestigated. For the time being, I am only able to provide mostly indirect experimental evidence. Reviews on both theory [4, 5] and experiment [3, 6] have been presented elsewhere. Data are quoted for illustrative purposes only.

1. *Maximum scattered intensity* (*light scattering*): For the system aniline-cyclohexane, Chow [7] observed a pronounced peak at a scattering angle θ of about 90° from a plot of scattered intensity versus θ at intermediate temperature distances from the critical solution temperature ($T-T_c < 0.3°$). Debye, Chu, and Kaufmann [8] reinvestigated the system and concluded from measurements at one concentration that the maximum scattered intensity reported by Chow was an experimental effect. It should be noted that, in critical opalescence studies, scattering measurements at one concentration seldom provide definitive answers. This is even more so for the system aniline-cyclohexane partly because aniline cannot be purified easily and it undergoes photochemical decomposition; and partly because the system scatters light very strongly near its critical mixing point. As the shape of the coexistence curve changes markedly in the presence of impurities, it is not certain whether the results reported by Debye, Chu and Kaufmann [8] was indeed measured at the critical solution concentration. Furthermore, the horizontal curves in reference 8 of figure 3 may partially be the result of an over correction on the alinement of the light scattering photometer as indicated by the slightly negative slope of LUDOX in the same figure [3].

It seems that further investigation on the system aniline-cyclohexane becomes necessary. Such experiments have been performed at Kansas with better instruments [3, 6, 9]. We have measured the critical opalescence of the aniline-cyclohexane system at three concentrations, 39.6, 40.6, 41.6 vol. percent of aniline. The corresponding phase separation temperatures are respectively 29.89°_{6}, 29.89°_{3}, 29.89°_{5} which are about 0.5° above the values reported in the literature [10]. A typical plot of reciprocal relative scattered intensity versus $\sin^2 \theta/2$ at $\lambda_0 = 578$ mμ is shown in figure 1. For such a

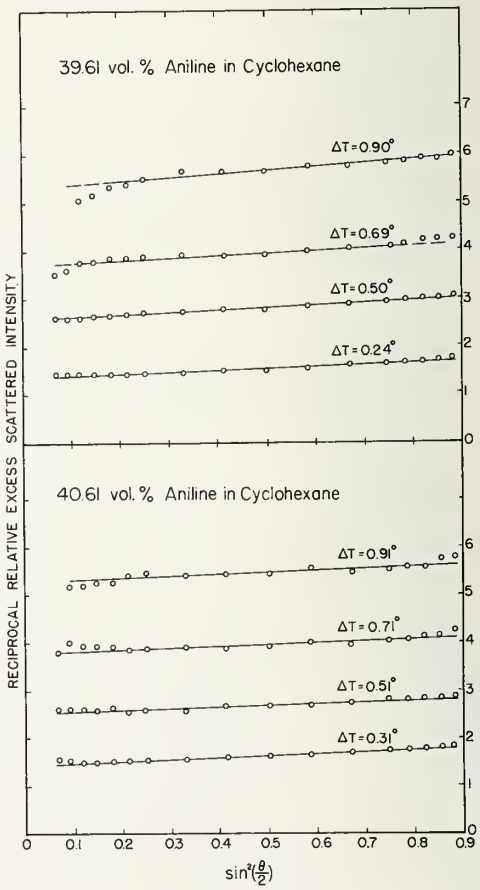

FIGURE 1. *Plot of reciprocal relative excess scattered intensity versus* $\sin^2 \frac{\theta}{2}$.

39.6$_1$ and 40.6$_1$ vol. percent aniline in cyclohexane. Observed phase separation temperature $= T_p = 29.89$ °C. I excess $(\theta, T) = I(\theta, T) - I(\theta, T - T_p \sim 10°)$. $\lambda_0 = 578$ mμ.

appreciable with cylindrical cells of about 8 mm in inside diameter even at relatively large temperature distances. For this reason, we used an incident wavelength of 578 mμ and performed our measurements not very close to the critical solution temperature so that the effects of multiple scattering were reduced. The results illustrate that the scattering behavior of this binary fluid system is similar to that of other binary liquid mixtures [3, 6]. It is quite certain that both the maximum scattered intensity and the lack of dissymmetry [8] for this system are experimental artifacts. The Debye l-parameter was estimated to be in the same range as those of other binary liquid mixtures [3, 6].

2. *Upward curvature* (*light scattering*): Virtually all binary fluid mixtures in the strongly opalescent region exhibit upward curvatures at large angles in a plot of reciprocal scattered intensity versus $\left(\frac{s}{\lambda}\right)^2$ (or $\sin^2 \theta/2$). Such a plot is sometimes referred to as an OZD plot. Closer inspection shows that the cylindrical scattering cells are either so large (e.g., 10 mm diam) that multiple scattering becomes appreciable or so small (e.g., 2 mm diam) that reflection and refraction problems are no longer avoidable. The only exception was Zimm's classical work [11] in which a different geometry for his photometer was used. The most convincing test for multiple scattering consists of a tedious procedure involving collimation and detector slits of various cross sections, scattering cells of different diameters and geometry, and composite scattering curves by means of both light and small-angle x-ray scattering [12, 13]. With those parameters, especially from a composite curve of light and small-angle x-ray scattering of polystyrene in cyclohexane [13], we have shown that the scattering curves continue from the visible light to the x-ray region without abrupt bends. Similarly, the same conclusion can be drawn from a superimposition of the scattering curves using three wavelengths (λ_0 = 365, 436, and 578 mμ) in the visible region [3, 6]. Therefore, the upward sweep has to be an experimental effect. In addition, the scattering due to fluctuations seems to behave differently from that due to particles, as a binary fluid mixture could show an upward curvature in an OZD plot indicating the presence of multiple scattering while a LUDOX (colloidal silica) solution of comparable scattering power may reveal only a horizontal straight line in the same plot [14].

3. *Attenuation correction* (*light scattering*): For very intense opalescence, the extinction of both incident and scattered light as the beam goes through the critical fluid mixture has to be taken into account [6]. Multiple scattering usually changes the shape of the scattering curves, such as an upward sweep in an OZD plot. Even in the absence of multiple scattering, attenuation correction becomes important especially when we want to know the temperature dependence of the extrapolated zero-angle scattered intensity over large temperature ranges.

According to the Debye theory, [2] we may assume that in the visible region, the scattered intensity I at constant wavelength has the form:

$$\frac{1}{I} = A(T) + B \sin^2 \frac{\theta}{2} \tag{1}$$

while, in fact, we have for the measured scattered intensity I* after correction for effective scattering volume:

$$\frac{1}{I^*} = F'(T) \left[A(T) + B \sin^2 \frac{\theta}{2} \right] \tag{2}$$

$F'(T)$ is an experimental correction factor based on the temperature dependence of the observed extinction coefficient and the size of the scattering cell. We have assumed that $F'(T)$ is independent of the scattering angle. In an OZD plot, we should not get parallel straight lines corresponding to different temperature distances since, according to eq (2), the measured slope is $F'(T) \cdot B$. Instead, a small increase in slope may be detected for strongly opalescent systems as the critical solution temperature is approached. This could be one of the reasons which may contribute appreciably the changing slopes reported by R. Pancirov and H. Brumberger [15] and by D. McIntyre, A. Wims, and M. S. Green [16] since neither articles have discussed this experimental effect. The same correction was also ignored in Zimm's work [6, 11].

4. *Downward bend in an OZD plot* (*light scattering*): Eskin [17] found a downward bend at relatively large temperature distances from the phase separation temperature (T_p) for the system polystyrene-cyclohexane away from the critical solution concentration, while McIntyre, et al. [16], found a downward bend at only small temperature distances from T_p. Furthermore, the pronounced downward dips reported by McIntyre, et al., appear only after the presence of upward sweeps for which

multiple scattering is responsible. With unaccountable effects due to polydispersity, it should be emphasized that only binary liquid mixtures of small molecules or one component systems are appropriate if we are interested in testing theories. On the other hand, polymer fluid mixtures are of interest in terms of the Debye l-parameter which is related to the cohesive energy densities. We have shown that, in an OZD plot, at very small temperature distances, say $T-T_p=0.002°$, the system n-dodecane and β,β' dichloroethyl ether, [18] indeed exhibits a gentle downward curvature virtually extending over the whole range of s/λ. More extensive studies are still in progress.

5. *Temperature dependence of extrapolated zero-angle scattered intensity:* Plots of reciprocal extrapolated zero-angle scattered intensity versus temperature are slightly concave upwards and tend to level off or to extrapolate to a nonzero value at T_c. For a binary liquid mixture, it is very difficult to obtain this extrapolation in view of the fact that the measured scattered intensity depends not only on the attenuation correction factor but it is also a sum of two terms, one due to concentration fluctuations, and the other due to density fluctuations. When we want to compare the observed data with theory, it is the concentration term that is of interest. The density term is usually, but not always, negligible over large temperature ranges. A plot of the reciprocal extrapolated zero-angle scattered intensity due to concentration fluctuations, $\frac{1}{I_c(0)}$, versus temperature shows that the straight line behavior, predicted by the approximate Debye theory, holds over short temperature ranges [6]. It is conceivable that deviations from the form $\frac{1}{I_c(0)}=C(T-T_p)$ exist over large ranges of temperature, i.e., over decades of the temperature distance from T_p. We have identified the maximum phase separation temperature on the coexistence curve as the critical solution temperature. Under these conditions, a correction term for density fluctuations, in addition to the attenuation correction, should be taken into account. So far, all the reported data on the temperature dependence of extrapolated zero-angle scattering, except for the system n-decane and β,β' dichloroethyl ether [6], have ignored both corrections.

6. *Extrapolation to zero-angle from OZD plots (small angle x-ray scattering):* It may be justified to extrapolate the reciprocal of scattered intensity to zero angle by means of light scattering where the values of $\frac{s}{\lambda}$ go down to about 1×10^{-4} Å^{-1}. The validity of this extrapolation by means of small-angle x-ray scattering often becomes questionable at small temperature distances from the critical solution temperature. It is my belief that the abnormally small l (~ 2.6 Å) for the system nitrobenzene-n-heptane [19] is in error.

7. *Constant intensity (small-angle x-ray scattering):* The usual critical opalescence behavior clearly contradicts the *constant* intensity results of G. W. Brady and H. L. Frisch [20]. The same system, n-perfluoro-heptane and isooctane, has been reinvestigated by light- and small-angle x-ray scattering [21]. Our light scattering data, although partially qualitative in nature because of multiple scattering, showed no region of constant intensity. Instead, they were found to be similar to the behavior observed in other binary liquid mixtures.

Plan of Attack

Once we know the difficulties, it takes a little planning before we should start our experiments. In principle, we want to select a critical binary fluid mixture which satisfies the following conditions:

1. *Purification:* Both components could be purified by preparative gas chromatography.

2. *Stability:* Both components are stable and do not undergo photo-chemical reactions.

3. *Temperature control and measurements:* The phase separation temperature by means of visual observation could be determined to about 0.001° without excessive patience. The same temperature limit applies to its controls (proportional temperature controller) and measurements (G–2 Mueller bridge). Therefore, it is reasonable to aim at a $(T-T_p)$ value of 0.001°. We also try to select a system which has a critical mixing temperature near the room temperature.

4. *Multiple scattering:* For strongly opalescent systems, multiple scattering invariably becomes the most serious and difficult obstacle to overcome. As we have mentioned earlier, one way is to reduce the sample cell size and the effective scattering volume. A cleverer approach (in my opinion) is to select a system which is not strongly opalescent. Even then, we are limited to cylindrical cells no larger than about 6–10 mm in diameter. A small

value of Δn, which implies a small $\left(\frac{\partial n}{\partial c}\right)$, is a suitable criterion. The symbols n and c refer to the index of refraction and the concentration of the fluid mixture respectively.

5. *Large electron density differences:* We want a system which scatters x rays as strongly as possible. It will be helpful if the two components possess a large difference in their electron densities.

6. *"Gravitational" effect:* In one component systems, the effect of gravity very near the critical point has to be taken into account. This effect is negligible for critical binary fluid mixtures where the scattering due to concentration fluctuations is predominant. Since, in many respects, the behavior of two-component systems is closely analogous to the condensation of simple fluids, we choose to begin our investigation on two-component systems. One-component systems are much more satisfying in terms of theory, although they are experimentally more difficult.

In view of the above conditions which I have imposed, we start looking for a two-component system in which both components can be purified by preparative gas chromatography, and are stable; has a convenient critical solution temperature, a small difference in the index of refraction of the two components, and a large difference in their electron densities. Fortunately, we have found not one two-component system but a homologous series of saturated paraffins as one of the two components with β,β'-dichloroethyl ether or chlorex as the other component. The paraffin-chlorex systems satisfy all of the imposed conditions. In addition, the homologous series provides us a series of systems with increasingly smaller refractive index differences as the molecular weights of the alkanes increase. Therefore, it is within reason to expect that experimental data on critical binary liquid mixtures very close to the critical point by means of light scattering are accessible with existing techniques. We may also take advantages of the homologous series for molecular interaction studies in terms of the Debye theory.

Experimental Details

Detailed descriptions of the light scattering photometer, [9] purification of materials, preparation of solutions, phase separation temperature determinations are discussed elsewhere [6, 18]. Only the changes will be specified.

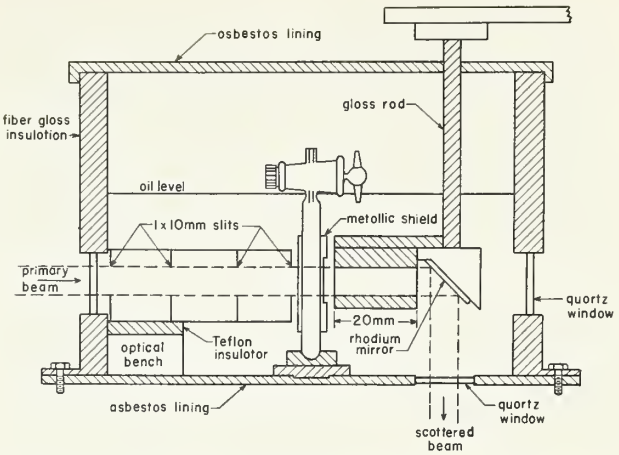

FIGURE 2. *A schematic diagram of the modified constant temperature bath and slit systems in the light scattering photometer.*

Further insulation on the thermostat-tank inside the light scattering photometer was necessary. The modifications are shown in figure 2. We favored the immersion tank technique because the bath had a reasonably large heat capacity, and the immersion oil, which matched the index of refraction of glass, reduced both refraction and reflection difficulties of a small light scattering cell. The bath temperature was controlled to better than 0.0005°. All metal parts in the tank were insulated, and there was a metallic shield around the light scattering cell to insure uniformity of temperature over the whole fluid mixture. The phase separation temperature of the sample was measured in a separate constant temperature bath and inside the photometer by means of a telescope. The observed phase separation temperatures agreed to within 0.001° for each liquid mixture.

Results and Discussion

The Debye theory provides an excellent representation of experimental facts in the intermediate temperature distances over large ranges of s/λ. Even deviations from the straight line behavior in plots of reciprocal scattered intensity versus $(s/\lambda)^2$ (or $(\theta/\lambda)^2$), by means of small-angle scattering of x rays, has been interpreted in terms of the Debye theory [12, 13, 22]. On the other hand, deviations from the straight line behavior in an OZD plot at small values of s/λ and very close to the critical solution temperature do exist [18]. Figure 3 shows a plot of reciprocal scattered intensity versus $(s/\lambda)^2$ using a cylindrical cell of approximately 6 mm

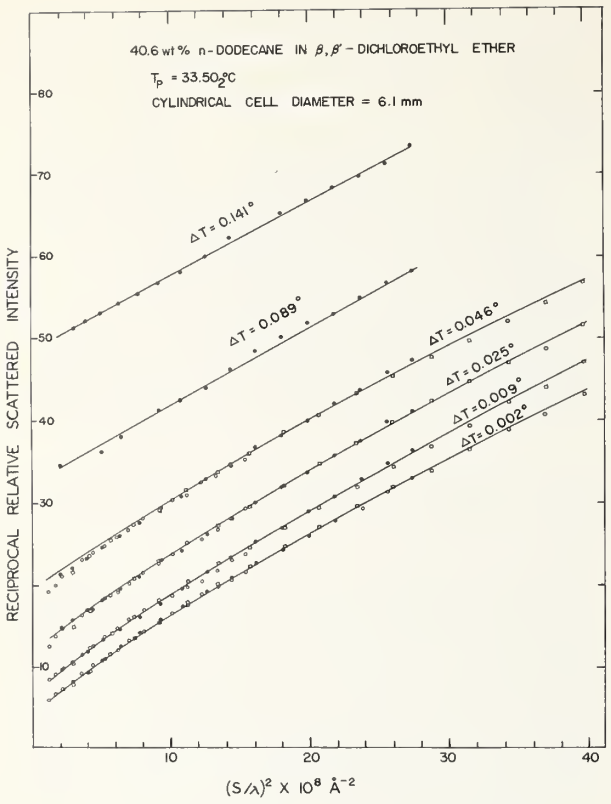

FIGURE 3. *Plot of reciprocal relative scattered intensity versus* $\left(\frac{s}{\lambda}\right)^2$.

Values of scattered intensities are denoted by hollow squares, solid circles and hollow circles for λ_0 values of 365, 436, and 578 mμ respectively.

in inside diameter. The curve with $\Delta T = 0.002°$ has been reproduced, and results from cells of different diameters and incident light of different wavelengths agree. A careful examination of figure 3 reveals that the curvature at $\Delta T = 0.046°$ is almost as large as that at $\Delta T = 0.002°$. This could partially be attributed to the fact that only the scattered intensities measured at $\lambda = 3023$ Å had been corrected for dust and stray light, while measurements from the other two wavelengths ($\lambda = 2516$ Å, 4027 Å) were not corrected for these effects. Note that the three hollow circles for the curve at $\Delta T = 0.046°$ for the smallest values of $(s/\lambda)^2$ were much lower than the general trends of the other points belonging to the same curve. When the system is more strongly opalescent, contributions due to dust and stray light become negligible as shown by the first few hollow circles at small values of s/λ ($\lambda = 4027$ Å) for the curve at $\Delta T = 0.002°$. We believe that, for the system *n*-dodecane and β,β'-dichloroethyl ether, there exists a gentle downward curvature in an OZD plot at small values of s/λ and at very small temperature distances from the phase separation temperature. However, the magnitude of the curvature is yet uncertain as the measured scattered intensity has to be corrected for both attenuation and density fluctuations. Furthermore, we do not know the range of s/λ in which any of the modified theories [5] are expected to hold. According to the equation [5] $\frac{1}{I} = D_0[\kappa^2 + (s/\lambda)^2]^{1-\eta/2}$, where D_0, κ, and η are assumed to be three adjustable parameters, η is estimated to be in the range 0.2–0.3 when $T - T_p$ is small. It is expected that η should be smaller after the intensities have been corrected for attenuation and density fluctuations. The temperature dependence of the extrapolated zero-angle scattered intensity is sketched in figure 4. It is quite certain that $\frac{1}{I_c(0)}$ is approximately proportional to the temperature distance. Deviations do exist and seem to concave upwards. On the other hand, there is perhaps an uncertainty on the critical solution concentration of about 1–2 wt percent in our preliminary measurements of the coexistence curve for the *n*-dodecane-chlorex system. Further scattering experiments with several concentrations near and at the critical solution concentration are in progress. We must also remember that, in an OZD plot, extrapolation to zero scattering angle is permissible only in the absence of very long range correlation, i.e., no abrupt change in curvature in the extrapolated region is present. For this reason, measurements at even lower angles by means of "long-wavelength" light scattering become desirable.

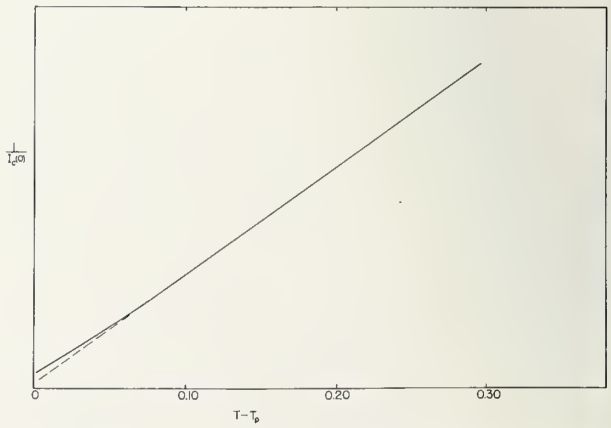

FIGURE 4. *Schematic variation of the inverse extrapolated zero-angle scattering due to concentration fluctuations estimated from preliminary results on the system* n-*dodecane and* β, β' *dichloroethyl ether.*

This work was supported by the National Science Foundation (GP–3922). The author wishes to thank W. P. Kao and J. S. Lin who performed the measurements.

References

[1] L. S. Ornstein and F. Zernike, Proc. Acad. Sci. Amsterdam **17,** 793 (1914); Physik. Z. **19,** 134 (1918); ibid. **27,** 761 (1926).
[2] P. Debye, in Non-Crystalline Solids, ed. by V. D. Frechette (John Wiley & Sons, Inc., New York, 1960) p. 1; J. Chem. Phys. **31,** 680 (1959); in Electromagnetic Scattering, ed. by M. Kerker (The Macmillan Company, New York, 1963) p. 393.
[3] B. Chu, J. Am. Chem. Soc. **86,** 3557 (1964).
[4] M. Fixman, Advan. Chem. Phys. **6,** 175 (1964).
[5] M. E. Fisher, J. Math. Phys. **5,** 944 (1964).
[6] B. Chu, J. Chem. Phys. **41,** 226 (1964).
[7] Q. Chow, Proc. Roy. Soc. (London) **A224,** 90 (1954).
[8] P. Debye, B. Chu, and H. Kaufmann, J. Chem. Phys. **36,** 3373 (1962).
[9] B. Chu, Rev. Sci. Instr. **35,** 1201 (1964).
[10] O. K. Rice and R. W. Rowden, J. Chem. Phys. **19,** 1423 (1951); D. Atack and O. K. Rice, Discussions Faraday Soc. **15,** 210 (1953), J. Chem. Phys. **22,** 382 (1954); F. R. Meeks, R. Gopal, and O. K. Rice, J. Phys. Chem. **63,** 992 (1959).
[11] B. Zimm, J. Phys. Colloid Chem. **54,** 1306 (1950).
[12] B. Chu, J. Chem. Phys. **42,** 2293 (1965).
[13] B. Chu, J. Chem. Phys. **42,** 426 (1965).
[14] P. Debye, H. Kaufmann, K. Kleboth, and B. Chu, Trans. Kansas Acad. Sci. **66,** 260 (1963).
[15] R. Pancirov and H. Brumberger, J. Am. Chem. Soc. **86,** 3562 (1964).
[16] D. McIntyre, A. Wims, and M. S. Green, J. Chem. Phys. **37,** 3019 (1962).
[17] V. E. Eskin, Vysokomolekul. Soedin. **2,** 1049 (1960); V. N. Tsvetkov, V. E. Eskin, and V. S. Skazka, Ukr. Fiz. Zh. **7,** 923 (1962).
[18] B. Chu and W. P. Kao, J. Chem. Phys. **42,** 2608 (1965).
[19] H. Brumberger and W. C. Farrar, in Electromagnetic Scattering, ed. by M. Kerker, (The Macmillan Company, New York, 1963), p. 403.
[20] G. W. Brady and H. L. Frisch, J. Chem. Phys. **35,** 2234 (1961).
[21] B. Chu, M. Pallesen, W. P. Kao, D. E. Andrews and P. W. Schmidt, J. Chem. Phys. **43,** 2950 (1965).
[22] P. Debye, D. Caulfield, and J. Bashaw, J. Chem. Phys. **41,** 3051 (1964).

Discussion

F. H. Stillinger: Dr. Fisher has very lucidly pointed out that the long range behavior of the critical pair correlation function doesn't tell one very much about specific heat anomalies. I would like to point out that there is, however, an analogous quantity which gives direct information on the specific heat anomalies by virtue of its long range behavior in the critical region. It is well known that the specific heat C_V is a fluctuation of potential energy. If one writes out the fluctuation formula in terms of spin distribution functions for an Ising model, one encounters a combination amounting to a quadruplet distribution function for two pairs of spins, the spins in each pair being close together, minus the product of the two pair correlation functions. The implication of a logarithmically divergent specific heat is that the critical point long range distance behavior of this combination would have to be as r^{-d}, where d is the dimensionality. Here the long range distance r is the distance between the centers of the two pairs.

If one goes ahead naively and attempts to evaluate this combination of distribution functions using a Kirkwood superposition approximation, or something roughly equivalent to it, one arrives at the conclusion that the long range distance behavior should vary as the square of the critical pair correlation function. Since we have seen that the exponent η is positive but small relative to unity this leads to a rather remarkable conflict with the requirement that this combination should vary as r^{-d} as mentioned above. It is rigorously known, of course, that the specific heat for an Ising model in two dimensions diverges logarithmically. I think the situation in three dimensions is in a state of flux. One would have at worse a small positive index α, perhaps of the order of $1/10$. In three dimensions, therefore, there could be some slight deviation of the index d from 3 for this quadruplet distribution function long range behavior, but it certainly would not become equal to the long range behavior of the square of the pair correlation function.

M. E. Fisher: May I make one comment on that? What Dr. Stillinger said is, of course, correct. If I look in the Ising model at $s_0 s_1$, where 0 and 1 are nearest neighbors, and at $s_r s_{r+\delta}$, where r and $r+\delta$ are near neighbors, then the behavior of $\langle s_0 s_1 s_r s_{r+\delta}\rangle - \langle s_0 s_1\rangle \langle s_r s_{r+\delta}\rangle$ for large r should tell me how the specific heat diverges. John Stephenson, a student of mine, has actually evaluated this correlation function explicitly which is not too difficult to do in the Ising model [1]. He finds in fact, as one might anticipate, that the behavior is as $e^{-2\kappa r}/r^2$ in this case. His correction factor $[1+Q_4(\kappa r)]$ satisfies $Q_4(x)\to 0$ as $x\to 0$ and $1+Q_4(x)\to \frac{\pi}{2}$ as $x\to\infty$. Once you can express the problem in terms of the long range behavior and you have a good theory for the long range behavior, it is fine. However, as Dr. Stillinger pointed out again, although formally all the information is contained in this quantity (indeed one could also get the pair correlation function from it), it is a different set of asymptotic limits that are required.

G. S. Rushbrooke: May I make a comment which is due to Dr. Widom? It concerns the things that Dr. Fisher talked about, but below the critical temperature rather than above. Widom simply takes the equation which relates the compressibility to the density fluctuations. Suppose the system is separated into two phases. Then in a small volume of dimensions of $1/\kappa$, the range of the correlation function, we ought to have fluctuations in the density equal to the width of the phase boundary. Now, if one just introduces this idea, one obtains the relation:

$$\gamma' = \nu' d - 2\beta \tag{1}$$

where γ' is the exponent of the susceptibility below the critical point, ν' the exponent of κ (T) below the critical point, β the exponent for the phase boundary and d the number of dimensions.

This works exactly for the Ising model in two dimensions. In three dimensions it depends what you take for ν'. If you take β and δ as given by Fisher and introduce the relation $\gamma' = \beta(\delta - 1)$ into (1), you get exactly $\nu' = 0.646$ below the critical point, equal to the value for ν above the critical point as given by Dr. Fisher. So for the Ising problem it looks as if these ideas which work above the critical point might also work below the critical point. I would like to ask Dr. Fisher whether he thinks this is reasonable.

The other point I want to ask Dr. Fisher is how far he thinks the conclusions about exponential decay depend on short range forces. This is established for the Ising model. However, quite a lot of people argue that the direct correlation function goes off like the pair potential. This is not a very strong argument. However, when the pair potential and consequently $C(r)$ decays as $1/r^6$, you cannot have the direct correlation function decaying more rapidly than the total correlation function, if the Ornstein-Zernike theory is true.

M. E. Fisher: Well, that last question is one which I suppose I have to answer since it was asked. However, I think it is a rather difficult question!

If one thinks of Coulomb forces, then of course, they do not make sense unless one has some counter-charge. But then we have the phenomena of screening and the correlations are presumed to decay more rapidly. This seems to be a property of the fact that Coulomb forces obey the Poisson equation. This is, I think, one way of interpreting it. But if you try and work the arguments which would give you that result with a force which is like a Coulomb force and even has counter-charges, but which decays a little faster than $1/r$, you would not get out complete screening. Now in as far as the Van der Waals

forces can be thought of as originating through the electromagnetic interactions of matter, it seems to me still possible, in principle, that you have some overall screening effects and that you still do have an exponential damping. But if you just take a completely radially symmetric fixed $1/r^6$ potential without any corrections, then I agree you cannot expect pure exponential damping since the direct correlation function would presumably go down in this way. So I am thinking here of models which have a potential that cuts off either exponentially or goes strictly to zero, if one really wants to prove it. But I would think that for real systems it is something of an open question.

W. Marshall: Dr. Fisher mentioned that the old theories can give very misleading results about the specific heat because you essentially take the long range behavior and extrapolate that into small distances. This, of course, is correct but one must be rather careful about the precise meaning. It is not a necessary consequence of the theories that you must get the wrong answer. In particular in the Elliott-Marshall theory [2] you get a difference equation for the correlation function and that difference equation happens to be valid at small distances as well as large distances. Therefore, that particular theory just reproduces the usual Bethe-Peierls result for the energy.

P. Debye: I would like to go back to some experimental facts. For instance the theoretician says, "Now I am at the critical temperature." Well, I do not know the critical temperature. Nobody can determine what the critical temperature really is. So how is there going to be an experiment at the critical temperature? Any experiment is a little bit away from the critical temperature and I cannot even define how far it is away from the critical temperature.

M. E. Fisher: Well, for example, some of the experiments discussed yesterday on the magnetic systems give you T_c very accurately.

P. Debye: I don't know of an equivalent experiment in liquids.

M. E. Fisher: Well, liquids are more difficult. The coexistence curves, I think, will tie down the critical points sufficiently accurately. Within a few millidegrees, to which some experiments seem to pin it down, I would not worry about the differences.

P. Debye: I would like that the theoretical people tell me when I am so and so far away from the critical point, then my curve should look so and so.

I would like to make two remarks in connection with the paper of Dr. Brumberger.

One remark is that I am not so pessimistic as Dr. Brumberger. If one wants to find deviations which appear in the immediate neighborhood of the critical point, one should not use x rays because the relevant variable is not $s = 2 \sin(\theta/2)$, but s/λ. Thus when λ is very small, one must go to extremely small angles θ in order to obtain some information. Thus if one wants to find deviations in the neighborhood of the critical point, one has to use light where s/λ can be small for reasonable values of θ. In the paper of Dr. Chu, it is shown that there are probably deviations from the Ornstein-Zernike theory near the critical point. However, if one goes to large values of s/λ, one should also find deviations from a straight line in an Ornstein-Zernike plot. The straight line is only a first approximation. So if one measures for large values of s/λ, one obtains information on the second moment of interaction and, if one goes farther, on the fourth and sixth moment of the interaction. Thus from the molecular point of view it is also interesting to go to large values of s/λ and there one has to use x rays.

It is really true, as Dr. Brumberger said, that you should connect the light experiments and the x-ray experiments with each other. This has been done at several places and we have done it too. For this purpose, I present two curves for I^{-1} as a function of $(s/\lambda)^2$ in figure 1 and figure 2 for a polymer, which Dr. Brumberger does not like. I do like polymers, as one obtains information about their interaction, which cannot be predicted easily. If you ask me what the interaction of two argon atoms is,

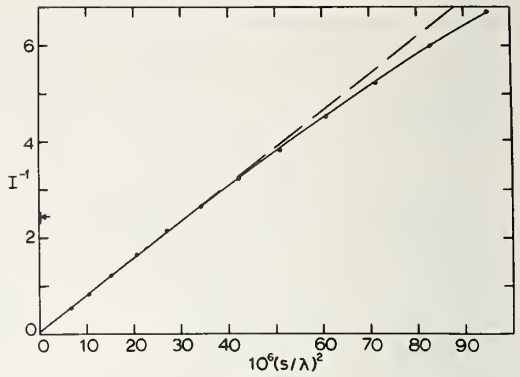

FIGURE 1

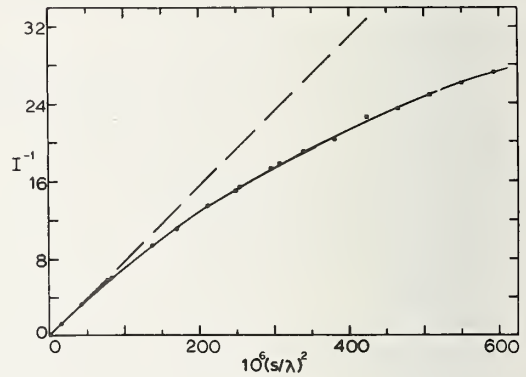

FIGURE 2

I know approximately the answer. However, if you ask me what the interaction between two polymers is which go through each other, I do not know the answer and I must do the experiment. Figure 1 shows I^{-1} as a function of $(s/\lambda)^2 \times 10^6$. One sees small deviations of a straight line if you go to large values of s/λ. And if one really wants deviations which give the value for the fourth moment of interaction, one has to go to considerably larger values of s/λ as shown in figure 2. From these data one can obtain the second moment and the fourth moment but not the sixth moment. The maximum value of s/λ possible with light is 5×10^{-4} Å^{-1}; the x-ray measurements covered the range from 2.6×10^{-3} Å^{-1} to 2.5×10^{-2} Å^{-1}. Over this range the scattered intensity changed by a factor of 56.

Dr. Brumberger made a nice remark when he said that other experiments of another kind should be done. It has been said and also Uhlenbeck made this remark at the beginning of this conference that in the neighborhood of the critical point the system can be disturbed rather easily from the outside. In this connection I remark that we studied the effect of an electrical field on the critical opalescence of a binary liquid mixture. For the details we refer to the publication [3]. Also here it is apparent that the Ornstein-Zernike theory is only correct if one is not too near to the critical point.

So I want to emphasize that one has a straight line I^{-1} as a function of $(s/\lambda)^2$ over a large distance, but if you go to very large values of s/λ, you get deviations as has to be expected. If you go to small values, which you can only do with light, then you can expect to find the things which are the subject of this afternoon.

W. Marshall: Dr. Brumberger explained the difficulties that you frequently get with light and x rays. I would like to emphasize the fact that in looking at these systems many of the difficulties are very much eliminated if you did the experiment with neutrons. This is a technique about which many people who have worked traditionally in this field do not think of because it is something new. Indeed Egelstaff and Enderby [4] have already verified that the structure factor of simple liquid metals as given by the x rays is not quite correct. The correction is quite important in the region of small s/λ. I would support very strongly, as Dr. Brumberger said, that neutron experiments also must be done. It would be nice to do it on the same material which means that almost all systems which Dr. Brumberger discussed have to be ruled out because they contain hydrogen and they all have to be deuterated.

M. S. Green: I would like to ask Dr. Marshall: What are the smallest values of k that you can reach with neutrons as compared with light and with x rays?

W. Marshall: That depends on which experimentalist you talk to. It is important to go from one to the other and get them into competition. The usual kind of k-vectors that are easy are those covered by x rays. But there is no reason why one should not build a special small angle scattering apparatus like that which Lowde or Jacrot have used [5]. Then you can get very small k-values. I think Jacrot can probably tell us exactly what it would be.

B. Jacrot: I think you can go to 10^{-3} Å^{-1} or maybe slightly lower.

W. Marshall: Thus then the neutron experiments would be as good as light experiments in this respect.

A. Arrott: I want to ask Dr. Debye what is meant by the critical region. When the susceptibility or compressibility obeys a $^4/_3$ power law already for $(T-T_c)/T_c=0.1$, should you not say that you are already in the critical region when the temperature is $T_c/10$ away from the critical? In discussing possible deviations from the Ornstein-Zernike theory you consider what happens at temperatures hundredths or thousandths of a degree away from the critical temperature. However you did not mention what is found for the power law of $I^{-1}(0)$ which is inversely proportional to the compressibility: $I^{-1}(0)$ means the inverse extrapolated zero angle intensity.

P. Debye: It is hard to find a deviation from linearity for $I^{-1}(0)$ as a function of T, because you are not certain that the extrapolation is correct.

H. Brumberger: The behavior of $I^{-1}(0)$ as a function of temperature does deviate from linearity in many cases over a wider temperature region.

M. S. Green: I think we have a real problem here. Although I don't know whether Dr. Debye would agree, I believe that light scattering experiments do in fact show a curvature for $I^{-1}(0)$ as a function of temperature many degrees away from the critical temperature. On the other hand, any deviations from the Ornstein-Zernike theory (one should also say Debye theory) do not occur unless the temperature is within 0.01 °K from the critical temperature. Perhaps this means there are two critical regions. I don't know the answer, but it is a problem which needs to be resolved. Perhaps it is related to the fact that the logarithmic singularity of the specific heat does not show up until one comes within a hundredth of a degree of the critical point, although the behavior of C_v is nonclassical in a much wider region.

D. McIntyre: I see no essential disagreement between Dr. Chu's new results for the cyclohexane-aniline system and our results with the same size cell in the same temperature range. I personally believe on the basis of our data that the plot of $I^{-1}(0)$ against ΔT is gradually curved upwards over the whole temperature range. Now I would like to enter a slight quibble. I am a little surprised at the form of your uncorrected scattering curves. There are some wiggles in your curves at 0.1 to 0.2 °C above T_c. They are sometimes straight, sometimes a little erratic, and even seem to have a little s shape.

B. Chu: The data on the aniline-cyclohexane system as I have shown in figure 1 of my paper demonstrate the experimental difficulties which one encounters in critical opalescence studies whenever multiple scattering becomes appreciable. These measurements on such a strongly opalescent system (aniline-cyclohexane) were performed at relatively large temperature distances ($\Delta T \cong 0.2°$ to 1°) and at a longer wave length ($\lambda_0=578$ mμ rather than the usual blue or green lines of a mercury arc) so that the effect of multiple scattering remains negligible. On the other hand, the wiggles in figure 3 of my paper refer to the scattering of a weakly opalescent system, namely, n-dodecane and β,β-dichlorodiethylether. Furthermore, the plot is reciprocal scattered intensity versus $(s/\lambda)^2$, and thus, the experimental "fluctuations" in the data seem to have been magnified.

D. McIntyre: But even 0.1 °C away from T_c?

B. Chu: Yes. The critical scattered intensity for the system, n-dodecane and β,β-dichlorodiethylether at 0.1° away from T_c is quite weak, especially when we have used very narrow slit systems. However, our main interest here was to try to determine the shape of the scattering curve very near the critical mixing point, not at temperature distances 0.1° away from the critical mixing point. In fact, such wiggles disappear whenever we increase the sensitivity of our detection scheme.

D. McIntyre: Examining your papers, I find that you suggest that you have corrected in some manner for the multiple scattering. Is this so? We have always found that what we thought to be multiple scattering in this range of ΔT was exhibited as a convexity to the abscissa at the ends of a conventional O-Z plot of a light scattering curve. In your systems I should think that you would get the same behavior.

B. Chu: No. I do not believe that with our experimental setup, multiple scattering is appreciable for this weakly opalescent system. We have tried to correct for attenuation and to *avoid* multiple scattering. I do agree with you that whenever multiple scattering does become appreciable, it invariably destroys the linear behavior in an O-Z-D plot.

D. McIntyre: In one of your curves it appeared.

B. Chu: This is not multiple scattering.

D. McIntyre: What is it?

B. Chu: I do not believe that the curvature in figure 3 is due to multiple scattering because we have performed our experiments with cylindrical cells of two different diameters, and the shape of such curves can be superimposed. This may not be fool proof. We also hope to carry our studies further with more variations in the geometry of our optical system. I would also like to make another remark. It is difficult to determine the behavior of $I^{-1}(0)$ as a function of temperature. For one thing, most investigators have neglected correcting for the attenuation of light as it goes through the sample cell. Since the turbidity of the sample depends strongly on temperature as we approach the critical temperature, a plot of the extrapolated reciprocal zero angle scattered intensity (without attenuation corrections) versus temperature does not represent the *true* behavior of $I^{-1}(0)$ versus T. Now, all I can say is that the curvature in a plot of $I^{-1}(0)$ versus T for our system is very small if there is any. As far as I can see, it is very straight as shown in figure 4 of my paper. Yet, we must remember that I remarked on its nearly straight line behavior over a temperature range of about only 0.3°. The nonlinear behavior over a whole temperature range (say 10°) remains to be examined.

209-493 O-66—10

D. McIntyre: I think that there is actually experimental concurrence in the fact that when measurements are made at small ΔT's and low angles a downward curvature in the O-Z plot, such as yours, will be found. So I think that the scattering experiments made by various people are in agreement on this point.

P. Debye: I think everybody is now convinced that there is curvature in the immediate neighborhood of the critical point and that the curvature is in the expected direction.
A. Isihara: Could you explain why the I^{-1} versus $(s/\lambda)^2$ plot curves downwards for small values of s/λ?

M. S. Green: I would like to comment on this question. As Dr. Fisher emphasized, the essential approximation of the Ornstein-Zernike theory is that the direct correlation function is short ranged which means it has a finite second moment. The second moment of the direct correlation function is essentially the slope of the I^{-1} versus $(s/\lambda)^2$ curve. The fact that this curve turns downwards means that the second moment is increasing. The truly significant prediction would be that the second moment of the direct correlation function not only increases but becomes infinite at the critical point. Nobody can actually show that, but this seems to be indicated by the experiments.

M. E. Fisher: The value of η estimated by Dr. Chu is much bigger than I would have expected. As far as I am concerned there are still some puzzles, because the curve of $I^{-1}(0)$ versus temperature does not go to zero if you extrapolate to the critical temperature. I think if you had done *P-V-T* measurements you would have observed that the fluctuations-of-composition-compressibility would go up to infinity while your $I^{-1}(0)$ still seems to stick to a small finite value. Maybe there is some reason why the real critical temperature is lower, but from what Dr. Chu has said, I don't see it!

A. Arrott: Returning to my previous question, it seems that for a binary mixture the critical region is much smaller than for a magnetic system. Why is there such an order of magnitude difference when you consider the critical region for a binary mixture and that for a magnetic system?

E. Helfand: I believe the size of the critical region is related to the range of the forces. This conclusion emerges in the study of systems with long range forces. The shape of the particles in the binary systems about which we are speaking may cause these systems to be less in corresponding states with the Ising or Heisenberg models than one component fluids or magnets.

M. S. Green: I don't think your answer is correct. I don't think we really have a narrow critical region in a binary system. The phenomena which Dr. Chu showed take place within indeed a range of one hundredth of a degree. However, there are other phenomena in the two phase region which occur over a much wider temperature range. For instance, the $(\Delta T)^{1/3}$ power law for the phase boundary curve, which is a nonclassical phenomenon, is just as much true for these systems as it is for a magnetic system or for a one component fluid. I guess the question of the $^4/_3$ power law for the compressibility is still a matter of controversy, but in my opinion (and I think Dr. McIntyre agrees with me), there are deviations from the straight line for the compressibility as a function of temperature in a much larger temperature range than we are talking about here.

E. Helfand: The degree of the coexistence curve is not as clearly related to the distance parameter of the correlations as are phenomena above the transition such as the compressibility (or its analogue for mixtures or magnets) and the critical scattering curves.

P. W. Anderson: To answer the question of Dr. Arrott, is not the reason why the critical region appears to be so terribly narrow, that you are studying terribly long range effects. A light scattering experiment is sensitive to distances between 4000 Å and 10,000 Å and the temperature differences $T-T_c$, which corresponds to such ranges are expected to be in the millidegree range. If one were to look in the intermediate range between light and x rays, I would guess one would see curvature in a range $T-T_c$ of one degree. In the x-ray results one sees curvature in the 10 deg range. Thus I think you have to look in the temperature range that corresponds to the range of the wavelength used in the scattering experiment. Unless the experiments show otherwise, this interpretation answers the question of the size of the critical range.

P. Debye: If one wants to investigate something characteristic for the immediate neighborhood of the critical point for a given angle θ, one has to go to longer and longer wavelengths because the characteristic variable is not s, but s/λ.
P. Anderson: I am not talking about s/λ, but I am talking about a physical range, in particular, about the correspondence between ranges in temperature and ranges in space. If you were 1 deg away from the critical point, you would find curvature at much shorter wavelengths.

P. Debye: No.

M. E. Fisher: I will attempt *not* to add anything to the confusion! First of all, I think it is a question of pure semantics. Unless you have some theory of the critical point you cannot talk about the critical region except in terms of deviations from this theory. We are talking in terms of the Ornstein-Zernike theory here, where there is a k-dependence and a temperature dependence to be considered. Now, if we look at the magnetic case, there is no doubt that for the susceptibility deviations can be seen very far away from the critical point. I find it puzzling that one does not seem to see these deviations in the binary system. As far as one does not see these deviations here, one has not really understood the difference between these two systems.

However, looking at the k-dependence, it is perfectly possible that you can have an Ornstein-Zernike k-dependence absolutely correct right up to the critical point even if the thermal behavior is not correct. The index η I find theoretically is very small. Because η is small you would expect, I think, to see deviations only in a small region. So I think to talk about the critical region is not too helpful. What Dr. Debye said is correct, namely, that when one is talking about some deviation one must attach to it a magnitude and a range of temperatures where it is to be observed, which can be different for one phenomenon compared to another. When these ranges differ from one system to another for the same phenomenon, we have a real challenge.

Dr. Sette: I want to point out that the results of sound absorption measurements for a liquid vapor critical system and a binary mixture are different. In a one-component system the absorption increases sharply only in a temperature range of one degree from the critical temperature. In the case of a binary mixture the absorption increases rapidly starting at $T-T_c=30$ °C. This indicates that the two systems behave in a different way. I believe that a comparison between the magnetic system and the binary system should be made with some precaution.

References

[1] J. Stephenson, preprint, Ising-model spin correlations on the triangular lattice. II. Fourth order correlations, to be published.
[2] R. J. Elliott and W. Marshall, Rev. Mod. Phys. **30,** 1 (1958
[3] P. Debye and K. Kleboth, J. Chem. Phys. **42,** 3155 (1965).
[4] P. A. Egelstaff and J. E. Enderby, to be published.
[5] B. Jacrot and T. Riste, Thermal Neutron Scattering, ch. VI, ed. P. A. Egelstaff, (Academic Press, 1965).

SCATTERING: INELASTIC

Chairman: K. S. Singwi

Critical Scattering of Neutrons by Ferromagnets

W. Marshall

Atomic Energy Research Establishment

Harwell, Great Britain

1. Introduction

Recently a number of authors have discussed the theory of critical phenomena in magnetic materials and produced results differing from the conventional and simple theory as described in many textbooks [1–4]. Some predictions of the new theories have already been verified experimentally. Neutron scattering techniques can be used to give a thorough investigation of critical phenomena and this paper discusses the theory needed in the interpretation of the experiments.

In section 2 the cross section formulae are written down in various forms and it is shown how the cross section is related to the generalized wave vector dependent susceptibility. In section 3 special attention is given to the time dependence of fluctuations near the critical point and it is shown that the conventional theory fails. A modified theory is described in section 4. Because of the difficulty of the problem this theory is only qualitative but it points to the existence of damped spin waves, or some similar phenomena, even above T_c. Section 5 mentions two other experiments indicating the existence of spin waves above the critical temperature. Section 6 gives conclusions.

2. Formulae and Definitions

The neutron has initial wave vector $\mathbf{k}$ and initial energy E. It is scattered into a state of wave vector $\mathbf{k}'$ and energy E'. The wave vector change and energy change are, respectively:

$$\mathbf{K}=\mathbf{k}-\mathbf{k}'$$

$$\hbar\omega=E-E'=(h^2/2m_0)(k^2-k'^2). \tag{2.1}$$

The cross section is then

$$\frac{d^2\sigma}{d\Omega' dE'}=\frac{N}{\hbar}\left(\frac{e^2\gamma}{mc^2}\right)^2\frac{k'}{k}\,|F(\mathbf{K})|^2(\delta_{\alpha\beta}-\hat{k}_\alpha\hat{k}_\beta)\mathscr{S}^{\alpha\beta}(\mathbf{K},\,\omega) \tag{2.2}$$

where

$$\mathscr{S}^{\alpha\beta}(\mathbf{K},\,\omega)=\frac{1}{2\pi}\int_{-\infty}^{\infty}dt\sum_{\mathbf{R}}e^{i\mathbf{K}\cdot\mathbf{R}-i\omega t}\langle S_0^\alpha(0)S_R^\beta(t)\rangle. \tag{2.3}$$

Only the terms with α and β equal contribute to (2.2) if the sample has only scalar interactions between the spins. Throughout this paper we shall assume this, i.e., ignore dipolar interactions and anisotropic exchange.

Define

$$\mathbf{S}(\mathbf{K},\,t)=\sum_{\mathbf{n}}e^{i\mathbf{K}\cdot\mathbf{n}}\mathbf{S}_\mathbf{n}(t) \tag{2.4}$$

then

$$\mathscr{S}^{xx}(\mathbf{K},\,\omega)=\frac{1}{2\pi N}\int_{-\infty}^{\infty}dte^{-i\omega t}\langle S^x(-\mathbf{K},\,0)S^x(\mathbf{K},\,t)\rangle \tag{2.5}$$

with similar definitions for the y and z-directions.

Below the critical temperature the correlation function in (2.3) has a nonzero value at infinite time and this gives the Bragg scattering contribution $\mathscr{S}_B^{\alpha\beta}(\mathbf{K},\,\omega)$.

$$\mathscr{S}_B^{\alpha\beta}(\mathbf{K},\,\omega)=\frac{1}{N}\,\delta(\omega)\langle S^\alpha(-\mathbf{K})\rangle\langle S^\beta(\mathbf{K})\rangle. \tag{2.6}$$

The remainder is the "diffuse" contribution

$$\begin{aligned}\mathscr{S}_D^{\alpha\beta}(\mathbf{K},\,\omega)&=\mathscr{S}^{\alpha\beta}(\mathbf{K},\,\omega)-\mathscr{S}_B^{\alpha\beta}(\mathbf{K},\,\omega)\\&=\frac{1}{2\pi N}\int_{-\infty}^{\infty}dte^{-i\omega t}\{\langle S^\alpha(-\mathbf{K},\,0)S^\beta(\mathbf{K},\,t)\rangle\\&\qquad-\langle S^\alpha(-\mathbf{K})\rangle\langle S^\beta(\mathbf{K})\rangle\}.\end{aligned} \tag{2.7}$$

We notice that

$$\begin{aligned}\int_{-\infty}^{\infty}d\omega\mathscr{S}_D^{\alpha\beta}(\mathbf{K},\,\omega)&=\frac{1}{N}\{\langle S^\alpha(-\mathbf{K},\,0)S^\beta(\mathbf{K},\,0)\rangle\\&\qquad-\langle S^\alpha(-\mathbf{K},\,0)\rangle\langle S^\beta(\mathbf{K},\,0)\rangle\}\end{aligned} \tag{2.8}$$

and in the limit $\kappa \to 0$ this is proportional to the mean square fluctuation in magnetization which, by elementary thermodynamics, is proportional to the magnetic susceptibility. Hence

$$\lim_{\kappa \to 0} \int_{-\infty}^{\infty} d\omega \mathcal{S}^{\alpha\beta}(\mathbf{K}, \omega) = kT\chi^{\alpha\beta}/g^2\mu^2 \qquad (2.9)$$

where the susceptibility tensor $\chi^{\alpha\beta}$ is defined in the usual way. For the correct choice of principle axes, $\chi^{\alpha\beta}$ has two values χ^{zz} and $\chi^{xx} = \chi^{yy}$ below T_c, and one value, $\chi^{zz} = \chi^{xx} = \chi^{yy}$, above T_c.

The form of (2.9) suggests that we seek a more general relation, valid at all $\mathbf{K}$, by introducing the quantity $\chi^{\alpha\beta}(\mathbf{K})$ which describes the response to a field of wave vector $\mathbf{K}$. The idea of this is well known but, so far as the author is aware, the first formulation for an explicitly neutron scattering problem was given in a recent paper by Mori and Kawasaki [5]. Following the latter paper we introduce a relaxation function

$$R^{\alpha\beta}(\mathbf{K}, t) = \int_0^{\beta} d\lambda \langle e^{\lambda \mathcal{H}} S^{\alpha}(-\mathbf{K}, 0) e^{-\lambda \mathcal{H}} S^{\beta}(\mathbf{K}, t) \rangle - \beta \langle S^{\alpha}(-\mathbf{K}, 0) \rangle \langle S^{\beta}(\mathbf{K}, t) \rangle. \qquad (2.10)$$

It can then be shown that

$$\mathcal{S}^{\alpha\beta}(\mathbf{K}, \omega) - \mathcal{S}^{\alpha\beta}(\mathbf{K}, \omega)_{\text{Bragg}} = \frac{\hbar\omega}{1 - e^{-\hbar\omega\beta}} \frac{1}{2\pi N} \int_{-\infty}^{\infty} dt e^{-i\omega t} R^{\alpha\beta}(\mathbf{K}, t) \qquad (2.11)$$

and also that

$$\chi^{\alpha\beta}(\mathbf{K}) = \frac{g^2\mu^2}{N} R^{\alpha\beta}(\mathbf{K}, 0). \qquad (2.12)$$

Hence

$$\mathcal{S}^{\alpha\beta}(\mathbf{K}, \omega) - \mathcal{S}^{\alpha\beta}(\mathbf{K}, \omega)_{\text{Bragg}} = \frac{kT}{g^2\mu^2} \chi^{\alpha\beta}(\mathbf{K}) \frac{\hbar\omega\beta}{1 - e^{-\hbar\omega\beta}} F^{\alpha\beta}(\mathbf{K}, \omega) \qquad (2.13)$$

where

$$F^{\alpha\beta}(\mathbf{K}, \omega) = \frac{1}{2\pi} \int_{-\infty}^{\infty} dt e^{-i\omega t} f^{\alpha\beta}(\mathbf{K}, t) \qquad (2.14)$$

and

$$f^{\alpha\beta}(\mathbf{K}, t) = \frac{R^{\alpha\beta}(\mathbf{K}, t)}{R^{\alpha\beta}(\mathbf{K}, 0)} = \frac{g^2\mu^2}{N\chi^{\alpha\beta}(\mathbf{K})} R^{\alpha\beta}(\mathbf{K}, t). \qquad (2.15)$$

By definition $f^{\alpha\beta}(\mathbf{K}, 0)$ is unity and hence, from (1.14),

$$\int_{-\infty}^{\infty} d\omega F^{\alpha\beta}(\mathbf{K}, \omega) = 1. \qquad (2.16)$$

Therefore (2.13) gives

$$\frac{kT}{g^2\mu^2} \chi^{\alpha\beta}(\mathbf{K}) = \int_{-\infty}^{\infty} d\omega \frac{1 - e^{-\hbar\omega\beta}}{\hbar\omega\beta} \{\mathcal{S}^{\alpha\beta}(\mathbf{K}, \omega) - \mathcal{S}^{\alpha\beta}(\mathbf{K}, \omega)_{\text{Bragg}}\}. \qquad (2.17)$$

This is an important relation because it is the generalization of (2.9) and because it unambiguously relates the observed cross sections to a quantity of theoretical interest. Whether or not we understand the full ω dependence of the cross section we can deduce $\chi^{\alpha\beta}(\mathbf{K})$ provided the experimental results are known with sufficient accuracy to evaluate the integral on the right-hand side of (2.17).

Frequently it is more convenient to measure the total count rate at a fixed scattering angle instead of the full $\mathcal{S}(\mathbf{K}, \omega)$; to deduce $\chi(\mathbf{K})$ from such measurements involves two approximations. First, the integral in (2.17) should be performed at fixed $\mathbf{K}$ not at fixed scattering angle. The error introduced by this is small if the incident neutron energy is large compared with the energy changes, $\hbar\omega$. Second, the count rate is not weighted with the factor $\{1 - e^{-\hbar\omega\beta}\}/\hbar\omega\beta$ and therefore we require that $\hbar\omega \ll kT$. If this last condition is satisfied the factor becomes unity and the experiments give $\chi^{\alpha\beta}(\mathbf{K})$ directly.

The molecular field theory for a ferromagnet above T_c predicts $\chi(\mathbf{K})$ to have the form:

$$\chi^{xx}(\mathbf{K}) = \chi^{zz}(\mathbf{K}) = \frac{\chi_c}{r_1^2(\kappa_1^2 + q^2)} \qquad (2.18)$$

where

$$\mathbf{K} = \boldsymbol{\tau} + \mathbf{q} \qquad (2.19)$$

and $\boldsymbol{\tau}$ is the nearest reciprocal lattice vector,

$$\chi_c = g^2\mu^2 S(S+1)/3kT_c. \tag{2.20}$$

r_1^2 gives a measure of the range of the exchange interaction

$$r_1^2 = \frac{1}{6}\frac{\sum_R J(R)R^2}{\sum_R J(R)} \tag{2.21}$$

and κ_1 is an inverse correlation range defined above T_c by

$$r_1^2\kappa_1^2 = \frac{\chi_c}{\chi^{zz}(0)} = \frac{T-T_c}{T_c}. \tag{2.22}$$

Other simple theories of ferromagnets give results qualitatively similar.

These predictions have been tested by Passell et al. [6], by neutron experiments on metallic iron. They conclude that the general form (2.18) is correct within the limits of experimental error but that $r_1^2\kappa_1^2$ does not have a linear variation with $T-T_c$, as predicted by (2.22) but instead

$$r_1\kappa^2 \sim (T-T_c)^{4/3} \qquad \text{for } T \sim T_c \tag{2.23}$$

This 4/3 law is in agreement with recent theoretical work by Domb [1] and by Gammell, Marshall, and Morgan [2] who found a 4/3 law for the divergence of $\chi^{zz}(0)$ using the mathematical technique of successive Padé approximants.

Below T_c the molecular field theory again gives the general form (2.18) but with

$$r_1^2\kappa_{1z}^2 = 2\,\frac{T_c-T}{T_c} \qquad \text{for } T < T_c$$

$$\kappa_{1x}^2 = 0 \tag{2.24}$$

Because this simple theory gives the incorrect power law above T_c we would expect it also to be incorrect below T_c but, to date, no experimental results of sufficient accuracy are available below T_c. The theory due to Elliott and Marshall [7] gives results virtually identical with (2.18) to (2.24) with one important difference, they predict a nonzero κ_{1x}^2 below T_c. The precise reason why the theories differ in this way is not yet understood; noninteracting spin waves also give $\kappa_{1x}^2 = 0$ and therefore it appears that in the theory of Elliott and Marshall a diffusive-like behavior is built into the perpendicular correlation function $\langle S_0^x(0)S_R^x(t)\rangle$. We will return to this point in the next section.

3. The Inelasticity of the Scattering

To consider this problem we concentrate attention on $F^{xx}(\mathbf{K}, \omega)$. Above T_c this is identical to $F^{zz}(\mathbf{K}, \omega)$ and therefore gives a complete description of the ω-dependence, while below T_c it gives the single spin wave scattering. We are not able to calculate $F^{xx}(\mathbf{K}, \omega)$ rigorously but we can get some information about the moments of it. We first note that

$$\frac{\partial}{\partial t}R^{xx}(\mathbf{K}, t) = \frac{i}{\hbar}\langle[S^x(-\mathbf{K}, 0), S^x(\mathbf{K}, t)]\rangle. \tag{3.1}$$

Hence

$$\frac{\partial^2}{\partial t^2}R^{xx}(\mathbf{K}, t) = \frac{i}{\hbar}\left\langle\left[S^x(-\mathbf{K}, 0), \frac{\partial}{\partial t}S^x(\mathbf{K}, t)\right]\right\rangle$$

and

$$\frac{\partial^n}{\partial t^n}R^{xx}(\mathbf{K}, t) = \frac{i}{\hbar}\left\langle\left[S^x(-\mathbf{K}, 0), \frac{\partial^{n-1}}{\partial t^{n-1}}S^x(\mathbf{K}, t)\right]\right\rangle. \tag{3.2}$$

It is easy to show that $F^{xx}(\mathbf{K}, \omega)$ is even in ω so only the even moments are nonzero. Then

$$\begin{aligned}\langle\omega^2\rangle &= \int_{-\infty}^{\infty} d\omega\omega^2 F^{xx}(\mathbf{K}, \omega)\\ &= -\left\{\frac{\partial^2}{\partial t^2}f^{xx}(\mathbf{K}, t)\right\}_{t=0}\\ &= \frac{-g^2\mu^2}{N\chi^{xx}(\mathbf{K})}\left\{\frac{\partial^2}{\partial t^2}R^{xx}(\mathbf{K}, t)\right\}_{t=0}\end{aligned} \tag{3.3}$$

and similarly

$$\langle\omega^4\rangle = \frac{g^2\mu^2}{N\chi^{xx}(\mathbf{K})}\left\{\frac{\partial^4}{\partial t^4}R^{xx}(\mathbf{K}, t)\right\}_{t=0}. \tag{3.4}$$

If we now assume a nearest neighbor model these two expressions can be evaluated. We find, using (3.2) and (3.3),

$$<\omega^2> = \frac{2g^2\mu^2 J}{\hbar^2\chi^{xx}(\mathbf{K})}(\gamma_0-\gamma_K)\langle S^yS_a^y + S^zS_a^z\rangle \tag{3.5}$$

where

$$\gamma_K = \sum_{\boldsymbol{\rho}} e^{i\mathbf{K}\cdot\boldsymbol{\rho}} \tag{3.6}$$

The expression for $\langle\omega^4\rangle$ is very long and will not be repeated here. It is of a similar form to (3.5) with a denominator $\chi^{xx}(\mathbf{K})$ and a numerator involving correlation functions between four spins which are close together. This numerator is also proportional to $(\gamma_0-\gamma_K)$, as is (3.5).

From these remarks we can now reconstruct the general character of the moments $\langle\omega^n\rangle$ as a function of n.

(a) $\langle\omega^0\rangle$ is unity.

(b) $\langle\omega^2\rangle$, $\langle\omega^4\rangle$ and all higher moments are inversely proportional to $\chi^{xx}(\mathbf{K})$.

(c) $\langle\omega^2\rangle$, $\langle\omega^4\rangle$ and all higher moments are proportional to $(\gamma_0-\gamma_K)$. This follows as a general rule from the remark that $f^{xx}(\mathbf{K}, t)$ is independent of t in the limit $K\to 0$.

(d) $\langle\omega^2\rangle$, $\langle\omega^4\rangle$ etc., are proportional to correlation functions between spins which are close together. This follows from (3.1), (3.2), which involve a commutator, and therefore reduce, at $t=0$, to short range correlation functions.

We now note that effect (d) cannot produce important qualitative effects near the critical temperature. For example we note that (3.5) can be rewritten, above T_c, as

$$\langle\omega^2\rangle = \frac{-2g^2\mu^2}{3\hbar^2\chi(\mathbf{K})}(\gamma_0-\gamma_K)\epsilon(T) \tag{3.7}$$

where $\epsilon(T)$ is the thermal energy for a typical pair of spins

$$\epsilon(T) = -2J\langle\mathbf{S}\cdot\mathbf{S}_a\rangle. \tag{3.8}$$

We know that the specific heat has a weak singularity (probably logarithmic) at T_c, and hence $\epsilon(T)$ is continuous, but with an infinite slope, at T_c. This is a weak singularity compared to the divergence in $\chi(0)$; this essential difference is because any short range correlation function can have only weak singularities whereas $\chi(\mathbf{K})$ involves long range correlation functions. We conclude that effect (d) produces numerical factors slowly varying with T.

Effect (b), the thermodynamic slowing down of fluctuations, shows that the scattering becomes more nearly elastic near T_c. Effect (c), the kinematic effect, shows that long wavelength fluctuations are slow.

At infinite temperature the discussion is straightforward. From (2.18) and (2.22) we get

$$\chi(\mathbf{K}) \to \chi_c T_c/T = g^2\mu^2 S(S+1)/3kT = \chi_0 \tag{3.9}$$

where we use χ_0 to stand for the Curie susceptibility. The short range correlation functions appearing in the moment formulae are also inversely proportional to T and a tedious calculation gives the results

$$\langle\omega^2\rangle \to \left(\frac{2J}{\hbar}\right)^2 \frac{2}{3} S(S+1)(\gamma_0-\gamma_K) \tag{3.10}$$

$$\langle\omega^4\rangle \to \left(\frac{2J}{\hbar}\right)^4 \frac{4}{9}\{S(S+1)\}^2(\gamma_0-\gamma_K)$$

$$\left\{\frac{7}{2}\gamma_0 - \frac{3}{2}\gamma_K - 2 - \frac{3}{4S(S+1)}\right\}. \tag{3.11}$$

In an earlier discussion de Gennes [8] evaluated these moments at infinite temperature working directly from the correlation function (2.5). His discussion is rather more difficult than that given here because he had to take four commutation operations with $\mathscr{H}$ to evaluate the fourth time derivative. In the present approach (3.2) shows that the fourth moment involves only three time derivatives and therefore three commutation operations with $\mathscr{H}$ furthermore the final commutation simplifies the formulae. de Gennes quoted only $\langle\omega^4\rangle$ for the simple cubic lattice averaged for a polycrystal. For that special case (3.11) gives the same answer except for the sign of the term 3/4 $S(S+1)$ which it appears de Gennes gave incorrectly. The subsequent discussion given by de Gennes is still valid because this term is very small.

In the forward direction we notice, since both $\langle\omega^2\rangle$ and $\langle\omega^4\rangle$ are proportional to K^2, that $\langle\omega^4\rangle$ is much larger than $\langle\omega^2\rangle^2$. It follows that although the half width at half height of $F(\mathbf{K}, \omega)$ must be small the shape must have large wings to it, i.e. $F(\mathbf{K}, \omega)$ must be something like a cutoff Lorentzian. We therefore assume

$$F(\mathbf{K}, \omega) = \frac{1}{\pi}\frac{\Gamma_K}{\omega^2+\Gamma_K^2} \qquad \text{for } |\omega| < s \tag{3.12}$$

$$= 0 \qquad \text{for } |\omega| > s$$

where

$$\Gamma_K=\frac{\pi}{2\sqrt{3}}\left\{\frac{\langle\omega^2\rangle^3}{\langle\omega^4\rangle}\right\}^{1/2} \tag{3.13}$$

and

$$s=\left\{\frac{3\langle\omega^4\rangle}{\langle\omega^2\rangle}\right\}^{1/2} \tag{3.14}$$

are chosen to give the second and fourth moments correctly. Substituting from (3.10) and (3.11) gives, to leading order in K^2,

$$\Gamma_K=\frac{J\pi}{3\hbar}(\gamma_0-\gamma_K)\left[\frac{S(S+1)}{\{r-1-3/16S(S+1)\}}\right]^{1/2} \tag{3.15}$$

$$s=\frac{4J}{\hbar}\,[S(S+1)]^{1/2}[r-1-3/16S(S+1)]^{1/2} \tag{3.16}$$

where r is the number of nearest neighbors. If we write

$$\Gamma_K=\Lambda K^2 \qquad \text{at } T=\infty \tag{3.17}$$

and use molecular field theory to give J in terms of T_c, we can now evaluate Λ. For Fe we find

$$2m_0\Lambda/\hbar=19 \qquad \text{at } T=\infty \tag{3.18}$$

[The factors on the left-hand side of (3.18) are convenient and give a dimensionless number.] (3.18) is only a rough estimate because we have used a nearest neighbor Heisenberg model to represent metallic Fe and furthermore we used molecular field theory to relate J to T_c. Nevertheless it should be of the correct order of magnitude. It should be noted that the only significant singularities of (3.12) are poles on the imaginary axis, at $\omega=\pm i\Gamma_K$.

At low temperatures the discussion is also straight forward. In a ferromagnet the last factor of (3.5) becomes S^2 and both molecular field theory and spin wave theory give

$$\chi^{xx}(\mathbf{K})=\frac{g^2\mu^2}{2J(\gamma_0-\gamma_K)}. \tag{3.19}$$

Hence

$$\langle\omega^2\rangle\to 4J^2S^2(\gamma_0-\gamma_K)^2/\hbar^2 \qquad \text{at } T=0. \tag{3.20}$$

The general expression for $\langle\omega^4\rangle$ can be used to give

$$\langle\omega^4\rangle=\langle\omega^2\rangle^2 \qquad \text{at } T=0. \tag{3.21}$$

The only distribution which satisfies (3.21) is a δ-function. Hence (3.20) and (3.21) together give

$$F^{xx}(\mathbf{K},\omega)=\tfrac{1}{2}\,\delta(\omega-\omega_K)+\tfrac{1}{2}\,\delta(\omega+\omega_K) \qquad [T=0] \tag{3.22}$$

where

$$\omega_K=2JS(\gamma_0-\gamma_K)/\hbar \tag{3.23}$$

is the correct spin wave frequency. As the temperature is raised the spin waves get damped and the δ-functions of (3.22) become broadened into cutoff Lorentzians, i.e., the singularities of $F^{xx}(\mathbf{K},\omega)$ move slightly off the real axis.

As the temperature is raised still further the spin wave interactions result in an energy renormalization. It is well known that at low temperatures this energy renormalization follows a $T^{5/2}$ law. Up to, say $0.8T_c$, it is probably reasonable to use (3.5) directly to give a rough estimate of the spin wave energy. Hence, very roughly,

$$\omega_K\sim 2J(\gamma_0-\gamma_K)\{\langle S^yS_a^y+S^zS_a^z\rangle\}^{1/2}/\hbar \qquad \text{for } 0<T<0.8\,T_c. \tag{3.24}$$

In the neighborhood of T_c we expect

$$\langle S^yS_a^y\rangle\sim\langle S^yS_a^z\rangle\sim\frac{S(S+1)}{3(r-1)}. \tag{3.25}$$

Hence

$$\omega_K=AK^2 \tag{3.26}$$

where

$$A\sim(2Ja^2r/6\hbar)\{2S(S+1)/3(r-1)\}^{1/2}. \tag{3.27}$$

Substituting for J as before we find for Fe [$S=1$, $r=8$] the result

$$2m_0A/\hbar\sim 30. \tag{3.28}$$

This last estimate is rough because we have made no real attempt to calculate the renormalized ω_K within, say, a factor of 2. Nevertheless within this kind of uncertainty it should be satisfactory

up to about $0.8T_c$ and beyond that temperature the spin wave interaction problem is too difficult to discuss here.

We now notice by comparing (3.17) and (3.28) that the separation between the spin wave peaks at about $0.8T_c$ is roughly the same as the width of the scattering curve at infinite temperature. The shape of $F^{xx}(\mathbf{K}, \omega)$ is very different at the two temperatures but the scale of the dependence on ω is roughly the same.

We now turn to a discussion of $F^{xx}(\mathbf{K}, \omega)$ near T_c. Several authors [5, 9, 10] have discussed this or a similar problem using various theories; all of these theories are, however, basically the same as that which we will now summarize. Because of the slow T dependence of effect (d), near but just above T_c we may estimate moments as

$$<\omega^2>_{K,T} \sim <\omega^2>_{K,\infty} \chi_0/\chi(\mathbf{K}, T) \qquad (3.29)$$

$$<\omega^4>_{K,T} \sim <\omega^4>_{K,\infty} \chi_0/\chi(\mathbf{K}, T)$$

where χ_0 is the Curie susceptibility. By comparison with the discussion of $F(\mathbf{K}, \omega)$ at infinite temperature we see this has the effect of replacing K^2 by $K^2\ \chi_0/\chi(\mathbf{K}, T)$. The ratio $<\omega^4>/<\omega^2>^2$ is now even larger than at infinite temperature because $\chi(\mathbf{K}, T)$ is large near T_c. In the absence of any other information about $F(\mathbf{K}, \omega)$ we assume it is a cutoff Lorentzian just as at infinite temperature; by analogy to (3.17) we get immediately

$$\Gamma_K = \frac{\Lambda K^2 \chi_0}{\chi(\mathbf{K}, T)} = \Lambda K^2 r_1^2 (\kappa_1^2 + k^2)\, T_c/T. \qquad (3.30)$$

From either (1.22) or (1.23) we see that $r_1^2\kappa_1^2$ is small near T_c and in typical neutron experiments the observations are made at angles such that $K^2 \sim \kappa_1^2$. Thus, for an experimental situation such as that used by Passell et al. [6], or Jacrot et al. [11], the expression (3.30) is some two orders of magnitude smaller than the appropriate expression for infinite temperature, (3.17). Hence the theoretical prediction is that there is a very substantial narrowing of the scattered neutron distribution as the temperature is reduced towards T_c.

However, in both the experiments by Passell et al., and by Jacrot et al., none of the features of (3.30) are observed. In particular the experiments suggest:

(1) The order of magnitude of Γ_K is given by an expression like (3.17) with

$$2m_0\Lambda/\hbar \sim 11.4 \qquad [\text{Experiment } T \sim T_c]. \qquad (3.31)$$

This is about two orders of magnitude larger than (3.30)

(2) Γ_K is approximately independent of temperature. This is in contrast with (3.30) which varies sensitively with T because of the $r_1^2\kappa_1^2$ dependence.

(3) Γ_K is proportional to K^2 within experimental error. No term proportional to K^4, as predicted by (3.30), is observed.

We are forced to conclude that the conventional theory as we have just summarized it, fails substantially. Therefore, in the next section, we look for an improvement.

4. Theoretical Discussion for $T \sim T_c$

The discussion of section 3 has shown that the inelasticity near T_c is hard to understand and therefore in this section we shall discuss the qualitative features which it now appears a good theory of the critical region must have.

We first note that the calculation for infinite temperature (3.18), the spin wave calculation at about 0.8 T_c, i.e., (3.28), and experiment near T_c, (3.31), all give results roughly in agreement as regards the dependence of $F^{xx}(\mathbf{K}, \omega)$ on ω. This suggests that the ω scale of $F^{xx}(\mathbf{K}, \omega)$ does not in fact change significantly from 0.8 T_c up to infinite temperature but that the *shape* of $F^{xx}(\mathbf{K}, \omega)$ changes considerably from two distinct spin wave peaks below T_c into a single Lorentzian at infinite temperature. But calculations which rely upon moment calculations are quite unable to give sensitive information on *shapes* and therefore the theory as described in section 3 is suspect.

We now examine more carefully the behavior of (3.29). Using (2.18) gives

$$<\omega^2>_{K,T} = <\omega^2>_{K,\infty} (r_1^2\kappa_1^2 + r_1^2 K^2)\, T_c/T \qquad (4.1)$$

$$<\omega^4>_{K,T} = <\omega^4>_{K,\infty} (r_1^2\kappa_1^2 + r_1^2 K^2)\, T_c/T \qquad (4.2)$$

(4.1) is proportional to K^2 at infinite temperature, because $<\omega^2>_{K,\infty}$ is proportional to K^2 but as the temperature is lowered (4.1) becomes smaller and becomes proportional to K^4 at temperatures sufficiently close to T_c that $\kappa_1^2 \ll K^2$. If we assume that $F^{xx}(\mathbf{K}, \omega)$ remains a cutoff Lorentzian we are

immediately led to (3.30). But the above behavior is quite consistent with a gradual change of shape in $F^{xx}(\mathbf{K},\omega)$ from a Lorentzian at infinite temperature to one which is dominated by two peaks at $\omega=\pm AK^2$ for temperatures such that $\kappa_1^2 \ll K^2$. These peaks would make a negligible contribution themselves to $<\omega^4>$ and the higher moments. Such peaks, if they existed, would have the obvious interpretation of quasi-spin waves above T_c. However we notice that a rectangular distribution bounded by $\omega=\pm AK^2$ would serve equally well as a dominant distribution near T_c. We also recall that, above T_c, $F^{xx}(\mathbf{K},\omega)$ and $F^{zz}(\mathbf{K},\omega)$ are identical and we cannot possibly associate single spin wave processes with $F^{zz}(\mathbf{K},\omega)$. Nevertheless the general point remains valid, it is quite consistent with (3.32) and (3.33) for any curve whether double peaked or not, to be sharply confined to limits $\omega=\pm AK^2$ provided it also has weak "tails" which can give large values to $<\omega^4>$ and higher moments.

This argument can be summarized as follows:

(i) The moment calculations are sensitive to the tails of the distribution $F^{xx}(\mathbf{K},\omega)$ whereas the neutron experiments measure only the central portion of $F^{xx}(\mathbf{K},\omega)$.

(ii) This central portion has a width, $\sim AK^2$, roughly independent of T from 0.8 T_c to infinite temperature but with a shape varying from a double peak (representing spin waves) at the lower limit to a single peak at high T. This central portion always contains the major part of the area of $F^{xx}(\mathbf{K},\omega)$.

(iii) The tails of the distribution $F^{xx}(\mathbf{K},\omega)$ are sensitive to T and vary so as to give agreement with the moment calculations. They are difficult to observe experimentally.

(iv) Above T_c, $F^{zz}(\mathbf{K},\omega)$ is identical to $F^{xx}(\mathbf{K},\omega)$ but below T_c does not show distinct spin wave peaks. However the ω-scale is roughly similar.

The above conclusions appear to be dictated by the experimental results which were obtained for the general range $K\sim\kappa_1$. For either $K\ll\kappa_1$ or $K\gg\kappa_1$ the neutron experiments give no information and therefore it is possible that in these regions the ω dependence is qualitatively different.

The clearest way of describing the situation is in terms of the singularities of $F^{xx}(\mathbf{K},\omega)$ in the complex ω plane. We have already remarked that the high temperature theory, (3.17), gives two significant poles at $\pm i\Lambda K^2$; the other singularities of $F^{xx}(\mathbf{K},\omega)$, [which are needed to describe the cutoff procedure for $|\omega|>s$], are distant $\sim J/\hbar$ from the origin. The conventional theory, (3.30), near T_c tells us that the two significant poles have moved along the imaginary axis to $\pm i\Lambda K^2\chi_0/\chi(\mathbf{K},T)$ and the other singularities of $F^{xx}(\mathbf{K},\omega)$ remain at a long distance from the origin. However, the neutron experiments insist that this is not correct, there must be singularities of some type distributed at distances $\sim\Lambda K^2$ from the origin; the poles predicted by (3.30) may or may not exist but if they do exist they must have a weight small compared to those at distances $\sim\Lambda K^2$.

The form of $F^{xx}(\mathbf{K},\omega)$ below T_c is of speeial interest. Well below T_c we know that $F^{xx}(\mathbf{K},\omega)$ is dominated by two spin wave peaks centered at $\pm\omega_K$, where ω_K is the renormalized spin wave energy, and with a width dependent on the spin wave lifetime. As the temperature is raised does $F^{xx}(\mathbf{K},\omega)$ retain this form or does a distinct diffusive mode appear in addition? We may speculate that an analogy to the classical fluid may exist. A classical fluid, at small K, may be described by the usual equations of hydrodynamics. In the absence of any dissipative effects, viscosity or thermal conductivity, the relaxation function [equivalent to $F^{xx}(\mathbf{K},\omega)$] has two δ-function peaks at $\pm c_sK$ where c_s is the velocity of sound. The introduction of viscosity or thermal conductivity damps these sound waves and simultaneously a diffusive mode also appears in the relaxation function. In other words, in the complex ω plane, as soon as the sound wave poles move off the real axis, a new pole appears on the imaginary axis. In suitable cases therefore, the relaxation function as measured by experiment as a function of real ω, can have three maxima, one at $\omega=0$ and two symmetrically placed either side at the appropriate renormalized frequencies [12, 13]. In the magnetic system the same phenomena might take place as the spin waves are damped. This possibility is intimately linked with the problem of the energy renormalization of spin waves very close to T_c and in view of the extremely speculative nature of this particular discussion we shall not pursue it further other than to remark that it is also connected with the behavior of κ_{1x}^2 below T_c (this problem was mentioned in sec. 2).

The discussion of this section is most clearly summarized in figure 1 which shows the positions of the singularities of $F^{xx}(\mathbf{K},\omega)$ in the complex ω plane according to the conventional theory and also two possibilities which would be consistent with the neutron results. In this figure singularities

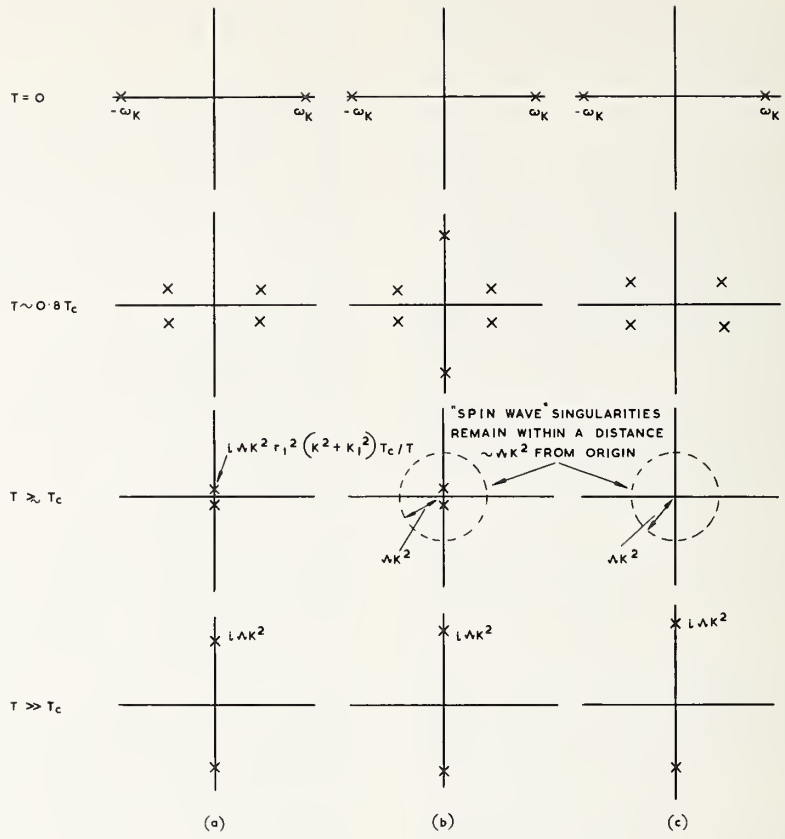

FIGURE 1. *Possible singularities of* $F^{xx}(\mathbf{K}, \omega)$ *in the complex* ω*-plane.*
Figure 1a shows the results of conventional theory. Figure 1b indicates the qualitative nature of the singularities of the analogy to hydrodynamics holds. Figure 1c indicates an alternative possibility in which poles do not collapse to the origin at T_c. In all diagrams the singularities at distances $\sim J/\hbar$ from the origin are ignored.

which are a long distance $\sim J/\hbar$ from the origin are not shown. Figure 1a gives the conventional theory, figure 1b the theory we would expect by analogy to hydrodynamics and figure 1c the theory we might expect if no "diffusive" mode appears below T_c. At the present time we are not able to tell whether possibility, (b) or (c) is correct.

5. Further Experiments

In this section we shall list briefly other experiments which give information on the form of $F^{xx}(\mathbf{K}, \omega)$.

(a) In experiments on Fe_3O_4, Riste [14] observed that spin waves existed above T_c and plotted their lifetime as a function of temperature. His results can be taken as experimental evidence in favor of the existence of spin waves above T_c. Unfortunately his experiments did not cover a wide enough range of scattering surfaces to distinguish between figures 1b and 1c.

(b) Although all the discussion of this paper has concerned ferromagnets we would naturally expect to carry over some results to antiferromagnets. In particular if spin waves exist above T_c in a ferromagnet we would expect them to exist above the Neél temperature of an antiferromagnet. It is therefore worth noting that Murthy et al. [15], have observed spin waves in MnO above the Neél temperature. As we would expect, these spin waves peaks are broad. MnO is an unusual antiferromagnet in that $T_N \sim 120$ °K but $\theta \sim 600$ °K; therefore at the Neél temperature we expect an exceptional amount of short range order to exist. In the presence of this large short range order we would expect the spin waves to be better defined than in the typical antiferromagnet and therefore in figures 1b and 1c the "spin wave" singularities would approximate closer to simple spin wave poles. This is probably why these neutron experiments observed them whereas experiments on other antiferromagnets, for example, Turberfield et al. [16], on MnF_2 do not see distinct spin waves above T_N.

6. Conclusions

The theory of neutron scattering from ferromagnets has been reviewed and it is shown how the experiments give the wavelength dependent susceptibility unambiguously. The experiments show that the conventional theory of the time dependence of the fluctuations near T_c, is incorrect. It is too difficult to construct an alternative theory immediately but to explain the results it is necessary that some remnant of "spin-wave motion" remains above T_c. Two possibilities are described in terms of the singularities of the relaxation function in the complex ω-plane.

7. References

[1] C. Domb and M. F. Sykes, Phys. Rev. **128**, 168, (1962).
[2] J. Gammel, W. Marshall and L. Morgan, Proc. Roy. Soc. **275**, 257 (1963).
[3] M. E. Fisher and M. F. Sykes, Physica **28**, 939 (1962).
[4] M. F. Sykes and M. E. Fisher, Physica **28**, 919 (1962).
[5] H. Mori and K. Kawasaki, Prog. Theor. Phys. **25**, 723 (1962).
[6] L. Passell, K. Blinowshi, P. Nielsen and T. Brun, Proc. International Conference on Magnetism.[1]
[7] R. Elliott and W. Marshall, Rev. Mod. Phys. **30**, 75 (1958).
[8] P. G. de Gennes, J. Phys. Chem. Solids **4**, 223 (1958).
[9] L. Van Hove, Phys. Rev. **95**, 1374 (1954).
[10] P. G. de Gennes and J. Villain, J. Phys. Chem. Solids **13**, 10 (1960).
[11] B. Jacrot, J. Kostantinovic, G. Perette and D. Cribier.[2]
[12] L. D. Landau and E. M. Lifshitz, Fluid Mechanics, Pergamon Press.
[13] W. Marshall, Lectures on Critical Phenomena, A.E.R.E.–L. 144 (1964).
[14] T. Riste, Journal Phys. Soc. Japan **17**, Supplement Bill, 60 (1962). Proc. of International Conference on Magnetism and Crystallography.
[15] N. S. Satya Murthy, G. Venkataraman, K. Usha Denig, B. A. Dasannacharya and P. K. Iyengar, Symposium on Inelastic Neutron Scattering, Bombay, 1964.
[16] K. C. Turberfield, A. Okazaki, and R. W. H. Stevenson, Proc. Phys. Soc. **85**, 743 (1965).

[1] Nottingham 1964, 99.
[2] Symposium on Inelastic Scattering of Neutrons in Solids and Liquids, Chalk River, 1962.

Critical Magnetic Scattering of Neutrons in Iron

L. Passell

Brookhaven National Laboratory, Upton, N.Y.

Abstract

Measurements of the angular and energy distributions of 4.28 Å neutrons scattered at small angles from iron at temperatures above the Curie temperature are described. The results are interpreted in terms of Van Hove's theory of critical magnetic scattering and yield information on the range of spin correlations and the dynamics of the spin ordering process. For the dimensionless parameter, $2m\Lambda/\hbar$, which describes the time dependence of the spin fluctuations, we obtain the value 11.0 ± 0.6 at $T-T_c=2$ and 18 °C. The zero field magnetic susceptibility, as determined by the parameters κ_1 and r_1 (which represent the range and strength respectively of the spin correlations), is found to vary as $(T-T_c)^{-1.30\pm0.04}$. Near the Curie temperature there was sufficient intensity to measure the ratio of the coefficients of the K^4 and K^2 terms of the angular distribution. The value of this ratio, 29 Å^2, is related to the existence of long range couplings within the spin system. Details of certain recent modifications of the theory of critical systems are discussed and compared with the experimental results.

This work is described in detail in a paper by L. Passell, K. Blinowski, T. Brun and P. Nielsen, Phys. Rev. **139A**, 1886 (1965).

Critical Neutron Scattering From Beta-Brass

O. W. Dietrich and J. Als-Nielsen

Research Establishment Risö, Roskilde, Denmark

Introduction

Beta-brass, which is an approx. 50 percent to 50 percent alloy of Cu and Zn, forms at low temperatures an ordered B.C.C. lattice. A B.C.C. lattice can be thought of as composed of two S.C. lattices — so-called superlattices, denoted respectively A and B — displaced half a cube diagonal with respect to each other. Perfect order means that all Cu atoms are at A sites, all Zn atoms at B sites. The order gradually decreases with increasing temperature; at the critical temperature T_c ($T_c \simeq 468$ °C) the average occupation of say an A site is entirely random, i.e., the long range order (abbr. LRO) has disappeared. Above T_c, however, local order still exists: If a certain A site is occupied by say a Zn atom there will be an excess probability over randomness that the nearest site — a B site — is occupied by a Cu atom and so on. This local order or short range order is described by a pair correlation function (abbr. pcf.)

In a diffraction experiment the LRO will give rise to narrow diffraction peaks (Bragg scattering peaks), whereas the SRO will give rise to broader and less intense peaks (critical scattering) provided that the radiation is scattered sufficiently different from a Cu atom and a Zn atom. This criterion make neutrons more suitable than x rays in case of β-brass. Walker and Keating have previously reported on a neutron scattering experiment from a β-brass crystal [1], which was furthermore enriched with Cu^{65} to enhance the difference in scattering amplitudes. Due to rapid Zn-evaporation from their crystal, it is however not possible to draw detailed quantitative conclusions from this experiment. From our present experiment, where a β-brass single crystal with normal isotopic abundance was used, the following can be deduced:

(1) The temperature dependencc of LRO in the close vicinity of T_c,

(2) the absolute value and the temperature dependence of the SRO correlation range, and

(3) some conclusions concerning the shape of the pair correlation function.

Cross Section

The changes in occupation of lattice sites are believed to be so slow that a static approximation is rigidly valid in deriving the relevant cross section. The cross section for a scattering vector $\boldsymbol{\kappa}$ close to a superlattice point $\boldsymbol{\tau}$ in the reciprocal space is

$$\frac{d\sigma}{d\Omega} \sim e^{-2W}\left(\frac{a-b}{2}\right)^2\left[\mathrm{LRO}^2\delta(\boldsymbol{\kappa}-\boldsymbol{\tau}) + \Sigma_{\mathbf{R}}\,\mathrm{pcf}\,(\mathbf{R})e^{-i\boldsymbol{\kappa}\cdot\mathbf{R}}\right] \quad (1)$$

a and b denote respectively the scattering amplitudes for Cu and Zn nuclei, $\mathbf{R}$ is a direct lattice vector and the Debye-Waller factor e^{-2W} accounts for the influence of the thermal vibrations on elastic scattering.

For $T < T_c$ the temperature dependence of $(\mathrm{LRO})^2$ is deduced from the Bragg peak intensities. For $T > T_c$ this kind of scattering disappears and only critical scattering remains. It will later be shown that the Ornstein-Zernike pcf $\sim \frac{1}{r_1^2} e^{-\kappa_1 R}/R$ fits the critical scattering data excellently, and with this shape of the pcf the critical scattering cross section becomes:

$$\left(\frac{d\sigma}{d\Omega}\right)\mathrm{crit} \sim \frac{1}{r_1^2}\frac{1}{|\kappa-\tau|^2+\kappa_1^2} \quad (2)$$

κ_1 is called the inverse correlation range, r_1 the strength parameter.

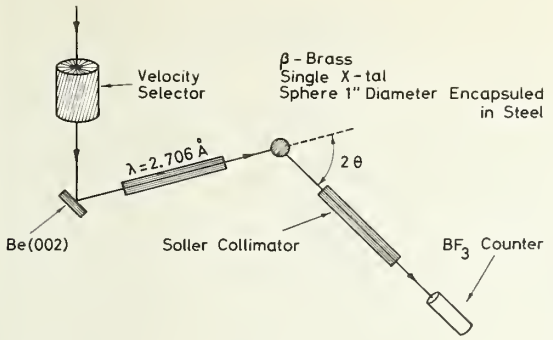

FIGURE 1. *Experimental setup in the (1, 0, 0) reflection.*
The angle between vertex and (0, 0, 1) is approx. 12°, whereby the occurrence of multiple scattering is prohibited.

The Experimental Setup

Monochromatic neutrons were extracted from the polyenergetic reactor beam by (0,0,2)—Bragg reflection in a Be single crystal (mosaic spread 5′ s.d.). Higher order neutrons were filtered out by means of a mechanical velocity selector (see fig. 1). A rather long wavelength of 2.70 Å was chosen to safely avoid parasitic multiple Bragg reflections in the β-brass single crystal, which in the (1,0,0) reflection was oriented with (0,0,1) approx. 12° from vertex. Also the instrumental resolution could be made quite narrow at this wavelength, which is essential for the interpretation of the critical scattering as shown below. The reactor beam was only collimated by the beam tube dimensions, the monochromatic beam was cylindrically collimated (30 mm diam per m) and the scattered beam was horizontally collimated by Soller slits (3.5 mm per m). The monochromatic beam intensity was $2.5 \cdot 10^5$ neutrons/sec. The counting time was mastered from a preset count on a monochromatic beam monitor (abbr. BMc in figures).

The spherical crystal (1 in. diam) was tightly encapsuled in a thin stainless steel container to avoid Zn evaporation. A 5 percent variation of the Zn content changes T_c 14 °C, [2] but in the six-months duration of the experiment T_c remained constant within a few tenth's of a degree. The crystal was mounted in an oven of sufficiently wide diameter so neutrons scattered from irradiated parts of the walls of the heating coil could not possibly hit the BF_3-detector. The crystal table could be turned around a horizontal and a vertical axis: the latter could also be coupled in the ratio 1:2

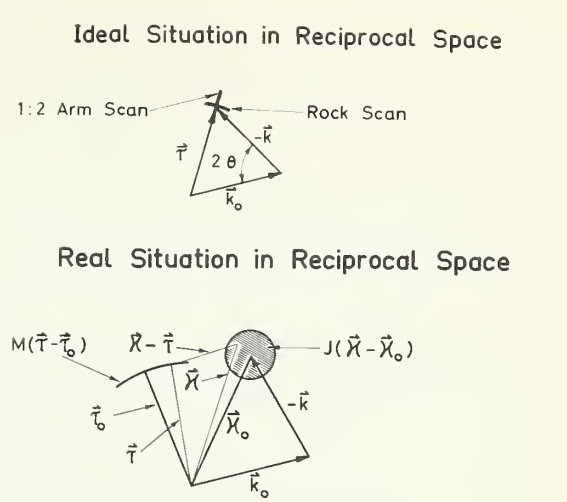

FIGURE 2. *Upper part: Wavevectors in reciprocal space corresponding to figure 1 (idealized resolution).*
Lower part: Definitions of distribution function with finite resolution.
The contour of $J(\kappa - \kappa_0)$ indicates f.i. a horizontal cut in the surface of half widths.

to the spectrometer arm. Two different scan types through a superlattice reflection in reciprocal space is sketched in figure 2.

Instrumental Resolution

Due to instrumental resolution the endpoint of the scattering vector κ is smeared, which is indicated by the distribution function $J_{\kappa_0}(\kappa)$. In the limited region in reciprocal space, where $J_{\kappa_0}(\kappa)$ will be used in the calculations below it is assumed that J is only dependent on the difference $\kappa - \kappa_0$, i.e., $J_{\kappa_0}(\kappa) = J(\kappa - \kappa_0)$. Also the endpoint of the τ-vector is smeared due to the mosaic spread, indicated by the distribution function $M(\tau - \tau_0)$(see fig. 2). The intensity $I(\kappa_0, \tau_0)$ with the spectrometer and crystal set at the average values κ_0 and τ_0 of the scattering vector and τ-vector respectively is found as the 6-dimensional convolution integral:

$$I(\kappa_0, \tau_0) = \int\int J(\kappa - \kappa_0) \cdot M(\tau - \tau_0) \cdot \sigma(\kappa, \tau)\, d\kappa d\tau, \qquad (3)$$

where the cross section $\frac{d\sigma}{d\Omega}(\kappa, \tau)$ has been abbreviated to $\sigma(\kappa, \tau)$.

For Bragg scattering $\sigma(\kappa, \tau) = \delta(\kappa - \tau)$ and

$$I_{\text{Bragg}}(\kappa_0 - \tau_0) = \int\int J(\kappa - \kappa_0) M(\tau - \tau_0) \delta(\kappa - \tau) d\kappa d\tau. \quad (4)$$

For critical scattering $\sigma(\kappa, \tau) = \sigma(\kappa - \tau) = \int \sigma(\epsilon) \delta(\kappa - \tau - \epsilon) d\epsilon$ and

$$I_{\text{crit}}(\kappa_0 - \tau_0) = \int \sigma(\epsilon) d\epsilon \int\int J(\kappa - \kappa_0) M(\tau - \tau_0) \cdot \delta(\kappa - \tau - \epsilon) d\kappa d\tau$$

$$= \int \sigma(\epsilon) d\epsilon \int\int J(\kappa^* - (\kappa_0 - \epsilon)) M(\tau - \tau_0) \cdot \delta(\kappa^* - \tau) d\kappa^* d\tau$$

$$I_{\text{crit}}(\kappa_0 - \tau_0) = \int I_{\text{Bragg}}(\kappa_0 - \epsilon - \tau_0) \sigma(\epsilon) d\epsilon \quad (5)$$

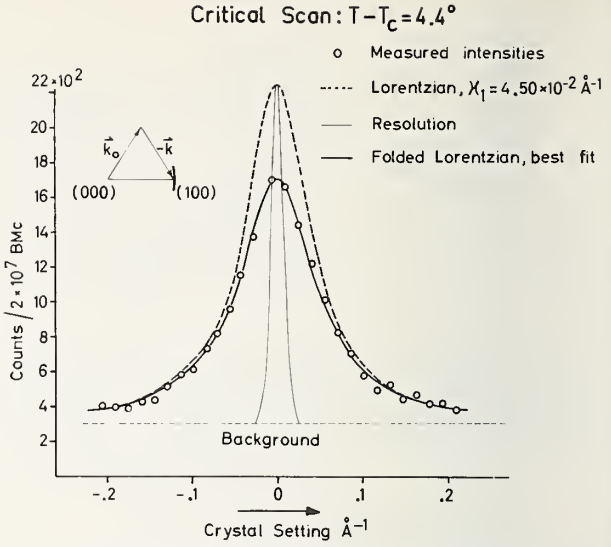

FIGURE 3. *A rock-scan through (1, 0, 0) 4.4° above* T_c. The excellent fit of an Ornstein-Zernike correlation function is apparent.

The measured critical scattering is thus the 3-dimensional convolution integral of a measurable function $I_{\text{Bragg}}(\kappa_0 - \tau_0)$ and the cross section σ, and an exact convolution can be performed without any assumptions of the shape of the distribution functions $J(\kappa - \kappa_0)$ and $M(\tau - \tau_0)$, apart from the already mentioned approximation $J_{\kappa_0}(\kappa) \simeq J(\kappa - \kappa_0)$.

Analysis of Critical Diffraction Peaks

In practice, the unfolding calculation was performed in the following way with the aid of a digital computer:

Three mutual perpendicular scans through the Bragg peak were measured below T_c and approximated by three normalized Gaussians. The product of these was used as $I_{\text{Bragg}}(\kappa_0 - \tau_0)$. In f.i. a rock scan measurement the computer calculated the ratio between $\sigma(\kappa_0, \tau_0)$ from (2) and $I(\kappa_0, \tau_0)$ from (5) for different directions of τ_0 and for a certain value of κ_1. For this value of κ_1 the sum of weighted, squared deviations between $I(\kappa_0, \tau_0)$ and the measured intensities was calculated, and by iteration in κ_1-values this sum was finally minimized.

An example is demonstrated in figure 3, where a scan perpendicular to (1, 0, 0) was measured 4.4 °C above T_c. The circular points are measured intensities as function of crystal setting. The narrow curve is the corresponding normalized Bragg reflection peak, measured below T_c, and the dashed curve is the Lorentzian (2) for the best κ_1-value. These curves are drawn upon a constant background, which was measured at several points far from the superlattic point (1, 0, 0). A scan at a high temperature (70° above T_c) showed the same constant background, when corrected for the remaining small amount of critical scattering. This justifies to some extent a constant background subtraction, which was used throughout the analysis of all critical data.

It is seen that the Ornstein-Zernike pair correlation function fits the data excellently. The scatter of measured points around the folded Lorentzian (solid line) is random and in statistical agreement with the uncertainties on the count rates.

Best Fit for Different Correlation Functions

Pair Correlation Function			$T-T_c$ 2.0°	4.4°	5.7°	12.1°
Ornstein Zernike	$\frac{e^{-\chi_1 R}}{R}$	χ_1	2.38×10^{-2}	4.54×10^{-2}	5.12×10^{-2}	6.82×10^{-2}
Fisher	$\frac{e^{-\chi_1 R}}{R^{1+\eta}}$	χ_1	2.38×10^{-2}	4.54×10^{-2}	5.12×10^{-2}	6.82×10^{-2}
		η	0.0000	0.0000	0.0000	0.0000
Hort	$\frac{e^{-\chi_1 R}}{R}\left[1-e^{-(\eta-\chi_1)R}\right]$	χ_1	2.38×10^{-2}	4.54×10^{-2}	5.12×10^{-2}	6.82×10^{-2}
		η	1.00×10^{6}	1.08×10^{6}	2.97×10^{5}	2.32×10^{6}

Temperature Dependence of LRO and SRO

Theoretically (LRO), which is proportional to the Bragg peak intensity, is proportional to $(T_c - T)^{2\beta}$ with $\beta \simeq 5/16 = 0.3125$ for the Ising Model [5].

Figure 4 shows the peak intensity from the (1,1,1) reflection as function of the temperature from 10° below the critical temperature to a little above this point. When the intensities are plotted as function of $\Delta T \equiv T_c - T$ in a double log plot, it is seen that a power law is valid near T_c and that $\beta \simeq 0.325$.

The intersection of the long-range order curve with the abscissa gives the thermocouple voltage when the crystal is in the critical state. The temperature dependence of all the parameters to be discussed is expressed by the temperature difference ΔT and this is measured as the corresponding difference in thermocouple voltage multiplied with the scaling factor 0.103 °K/μV. The uncertainty of the intersection contributes the main part of the uncertainty of 0.1 °K on ΔT.

A possible temperature gradient can be found by measuring similar curves with reduced beam hitting different parts of the crystal. The currents in the heating coils in the oven were adjusted until all curves intersected the abscissa at the same thermocouple voltage, and it was then concluded that temperature gradients could be neglected.

Figure 5 shows similar curves for the (1,0,0) reflection. β is here found to be 0.27 which differs significantly from the value 0.325 obtained from the (1, 1, 1) reflection. This might be due to a different degree of extinction in the two cases. The extinction correction will be relatively larger for big values of ΔT than for small values, since the cross section and thereby the beam attenuation through the crystal increases with increasing values of ΔT. The extinction correction will therefore qualitatively have the effect of increasing the slope of the line in the double log plot. At present we have not investigated this problem in detail, and the figures show uncorrected Bragg peak intensities.

The tail of the curve for temperatures above the critical point is the peak intensity of the critical scattering, and the difference in order of magnitude from the Bragg peak intensity should be noted.

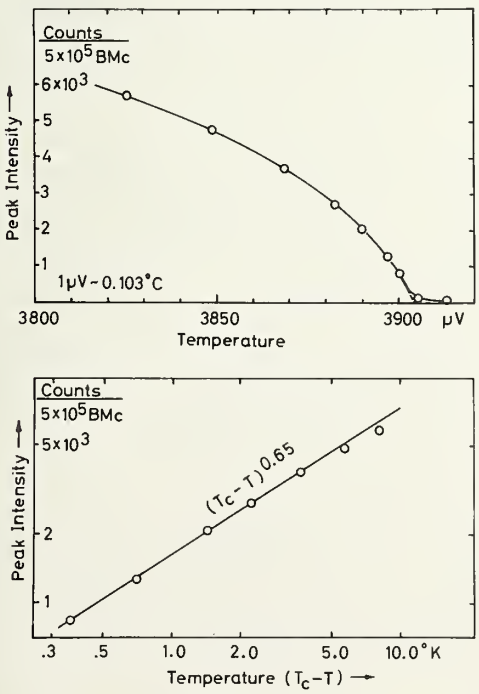

FIGURE 4. *Bragg peak intensity versus temperature for the (1, 1, 1) reflection.*

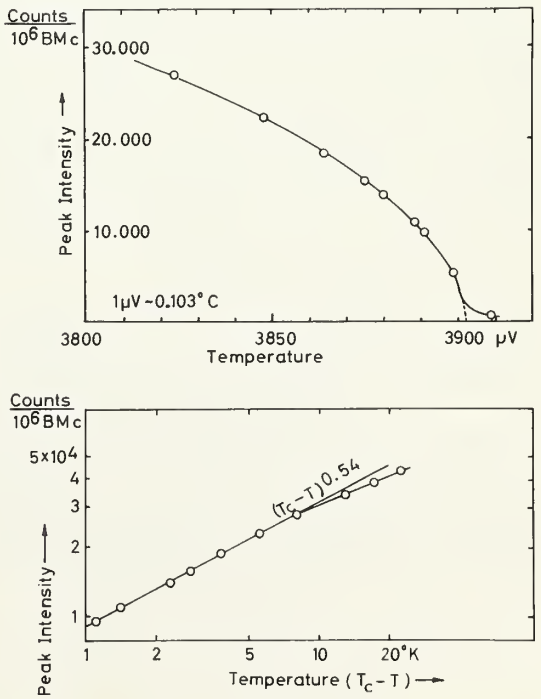

FIGURE 5. *Bragg peak intensity versus temperature for the (1, 0, 0,) reflection.*

209-493 O-66—11

Also the temperature dependence of the SRO has been calculated in the Ising Model. For a ferromagnet it has been found that the susceptibility χ obeys a power law being proportional to $\left(\frac{T-T_c}{T}\right)^{\gamma}$ with γ equal to 1.25 [5]. It is a well known fact that the susceptibility χ is related to the pair correlation function through ($\chi \propto \Sigma_R$ pcf (R)).

On the other hand the peak intensity I_0 for $T > T_c$ is also proportional to this sum as seen from the cross section formula (1). Recalling the close analogy of the order-disorder transition in alloys and magnetic materials, it is therefore expected that $I_0 \propto \left(\frac{T-T_c}{T}\right)^{-\gamma}$. γ can therefore be determined from the measured temperature dependence of the peak intensity, *independently* of any shape that the pair correlation function might have, provided of course that the resolution correction is correct.

Figure 6 shows the peak intensities of critical scattering from the (1, 0, 0) and from the (1, 1, 1) reflections for temperatures up to about 35° above T_c. The intensities are corrected for reduction due to resolution and the curves shown in the lower part of the figure show the corrections. The peak value reduction amounts to as much as a factor of 2 at the lowest temperatures and since the corrected intensities for both reflections obey the same power law, this gives confidence in the calculations on resolution corrections.

The difference between peak intensities for the (1, 0, 0) and the (1, 1, 1) reflections is due to different Debye-Waller factors. The measured ratio is seen to be 1.28 and, using Chipmann's data for the Debye temperature around 750 °K [6], the ratio of the Debye-Waller factors is 1.32.

The weighted average value of the power γ is 1.11 ± 0.01, which should be compared with the theoretical value of 1.25.

Figure 7 shows the values of κ_1 obtained at different temperatures in different scan types through different superlattice points in the reciprocal lattice. It is worthwhile to note the consistency of the results. Each point represents one diffraction peak, which takes, on an average, 48 hrs of measuring time.

For comparison with theory, the value of κ_1 at 75° above T_c calculated from the theory of Elliott and Marshall is also shown.

The peak intensity I_0 is with the Ornstein-Zernike pcf proportional to $(r_1 \cdot \kappa_1)^{-2}$.

r_1 is theoretically expected to decrease slightly with increasing temperature [7]. This implies that twice the slope of the least square fitted line to the κ_1-values is an upper limit of the parameter γ already discussed. It is concluded therefore that γ is less than 1.18 ± 0.02, in consistency with the value found from the peak value runs.

On the other hand, the measured values of κ_1 together with the experimental result that

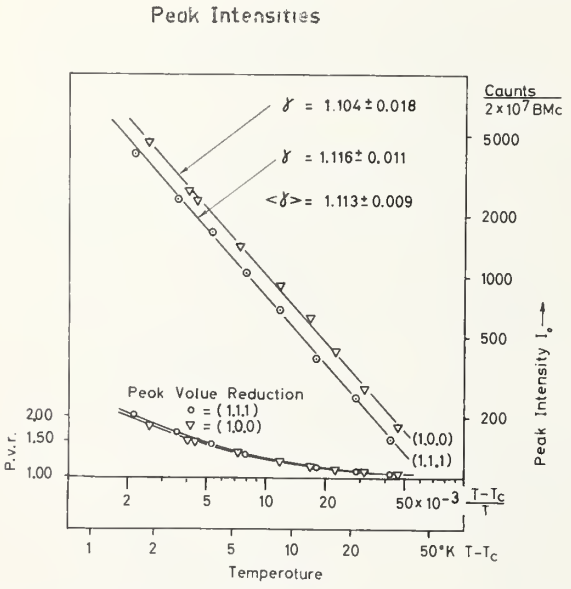

FIGURE 6. *Critical peak intensities, corrected for resolution reduction, for (1, 0, 0) and (1, 1, 1) reflections.*

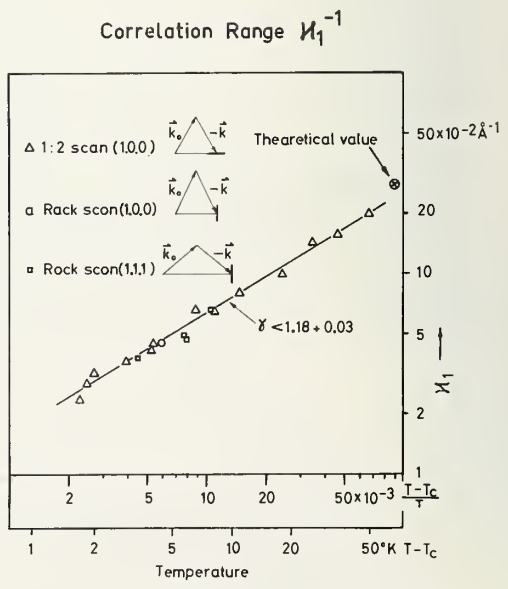

FIGURE 7. *Inverse correlation ranges κ_1 versus temperature.* Each point represents the result of a scan as shown in figure 3.

$(r_1 \cdot \kappa_1)^{-2} \propto \left(\frac{T-T_c}{T}\right)^{-1.11}$, can be used to deduce the temperature dependence of r_1. In a linear approximation with $r_1^2 = r_{1c}^2\left(1-\alpha\frac{\Delta T}{T}\right)$, it was found that α was equal to 3.6 ± 1.2, which is compared with the temperature dependence of r_1 given by Elliott and Marshall [7], who found that $\alpha \simeq 1.2$.

After completion of these measurements it was concluded that the most accurate information could be obtained from rock-scans through the (1, 0, 0) reflection. A series of such scans were therefore measured, but the inverse correlation ranges were now found to be 20 percent lower than the previous data over the entire temperature region as shown on figure 8.

The (1, 1, 1) reflection data, which was obtained at the end of the previous run, tends toward the data of the latest (1, 0, 0) reflection run. The critical temperature, as well as the Bragg peak intensities, were still exactly reproducible. Also the temperature dependences of κ_1 and I_0 as well as $I_0(\kappa_1)$ are in agreement with the previous data. It must therefore be concluded that some properties of the crystal have changed during the long period at elevated temperatures, but we are unable to give any detailed explanation of the change. Future experiments on other β-brass crystals might shed light on the problem.

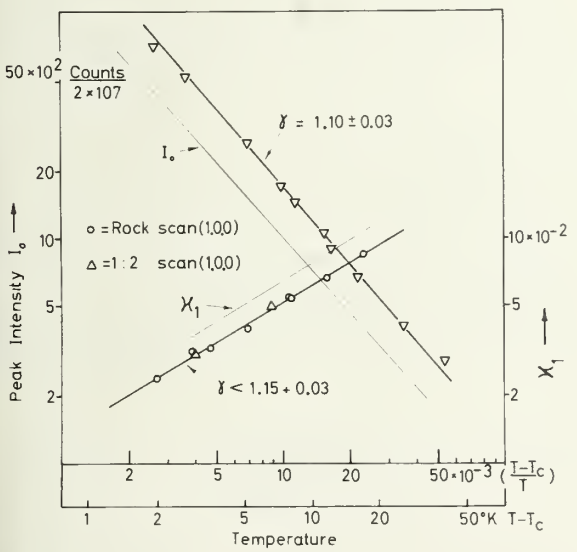

FIGURE 8. *Later results of critical scattering around the (1, 0, 0) reflection.*

These results are not consistent with the results in figure 6 and figure 7. Note, however, that T_c, β, γ, and $I_0(\kappa_1)$ are the same.

Conclusion

The following conclusions can be drawn from the present experiment:

(1) The Ornstein-Zernike correlation function is in excellent agreement with the data. A complete Fourier analysis to obtain all SRO parameters is not possible due to the very limited regions of the reciprocal space where the critical scattering is sufficiently intense for experimental access.

(2) The absolute value of the short range order correlation range is roughly in agreement with theory, but could possibly be an individual property of a given crystal.

(3) The temperature dependence of LRO is not in contradiction to the latest Ising model results, but definitely outrules the results of older theories $\left(\text{f.i. Bethe-Peierls theory, } \beta = \frac{1}{2}\right)$.

(4) The temperature dependence of SRO is in slight but definite disagreement with the Ising model in the nearest-neighbor interaction approximation.

Note added in proof. Later measurements have indicated that the β-brass crystal contains a few percentages of γ-phase. Recent measurements on a pure β-brass crystal gave an exponent in the temperature law for the susceptibility of $\gamma = 1.25 \pm .02$.

References

[1] Walker, C. B., and Keating, D. T., Phys. Rev. **130**, 1726 (1963).

[2] Hansen, M., Constitution of Binary Alloys (McGraw-Hill Book Co., New York., N.Y., 1958).

[3] Fisher, M. E., Physica **28**, 172 (1962).

[4] Hart, E. W., J. Chem. Phys. **34**, 1471 (1961).

[5] Essam, I. M., and Fisher, M. E., J. Chem. Phys. **38**, 802 (1963).

[6] Chipman, D. R., MRL Report No. 67, Watertown Arsenal, Massachusetts (1959).

[7] Elliott, R. I., and Marshall, W., Rev. Mod. Phys. **30**, 1 (1958).

The Spectrum of Light Inelastically Scattered by a Fluid Near Its Critical Point*

N. C. Ford, Jr.,[1] and G. B. Benedek

Massachusetts Institute of Technology, Cambridge, Mass.

If a light beam passes through a perfectly homogeneous medium we expect no scattering of the light in directions other than the forward direction. This conclusion results from the fact that waves scattered from each point in a homogeneous medium interfere destructively in every direction other than the forward direction. Of course, if the wavelength of the radiation is of the order of the interatomic distances then on this scale the medium will be nonhomogeneous and scattering can be expected to occur in conformity with the Bragg conditions. However, for light waves the Bragg equations cannot be satisfied.

Despite this argument there is considerable light scattering even from the most highly purified liquids. This scattering grows stronger as one approaches the liquid-gas critical point. In fact, in this critical region the scattering is so impressive that it is called "critical opalescence." Von Smoluchowski [1] was the first to suggest that in a real liquid the density is not perfectly uniform but that over regions of the order of the wavelength of light there were fluctuations in the density of the liquid. At each instant of time, he suggested, the liquid is not of a single density, but instead there is a distribution of density around the average density. The light is then scattered off the fluctuation in the density around the average.

Stimulated by Von Smoluchowski's suggestion, Einstein [2] undertook a quantitative calculation of the scattering of light from the fluctuations in a liquid with special attention to the situation near the critical point. If we take the wave vector of the incident light beam as $\mathbf{k}$, and that of the scattered beam as $\mathbf{k}'$, then Einstein was able to show that the electric field scattered a distance R away from the illuminated region is given by

$$\mathbf{E}(R, \mathbf{K}, t) = -\mathbf{E}_0\left(\frac{\omega_0}{c}\right)^2 \frac{\sin\varphi}{4\pi} \frac{e^{i(\mathbf{k}'\cdot\mathbf{R}-\omega_0 t)}}{R}(2\pi)^{3/2}\,\delta\epsilon(\mathbf{K}, t) \tag{1}$$

where:

$$\mathbf{K} = \mathbf{k}' - \mathbf{k} \tag{2}$$

and where $\mathbf{E}_0$ is the amplitude of the incident plane wave, ω_0 is the angular frequency of the incident radiation, $\sin\varphi$ is the angle between the direction of polarization of the incident light and the direction of $\mathbf{k}'$. $\delta\epsilon(\mathbf{K}, t)$ is the fluctuation of the dielectric constant having the wave vector equal to the scattering vector $\mathbf{K}$. Equation (1) signifies that scattering in the direction $\mathbf{k}'$ is produced by a fluctuation in dielectric constant having wave vector $\mathbf{K} = \mathbf{k}' - \mathbf{k}$. This corresponds classically to a Bragg reflection off the fluctuation having wave vector $\mathbf{K}$. Quantum mechanically eq (1) and (2) signify that constructive interference of the scattered wavelets occurs only when the momentum is conserved between the photons and the scattering fluctuation.

In order to determine the intensity of the scattered light Einstein then went on to calculate the mean squared scattered field:

$$\langle|\mathbf{E}(R, \mathbf{K}, t)|^2\rangle = E_0^2\left(\frac{\omega_0}{c}\right)^4 \frac{\sin^2\varphi}{(4\pi R)^2}(2\pi)^3\langle|\delta\epsilon(\mathbf{K}, t)|^2\rangle. \tag{3}$$

The fluctuation in the dielectric constant can be taken as arising out of the fluctuation of the density $\delta\rho$ viz:

$$\delta\epsilon(\mathbf{K}, t) \cong \left(\frac{\partial\epsilon}{\partial\rho}\right)_T \delta\rho(\mathbf{K}, t) \tag{4}$$

and Einstein evaluated the mean squared amplitude of the fluctuation in the density for $\mathbf{K} = 0$ using the

*This research was supported by the Advanced Research Projects Agency under Contract SD 90.

[1] Present address: University of Massachusetts, Amherst, Mass.

Boltzmann principle which weights a fluctuation by the work required to produce it. In this way Einstein found for $\mathbf{K}=0$

$$(2\pi)^3\langle|\delta\epsilon(\mathbf{K},\,t)|^2\rangle \underset{K\equiv 0}{\cong} V\rho_0\left(\frac{\partial\epsilon}{\partial\rho}\right)^2\left[\frac{\rho_0 kT}{B_T}\right] \qquad (5)$$

where V is the volume of the illuminated region, ρ_0 is the mean density, B_T is the isothermal bulk modulus, kT is Boltzmann's constant times the absolute temperature. The phenomenon of critical opalescence follows simply from (5) since as $T\rightarrow T_c$ the isothermal bulk modulus goes to zero, or perhaps more strikingly, the compressibility grows very large indeed and hence $\langle|\delta\epsilon(0,\,t)|^2\rangle$ gets very big. Physically the enormous increase in the scattering results because large density fluctuations become energetically very easy to produce since the compressibility is very large. The large density fluctuations in turn produce large fluctuations in the dielectric constant and hence a great deal of light scattering.

The work of Einstein was later extended by Ornstein and Zernike [3]. They noted that eq (5) was a good approximation for $\delta\epsilon(\mathbf{K},\,t)$ provided that one was not too near T_c. As $T\rightarrow T_c$, however, it becomes necessary to evaluate $\langle|\delta\epsilon(\mathbf{K},\,t)|^2\rangle$ for $K\neq 0$. Their result, which has also been obtained in other ways [4, 5], has the form for small K

$$(2\pi)^3\langle|\delta\epsilon(\mathbf{K},\,t)|^2\rangle \simeq V\rho_0\left(\frac{\partial\epsilon}{\partial\rho}\right)^2\left(\frac{\rho_0 kT}{B_T+(aK)^2}\right) \qquad (6)$$

where a is a length of the order of the interatomic distance. Thus, the scattered light intensity grows extremely large only in the forward direction $\mathbf{K}=0$. For other directions the scattered intensity will not in fact diverge.

Following the work of Einstein, and Ornstein and Zernike, much experimental effort was devoted to a study of the temperature dependence and the $\mathbf{K}$ dependence of the scattered light intensity. Work continues to the present day and in fact is being reviewed at the present conference. Despite this activity, there exists no experimental information on the *spectrum* of the scattered light in the critical region of a fluid.

The first person to investigate theoretically the spectrum of light scattered from a liquid or solid was L. Brillouin. His first investigation [6] of this subject was in 1914. This was followed by a more complete analysis in 1922 [7]. The spectrum of the scattered light depends upon the form of the time dependence of the fluctuation in the dielectric constant. In fact, the spectrum is obtained if the time correlation function $\langle E(\mathbf{K},\,t+\tau)\cdot E^*(\mathbf{K},\,t)\rangle$ is known [8]. This correlation function is related to the temporal fluctuations in the scattered field by

$$\langle E(\mathbf{K},\,t+\tau)\cdot E^*(\mathbf{K},\,t)\rangle$$

$$\equiv \lim_{T\rightarrow\infty}\frac{1}{2T}\int_{-T}^{T} E(\mathbf{K},\,t+\tau)\cdot E^*(\mathbf{K},\,t)dt \qquad (7)$$

where we have dropped the distance R in the designation of the functional dependence in E. The correlation function for the scattered field is related to the correlation function for the fluctuations in the dielectric constant by

$$\langle\mathbf{E}(\mathbf{K},\,t+\tau)\cdot\mathbf{E}^*(\mathbf{K},\,t)\rangle = E_0^2\left(\frac{\omega_0}{c}\right)^4$$

$$\frac{\sin^2\varphi}{(4\pi R)^2}(2\pi)^3\langle\delta\epsilon(\mathbf{K},\,t+\tau)\delta\epsilon^*(\mathbf{K},\,t)\rangle e^{-i\omega_0\tau} \qquad (8)$$

and the spectrum of the scattered light is given by

$$S(\mathbf{K},\,\omega')\equiv\frac{1}{2\pi}\int\langle\mathbf{E}(\mathbf{K},\,t+\tau)\cdot\mathbf{E}^*(\mathbf{K},\,t)\rangle e^{i\omega'\tau}d\tau \qquad (9)$$

and the total intensity under the spectrum S is just

$$\langle|E(\mathbf{K},\,t)|^2\rangle=\int_{-\infty}^{\infty} s(\mathbf{K}\omega')d\omega'. \qquad (10)$$

The question thus arises, what is the time correlation function for the fluctuations in the dielectric constant? To answer this we must have some model for the origin of the fluctuations in ϵ. Brillouin pointed out that one such origin was to be found in the thermally excited sound waves which continuously travel through the medium. These sound waves are fluctuations in pressure at constant entropy. The pressure fluctuations in turn modulate the dielectric constant and so produce scattering. To calculate the modulation of the dielectric constant produced by the thermally excited sound waves, we observe that:

$$(\delta\epsilon(\mathbf{K},\,t))_s=\left(\frac{\sigma\epsilon}{\partial p}\right)_s(\delta p(\mathbf{K},\,t))_s \qquad (11)$$

where $\delta p(\mathbf{K},\,t)$ is the Fourier amplitude for the pressure fluctuation in the sound wave having wave vector $\mathbf{K}$. Since the sound wave travels as a wave with frequency $\pm\Omega(\mathbf{K})$ and has a finite lifetime

$1/\Gamma(\mathbf{K})$ we may expect that the correlation function for the pressure fluctuations is

$$\langle \delta p(\mathbf{K}, t+\tau)\delta p^*(\mathbf{K}, t)\rangle = \langle |\delta p(\mathbf{K}, t)|^2\rangle e^{\pm i\Omega(\mathbf{K})\tau} e^{-\Gamma\tau}. \tag{12}$$

From this it follows at once that the spectrum of the scattered radiation is given using equations 12, 11, 9, 8, by

$$[S(\mathbf{K}, \omega')]_{\text{sound waves}} = E_0^2 \left(\frac{\omega_0}{c}\right)^2 \frac{\sin^2\varphi}{(4\pi R)^2}$$

$$(2\pi)^3 \left(\frac{\partial \epsilon}{\partial p}\right)_s^2 \langle |\delta p(\mathbf{K}, t)|^2\rangle$$

$$\frac{1}{\pi}\left\{\frac{\Gamma(\mathbf{K})}{[\omega' - (\omega_0 \pm \Omega(\mathbf{K}))]^2 + \Gamma^2(K)}\right\}. \tag{13}$$

Thus the spectrum of light scattered by the sound waves in liquid consists of a doublet. Each component of the doublet is shifted away from the incident frequency ω_0 by an amount $\pm\Omega(\mathbf{K})$. This shift is simply the frequency of the sound wave which was responsible for the scattering. The Brillouin doublets can be regarded as a Doppler shift in the frequency of the incident light as a result of a reflection off the moving sound waves. Or equivalently the condition

$$\omega' = \omega_0 \pm \Omega(\mathbf{K}) \tag{14}$$

can be looked upon as a conservation of energy between the incident photon, the emergent photon, and the scattering phonon. The plus sign corresponds to phonon annihilation and the negative sign to phonon creation.

The existence of the Brillouin doublets for light scattered by a liquid was first shown by the experiments of Gross in 1930 [9, 10]. This subject has since expanded considerably and the experimental information on liquids has been well reviewed by I. Fabelinskii [11]. The experiments showed, even in the most carefully purified liquids, that the spectrum also contained light whose frequency was equal to that of the incident radiation. That is, in addition to the Brillouin doublets, there is a central component in the spectrum of the scattered light. The existence and relative magnitude of the central components and the Brillouin doublets was explained by Landau and Placzek [12, 4]. They pointed out that the fluctuations in the dielectric constant are produced not only by the adiabatic pressure fluctuations (the sound waves) but also by the isobaric entropy fluctuations. Putting the matter very explicitly, the dielectric constant can be regarded as a function of the entropy (s) and the pressure (p) and fluctuations in either of these quantities will cause fluctuations in the dielectric constant. Thus

$$\delta\epsilon(\mathbf{K}, t) = \left(\frac{\partial \epsilon}{\partial s}\right)_p (\delta s(\mathbf{K}, t))_p + \left(\frac{\partial \epsilon}{\partial p}\right)_s (\delta p(\mathbf{K}, t))_s. \tag{15}$$

The second term on the right hand side of eq (15) was considered by Brillouin. Landau and Placzek stressed the importance of the first term. In order to obtain the time dependence of the entropy fluctuations they argued that the fluctuations in entropy were proportional to those of temperature through

$$T(\delta s)_p = c_p(\delta T)_p. \tag{16}$$

But the time dependence of a temperature fluctuation is governed by the Fourier heat flow equation viz:

$$\frac{d}{dt}\delta T(r, t) = \frac{\lambda}{c_p^*}\nabla^2 \delta T(r, t) \tag{17}$$

where c_p^* is the specific heat per unit volume, λ is the thermal conductivity, $\delta T(r, t)$ is the temperature fluctuation at the point r and time t. To obtain the time dependence of the temperature fluctuations with wave vector $\mathbf{K}$, we compute the Fourier transform of eq (17) and find that

$$\frac{d}{dt}\delta T(\mathbf{K}, t) = \frac{-\lambda K^2}{c_p^*}\delta T(\mathbf{K}, t). \tag{18}$$

Thus the temperature fluctuations do not propagate, they are diffusion like in their decay, and a fluctuation will die away exponentially with time. Thus we have that the correlation function for the entropy fluctuation will have the form

$$\langle \delta s(\mathbf{K}, t+\tau)\delta s^*(\mathbf{K}, t)\rangle = \langle |\delta s(\mathbf{K}, t)|^2\rangle e^{-\Gamma_e(\mathbf{K})\tau}, \tag{19a}$$

where

$$\Gamma_e(\mathbf{K}) \equiv \frac{\lambda K^2}{c_p^*} \tag{19b}$$

Since the entropy fluctuations are independent of the pressure fluctuations we may calculate the spectrum of light scattered by the entropy fluctuations alone and we obtain using 8, 9, 15, and 19 that

$$(S(\mathbf{K}, \omega'))_{\substack{\text{entropy} \\ \text{fluctuation}}} = \left[E_0^2 \left(\frac{\omega_0}{c}\right)^2 \frac{\sin^2 \varphi}{(4\pi)R^2} (2\pi)^3 \left(\frac{\partial \epsilon}{\partial s}\right)_p^2 \langle |\delta s(\mathbf{K}, t)|^2 \rangle\right] \times \left[\frac{1}{\pi} \left\{\frac{\Gamma_c(\mathbf{K})}{(\omega' - \omega_0)^2 + \Gamma_c^2(\mathbf{K})}\right\}\right]. \quad (20)$$

Since the entropy fluctuations do not propagate, they appear in the spectrum with the same frequency as the incident light frequency. The width of this central component gives the lifetime for the entropy fluctuation with wave vector $\mathbf{K}$.

The entire spectrum of the scattered light is the sum of the spectrum due to the sound waves and the entropy fluctuations, i.e.,

$$S(\mathbf{K}, \omega)_{\text{total}} = (s(\mathbf{K}, \omega))_{\substack{\text{entropy} \\ \text{fluctuation}}} + (s(\mathbf{K}, \omega))_{\substack{\text{sound} \\ \text{waves.}}} \quad (21)$$

By evaluating $\langle |\delta s(\mathbf{K}, t)|^2 \rangle / \langle |\delta p(\mathbf{K}, t)|^2 \rangle$ for $\mathbf{K} \sim 0$ Landau and Placzek could show that the intensity in the central component is greater than that in the Brillouin components by the ratio $(c_p - c_v)/c_v$.

As we can see from eqs (13) and (20), the spectrum of the light scattered by a liquid contains a great deal of information of importance in the critical region. In particular we should mention the following points. The width of the Brillouin components provides the sound wave lifetimes as a function of temperature and wavelength. The spectral position gives the sound velocity as a function of wavelength and temperature. Note that since the adiabatic bulk modulus approaches zero as $T \to T_c$ the Brillouin doublets should move in toward the center as one approaches T_c. The intensity of the Brillouin components gets large like the adiabatic compressibility. The central component contains the following information. The width gives the lifetime for decay of the nonpropagating fluctuations of the entropy. The precise shape of the central component gives the time dependence of the correlation function. The intensity gives $(c_p - c_v)$ as a function of the temperature.

Despite the information contained in the spectrum, until very recently, there have been no observations of the spectrum of light scattered near the critical point of a fluid. The reason for this is that the line width of the conventional light sources were so broad that its spectrum spread out well beyond the Brillouin doublets thus preventing resolution of the spectrum near the critical point.

The invention of laser light sources with high intensity and very narrow spectral width has made it possible to study [13, 14] the spectrum of light scattered from a normal liquid with much greater resolution than was previously possible. In view of the information contained in the Brillouin components we undertook a study of the spectrum of light scattered from the fluid sulfur hexafluoride (SF_6) in the vicinity of the critical point $T_c = 45.55$ °C. The critical pressure and density of this fluid of nearly spherical molecules is $p_c = 37.11$ atm and $\rho_c = 0.730$ g/cm^3. We used as a spectrograph a high resolution Fabry-Perot interferometer which could resolve lines spaced as closely at 50 Mc/s. The expected splitting of the Brillouin components was about 500 Mc/s. The light source was a single moded, helium neon laser, whose frequency was constant to within about 10 Mc/s. We searched along the critical isochore over a temperature range $0.1\ °\text{K} < T - T_c < 20\ °\text{K}$ without finding any resolved Brillouin doublets. While this experiment must be repeated with greater sensitivity, we feel that the negative result may indicate that the widths of the Brillouin doublets in this critical region are much broader than the displacement of each line from the central component. In other words, the sound wave lifetimes for sound waves with a frequency of ~ 500 Mc/s is actually shorter than the period of the wave. These considerations are supported by an ω^2 extrapolation of measurements of the low frequency sound wave attenuation in SF_6 near the critical point [15]. As a result of these observations it appears that the most striking feature of the spectrum is the central component which grows in intensity and gets extremely narrow as $T \to T_c$.

Very recently Alpert, Yeh, and Lipworth [16] have reported the observation of the width of the central component in the spectrum of light scattered from a critical mixture of cyclohexane and aniline. They used an elaborate "homodyne spectrometer" [17] which analyzed the beat between the scattered light and part of the incident light.

We report here the first measurements of the width of the central component for light scattered from a pure fluid, SF_6, near its critical point. We use for this study the very simple detection scheme shown in figure 1.

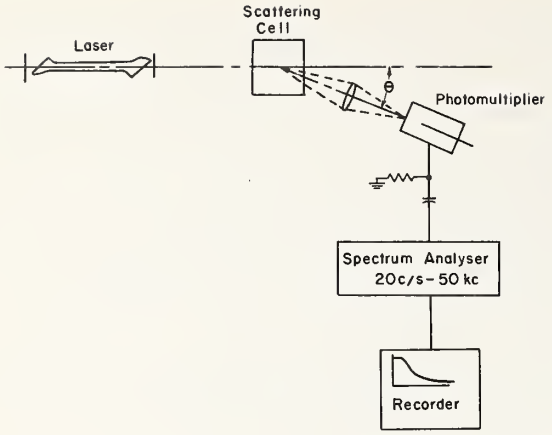

FIGURE 1. *Block diagram of "self beating" or "square law" spectrometer.*
This spectrometer provides the frequency spectrum of the fluctuations in the scattered electromagnetic field.

The light scattered in the angular range between θ and $\theta+\Delta\theta$ is collected by a lens and focused onto the surface of a phototube. The phototube current is proportional to the square of the incident electric field. Thus the fluctuations in the output current of the phototube gives the fluctuations in $E(t)E^*(t)$. This fluctuating current is analyzed into its spectrum using a spectrum analyzer and the spectrum is displayed on a recorder.

The spectrum, as obtained by this "self beat" or square law detection system, gives the spectrum of the fluctuations in $|E(t)|^2$. We may relate this spectrum to the spectrum of $E(t)$ by making use of the fact that if $E(t)$ is a Gaussian random variable, the correlation function for $|E(t)|^2$ is related to the time dependence of $E(t)$ by the equation

$$\langle |E(\mathbf{K}, t+\tau)|^2 |E(\mathbf{K}, t)|^2 \rangle = (\langle |E(\mathbf{K}, t)|^2 \rangle)^2 + \langle E(\mathbf{K}, t+\tau)E(\mathbf{K}, t) \rangle \langle E^*(\mathbf{K}, t+\tau)E^*(\mathbf{K}, t) \rangle + |\langle E(\mathbf{K}, t+\tau)E^*(\mathbf{K}, t) \rangle|^2 \quad (22)$$

where we have explicitly written $\mathbf{K}$ the scattering vector in the expression for the correlation functions to emphasize that these functions depend on the scattering vector. We now use the fact that the time dependence $E(\mathbf{K}, t)$ for the scattering from the entropy fluctuations is given by

$$(E(\mathbf{K}, t))_{\text{entropy}} = -E_0 \left(\frac{\omega_0}{c}\right)^2 \frac{\sin\varphi}{4\pi} \frac{e}{R} e^{i\mathbf{k}\cdot\mathbf{R}} (2\pi)^{3/2} \left(\frac{\partial\epsilon}{\partial s}\right)_p (\delta s(\mathbf{K}, t))_\mu e^{-i\omega_0 t}. \quad (23)$$

With this time dependence of $E(\mathbf{K}, t)$ it follows that the second term on the right-hand side of eq (22) is zero and the correlation function for the output of the phototube is determined entirely by the correlation function of the scattered field viz:

$$R_e(\tau) \equiv \langle E(\mathbf{K}, t+\tau)E^*(\mathbf{K}, t) \rangle_{\text{entropy}} = E_0^2 \left(\frac{\omega_0}{c}\right)^4 \frac{\sin^2\varphi}{(4\pi R)^2} (2\pi)^3 \left(\frac{\partial\epsilon}{\partial s}\right)_p^2 \langle |\delta s(\mathbf{K}, t)|^2 \rangle e^{-i\omega_0\tau} e^{-\Gamma_e(\mathbf{K})\tau} \quad (24)$$

where we have used the Landau-Placzek assumption, eq (19), to obtain the form of the correlation function for the entropy fluctuations. Thus the correlation function for the output of the phototube has the form:

$$\langle |E(\mathbf{K}, t+\tau)|^2 |E(\mathbf{K}, t)|^2 \rangle = (R_e(0))^2 + |R_e(\tau)|^2 \quad (25)$$

and the spectrum of this fluctuation, i.e., the spectrum of the input to the spectrum analyzer has the form $S_2(\mathbf{K}, \omega)$:

$$S_2(\mathbf{K}, \omega) = \frac{1}{2\pi} \int_{-\infty}^{\infty} \langle E(\mathbf{K}, t+\tau) E^*(\mathbf{K}, t) \rangle e^{+i\omega\tau} d\tau \quad (26)$$

$$= R_e^2(0) \left\{ \delta(\omega) + \frac{1}{\pi} \frac{2\Gamma_e(\mathbf{K})}{(\omega^2 + (2\Gamma_e(\mathbf{K}))^2)} \right\}^2. \quad (27)$$

The first term on the right side of eq (27) corresponds to the d-c photocurrent. This d-c current does not enter the spectrum analyzer as it is removed with an RC blocking filter as shown in figure 1. Thus the power spectrum of the current fluctuations entering the spectrum analyzer is given by the second term on the right side of eq (27). The spectrum analyzer uses a linear full wave rectifier as its detector element. As a result,

it can be shown [8] that the output current $I(\omega)$ as a function of frequency ω is directly proportional to the square root of the input power spectrum. $I(\omega)$ is displayed on the recorder, and from the discussion above we see that $I(\omega)$ is given by:

$$I(\omega)=(\text{const})\,\frac{R_e(0)}{\pi^{1/2}}\left(\frac{2\Gamma_e(\mathbf{K})}{(\omega^2+(2\Gamma_e(\mathbf{K}))^2)}\right)^{1/2}. \quad (28)$$

We can therefore use eq (28) to analyze the shape of the $I(\omega)$ spectrum and thereby determine the decay rates of the entropy fluctuations $\Gamma_e(\mathbf{K})$. Of course, if the output spectrum $I(\omega)$ does not have the form predicted by the Landau theory we can obtain from $I(\omega)$ information on the form of the time dependence of the correlation function for the entropy fluctuation.

We show in figure 2 the spectrum analyzer output $I(\omega)$ as observed at $T=45.78$ °C, about 0.2 °C from the critical point, and near the critical isochore. The scattering angle was about 8.7°. We estimate that the half width at half height of this spectrum is about 350 c/s. This measurement is remarkable in that it shows that lasers now make it possible to detect shifts in the frequency of the scattered light as small as a few hundred cycles per second out of the incident light frequency of 5×10^{14} c/s. In figure 3 we show similar spectra taken at fixed temperature for different scattering angles to check the K^2 dependence of the half width of the line. The results of this investigation are shown in figure 4 for two different temperatures. Within the error limits imposed by these early measurements we see that the width of the scattered spectral line is indeed proportional to K^2. In figure 5 we show the temperature dependence of the half width for fixed scattering angle in order to examine the temperature dependence of λ/c_p^*.

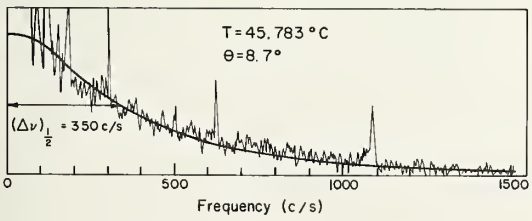

FIGURE 2. *The spectral distribution of the light scattered by the nonpropagating entropy fluctuations in* SF_6 *very near the critical point.*

Note that the width of this spectral distribution is only a few hundred cycles per second. The incident light frequency is 5×10^{14} c/s. The resolving power of the spectrometer ($\nu/\Delta\nu$) is about 1×10^{12}.

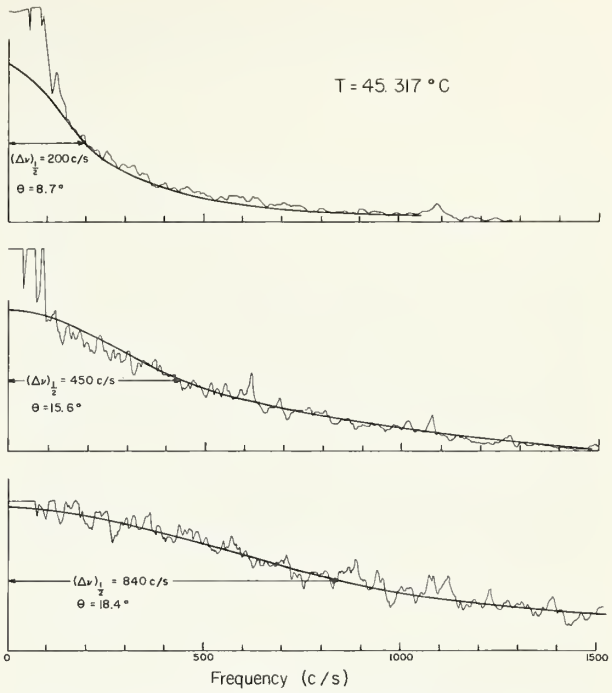

FIGURE 3. *The spectral distribution of light scattered from* SF_6 *near its critical point for different scattering angles.*

Observe the broadening at the larger scattering angles.

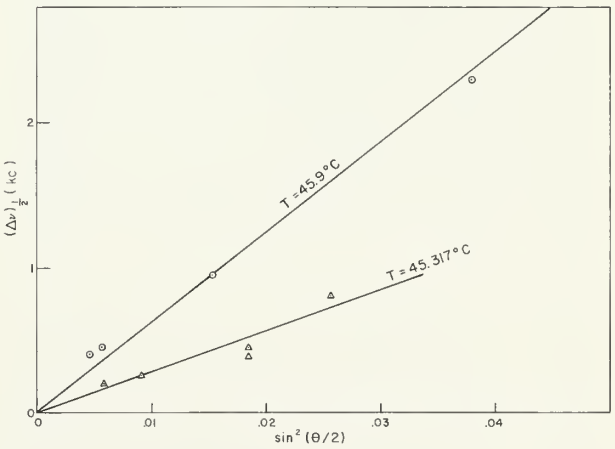

FIGURE 4. *The dependence of the half width of the scattered spectrum on the square of the scattering vector* $K \equiv k_0 \sin\theta/2$ *for two different temperatures near the critical point.*

Finally we may inquire as to whether the value of $\Gamma_e(\mathbf{K})$ as deduced from $I(\omega)$ and eq (28) is in agreement with the formula of Landau. Along with J. V. Sengers [18] we have estimated the temperature dependence of λ and c_p^* for SF_6 at the critical isochore and thus obtain a theoretical estimate for the temperature dependence of $\Gamma_e(\mathbf{K})$. This esti-

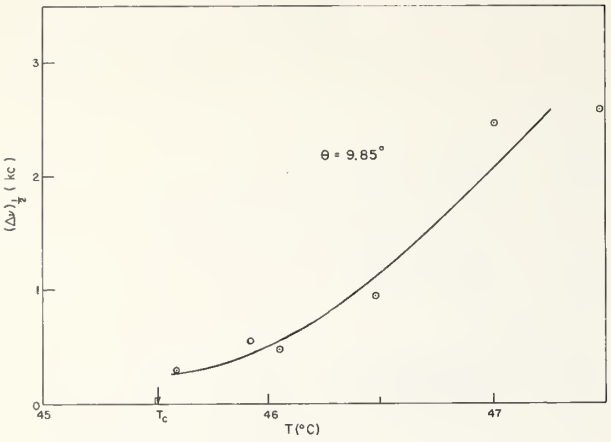

FIGURE 5. *The temperature dependence of the half width of the scattered spectrum of light from SF_6 for a density near the critical isochore.*

The critical point is at 45.55 °C.

mate is in a good qualitative agreement with the present observations [19].

In conclusion we wish to stress the following points. First, that the present experiments demonstrate that it is possible to study the spectral distribution of the light scattered from entropy fluctuations near the critical point. These studies can be carried out using a very simple "self beating" or "square law" spectrometer whose operation has been described. The spectrometer, which uses a laser beam as a light source, permits a measurement of the spectral distribution in the scattered light which is as narrow as a few tens or hundreds of cycles per seconds out of the incident light frequency of 5×10^{14} c/s. By studying the detailed shape of the spectrum and its temperature dependence we can obtain information on the time and temperature dependence of the correlation function for the entropy fluctuations in the critical region. Finally, we have presented the first measurements of these fluctuations in a pure fluid (SF_6) near its critical point.

References

[1] M. Von Smoluchowski. Ann. d. Phys. **25**, 205 (1908).
[2] A. Einstein. Ann. d. Physik **38**, 1275 (1910).
[3] L. F. Ornstein and F. Zernike. Proc. Acad. Sci. Amsterdam **17**, 793 (1914–1915).
[4] L. Landau and E. M. Lifshitz. Electrodynamics of Continuous Media. pp. 393ff. (Addison Wesley, Reading, Massachusetts, 1960).
[5] M. E. Fisher. J. Math. Phys. **5**, 944 (1964).
[6] L. Brillouin, Comptes Rendus de l'Academie des Sciences **158**, 1331 (1914).
[7] L. Brillouin. Ann. de Physique **17**, 88 (1922).
[8] W. B. Davenport and W. Root. An Introduction to the Theory of Random Signals and Noise (McGraw-Hill Book Co., New York, N.Y., 1958).
[9] E. Gross. Nature **126**, 201, 400, 603 (1930).
[10] E. Gross. Zeit. f. Phys. **63**, 685 (1930).
[11] I. Fabelinskii. Usp. Fiz. Nauk **63**, 355 (1957).
[12] L. Landau and G. Placzek. Physik Z. Sowjetunion **5**, 172 (1934).
[13] G. Benedek, J. B. Lastovka, K. Fritsch, and T. Greytak. J.O.S.A. **54**, 1284 (1964).
[14] R. Y. Chiao and B. P. Stoichieff, J.O.S.A. **54**, 1286 (1964).
[15] W. G. Schneider, Can. J. Chem. **29**, 243 (1951).
[16] S. S. Alpert, Y. Yeh, and E. Lipworth, Phys. Rev. Letters **14**, 486 (1965).
[17] H. Z. Cummins, N. Knable and Y. Yeh, Phys. Rev. Letters **12**, 150 (1964).
[18] J. V. Sengers, private communication.
[19] N. C. Ford and G. B. Benedek, Phys. Rev. Letters **15**, 649 (1965).

Time-Dependent Concentration Fluctuations Near the Critical Temperature*

S. S. Alpert

Columbia University, New York, N.Y.

The title of this talk which is printed in the conference program as "Time-Dependent Density Fluctuations Near the Critical Temperature" is incorrect and should be altered to read "Time-Dependent Concentration Fluctuations Near the Critical Temperature." This is readily apparent when one considers the differential element of scattered energy given by the expression

$$\frac{dE_{sc}}{I_0} \propto \frac{d\Omega}{\lambda^4}\left[\left(\frac{\partial\epsilon}{\partial\rho}\right)^2\overline{\delta\rho^2}+\left(\frac{\partial\epsilon}{\partial c}\right)^2\overline{\delta c^2}\right]B(\theta,\lambda).$$

Here dE_{sc} is the differential element of scattered energy which is normalized to the incident intensity I_0: $d\Omega$ is the element of solid angle into which the light of wavelength λ is scattered. The factor $B(\theta, \lambda)$ gives the dependence of the scattered energy on the scattering angle θ and on the wavelength λ. It is seen that the scattered intensity depends on the change of the dielectric constant ϵ of the medium with respect to both the density ρ and the concentration c. For a binary system such as aniline-cyclohexane, which is the system studied, there is reason to believe that the mean square fluctuation of concentration $\overline{\delta c^2}$ becomes very large as the critical temperature is approached. This point will be discussed later in this talk. However, since the compressibility of the binary system is nonsingular in the region of the critical temperature, the mean square of the density fluctuation remains finite and small; hence it is reasonable to assume that it is the concentration fluctuations which are responsible for the light scattered from binary systems near the critical temperature.

In the preceding talk, Professor Benedek clearly outlined the nature of the light scattered from a pure liquid system. The scattered light from a binary mixture is a triplet where the outer two components, the Brillouin doublet [1], result from thermally excited acoustic modes and where the central unshifted component [2] results from fluctuations of concentration and temperature at constant pressure. It is this central unshifted line which my colleagues, Dr. Y. Yeh and Dr. E. Lipworth, and myself have experimentally observed, using a laser homodyne spectrometer of high resolving power.

Before discussing the results of our experiment, I should like to digress for a few minutes and to sketch for you the general functioning of the laser homodyne spectrometer developed at Columbia University by Cummins, Knable, and Yeh [3] in the early part of 1964.

The laser homodyne spectrometer [3] has a resolving power of one part in 10^{14} and is capable of scanning the spectral profile of the central component of the scattered triplet. The essential functional components of this spectrometer are the laser light source, a divided optical path, the externally driven Bragg tanks, and the detection apparatus and associated data-processing electronic equipment. (See figs. 1 and 2). These functional components are presented in outlined form below:

1. *Laser source.* As previously noted in this report it was desired to observe the spectral profile of the central component of the scattered light triplet. This profile was expected to be on the order of a few hundred cycles per second. Clearly the spectrometer light source must be inherently more narrow than the desired spectrum. The only available light source fulfilling this requirement at the present time is the He-Ne laser. Jaseja [4] has shown that under highly controlled conditions and for short times, the line width of a single mode of the He-Ne laser is less than 1 c/s. This was the reason underlying the use of a He-Ne laser capable of a power output of about 15 mW with an intermodular spacing of 60 Mc/s.

2. *Divided optical path.* Although the frequency output of the He-Ne laser is instantaneously quite narrow, over any reasonable time interval of observation (≈ 1 sec) the line width is broadened to the bandpass of the optical cavity which is about 10 kc/s. This broadening results from thermal vibration effects on the mirrors and also any microphonic effects present. It thus becomes

*This work was supported in part by the Army Research Office—Durham under Contract DA-31-124-ARO-D-296, and in part by the Joint Services Electronics Program under Contract DA-28-043 AMC-00099 (E).

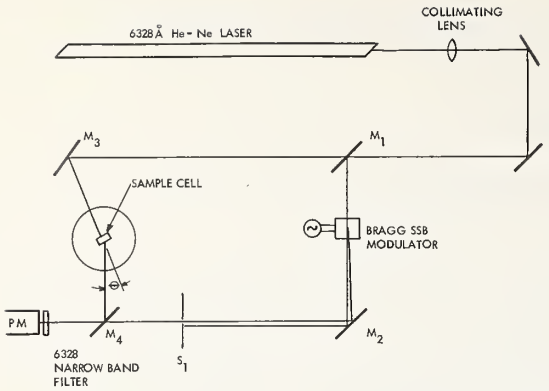

FIGURE 1. *Schematic arrangement of optical components of laser homodyne spectrometer.*

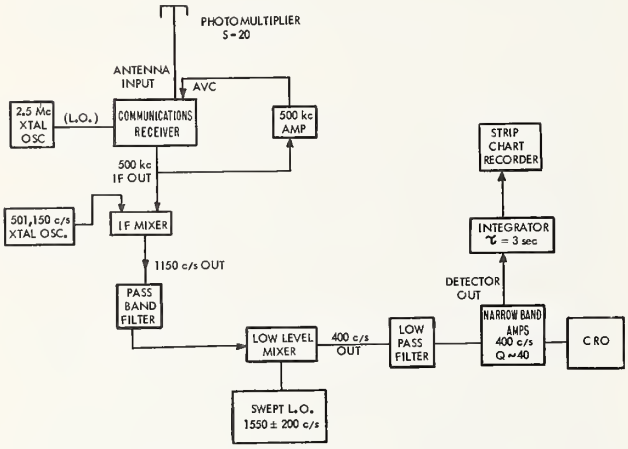

FIGURE 2. *Block diagram of electronic equipment used in laser homodyne spectrometer.*

essential to avoid this cavity broadening by a "beating" or heterodyning technique. This is accomplished by dividing the laser light into two separate optical beams. One beam falls directly on the photocathode detector, together with light from the other beam which is first scattered off to sample being studied.

3. *Bragg tanks.* The heterodyning technique suggested under the previous heading is difficult to detect because the resulting "beats" occur at ultraviolet frequencies and at dc. For practical detection a "beat" should occur at radio frequencies. The "beat" can be made to occur at radio frequencies by shifting the frequency of each arm of the optical path by known amounts. This was done by the use of two Bragg tanks [5] filled with water and acoustically driven with quartz transducers at 18 Mc/s and at 30 Mc/s.

4. *Detector and data handling electronics.* The 12-Mc/s "beat" falls on an S–20 photocathode and appears in the photomultiplier output current (fig. 2). The photomultiplier output which contains the spectral-profile information centered about a frequency of 12 Mc/s is fed into a radio receiver tuned to that frequency. The resulting i.f. signal is further "mixed" in two sequential stages so that the resulting signal is greatly reduced in frequency. The last mixer is provided with a mechanically scanned local oscillator input. The output of the final mixing stage is passed through a narrow-band amplifier centered at a frequency of 400 c/s. Since the narrow-band amplifier will only amplify in this range and since the local oscillator input to the final mixer is swept, the final output will yield a frequency profile of the original 12-Mc/s beat. The instrumental bandwidth of such a system was 13 c/s.

The system studied in the present experiment was a cyclohexane-aniline mixture, 53 percent cyclohexane and 47 percent aniline by weight. The mixture was contained in a cylindrical glass cell in a constant-temperature enclosure, the temperature of which could be adjusted and held constant to about 1×10^{-3} °C over extended periods of time.

Some characteristic spectra are shown in figure 3. These are typical of the spectra observed with the laser homodyne spectrometer; I might add that the word "typical" is not used here in the sense that Miss America is the "typical" American girl, but to indicate the ordinary performance of our spectrometer. The spectra shown in figure 3 are normalized to give the same magnitude on our final recorder. In actuality the signals become less intense

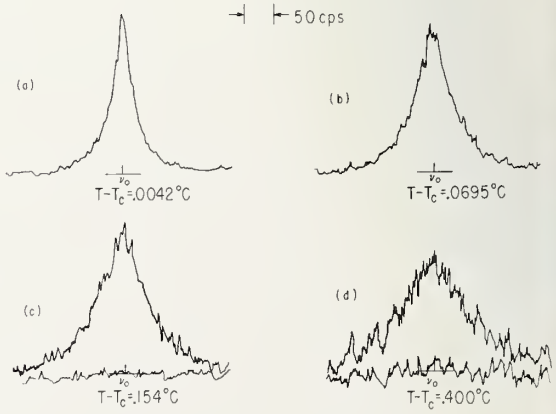

FIGURE 3. *Characteristic spectra observed at a scattering angle of 20.5° and at varying temperatures.*
Signals are normalized to give recorder traces of approximately the same magnitude.

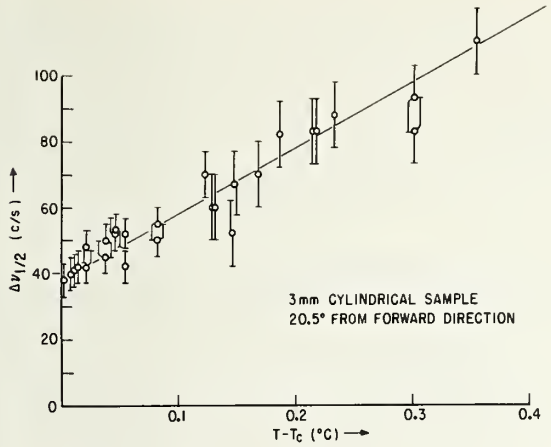

FIGURE 4. *The halfwidth at half-intensity versus* $T-T_c$. Included in observed halfwidths is an instrumental error of 13 c/s which can be directly subtracted out. Note that at $T=T_c$ the extrapolated halfwidth does not vanish.

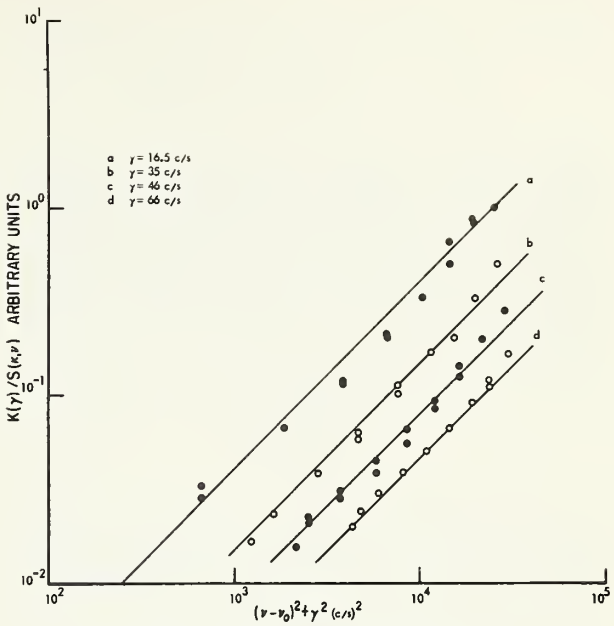

FIGURE 5. *Log-Log plot for Lorentzian fit.*

as the temperature above critical is increased, as can be deduced from figure 3, by the increasing presence of noise superposed on the signal. As the sample approached its critical temperature from above, a definite narrowing of the width of the scattered profile was observed as shown in figure 4 where the scattering angle was 20.5° from the forward direction; T_c was defined as the temperature at which a meniscus was first seen to appear visually. It is to be noted that at $T=T_c$, the halfwidth of the scattered spectrum is 38 c/s. This includes a 13-c/s instrumental line width which can be directly subtracted out if the scattered spectrum is Lorentzian, which seems to be the case. Thus for $T=T_c$, a half width of 25 c/s was observed for the corrected spectrum.

A question to be answered is what is the line shape of the observed spectra. At first glance it would seem (see fig. 3) that the lines are Lorentzian. The curves do, indeed, match an assumption of being Lorentzian as is shown in figure 5. Such an assumption would predict a concentration fluctuation decay of the form $\sqrt{\delta c^2}\, e^{-t/\tau}$ which would correspond to a $\tau=0.013$ sec for our sample at the critical temperature.

The scattering angle θ was varied between 20° and 40° and the width at half intensity was observed. The results are shown in figure 6 where it is seen that $\Delta\nu_{1/2} \propto \sin^2\frac{\theta}{2}$. The intercept corresponding to $\theta=0$ represents the instrumental line width which can be directly subtracted out.

Since it is assumed that

$$S(K,\nu)=\frac{K(\gamma)}{(\nu-\nu_0)^2+\gamma^2},$$

the log of $\frac{K(\gamma)}{S(K,\nu)}$ is plotted versus log $(\nu-\nu_0)^2+\gamma^2$. Here γ is the halfwidth at half-intensity.

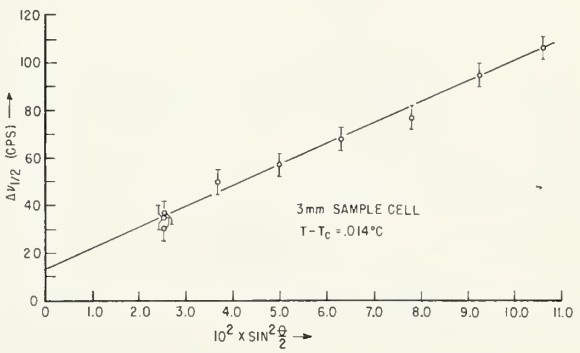

FIGURE 6. *Plot of* $\Delta\nu$ *versus* $\sin^2(\theta/2)$ *for a 3-mm sample cell at* $T-T_c=0.014$ *°C.*

To indicate that our overall results are reasonable, I would like to invoke the following argument based on published work of Landau and Lifshitz [6]. From hydrodynamical considerations these authors deduce the following coupled equations for a binary system:

$$\frac{\partial}{\partial t}\delta c = D\left(\nabla^2\delta c+\frac{k_T}{T}\nabla^2\delta T\right) \qquad (1)$$

and

$$\frac{\partial}{\partial t}\delta T-\frac{k_T}{c_p}\left(\frac{\partial \mu}{\partial c}\right)_{p,T}\frac{\partial \delta c}{\partial t}=\chi\nabla^2\delta T$$

where D is the diffusion constant k_T is the thermal-diffusion ratio, χ is the thermal diffusivity, and μ is a suitably defined chemical potential. The other symbols have been previously defined. Landau and Lifshitz [7] have also shown that for a binary mixture,

$$\overline{\delta c^2}=\frac{kT}{N\left(\frac{\partial \mu}{\partial c}\right)_{p,T}} \tag{2}$$

As the critical temperature is approached, the chemical potential and its first and second derivatives with respect to concentration vanish. Thus near the critical temperature $\overline{\delta c^2}$ goes to a large value and since δT remains nonsingular $\overline{\delta c^2} \gg \overline{\delta T^2}$. Under these simplifying assumptions we derive from eqs (1) the single diffusive expression

$$\frac{\partial}{\partial t}\delta c=D\nabla^2\,\delta c.$$

The solution of this equation is

$$\delta c=\frac{1}{(4\pi Dt)^{3/2}}\exp\left[-\frac{r^2}{4Dt}\right]$$

which has a Fourier transform of the form

$$\Gamma(K,\,\omega)=\frac{2DK^2}{(DK^2)^2+\omega^2} \tag{3}$$

where K is $\frac{4\pi}{\lambda}\sin\theta/2$. Hence we would, indeed, expect a Lorentzian line shape at a fixed scattering angle and also a line width dependence on $\sin^2\theta/2$ at fixed temperature.

Dr. Raymond Mountain [8] of the National Bu reau of Standards has solved the eqs (1) using Fourier and Laplace transform techniques and gets the same results for the line shape in expression (3).

In closing I would like to point out that in the past, researchers have only been able to measure scattered intensities. We now have available techniques as demonstrated in this paper of measuring spectral profiles. Hopefully, as our techniques become more refined and our results more quantitative, studies of the spectral profile of scattered light such as we have performed can be used as a new experimental basis with which to construct theoretical models of the nature of liquids.

References

[1] L. Brillouin, Ann. Phys. (Paris) **17**, 88 (1922).
[2] E. Gross, Nature **126**, 201 (1930).
[3] H. F. Cummins, N. Knable, and Y. Yeh, Phys. Rev. Letters **12**, 150 (1964).
[4] T. S. Jaseja, A. Javan, and C. H. Townes, Phys. Rev. Letters **10**, 165 (1963).
[5] H. F. Cummins and N. Knable, Proc. IEEE **51**, 1246 (1963).
[6] L. D. Landau and E. M. Lifshitz, Fluid Mechanics (Addison-Wesley Publishing Co., Inc., Reading, Mass., 1959).
[7] L. D. Landau and E. M. Lifshitz, Statistical Physics (Addison-Wesley Publishing Co., Inc., Reading, Mass., 1958).
[8] R. Mountain, J. Res. NBS **69A** (Phys. and Chem.), No. 6, 523 (1965).

Discussion

B. Jacrot: I would like to comment on Dr. Marshall's explanation of the inelastic neutron scattering by assuming that the spin waves persist even close to the Curie point. Indeed the line width which I observed experimentally is in good agreement with the contribution estimated from spin waves as shown by Dr. Marshall. At this time I think it is just a coincidence, but the explanation may well be correct.

E. Callen: I am uncomfortable with the application of the beautiful analysis of Dr. Marshall to metals, because I see no evidence of a large line width mechanism, the complex susceptibility arising from excitation of electrons among Landau states.

W. Marshall: I certainly agree with you, that we must be cautious in applying the theory to metals, which, of course, is the only thing I have done. I would answer your remark in the following way. What I am really trying to say is that as soon as you stop damping the spin waves a diffusive mode will appear on the imaginary axis. There are various ways in which you could describe this. You may prefer to describe it in terms of spin waves and the damping of spin waves. That is perfectly satisfactory. But we have also to look, in this particular formulation, at what this pole is on the imaginary axis, and on the effect of this diffusive motion. In the case of a liquid we know that the sound waves are damped by thermal conductivity and viscosity. Similarly we can explain our results in terms of the damping of spin waves. But as soon as we put in the thermal conductivity, a third pole appears in the expression on the imaginary axis. And that pole becomes largest in the proximity of the critical temperature.

H. B. Callen: A simple analogy may make this diffusive mode a little less mysterious. The excitations of a noninteracting Fermi gas at very low temperatures are oscillations of the Fermi surface which are coherent excitations of the whole system which occur at high frequency. I think they are the analog of the spin waves. When the temperature becomes large enough so that the relaxation term becomes appreciable these high frequency excitations disappear, being replaced by one-particle excitations (at very low frequencies). These one-particle excitations seem to correspond to the diffusive mode. In the transition region the one-particle and the collective mode may coexist, although the collective oscillations of the Fermi surface are then damped.

R. Nathans presented measurements of neutron scattering in antiferromagnetic potassium manganese fluoride [1].

B. Jacrot: In connection with the work of Dr. Nathans, I want to remark that the inelasticity for an antiferromagnetic system like manganese fluoride should be ten or twelve times larger than for iron due to the absence of kinematical slowing down. This has been confirmed qualitatively by some unpublished results obtained a few years ago at Saclay. New experiments are now in progress.

R. Nathans: Well, that may be possible. We have only seen the data of Turberfield in manganese fluoride, which indicate a small inelasticity in the critical region.

M. S. Green: Dr. Passell, why did you expect to observe elastic scattering before you started the experiment?

L. Passell: Because the parameter Λ which describes the time dependence of the spin fluctuations should be inversely proportional to the susceptibility as indicated by Dr. Marshall. This was the argument which Van Hove used in his original formulation of the theory. On this basis we assumed that we were going to have essentially quasi-elastic scattering at the ordering temperature.

M. S. Green: Did not Van Hove predict a finite inelastic scattering for finite k-values?

L. Passell: Yes, that is right. But that would give only a small correction.

W. Marshall: May I comment on this point? First, if you use what I call the conventional theory and which Van Hove gave, then of course the scattering is inelastic. And this gives you the difference between say a neutron experiment and a N.M.R. experiment. However, when you ask theoretically how inelastic the scattering is, you discover that so far as neutrons are concerned the spectral distribution looks like a sharp δ-function. So if that were true, we could say that for experimental purposes the scattering is as elastic as we could possibly want it to be.

Secondly, Dr. Passell was much more polite in describing the situation than I would have been. We knew about Jacrot's results and that he had found the scattering to be inelastic, but we did not believe it could be true. So we felt that there probably was some experimental flaw in these experiments; I now apologize to Dr. Jacrot for thinking that to be the case.

I also like to make another point. It is true, of course, that we would expect proportionally very much greater inelasticity in an antiferromagnet than in a ferromagnet, simply because we do not have the kinematic narrowing. However, we also have the fact that the Curie temperature of iron is 1042 °K compared to 80 °K for manganese fluoride, so that the higher exchanges energies in iron compensate the difference to a certain extent.

J. Villain: As a theoretician, I would be very interested in the temperature dependence of the inelasticity parameter Λ. In fact, de Gennes [2] has predicted a thermodynamic slowing down which must be added to the kinematic slowing down. It is predicted that the line width close to the critical temperature is smaller than at the temperatures higher than the Curie temperature. I think that the original treatment of de Gennes and myself [2] is not correct and that this thermodynamic slowing down is perhaps weaker, but it must exist. Our present theory [3] to account for this effect is in good argeement with the results of Jacrot for the temperature dependence of Λ. However, the results of Jacrot do not allow a detailed comparison with the theory. I think it would be very interesting to go also to higher temperatures. Perhaps, it is necessary to work with a higher precision for this purpose.

L. Passell: May I make a brief comment on that? When we tried to do an energy analysis, we ran out of intensity very rapidly as we went up in temperature. With the facilities we had in Denmark, we could never hope to get much at temperatures higher than 30 °K above the Curie temperature. We do not have a sufficient intensity for that purpose. On the other hand, I believe that in Saclay you do have the possibility to cover a larger temperature range, because you have a cold neutron source. We could not see any difference between the value of the parameter Λ at 2 °K above the Curie temperature and that at 18 °K above the Curie temperature. It may be that there is a small change of Λ with temperature, which begins to occur at higher temperatures. Would you care to comment on this, Dr. Jacrot?

B. Jacrot: I agree that it is extremely difficult to observe any effect of the temperature. In the curve which we first published, we showed a temperature effect for Λ. However, that were just crude data and after a careful analysis with the computer, it turned out that Λ is practically the same at the Curie point and at 30 °K above the Curie point. This means that we have to carry out experiments with much higher accuracy. It is very doubtful that this is possible. In order to observe the variation of Λ with temperature it is better to do the experiments on nickel where the effect is bigger.

P. Debye: In connection with the paper of Dr. Ford and Dr. Benedek, I want to remark that already 30 years ago the spectral distribution of light scattered in liquids was photographed by Ramm using an echelon [4]. I think this work should not be forgotten in any historical review.

P. Debye gave also theoretical argumenis as to why the line width of light scattered by a binary mixture in the vicinity of the critical point, as observed by Dr. Alpert and coworkers, should

a. increase proportional to $s^2 = 4 \sin^2(\theta/2)$ with increasing scattering angle θ;

b. increase proportional to the temperature distance $T - T_c$.

The substance of this discussion remark has been published in Phys. Rev. Letters **14**, 483 (1965).

W. Marshall: I wonder why the line width observed by Dr. Alpert does not go to zero when the temperature approaches the critical temperature.

S. S. Alpert: There is a possibility that we were not exactly at the critical point.

W. Marshall: That is one suggestion which I was going to make. However, I want to bring up another suggestion. We are used to the assumption that the scattering from a particular molecule can be taken as a constant. We associate with each molecule a given scattering power which we allow to vary with angle. However, suppose that the scattering power of each molecule is slightly dependent on its neighboring molecules. Then the scattering power would depend on short range order. You may then get a term which is in fact not divergent. This might be something that would have to be taken into account in these very delicate experiments. It is really a question; I do not know whether it is sensible or whether the orders of magnitude are right.

Commenting on the neutron scattering from β-brass. I would like to congratulate Dr. Dietrich and Dr. Als-Nielsen on two facts:

(1) They did some very beautiful experiments which other people have attempted and have failed to do.

(2) They were very good politicians because on the last day of their experiments, they managed to destroy their crystal, which was probably the only good crystal of β-brass in the world. We may have to wait a long time before we get any better results.

I would like to make also some comments which are stimulated by Dr. Benedek's talk. He commented and in my talk I referred to the fact that as soon as the sound waves get damped a diffusive type mode appears. Some of you may think that sound waves are not only damped by the thermal conductivity but also by the viscosity, which, of course, is true. You may then ask why the viscosity did not appear in the formula for the line width of the central line. The reason for that is that the viscosity and thermal conductivity appear quite differently in the hydrodynamic equations. Indeed there is another mode which appears as soon as you introduce damping through viscosity, but it is a mode which stays on the imaginary axis and never comes down to the origin even at the critical point. Therefore, it does not produce any appreciable effects at the kind of wave vectors we are talking about. If we indeed go to higher k-values in these systems which seems possible by pushing the laser technique further, and certainly when we use neutrons where we have higher k-values, it is very important to modify the discussion of the fluid to include rigidity. At the higher frequencies the liquid is just as rigid as the solid. In Egelstaff's neutron experiments on liquids already you can see that you must include rigidity to get the right results. Thus the rigidity of the liquid will affect the shape of the curve for the higher k-values. Whether the laser will reach that region, has to be found out in the future.

References

[1] R. Nathans, M. Cooper and A. Arrott, Proc. Conference on Magnetism, San Francisco, 1965, to be published.

[2] P. G. de Gennes and J. Villain, J. Phys. Chem. Solids **13**, 10 (1960).

[3] J. Villain, J. Phys. **26**, 405 (1965).

[4] W. Ramm, Physik Z. **35**, 111, 756 (1943); E. H. L. Meyer and W. Ramm, Physik Z. **33**, 270 (1933).

TRANSPORT AND RELAXATION PHENOMENA

Chairman: R. W. Zwanzig

209-493 O-66—12

Behavior of Viscosity and Thermal Conductivity of Fluids Near the Critical Point

J. V. Sengers

Institute for Basic Standards, National Bureau of Standards, Washington, D.C.

1. Introduction

This paper reviews the experimental information on the behavior of the viscosity and thermal conductivity of fluids near the critical point. Section 2 presents some general remarks on experimental complications associated with the measurement of these properties in the critical region. Experimental work on the viscosity of one component fluids near the liquid-vapor critical point is reviewed in section 3. The thermal conductivity of one component fluids is considered in section 4. The behavior of the viscosity and thermal conductivity in binary liquid mixtures near the critical mixing point is discussed in sections 5 and 6, respectively. Section 7 is a summary of conclusions based on these experimental results.

2. Some General Remarks

In addition to the usual difficulties associated with experiments in the critical region, measurements of the transport coefficients are hampered by the fact that they are nonequilibrium quantities. Most accurate measurements have been carried out by introducing macroscopic gradients into the system. In order to obtain the transport coefficients the hydrodynamic equations must be solved under certain imposed boundary conditions. Exact solutions of these equations are known only for fluids with constant properties in idealized geometrical situations. However, in the critical region a number of physical properties like local density and specific heat vary appreciably with position as a result of the gradients. This complicates the analysis considerably. Close to the critical point even the validity of the Navier-Stokes equations [41] and of the linear laws has been questioned [38, 42, 59].

If in a fluid near the liquid-vapor critical point the temperature is not uniform, gravity can easily generate convection currents and convective heat flow which must be distinguished from the irreversible fluxes associated with the thermodynamic forces by the linear laws. This is the most serious difficulty encountered in measuring the thermal conductivity and will be further discussed in section 4. As is well known, equilibrium or a steady state is approached very slowly by a physical system near a critical point. Consequently, some authors have observed hysteresis effects in their experimental observations of the viscosity [2, 6, 50].

A prerequisite for the study of the behavior of any physical property in the critical region is a knowledge of the values of the appropriate thermodynamic variables at which the property is measured. Near the liquid-vapor critical point the temperature and density and near the critical mixing point of a binary liquid mixture the temperature and concentration should be known. If a P-V-T relationship is known, one can calculate the density from the measured pressure and temperature. Close to the critical point, where the isotherms become very flat, this procedure becomes inaccurate. This inaccuracy is greatly increased by uncertainties in the absolute value of the temperatures at which either the transport coefficients or the isotherm data were measured. Uncertainties in the temperature also hamper a comparison with other properties near the critical point. Such a comparison for a binary liquid mixture is complicated by the fact that the critical parameters are very sensitive to impurities.

If one measures the transport coefficients as a function of pressure and temperature, care should be taken to work at small enough pressure and temperature intervals as otherwise the whole critical region is easily overlooked. In experimental work on transport coefficients this has led to considerable confusion, which will be discussed further in section 4 in connection with thermal conductivity measurements. It is equally important for the study of any other property near the liquid-vapor critical point.

Another procedure consists in following an isochoric method where the temperature is varied

while the total amount of gas is kept constant. However, this method also has its pitfalls. First, if one lowers the temperature at constant density, phase transition occurs at a certain temperature which is equal to the critical temperature at the critical density. Below this transition temperature one measures either in the vapor or in the liquid, depending on the experimental arrangement. As a consequence the density, at which the properties under consideration actually are measured, does change rapidly as a function of temperature, although the density averaged over vapor and liquid phase is kept constant. The temperature at which this transition occurs should be determined accurately. Moreover, even above this temperature a large density gradient is developed close to the critical temperature so that the local density at a certain position in the vessel is still not independent of the temperature. Ultimately, close to the liquid-vapor critical point a knowledge of the local value of the density is required.

The influence of critical phenomena is not restricted to the immediate vicinity of the critical point. For instance, an anomaly in the specific heat can be detected at temperatures considerably higher than the critical temperature. In this paper the qualitative properties of viscosity and thermal conductivity regarding the existence of similar anomalies in the critical region will be discussed. However, the precise mathematical character of such anomalies can only be obtained from measurements very close to the critical point. In view of the difficulties mentioned above an analysis of the latter kind is not yet possible for the transport coefficients.

3. The Viscosity of a One Component Fluid Near the Liquid-Vapor Critical Point

Accurate measurements of the viscosity of compressed gases have been mainly carried out either by a transpiration method or by the oscillating disk method. In the first method the gas is caused to flow through a capillary and the viscosity is obtained from the flow rate. In the latter method the damping of an oscillating disk due to the viscosity of the surrounding medium is determined. Both methods have been used to measure the viscosity in the critical region. Close to the critical point the oscillating disk method has the advantage that it allows the measurement of the viscosity at a certain horizontal level in the fluid and consequently, in principle, at a certain local density. In the capillary flow method the density varies along the capillary.

An example of the "normal" behavior of the viscosity outside the critical region is shown in figure 1; the viscosity coefficient of argon [4, 7] at three temperatures, high relative to the critical temperature ($t_c = -122.3$ °C), as a function of density. One amagat unit of density is the density at 0 °C and 1 atm.[1] At a given temperature the viscosity coefficient increases monotonically with the density; $(\partial\eta/\partial\rho)_T$ and $(\partial^2\eta/\partial\rho^2)_T$ are both positive. The temperature derivative $(\partial\eta/\partial T)_\rho$ is positive up to a density well beyond the critical. At very high densities $(\partial\eta/\partial T)_\rho$ becomes negative [3, 8], but this is not relevant for our present discussion. Sometimes the excess viscosity $\eta - \eta_0$, where η_0 is the viscosity coefficient in the dilute state at the given temperature, is considered to be only a function of the density. This is, however, not true in general.

Most measurements of the viscosity and thermal conductivity in the critical region have been carried out for carbon dioxide because of its easily accessible critical temperature.[2] The discussion will therefore be mainly based on the phenomena observed for CO_2. The few investigations on other substances sustain the conclusions obtained for CO_2

The experimental investigation of the viscosity of CO_2 in the supercritical region started with the work of WARBURG and VON BABO in 1882 using a capillary flow method [15]. Even that early these authors were aware that knowledge of the density is essential and were careful to determine the density as well as pressure and temperature. They realized that the pressure difference along the capillary should be kept small and applied corrections for the variation of the density along the capillary. In an illuminating discussion of this experimental work M. BRILLOUIN [1] remarked that these corrections are practically canceled by the variation of the viscosity associated with the variation of the density. The data of Warburg and von Babo at 32.6 °C

[1] One amagat unit of density for argon corresponds to 0.0017834 g/cm³.

[2] In this review the values given by Michels et al. [60], are used as critical parameters of CO_2:

$t_c = 31.04$ °C. $P_c = 72.85$ atm. $\rho_c = 0.468$ g/cm³ = 236 amagat.

An alternative possible set of critical values was given by Schmidt and Traube [65]:

$t_c = 31.00$ °C. $P_c = 72.86$ atm. $\rho_c = 0.468$ g/cm³ = 236 amagat.

One amagat unit of density for CO_2 corresponds to 0.0019764 g/cm³.

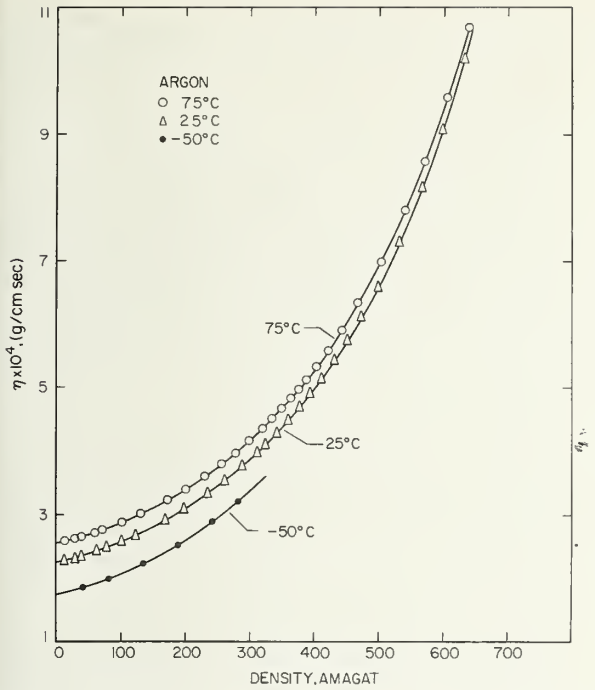

FIGURE 1. *The viscosity of argon as a function of density at temperatures high relative to the critical.*

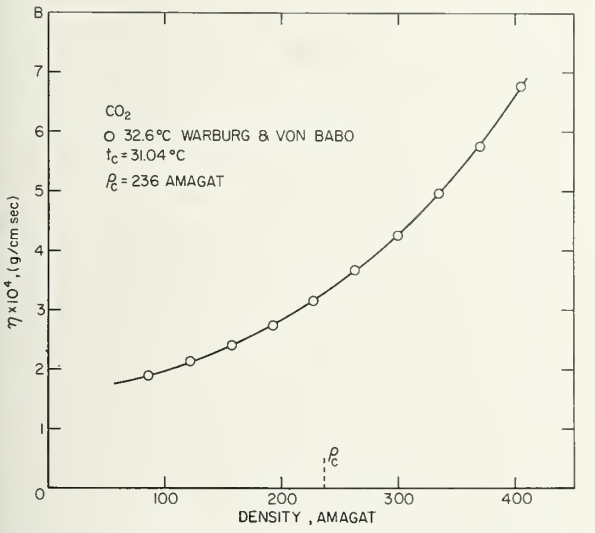

FIGURE 2. *The viscosity of CO_2 at 32.6 °C according to Warburg and von Babo.*

are shown in figure 2. They also measured viscosity isotherms at 35.0 and 40 °C which have not been included in figure 2 since the temperature effect turned out to be small. Since the viscosity isotherms at 35 and 40 °C are nearly parallel to the one at 32.6 °C. the authors conclude that the viscosity does not show any anomaly at supercritical temperatures down to 32.6 °C (about 1.6 °C above the critical temperature). Although the absolute accuracy of these old measurements may be limited, the relative precision is sufficiently good to warrant this conclusion.

After some inconclusive work on the subject by PHILLIPS [11], CLARK [2], and SCHRÖER and BECKER [13], an experimental investigation of the viscosity near the critical point of CO_2 was undertaken by NALDRETT and MAASS [10] using an oscillating disk [6]. The critical region was approached by the isochoric method. One viscosity isotherm at 31.14 °C was also determined. The authors conclude that the viscosity coefficient shows a small anomalous increase close to the critical point. At the critical density this anomalous increase is about 1 percent at 32.0 °C and about 10 percent at 31.1 °C. The results confirm the conclusion of Warburg and von Babo that at 32.6 °C any anomaly is smaller than 0.5 percent. The authors did not consider the influence of the variation of the density as a function of the height in the fluid. A cell with a height of about 13 cm was used, the oscillating disk being located in the lower end of the vessel, and an estimate from the density versus height relationship published in the literature [65, 67] shows that this effect could have caused an apparent increase of the same order as the anomaly observed. Therefore, the conclusion that the viscosity exhibits an anomalous increase near the critical point is not justified.

A pronounced anomalous increase in a wider temperature range and with the viscosity increased by a factor 2 at 31.1 °C was reported by MICHELS, BOTZEN, and SCHUURMAN [8]. Their data were obtained with a capillary flow method which was known to be accurate outside the critical region. As pointed out by the authors, the method is not reliable in the critical region due to the large density gradient in the capillary resulting from the use of a pressure difference of about 0.5 atm. Nevertheless, they conjectured that the anomalous behavior observed was essentially real [8, 9].

In order to resolve the discrepancy between these results, new measurements of the viscosity of CO_2 were carried out by KESTIN, WHITELAW, and ZIEN using an oscillating disk method [5]. They approached the critical region along different isochores as did Naldrett and Maass. Their results show convincingly that any anomalous increase is much smaller than that reported by Michels et al. Close to the critical point they find an anomalous increase of the same order of magnitude as that

reported by Naldrett and Maass. The data obtained by Kestin et al., at 31.1 °C and at 34.1 °C are shown in figure 3a, b as a function of density. For comparison the behavior of the viscosity isotherm at 50 °C is indicated and data obtained by Naldrett and Maass and a few data of Michels et al., outside the critical region are included in the figure.

Recently the viscosity of CO_2 was also measured by BARUA and ROSS with a capillary flow method [12]. By using a horizontal capillary and extrapolating to zero flow rate [4], they were able to avoid the difficulties inherent in the viscometer of Michels et al. The analysis of their experimental data has not yet been completed, yet it seems that their results are in agreement with those of Kestin et al.

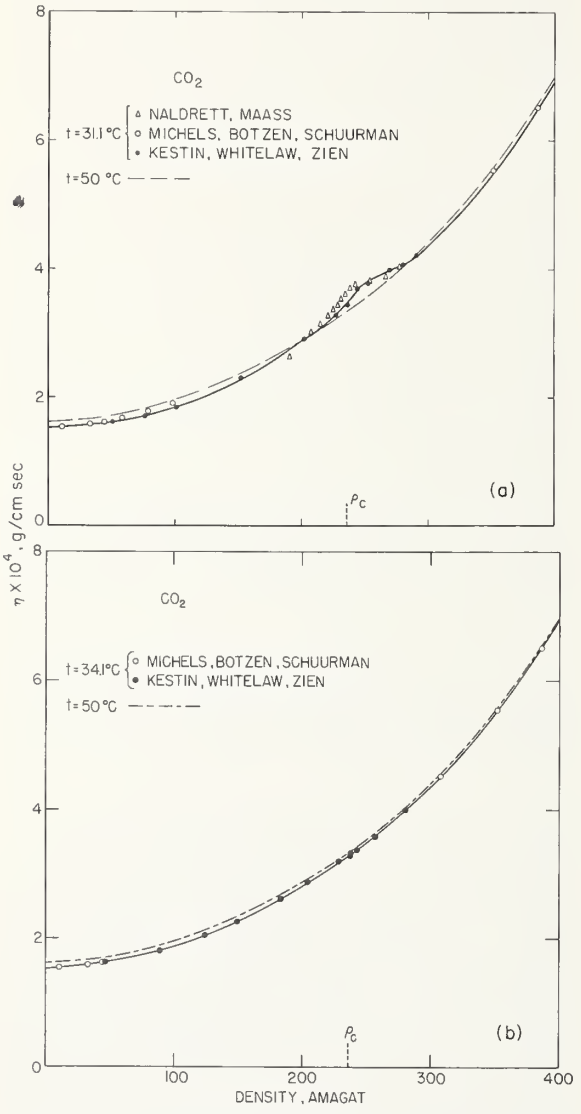

FIGURES 3a, b. *The viscosity of CO_2 as a function of density near the critical temperature.*

Close to the critical temperature they find an increase of 1 to 2 percent on one isotherm, which is of the order of the measuring accuracy in this difficult region.

From the experimental work described, we can draw the following two conclusions.

1. Measurements of the viscosity of CO_2 with the oscillating disk method [5, 10] as well as measurements with the capillary flow method [12, 15] have shown that the viscosity coefficient does not show any anomalous behavior at supercritical temperatures down to a temperature $(T - T_c)/T_c = 1$ percent from the critical.

2. The significance of the small anomalous increase at temperatures closer to the critical is not clear at present. A correction should be subtracted from the data of Naldrett and Maass in this region which in magnitude might be comparable to the anomaly reported. Using the same apparatus Mason and Maass did not find an anomalous increase of the viscosity of ethylene near the critical point, although the data are somewhat preliminary. It is interesting that the difference between the data of Kestin et al., and the uncorrected data of Naldrett and Maass is also of the same order as the anomaly. Kestin et al., have discussed the possible influence on their measurements of the variation of the density with height. Because their oscillating disk is located at a position somewhat higher than the center, the variation of density leads to a correction in the opposite direction from that to be applied to the data of Naldrett and Maass and therefore tends to enlarge the anomalous effect. The authors point out that their data become less reliable in this difficult region and they are taking the attitude that their data prove only the absence of the pronounced anomaly suggested by Michels et al., and that any anomaly is smaller than 20 percent. The reality of the small anomaly can be decided definitely only if the local value of the density is determined simultaneously and the effect of a variable density on the interpretation of the viscosity measurements is carefully analyzed.

This picture of the viscosity in the critical region is sustained by the work on other substances. STARLING, EAKIN, DOLAN, and ELLINGTON have measured the viscosity of ethane, propane and *n*-butane with a capillary flow method [14]. Although the authors did not analyze their measurements as a function of density, they have measured at sufficiently small pressure intervals to conclude that

the viscosity does not show a pronounced anomaly in the critical region. However, near the critical point neither the density at which the viscosity was determined nor the precision of the values for the viscosity coefficient is sufficiently well known to decide whether a small increase, as observed by Kestin et al., exists.

Recently DILLER reported that the viscosity of parahydrogen does not show any anomaly near the critical point [3]. Measurements at temperatures for which $T-T_c$ is ten times smaller than in the case of CO_2 are required, because the critical temperature of parahydrogen is only 32.976 °K. Consequently, only the measurements at one isotherm ($T=33.000$ °K) are relevant for our present discussion. Indeed, the data on this isotherm do not show any appreciable anomaly near the critical density. However, this conclusion is based only on a few experimental points for which calculations of the density from the *P-V-T* data are difficult. An analysis of the viscosity data on adjacent isotherms shows that the precision is only a few percent. Therefore, no decisive conclusion can be drawn from this work regarding the existence of a small anomaly.

4. The Thermal Conductivity of a One Component Fluid Near the Liquid-Vapor Critical Point

Outside the critical region the behavior of the thermal conductivity is very similar to that of the viscosity described in the previous section. However, there exists a serious controversy in the literature whether the thermal conductivity, contrary to the viscosity, exhibits a pronounced anomaly in the critical region. An introductory survey on the subject has been presented by Ziebland [37].

The thermal conductivity is sometimes studied either as a function of pressure at constant temperature or as a function of temperature at constant pressure, without considering the dependence on the density. The region around the critical density is restricted to very narrow pressure and temperature intervals in this procedure, because both $(\partial\rho/\partial p)_T$ and $(\partial\rho/\partial T)_p$ become infinite at the critical point. Measurements at the critical pressure are not equivalent to measurements near the critical density unless the temperature is equal to the critical temperature within a tenth of a degree. For instance, considering the density dependence along an isobar, in CO_2 at a temperature 0.15 °C from the critical temperature the density is only 185 amagat at the critical pressure, whereas the critical density is 236 amagat. Consequently extrapolation of data at constant pressure as a function of temperature easily overlooks the critical region entirely and therefore does not reveal any anomaly in the critical region. Along an isotherm the density is similarly sensitive to a small change in pressure.

Another procedure sometimes used to obtain a thermal conductivity value associated with the critical point is based on the assumption that the excess thermal conductivity $\lambda-\lambda_0$, where λ_0 is the thermal conductivity at 1 atm at the temperature considered, is only dependent on the density and not on the temperature. However, this relation actually has been verified outside the critical region only and therefore cannot be used legitimately in the critical region. "Critical thermal conductivity values," obtained in this way, are often used as reduction parameters for correlation of the thermal conductivity of different substances [66]. It must be kept in mind that these reduction parameters do not necessarily represent the actual thermal conductivity near the critical point. Similar procedures have been used to obtain critical values of the viscosity. The reduction parameters for the viscosity obtained in this way are closer to the actual viscosity in the critical region, because any anomaly in the viscosity near the critical point is small. With few exceptions, values for the transport coefficients in the critical region which are based on data outside the critical region are not discussed in this review.

Two methods for the measurement of the thermal conductivity of compressed gases have had wide acceptance, the concentric cylinder and the parallel plate method. In the first the fluid is enclosed between two coaxial cylinders, either in horizontal or in vertical position, and the heat flow through the gas layer is determined as a function of the temperature difference between the cylinders. In the latter method the fluid is contained between two horizontal plates and the heat flowing from the upper plate to the lower plate is determined as a function of the temperature difference. A special case of the concentric cylinder method is the hot wire method. This method is not suitable for the critical region because the heat transfer analysis is complicated, too large temperature differences are usually involved and, most importantly, convection cannot be avoided.

Papers reporting an anomalous increase of the thermal conductivity in the critical region are generally considered with much skepticism due to the high probability of convection. An exact theoretical analysis of convection is very complicated and has been carried out only in very special cases. We do not go into the details here, but remark that the presence of convection can be detected by varying the thickness of the gas layer or the temperature difference across this layer. The heat transfer coefficient or so-called apparent thermal conductivity coefficient, which includes a contribution from convection, depends on the geometry of the apparatus and of the boundary conditions involved.

Heat transferred by convection is usually related to the Rayleigh number R defined as

$$R = g\alpha\rho^2 c_p d^3 \Delta T/\lambda\eta \qquad (1)$$

where g is the gravitation constant, α the expansion coefficient, ρ the density, c_p the specific heat at constant pressure, d the thickness of the gas layer, ΔT the temperature difference, λ the thermal conductivity and η the viscosity coefficient. In the critical region the Rayleigh number becomes extremely large [26, 30]. By the use of many approximations and assuming that the convection is small, the error introduced by convection can be derived explicitly:

$$\frac{\lambda' - \lambda}{\lambda} = CR\frac{d}{l}\sin\epsilon \qquad (2)$$

where λ' is the apparent thermal conductivity coefficient as measured, l the length of the gas layer, ϵ the angle between the temperature gradient and the vertical, and C a proportionality constant. In order to obtain (2) one neglects the variation with temperature of the fluid properties other than the density, linearizes the hydrodynamic equations, assumes a spatially uniform temperature gradient and considers the limiting solution for $\frac{d}{l} \ll 1$. Without these approximations the error may well depend on d and ΔT in a more complicated way. The absence of convection is verified, nevertheless, if the measured thermal conductivity coefficient at a given density and temperature does not change under sufficient variation of ΔT or d.

If convection is present, one sometimes tries to obtain the correct value of λ by extrapolating to $\Delta T = 0$ from the experimental data obtained for λ' using various values of ΔT. In the critical region the contribution of convection becomes very large and such an extrapolation can diminish the accuracy considerably even when care is taken that only values for λ' corresponding to the same average density and average temperature are used. In some cases, such as a horizontal fluid layer heated from below, convection only seems to start if the Rayleigh number becomes larger than a certain critical value [64]. This has also been reported for a concentric cylindrical layer in horizontal position [23, 58]. When this instability occurs, extrapolation to $\Delta T = 0$ is not legitimate and can lead to overcorrections.

The controversy over the existence of a thermal conductivity anomaly started in 1934. KARDOS attempted to measure the thermal conductivity of CO_2 using a hot wire method [21]. He found a tremendous increase of heat transfer in the critical region, which was later recognized as an effect of convection [28]. SELLSCHOPP measured the thermal conductivity of CO_2 with two concentric cylinders in horizontal position [29]. He observed an increase in the apparent thermal conductivity near the critical density at supercritical temperatures, but his measurements were also influenced by convection. The whole effect was attributed to convection and it was assumed, without experimental justification however, that in the critical region the thermal conductivity was only dependent on the density and not on the temperature [18, 29].

TIMROT and OSKOLKOVA [33] reported that the thermal conductivity of CO_2 did not show any anomaly in the supercritical region, but their measurements obtained with a hot wire method were actually carried out too far away from the critical point.

COMINGS et al., measured the thermal conductivity of several gases using two concentric cylinders in horizontal position. Anomalies in the supercritical region were reported for ethane, propane, and butane [22] but the reality of the effect could not be established again due to the possibility of convection. An anomalous increase of the thermal conductivity of argon at 0 °C, originally reported by the present author among others, later turned out to be entirely caused by convection [24].

The first critical study of the existence of a thermal conductivity anomaly was carried out by GUILDNER [19]. He measured the thermal conductivity of CO_2 using a vertical cylindrical gas

layer with a thickness of 0.68 mm. Convection could not be avoided in this apparatus so that λ was determined from measurements at various temperature differences by extrapolation to $\Delta T = 0$ at constant average temperature. He concluded that the thermal conductivity itself exhibits a pronounced anomaly. This anomalous increase is already 30 percent at 40 °C at the critical density. He approached the critical temperature to within 1 °C. Although at 75 and 40 °C the influence of convection was small, closer to the critical temperature the influence of convection became large diminishing the accuracy of the data.

On the other hand, VARGAFTIK stated that the thermal conductivity did not exhibit an anomaly in the critical region [34]. This assertion was based on experimental wotk of SHINGAREV, which unfortunately, has not been made available and therefore cannot be critically examined. According to the discussion given by Vargaftik, these conclusions were drawn after applying corrections for convection by extrapolation to zero temperature difference.

It is clear that measurements in the critical region free of convection are highly desirable. For this purpose a detailed study of the thermal conductivity of CO_2 was carried out by MICHELS, SENGERS, and VAN DER GULIK using a parallel plate method [25, 26, 30]. Contrary to the concentric cylinder method the horizontal flat layer method has the advantage that the angle between temperature gradient and the vertical can be made very small to suppress convection. The experimental results obtained for the thermal conductivity as a function of density are presented in figure 4. The thermal conductivity shows indeed a pronounced anomaly at the critical point. An anomalous increase can be detected as much as 20 °C above the critical temperature which becomes 250 percent at 1 °C above the critical temperature. Convection was avoided by the use of a small distance between the plates ($d = 0.4$ mm) and small temperature differences (ΔT varied from 0.03 to 0.25 °C). The absence of convection was verified experimentally; in the whole critical region the thermal conductivity values measured were independent of the temperature difference used. Of course, one should compare measurements with different ΔT, but at the same average density and temperature. For the details we refer to the previous publication. The reality of the anomaly was independently confirmed by a few measurements with a larger plate distance. An attempt was made to include a measurement of the thermal conductivity isotherm at 31.2 °C using even smaller temperature differences. These results are shown in figure 5. Obviously the values at this temperature are less

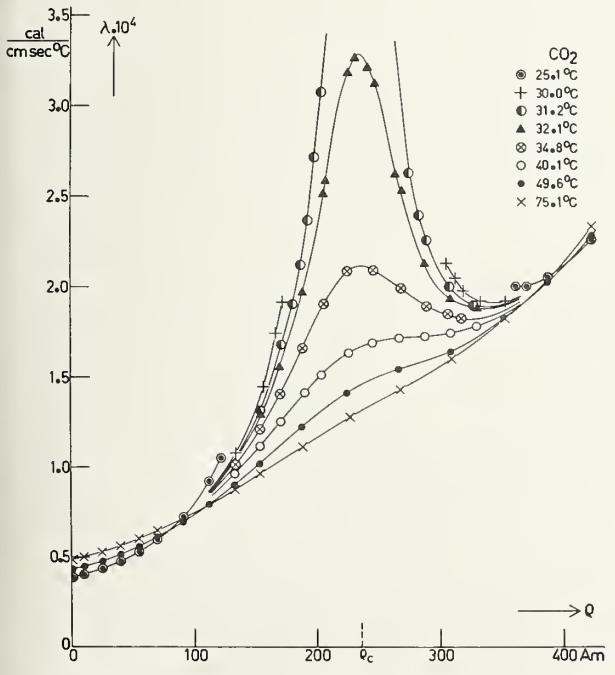

FIGURE 4. *The thermal conductivity of CO_2 as a function of density.*

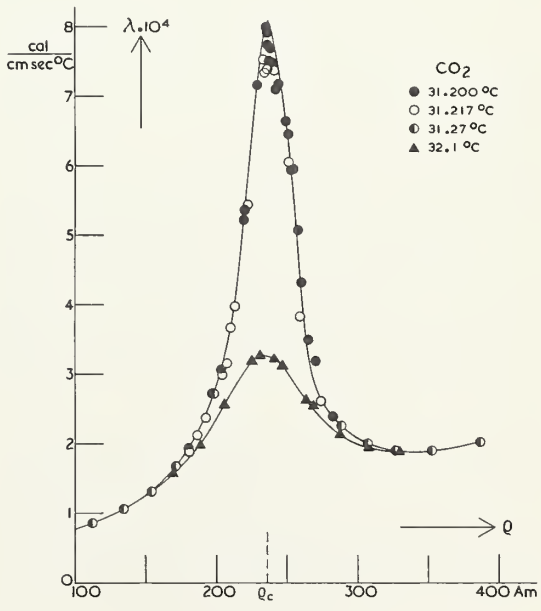

FIGURE 5. *The thermal conductivity of CO_2 at 31.2 and 32.1 °C as a function of density.*

accurate than those of figure 4, since the experimental verification of the absence of convection becomes more difficult due to the inaccuracy in the density.

Due to the variation of temperature, the density variation in the pressure vessel is very complicated. It is therefore difficult to approach the critical region by the isochoric method. The density must be calculated from the experimental pressure and temperature, which may introduce systematic errors at each isotherm. Thus the detailed behavior along the critical isochore, particularly the character of the divergence of the thermal conductivity, cannot accurately be deduced from the data.

It is notable that at 75 and 40 °C, where the amount of convection in the apparatus of Guildner was reasonably small, there is a satisfactory agreement with the data of Guildner, confirming the anomaly of 30 percent at 40 °C. It turned out, however, that closer to the critical temperature the anomalous increase is considerably smaller than that reported by Guildner.

The fact that the thermal conductivity measured was independent of the temperature difference used not only guarantees the absence of convection, but also verifies the validity of the law of Fourier in the temperature range considered. The validity of the law of Fourier in the critical region was questioned by SIMON and ECKERT [32]. From interferometric studies of laminar free convection near a vertical wall a quantity k was derived, which they identified with the thermal conductivity coefficient of the fluid. This quantity k turned out to increase with increase of heat rate and it was conjectured that the anomaly in the thermal conductivity would disappear in the limit of zero heat rate. However, an analysis of their data shows that this quantity k remained dependent on the heat rate outside the critical region as well, where the validity of the law of Fourier cannot reasonably be questioned. Therefore, this quantity k should not be identified with the thermal conductivity coefficient.

The existence of an anomaly in the thermal conductivity near the critical point was denied by Abas-Zade [16] and by Amirkhanov and Adamov [17]. These authors do not base this assertion on measurements in the supercritical region, but on data obtained at temperatures below the critical which they claim are associated with the coexistence line. ABAS-ZADE performed his measurements using a hot wire apparatus at various temperatures, but at constant pressure. As mentioned before data at constant pressure as a function of temperature do not approach smoothly the critical density. Consequently, the measurements were not carried out near the critical density. The interpretation of Abas-Zade that he followed the coexistence line up to the critical temperature is erroneous.

Very careful thermal conductivity measurements were carried out by AMIRKHANOV and ADAMOV using both a horizontal parallel plate method and a vertical concentric cylinder method [17]. Using the parallel plate apparatus, a series of measurements was carried out with plate distances of 0.3 mm and of 0.6 mm, and the temperature difference was varied from 0.07 to 1 °C. With the smaller plate distance the data turned out to be independent of ΔT, which guarantees absence of convection. Data obtained with the larger plate distance and also those obtained using the concentric cylinder apparatus were dependent on ΔT showing the presence of convection. The results obtained with the smallest value of ΔT agreed for all 3 series of measurements. The values obtained for the thermal conductivity therefore seem to be very reliable. As has been pointed out repeatedly before, it is equally important to verify whether the measurements were carried out sufficiently close to the critical density. Unfortunately, the authors do not describe their experimental procedure. They do not report whether and how either pressure or density was determined. In addition, although they measure the temperature difference ΔT carefully, no device was presented for measuring the absolute average temperature of the gas layer, which obviously differs from the temperature of the surrounding thermostat. It is not clear at which temperatures and densities the thermal conductivity actually was determined. If the measurements were carried out at the coexistence line, one would expect a large variation of the density when the temperature difference was varied from 0.1 to 1.0 °C, at the liquid side even leading to evaporation of the liquid. On the contrary, their results indicate that even up to a few hundredths of a degree below the critical temperature the density did not change when ΔT was varied from 0.1 to 1 °C. Thus it seems that the measurements were not carried out near the critical density.

From the data given in figure 4 it is evident that the first indication of the existence of the thermal

conductivity anomaly can be noticed from the occurrence of intersections of the thermal conductivity isotherms as a function of density at temperatures considerably higher than the critical temperature. It is interesting therefore to study as a function of density data given in the literature somewhat remote from the critical point. As an example, we considered the experimental data obtained by ZIEBLAND and BURTON [35] for the λ of nitrogen. These data were originally plotted along isobars and consequently did not reveal any anomaly. However, if the data are plotted as a function of density the thermal conductivity isotherms shown in figure 6 are obtained.[3] A pronounced increase in the thermal conductivity can be noticed at -140 °C (7 °C above the critical temperature). This observation is based on only two experimental points, but the crucial experimental value at -140 °C, showing an anomalous increase of 35 percent, was obtained with two different values of ΔT, which excludes the possibility of convection. This is a clear illustration of how one can be misled if the density dependence of λ is not considered explicitly.

[3] One amagat unit of N_2 corresponds to 0.0012502 g/cm³.

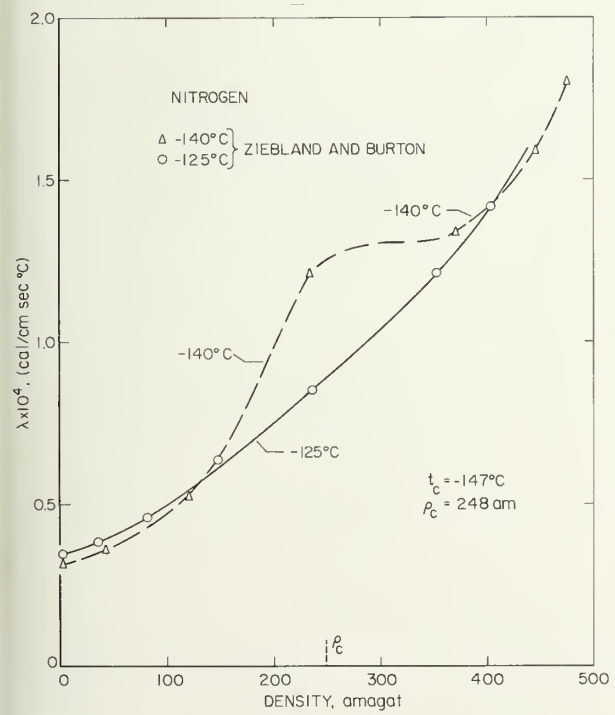

FIGURE 6. *The thermal conductivity of nitrogen at -125 and -140 °C as a function of density.*

A similar result is obtained [31] if one analyzes the thermal conductivity data obtained by IKENBERRY and RICE for argon [20]. However, since these authors did not adequately examine the absence of convection, we cannot rely on their results as decisive.

In view of these results NEEDHAM and ZIEBLAND studied the thermal conductivity of ammonia in more detail [27, 37] than before [36]. The data were obtained using an apparatus consisting of two concentric cylinders with a gap of 0.2 mm. The results obtained at two supercritical temperatures are shown as a function of density[4] in figure 7. An anomalous increase can be noticed near the critical density even at 157.1 °C. The absence of convection was verified by measurements with different values of ΔT. At 138.8 °C the thermal conductivity goes through a maximum. The densities were estimated by Needham and Ziebland from $P-V-T$ data published in the literature. However, at 138.8 °C these $P-V-T$ data are virtually unknown, so that the densities cannot be calculated with sufficient accuracy to conclude that the maximum does not occur at the critical density.

We conclude that the existence of a pronounced anomaly in the thermal conductivity has been verified by convection free measurements obtained both with a parallel plate method and with a concentric cylinder method.

[4] One amagat unit of NH_3 corresponds to 0.0007714 g/cm³.

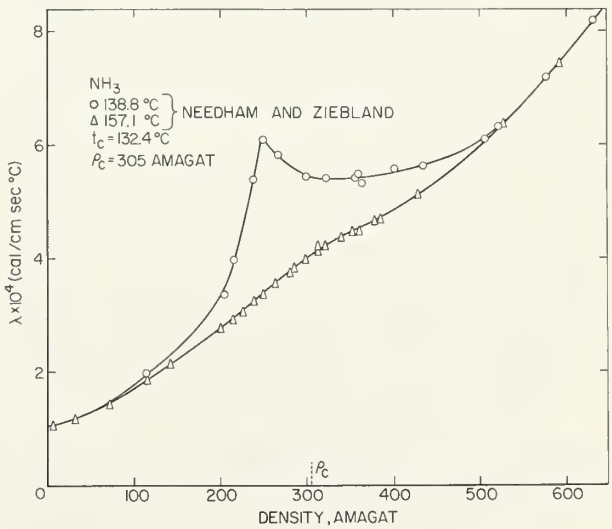

FIGURE 7. *The thermal conductivity of ammonia as a function of density.*

TABLE 1. *Comparison of the thermal conductivity with the specific heat along the critical isochore of* CO_2 ($\rho_c = 236$ *amagat*)

t	λ/λ_{75}	$\dfrac{\lambda/c_v}{(\lambda/c_v)_{75}}$	$\dfrac{\lambda/c_p}{(\lambda/c_p)_{75}}$
°C			
75	1.0	1.0	1.0
50	1.1	1.0	0.5
40	1.3	1.0	.3
34.8	1.6	1.1	.1
32.1	2.5	1.3	.05
31.2	6.1	1.6	.02

An interesting question is whether the anomaly in the thermal conductivity is related to that in the specific heat. For this reason the variation of λ of CO_2 as a function of temperature at the critical isochore is compared with the variation of c_v and c_p in table 1. For c_v the experimental data [62] are supplemented with values calculated from the P–V–T data at temperatures where no experimental data for c_v are available [61]. The values for c_p are obtained by adding the calculated difference $c_p - c_v$ to the values for c_v obtained as mentioned above. It is evident that c_p increases much faster in the critical region than λ, so that the ratio λ/c_p decreases by two orders of magnitude when the temperature is varied from 75 to 31.2 °C. On the other hand the variation of λ/c_v is an order of magnitude smaller than that of λ itself. Very close to the critical point c_v as well as λ is not accurately known. A relationship between the anomaly in λ and c_v is well possible. In view of the recent work on the c_v anomaly, it is natural to ask whether λ diverges logarithmically. Such questions about the detailed behavior cannot be decided at present and further experimental research is required.

According to the classical theory the line width of the central component of the spectrum of the scattered light is determined by the thermal diffusivity $\lambda/\rho c_p$ [57, 63]. The line width to be expected for CO_2 from the static measurements of λ is presented in figure 8 for $k = 10^5$ cm, which corresponds to light from a He-Ne laser scattered through an angle of 60°. Because c_p diverges much faster than λ, the thermal diffusivity [31] and consequently the line width of the central component decreases rapidly in the critical region.

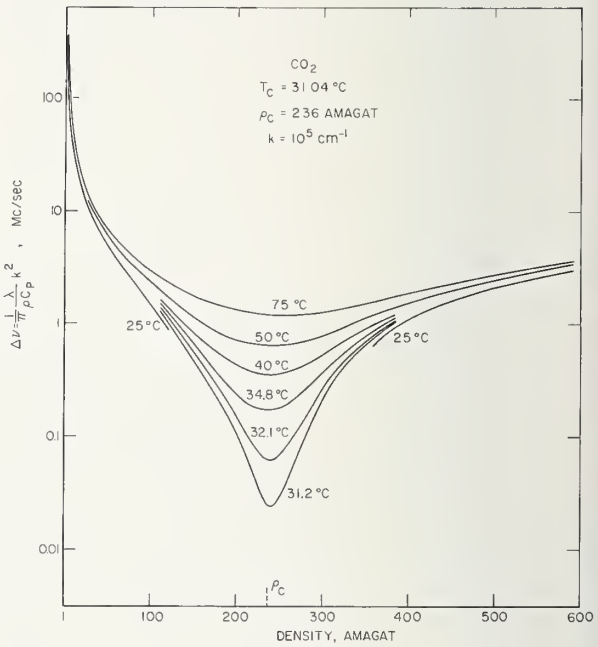

FIGURE 8. *Expected line width of the central component of light scattered by* CO_2 *for* $k = 10^5$ *cm*$^{-1}$.

5. The Viscosity of a Binary Liquid Mixture Near the Critical Mixing Point

Many binary liquid mixtures exhibit a critical mixing point near room temperature. The viscosity of a number of different mixtures of this type has been studied. There are not enough data obtained by different authors for the same substance. Moreover, the critical parameters are very sensitive to the purity of the components. Although some attention has been given to the influence of a third component on the viscosity in the critical mixing region [43, 47, 50, 51, 53], the influence of any impurity on this anomaly is not clear. It seems that the effect depends on the binary system as well as on the character of the impurity.

Most viscosity measurements for binary liquid mixtures have been carried out with some version of the capillary flow method. We have not made a critical analysis of the experimental procedures used by the various authors. However, there is sufficient agreement to establish the existence of an anomaly in the viscosity near the critical mixing point for systems with either an upper or lower critical solution point [39, 40, 43–53].

In the beginning of the century, an anomalous increase of the viscosity near the critical mixing point was reported by various authors, among others by FRIEDLANDER [43] for the systems isobutyric acid-water and phenol-water, by SCARPA [48] for phenol-water, by DRAPIER [40] for nitrobenzene-hexane and cyclohexane-aniline, and by TSAKALOTOS [52] for isobutyric acid-water, trimethylethylene-aniline, triethylamine-water and nicotine-water.

For simple binary liquid mixtures the anomalous increase of the viscosity is of the order of 15 to 25 percent at the critical mixing point.

REED and TAYLOR observed an anomalous increase in the viscosity of the mixtures isooctane-perfluorocyclic oxide, *n*-hexane-perfluorocyclic oxide, isooctane-perfluoroheptane [46]. The effect was most pronounced in the mixture isooctane-perfluoroheptane; their results for this system are shown in figure 9. The viscosity exhibits an anomalous increase up to 25 percent. According to these data the anomalous behavior can be detected as far away as 10 °C from the critical temperature. However, other authors found that for some systems the anomaly occurs only at temperatures much closer to the critical.

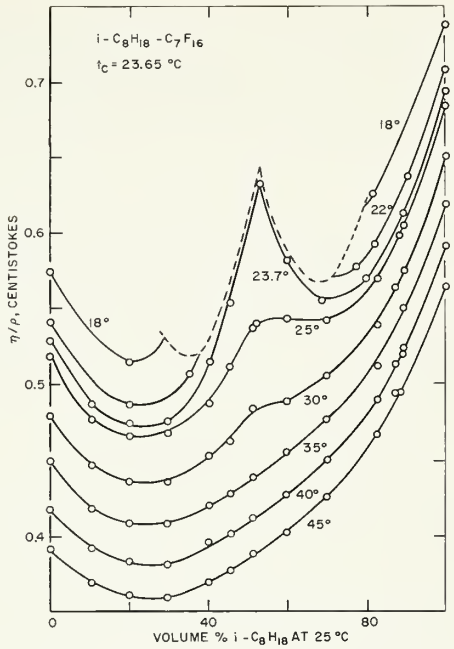

FIGURE 9. *The viscosity of the mixture isooctane-perfluoroheptane as a function of concentration according to Reed and Taylor* [46].

SEMENCHENKO and ZORINA investigated the viscosity of the systems triethylamine-water and nitrophenol-hexane [49]. The first mixture has a lower critical mixing temperature. For both systems an anomalous increase of the viscosity up to 20 percent was found. The anomalous phenomenon only occurred at temperatures within 1.0 or 1.5 °C from the critical and in a concentration range of 10 mole percent.

Recent measurements of the viscosity of the nitrobenzene-isooctane mixture obtained by PINGS et al., confirmed that for this system also a viscosity anomaly occurs in a very small temperature range [45]. No anomaly could be detected at 4.5 °C above the critical temperature, but an anomalous increase of 5 to 7 percent was noticed at 0.45 °C above the critical temperature.

We conclude that the viscosity does show an anomalous increase near the critical mixing point, but for a number of simple mixtures the anomalous behavior occurs only at temperatures within 2 °C of the critical temperature.

6. Thermal Conductivity of a Binary Liquid Mixture Near the Critical Mixing Point

Experimental investigations of the thermal conductivity of binary liquid mixtures near the critical

mixing point are very scarce. This is surprising since the experimental complications are somewhat less difficult than those encountered in the measurement of the thermal conductivity near the liquid-vapor critical point.

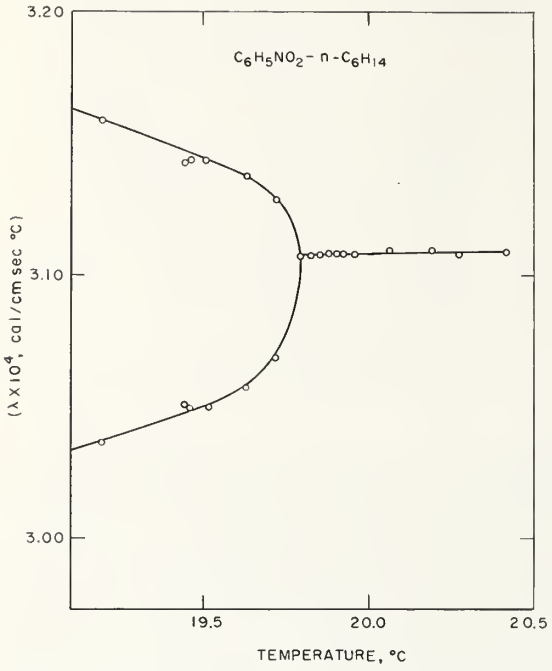

FIGURE 10. *The thermal conductivity of the system nitrobenzene-n-hexane according to Gerts and Filippov [54].*
(63.0 wt % $C_6H_5NO_2$.)

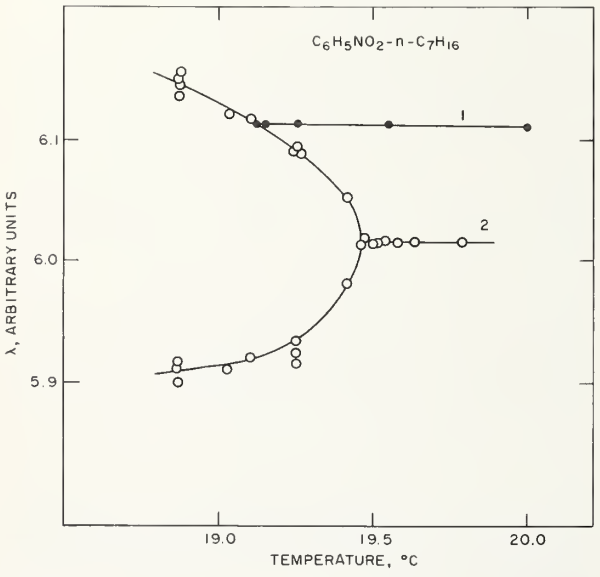

FIGURE 11. *The thermal conductivity of the system nitrobenzene-n-heptane according to Gerts and Filippov [54].*
(Curve 1: 62 wt % $C_6H_5NO_2$; curve 2: 52.3 wt % $C_6H_5NO_2$.)

The most extensive study was carried out by GERTS and FILIPPOV, who measured the thermal conductivity of a number of binary liquids using a hot wire apparatus [54]. Measurements of the thermal conductivity of the system nitrobenzene-*n*-hexane were carried out with four different temperature differences: 0.01, 0.05, 0.15, and 0.3 °C and found to be independent of this temperature difference. In addition the systems nitrobenzene-*n*-heptane, methanol-*n*-hexane and triethylamine-water were investigated. The results obtained by Gerts and Filippov for the nitrobenzene-*n*-hexane mixture are shown in figure 10 and those for the nitrobenzene-*n*-heptane system in figure 11. It is evident that, contrary to the behavior near the liquid-vapor critical point, the thermal conductivity of these binary liquid mixtures does not show any pronounced anomaly near the critical mixing point. Similar results were obtained for the other two systems mentioned. An anomaly even as small as that found for the viscosity of binary mixtures seems to be absent. The data were not obtained at enough different concentrations to study the behavior in detail and the results cannot be plotted as a function of concentration as was done for the viscosity in figure 9. The absence of a pronounced anomaly near the critical mixing point seems to be established. This difference between the behavior of the thermal conductivity near the liquid-vapor critical point and that near the critical mixing point was noticed before by SKRIPOV [56]. Additional experimental data are highly desirable to verify this conclusion and to study smaller details.

On the other hand an anomalous increase of the thermal conductivity was reported by OSIPOVA for the phenol-water system [55]. The data were obtained with a parallel plate method. The uncertainty in the temperature difference and the scatter of the experimental data suggest that these results should be considered with some reservations. No experimental verification for the absence of convection was presented.

7. Summary

The experimental information on the viscosity and thermal conductivity in the critical region can be summarized as follows:

1. Measurements of the viscosity with the oscillating disk method as well as with the capillary flow

method have shown that the viscosity does not show any anomaly near the liquid-vapor critical point if the temperature is not within $(T-T_c)T_c = 1$ percent of the critical temperature. Whether an anomalous behavior of the viscosity occurs at temperatures closer to the critical point is not clear at present. If such an anomaly does occur it is probably smaller than 20 percent.

2. Measurement with the parallel plate method as well as with the concentric cylinder method have shown that the thermal conductivity exhibits a pronounced anomaly near the liquid-vapor critical point. Further experimental work is required to study the precise character of the anomaly and to investigate whether the anomaly of λ is related to the anomaly of the specific heat c_v.

3. The viscosity of binary liquid mixtures shows an anomalous increase near the critical mixing point. For simple systems this increase is between 15 percent and 25 percent at the critical point. For a number of liquid mixtures, however, this phenomenon is only observed at temperatures within 2 °C of the critical temperature.

4. It seems evident that the thermal conductivity of a number of binary liquid systems does not show an appreciable anomaly near the critical mixing point. Additional experimental information is highly desirable, since this assertion can only be based on the results of one experimental investigation.

The author is indebted to Dr. H. Ziebland who presented the thermal conductivity data for ammonia shown in figure 7. The author also acknowledges the stimulating interest of several colleagues at the National Bureau of Standards and in particular that of Dr. M. S. Green.

References

Viscosity of One-Component Fluids

[1] M. Brillouin, Leçons sur la viscosité des liquides et des gaz. 1., pp. 184–195 (Gauthier-Villars, Paris, 1907).
[2] A. L. Clark, Trans. Roy. Soc. Canada III **9** (1915) 43; **18** (1924) 329; Chem. Revs. **23** (1938) 1.
[3] D. E. Diller, J. Chem. Phys. **42** (1965), 2089.
[4] G. P. Flynn, R. V. Hanks, N. A. Lemaire and J. Ross, J. Chem. Phys. **38** (1963), 154.
[5] J. Kestin, J. H. Whitelaw and T. F. Zien, Physica **30** (1964), 161.
[6] S. G. Mason and O. Maass, Can. J. Research **18B** (1940), 128.
[7] A. Michels, A. Botzen and W. Schuurman, Physica **20** (1954), 1141.
[8] A. Michels, A. Botzen and W. Schuurman, Physica **23** (1957), 95.
[9] A. Michels, Proc. Intern. Symposium Transport Processes in Stat. Mech., Brussels, 1956, p. 365.
[10] S. N. Naldrett and O. Maass, Can. J. Research **18B** (1940), 322.
[11] P. Phillips, Proc. Roy. Soc. (London) **A87** (1912), 48.
[12] J. Ross, private communication.
[13] E. Schröer and G. Becker, Z. physik. Chem. **A173** (1935), 178.
[14] K. E. Starling, B. E. Eakin, J. P. Dolan and R. T. Ellington, Progress Intern. Research Thermodynamic Transport Properties, A.S.M.E., Princeton, 1962, p. 530.
K. E. Starling, Critical region viscosity behavior of ethane, propane and *n*-butane, Master thesis, Institute of Gas Technology, Chicago, 1960.
[15] E. Warburg and L. von Babo, Ann. Phys. Chem. **253** (1882), 390.

Thermal Conductivity of One-Component Fluids

[16] A. K. Abas-Zade, Doklady Akad. Nauk SSSR **68** (1949) 665; **99** (1954) 227. A. K. Abas-Zade and A. M. Amuraslanov, Zh. Fiz. Khim. **31** (1957) 1459.
[17] Kh. I. Amirkhanov and A. P. Adamov, Teploenergetika **10**, No. 7 (1963) 77; Primenenie Ultraakustiki k Issledovan Veschestva **18** (1963) 65. Kh. I. Amirkhanov, A. P. Adamov and L. N. Levina, Teplo i Massoperenos, Pervoe Vses. Svesch., Minsk **1** (1961) 105.
[18] E. Borovik, Zh. eksp. teor. Fiz. U.S.S.R. **19** (1949) 561.
[19] L. A. Guildner, Proc. Nat. Acad. Sci., **44** (1958) 1149; J. Res. NBS **66A** (Phys. and Chem.) No. 4. (1962) 333, 341.
[20] L. D. Ikenberry and S. A. Rice, J. Chem. Phys. **39** (1963) 1561.
[21] A. Kardos, Z. gesamte Kälte-Ind. **41** (1934) 1, 29; Forsch. Gebiete Ingenieurwesens **5** (1934) 14.
[22] F. R. Kramer and E. W. Comings, J. Chem. Eng. Data **5** (1960) 462. D. E. Leng and E. W. Comings, Ind. Eng. Chem. **49** (1957) 2042. J. M. Lenoir, W. A. Junk and E. W. Comings, Chem. Eng. Progress **49** (1953) 539.
[23] J. M. Lenoir and E. W. Comings, Chem. Eng. Progress **47** (1951) 223.
[24] A. Michels, A. Botzen, A. S. Friedman and J. V. Sengers, Physica **22** (1956) 121.
A. Michels, J. V. Sengers and L. J. M. van de Klundert, Physica **29** (1963) 149.
[25] A. Michels, J. V. Sengers and P. S. van der Gulik, Physica **28** (1962) 1201, 1216.
[26] A. Michels and J. V. Sengers, Physica **28** (1962) 1238.
[27] D. P. Needham and H. Ziebland, Int. J. Heat Mass Transfer **8** (1965) 1387.
[28] R. Plank and O. Walger, Forsch. Gebiete Ingenieurwesens **5** (1934) 289.
[29] W. Sellschopp, Forsch. Gebiete Ingenieurwesens **5** (1934) 162.
[30] J. V. Sengers, Thermal conductivity measurements at elevated gas densities including the critical region, thesis, van der Waals Laboratory, Amsterdam, 1962.
J. V. Sengers and A. Michels, Progress Intern. Research Thermodynamic and Transport Properties, A.S.M.E., Princeton, 1962, p. 434.
[31] J. V. Sengers, Int. J. Heat Mass Transfer **8** (1965) 1103.
[32] H. S. Simon and E. R. G. Eckert, Int. J. Heat Mass Transfer **6** (1963) 681.
[33] D. L. Timrot and V. G. Oskolkova, Izvestia V.T.I. No. 4 (1949).
[34] N. B. Vargaftik, Proc. joint Conference Thermodynamic Transport Properties Fluids, London, 1957, p. 211.
[35] H. Ziebland and J. T. A. Burton, Brit. J. Appl. Phys. **9** (1958) 52.
[36] H. Ziebland and D. P. Needham, Progress Intern. Research Thermodynamic and Transport Properties, A.S.M.E., Princeton, 1962, p. 441.
[37] H. Ziebland, N.P.L. Thermal Conductivity Conference, Teddington, England 1964.

Viscosity of Binary Liquid Mixtures

[38] W. Botch and M. Fixman, J. Chem. Phys. **36** (1962) 310.
[39] P. Debye, B. Chu and D. Woermann, J. Polymer Science **A1** (1963) 249.
[40] P. Drapier, Bull. Acad. Belg. Cl. Sci. 1911, p. 621.
[41] M. Fixman, J. Chem. Phys. **36** (1962) 310.
[42] M. Fixman, Adv. Chem. Phys. **6** (1964) 175.
[43] J. Friedlander, Z. physik. Chem. **38** (1901) 385.
[44] W. Ostwald and H. Malss, Koll. Z. **63** (1933) 61.
[45] C. J. Pings, private communication.
[46] T. M. Reed III and T. E. Taylor, J. Phys. Chem. **63** (1959) 58.
[47] V. Rothmund, Z. physik. Chem. **63** (1908) 54.
[48] O. Scarpa, Nuovo Cimento (5) **6** (1903) 277; J. Chim. Phys. **2** (1904) 447.
[49] V. K. Semenchenko and E. L. Zorina, Doklady Akad. Nauk SSSR **73** (1950) 331; **80** (1951) 903; Zh. Fiz. Khim. **26** (1952) 520.
[50] V. K. Semenchenko and E. L. Zorina, Doklady Akad. Nauk SSSR **84** (1952) 1191.
[51] V. P. Solomko and S. M. Smiyun, Dopovidi Akad. Nauk Ukrains'koi RSR 1961, 649.
[52] D. E. Tsakalatos, Bull. Soc. Chim. France [4] **5** (1909) 397; Z. Physik. Chem. **68** (1910) 32.
[53] E. L. Zorina and V. K. Semenchenko, Zh. Fiz. Khim. **33** (1959) 523, 961.

Thermal Conductivity of Binary Liquid Mixtures

[54] L. G. Gerts and L. P. Filippov, Zh. Fiz. Khim. **30** (1956) 2424.
[55] V. A. Osipova, Doklady Akad. Nauk Azerbaidzhan S.S.R. **13** (1957) 3.
[56] V. P. Skripov, Conference Critical Phenomena and Fluctuations in Solutions, Akad. Nauk SSSR, Moscow, 1960, p. 117.

Miscellaneous

[57] N. C. Ford and G. B. Benedek, Conference Phenomena Neighborhood Critical Points, N.B.S., Washington, D.C., 1965.
[58] H. Kraussold, Forsch. Gebiete Ingenieurwesens **5** (1934) 186.
[59] I. R. Krichevskii, N. E. Khazanova and L. S. Lesnevskaya, Inzh.-Fiz. Zh., Akad. Nauk SSR **5** (1962) 101.
[60] A. Michels, B. Blaisse and C. Michels, Proc. Roy. Soc. (London) **A160** (1937) 358.
[61] A. Michels and S. R. de Groot, Appl. Scient. Research **A1** (1948) 94.
[62] A. Michels and J. C. Strijland, Physica **18** (1952) 613.
[63] R. D. Mountain, Rev. Mod. Phys. **38** (1966) 205.
[64] A. Pellew and R. V. Southwell, Proc. Roy. Soc. (London) **A176** (1940) 312.
[65] E. H. W. Schmidt and K. Traube, Progress Intern. Research Thermodynamic Transport Properties, A.S.M.E., Princeton, 1962, p. 193.
[66] L. I. Stiel and G. Thodos, Progress Intern. Research Thermodynamic Transport Properties, A.S.M.E., Princeton, 1962, p. 352.
[67] S. A. Ulybin and S. P. Malyshenko, Advances Thermophysical Properties at Extreme Temperatures and Pressures, A.S.M.E., Purdue Univ., 1965, p. 68.

Nuclear Magnetic Resonance Measurements Near the Critical Point of Ethane

M. Bloom[1,2]

Harvard University, Cambridge, Mass.

In this talk I shall discuss the application of nuclear magnetic resonance (NMR) techniques to the measurement of two transport properties of fluids near the critical point. The two transport properties we shall discuss are the nuclear spin-lattice relaxation time T_1 and the self-diffusion constant D of the fluid. Both of these observables are easy to measure using the NMR pulse technique of E. L. Hahn [1].

The Hahn pulse technique: A simple version of the NMR pulse technique is illustrated schematically in figure 1. Suppose that a time independent magnetic field

$$\mathbf{H} = H_0\mathbf{k} + G_z\mathbf{k} - G_x\mathbf{i} \qquad (1)$$

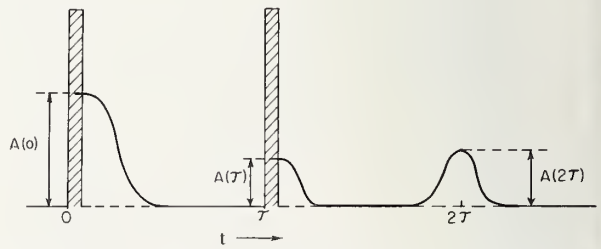

FIGURE 1. *Drawing of an oscilloscope display amplitude of the detected r-f signal as a function of time for the two-pulse nuclear magnetic resonance experiment.*
Following the pulses at times 0 and τ indicated by shaded regions are induction signals of maximum amplitude $A(0)$ and $A(\tau)$ respectively. The echo has a maximum amplitude $A(2\tau)$.

[1] Alfred P. Sloan Fellow.

[2] Permanent address: Department of Physics, University of British Columbia, Vancouver, British Columbia, Canada. On sabbatical leave 1964–65 while holding a John Simon Guggenheim Memorial Fellowship.

is applied to the nuclear spin system such that the gradient G is small so that

$$Gx,\ Gz \ll H_0 \tag{2}$$

over the entire volume of the sample. **i** and **k** are unit vectors in the x- and z-directions respectively. The spin system is assumed to be in equilibrium before the first of the two r-f pulses applied at times $t=0$ and $t=\tau$ respectively. Assume that the r-f pulses are sufficiently intense and that their frequency is sufficiently close to the Larmor frequency $\omega_0=\gamma H_0$, where γ is the nuclear gyromagnetic ratio, that the lengths of the pulses can be chosen such that the z-component of magnetization is rotated by an angle $\frac{\pi}{2}$ by each of the pulses. Then, if the z-component of the nuclear magnetization relaxes towards its equilibrium value exponentially with a time constant T_1, the maximum amplitudes of the detected nuclear induction signals $A(0)$ and $A(\tau)$ following the pulses are related by [1]

$$\frac{A(0)-A(\tau)}{A(0)}=\exp\left[-\frac{\tau}{T_1}\right]. \tag{3}$$

If the x and y components of the nuclear magnetization relax towards their equilibrium value of zero exponentially with a common time constant T_2 and if the spatial motion of the spins in the sample is adequately described by the solution to the diffusion equation, the maximum amplitude of the "spin-echo" at time 2τ is given by [2]

$$A(2\tau) \propto \exp\left[-\frac{2\tau}{T_2}-\frac{2}{3}\gamma^2G^2D\tau^3\right]. \tag{4}$$

Equation (4) correctly gives relative values of $A(2\tau)$ in terms of T_2, G, D and τ for any given angles of rotation by the r-f pulses [3]. For systems with strong NMR signals, it is easy to measure T_1 and D to an accuracy of ± 5 percent and with care an accuracy of ± 1 percent can be attained.

Note that the self-diffusion constant measured here is the "spin self-diffusion constant." The interpretation of this type of self-diffusion constant has been given by Emery [4] and by Fukuda and Kubo [5].

Interpretation of T_1 measurements: For most simple systems there are three main types of interactions which enable the nuclear spin system to exchange energy with the translational and rotational degrees of freedom of the system so that one can usually write

$$\frac{1}{T_1}=R_A+R_B+R_C. \tag{5}$$

R_A is the relaxation rate due to intramolecular dipole-dipole and/or electric quadrupolar interactions [6]: i.e., those interactions which transform as $Y_{2m}(\Omega_i)$, where Ω_i is the orientation of a vector fixed in the molecule i. R_B is the relaxation rate due to dipole-dipole interactions between nuclear spins on different molecules, i.e., those interactions which vary as $Y_{2m}(\Omega_{ij})/r_{ij}^3$, where $\mathbf{r}_{ij}=(r_{ij},\ \Omega_{ij})$ is the vector joining a pair of spins on different molecules [7]. R_C is the relaxation rate due to the interaction between the nuclear spins and the rotational angular momentum $\mathbf{J}_i$ of the same molecule [8] (the spin-rotation interaction).

Of the three terms contributing to T_1^{-1} in eq (5), a molecular theory is available only for R_B [7], which is expressed in terms of Fourier transforms of the correlation functions

$$J(\omega)=\iint d\mathbf{r}d\mathbf{r}'e^{-i\omega\tau}g(\mathbf{r},\ \mathbf{r}',\ \tau)\frac{Y_{2m}(\Omega)}{r^3}\frac{Y_{2m}^*(\Omega')}{r'^3}d\tau \tag{6}$$

where $g(\mathbf{r},\ \mathbf{r}',\ \tau)$ is a time dependent pair distribution function for the system; $g(\mathbf{r},\ \mathbf{r}',\ \tau)\ d\mathbf{r}d\mathbf{r}'$ is the probability that the vector joining a *pair* of molecules is between $\mathbf{r}$ and $\mathbf{r}+d\mathbf{r}$ initially and between $\mathbf{r}'$ and $\mathbf{r}'+d\mathbf{r}'$ at a time τ. For a system of identical nuclear spins R_B is expressed in terms of $J(\omega_0)$ and $J(2\omega_0)$. Note that typical values of ω_0 are $\omega_0 \leqslant 10^8$ sec^{-1} which is an extremely low frequency insofar as the dynamical motions of fluids are concerned. The other important point to notice about eq (6) is that $J(\omega)$ gets its major contribution from pairs of molecules which are very close together, because of the r^{-3} dependence of the dipole-dipole interaction.

Physically, one can say that R_B gives a measure of a specific type of inelastic scattering cross section corresponding to collisions between pairs of molecules in which the total nuclear Zeeman energy is changed. The low frequency ω_0 corresponds to the fact that the energy exchanged between the spin system and the translational degrees of freedom is very small ($< 10^{-7}$ eV).

There are no detailed molecular theories for R_A and R_C in dense fluids, except for liquid H_2 [9], and this has inhibited the interpretation of the many T_1 measurements already performed on liquids

209-493 O-66—13

in molecular systems. R_A and R_C are related to low-frequency Fourier transforms of correlation functions of $Y_{2m}(\Omega_i(t))$ and $\mathbf{J}_i(t)$. Since the interactions responsible for molecular reorientation are the anisotropic intermolecular interactions, the correlation functions of $Y_{2m}(\Omega_i(t))$ and $\mathbf{J}_i(t)$ are each related to correlation functions of these (short range) anisotropic interactions in a manner which has been defined for one system [9], that of H_2. It is very likely, in the light of the theory for H_2, that R_A and R_C can be expressed in terms of Fourier transforms of correlation functions similar to that of eq (6), for interactions of shorter range than r^{-3}.

The behavior of T_1 near the critical point; From the preceding discussion, we can see that the quantity of interest in the interpretation of T_1 is $g(\mathbf{r}, \mathbf{r}', \tau)$ *at short range*, i.e., for $r, r' \lesssim R_0$, the range of the *inter*molecular interactions. Defining $j(\mathbf{r}, \mathbf{r}', \omega)$ by

$$j(\mathbf{r}, \mathbf{r}, \omega) = \int_{-\infty}^{\infty} e^{-i\omega\tau} g(\mathbf{r}, \mathbf{r}'\tau) d\tau \qquad (7)$$

the quantity of interest *in the low-frequency limit* is $j(\mathbf{r}, \mathbf{r}', 0)$, i.e., the area under the time dependent pair distribution function for $r, r' \lesssim R_0$. This problem is analogous to the calculation of the area under the correlation function for relative orientations of neighboring spins near the ferromagnetic Curie temperature. The interpretation of T_1 near the critical point may be compared with the inelastic scattering of neutrons, which is dominated by the long range correlations. Unlike the short range parts of $g(\mathbf{r}, \mathbf{r}', \tau)$ of interest here, the long range parts can be studied explicitly near the critical point by the methods of macroscopic fluctuation theory [10].

Experimental results for T_1: The simplest type of system in which to investigate T_1 near the critical point is a system such as He^3 in which $R_A = R_C = 0$. However, because of the smallness of R_B near the critical point, special precautions would have to be taken to eliminate spin relaxation due to collisions with the walls of the container and such a study has not yet been carried out. For all the systems studied near the critical point thus far $R_A + R_C \gg R_B$.

The first study of T_1 near the critical point was conducted on SF_6 by Schwartz [11]. Since then several substances have been studied including benzene and some of its derivatives [12], HCl and HBr [13], and ethane [14] (C_2H_6). The results obtained are qualitatively similar for all the cases studied, but the study of ethane by Noble is the only one in which care was taken to ensure that the sample was in thermodynamic equilibrium near the critical point. He usually kept the sample at constant temperature for 24 hrs before making T_1 measurements and then made a second set of measurements after waiting for an additional 24 hrs. The temperature gradient across the sample was less than 0.004 °C.

As may be seen from figure 2, Noble's critically loaded samples were in *vertically mounted* glass tubes and he made measurements on two regions,

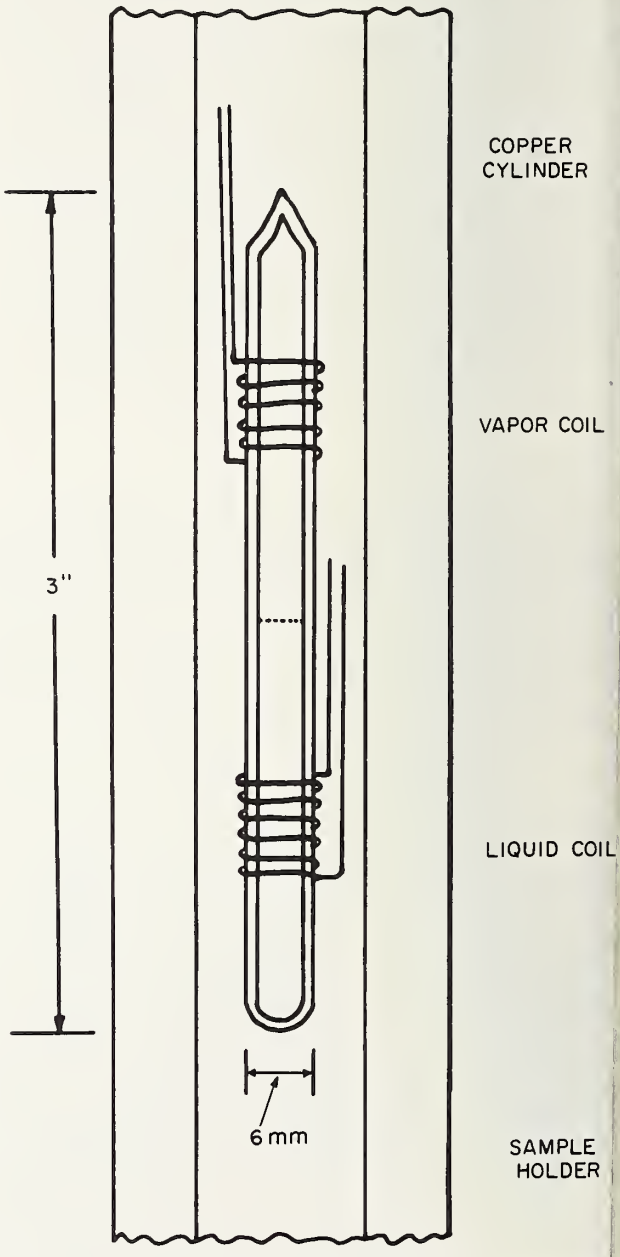

FIGURE 2. *Drawing of sample holder used by J. D. Noble showing location of r-f coils.*

one in the lower half and the other in the upper half of the tube so that none of his measurements actually corresponds to the critical point. The amplitude of the NMR signal for each of the coils is proportional to the density of the sample within the coil. The effect of gravity on the ratio of densities in the two coils ρ_L/ρ_V, corresponding to the ratio of the liquid to vapor densities below the critical temperature T_C, is important as may be seen from figure 3. ρ_L/ρ_V in the pure sample is compared with those obtained by other techniques [15]. The measurements in the impure sample will be used later in interpreting the measurements of D made in that sample.

It should be noted that for the critically loaded samples, the meniscus separating the liquid and solid phases below T_C is observed to remain in a fixed position midway up the sample tube in the region of temperature not too far below T_C. Thus, in this temperature range, one can say that $\rho_L + \rho_V \approx 2\rho_C$ independent of temperature, where $\rho_C = 0.207$ g/cm^3 is the critical density. Therefore, the measurement of ρ_L/ρ_V is sufficient to determine the densities ρ_L and ρ_V in the region of temperature in which the meniscus is constant.

It was found that for the region $T < T_C$, the value of T_1 obtained for the liquid was always longer than that obtained for the vapor in equilibrium with the liquid. This indicates that the time required for molecular reorientation in the liquid is always shorter than for the less dense gas. The results are qualitatively similar to those obtained for other systems [11, 12, 13] and have been obtained over a wide range of temperatures [14]. Figure 4 shows T_1 for the sample in each of the two coils in the vicinity of T_C.

Experimental results for the diffusion constant D: Noble has also measured the diffusion constant in ethane with approximately 1 percent O_2 impurity added [14, 16] (see fig. 3) The O_2 was added to reduce T_1 and thereby enable more accurate results to be obtained for D since the experiment could be repeated more often. The measurements of D as a function of temperature near T_C are shown in figure 5. The estimated maximum error in the measurements is ± 5 percent including systematic

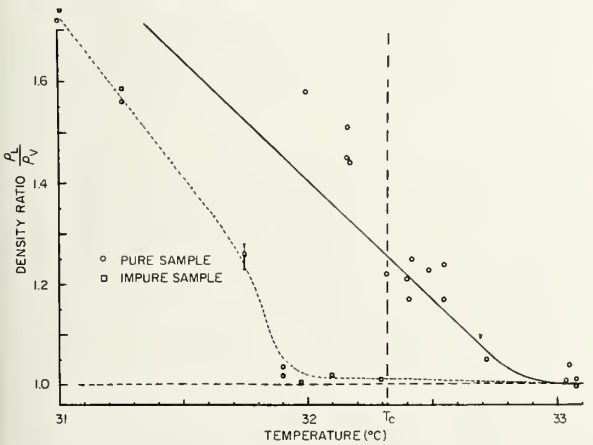

FIGURE 3. *The ratio ρ_L/ρ_V of the average density of the ethane within the lower coil to the average density within the upper coil as measured by the relative amplitudes of the NMR signals using each of the coils.*
Measurements are shown for pure ethane and for ethane with 1 percent O_2 added. The measurements for pure ethane are in good agreement with those of Palmer [13].

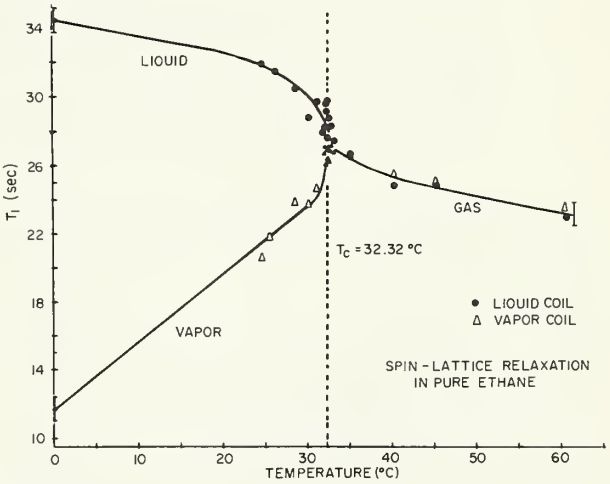

FIGURE 4. T_1 *as a function of temperature in a pure sample of ethane which was critically loaded and mounted vertically.*
Values are shown for the region of temperature near T_C for nuclei in the upper and lower parts of the sample tube respectively.

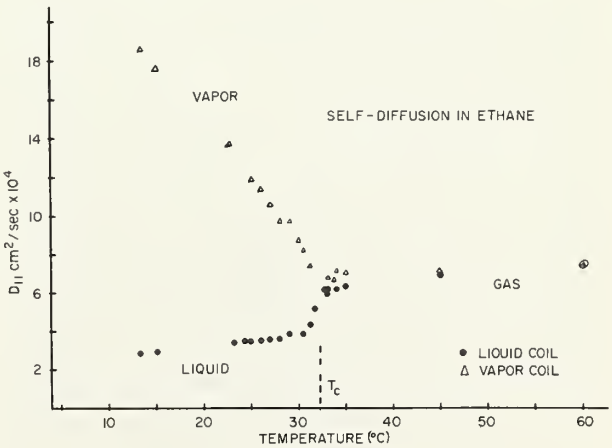

FIGURE 5. *Self-diffusion constant* D *as a function of temperature in ethane with approximately 1 percent O_2 added as an impurity.*
The sample was critically loaded and mounted vertically. Values of D are shown for nuclei in the upper and lower parts of the sample tube respectively.

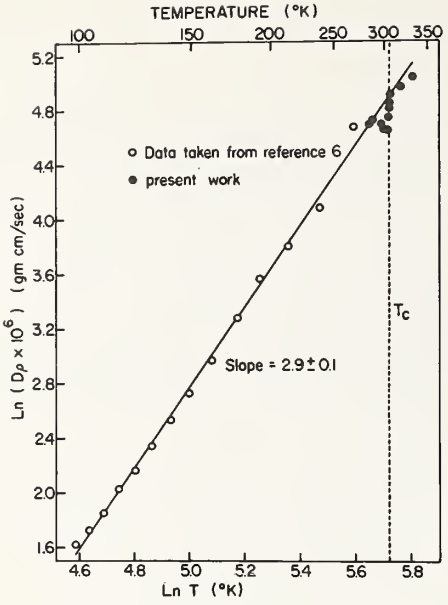

FIGURE 6. *Plot of* ln (Dρ) *versus* ln T.
The points below 0 °C are based on the smooth curve drawn through the diffusion constant data of reference 17.

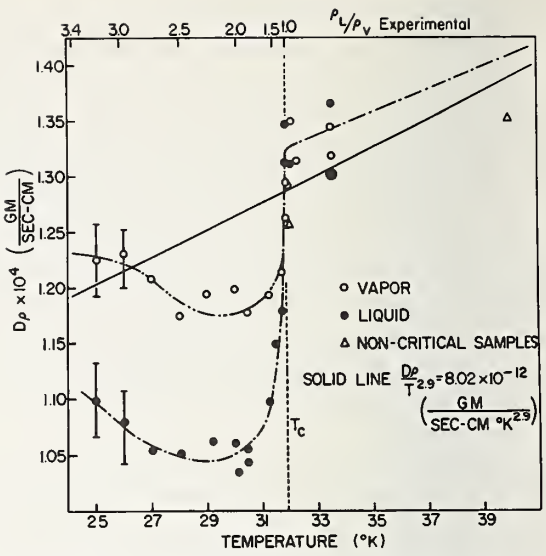

FIGURE 7. *Plot of* D_ρ *versus temperature near* T_C.
Measured values of ρ_L/ρ_V are also shown. The samples used were loaded to the critical density. Measurements of D_ρ based on the slopes of $1/D$ versus ρ plots at 32 and 40 °C using noncritically loaded samples are also shown. The dotted line at 31.9 °C labeled T_C is an upper limit for the critical temperature since it is the lowest temperature at which $\rho_L/\rho_V = 1$, within experimental error.

errors, while the measurements of ρ_L/ρ_V are accurate to ± 2 percent.

Interpretation: Experiments performed at 32 and 40 °C *in noncritically loaded samples* showed that $D \propto \rho^{-1}$ in the range $\rho_C/2 < \rho < 2\rho_C$. *Thus* $D\rho$ *is a function of temperature only in this density range* far from the critical point. A plot of ln $(D\rho)$ versus ln T from just above the melting point at 89.9 to 333 °K approximately 30 °K above the critical point, is shown in figure 6. The results of Gaven, Stockmayer, and Waugh [17] far from the critical point are included. The resulting straight line gives $D\rho \propto T^{2.9 \pm 0.1}$. This is an empirical relationship which does not necessarily hold for other substances. Figure 7 gives a plot of $D\rho$ versus T in the temperature region within a few degrees of T_C. A comparison with the results of figure 6, as given by the solid line of figure 7, shows that $D\rho$ goes through a pronounced minimum for the liquid near T_C with its minimum value about 20 percent below the solid line. A similar but smaller effect is observed for the vapor but, unlike the data for the liquid, we cannot say definitely that the vapor minimum is not due to a systematic error, which we estimate to be less than 5 percent. A single measurement of D for a pure sample at 24 °C, having an error of ± 10 percent agrees with D for the impure sample.

The interpretation which we propose for the data of figures 6 and 7 is that whereas, for systems not too close to the region of the critical point $D\rho$ is a function of temperature only, the diffusion constant decreases anomalously near the critical point.

In figures 6 and 7, T_C for the impure sample used has been nominally given as 31.9 °C as compared with 32.32 °K. *This actually represents an upper limit for* T_C since it is the temperature at which $\rho_L/\rho_V = 1.0$ within experimental error. Since we do not know the equation of state for the impure sample, we cannot take into account the influence of gravity in a reliable fashion, but an examination of figure 3 indicates that the true value of T_C (or region of T_C) is probably close to the temperature at which $D\rho$ goes through its minimum value.

As far as we know these are the first measurements of a *self* diffusion constant near the critical point. Dr. B. Jacrot has, however, drawn our attention to some published measurements of the diffusion constant of Iodine in CO_2 near the critical point [18], where it is found that the diffusion constant is practically zero. This is consistent with the anomalous decrease observed by Noble for $D\rho$ for ethane near T_C as shown by figures 6 and 7. Obviously, it would be desirable to make further measurements of D near the critical point for samples having better geometry (flat, horizontal samples) and a higher degree of purity, e.g., SF_6 would be a good system to study since the relaxation time T_1 of pure SF_6 is reasonably short [11].

References

[1] E. L. Hahn, Phys. Rev. **80**, 580 (1950).
[2] H. Y. Carr and E. M. Purcell, Phys. Rev. **94**, 630 (1954).
[3] B. H. Muller and M. Bloom, Can. J. Phys. **38**, 1318 (1960).
[4] V. J. Emery, Phys. Rev. **133**, A661 (1964).
[5] E. Fukuda and R. Kubo, Prog. Theor. Phys. **29**, 621 (1963).
[6] A. Abragam, The Principles of Nuclear Magnetism, pp. 298–300, 313–315 (Oxford University Press, 1961).
[7] H. C. Torrey, Phys. Rev. **92**, 962 (1953); M. Eisenstadt and A. G. Redfield, Phys. Rev. **132**, 635 (1963); reference 6, pp. 300–305, 458–466; I. Oppenheim and M. Bloom, Can. J. Phys. **39**, 845 (1961).
[8] P. S. Hubbard, Phys. Rev. **131**, 1155 (1963).
[9] T. Moriya and K. Motizuki, Prog. Theor. Phys. **18**, 183 (1957); T. Moriya, Prog. Theor. Phys. **18**, 567 (1957); M. Bloom and I. Oppenheim, Can. J. Phys. **41**, 1580 (1963).
[10] L. van Hove, Phys. Rev. **95**, 249 (1954).
[11] J. Schwartz, Ph. D. Thesis, Harvard University, (1958), unpublished.
[12] D. K. Green and J. G. Powles, Proc. Phys. Soc. **85**, 87 (1965).
[13] J. S. Blicharski and K. Krynicki, Acta Phys. Pol. **22**, 409 (1962); K. Krynicki and J. G. Powles, Phys. Letters **4**, 260 (1963).
[14] J. D. Noble, Ph. D. Thesis, University of British Columbia (1965).
[15] H. B. Palmer, J. Chem. Phys. **22**, 625 (1954).
[16] J. D. Noble and M. Bloom, Phys. Rev. Letters **14**, 250 (1965).
[17] J. V. Gaven, W. H. Stockmayer and J. S. Waugh, J. Chem. Phys. **37**, 1188, (1962).
[18] I. R. Krichevskii, N. E. Khazanova and L. R. Linshitz, Doklady Acad. Nauk. SSSR **141**, 397 (1961) (in Russian).

Ultrasonic Investigation of Fluid System in the Neighborhood of Critical Points

D. Sette

Instituto di Fisica, Facolta' Ingegneria, University of Rome, Rome, Italy

1. Introduction

It is the intention of this paper to examine the research that has been so far carried out in fluid critical systems by means of sound waves. Since 1940 several authors have attempted to study the propagation of sound waves in order to find information on the nature and the behavior of these particular media: various indications and suggestions have been obtained, which have contributed to a better definition of the problems concerning critical systems. The solution of these problems is however far from complete.

The quantities which are usually measured are the velocity and the sound absorption coefficient; they may be determined as functions of temperature, frequency and, in the case of mixtures, of composition. It must be observed that the information available at present for the systems in which sound measurement have been performed, is only partial because it usually refers to only one of these quantities (i.e., velocity or absorption coefficient) determined in a limited range of one of the variables, temperature, frequency, and composition.

Strong similarities exist between liquid-vapor and liquid-liquid critical systems as well as some dissimilarities. It is preferable for a clearer exposition to review separately the work made on each of the two types of systems, though this procedure will require some repetition. We consider first the case of liquid-vapor critical media.

2. Liquid-Vapor Critical Systems

Table I, although it is not complete,[1] indicates the substances which have been the object of the more extensive experiments. Together with pure liquids, few binary or ternary mixtures have been investigated in the liquid-vapor critical region. The experiments have been performed either at a single frequency or in a rather limited frequency range. Moreover velocity and absorption coefficient determinations have usually not been made on the same system.

Figure 1 gives the results of Tielsch and Tanneberger [5] for the sound velocity in gaseous CO_2 as a function of pressure at constant temperature. In the examined frequency range (0.4–1.2 Mc/s) and in the limits of error (0.2%) no dispersion has been found. The same conclusion was reached by Parbrook and Richardson [3] in the range 0.5–2 Mc/s. The velocity goes through a minimum which becomes sharper and sharper as the temperature approaches the critical one: the minimum velocity

[1] In particular much research of Russion authors is included in thesis not easily available; some results are reported in quotation [9].

TABLE I. *Sound Propagation in Liquids-Vapor Critical Systems*

Substance	T_c	P_c	Temperature	Pressure	Frequency	Quantity measured	Author
Helium	5.1994 °K	1718 mm Hg	$T_c-0.03$ $T_c+0.04$ °K	$p-40$ p_c-35 mm Hg	1 *Mc/s*	c	Chase-Williamson-Tisza [1].
Xenon	16.74 °C	58.2 atm	15–19 °C	.....	0.25–1.25	c,α	Chynoweth-Schneider [2].
Carbon dioxide	31.4 °C	73 atm	19–38 °C	up to 100 atm	0.5–2	c,α	Parbrook-Richardson [3].
.....	.....	.....	28–38 °C	5–98 atm	0.270	c,α	Herget [4].
.....	.....	.....	25–48 °C	35–120 atm	0.410	c,α	Tielsch-Tannaberger [5].
Ethylene	9.7 °C	50.9 atm	7–18.7 °C	up to 100 atm	0.5–2 0.27–0.6	c,α	Parbrook-Richardson [3].
.....	.....	.....	9.7–23 °C	35–75 atm	0.27–0.6	c	Herget [4].
Hydrogen chloride	51.4 °C	81.6 atm	38–62 °C 52–62 °C		1.9 1–9	c α	Breazeole [6]. Breazeole.
N_2O Nitrous oxide	36.5 °C	71.7	32–37 °C	55–150 atm	0.96	c	Noury [7].
n-hexane	234.8	29.5 atm	along the saturation curve		2–3	c	Nozdrev [8].
n-heptane	266.8 °C	26.8 atm	.....		2–3	c	Nozdrev.
Methyl acetate	233.7 °C	46.3 atm	along the saturation curve		2–3	c	Nozdrev.
.....	.....	.....	.....		5–13	c	Kal'ianov [10].
.....	.....	.....	.....		.....	.....	Nozdrev [9].
Ethyl acetate	250 °C	37.8 atm	along the saturation curve		2–3	c	Nozdrev [8].
.....	.....	.....	.....		5–9	c	Nozdrev-Sobolev [11].
Propyl acetate	276.2 °C	32.9 atm	along the saturation curve		2–3	c	Nozdrev [8].
Methyl alcohol	240–240.5	78.7 atm	along the saturation curve		2–3	c	Nozdrev.
Ethyl alcohol	243.1	63.1 atm	along the saturation curve		2–3	c	Nozdrev.
Isobuthyl alcohol	283.4	.....	along the saturation curve		2–3	c	Nozdrev.
Sulphur hexafluoride	45.6 °C	36 atm	.....		0.6	c,α	Schneider [12].
Water	374 °C	217.5 atm,	along the saturation curve		2	c	Nozdrev-Osadchii-Rubtsov [13].
Benzene methyl alcohol	239 °C for 10% benzene	.....	along the saturation curve		.....	c	Nozdrev-Taraitova [14].
Benzene methyl-alcohol-toluene	240–320 °C	.....	along the saturation curve		.....	c	Grechkin-Nozdrev [15].

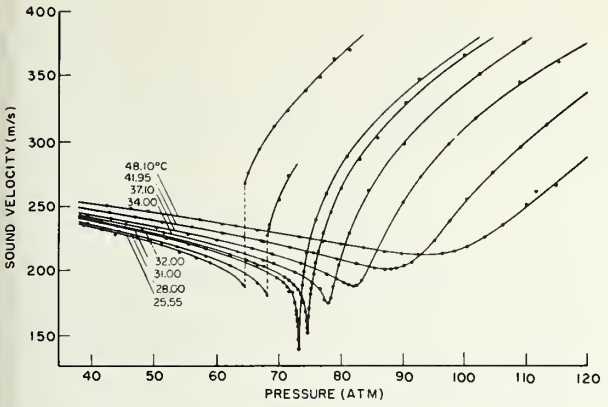

FIGURE 1. *Sound velocity in CO_2 versus pressure, at constant temperature*
(H. Tielsh and H. Tanneberger [5]).

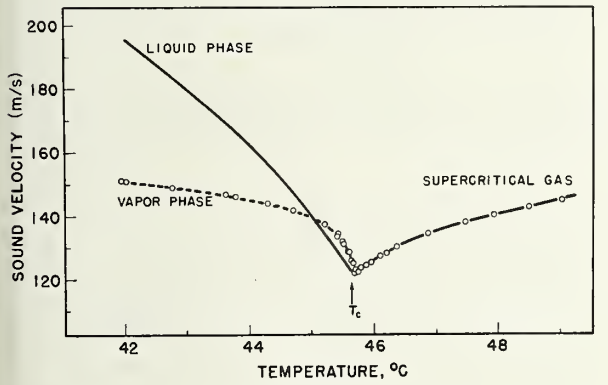

FIGURE 2. *Sound velocity for the liquid and the vapor phase of sulfur hexafluoride (W. G. Schneider [12]).*

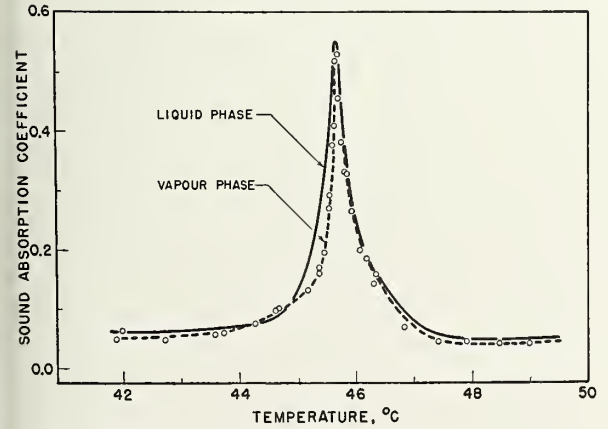

FIGURE 3. *Sound absorption for the liquid and the vapor phase of sulfur hexafluoride (W. G. Schneider [12]).*

measured at 31 °C is about one half of the value in normal conditions.

Figures 2 and 3 give Schneider's results (600 kc/s) on velocity and absorption in sulfur hexafluoride, a nonpolar compound with spherically symmetric molecules [12]: the data are in this case available for the liquid phase as well as for the vapor on both sides of critical temperature (T_c).[2] The velocity in the liquid and in the gas seems, in the limits of experimental errors, to reach a common minimum at a temperature which coincides with T_c; the absorption coefficient in both phases increases very rapidly approaching T_c.[3] The last circumstance has been observed in all systems examined and the various researchers have not succeeded in making a measurement at T_c.

Figures 4 and 5 give the results of Chynoweth and Schneider in xenon [2]. The absorption coefficient was measured at 250 kc/s and it shows a behavior similar to that observed in sulfur hexafluoride when T approaches T_c. The velocity instead was measured in the range 250 kc/s−1,250 Mc/s: a dispersion has been detected whose magnitude is largely higher than the experimental error ($0.2 \div 0.7\%$). We will discuss the inferences of this result shortly. At present we call attention to the fact that Chynoweth and Schneider have not noticed any tendency of velocity towards a discontinuity or a sudden drop to zero when T approaches T_c. Until recently, this has been a general conclusion of experiments. Nozdrev [8], for instance, who has made velocity measurements using light diffraction by sound waves, claims to have been able to visually follow the continuous change of sound velocity through the critical point.

The fact that the velocity of sound remains finite at the critical point is in agreement with standard thermodynamics [16]. In this state, the derivative of pressure respect to volume at constant temperature vanishes: $\left(\frac{\partial p}{\partial v}\right)_T = 0$. Consequently, the specific heat at constant pressure (C_p) is infinite while C_v, the adiabatic compressibility and the sound velocity stay finite.

It may be of some interest, at this point, to mention some results that have been obtained by Nozdrev [8, 9] who has performed extensive velocity

[2] The full and broken lines above T_c in figure 3 correspond to measurements in the supercritical gas performed respectively near the sound source and far from it.

[3] The velocity and absorption curves for liquid and vapor as obtained by Schneider cross at about 0.6 °C below T_c. This fact, which has no simple explanation, has not been found in any other case although some systems have been purposely investigated [8].

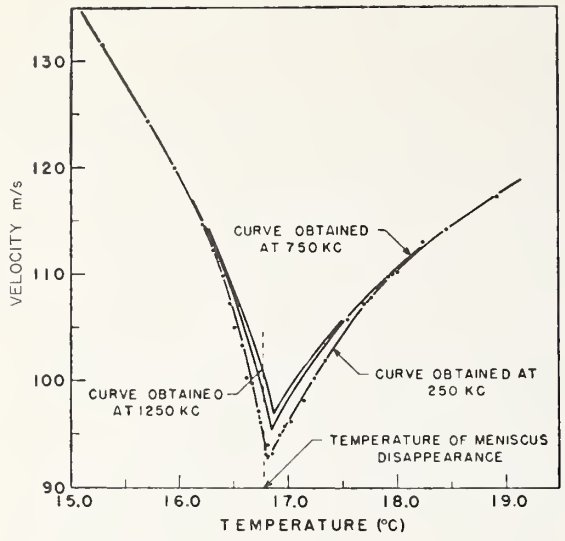

FIGURE 4. *Sound velocity versus temperature in xenon (A. G. Chynoweth and W. G. Schneider [2]).*

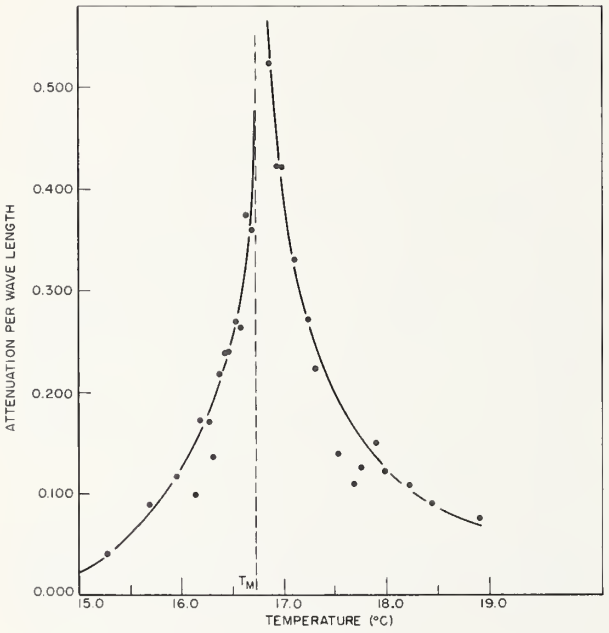

FIGURE 5. *Absorption per wavelength ($\alpha \cdot \lambda$) versus temperature in xenon (A. G. Chynoweth and W. G. Schneider [2]).*

measurement in critical fluids along the saturation curve. He has found, in the limits of error of his instrument, that the velocity variation along the saturation curve in both vapor and liquid near the critical temperature can fairly well be expressed by using van der Waals equation of state in the case of organic unassociated substances. This conclusion is not true for the liquid phase of associated liquids (e.g., ethyl alcohol) which proves that associations may persist up to the critical point. Moreover, in the absence of dispersion and in the limits of experimental errors, Nozdrev establishes an empirical simple relation between the arithmetical average of sound velocities in the gas (c_v) and in the liquid (c_L) and ($T-T_c$)

$$\frac{c_v+c_L}{2}=c_{cr}+a(T_c-T) \qquad (1)$$

being c_{cr} the common velocity at T_c and a a constant. This relation would be valid in the range between T_c and a temperature 15 to 30 °C below.

The standard thermodynamical treatment of critical state from which the conclusion on C_p, C_v, and c have been deduced, derives from some assumptions on the behavior of thermodynamical functions near the critical point:[4] in particular it is assumed that the thermodynamical quantities (as function of V and T) do not show mathematical singularities along the curve which limits the region in which the substance can not exist as a homogeneous phase either in stable or in metastable equilibrium. Only in such case the above-mentioned limit curve is determined by $\left(\frac{\partial p}{\partial v}\right)_T=0$ at the critical point alone.

The truth of this treatment has been seriously questioned recently. Some experimental results on C_v in argon [17] and in oxygen [18] have been obtained which indicate a logarithmic temperature dependence of such a specific heat near the critical point. If this behavior remains unchanged up to the critical point, C_v and the adiabatic compressibility would be ∞ and $c=0$ at $T=T_c$ [19].

To obtain further information, Chase, Williamson, and Tisza [1] have performed sound velocity measurements in helium much more carefully and precisely than used in previous investigation near the critical point. The temperature was regulated to $\pm 10^{-4}$ °K (instead of $\pm 2.10^{-3}$ °K in Chynoweth and Schneider measurements in Xenon), the pressure to ± 0.1 mm Hg; the velocity measurements were performed with a phase sensitive method having a resolution of 0.01 percent (the error in the Chynoweth-Schneider setup was ± 0.2 -0.7%). Figure 6 gives the results obtained for the velocity both as a function of temperature (at a pressure $p=1718\pm 1$ mm Hg practically coinci-

[4] Quotation [16] p. 262.

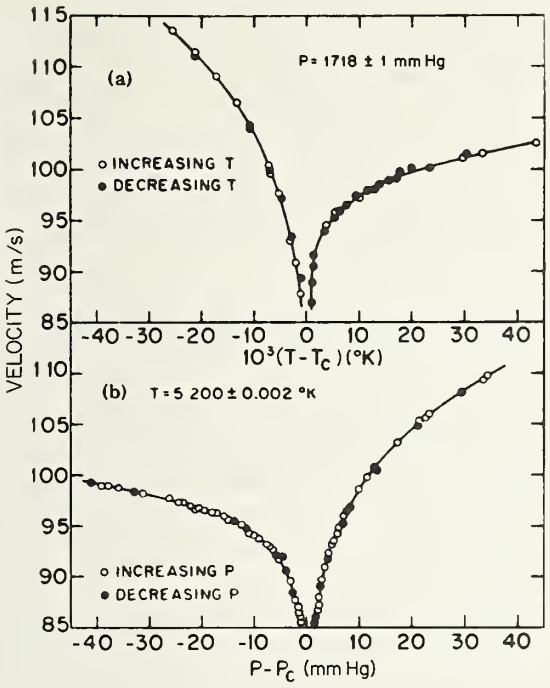

FIGURE 6. *Sound velocity as a function of temperature (a) and pressure (b) in the critical region of helium (C. E. Chase, R. C. Williamson, and L. Tisza [1]).*

dent with p_c) and as a function of pressure (at temperature 5.200 ± 0.0002 °K practically coincident with $T_c = 5.1994$ °K). The velocity decreases rapidly approaching the critical point. High absorption has not allowed measurements over a region of about 2.10^{-3} °K or 2.5 mm Hg.

The fast decrease of c approaching the critical point in the range of temperature or pressure examined makes Chase, Williamson, and Tisza think the limit zero for c at T_c to be possible. The adiabatic compressibility K_S as a function at T or p has been calculated making suitable approximations for density: in the range examined, K_S seems to have a logarithmic singularity similar to that found for C_v in argon and oxygen.

This recent research, having questioned the standard thermodynamical treatment of critical states, opens a new exciting field of investigation. It must be observed, however, that the experimental results so far obtained, although they have caused serious doubts on the exactness of traditional thermodynamical treatment have not yet definitely proved it wrong. The measurement of c in helium for instance, shows a fast decrease of velocity when T approaches T_c, but at a separation of 10^{-3} °K from T_c the velocity has still a value quite different from zero. The possibility of a leveling off at a much lower but finite value has not yet been excluded.

The behavior of velocity, C_v and adiabatic compressibility at the critical point remains a very interesting and exciting problem, which may clarify in depth the nature of systems in the critical state: it requires further experimental as well as theoretical research.

Closely related to the nature of liquid-vapor critical systems is also the enormous absorption that these media show. Two mechanisms have been proposed: [5] scattering and relaxation.

A. G. Chynoweth and W. G. Schneider [2] have studied sound propagation in xenon in the hope of finding out which is the more important dissipative process. On the basis of an approximate calculation of scattering losses produced by inhomogeneities due to density fluctuations in the medium, they conclude that these losses do not appear sufficiently large to explain the experiment. They believe therefore that, as Schneider had already suggested in the case of sulfur hexafluoride, the more important dissipative mechanism is structural relaxation caused by sound-induced perturbation of equilibrium among molecular aggregates (clusters) present in the medium. The sound dispersion found in xenon (fig. 4) gives support to this explanation of high absorption. The relaxation phenomena would be characterized by a distribution of relaxation times.

Different conclusions were reached by H. D. Parbrook and E. G. Richardson [3] studying CO_2 and by M. A. Breazeale [6] in hydrogen chloride. The last author was unable to detect dispersion in the range 1 to 3 Mc/s; the absorption results could be interpreted as produced by relaxation processes with a wide distribution of relaxation times, but it seems also possible to explain them on the basis of a scattering mechanism if correlations between density fluctuations in adjacent volumes are taken into account. To evaluate the scattering losses, Breazeale, as already Chynoweth and Schneider had indicated, chooses the Libermann-Chernow [20, 21] formula, which was developed to deal with sound absorption caused by temperature inhomogeneities in the ocean. In the calculation of this formula the validity of an exponential autocorrela-

[5] It seems that losses due to finite amplitude of waves cannot have importance, as experiments have shown that the signal detected by a sound receiver depends exponentially on the source-receiver distance.

tion function is assumed. The absorption coefficient due to scattering by inhomogeneities of diameter a is

$$\alpha_S = 8 \left(\frac{\Delta c}{c}\right)^2 \frac{k^4 a^3}{1+4a^2k^2} \qquad (2)$$

where $k=\frac{2\pi}{\lambda}$ and $\frac{\Delta c}{c}$ is the fractional change of sound velocity. In order to make a numerical calculation a was chosen 10^{-4} cm, i.e., approximately 10^3 molecular diameters as suggested by light scattering in various substances near the critical point; moreover, the value 0.25 was used for $\frac{\Delta c}{c}$. Figure 7 gives Breazeale's experimental results at various temperatures; the flags indicate the limits of errors. These results seem to depend upon the square of the frequency (dotted lines). The solid line on the same figure gives α_S calculated from (2) with above mentioned values of a and $\frac{\Delta c}{c}$; the correct order of magnitude of α is obtained; according to Breazeale the deviation of the experimental curves from the Libermann-Chernow curve, which essentially corresponds to a dependence of α from ν^4, could be explained by using an adequate correlation between density fluctuations in neighboring volumes. Breazeale is therefore of the opinion that, while relaxation may be important at lower frequencies, scattering is most likely the main source of absorption in the range 1 to 9 Mc/s.

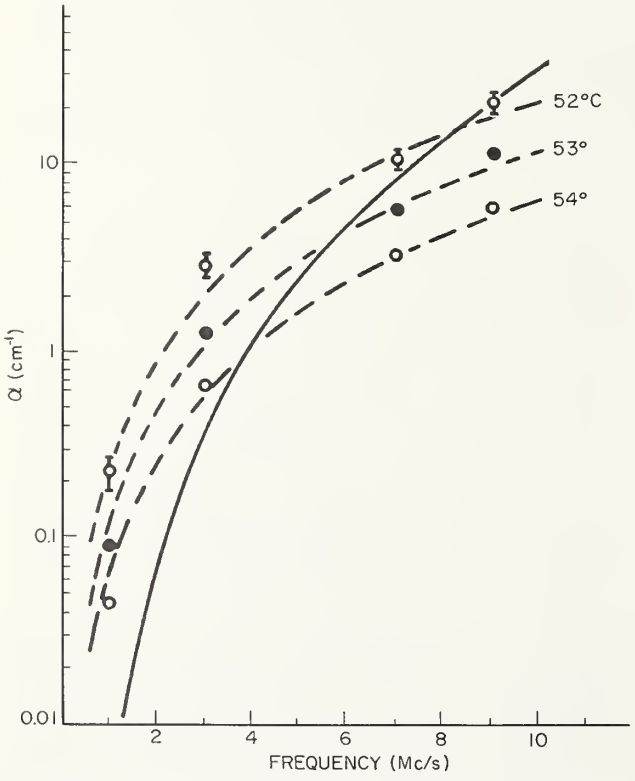

FIGURE 7. *Absorption coefficient versus frequency at different temperature in the super critical region of hydrogen chloride (M. A. Breazeale [6]).*

3. Mixtures of Partially Soluble Liquids

Table II indicates the few systems which have been studied in some way in the critical region of solubility. Almost all research has been limited in each system to only one mixture with a composition close to that of the maximum (or minimum) of the solubility curve.

Figure 8 is relative to a mixture having 47.6 wt percent of n-hexane in aniline [2]. The velocity was measured at 600 kc/s. The values of c in the two separate phases approach each other as T tends to T_c. On this basis, Chynoweth and Schneider formulated the tentative conclusions that the velocity in the three phases gradually tends to the same value as T approaches T_c and that no anomalous behavior is present. A different indication, however, emerges from the work of M. Cevolani and S. Petralia [23] in the aniline-cyclohexane mixture (49 wt % of cyclohexane) (fig. 9).

More research is needed to determine the exact behavior of velocity in the three phases in the immediate proximity of T_c; the use of apparatus today available with smaller errors than those so far used in this kind of experiment should allow precise information.

No great effort, so far, has been made to investigate dispersion in the critical region of solubility and the few indications available [26] do not allow to reach any conclusion on the subject.

A common experimental finding is the high attenuation of sound waves in the critical region. Figure 10 [22] shows the typical behavior of the absorption coefficient per wavelength ($\alpha \cdot \lambda$) as a function of temperature through the critical region of solubility: it refers to the triethylamine-water system (44. 6 wt % of amine) at 600 kc/s. Figure 11 [25] gives the parameter $\frac{\alpha}{\nu^2}$ for mixtures n-hexane-nitrobenzene as a function of composition;

TABLE II. *Sound Propagation in Mixtures of Partially Soluble Liquids*

System	Composition	T_c	Quantity measured	Temperature range	Frequency range	Author
		°C		°C	*Mc/s*	
Aniline *n*-hexane	47.6% w *n*-hex	68.3	c, α	55–74	0.6	Chynoweth-Schneider [22].
Aniline cyclohexane	51% w an.	.....	c, α	15–55	3	Cevolani-Petralia [23].
Do.....	20–63% mole an	30.7	c, α scattering	29–34	1.5–5	Brown-Richardson [24].
Nitrobenzene *n*-hexane	0–100	21.02 °C	α	25	8	Sette [25].
	53.2 w% nitrob.	23.2	.....	23–28	1–9	Alfrey-Schneider [24].
Water-triethylamine	44.6 w% am.	17.9	c, α	10–28	0. 6	Chynoweth-Schneider [22].
	44.6 w% am.	.....	α	15	7–54	Sette [25].
	34 w% am.	19.5	.....	10–20	1–9	Alfrey-Schneider [24].
Water-phonol	34 w% Ph.	66	c, α	51–80	3	Cevolani-Petralia [23].

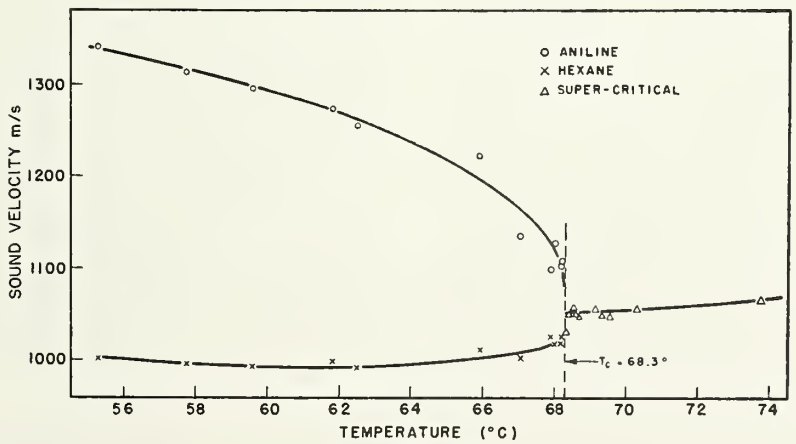

FIGURE 8. *Sound velocity through the critical region of the aniline-hexane system (A. G. Chynoweth and W. G. Schneider [2]).*

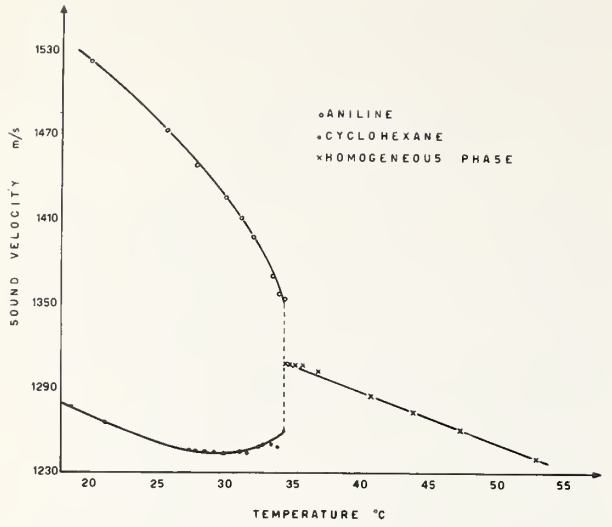

FIGURE 9. *Sound velocity through the critical region of the aniline-cyclohexane system (M. Cevolani and S. Petralia [23]).*

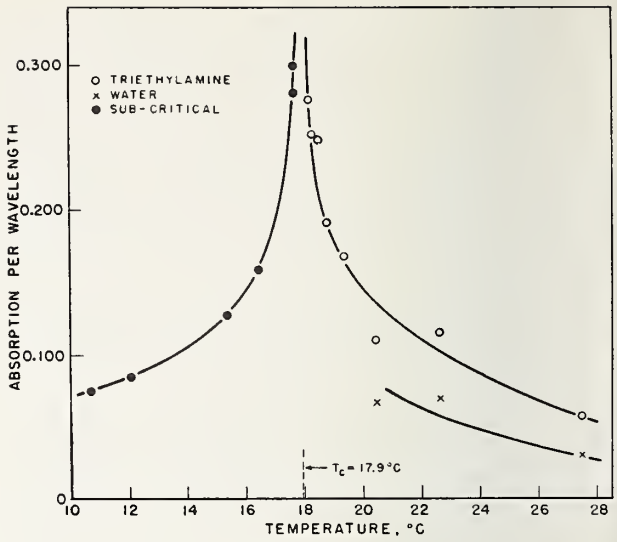

FIGURE 10. *Sound absorption per wavelength ($\alpha \cdot \lambda$) versus temperature for the water-triethylamine system (A. G. Chynoweth and W. G. Schneider [22]).*

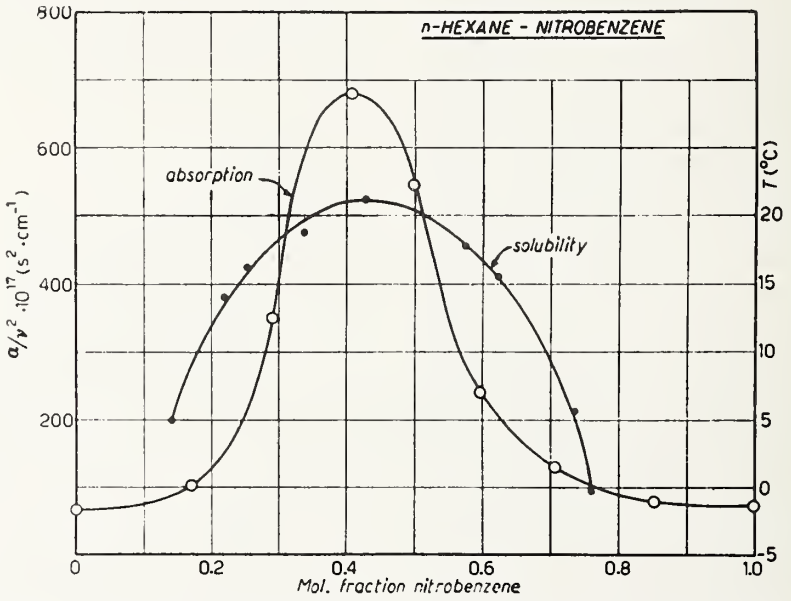

FIGURE 11. *Sound absorption versus composition and coexistence curve for* n *hexane-nitrobenzene mixtures (D. Sette [25]).*

the experiment was performed at 25 °C, i.e., at a temperature 4 °C higher than the consolute temperature. The comparison of the results in figures 10 and 11 with those obtained in the liquid-vapor critical region (figs. 3 and 5) shows that in the critical solubility case the processes which give rise to additional losses operate in a wider range of temperature around the critical one. This fact indicates an essential difference between the two types of systems.

Various attempts have been made to find out what the process responsible for the largest part of losses in these systems is. The dissipative causes which have been examined are viscosity, relaxation, and scattering. Let us briefly review the research made on this subject.

3.1. Viscosity and Thermal Conductivity

Different from the case of liquid-vapor critical media, the viscosity coefficient (η) of mixtures formed by partially soluble liquids undergoes a large increase when temperature approaches the critical one. However, the classical losses due to this fact, i.e., calculated with Stokes' formula for an homogeneous medium, would be still inadequate to explain the experiment: the total viscosity absorption coefficient would amount to a few per mille of the observed value.

The fluid however is not homogenous. R. Lucas [27] has calculated the sound absorption coefficient when density fluctuations are present in the liquid. Lucas assumes that the density fluctuations are time independent and isotropic and that the sound velocity does not vary along the direction of propagation. Moreover he maintains Stokes' relation between the two viscosity coefficients. The absorption coefficient then results

$$\alpha_{\eta}^{*} = A\nu^2 + B \tag{3}$$

where

$$A = \frac{8\pi^2}{3}\frac{\eta}{\rho_0 c^3}\left(1 + \frac{1}{\tau}\int_0^{\tau} s^2 d\tau\right)$$

$$B = \frac{10}{9}\frac{\eta}{\rho_0 c}\frac{1}{\tau}\int_0^{\tau}\left(\frac{\partial m}{\partial x}\right)^2 d\tau$$

and ρ_0 the average density; ρ the local density; $m = \frac{\rho_0}{\rho}$; s, the condensation, given by $\rho = \rho_0 (1+s)$; $d\tau = dxdydz$ the volume element of the liquid. A and B depend upon the properties of the liquid and the density fluctuations in it, but they are frequency-independent. As a consequence of the presence of density fluctuations, the expression of the absorption coefficient has two corrective terms for Stokes' expression

$$\alpha_{\eta} = \frac{8\pi^2}{3}\frac{\eta}{\rho_0 c^3}. \tag{4}$$

The first corrective term has the same frequency dependence of the Stokes' term, the second one is constant with frequency. The parameter $\frac{\alpha_{\eta}^{*}}{\nu^2}$ therefore decreases with frequency. Such behavior is generally found in these kinds of mixtures; figure 12 [25] gives some results for a mixture water-triethylamine with 44.6 wt percent of amine. Unfortunately, however, a similar decrease of $\frac{\alpha}{\nu^2}$ with frequency can be expected also in the case of other dissipative effects, mainly of the relaxation type.

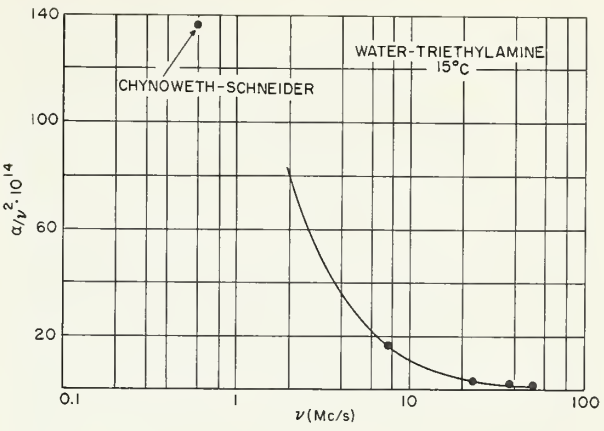

FIGURE 12. *α/ν^2 versus frequency far a water-triethylamine mixture at 15 °C (D. Sette [25]).*

A calculation using the Lucas' formula has been carried out for the water triethylamine mixture for which data on the thermodynamic behavior of the system are available. Rough approximations were introduced; the results seem to indicate however that, though the viscosity losses in the inhomogenous medium are higher than those given by Stokes' formula and may become of some importance at low frequencies, they are still insufficient to explain the largest part of the observed attenuation.

Another cause of losses is the existence of thermal conductivity. The corresponding contribution to absorption coefficient in normal liquids is much smaller than the viscosity term. Although thermal conductivity determinations in critical region are missing in the literature, it seems unlikely that thermal conductivity substantially contributes to the large absorption found in the critical media.

3.2. Scattering

A rough description of the medium is obtained by thinking of the system as formed by a mother phase in which clusters of various sizes and compositions are dispersed. The presence of inhomogeneities may lead, as in the case of liquid-

vapor critical systems, to scattering of sound energy. On the importance of this process the opinions do not entirely agree.

The dimensions of individual clusters as determined by light scattering experiments are of the order of wavelength of visible light ($0,5 \cdot 10^{-6}$ m), i.e., much smaller than the sound wavelength ($\sim 10^{-3}$ m at 1 Mc/s) in the frequency range of experiments: if the clusters acted as individual scatters the contribution of scattering to sound energy loss would be very small. It is however necessary to assume, as in the case of liquid-vapor critical systems, that there actually are strong correlations between fluctuations in adjacent volumes. If one considers Liebermann's theory in which an exponential autorrelation is assumed one finds a dependence of α on frequency which is not much different from proportionality to the fourth power of ν, i.e., $\frac{\alpha}{\nu^2}$ should increase with frequency. This is contrary to some experiments where this parameter has been found decreasing within the range examined: figure 12 refers to water-triethylamine mixtures and similar results have been obtained in nitrobenzene-*n*-hexane (5 to 95 Mc/s).

Liebermann's theory therefore does not seem satisfactory for an explanation of the experimental results, and it is at the present difficult to see whether by using an adequate correlation function, it is possible to explain the entire increase of absorption in the critical mixture by means of scattering.

Some experiments however have definitely shown the existence of scattered energy in a critical mixture when sound goes through it. Recently A. E. Brown and E. G. Richardson [26] have shown this effect in aniline-cyclohexane mixtures. These authors have measured the energy received by a probe whose axis forms an angle θ with the sound beam radiated from the source. At 1.5 and 2.5 Mc/s a broadening ($4 \div 5°$ at 2.5 Mc/s) of the beam radiated has been observed when the source is in the critical mixture. At 5 Mc/s, while the intensity falls to zero (first minimum) at an angle θ of 1.5° if the medium does not contain inhomogeneities when the radiation takes place in a critical mixture one obtains patterns of relative intensities at various angles θ as those shown in figure 13. From the position of maxima and minima the authors calculate dimensions of effective scatters, which are of the order of magnitude of 100 to 400μ (compared with $\lambda = 500\mu$). Table III gives the experimental

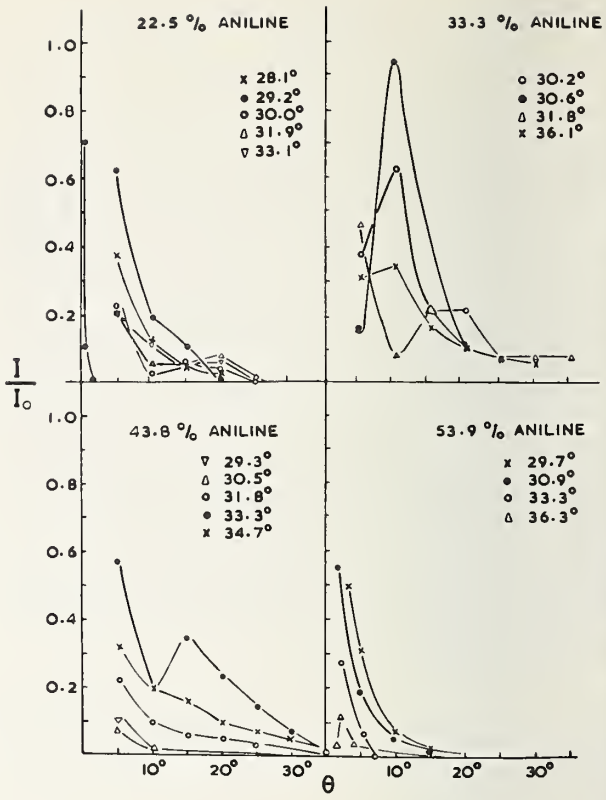

FIGURE 13. *Angular distribution of scattered sound at 5 Mc/s in aniline-cyclohexane mixtures (A. E. Brown and E. G. Richardson [26]).*

TABLE III

Temperature °c	$f = 1{\cdot}5$ Mc/s			$f = 2{\cdot}5$ Mc/s			$f = 5{\cdot}0$ Mc/s		
	α	α_s	c	α	α_s	c	α	α_s	c
22·5% aniline									
34				0·057	0·011	1262	0·145	0·11	1260
33				0·070	0·030	1262	0·15	0·11	1260
32				0·080	0·035	1262	0·15	0·11	1262
31				0·097	0·023	1262	0·155	0·11	1264
30·5				0·115	0·023	1262	0·17	0·12	1266
30				0·140	0·011	1262	0·185	0·14	1268
29·25				0·105	0·06	1262	0·26	0·145	1270
33·3% aniline									
34	0·042	0·006	1281	0·09	0·055	1282	0·23	0·20	1288
33	0·045	0·007	1284	0·105	0·055	1282	0·23	0·20	1291
32	0·057	0·011	1288	0·130	0·055	1289	0·25	0·17	1288
31	0·060	0·02	1294	0·160	0·055	1289	0·40	0·17	1294
30·5	0·057	0·007	1296	0·132	0·055	1296	0·25	0·20	1297
43·8% aniline									
34	0·050	0·035	1312	0·080	0·063	1318	0·24	0·17	1310
33	0·057	0·035	1317	0·086	0·063	1319	0·27	0·20	1316
32	0·092	0·035	1323	0·130	0·070	1322	0·30	0·15	1322
31	0·083	0·04	1323	0·160	0·046	1319	0·38	0·05	1333
30·5	0·077	0·052	1323	0·140	0·046	1318	0·32	0·03	1342
53·9% aniline									
34	0·040	0·035	1355	0·070	0·052	1360	0·14	0·023	1356
33	0·040	0·035	1355	0·075	0·046	1360	0·16	0·023	1361
32	0·040	0·035	1356	0·087	0·043	1361	0·18	0·023	1360
31	0·055	0·030	1359	0·14	0·058	1371	0·23	0·035	1359
30·5	0·054	0·030	1360	0·115	0·050	1375	0·23	0·029	1365
30	0·080	0·023	1360	0·092	0·058	1379	0·26	0·035	1376

absorption coefficient (α) and the coefficient that Brown and Richardson determine as due to scattering (α_s) for mixtures of the composition examined and at the frequencies used. These results indicate a substantial contribution of scattering to the total losses: in this case, scattering appears to be the most important dissipative process. The authors observe however that, in the limits of experimental error, scattering does not seem satisfactory to explain the totality of losses experimentally found. Using the roughly approximate procedure of subtracting the scattering absorption coefficient from the experimental one, an unexplained part remains which has the same order of magnitude as the absorption coefficient in pure liquids. $\left(\frac{\alpha}{\nu^2}=50\times10^{-17}\,\mathrm{sec^2\ cm^{-1}}\right.$ in aniline and 200 10^{-17} in cyclohexane$\left.\right)$.

3.3. Relaxation Processes

Various researchers have thought that relaxation processes of various kinds may be involved in the propagation of sound waves in critical mixtures and could be responsible for the large absorption experimentally found.

The existence of clusters of various compositions dispersed in a mother phase induces the presence of a great number of equilibria which may be perturbed by the temperature variations due to the sound wave. The kinetics of the system is to be described by reactions which take place either among clusters of different kinds or between clusters and molecules of the mother phase to generate clusters having a new composition. The situation is similar to the one found in binary mixtures of the water-alcohol type when a maximum of the absorption coefficient versus composition is present: in such case, most of the absorption increase seems connected with equilibria which exist among various molecular associations of the two components, and are altered by temperature changes produced by sound waves.

The relaxation processes which arise are of the same kind as those found in liquids where a low rate chemical equilibrium is present and can be described by means of a specific heat function of frequency. Owing to the great number of equilibria present among clusters of various sizes and compositions, a very broad distribution of relaxation times is to be expected. This indication is in agreement with experimental findings: in the case of the water-triethylamine mixture the experimental results (fig. 12) when interpreted on the basis of the relaxation theory, clearly show this fact; a very rough estimation of the range of relaxation frequencies indicates that it extends at least from 2 to 30 Mc/s.

M. Fixman [28, 29, 30] has recently considered in some detail the manner in which the characteristic fluctuations of critical mixtures may cause a frequency dependence of one or more of the thermodynamical quantities which are of importance in sound propagation; he too has reached the conclusion that the specific heat is the quantity most likely to be involved in the observed behavior. In an early attempt [28], he considered a fluctuating heat capacity associated with density fluctuations; adjacent volumes of the liquid reach different temperatures when passed through by a sound wave: sound energy absorption would appear as a consequence of the heat flow in the equalization of temperature gradients. Such a process however can produce a much smaller absorption than observed experimentally and therefore can not be responsible for the high losses observed. The dissipative effect just mentioned is described in the nonlinear equation of motion and energy transport by a term linear both in the temperature variation produced by the sound wave and in the density or composition fluctuations; in Fixman's early treatment other terms which are either quadratic or of higher order in local fluctuations, were neglected.

In a later study Fixman has found the way to handle the quadratic terms and he was able to show that they are strongly coupled with local temperatures; these terms originate an anomalous static heat capacity in agreement with experiment [31] and a frequency dependent heat capacity which could be responsible for the sound absorption increase in the critical region. In this calculation, the composition is expressed as a function of position by means of a Fourier series or integral, with suppression of all Fourier components having a wave number (k) greater than some $k_{\max}$. It is then possible to obtain a fluctuating entropy density $\langle \delta s \rangle$ associated with critical composition fluctuations which is perturbed by the temperature variation produced by sound and gives rise to an excess heat capacity per unit volume

$$\Delta = T_c \frac{\langle \delta s \rangle}{\delta T}. \tag{5}$$

In the expression of $\langle \delta s \rangle$ enters the radial distribution function $g(r)$ at time t expressed by means of the Fourier components up to k_{max}. The dynamics of the long range part of $g(r)$ is assumed to satisfy the diffusion equation

$$\frac{dg}{dt} = h[\kappa^2 \nabla^2 g - \nabla^2 \nabla^2 g] \tag{6}$$

being h a diffusion constant which may be related to more usual parameters and κ the reciprocal of an "indirect" correlation length. For a mixture at the critical composition κ can be expressed by means of a short-range correlation length l

$$\kappa^2 = 6 \frac{T - T_c}{l^2 T_c}. \tag{7}$$

Fixman's analysis led him to conclude that κ^2 is strongly coupled with local temperature and that this circumstance can be the reason for both the increase of static heat capacity and the appearance of a frequency dependence of specific heat. Therefore he substitutes κ^2 with

$$\kappa^2 + \left(\frac{\partial \kappa^2}{\partial T}\right) \delta T \tag{8}$$

and supposes δT to be sinusoidal function of time. Fixman obtains for the complex dynamic heat capacity per unit volume an expression and furnishes a numerical integration of the real and imaginary part close to the critical point.[6]

This expression can be used to calculate the complex speed of sound from which velocity and absorption are derived. The comparison of these theoretical values with experiment requires the knowledge of: (1) the correlation distance 1; (2) a friction constant, β, which enters in the expression of the diffusion constant; (3) the specific heat per mole in the absence of fluctuation C_p^0; (4) the ratio of specific heat $\gamma_0 = \dfrac{C_p^0}{C_v^0}$ in the same conditions. The results of the comparison between theory and and experiment in the case of the mixture *n*-hexane-aniline (47.6 wt % of hexane) studied by Chynoweth and Schneider are indicated in figure 14. C_p^0 and γ_0 were approximately evaluated by the Author while $\beta = 9.10^{13}$ sec^{-1} and $l = 4$ Å were assumed as reasonable values. It appears that the numerical values of the observed absorption as well as its

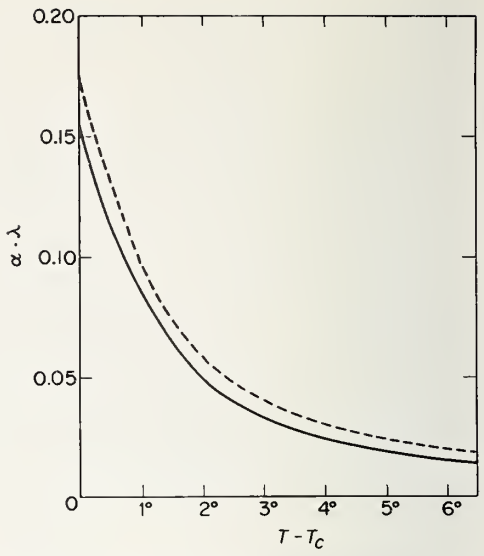

FIGURE 14. *Absorption per wavelength versus* $(T - T_c)$ *for aniline-n hexane critical*
Solid line theoretical, dashed line experimental. (M. Fixman [29]).

variation with temperature could be explained by Fixman's theory. The theory should be tested for the variation of absorption coefficient with frequency.

Fixman's calculation predicts a very small velocity dispersion and this result could be in agreement with experiment because no dispersion has been so far detected in the limits of errors. The variation of velocity with temperature indicated by the theory (3% for a temperature increase of 5 °C above the critical point) is about twice the change observed. Fixman's theory, which could be extended to a liquid-vapor critical system supports the idea that relaxation processes may be an important, if not the most important, dissipation process in the critical systems.

4. Conclusions

At the present status of research, most of the high absorption found in liquid-vapor and liquid-liquid critical systems is most likely due to one or both of the two processes: (1) scattering by inhomogeneities due to density or composition fluctuations, (2) relaxation in the cluster equilibria perturbed by the temperature variations induced by sound waves. It is not possible, at present, to go much further in specifying what the most important process may be in particular cases.

[6] The function has been tabulated by Kendig, Bigelow, Edmunds, and Pings [32].

It is to be mentioned at this point that recently A. S. Sliwinski and A. E. Brown [33] have stressed the importance of a strong difference existing between critical mixtures and liquid-vapor critical systems. In the first case, in fact, the equalization of composition fluctuations must proceed through a diffusion mechanism which is particularly slow near the critical point: instead, the merging of two or more density fluctuations to form a uniform region in a liquid-vapor critical medium does not require diffusion. Such a difference could play an important role when the sound wavelength is either smaller or of the same magnitude than the linear dimension of assemblies: this is the normal case when ultrasonic waves interact with critical systems. The sound wave produces a variation of the pressure and temperature of assemblies around values which are near the critical ones: in the case of liquid-liquid system, as a consequence of the slowness of diffusion in the short time in which the interface between assemblies disappears, the passage of sound does not strongly affect the form and size of assemblies; in the case of liquid-vapor the assemblies lose their identity when the surface tension disappears and they may reappear successively in a form quite different from the original configurations.[7] To support this point of view, Sliwinski and Brown have considered some other experiments which indicate the different ways of interaction of sound waves with a liquid-liquid critical mixture and a liquid-vapor critical system. The striations which can be observed with a Schlieren setup in a medium at rest are not significantly changed when sound is applied in the liquid-liquid case, while they are broken in liquid-vapor systems as though a pulverization of assemblies had taken place. A similar effect is evident when one follows the light diffraction patterns produced by a sound wave in the medium with time after sound application. In figure 15 the light diffraction pattern in an aniline-cyclohexane mixture at 31 °C, in carbon dioxide at 3.5 °C and 72 atm, and in ethylene at 9.6 °C and 52 atm are shown at 1/12 sec intervals from the instant when sound (1 Mc/s) is switched on (arrow). While the patterns remain unchanged in the liquid-liquid critical mixture: they rapidly become blurred in the liquid-vapor case.

[7] The existence of substantial differences between assemblies in the two types of critical systems is also shown by the temperature dependences of α experimentally found (figs. 3, 5, and 10).

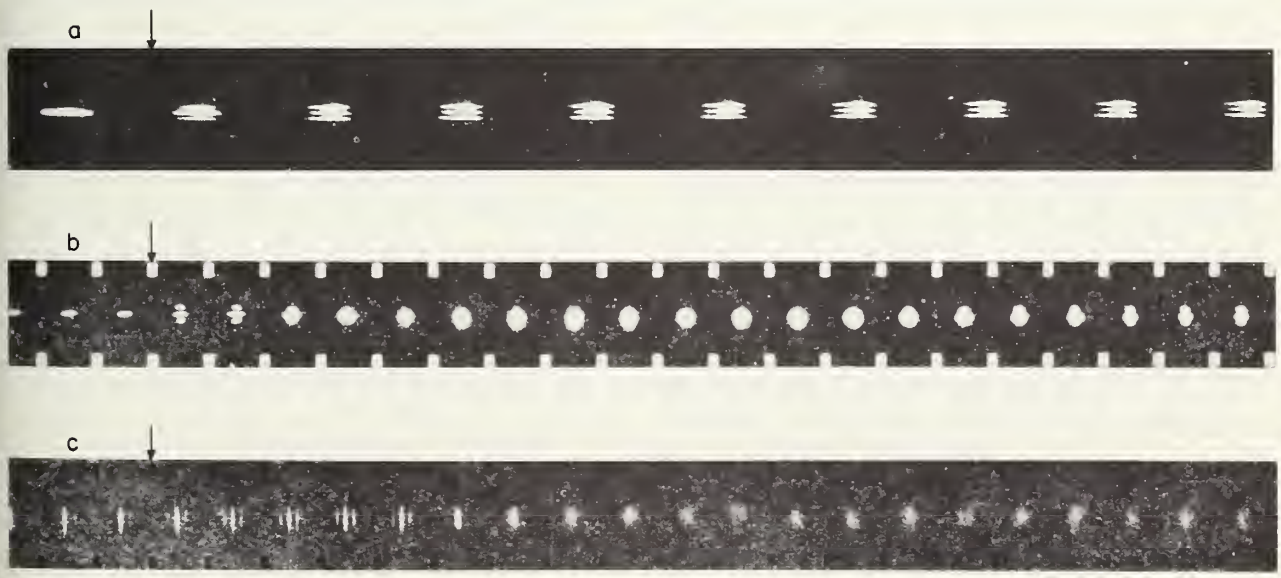

FIGURE 15. *Light diffraction pattern produced by sound (1 Mc/s) in aniline-cyclohexane mixture at 31 °C (a) in CO_2 at 31.5 °C and 72 atm (b), in ethylene at 9.6 °C and 52 atm (c) the photographs were taken at 1/12 sec intervals.*
Arrows show turning on of the sound. (A. S. Sliwinski and A. E. Brown [33]).

209-493 O-66—14

It would seem therefore that sound has a tremendous effect on the structure of assemblies in the liquid vapor case while it does not practically affect the configuration of clusters in critical mixtures. Sliwinski and Brown think that this could be an indication of the fact that scattering is particularly important in critical mixtures while it must be less significant in liquid vapor media: in the last case structural relaxation effects would be the main cause of absorption.

The survey of the work so far carried out in critical systems has shown how the problems associated with the propagation of sound waves in critical media have not yet been solved. At present, they seem to be posed in clearer terms than some years ago, but much theoretical and experimental research is needed. The important areas of research are essentially two: (a) the low-frequency sound velocity at the critical point; (b) the analysis of absorption and possibly, of dispersion of sound waves. The progress of experimental techniques should today allow more precise determinations of sound velocity and of the absorption coefficient: moreover, it is important to extend the ranges of temperature, frequency and composition in which the measurements are made. From the theoretical side, we expect progress in the thermodynamical treatment of critical systems, in scattering theories adequately considering correlation between fluctuation in adjacent volumes, in separating the contributions to absorption due to relaxation and scattering processes when they are of comparable importance.

The profit of these researches will surely be rewarding in establishing the characteristics and the behavior of critical systems since sound propagation is so intimately connected with the particular nature of these media.

5. References

[1] C. E. Chase, R. C. Williamson, and L. Tisza, Phys. Rev. Letters **13**, 467 (1964).
[2] A. G. Chynoweth and W. G. Schneider, J. Chem. Phys. **20**, 1777 (1952).
[3] H. D. Parbrook and E. G. Richardson, Proc. Phys. Soc. (London) **B65**, 437 (1952).
[4] C. M. Herget, J. Chem. Phys. **8**, 537 (1940).
[5] H. Tielsch and H. Tanneberger, Z. Physik. **137**, 256 (1954).
[6] M. A. Breazeale, J. Chem. Phys. **36**, 2530 (1962).
[7] J. Noury, Compt. Rend. Acad. Sci. Paris **233**, 516 (1951).
[8] V. F. Nozdrev, Soviet Phys. Acoustics **1**, 249 (1955).
[9] V. F. Nozdrev. Application of Ultrasonics in Molecular Physics (Gordon and Breach, New York, 1963).
[10] B. I. Kal'ianov and V. F. Nozdrev, Soviet Phys. Acoustics **4**, 198 (1958).
[11] V. F. Nozdrev and V. D. Sobolev, Soviet Phys. Acoustics **2**, 408 (1956).
[12] W. G. Schneider, Canadian J. Chem. **29**, 243 (1951).
[13] V. F. Nozdrev, A. P. Osadchii, and A. S. Rubtsov, Soviet Phys. Acoustics **7**, 305 (1962).
[14] V. F. Nozdrev and G. D. Tarantova, Soviet Phys. Acoustics **7**, 402 (1962).
[15] V. I. Grechkin and V. F. Nozdrev, Soviet Phys. Acoustics **9**, 304 (1964).
[16] L. D. Landau and E. M. Lifshitz, Statistical Physics (Pergamon Press, 1959).
[17] M. I. Beyatskii, A. V. Voronel, and V. G. Gusak, Soviet Phys. JEPT **16**, 517 (1963).
[18] A. V. Voronel, Yu. R. Chashkin, V. A. Popov, and V. G. Simkin, Soviet Phys. JEPT **18**, 568 (1964).
[19] C. N. Yang, and C. P. Yang, Phys. Rev. Letters **13**, 303 (1964).
[20] L. Liebermann, J. Acoust. Soc. Am. **23**, 563 (1951).
[21] L. Chernov, Wave Propagation in a Random Medium (McGraw-Hill Book Co., New York, 1960).
[22] A. G. Chynoweth and W. G. Schneider, J. Chem. Phys. **19**, 1566 (1951).
[23] M. Cevolani and S. Petralia, Atti Accad. Naz. Lincei **2**, 674 (1952).
[24] G. F. Alfrey and W. G. Schneider; Disc. Far. Soc. **15**, 218 (1953).
[25] D. Sette, Nuovo Cimento **1**, 800 (1955).
[26] A. E. Brown and E. G. Richardson, Phys. Magazine **4**, 705 (1959).
[27] R. Lucas, J. Phys. Rad. **8**, 41 (1937).
[28] M. Fixman, J. Chem. Phys. **33**, 1363 (1960).
[29] M. Fixman, J. Chem. Phys. **36**, 1961 (1962).
[30] M. Fixman, Advance in Chemical Physics Vol. **VI** (Interscience Publ., New York, N.Y., 1964).
[31] M. Fixman, J. Chem. Phys. **36**, 1957 (1962).
[32] A. P. Kendig, R. H. Bigelow, P. D. Edmonds, C. J. Pings, J. Chem. Phys. **40**, 1451 (1964).
[33] A. S. Sliwinski, A. E. Brown, Acustica **14**, 280 (1964).

Ultrasonic Investigation of Helium Near its Critical Point

C. E. Chase* and R. C. Williamson**

Massachusetts Institute of Technology, Cambridge, Mass.

The recent discovery of a logarithmic singularity in the specific heat at constant volume C_V of fluids at the critical point [1–3] has stimulated renewed interest in this region. A consequence of this singularity that was soon demonstrated [4, 5] is that the adiabatic compressibility κ_s must likewise be singular and the velocity of sound, given by $u^2=1/\rho\kappa_s$, must go to zero. We have accordingly measured the sound velocity in He^4 at a frequency of 1 Mc/s in the critical region. Some of the results of these measurements are reported herein.

Figure 1 shows the velocity as a function of temperature along an isobar and as a function of pressure along an isotherm passing approximately through the critical point. These measurements have been reported previously [5, 6] (together with a description of the experimental techniques, which will not be repeated here). However, we have subsequently found that, as a result of slight hysteresis and lack of reproducibility in the pressure gauge used in the experiment, the pressure and temperature of this isobar and isotherm should probably be increased by about 4 mm Hg and 0.003 °K, respectively. We are currently making measurements along families of closely spaced isotherms passing through the critical region, and find that the shape of an isotherm is substantially independent of its temperature over a range of several millidegrees. We therefore believe that our conclusions will not be seriously affected by the above-mentioned correction, but final judgement must be reserved until our measurements are complete.

It can be seen from figure 1 that the general behavior is in agreement with expectation; the velocity falls rapidly as the critical point is approached from any direction, and it is not unreasonable to suppose that it goes to zero at the critical point itself. Unfortunately, the large attenuation in this region makes it impossible to approach the critical point more closely with the present apparatus. We can thus only draw inferences about the behavior closer to the critical point by interpretation of the data we have; this is the subject of the following paragraphs.

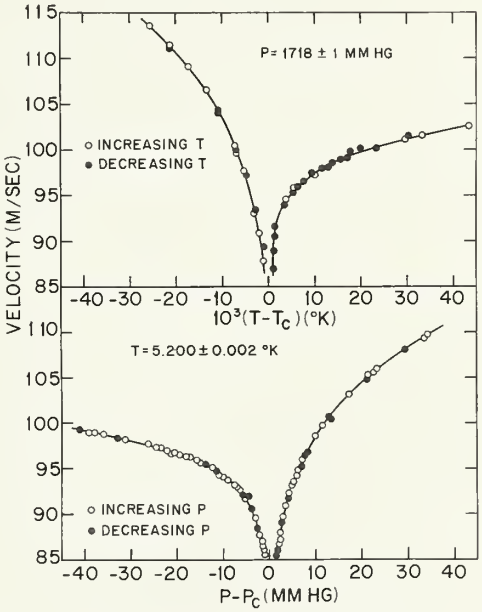

FIGURE 1. *Sound velocity as a function of temperature (a) and pressure (b) in the critical region.*

We note first that a plot of $1/u^2$ as a function of $\log|T-T_c|$ or $\log|P-P_c|$ is very nearly linear over the range of our data; there thus appears to be a logarithmic singularity in this quantity at the critical point. This fact is of interest as an experimental result independent of any theory. However,

*National Magnet Laboratory, supported by the U.S. Air Force Office of Scientific Research.

**Department of Physics.

in order to make a more meaningful comparison with the results of specific-heat measurements and with theory, we would like to know the adiabatic compressibility. This requires knowledge of the density, which has never been measured close to the critical point in He^4; the only measurements in this region are those of Edwards and Woodbury [7] along the coexistence curve, which extend to within 36 mdeg of T_c in the liquid and 50 mdeg in the vapor. It is therefore necessary to find an appropriate equation of state from which values of the density can be calculated.

Inasmuch as classical treatments such as the van der Waals equation are only approximate, and more recent approaches have not yet succeeded in yielding an equation of state suitable for our purposes, we have resorted to the technique of expanding in power series about the critical point. This procedure has to be used with caution because of the nonanalytic character of the thermodynamic functions at the critical point [8]; nevertheless we believe that the following developments could be used as a point of departure to be corrected by a singular function becoming significant in the immediate neighborhood of the critical point. In particular, this procedure has shed light on the proper choice of thermodynamic variables in the critical region, and has disclosed previously unreported inconsistencies in the standard treatment of the critical point given by Landau and Lifshitz [9] and modified by Edwards and Woodbury [7].

Landau and Lifshitz expand the slope of an isothermal as a power series in $t=T-T_c$ and $v'=V-V_c$ according to the equation

$$N^{-1}(\partial^2 F/\partial V^2)_{T,N}=-(\partial P/\partial V)_T=At+Bv'^2+\ldots \tag{1}$$

where A and B are positive constants. This procedure leads to a coexistence curve symmetrical about the critical point when plotted as a function of the volume:

$$v'_G=-v'_L=(-3At/B)^{1/2}. \tag{2}$$

The fact that the exponent of the coexistence curve is 1/2, as is nearly always the case with such expansions, does not present a problem in the present case; in contrast to the behavior of most other substances (for which an exponent of 1/3 is observed), He^4 obeys the 1/2-power law experimentally from the above-mentioned closest approach to within 110 mdeg of T_c [7, 10]. However, eq (1) can be criticized on other grounds: e.g., the coexistence curve is actually much more nearly symmetric in the density than in the volume (for He^4 departures from perfect symmetry in density amount to only 2% per degree Kelvin). This difficulty was noted by Edwards and Woodbury [7], who eliminated the spurious volume symmetry of eq (1) and obtained agreement with their measured orthobaric densities within 110 mdeg of T_c by adding two higher terms to the expansion, obtaining

$$-(\partial P/\partial V)_T=At+Bv'^2+Ctv'+Dt^2. \tag{3}$$

There are, however, further difficulties that are not eliminated, but rather compounded, by this procedure. This can be shown by integrating eqs (1) and (3) to obtain families of isotherms. For $T<T_c$, the resulting temperature-dependent constant of integration can be chosen to yield the observed $P-T$ relation along the vapor-pressure curve; above T_c it is plausible to choose this constant so that the critical isochore lies on the extrapolated vapor pressure curve. The results of such a calculation are shown in figures 2 and 3. The calculated isotherms are observed to cross in both cases; moreover this crossing is worse (in the sense of occurring closer to the critical point) for the Edwards-Woodbury expansion than for that of Landau and Lifshitz. The anomalies are so pronounced that they could scarcely be removed by any reasonable adjustment of the parameters P_c, T_c, V_c, or the constants $A-D$. These expansions are thus unsuitable for quantitative calculations.

The way out of this difficulty is found by a simple interchange of the role of the variables N and V in eq (1). This leads to a description in terms of the conjugate pair of variables μ, ρ (where μ is the chemical potential), as opposed to the traditionally preferred pair $-P$, V, and in fact represents a nontrivial change in the definition of the thermodynamic system. The equation which is the analog of eq (1) is now

$$V^{-1}(\partial^2 F/\partial N^2)_{T,V}=(\partial\mu/\partial\rho)_T=\alpha t+\beta\rho'^2+\ldots \tag{4}$$

where $\rho'=\rho-\rho_c$, and the slope of the isothermals is given by

$$(\partial P/\partial\rho)_T=\rho(\partial\mu/\partial\rho)_T=\rho(\alpha t+\beta\rho'^2). \tag{5}$$

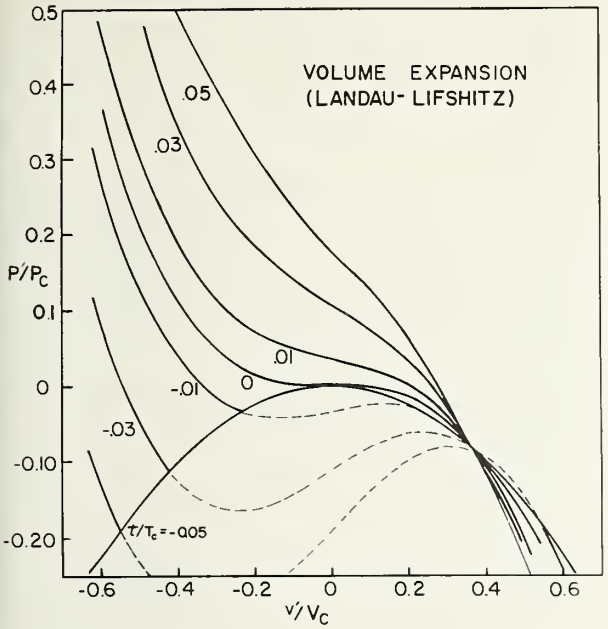

FIGURE 2. *Isotherms and coexistence curve calculated from the Landau-Lifshitz expansion (eq (1)) with* $A=7.95\times10^{4}$ *dyn mol cm*$^{-5}$ *deg*$^{-1}$, $B=62$ *dyn mol*^{3} *cm*$^{-11}$, $(dP/dT)_{sat}=1.7\times10^{6}$ *dyn cm*$^{-2}$ *deg*$^{-1}$, $P_c=2.288\times10^{6}$ *dyn cm*$^{-2}$, $T_c=5.200$ °K, $V_c=57.628$ *cm*^{3} *mol*$^{-1}$.

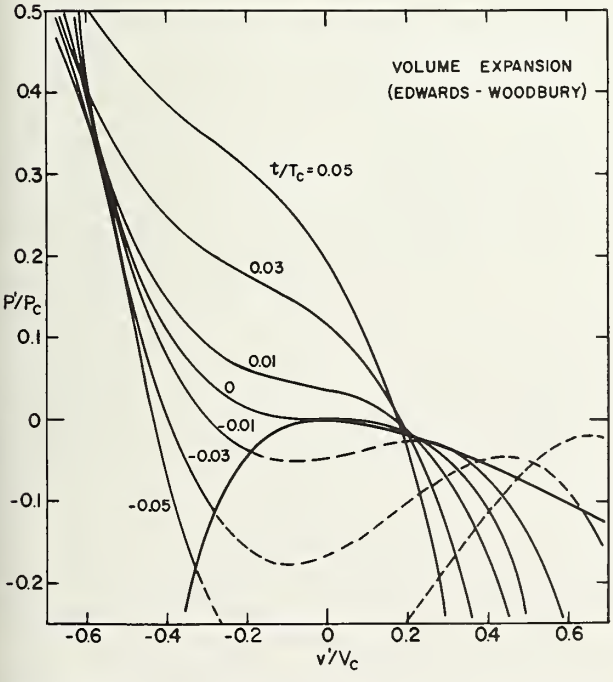

FIGURE 3. *Isotherms and coexistence curve calculated from the Edwards-Woodbury expansion (eq (3)), with* $c=8.16\times10^{3}$ *dyn mol*^{2} *cm*$^{-8}$ *deg*$^{-1}$, $D=1.78\times10^{5}$ *dyn mol cm*$^{-5}$ *deg*$^{-2}$, A, B, $(dP/dT)_{sat}$, P_c, T_c, V_c *as in figure 2.*

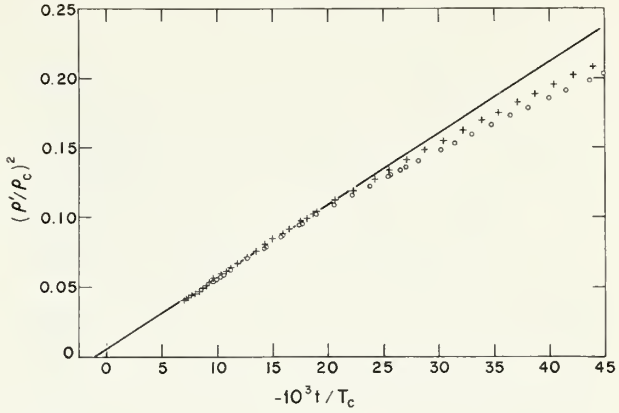

FIGURE 4. *Graph of* $(\rho_L'/\rho_c)^2$ *and* $(\rho_G'/\rho_c)^2$ *against* $-t/T_c$ *from data of reference 7.*
Equation (6) predicts a single straight line of slope $3\alpha/\beta$. $+(\rho_L'/\rho_c)^2$ $\circ(\rho_G'/\rho_c)^2$.

By development exactly parallel to that of reference 9, we now find that the coexistence curve is symmetric in the density:

$$\rho_L'=-\rho_G'=(-3\alpha t/\beta)^{1/2}. \tag{6}$$

To evaluate α and β we note that a plot of $\rho_L'^2$ and $\rho_G'^2$ against $-t$ should lie on a single straight line through the origin of slope $3\alpha/\beta$. Such a plot, based on the data of Edwards and Woodbury [7], is shown in figure 4, from which we find $\alpha/\beta=(1.03\pm0.02)\times10^{-4}$ mole^2/cm^6 °K. Note that the range of agreement with experiment is as wide as that achieved by Edwards and Woodbury with their four-parameter expansion [11]. As in reference [7], β can be evaluated approximately in terms of the measured density and isothermal compressibility [12] at 5 °K, yielding $\beta=(6.86\pm1.2)\times10^{13}$ dyne-cm^{10}/mol^4. The resulting isotherms in the μ, ρ plane are shown in figure 5. In this case the temperature-dependent integration constant that determines the separation of the isotherms was evaluated from the relation $Nd\mu=VdP-SdT$, using entropy values along the critical isopycnal derived by numerical integration of the specific-heat data of Moldover and Little [3]. Isotherms in the P, ρ plane, calculated with the same assumptions used in deriving figures 2 and 3, are shown in figure 6. In neither case are inconsistencies evident.

Although this expansion was derived for purely practical reasons, we believe it has significance beyond mere curve-fitting. In particular, the great improvement resulting from the proper choice of variables, and the natural way in which the sym-

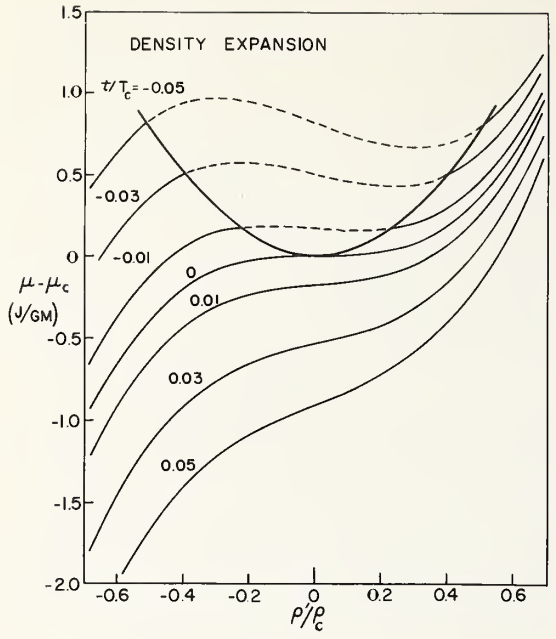

FIGURE 5. *Isotherms and coexistence curve in the* μ, ρ *plane calculated from the density expansion (eq (4)), with* $\alpha = 7.06 \times 10^9$ *dyn mol*$^{-2}$ *cm*^{4} *deg*$^{-1}$, $\beta = 6.86 \times 10^{13}$ *dyn mol*$^{-4}$ *cm*^{10}, *other parameters as in figure 2.*

For method of calculating spacing of isotherms see text.

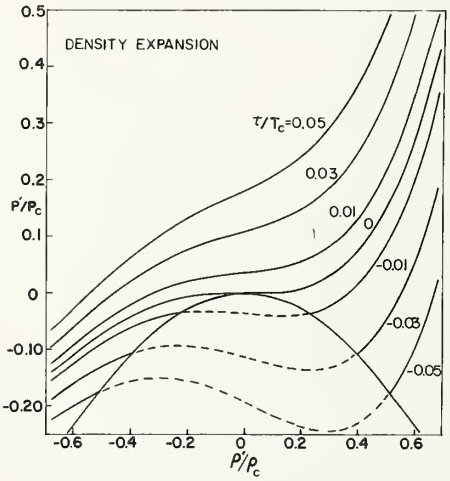

FIGURE 6. *Isotherms and coexistence curve in the* P, ρ *plane calculated from the density expansion (eq (5)); all parameters as in figure 5.*

metry of the problem enters when these variables are used, appear to us important. These features should survive even in a more sophisticated treatment that includes a proper handling of the singularity.

Values of the density along the critical isobar and isotherm, calculated in the same way as those plotted in figure 6, have been combined with our

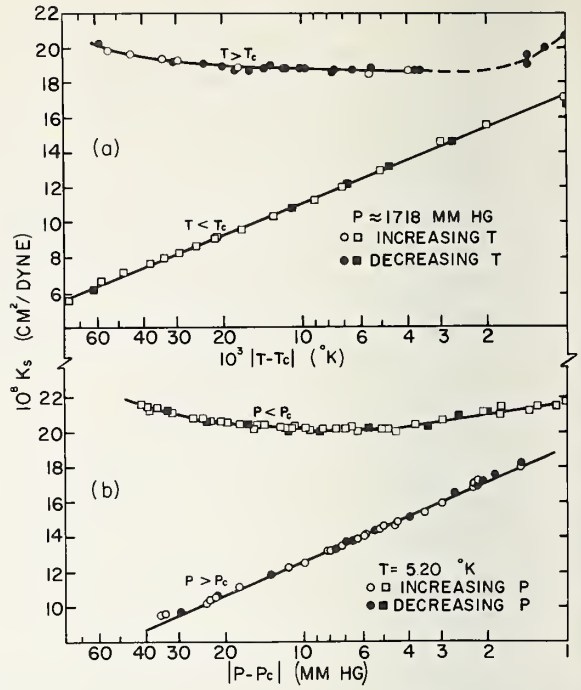

FIGURE 7. *Adiabatic compressibility (a) as a function of log* $|T - T_c|$ *and (b) as a function of log* $|P - P_c|$ *in the critical region, calculated from the results of figure 1 and the density expansion (eq (5) and fig. 6).*

velocity data to yield κ_s, which is plotted logarithmically as a function of $|T - T_c|$ or $|P - P_c|$ in figure 7. This figure is similar to one previously given, [5, 6] but the differences resulting from use of our improved expansion for the calculation of the density are significant. Results in the liquidlike modification ($P > P_c$ or $T < T_c$) are virtually unchanged, and the presence of a logarithmic singularity in κ_s over more than a decade is clearly indicated. However, in the gaslike modification κ_s now appears to be almost constant, and if a singularity is present at all, it must only show up within the last 4 or 5 mdeg (or millimeters) away from the critical point.

Velocity measurements have also been made along a number of isotherms above T_c. Some of these measurements are shown in figure 8. These curves all show pronounced minima as a function of pressure. It is perhaps important to point out that all these minima are rounded rather than cusp-shaped, even within about 10 mdeg of T_c (the closest point at which the velocity could be observed continuously through the minimum). The fact that the locus of these minima in the P, T plane falls approximately on the extrapolated vapor pressure

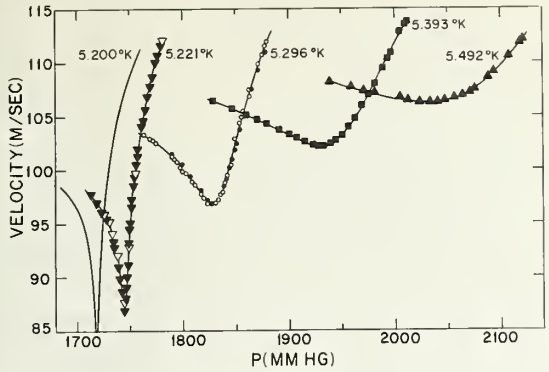

FIGURE 8. *Velocity as a function of pressure along isotherms above the critical temperature.*

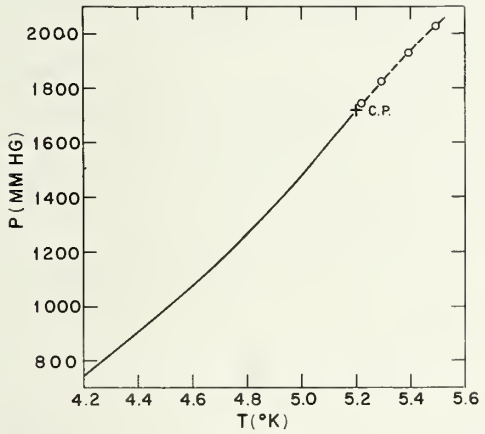

FIGURE 9. *Locus of velocity minima along the isotherms of figure 8 in the* P, T *plane.*
Full line: vapor pressure curve, + critical point.

curve, as is shown in figure 9, allows us to reach some further conclusions. According to Yang and Yang [4], the velocity of sound along the critical isopycnal above T_c should be given by

$$u^2 = \rho_c^{-2}(dP/dT)^2_{\text{sat}}(T/C_V), \tag{7}$$

where C_V is taken along the same isopycnal and $(dP/dT)_{\text{sat}}$ is the slope of the saturated vapor pressure curve just below T_c. Starting from the thermodynamic relation

$$(\partial P/\partial V)_s = (\partial P/\partial V)_T - (\partial P/\partial T)^2_V(T/C_V), \tag{8}$$

it is easy to see that eq (7) can be obtained from the exact expression

$$u^2 = (\partial P/\partial \rho)_T + \rho_c^{-2}(\partial P/\partial T)^2_V(T/C_V) \tag{9}$$

by neglecting $(\partial P/\partial \rho)_T$ (which vanishes as $T \to T_c$) and assuming that $(\partial P/\partial T)_{V,(T>T_c)} = (dP/dT)_{\text{sat},(T<T_c)}$.

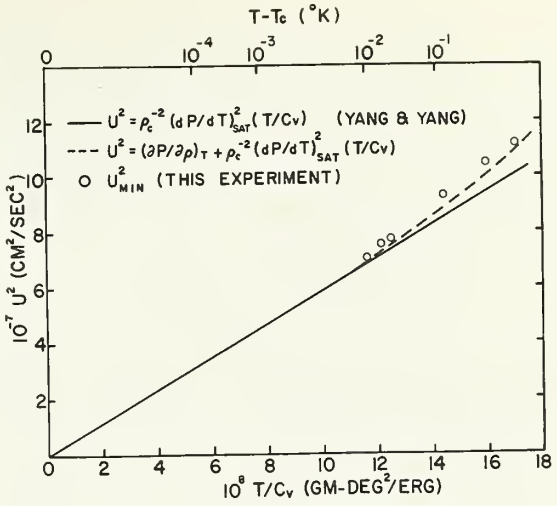

FIGURE 10. *Plot of* u^2_{min} *against* T/C_V *from data of reference 3.*

In this approximation a plot of u^2 versus T/C_V should be a straight line of slope $\rho_c^{-2}(dP/dT)^2_{\text{sat}}$. This is shown by the solid line in figure 10; the dotted line is a correction for the nonzero value of $(\partial P/\partial \rho)_T$ derived from our density expansion (eq 5). The circles represent our values of u^2_{min} at various temperatures plotted against the specific-heat measurements of Moldover and Little [3]; use of u_{min} is consistent with the assumption $(\partial P/\partial T)_V = (dP/dT)_{\text{sat}}$ and the fact that the observed minima lie on the extrapolated vapor pressure curve; i.e., we are assuming that the velocity minima lie along the line $\rho = \rho_c$. The agreement of these points with Yang and Yang's prediction, plus the small correction term $(\partial P/\partial \rho)_T$, is reasonably good, although all the points lie about 2 to 5 percent too high [13]. We ascribe this small systematic difference to errors either in the choice of $(dP/dT)_{\text{sat}}$, in the measured values of C_V, or in the temperature scales of the two experiments.

Since eq (7) ought to become more accurate as the critical point is approached, we can now estimate how low the velocity ought to fall along isotherms very close to T_c. As can be seen with the aid of the temperature scale at the top of figure 10, the minimum velocity along an isotherm just 10^{-4} °K above T_c would be ~55 m/sec, about 2/3 of the lowest value we have observed. Thus, even in an ideal experiment in which measurements could be made very close to the critical point in spite of the large attenuation there, it would hardly be possible to observe much lower values of u than we have done.

The authors are extremely grateful to Laszlo Tisza for suggesting this experiment, for playing a major part in the derivation of the density expansion and the elucidation of its significance, and for continued helpful advice and encouragement throughout the course of this work. Most of the numerical computations were carried out at the M.I.T. Computation Center.

References and Notes

[1] M. I. Bagatskii, A. V. Voronel', and V. G. Gusak, Zh. Eksperim. i. Teor. Fiz. **43**, 728 (1962) [translation: Soviet Phys.—JETP **16**, 517 (1963)].
[2] A. V. Voronel', Yu R. Chashkin, V. A. Popov, and V. G. Simkin, ibid. **45**, 828 (1963) [translation: Soviet Phys.—JETP **18**, 568 (1964)].
[3] M. Moldover and W. A. Little, Proc. 9th Intl. Conf. on Low Temp. Phys., Columbus, Ohio, 1964 (to be published).
[4] C. N. Yang and C. P. Yang, Phys. Rev. Letters **13**, 303 (1964).
[5] C. E. Chase, R. C. Williamson, and L. Tisza, Phys. Rev. Letters **13**, 467 (1964).
[6] C. E. Chase and R. C. Williamson, Proc. 9th Intl. Conf. on Low Temp. Phys., Columbus, Ohio, 1964 (to be published).
[7] M. H. Edwards and W. C. Woodbury, Phys. Rev. **129**, 1911 (1963).
[8] L. Tisza, Phase Transformations in Solids (John Wiley & Sons, Inc., New York, N.Y., 1951), p. 15; M. E. Fisher, J. Math. Phys. **5**, 944 (1964).
[9] L. D. Landau and E. M. Lifshitz, p. 259 ff. Statistical Physics, (Pergamon Press, New York, 1958).
[10] The deviations from a 1/3-power law observed by Edwards and Woodbury appear to be much too large to ascribe to experimental error. If these deviations are real, they might be attributed to quantum corrections to the law of corresponding states (J. de Boer, Physica **14**, 139, 149 (1948); J. de Boer and R. J. Lunbeck, Physica **14**, 509 (1948)), and similar behavior ought to be observed in He^3. Such appears to be the case (see paper by R. H. Sherman in this conference).
[11] The line in the figure actually has a finite intercept of +4.6 millidegrees on the abcissa. This may indicate flattening of the coexistence curve close to the critical point, or may be the result of errors in the measured temperatures in reference 7 or the assignment of T_c.
[12] M. H. Edwards and W. C. Woodbury, Can. J. Phys. **39**, 1833 (1961).
[13] Note that if the velocity minima did *not* fall exactly on the line $\rho = \rho_c$ the agreement would be worse, for a *smaller* value of u is required to fit the theoretical curve.

Ultrasonic Investigation of the Order-Disorder Transition in Ammonium Chloride

C. W. Garland and R. Renard

Massachusetts Institute of Technology, Cambridge, Mass.

Introduction

The lambda transition in solid ammonium chloride was discovered by Simon [1] from heat-capacity measurements. An x-ray analysis by Simon and von Simson [2] showed that ammonium chloride has a CsCl-type cubic structure both above and below the critical temperature; thus the transition could not be due to a change in lattice type. Hettich [3] found that ammonium chloride is weakly piezoelectric in the low-temperature modification, whereas it is not piezoelectric above the critical temperature. From this he concluded that the tetrahedral ammonium ions are oriented parallel in the low-temperature modification. Menzies and Mills [4] came to the same conclusion on the basis of the Raman effect. Pauling [5] suggested that the transition was related to the onset of free rotation of the ammonium ions, and quantitative refinements of this idea were carried through by Fowler [6] and by Kirkwood [7]. In opposition to this, Frenkel [8] interpreted the transition as being of the order-disorder type, involving the relative orientations of the tetrahedral ammonium ions; it was assumed that in both the ordered and the disordered states the ammonium ions liberate about an equilibrium position. This idea has been confirmed by many subsequent experiments.

In particular, Levy and Peterson [9] have carried out a neutron-diffraction determination of the hydrogen positions in both the low- and high-temperature modification, and Purcell [10] has analyzed the nmr data to obtain the relaxation time for an NH_4^+ ion to move from one orientation in its cubic cell to the other orientation. Both these investigations show that free rotation does not occur.

Indeed, in many respects NH_4Cl is an ideal crystal for studying cooperative order-disorder phenomena. The ordering is completely analogous to that for a simple-cubic ferromagnet in a zero external field. The change in interaction energy between parallel and antiparallel NH_4^+ ions is almost completely due to octopole-octopole terms between nearest and next-nearest NH_4^+ neighbors

[11], and thus NH_4Cl is quite a good example of an Ising lattice. Furthermore, the ordering process should have little effect on the dynamics of such an ionic lattice.

We wish to discuss here a variety of ultrasonic measurements which have been made on single-crystal ammonium chloride. Longitudinal and transverse (shear) acoustic velocities have been measured [12, 13] over a wide range of frequencies (5 to 60 Mc/s), temperatures (150 to 320 °K) and pressures (0 to 12 kbar). The attenuation of longitudinal ultrasonic waves has been measured [14] at 1 atm for frequencies between 5 and 55 Mc/s and temperatures from 200 to 270 °K. In all these investigations, special emphasis was given to the "anomalous" behavior near the lambda transition. As shown in figure 1, the transition temperature is a fairly strong function of pressure, increasing from ~ 242 °K at 1 atm to ~ 308 °K at 10 kbar. (Note the pronounced curvature of the lambda line and the hysteresis observed at low pressures.) At a constant pressure of 1 atm, the ultrasonic velocities were originally measured by a pulse-echo method as a function of frequency and temperature, and no dispersion was observed [12]. Recently, the McSkimin pulse-superposition method has been used at a fixed frequency of 20 Mc/s. The temperature dependence at 1 atm has been restudied, and the pressure dependence of the velocities were measured at five fixed temperatures spaced between 250 and 308 °K. Thus, we have very precise velocity data (±0.005%) on both the ordered and disordered phases. This experimental data will be described elsewhere [13] in detail, but is presented here in a graphical form.

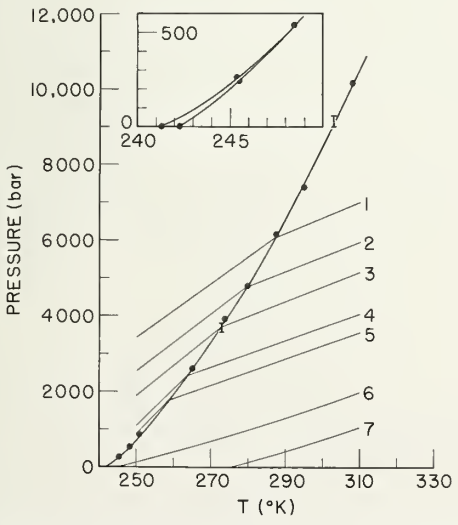

FIGURE 1. *Phase diagram for* NH_4Cl *(the high-pressure, low-temperature field corresponds to the ordered phase).*
The solid data points were obtained from the abrupt "break" in the ultrasonic shear velocities at the λ transition point (see figs. 2 and 3). The vertical bars indicate static measurements of Bridgeman [15]. The light lines numbered 1 through 7 represent various isochores.

All the results given below are in terms of the variation of one of the three elastic constants c_{11}, c_{44}, and $C' = (c_{11} - c_{12})/2$. Third-order elastic constants are not used, and at high pressures the quantities c_{11}, c_{44}, and C' are in a sense "effective" elastic constants. The constants c_{11} and c_{44} were calculated from the experimental longitudinal and transverse velocities (U) in the [100] direction with the relations $\rho U_l^2 = c_{11}$ and $\rho U_t^2 = c_{44}$; the constant C' was calculated from $\rho U_{t'}^2 = C'$, where $U_{t'}$ is the velocity in the [110] direction of a shear wave polarized perpendicular to the [001] axis.

Experimental Results

The variations of the shear constants c_{44} and C' and of the compressional constant c_{11} with pressure at five different temperatures are given in figures

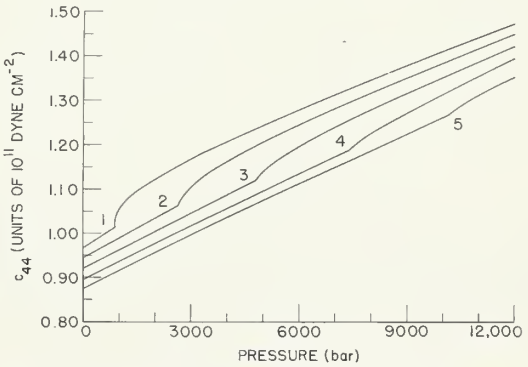

FIGURE 2. *Dependence of* c_{44} *on pressure at* $T_1 = 250$, $T_2 = 265$ $T_3 = 280$, $T_4 = 295$, *and* $T_5 = 308$ °K.

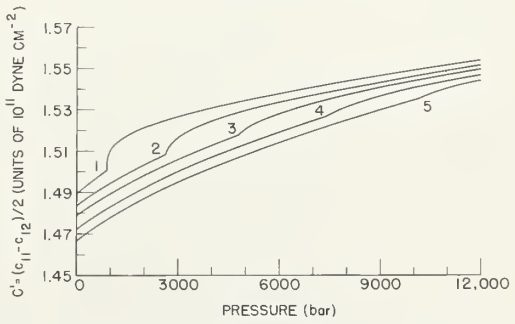

FIGURE 3. *Dependence of* C' *on pressure at various temperatures (see fig. 2 legend).*

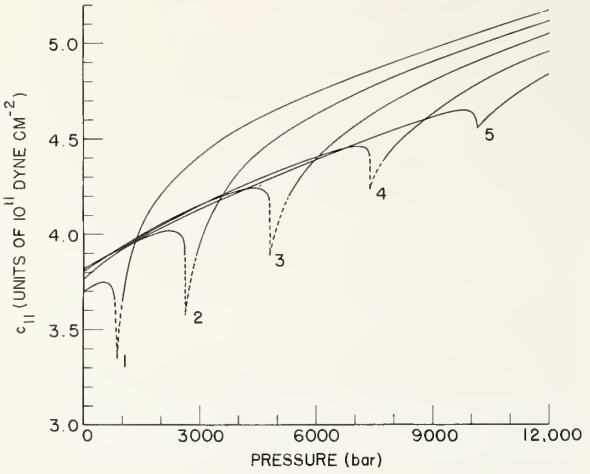

FIGURE 4. *Dependence of* c_{11} *on pressure at various temperatures (see fig. 2 legend).*

Dashed portions of the curves indicate regions where data are less accurate or are missing due to high attenuation.

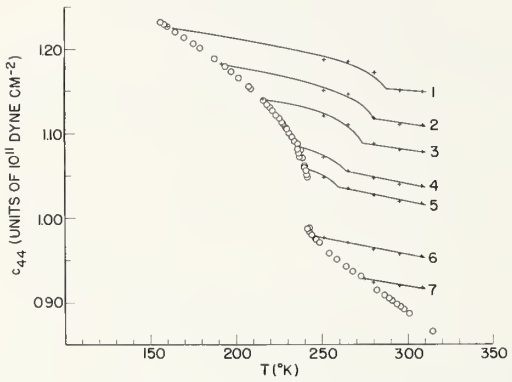

FIGURE 5. *Variation of* c_{44} *with temperature at 1 atm (open circles) and at* $V_1=34.00$, $V_2=34.15$, $V_3=34.27$, $V_4=34.43$, $V_5=34.51$, $V_6=34.77$, $V_7=34.93$ *cm³ mole⁻¹ (crosses).*

The transition temperature is known for each of these volumes, and thus the location of the change in slope for each of the constant-volume lines is fixed.

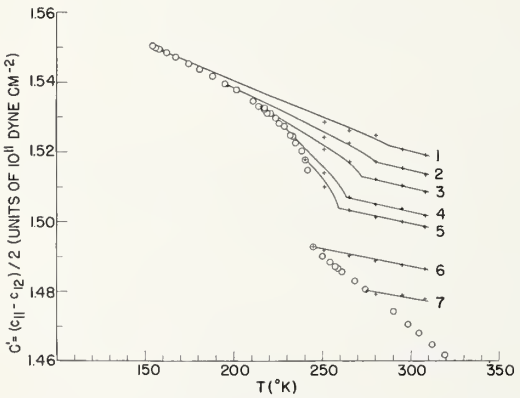

FIGURE 6. *Variation of* C' *with temperature at 1 atm (open circles) and at various constant volumes (see fig. 5 legend).*

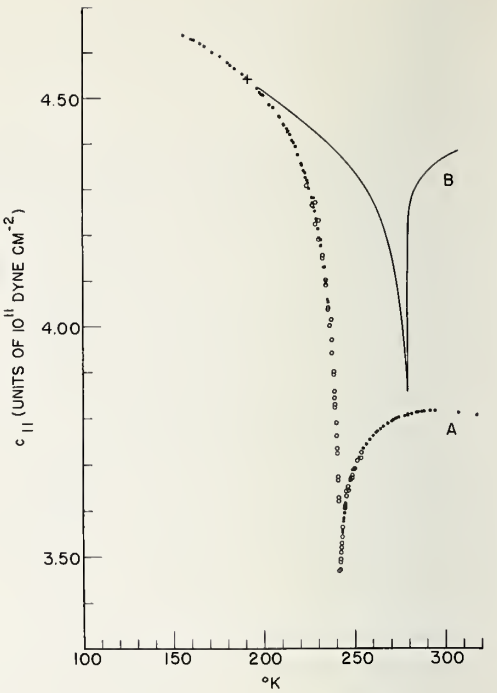

FIGURE 7. *Variation of* c_{11} *with temperature.*

Curve A: data at 1 atm (solid circles = pulse superposition method [13], open circles = corrected pulse-echo data [12]). Curve B: calculated curve at constant volume $V_2=34.15$ cm³ mole⁻¹; V_2 corresponds to V_λ at 280 °K and to the volume at 1 atm and 191.25 °K (marked by cross).

2, 3, and 4. Data points are not shown on these figures since a variety of corrections must be applied to the data, which requires some smoothing. Each isotherm is based on at least 30 experimental points which show very little scatter. Note that c_{44} is much more sensitive to pressure than C' but that the character of the anomalous variation near the lambda line is very similar for both these shear constants. Indeed, there is a marked reduction in the rapid variation just above the transition as the lambda line is crossed at higher pressures. This same reduction in anomalous behavior is also seen in the c_{11} data. The adiabatic compressibility β^S can be calculated from

$$1/\beta^S=\frac{1}{3}(c_{11}+2c_{12})=c_{11}-\frac{4}{3}C' \qquad (1)$$

and it is clear that β^S goes through a sharp maximum at a lambda point.

Experimental data points are shown in figures 5, 6, and 7 for the constants c_{44}, C', and c_{11} as functions of temperature at 1 atm. In addition, the variation of c_{44} and C' with temperature is given for seven different constant volumes, and the behavior of c_{11} at a single constant volume is also shown.

These constant-volume curves were obtained by determining the pressure required at a given temperature to give the desired volume (Bridgeman's data [15] and our own were used) and then reading the appropriate elastic constant values from figures 2 to 4.

For the shear constants, one can immediately see that most of the temperature change near T_λ at 1 atm is due to the rapid change in volume in the transition region. Our data permit us to completely analyze the effects of volume changes and temperature changes so that one can see the effect of ordering at a constant volume and temperature. For longitudinal waves, volume changes do have a significant effect on the velocity, but the anomalous dip in c_{11} is essentially due to ordering effects. In figure 7, the shift in the minimum between curves A and B is merely a result of the value chosen for the constant volume: the important difference between these curves is their shape near the minimum.

For shear waves there is no indication of excess ultrasonic attenuation near the lambda line, but for longitudinal waves there is a very sharp maximum in the attenuation coefficient α at the transition point. Quantitative measurements of α for longitudinal waves along [100] have been made at 1 atm as a function of frequency and temperature [14]. The results are shown in figure 8 for 15, 25, 45, and 55 Mc/s. Data have also been taken at 5 Mc/s, where a rather large (0.5 dB cm^{-1}), temperature-independent background attenuation is present (presumably due to beam-spread losses).

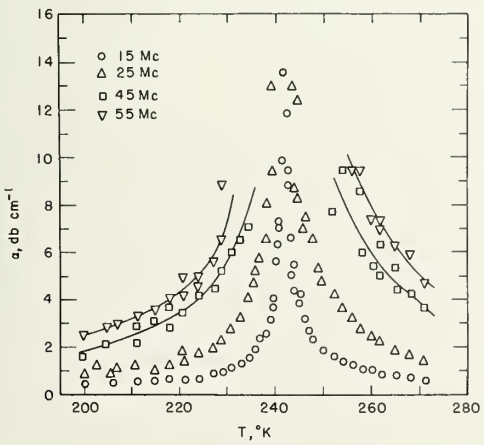

FIGURE 8. *Attenuation coefficient α at various ultrasonic frequencies.*
Data obtained on two samples with different path lengths were in excellent agreement at 15 and 25 Mc/s. Scatter in the 45 and 55 Mc/s data is caused by high α values and weak initial pulses (9th and 11th harmonics of 5 Mc/s transducer).

Further experimental work on attenuation is currently in progress.

Since there is no excess attenuation near the lambda point for shear waves, it is possible to follow the behavior of the shear velocities through the transition region. Both c_{44} and C' showed a small hysteresis, the magnitude of which is indicated in the insert on figure 1. We have not shown data points in this region on figures 5 and 6 since equilibrium was very difficult to achieve (slow changes in the shear velocities occurred even after 45 min). The presence of this hysteresis and the very abrupt change in shear velocities near T_λ are significant properties of our measurements at 1 atm. (Similar indications of hystersis and abrupt changes near T_λ are seen from volume measurements and cooling curves.)

Discussion

Equilibrium data. Because of the formal analogy between the ordering of NH_4Cl and of a ferromagnet in the absence of an external field, it is appropriate to consider the mechanical behavior of an Ising lattice. If the coupling between the lattice system and the "spin" system is sufficiently weak, an Ising lattice will become unstable in the immediate vicinity of its critical point and a first-order transition will occur. Furthermore, hysteresis will be expected in the critical region. This instability has been demonstrated for a two-dimensional square lattice [16, 17], where there is an analytic solution to the Ising problem. The important conditions for this instability are (1) weak lattice-spin coupling, (2) a finite compressibility for the disordered lattice, and (3) an infinite C_v for the "spin" system at the critical temperature. The effect will be large only when (a) the lattice is soft, (b) the critical temperature is large, and (c) dJ/dV is large (where J is the usual Ising interaction energy). Such an instability has been proposed previously for other models [18, 19] and discussed in general thermodynamic terms by Rice [20], but little attention seems to have been paid to this problem. It would appear that NH_4Cl is a much more appropriate system for observing these effects than most ferromagnetic solids would be.

To *illustrate* the instability and the possible hysteresis in order-disorder transitions, let us look at the two-dimensional case [16]. Figure 9 shows a plot of p_I and $-p_{dI}$ against the area σ at several temperatures $T_1 < T_2 \ . \ . \ . \ T_6 < T_7$. The pressure

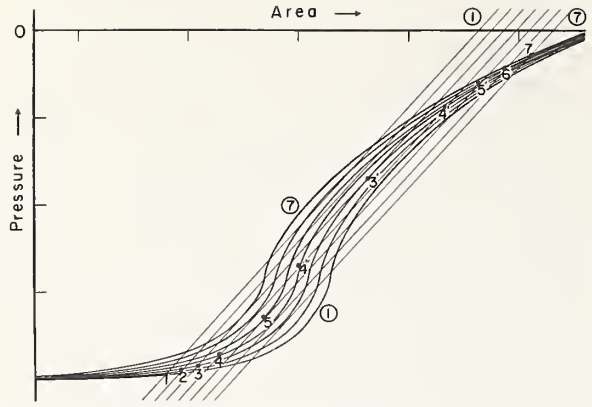

FIGURE 9. *Plot of* p_I *and* $-p_{dI}$ *versus the area* σ *for a two-dimensional Ising lattice.*

The family of *curves* p_I were calculated at seven evenly spaced temperatures from T_1 up to T_7. The family of *lines* $-p_{dI}$ were drawn to represent a disordered lattice with typical compressibility and thermal expansion coefficients. The encircled numbers 1 and 7 indicate the spin and lattice isotherms at T_1 and T_7.

p_{dI} is that of the completely disordered lattice, and p_I represents the attractive (negative) pressure due to the ordering of an Ising spin system. An intersection of the two appropriate isotherms (p_I and $-p_{dI}$) will correspond to $p=p_I+p_{dI}=0$ and will give an equilibrium area σ if the stability condition $(\partial^2 A/\partial\sigma^2>0)$ is satisfied. The stability condition requires that the slope of $-p_{dI}$ be greater than that of p_I; e.g., the system is unstable at a point such as 4″. Now consider the change in area with T for a system under zero external stress ($p=0$). As the temperature increases from T_1 to T_5, σ can increase continuously from σ_1 to σ_5 (points 1 to 5 on fig. 9) but as $T\rightarrow T_5$ *from below* the system becomes unstable ($\partial^2 A/\partial\sigma^2=0$) at point 5 and there must be a first-order change in area from σ_5 to $\sigma_{5'}$. On further heating, σ increases continuously from $\sigma_{5'}$ to σ_7. However, on cooling from T_7 to T_3 the area can decrease smoothly from σ_7 to $\sigma_{3'}$. As $T\rightarrow T_3$ *from above* the instability occurs at point 3′ and there is a first-order change from $\sigma_{3'}$ to σ_3. Below T_3, σ decreases smoothly on cooling. Thus, there can be a hysteresis loop near the critical point with a first-order jump in σ at T_5 on heating and a first-order drop in σ at T_3 on cooling. The values T_3 and T_5 determine the maximum width of this loop since the system becomes *mechanically* unstable at points 5 and 3′. Naturally, there is a temperature T_4 for which the free energy at point 4 equals that at point 4′; thermodynamic equilibrium would give a first-order transition at T_4 and no hysteresis. The region between 4 and 5 on heating or 4′ and 3′ on cooling is only metastable. Although the shape of the p_I curves will be different for a three-dimensional Ising lattice, the instability will still occur if C_v (and thus $\partial p_I/\partial V)\rightarrow\infty$ at the critical point. Thus the hysteresis described above can still occur.

As seen in figures 2, 3, 5, and 6, the shear constants of NH_4Cl are sensitive functions of volume. Thus the experimental hysteresis in c_{44} and C' can indicate the presence of the proposed hysteresis in V. Note that experimentally the hysteresis decreases for a transition higher up along the lambda line (i.e., at some finite external pressure). This would be expected from our analysis of the Ising lattice since the only difference between working at zero pressure and at some large constant pressure is in the lattice stiffness. For high external pressures, the slope of $-p_{dI}$ will be greater and the maximum width ΔT of the hysteresis will be less. Moreover, a semiquantitative estimate of the magnitude of ΔT at 1 atm is in reasonable agreement with experiment. Completely analogous considerations can be developed for an instability and hysteresis on compressing an Ising lattice at constant temperature. An elaboration of the effects of hysteresis and instability on measurements at either constant pressure or constant volume will be given in detail elsewhere [16]. In addition, our shear data strongly suggest a sluggish first-order transition in the critical region. For points taken at temperatures more than 1 °K away from T_λ and at pressures more than 100 bar away from p_λ, equilibrium was achieved within about 15 min after the temperature or pressure was adjusted. In the immediate vicinity of a critical point, very slow changes in velocity were still observed 45 min after the temperature or pressure was adjusted, as would be expected in a metastable region. Also the changes in c_{44} and C' in this narrow hysteresis region are extremely abrupt, even when compared with the very rapid variations observed in the ordered phase near the transition line.

Leaving aside the important but relatively narrow range where instability may occur, it is possible to discuss the effect of ordering at constant volume on the elastic constants in terms of an Ising model. We have carried out a general stress-strain analysis of the two-dimensional Ising lattice (using Onsager's analytic solution for the case $J\neq J'$) and have obtained explicit formulae for the *isothermal* stiffnesses c_{11}, c_{44}, and $C'=(c_{11}-c_{12})/2$. The details will be reported elsewhere [21], but the essential

features can be seen from the simpler formula for the isothermal volume compressibility β^T:

$$\frac{1}{V\beta^T}=\left(\frac{\partial^2 A}{\partial V^2}\right)_T=\left(\frac{1}{V\beta^T}\right)_{dl}-\frac{T}{J^2}C_l(0,H)\left(\frac{dJ}{dV}\right)^2+\frac{U_l(0,H)}{J}\left(\frac{d^2J}{dV^2}\right) \qquad (2)$$

where $C_l(0, H)$ and $U_l(0, H)$ are the Ising heat capacity and internal energy at zero field as a function of $H\equiv J/kT$. The subscript dl denotes the appropriate quantity for a completely *disordered lattice* (for which C_l and U_l equal zero). The elastic constants c_{ij} are given by $(\partial^2 A/\partial x_i\partial x_j)_T$ where the x's are the appropriate strains. Thus the expression for c_{11} will have a form similar to eq (2), and the dominant term in determining the shape of c_{11} near T_λ will involve C_l. For $C'=(c_{11}-c_{12})/2$ one requires a difference between two such expressions, and the singular part involving C_l will cancel out. The final expression for C' is complicated in its dependence on V and T, but it does predict a smooth variation through the transition region. For c_{44} the term containing C_l disappears identically since $dJ/d\gamma=0$ (γ is the change in angle during a c_{44} shear), but $d^2J/d\gamma^2\neq 0$ and the shape of c_{44} near T_λ is determined by U_l. In general terms these predictions are all fulfilled by our NH_4Cl data as functions of temperature at constant volume. In the case of c_{11} one must take account of the significant difference between the adiabatic and the isothermal constants near T_λ, but even so the shape of c_{11} is strikingly related to the shape of the heat capacity curve. In addition, the shape of c_{44} is what one would expect from an internal energy curve. No detailed discussion of C' will be given here, but in crude terms the effect of ordering is very small for this shear mode and this indicates that the "anomalous" variations in c_{11} and c_{12} almost completely compensate each other.

A final remark about the equilibrium properties of NH_4Cl can be made in connection with the Pippard equations. It is known that these phenomenological relations are fairly well obeyed [12] in NH_4Cl, but a generalization of them in terms of stress-strain variables [22] shows that there are some unexplained difficulties. We have recently discussed the Pippard equations [23] on the basis of a three-dimensional Ising model and can now give a better insight into the reasons for their behavior.

Dynamical data. In the past few years there has been increasing interest in the theory of the dynamical properties of substances near a lambda point. Landau and Khalatnikov [24] were the first to treat this problem by combining the thermodynamics of irreversible processes with an approximate equilibrium solution to the Ising problem. This approach has been extended and improved by others [25, 26] and a somewhat simplified result for the relaxation time τ for long-range ordering can be given in the form

$$\tau^{+,-}=A^{+,-}/|T-T_c| \qquad (3)$$

where + and − denote temperatures above and below T_c. The phenomenological constants A^+ and A^- depend on the substance involved but have a fixed ratio of $A^+/A^-=2$. A more general statistical-mechanical treatment of this problem has been given by Kikuchi [27]. For a temperature range close to the lambda point one can show that Kikuchi's results for the long-range relaxation times are still of the form given in eq (3). However, the constants A^+ and A^- now depend on microscopic transition probabilities and the ratio A^+/A^- near T_c is ~ 1.6 rather than 2.

An essential feature of our ammonium chloride data which requires explanation is the fact that the attenuation α has its maximum at T_λ. One would expect α to vanish at T_λ if τ becomes infinite there. However, the theories mentioned above deal with τ_{TV}, the relaxation time for ordering at constant temperature and volume. The experimental conditions for measuring attenuation are adiabatic rather than isothermal, and although the process is irreversible one can consider it to be essentially isentropic for small sound amplitudes. In this case the appropriate relaxation time is τ_{SV}, which can be related to τ_{TV} by

$$\frac{1}{\tau_{SV}}=\frac{1}{\tau_{TV}}+\frac{\bar{\bar{k}}T}{\tilde{C}_v}\left(\frac{\partial S}{\partial\xi}\right)^2_{T,V} \qquad (4)$$

where $\bar{\bar{k}}$ is a rate constant, $\tilde{C}_v$ is the specific heat at infinite frequency ("frozen" specific heat), and ξ is a progress variable characterizing the internal (nonequilibrium) state of the system at a given V and T.

The detailed behavior of $(\partial S/\partial\xi)^2$ is not known, but it seems likely that this quantity varies only slowly with temperature near T_λ. We shall *assume* below that the quantity $\bar{\bar{k}}T(\partial S/\partial\xi)^2/\tilde{C}_v$ has a constant value (call it B) over the temperature range of

interest. With this assumption and eqs (3) and (4), we find that

$$\frac{1}{\tau_{SV}}=\frac{\Delta T}{A}+B \tag{5}$$

for the relaxation time associated with long-range ordering, where $\Delta T=|T-T_\lambda|$ and the constant A has different values above and below T_λ. According to eq (5), τ_{SV} will have a finite maximum value at T_λ and if this value is reasonably small (i.e., $\omega^2\tau^2<1$) the attenuation will have its maximum at T_λ.

For a mechanism involving a single relaxation time, we have the usual expression

$$\alpha=\left[\frac{c\bar{\gamma}_1-c^0_{11}}{2Uc_{11}}\right]\frac{\omega^2\tau_{SV}}{1+\omega^2\tau^2_{SV}}. \tag{6}$$

Unfortunately the variation of $(c\bar{\gamma}_1-c^0_{11})/2Uc_{11}$ with temperature is not known, but it is unlikely that this could be an important factor in determining the temperature dependence of α. One would probably expect only a small and slowly varying dependence of $c\bar{\gamma}_1-c^0_{11}$ on temperature. We shall *assume* (as did Chase in his analysis of helium [28]) that $(c\bar{\gamma}_1-c^0_{11})/2Uc_{11}$ has a constant value throughout the transition region. We shall also assume (and can subsequently justify) that $\omega^2\tau^2_{SV}\ll 1$ for all temperatures near T_λ. With these assumptions and eq (5), we can rewrite eq (6) in the form

$$\frac{\omega^2}{\alpha}=\frac{2Uc_{11}}{c\bar{\gamma}_1-c^0_{11}}\frac{1}{\tau_{SV}}=\frac{2Uc_{11}}{c\bar{\gamma}_1-c^0_{11}}\left(\frac{\Delta T}{A}+B\right). \tag{7}$$

If all our assumptions are valid, then ω^2/α should be independent of frequency and should vary linearly with the temperature on both sides of T_λ.

Figure 10 shows a plot of ω^2/α, in units of cps^2 N^{-1} cm, *versus* temperature for all of our data close to T_λ. Various details concerning the correction for background attenuation and the justification of $\omega^2\tau^2<1$ are given elsewhere [14], but in a general way the data shown in figure 10 seem to agree with eq (7). The value of ω^2/α at its minimum (at ~ 242.0 °K) is 0.52×10^{16}; the slope above T_λ is 0.46×10^{16} and the slope below T_λ is 0.66×10^{16}. These slopes give a ratio $A^+/A^-=1.43$, as compared to ~ 1.6 expected on the basis of Kikuchi's model.

When the analysis is extended to data obtained at higher frequencies and at temperatures further away from T_λ, the deviations from eq (7) are not quite what one would expect [14] and new experimental work along these lines is currently in progress. Also if NH_4Cl undergoes a first-order transition very close to the "lambda point," then one would expect τ to undergo a discontinuous change between two finite values. This may supersede the explanation given above for the behavior of α [29].

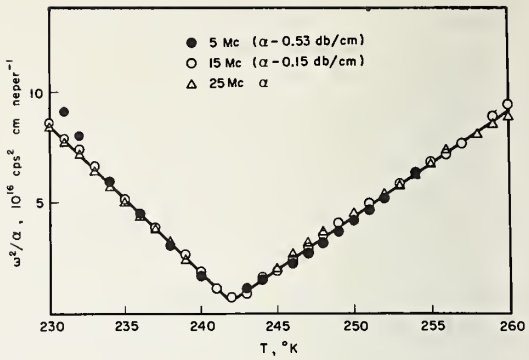

FIGURE 10. *Plot of ω^2/α versus temperature, close to the lambda point at* p = 1 *atm.*

Data at 45 and 55 Mc/s were not available over this temperature range. Note that the α values for 5 and 15 Mc/s have been corrected for a temperature-independent background attenuation (beam-spread losses).

References

[1] F. Simon, Ann. Physik **68**, 4 (1922).
[2] F. Simon and C. von Simson, Naturwiss. **14**, 880 (1926).
[3] A. Hettich, Z. Physik. Chem. **A168**, 353 (1934).
[4] A. C. Menzies and H. R. Mills, Proc. Roy. Soc. **A148**, 407 (1935).
[5] L. Pauling, Phys. Rev. **36**, 430 (1930).
[6] R. H. Fowler, Proc. Roy. Soc. **A149**, 1 (1935).
[7] J. Kirkwood, J. Chem. Phys. **8**, 205 (1940).
[8] J. Frenkel, Acta Physicochimica **3**, 23 (1935).
[9] H. A. Levy and S. W. Peterson, Phys. Rev. **86**, 766 (1952).
[10] E. M. Purcell, Physica **17**, 282 (1951).
[11] C. W. Garland and J. S. Jones, J. Chem. Phys. **41**, 1165 (1964).
[12] C. W. Garland and J. S. Jones, J. Chem. Phys. **39**, 2874 (1963).
[13] C. W. Garland, and R. Renard, J. Chem. Phys. **44**, 1130 (1966).
[14] C. W. Garland and J. S. Jones, J. Chem. Phys. **42**, 4194 (1965).
[15] P. W. Bridgeman, Phys. Rev. **38**, 182 (1931).
[16] C. W. Garland and R. Renard, J. Chem. Phys. **44**, 1120 (1966).
[17] C. Domb, J. Chem. Phys. **25**, 783 (1956).
[18] C. P. Bean and D. S. Rodbell, Phys. Rev. **126**, 104 (1962).
[19] D. C. Mattis and T. D. Schultz, Phys. Rev. **129**, 175 (1963).
[20] O. K. Rice, J. Chem. Phys. **22**, 1535 (1954).
[21] R. Renard and C. W. Garland, Phys. Rev. J. Chem. Phys. **44**, 1125 (1966).
[22] C. W. Garland, J. Chem. Phys. **41**, 1005 (1964).
[23] C. W. Garland and R. Renard, J. Chem. Phys. (in press).
[24] L. D. Landau and I. M. Khalatnikov, Akad. Nauk. S.S.S.R. **96**, 469 (1954).
[25] I. A. Yakovlev and T. S. Velichkina, Sov. Phys. Uspekhi **63**, 552 (1957).
[26] T. Tanaka, P. H. E. Meijer, and J. H. Barry, J. Chem. Phys. **37**, 1397 (1962).
[27] R. Kikuchi, Ann. Phys. (N.Y.) **10**, 127 (1960).
[28] C. E. Chase, Phys. Fluids **1**, 193 (1958).
[29] C. W. Garland and C. F. Yarnell, J. Chem. Phys. (in press).

Discussion

E. H. W. Schmidt presented some experimental observations on convective heat transfer near the critical point of CO_2 [1] emphasizing the difficulties which arise in measuring the thermal conductivity in the critical region.

J. J. M. Beenakker: I have a problem concerning the dimensions of the apparatus in which one tries to measure the transport properties near the critical point. As soon as one expects that any anomaly in viscosity or thermal conductivity is related to the long range correlations or fluctuations, care has to be taken that the dimensions are large compared to the magnitude of the correlation length.

M. E. Fisher: It seems to me there is no need to worry about the dimensions relative to the correlation length because all the light scattering and neutron scattering experiments show that even when you have what you call long range correlations, they are still of the order of 1000 Å when you come very close to the critical point. And that is for the pair correlation function. Most of these transport coefficients involve higher order correlation functions which one would expect to die out more rapidly. Thus although in principle one could get difficulties very close to the critical point, I don't think one has to worry about this in practice.

J. J. M. Beenakker: In the case of an oscillating disk viscometer one has to consider a penetration depth between oscillating plates and the gas layer. As in the critical region the density is changing rapidly with height, I wonder whether you can make a statement of the absence of an anomaly in the viscosity close to the critical point.

J. V. Sengers: That was one of the reasons why I made the statement that any anomaly in the viscosity is absent at temperatures more than 1 percent away from the critical temperature. At present I would rather leave open the question of the behavior of the viscosity closer to the critical point.

J. S. Rowlinson: I would like to raise the question whether the C_v of a binary mixture has an anomaly near the critical mixing point. There is certainly an anomaly in C_p, but as far as I know there is no anomaly in C_v in this case.

J. V. Sengers: I don't know. I looked for experimental data for C_v near the critical mixing point of binary mixtures in the literature, but I did not find any.

C. J. Pings: Dr. Sengers, did you not also run your experiments with two different distances between the plates? You seem to get the same results which proves the absence of an effect from convection.

J. V. Sengers: At the isotherms close to the critical temperature (31.2, 32.1, 34.8 °C) measurements were taken using only one plate distance, because it is difficult to do those measurements with a larger plate distance. However, the anomalous behavior is already present at higher temperatures where measurements with two different plate distances were indeed carried out, which give an additional proof of the reality of the anomaly.

M. S. Green: I want to point out that the difference in behavior between viscosity and thermal conductivity is theoretically very surprising. Both the viscosity and the thermal conductivity can be expressed as the time average correlation of relevant fluxes. As the flux for the thermal conductivity and the flux for the viscosity have a similar form, it is hard to imagine why there would be any difference in behavior.

R. Zwanzig: If you analyze these correlation function formulas for fluids which have internal degrees of freedom interacting weakly with the translational degrees, it turns out that the shear viscosity does not show any particular effect from the internal degrees of freedom. On the other hand the thermal conductivity shows some effect and the bulk viscosity even a bigger effect [2]. Thus there exists a counter example to Dr. Green's suggestion that the correlation function formulas should show roughly the same behavior.

E. Helfand: I think the anomaly in the thermal conductivity arises from the thermodynamic force involved. Any molecular model would speak in terms of energy transport. However, the thermal conductivity is related to a temperature gradient. Therefore to go from the energy gradient to the temperature gradient one has to introduce the specific heat. This is similar to the case of the diffusion coefficient where one has to transform a gradient of the chemical potential into a concentration gradient. For this reasion a connection between the anomaly in the thermal conductivity and in the C_v is not surprising.

R. Zwanzig: I would suggest to the experimentalists to study the dependence of the friction on the frequency with the oscillating disk viscometer as well as observing slow oscillations. If there were nonlocal effects involving a penetration length and a correlation length, one would perhaps be able to see from the frequency dependence of the friction whether any peculiar behavior would occur.

J. Kestin: One can regard all these experiments as having been performed at zero frequency. When one wants to go to higher frequencies, one must consider the possibility that hydrodynamic instabilities will be encountered.

As Dr. Sengers pointed out, I think one should measure the two quantities: density and viscosity or density and thermal conductivity, simultaneously. This does not seem to be impossible.

N. J. Trappeniers presented experimental data for the spin-lattice relaxation time of deuterated methanes [3].

N. J. Trappeniers: We have also made diffusion measurements in the critical region, but I did not present those, because one has to be extremely careful to find the density. I think that one cannot say much, if one does not have accurate density measurements. In the critical region the density varies extremely rapidly. Therefore I would like to ask Dr. Bloom the following: You make your measurements of the diffusion coefficients with an accuracy of about 5 percent in the critical region. If you would make an error in density of 5 percent or even 10 percent, which is easily made if one does not have accurate $P-V-T$ data, would it not be possible to accumulate the errors by plotting the product $D\rho$ so that the scattering in your points thus obtained would explain the anomaly which you think to detect in the critical region?

M. Bloom: I agree with you that it is dangerous. We have made density measurements in three different samples (these were the impure samples) and I showed the ratio ρ_L/ρ_V of the liquid and gas densities. These were obtained by making measurements at the top end of the tube and at the bottom end of the tube, while the density gradient was in the middle of the tube. We measured the ratio ρ_L/ρ_V to within 2 percent. The diffusion coefficient was measured within approximately 2 percent. An error of 5 percent has been assigned to D to take into account systematic errors and that is a conservative estimate. The anomalous decrease in $D\rho$ which we observed is about 20 percent. But I agree with you that it is dangerous. I think one should do measurements with a flat horizontal sample to eliminate gravitational effects.

C. J. Pings presented experimental data for the sound absorption in the nitrobenzene-iso-octane system [4].

L. Tisza: To Drs. Chase and Williamson should go the credit for their experiments. However, I have to assume the responsibility for the prediction that the sound velocity tends to zero as the critical point is approached. The argument is based on thermostatics and can be applied only to the real part of the sound velocity in the low frequency limit. Since the absorption of sound need not decrease, one can expect that the sound velocity would drop until the signal is lost. This seems to be the experimental finding.

R. Zwanzig: I would like to make one remark about the general interpretation of ultrasonic data. Many years ago Dr. Tisza pointed out that ultrasonic absorption data could be explained formally by the introduction of a volume viscosity or bulk viscosity into the hydrodynamic equations [5]. However, as far as I know, nobody ever does this in connection with ultrasonic relaxation, especially near the critical point. There is one good reason for this, namely that there is hardly any way of measuring the bulk viscosity. The only way you do it nowadays is to measure the sound absorption, so that it seems redundant. At present, however, there are theoretical expressions for the bulk viscosity (derived first, in fact, by Dr. Green) and there is at least a handle by which one can investigate theoretically what the magnitude of the bulk viscosity ought to be. Very little is known about this either, but one does not have as yet a good reason to disregard the classical hydrodynamics with the bulk viscosity.

K. F. Herzfeld: The situation is not so simple. It is completely correct, of course, that one can formally describe the sound absorption via a bulk viscosity. In a polyatomic gas the bulk viscosity is arising mainly from the relaxation of the internal degrees of freedom to their equilibrium distribution. In liquids, however, there are more processes contributing to a bulk viscosity. At low frequencies one can describe the relaxation of the different processes with one "bulk viscosity constant." However, at higher frequencies one has to take into account the fact that the different processes relax with different relaxation times and show resonances at different frequencies. Consequently the bulk viscosity is dependent on the frequencies and one has to analyze the different processes involved. The situation is analogous to that regarding the dielectric constant which only can be considered constant at low frequencies.

R. Zwanzig: That is right. The only reason why I raised the point is the fact that there are presumably rigorous statistical mechanical expressions for the frequency dependent viscosity. The question arises whether the ultrasonic absorption can be described by these formulas or whether the ultrasonic absorption is due to something more complicated like scattering by density fluctuations.

O. K. Rice: In connection with the paper of Dr. Garland and Dr. Renard, I might say that about 12 years ago I wrote a paper in which I showed by purely thermodynamical means that for a compressible lattice the transition will change into a first-order transition [6].

C. W. Garland: We agree that this can be proved in a phenomenological way, but we considered that doing it for an explicit model, in which the shape of the curve is given analytically by the Onsager solution, provided an additional way of looking at the problem with which people who like models can perhaps feel more confident.

M. E. Fisher: In this connection I would also like to draw attention to the work of Domb [7], Bean and Rodbell [8] and Mattis and Schultz [9] who reach similar conclusions to those first discussed by Dr. Rice but from a more microscopic view point. It seems to me that the general validity of all these treatments is open to doubt in respect of the conclusions drawn about the changed nature of the transition point. The physical reason is the neglect of the fluctuations in the lattice expansion and the consequent "renormalization" of the original interaction responsible for the phase transition. This difficulty can be seen explicitly in the case of a linear chain model which never has a phase transition (as shown by an exact solution) but for which the treatments referred to would predict a first order transition for certain parameter values. This has been demonstrated by Mattis and Schultz [9] (although the arguments they give as to why this might not matter in three dimensions are unconvincing).

N. J. Trappeniers presented experimental data for the C_v of ammonium chloride as a function of pressure along the λ-line.

References

[1] E. Schmidt, Int. J. Heat Man Transfer **1,** 92 (1960).
[2] R. Zwanzig, J. Chem. Phys. **43,** 714 (1965).
[3] N. J. Trappeniers, C. J. Gerritsma, P. H. Oosting, Physica **31,** 202 (1965); Phys. Letters **16,** 44 (1965).
[4] C. J. Pings and A. V. Anantaraman, Phys. Rev. Letters **14,** 781 (1965).
[5] L. Tisza, Phys. Rev. **61,** 531 (1942).
[6] O. K. Rice, J. Chem. Phys. **22,** 1535 (1954).
[7] C. Domb, J. Chem. Phys. **25,** 783 (1956).
[8] C. P. Bean and D. S. Rodbell, Phys. Rev. **126,** 104 (1962).
[9] D. C. Mattis and T. D. Schultz, Phys. Rev. **129,** 175 (1963).

SUPPLEMENTARY SESSION

209-493 O-66—15

Effect of Gravity on the Equilibrium Mass Distribution of Two-Component Liquid Systems. The Observation of Reversed Diffusion Flow

H. L. Lorentzen and B. B. Hansen

University of Oslo, Oslo, Norway

At the conference the similarity between the *coexistence curves* of one-component and two-component systems has been stressed. The similarities between the two systems have to be extended to the *equilibrium mass distributions* in vertical containers.

In one-component systems it is well known that close to the critical point the mass distributions at equilibrium are represented by sigmoid curves in the height versus density diagrams. This is caused by the effect of gravity. The same applies to the two-component systems. Thus in a vertical container filled with mixture at critical conditions, homogeneous mixtures do not represent equilibrium. Due to the effect of gravity—also in the two-component systems—equilibria in the critical region are represented by sigmoid curves in the height versus composition diagrams. (See fig. 1.)

In the experimental part of this paper will be shown exposures of curves of mass distribution, which spontaneously developed in two-component liquid systems. They are representing equilibrium mass distributions. One of the observations which support this is the observation of transport of material through the layers of the equilibrium distributions. The transport was towards greater composition differences.

It will be shown in three different ways that the equilibrium mass distribution in the critical region cannot be the homogeneous mixtures, but distributions represented by sigmoid curves in the height versus composition diagram. The developments are founded on the low values of the gradient of the chemical potential ($d\mu/dc$) in the critical region.

According to classical thermodynamical view the gradient of the chemical potential is zero at the critical point:

$$\frac{d\mu}{dc}=0. \tag{1}$$

Furthermore, according to modern views the gradient of chemical potential is the virtual force producing diffusion. Therefore, when the gradient of the chemical potential is zero, also the diffusion coefficient will be zero.

Bjørn Bergsnov Hansen [1] and I determined the diffusion coefficient at critical density as function of the temperature distance from the critical for the two systems: succinonitrile-ethanol and triethylamine-water. We found the diffusion coefficients to be close to linear functions of the temperature distance from critical, $\Delta T=T-T_c$, and approaching zero at the critical temperature.

Determinations of the diffusion coefficients as function of the composition difference from critical $\Delta c=c-c_c$, as well as the temperature difference from critical ΔT has shown the following relationship to be basically correct.

$$D=k_1\Delta T+|k_2\Delta c^n| \tag{2}$$

where k_1 and k_2 are constants (k_2 not the same on both sides of the critical composition) and n is close to 3.

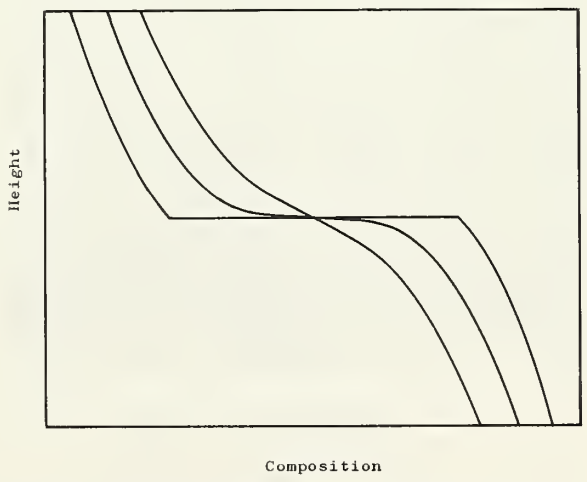

FIGURE 1. *Schematic drawing of equilibrium mass distributions in the height versus composition diagram.*

This is in agreement with theoretical considerations which Professor Joseph Mayer had pointed out to me [6].

When the diffusion coefficient approaches zero at the critical point the *thermal diffusion ratio* approaches infinite. In a binary system a temperature gradient leads to a flow which will ultimately separate the liquid in two layers. However, by this flow a composition gradient is built up and consequently a mass diffusion flow will counteract the effect of the temperature gradient. At the "Endzustand" the two effects are in balance. At the critical point the diffusion coefficient approaches zero and thus the composition gradient $\left(\frac{dc}{dh}\right)$ will approach infinite.

Studies of the thermodiffusions in the critical region of the system aniline-cyclohexane here have shown the Endzustände to be sigmoid curves with the greatest gradients at critical composition. The gradient increases where the temperature of the critical composition approaches the critical, and the gradient may well become infinite at this temperature. When this is so, it is obvious that, when the temperature gradient diminishes towards zero (T=constant) and the Endzustände goes towards that of an equilibrium, the mass distributions at this equilibrium will also be sigmoid curves in the height versus composition diagram.

In a binary mixture the molecules of the components will have different buoyancy relative to the mixture. Therefore, the molecules of one of the components will have a tendency to move upwards and the molecules of the other to move downwards in the liquid. Consequently, a composition gradient will develop and an inhomogeneous equilibrium distribution will be established, whereby these tendencies are balanced by diffusion flow towards homogeneity.

Because of the overwhelming influence of the diffusion flow such effect has not been observed at normal conditions. In the critical region, however, where the diffusion coefficients are very small, the effect will have to be remarkable, and at the critical point the effect will result in an equilibrium distribution of an infinitely great composition gradient.

In a liquid the potential energy increases with the height. In liquid mixtures—at equilibrium—the difference of potential energy of the layers at the various heights will be balanced by a change of the composition of the mixtures with height.

In a binary mixture the equilibrium condition will be governed by the equation

$$\frac{dx}{dh}=\frac{M_1-\rho V_1}{d\mu_1/dx}\cdot g \tag{3}$$

where x is the mole fraction n_1/n_1+n_2, h is the height, M is the molecular weight, ρ is the density of the mixture, V is the partial molar volume, $V_1=(dV/dn_1)_{pTn_2}$, μ is the chemical potential and g the acceleration of gravity. When in the critical region $d\mu/dx$ is very small, dx/dh will be great.

Reversed diffusion flow. It was mentioned in the introduction that diffusion flow towards greater composition differences has been observed. Fick's law is founded on the observation that at normal conditions the Endzustände of the diffusion process is that of a homogeneous mixture. When, however, homogeneous mixtures do not represent equilibrium, the diffusion process will not go towards homogeneity, but towards the equilibrium condition.

Fick's law then may have to be rewritten in the form:

$$J=-D^*\left(\frac{dc}{dh}-\left(\frac{dc}{dh}\right)^0\right) \tag{4}$$

where h is the direction of the diffusion flow in a vertical container. dc/dh is the concentration gradient of the liquid with respect to the height; dc/dh approaches the equilibrium distribution characterized for the temperature and composition in question by the gradient $(dc/dh)^0$ at equilibrium.

The term $\left(\frac{dc}{dh}-\left(\frac{dc}{dh}\right)^0\right)$ of eq (4) will be negative when $(dc/dh)^0$ is greater than dc/dh. The flow J is then negative, and we will observe a "reversed diffusion flow."

Reversed diffusion flow can also be observed independent of the effect of gravity. If a mixture is left at a temperature of the coexistence curve the mixture may be split in two phases divided by a surface. This is schematically shown on figure 2. The lines AB and B′A′ indicate equilibrium phases. When now the temperature is changed in the direction away from the critical temperature, then the compositions of the phases at the new temperature will be outside the compositions corresponding to the former temperature (dotted lines CD and D′C′).

Generally the formation of the new phases will be introduced by fog formation. In some cases,

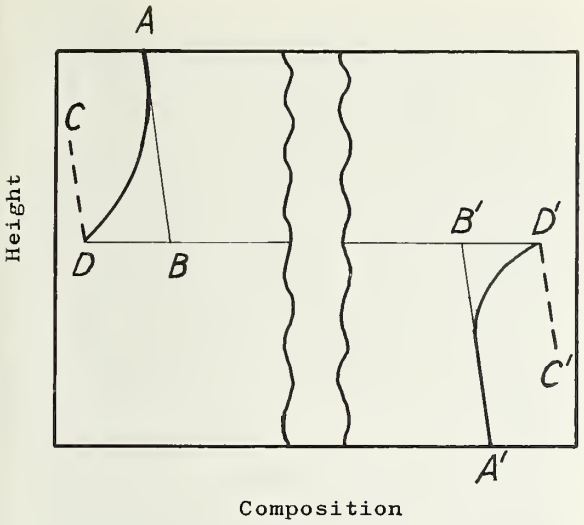

FIGURE 2. *A schematic drawing of the mass distribution at two temperatures* T_1 *and* T_2.

T_1 is the temperature closest to the critical, and the lines AB and A'B' indicate the two phases at equilibrium at T_1. The temperature difference between T_1 and T_2 is very small, and the dotted lines DC and D'C' indicate the equilibrium distribution at T_2.

When the temperature is changed from T_1 to T_2 no fog is formed. A diffusion flow of material passing the surface DD' will be observed as mass distribution curves of the form AD and A'D'.

however, when the phases remain "undercooled," the formation of fog does not take place, and a diffusion flow of material will take place. The diffusion flow is crossing the surface border and is a "reversed diffusion flow" towards greater differences in composition.

The two arched curves at the surface together with the straight lines at greater distance from the surface show the distributions observed after a period of time at the new temperature.

I have not been able to make an exact determination of the form of the arched curves. The form appears, however, to be close to the error function curve observed by free diffusion.

Experimental Procedures

The average compositions of the mixtures were close to the critical compositions.

The liquid mixtures were sealed in all-glass containers—ca. 15 mm high and of about 5 mm^2 cross section area. The liquid mixture almost completely filled the container.

The container was placed in a thermostat which allowed the temperature to be controlled with an accuracy better than ± 1 mdeg [2]. The temperature was determined by means of a platinum resistance thermometer.

The compositions of the mixture at the various heights inside the container were determined by means of an integral optical system [3]. This allowed visual observations and photographic recordings, which actually are diagrams with the height in the container as ordinate and the optical density as abscissa.

In the region of the critical solution points, one observes that the mass transports towards equilibrium distributions are using the formation of fog as vehicle. Thereby droplets of compositions at densities different from that of the mother liquid are formed and move by buoyancy upwards or downwards in the liquid mixture. After a period of time the fog has disappeared and a new mass distribution can be observed.

When the temperature of a nearly homogeneous mixture of a composition close to the critical, and at a temperature outside the coexistence curve, is changed to one of the temperatures *of the coexistence curve*, the material of the sample is then brought to a state of unattainable instability. Two phases must then develop and they do so probably instantaneously by the formation of fog.

Figure 3 shows an example whereby a nearly homogeneous mixture of succinonitrile-ethanol was cooled to about 50 mdeg below the critical. When the fog had disappeared the composition of both phases were inhomogeneous and had the form of two arms of a sigmoid curve.

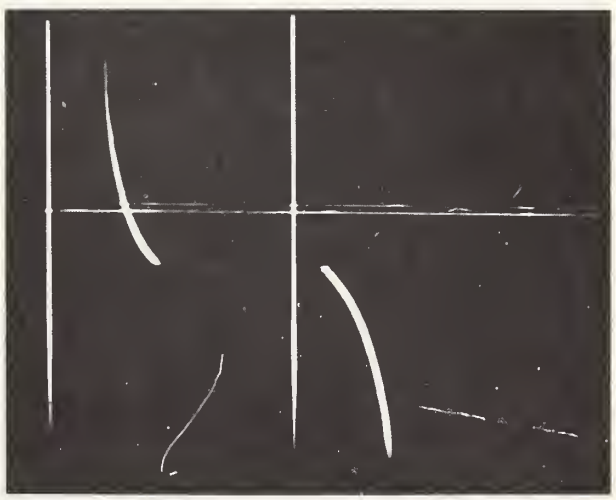

FIGURE 3. *System: Succinonitrile-ethanol.*
Ordinate: Height in container.
Abscissa: Composition.
Straight vertical and horizontal lines are orientation lines.

Figure 3 shows the composition which appeared when the near homogeneous mixture of succinonitrile-ethanol had been cooled from a temperature above the critical down to a temperature of about 50 mdeg below the critical and the fog had disappeared.

Figure 3 is representative for a great number of observations also with other liquid systems which have been studied here.

Figure 3, however, does not represent the sole form which the phases may show when the fog disappears. In some cases only one of the phases may be smoothly sigmoid and the other closer to homogeneous. This is explained by convection flow in this phase during the establishment.

When the temperature of the mixture is *not* brought to the temperature *of the coexistence curve*, a redistribution of the material can not be enforced. It happened, however, that in a mixture of triethylamine-water the reestablishment took place also at a temperature outside those of the coexistence curve and in the temperature range reaching from the critical temperature to about 100 mdeg outside the coexistence curve.

The system triethylamine-water was studied at the lower critical solution point of the system. At a lower solution point the temperatures outside the coexistence curve are below the critical temperature, and the temperatures of the coexistence curve above.

During the general study of this system the sample was left for one night at a temperature outside the coexistence curve. Next day the arbitrary mass distribution curve was found to have been partly reformed into a smoothly formed arched curve in the diagram height versus composition.

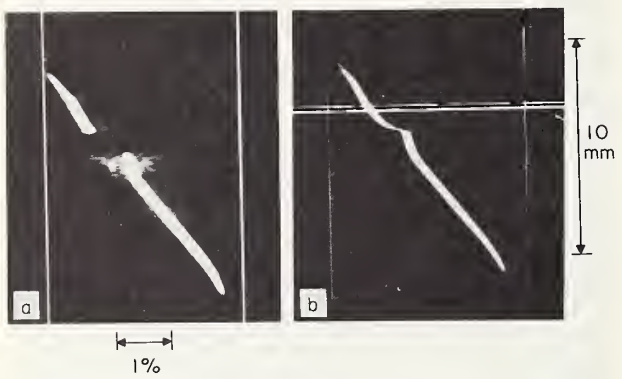

FIGURE 4. *System: Triethylamine-water.*
Ordinate: Height in the container, scale shown on the right side of the figure.
Abscissa: Composition of the mixture, scale unit below photograph 4.a.

Exposure 4.a shows the originally straight curve partly disrupted by layers of fog. Below this layer is another layer of fog, which, however, allows the light to pass and produces background illumination at these heights.

Exposure 4.b shows the composition curve after the fog had disappeared. The curve has attained a regular arched form where the upper layer of fog had been. When making the exposure a, the horizontal orientation lines were not illuminated. The photographically recorded composition curves do not represent the entire column of the liquid mixture.

This surprising reformation of the mass distribution was then systematically studied, and Bjørn Bergsnov Hansen and I subsequently found a temperature treatment of the sample—which was sealed inside an all-glass cell—whereby we could reproduce the phenomenon ad libitum. The temperature of the thermostat was set at a temperature below the critical (outside of the coexistence curve). The cell was then removed from the thermostat, warmed to room temperature and cooled to about 10° below the critical and carefully tilted. Thereby a certain concentration gradient was established in the liquid mixture. (Typical is the lower curve of fig. 5.) The container was then reinserted in the thermostat and it was observed that the composition curve remained unbroken.

After periods of time of different duration at constant temperature a belt of fog was spontaneously formed at varying levels in the liquid (in all cases but one in the upper middle section of the liquid column). The belt was at first fractions of a millimeter thick and gradually developed upwards as well as downwards in the liquid.

Figure 4a shows a photograph made after the fog had appeared. The fog consisted of two layers separated by a sharp boundary. The upper layer of fog entirely veiled this part of the liquid. The lower layer of fog allowed the light to pass and disclosed that the mixture at these levels had attained nearly homogeneous compositions. The nature of this fog, however, was such that light was scattered, and at these levels a background illumination was observed.

30 min later the fog had disappeared and, where the upper layer of fog had been, the curve had attained a smooth arched shape leading downwards to a kink from which the curve by a near-vertical section continued into the original curve. (Fig. 4b.)

The smooth arched curves represent layers with defined composition gradients. The gradient increases towards critical composition, and must be regarded as a section of an equilibrium distribution curve.

As mentioned the fog started as a very thin belt, which grew broader with time. In one series of experiments the temperature was immediately lowered just as the fog appeared. Thereby the fog disappeared, and a comparison between the curve, before and after the fog disappeared, showed that the fog was first formed where the original gradient and the gradient of the developed arched curve were equal (fig. 5) [5].

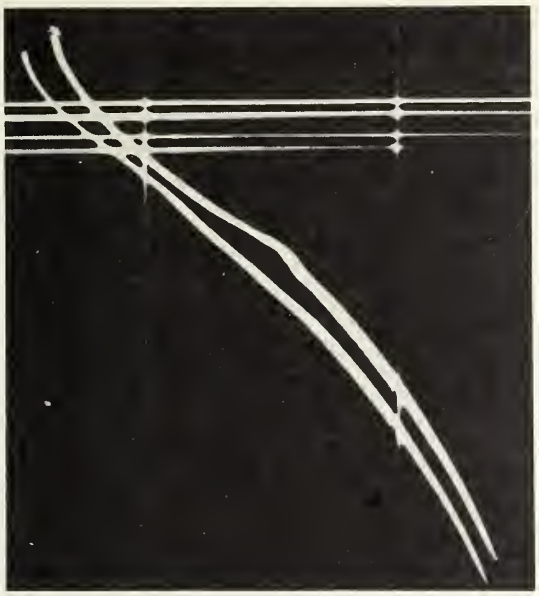

FIGURE 5. *System, ordinate, and abscissa as on figure 4, however, different scales.*

Two photographs are mounted together by dislocation along the ordinate. The lower is the original composition curve before the development of fog.

The upper curve shows the composition after the liquid mixture had been cooled and the fog had thus disappeared. Visual observation had disclosed that the formation of fog started at composition close to the left vertical orientation line, where the exposures show that the gradients of the original and the developed regular arched curves are the same.

The latter observation explains why the belt of fog appeared at compositions somewhat different from critical composition (in all cases but one at triethylamine richer mixtures).

The smooth arched curves which appeared after the fog had disappeared generally did not reach to the critical composition. When the system was left undisturbed at constant temperature after the fog had disappeared, the smooth arched curve grew in both directions. The form of the originally formed curve remained unchanged. It was, however, observed slowly to change its height in the container.

When enough time had gone, the smooth arched curve grew past the critical composition and passed a point of inflexion. From this point on the composition gradient decreased with increasing distance from critical composition. Maximum gradient was found at — or very close to — critical composition.

When the smooth arched curve was observed to grow in both directions this naturally was caused by an increase in the height of these layers upwards as well as downwards. This was a consequence of a transport of material through these layers, which transport was a diffusion flow towards increasing differences in composition, "reversed diffusion flow."

Figure 6 and figure 7 show exposures from two series in which the curves mentioned above had been established. (See legend.) In the series of figure 6 the temperature was lowered in steps (away from the critical). When the temperature changed, a fine fog veiled the regular arched section of the curve for a shorter period of time, and

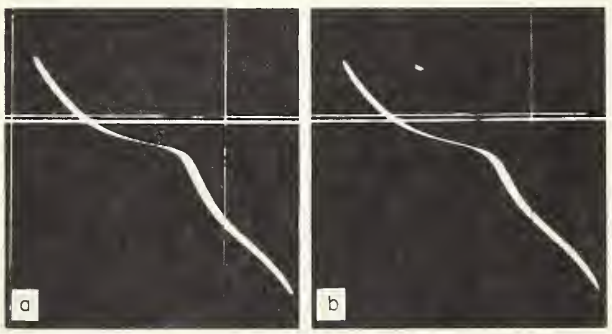

FIGURE 6. *System, ordinate, abscissa and scales as on figure 4*

Figure 6.a shows the regular arched curve developed to both sides of the critical composition during 10 hr at constant temperature, 41.5 mdeg below the critical.

The temperature was then lowered to 53 mdeg below critical, and figure 6.b shows the composition curve after 7 hr at this temperature. The composition gradients had decreased in the layers of the smooth arched composition curve. A comparison of the "lower arm" of the curve does indicate that a diffusion towards greater composition differences has taken place (towards a continuation of the regular arched curve).

FIGURE 7. *System, ordinate, abscissa and scales as on figure 4.*

Five photographs of the same series with stepwise increasing temperatures, mounted in successive sequence of time.

The opening of the concentration curve in figure 7a is due to the optics of the apparatus.

In figures 7b–e two phases are formed.

in this section the form of the curve changed basically by an increase of the composition gradients dc/dh.

Figure 7 shows exposures of a series with stepwise increase of temperature. Here too a faint fog was formed as in the series above. At the temperatures of the exposures 7a and 7b the smooth arched section of the curve changed basically at each step by a decrease of the gradients dc/dh at the various compositions.

At the step 7b the critical temperature is passed and the concentration curve is broken close to critical composition.

Exposure 7d is taken at a temperature 17 mdeg above critical. The left part of the curve is arched basically in the same way as shown on figures 1 and 3. The upper part of the right side leading to the surface dividing the phases is nearly vertical. The reason for this may be a convection flow in the lower phase during the establishment of this phase.

End Remarks

In the beginning of this paper it was said that the effect of gravity added to the analogy which is known to exist between the binary and the one-component systems. This may be further illuminated:

1. The presence of a temperature gradient in the binary systems leads to the Soret effect. In the one-component systems a temperature gradient will lead to mass distribution curves which will constitute isobars in the temperature-density diagram. In both cases it must however be remembered that the effect of the temperature gradient in the experiments will come in addition to the effect of gravity.

It may also be mentioned that when in the one-component systems the isobars are experimentally known, and also the gradient dp/dT at the critical density, the isotherms can be constructed. A similar relationship may be expected to hold in the binary systems between the Soret effect and the effect of gravity.

2. It was said that the effect of gravity in the binary systems was a necessary consequence of the small diffusion coefficient in the critical region, caused by the fall of the molecules of the heavier component towards the bottom of the container. In the same way the known sigmoid form of the mass distribution curves in the one-component systems can be regarded as a consequence of the fall of the molecules balanced by a diffusion upwards. This leads to the conclusion that the diffusion coefficients also of the one-component systems are very small in the critical region and will apply to an equation analogous to eq (2).

Hirschfelder [4] and Prigogine [5] have pointed out that diffusion measurements are of fundamental importance for the study of liquid mixtures on the molecular level.

By experimental determination of the equilibrium mass distributions in mixtures, preferably in fields of increased acceleration, one should have an additional method for the study of liquid mixtures — not only in the region of the critical solution points, but also for the study of liquid mixtures in general.

The reestablishment of the mixtures were observed in 1957. Professor Joseph Mayer kindly reviewed the reports from the experiments and showed that the form of the new established curves were related to the gradient of the chemical potential and consequently to the diffusion coefficient as function of the temperature and composition. I am very much in debt to Professor Mayer, who thereby gave me the clue to the problems.

I also express my thanks to Professor Odd Hassel for his interest and assistance. Furthermore, I express my thanks to Professor E. G. D. Cohen and Dr. J. M. H. Levelt Sengers, who have reviewed my paper.

References

[1] Hans Ludvig Lorentzen and Bjørn Bergsnov Hansen, Acta Chem. Scand. **12**, 139 (1958).
[2] Hans Ludvig Lorentzen, Acta Chem. Scand. **7**, 1335 (1953).
[3] Hans Ludvig Lorentzen, Acta Chem. Scand. **9**, 1724 (1953).
[4] Hirschfelder, Curtiss, Bird, Molecular Theory of Gases and Liquids, p. 539 (John Wiley & Sons, Inc., New York, N.Y., 1964).
[5] Prigogine, The Molecular Theory of Solutions, p. 51 (North-Holland Publ., 1957).
[6] Professor Joseph Mayer, private correspondence (Chicago, June 21, 1957).

Ferro- and Antiferromagnetism of Dilute Ising Model

S. Katsura and B. Tsujiyama

Tohoku University, Sendai, Japan

1. Introduction

The properties of alloys of magnetic substance and nonmagnetic substance are investigated experimentally and theoretically as problems of dilute magnetism. Here we consider Ising spins of $S=1/2$ as a magnetic substance and the energy of the system is assumed to be given by a sum of exchange energies between nearest neighbor Ising spins, positive or negative, corresponding to ferro- and antiferromagnetic coupling. That is, the interaction energy between nonmagnetic ions and that between nonmagnetic ions and Ising spins are neglected. This restriction can easily be removed. The calculation based on the inclusion of the interaction energy of nonmagnetic ions will be carried out in future.

The idealization of the preparation of the system can be classified into two limiting cases. We denote the spin average by $\langle\ \rangle_s$ and the configuration average by $\langle\ \rangle_c$.

The free energy of the system which was heated at infinitely high temperature and was cooled infinitely rapidly up to temperature T is given by

$$F_Q=-kT\langle\ln\langle Z\rangle_s\rangle_c. \tag{1.1}$$

In this system the true thermal equilibrium is not realized and it is a free energy of an idealized quenched system in which ions are frozen randomly at their positions.

On the other hand, if the temperature and external parameters are varied infinitely slowly and true thermal equilibrium is realized, the free energy of the system is given by

$$F_A=-kT\ln\langle Z\rangle_{s,c}. \tag{1.2}$$

Although the interaction energy of the nonmagnetic ions are to be taken into account, the system corresponds to an idealized annealed system.

The distinction between these two cases has been discussed by Brout [1], Mazo [2], and Morita [3]. Quenched random dilute magnetism has been investigated by Behringer [4], Sato, Arrott and Kikuchi [5], Brout [1], Rushbrooke and Morgan [6], Elliott and Heap [7], and Abe [8]. In experiments ideal randomness in Brout's sense is not realized an actual "randomness" depends on the history of the preparation of samples. Experimental situation lies, more or less, between two idealized limiting cases. Hence it seems worthwhile to compare physical properties of those two systems for exactly solvable cases.

On the other hand, Syozi [9] investigated a two-dimensional decorated lattice model of dilute magnetism, where Ising spins locate on lattice points of regular two-dimensional lattice, and nonmagnetic atoms or Ising spins locate on middle points between nearest neighbor lattice points (fig. 1). He obtained exactly thermal properties of two-dimensional lattices by reducing its partition function to Onsager's partition function. We can get thermal and magnetic properties of the one-dimensional Syozi's model since the original Ising model of a one-dimensional system is known in a magnetic field. We will also compare properties of Syozi's model with above mentioned two cases.

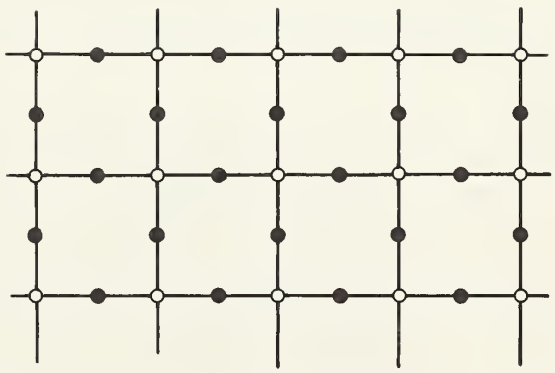

FIGURE 1. *Syozi's decorated lattice model of dilute Ising model.* ○ Ising spins, ● Ising spins or nonmagnetic atoms.

2. Annealed System: Formulation by Generating Function Method

In this and next sections, it will be shown that the problem of the annealed system is formulated by introducing a generating function in case of Ising spins, and that in the case of a one-dimensional problem evaluation of the generating function is reduced to an eigenvalue problem [10]. Moreover that eigenvalue equation is solved exactly and the free energy, the energy and the susceptibility are obtained.

A crystal lattice whose lattice point is named $i=1.2\ldots N$ is considered. On each lattice point there is either an Ising spin of $S=1/2$ or a nonmagnetic atom. If $\mu_i=1$, 0 or -1 is the state of each lattice point, the total energy of this system is given by

$$E=-\frac{J}{2}\sum_{\langle ij\rangle}\mu_i\mu_j-m\mathscr{H}\sum_i\mu_i. \tag{2.1}$$

Here m is magnetic moment ($=\frac{1}{2}g\mu_B$, g:g factor, μ_B: Bohr magnetron) of spin, $\mathscr{H}$ is external magnetic field. $J>0$ corresponds to ferromagnetic interaction and $J<0$ antiferromagnetic interaction. $\sum_{\langle ij\rangle}$ denotes summations over all pairs of neighboring lattice points. The second term is Zeeman energy. $\mu=1$ or -1 corresponds to Ising spin (up or down) and $\mu=0$ to a nonmagnetic atom, respectively. Instead of considering the problem of the system in which concentration of Ising spins is given by p (that of nonmagnetic atoms by $1-p$), the generating function Z with parameter D is calculated.

$$Z=\sum_{\mu_i=\pm1,\,0} e^{K\sum_{\langle ij\rangle}\mu_i\mu_j+C\sum\mu_i+D\sum\mu_i^2}, \tag{2.2}$$

where

$$K=\frac{J}{2kT},\qquad C=\frac{m\mathscr{H}}{kT}.$$

Since $\mu_i^2=1$ for spin states and 0 for nonmagnetic atoms,

$$\frac{1}{N}\frac{\partial\ln Z}{\partial D}=\langle\mu_i^2\rangle=p=p(K,D,C). \tag{2.3}$$

By solving D from (2.3) as a function of p and C,

$$D=D(K,p,C) \tag{2.4}$$

can be derived. D corresponds to chemical potential of spins divided by kT in an alloy of nonmagnetic atoms and spins. When (2.4) is substituted into

$$E=-\frac{J}{2}\left(\frac{\partial\ln Z}{\partial K}\right)=E(K,C,D) \tag{2.5}$$

and

$$M=m\left(\frac{\partial\ln Z}{\partial C}\right)_{K,D}=M(K,C,D), \tag{2.6}$$

energy E and magnetization M can be expressed as functions of K, p, and C. This problem is equivalent to the Ising model of $S=1$ with anisotropy.

3. Annealed System—Continued. Eigenvalue Problem in the Case of One-Dimensional System

The formulation in 2 leads to an eigenvalue problem in the case of one dimensional system. Generating function Z is given by

$$Z=TrV^N, \tag{3.1}$$

$$V=V_3^{1/2}V_2^{1/2}V_1V_2^{1/2}V_3^{1/2}, \tag{3.2}$$

under a periodic boundary condition. Here

$$V_1=\begin{pmatrix}e^K & 1 & e^{-K}\\ 1 & 1 & 1\\ e^{-K} & 1 & e^K\end{pmatrix},\quad V_2=\begin{pmatrix}e^C & & \\ & 1 & \\ & & e^{-C}\end{pmatrix},$$

$$V_3=\begin{pmatrix}e^D & & \\ & 1 & \\ & & e^D\end{pmatrix}. \tag{3.3}$$

If the maximum eigenvalue of $V=V_3^{1/2}V_2^{1/2}V_1V_2^{1/2}V_3^{1/2}$ is $\lambda_{\max}$, Z can be expressed in terms of $\lambda_{\max}$ in the limit of $N\to\infty$

$$\lim_{N\to\infty} Z^{1/N} = \lambda_{\max}. \tag{3.4}$$

The explicit expression for $\lambda_{\max}(K, C, p)$ which is a solution of a cubic equation is much too complicated to be differentiated analytically. It is sufficient, however, to derive $\lambda_{\max}$ exactly only up to the second order in powers of C since we are interested mainly in the energy and the susceptibility at zero field. From the symmetry of this matrix, the eigenvalue at $C=0$ and the coefficient of C^2 in the expansion of $\lambda_{\max}$ can be obtained simply by solving a quadratic equation. V can be written as a sum of even function and odd function of C.

$$V = \begin{pmatrix} k^2d^2 \operatorname{ch} C, & \alpha \operatorname{ch}\frac{C}{2}, & k^{-2}d^2 \\ d \operatorname{ch}\frac{C}{2}, & 1, & d \operatorname{ch}\frac{C}{2} \\ k^{-2}d^2, & \alpha \operatorname{ch}\frac{C}{2}, & k^2d^2 \operatorname{ch} C \end{pmatrix}$$

$$+ \begin{pmatrix} k^2d^2 \operatorname{sh} C, & d \operatorname{sh}\frac{C}{2}, & 0 \\ d \operatorname{sh}\frac{C}{2}, & 0, & -d \operatorname{sh}\frac{C}{2} \\ 0, & -d \operatorname{sh}\frac{C}{2}, & -k^2d^2 \operatorname{sh} C \end{pmatrix} \tag{3.5}$$

where

$$e^K = k^2 \qquad e^D = d^2.$$

By using similarity transformation matrices

$$S_1 = \frac{1}{\sqrt{2}}\begin{pmatrix} 1 & 0 & 1 \\ 0 & \sqrt{2} & 0 \\ 1 & 0 & -1 \end{pmatrix} = S_1^{-1} \tag{3.6}$$

and

$$S_2 = \begin{pmatrix} \sin\theta, & \cos\theta, & 0 \\ \cos\theta, & -\sin\theta, & 0 \\ 0, & 0, & 1 \end{pmatrix} = S_2^{-1}, \tag{3.7}$$

we have

$$S_2^{-1}S_1^{-1}VS_1S_2 = \mathsf{H}^{(0)} + \mathsf{H}^{(1)}$$

$$= \begin{pmatrix} H_{11}^{(0)} & 0 & 0 \\ 0 & H_{22}^{(0)} & 0 \\ 0 & 0 & H_{33}^{(0)} \end{pmatrix} + \begin{pmatrix} 0 & 0 & H_{13}^{(1)} \\ 0 & 0 & H_{23}^{(1)} \\ H_{31}^{(1)} & H_{32}^{(1)} & 0 \end{pmatrix}, \tag{3.8}$$

where θ is determined in such a way that $H_{12}^{(0)}$ vanishes. $H^{(0)}$ is an even function of C and $H^{(1)}$ an odd function.

In order to obtain $\lambda_{\max}$ in case of $C \simeq 0$, $H^{(0)}$ is regarded as an unperturbed term and $H^{(1)}$ as a perturbation. From second order perturbation theory (first order perturbation term vanishes)

$$\lambda_{\max} = H_{11}^{(0)} + \frac{(H_{13}^{(1)})^2}{H_{11}^{(0)} - H_{33}^{(0)}}. \tag{3.9}$$

Taking $C \simeq 0$ into consideration, $H_{11}^{(0)}$, $H_{33}^{(0)}$, and $H_{13}^{(1)}$ are expanded with respect to C,

$$H_{11}^{(0)} = \lambda^{00} + C^2\lambda^{01} + 0(C^4), \tag{3.10}$$

$$\frac{(H_{13}^{(1)})^2}{H_{11}^{(0)} - H_{33}^{(0)}} = C^2\lambda^{11} + 0(C^4). \tag{3.11}$$

The term of $0(C^2)$ does not appear from the third and higher order terms of the perturbation.

Thus the maximum eigenvalue of (3.2) is obtained exactly up to order of C^2.

When $\mathscr{H}=0$, the relation between p and D is represented by

$$e^{-D} = d^{-2} = \frac{p(p-1)(k^2+k^{-2})^2}{(k^2+k^{-2}-4)p(p-1)-1-(2p-1)\sqrt{2(2-k^2-k^{-2})p(p-1)+1}}. \tag{3.12}$$

The energy E and the susceptibility χ in case of $\mathscr{H}=0$ is expressed in terms of d^{-2}.

$$\frac{E}{NJ} = -\frac{1}{4}\frac{k+k^{-1}}{k-k^{-1}} \times \left[1 + \frac{k^2-4+k^{-2}-d^{-2}}{\sqrt{(k^2+k^{-2}-d^{-2})^2+8d^{-2}}}\right]. \tag{3.13}$$

$$\frac{kT\chi}{Nm^2}=\frac{2(\lambda^{01}+\lambda^{11})}{\lambda^{00}}$$

$$=\frac{1}{k^2+k^{-2}+d^{-2}+\sqrt{(k^2+k^{-2}-d^{-2})^2+8d^{-2}}}$$

$$\left[\frac{k^4+1-d^{-2}(k^2-2)}{\sqrt{(k^2+k^{-2}-d^{-2})^2+8d^{-2}}}+k^2\right.$$

$$\left.+\frac{4k^4+2d^{-2}+\dfrac{4\left\{(k^2+k^{-2}-d^{-2})\left(k^4\dfrac{d^{-2}}{2}\right)+4d^{-2}k^2\right\}}{\sqrt{(k^2+k^{-2}-d^{-2})^2+8d^{-2}}}}{3k^{-2}-k^2+d^{-2}+\sqrt{(k^2+k^{-2}-d^{-2})^2+8d^{-2}}}\right]. \tag{3.14}$$

d^{-2} in (3.13) and (3.14) is regarded as given by (3.12) in terms of p. Substituting $p=1$ into (3.13) and (3.14), well-known results on the Ising model

$$\frac{E}{NJ}=-\frac{1}{2}\,\mathrm{th}\,K, \qquad \frac{kT\chi}{Nm^2}=e^{2K} \tag{3.15}$$

are reproduced.

4. Quenched System

Next we consider the quenched system in one-dimension. The partition function for a given configuration of nonmagnetic atoms is given by

$$\langle Z\rangle_s=\sum\exp\left\{K\sum_{\langle ij\rangle}\mu_i\mu_j+C\sum\mu_i\right\} \tag{4.1}$$

$$=\mathrm{ch}^M K\mathrm{ch}^{N_s}C\sum_{\mu=\pm1}\prod^{N_s}(1+\mu_i\mu_j\mathrm{th}K)\prod^{N_s}(1+\mu_k\mathrm{th}C)$$

$$=\mathrm{ch}^M K\mathrm{ch}^{N_s}C\sum_{\mu=\pm1}\left(1+\sum_{\langle ij\rangle}\mu_i\mu_j\mathrm{th}K+\sum_{\langle ij\rangle}\sum_{\langle i'j'\rangle}\right.$$

$$\left.\times(\mu_i\mu_j)(\mu_{i'}\mu_{j'})\mathrm{th}^2K+\cdots\right)$$

$$\times(1+\Sigma\mu_k\mathrm{th}C+\Sigma\Sigma\mu_k\mu_{k'}\mathrm{th}^2C+\cdots) \tag{4.2}$$

Here $\mu=\pm1$, in contrast to the annealed system. N_s is the number of Ising spins. M is the number of bonds connecting Ising spins. The summation $\sum_{\langle ij\rangle}$ in (4.1) is carried out for only Ising spin pairs.

Expanding the product we have

$$\langle Z\rangle_s=\mathrm{ch}^M K\mathrm{ch}^{N_s}C\sum_{\mu=\pm1}\sum_m\sum_n(\mu_i\mu_j)(\mu_{i'}\mu_{i'})\cdots$$

$$\times(\mu_i^{(m)}\mu_j^{(m)})\mu_k\mu_{k'}\cdots\mu_k^{(n)}\mathrm{th}^mK\mathrm{th}^nC. \tag{4.3}$$

Carrying out the summation with respect to $\mu=\pm1$, we have

$$\langle Z\rangle_s=2^{N_s}\mathrm{ch}^M K\mathrm{ch}^{N_s}C\times\sum_m\sum_n[\text{Number of graphs which have } m \text{ bonds and of which the sum of the number of end points and odd junctions is } n \text{ in that configuration}]\times\mathrm{th}^mK\mathrm{th}^nC. \tag{4.4}$$

When we take the logarithm and divide by N, only the term proportional to N in the bracket survives. Restricting our interest in th^0C and in th^2C terms in the case of one dimension, we find that the average number of graphs which have m bonds and two end points is Np^{m+1}, since the probability of finding an Ising spin at each lattice point is p. Taking the configurational average by $\langle\ \rangle_c$, we have

$$[n=0,\ m=0]=1,$$

$$[n=0,\ m=1,\ 2,\ 3,\ \cdots]=0$$

$$\langle[n=2,\ m]\rangle_c=Np^{m+1},$$

$$\langle N_s\rangle_c=Np,$$

$$\langle M\rangle_c=Np^2.$$

Hence

$$\langle\ln\langle Z\rangle_s\rangle_c=Np^2\ln\mathrm{ch}K+Np\ln\mathrm{ch}C+Np\log2$$
$$+\ln\left[1+N\sum_m\mathrm{th}^2Cp^{m+1}\mathrm{th}^mK\right] \tag{4.5}$$

$$\lim_{N\to\infty}\frac{1}{N}\langle\ln\langle Z\rangle_s\rangle_c=p\log2+p^2\ln\mathrm{ch}K+p\ln\mathrm{ch}C$$

$$+\sum p^{m+1}\mathrm{th}^mK\mathrm{th}^2C+0(\mathrm{th}^4C). \tag{4.6}$$

Thus the energy is given by only the first term of the series and the series for the susceptibility

can be summed, giving

$$E=-\frac{J}{2}\frac{\partial\langle\ln\langle Z\rangle_s\rangle_c}{\partial K}=-\frac{NJ}{2}\,p^2\mathrm{th}K, \qquad (4.7)$$

$$\chi=\frac{m^2Np}{kT}\left\{1+2\sum p^m\mathrm{th}^mK\right\} \qquad (4.8)$$

$$=\frac{m^2Np}{kT}\frac{1+p\mathrm{th}K}{1-p\mathrm{th}K}.$$

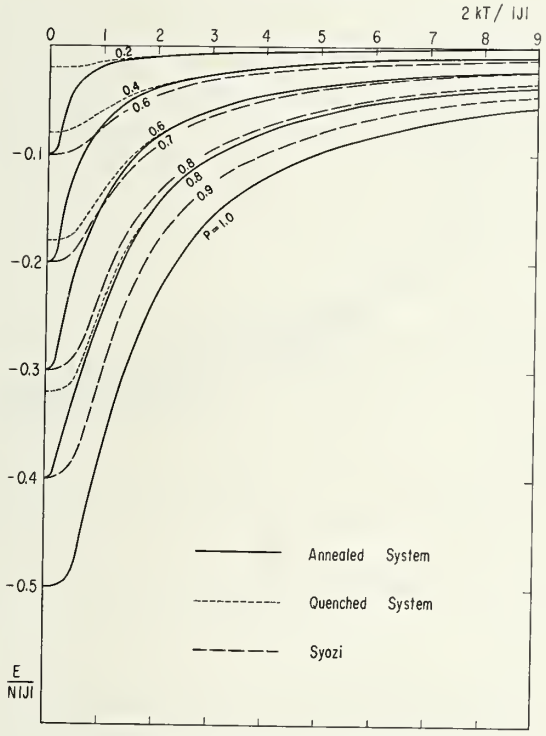

FIGURE 2. *Energy in zero magnetic field.*
Solid line: the annealed system. Dotted line: the quenched system ($0 \leq p \leq 1$). Dashed line: Syozi's model ($\frac{1}{2} \leq p \leq 1$).

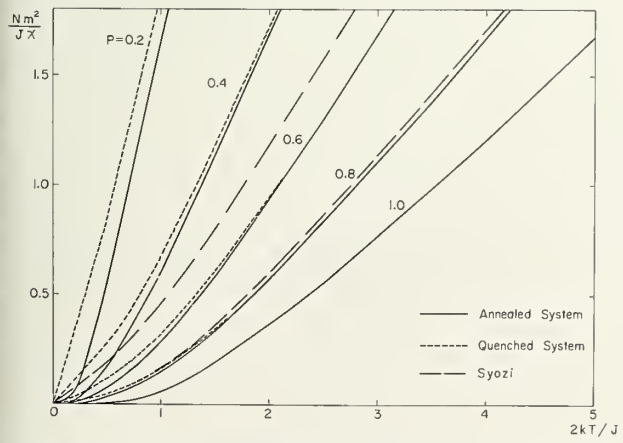

FIGURE 3. *Inverse susceptibility in the ferromagnetic case.*
Solid line: the annealed system. Dashed line: the quenched system. Long dashed line: Syozi's model.

5. Numerical Results and Discussions

Now we compare the numerical results of three cases, an annealed system, a quenched system, and Syozi's model.

Figure 2 shows the energy in zero magnetic field. The energy of Syozi's model for p is $-(p-\frac{1}{2})\times\tanh K$ for $\frac{1}{2}<p<1$. Figure 3 shows the inverse susceptibility of ferromagnetic case. Figure 4 shows the susceptibility of an antiferromagnetic case in the annealed system. Figure 5 is that for the quenched system and figure 6 shows that for Syozi's model. As the temperature goes to zero, the first tends to zero while the second and the third tends to infinity. Figure 7 shows the concentration dependenee of the antiferromagnetic susceptibility of the quenched system and the annealed system.

In the above results the difference in the low temperature susceptibility between the annealed system and the quenched system in the case of antiferromagnetic interaction is most drastic. In the quenched system the susceptibility at the concentration p is obtained by the arithmetic mean of each configuration corresponding to the same

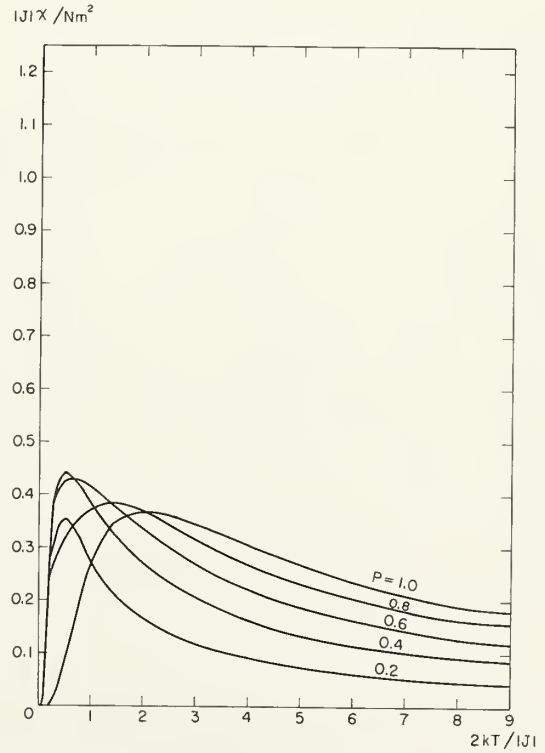

FIGURE 4. *Susceptibility of an antiferromagnetic case in the annealed system.*

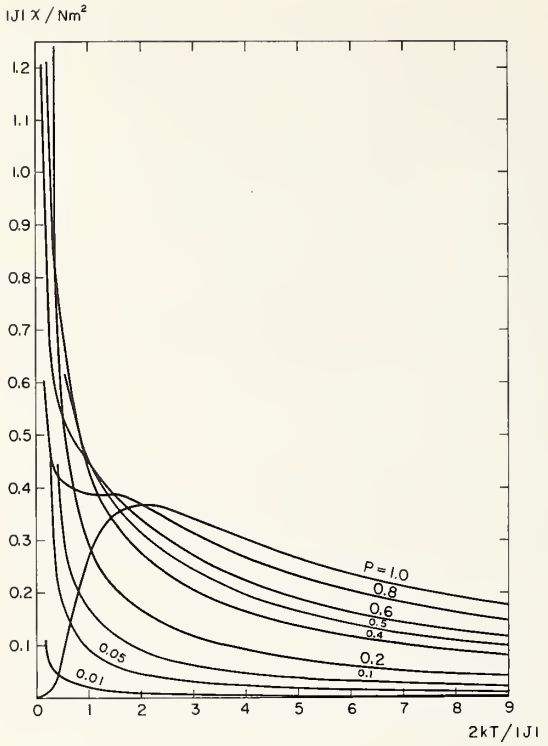

FIGURE 5. *Susceptibility of an antiferromagnetic case in the quenched system.*

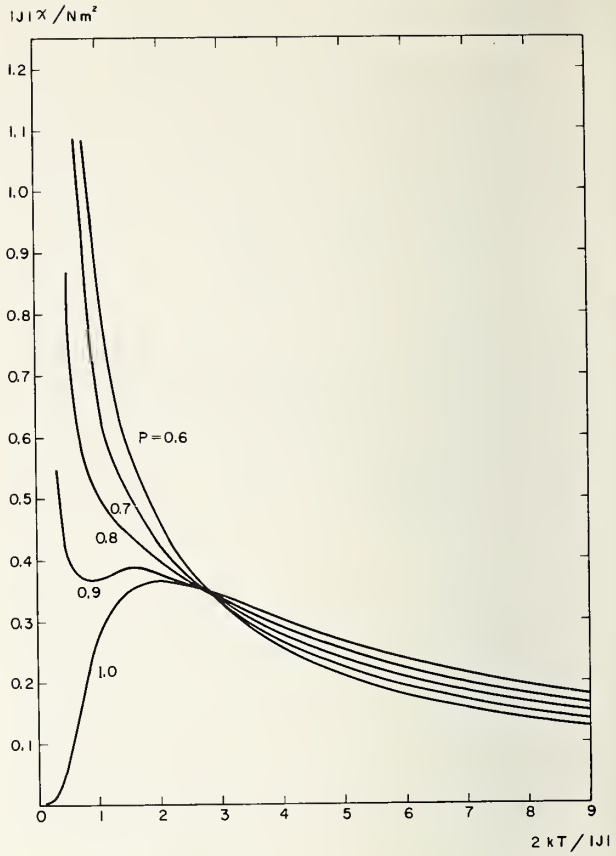

FIGURE 6. *Susceptibility of an antiferromagnetic case in Syozi's model.*

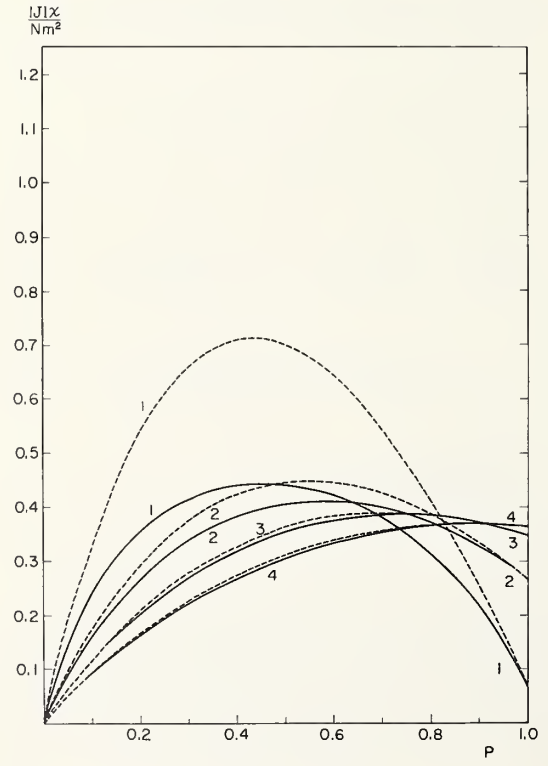

FIGURE 7. *Concentration dependence of the antiferromagnetic susceptibility.*
Solid line: the annealed system. Dashed line: the quenched system.
1: $T-|J|/4k$, 2: $T-2|J|/4k$,
3: $T-3|J|/4k$, 4: $T-4|J|/4k$.

concentration p, and the paramagnetic configuration gives the dominant contribution compared with the antiferromagnetic configuration. On the other hand, in the annealed system, the energy of the paramagnetic configuration is high compared with the antiferromagnetic configuration, and hence it dies and the susceptibility tends to zero.

The authors wish to thank for valuable discussions Professor R. Kubo, Professor M. E. Fisher, Dr. S. Inawashiro, and Dr. T. Kawasaki. The numerical calculation was carried out using NEAC 2230 in the computing center of Tohoku University and IBM 7090 in UNICON (University contribution of Japan IBM).

6. References

[1] R. Brout, Phys. Rev. **115**, 824 (1959).
[2] R. Mazo, J. Chem. Phys. **39**, 1224 (1963).
[3] T. Morita, J. Math. Phys. **5**, 1401 (1964).
[4] R. E. Behringer, J. Chem. Phys. **26**, 1504 (1957).
[5] H. Sato, A. Arrott, and R. Kikuchi, J. Phys. Chem. Solids. **10**, 19 (1959).
[6] G. S. Rushbrooke and D. J. Morgan, Mol. Phys. **4**, 1 (1961); ibid. **4**, 291 (1961); G. S. Rushbrooke, J. Math. Phys. **5**, 1106 (1964).
[7] R. J. Elliott and B. R. Heap, Proc. Roy. Soc. **A265**, 264 (1962).
[8] R. Abe, Prog. Theor. Phys. **31**, 412 (1964).
[9] I. Syozi, Prog. Theoret. Phys. **34**, 189 (1965).
[10] H. A. Kramers and G. H. Wannier, Phys. Rev. **60**, 252, 263 (1941).

The Statistical Mechanics of a Single Polymer Chain

S. F. Edwards

University of Manchester, Manchester, Great Britain

It is clear from the papers presented at this conference that near critical points thermodynamic functions and correlation functions take on forms which reflect only a very small amount of the detailed structure of the systems considered, and are rather manifestations of the three dimensionality of space and the short range of interactions. The configurational statistics of polymers shares this feature and is therefore interesting as an indication of how the critical behavior may be generated mathematically: in fact the problem is one way of approximating to the Ising lattice as was mentioned by Professor Domb [1]. In this talk I shall develop the theory applied to polymers themselves however, and comment on their critical behavior, since whether the analysis will really be useful for bulk systems remains to be seen. A polymer without interaction will have the well-known distribution

$$p(\mathbf{r}, L)=\left(\frac{2\pi Ll}{3}\right)^{-3/2}\exp\left(-\frac{3r^2}{2Ll}\right) \qquad (1.1)$$

for the probability that the end points are at $\mathbf{0}$, $\mathbf{r}$ when the length is L. This has the form

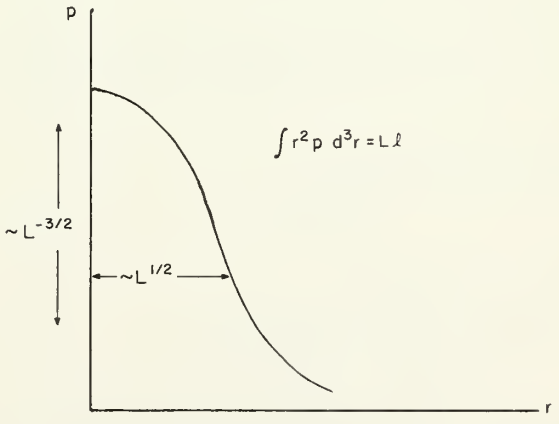

(1.2)

For the case of excluded volume i.e., a repulsion between elements of the polymer, p has no simple analytic form, but salient features are shown in

the diagram (schematic)

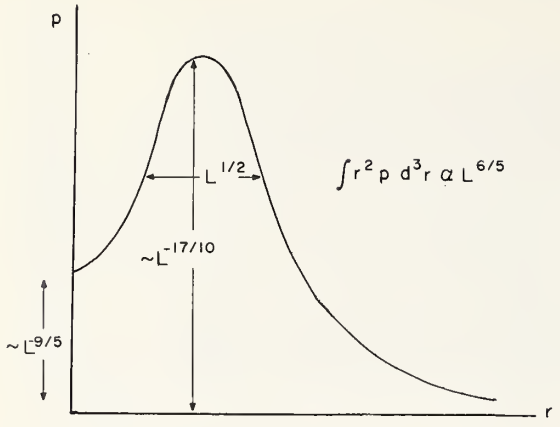

(1.3)

Expressions will also be obtained for the number of configurations allowed to the polymer.

2. Mathematical Formulation of the Problem

Firstly the problem is to be stated mathematically and brought down to its simplest form. Suppose the polymer consists of n identical molecules freely hinged in a chain, and there is a potential U between molecules. If the length of one molecule is l, and the coordinate of the end of the m^{th} molecule is $\mathbf{R}_m$, then the probability of finding a particular configuration $P(\mathbf{R}_1, \ldots \mathbf{R}_n)$ is given by

$$P(\mathbf{R}_1 \ldots \mathbf{R}_n) = \mathcal{N} \prod_i p(\mathbf{R}_i, \mathbf{R}_{i+1}) \exp\left[\frac{1}{kT} \sum_{m \neq l} U(\mathbf{R}_m - \mathbf{R}_l)\right] \tag{2.1}$$

where $\mathcal{N}$ is the normalization

$$\int P \Pi d^3R = 1 \tag{2.2}$$

and p is the constraint

$$p(\mathbf{R}_i, \mathbf{R}_{i+1}) = \delta(|\mathbf{R}_i - \mathbf{R}_{i+1}| - l). \tag{2.3}$$

(Note since normalizations are constantly occurring they will *all* be denoted by $\mathcal{N}$.) Of course, one can put structure into the molecules making U an integral over the molecule and one can put in bond flexibilities, but the basic problem is already in (1.1) including the case of hard exclusions in which

$$U = \infty \qquad |\mathbf{R}_m - \mathbf{R}_e| < a \tag{2.4}$$
$$= 0 \text{ otherwise.}$$

A lattice polymer, can also be included if the definition (1.3) is suitably modified, but it is again a complication not a simplification. The probability that starting at the origin, the polymer's nth link will end at $\mathbf{r}$, is given by

$$p(r, L) = \int P(\mathbf{R}_1, \ldots, \mathbf{R}_n) \delta(\mathbf{r} - \mathbf{R}_n) \Pi d^3R_i \tag{2.5}$$

where L, the length, is nl. A method of evaluating p for a slightly simpler problem, that of the infinite polymers, has been given by the author (reference [2], hereafter referred to as I) in a paper which develops a physical picture of what is going on and translates the physical picture into mathematics. A more formal but precise method of approach is given in an appendix to I, and in this paper, after reviewing the physical arguments, it is this formal development which will be given and extended to give a more complete theory of the single finite polymer.

Firstly it must be explained that the fact that there are n integrations in (1.1) is a nuisance; it is easier to consider a continuous function $\mathbf{R}(L')$ where $0 < L' < L$ and integrate over all functions $\mathbf{R}(L')$. The constraint $\prod_i p(\mathbf{R}_i, \mathbf{R}_{i+1})$ is the expression originally considered by Weiner when he introduced functional integration and can be expressed as

$$\mathcal{N} \exp\left(-\frac{3l}{2} \int_0^L \left(\frac{\partial \mathbf{R}}{\partial L'}\right)^2 dL'\right) \tag{2.6}$$

so that, putting $V = Ul^{-2}$

$$p(\mathbf{r}, L) = \mathcal{N} \int_{\mathbf{R}(0)=0}^{\mathbf{R}(L)=\mathbf{r}} d(\text{path } \mathbf{R}(L')) \exp\left(-\frac{3l}{2} \int_0^L \left(\frac{\partial \mathbf{R}}{\partial L'}\right)^2 dL' - \frac{1}{2kT} \int_0^L \int_0^L V\left(\mathbf{R}(L') - \mathbf{R}(L'')\right) \frac{dL'}{dL''}\right) \tag{2.7}$$

At this point a parametric representation can be

employed. It is well known that

$$e^{-a^2/2}=\int_{-\infty}^{\infty} e^{iax-x^2/2}dx \Big/ \int_{-\infty}^{\infty} e^{-x^2/2}dx. \quad (2.8)$$

This can be generalized to

$$\exp\left(-\sum_{ij} a_iA_{ij}a_j/2\right)$$
$$=\int_{-\infty}^{\infty}\int_{-\infty}^{\infty}\exp\left(i\sum_j a_jx_j-\sum_{i,k} x_iA_{ik}^{-1}x_k/2\right)$$
$$\Big/\int\int\int_{-\infty}^{\infty}\int_{-\infty}^{\infty} e^{-\Sigma xA_x^{-1}}\,\Pi dx, \quad (2.9)$$

where A^{-1} is the inverse matrix to A, and hence to the functional form

$$\exp\left(-\int a(\alpha)A(\alpha\beta)a(\beta)d\alpha d\beta\right)$$
$$=\int_{-\infty}^{\infty}\cdots\int_{-\infty}^{\infty}(\Pi dx)\exp\left[i\int a(\alpha)x(\alpha)d\alpha$$
$$-\frac{1}{2}\int\int x(\alpha)A^{-1}(\alpha\beta)x(\beta)d\alpha d\beta\right]$$
$$\times\left[\int_{-\infty}^{\infty}\int_{-\infty}^{\infty}\exp\left[-\int\int x(\alpha)A^{-1}(\alpha\beta)x(\beta)d\alpha d\beta\right]\Pi dx\right] \quad (2.10)$$

where A^{-1} is the inverse operator to A,

$$\int A^{-1}(\alpha\beta)A(\beta\gamma)d\beta=\delta(\alpha-\gamma). \quad (2.11)$$

This theorem allows one to write

$$\exp\left(-\frac{1}{2kT}\int_0^L\int_0^L V(\mathbf{R}(L')-\mathbf{R}(L''))dL'dL''\right)$$
$$=\mathcal{N}\int\delta\chi\exp\left[i\int_0^L\chi(\mathbf{R}(L'))dL'\right.$$
$$\left.-\frac{kT}{2}\int\int d^3r_1d^3S\chi(\mathbf{r})V^{-1}(\mathbf{r}-\mathbf{s})\chi/\mathbf{s})\right], \quad (2.12)$$

where

$$\int V^{-1}(rs)V(sr')d^3s=\delta(r-r'), \quad (2.13)$$

and $\int\delta\chi$ represents the integral over all functions. It is supposed that $\int\chi V^{-1}\chi$ is positive definite, corresponding to V being repulsive. If this is not the case one has to split V into a part with positive Fourier coefficients and a part with negative Fourier coefficients and parameterize them separately. This will be equivalent to χ becoming complex and the functional integration being over its real and imaginary parts independently. Although physical forces always do have attractions and repulsions it is well known from the study of the Ursell-Mayer cluster expansion, that provided the system remains of low density the effects of interparticle potentials can be simulated by pseudo potentials which will give rise to the correct virial coefficient. Thus if the excluded volume is defined by

$$v=\int[1-\exp(-U/kT)]d^3r \quad (2.14)$$

the effective pseudo potential is $v\delta(r)$, whose inverse is $v^{-1}\delta(r)$. It will be assumed now that v is positive, i.e., the mean effect of the forces is a repulsion. Then finally

$$p(\mathbf{r},L)=\mathcal{N}\int_0^r\exp\left[-\frac{3l}{2}\int_0^L\left(\frac{\partial\mathbf{R}}{\partial L'}\right)^2dL'\right.$$
$$\left.-i\int_0^L\chi(\mathbf{R}(L'))dL'-\frac{l^2}{2v}\int\chi^2(S)d^3S\right]\delta\chi\delta R$$

(δR for the integral over all paths). (2.15)

The theorem states that the probability p is that of diffusion in the presence of a potential $i\chi$ (a Markov process), averaged over all potentials with a Gaussian weight. It is a well-known theorem elsewhere in physics. Since the evaluation of the functional integral over δR is equivalent to solving the diffusion equation, one can obtain the final form

$$p(r,L)=\mathcal{N}\int\delta\chi G(\mathbf{r},L,[\chi])W([\chi])\delta\chi \quad (2.16)$$

where

$$W([\chi])=\exp\left(-\frac{l^2}{2v}\int\chi^2d^3s\right), \quad (2.17)$$

$$\left(\frac{\partial}{\partial L}-\frac{l}{6}\nabla^2+i\chi(\mathbf{r})\right)G(\mathbf{r},L,[\chi])=\delta(\mathbf{r})\delta(L) \quad (2.18)$$

and $\mathcal{N}=\mathcal{N}(L)$ is defined from $\int pd^3r=1$.

209-493 O-66—16

3. The Solution

Two problems have presented themselves in (2.16). Firstly one has to get G from (2.18) and then do the integral over χ. It will be argued that the mathematical tools for these problems are already available, at least within reasonable stretching: the Green function can be got by the JWKB method, and the χ integration by the method of steepest descent. Physically one can argue that, since one knows that the polymer starts at the origin, on an average a "polymer density" will build up having its maximum at the origin. It is this field which will be uncovered by the steepest descent calculation, and it will be a field with a long range effect, slowly varying in space so that the JWKB method will be the correct method to assess its effect on the diffusion. That this mean field can be expected to be long range is seen at once from the noninteracting distribution (1.1). From (1.1) the probability that a very long noninteracting polymer goes through $\mathbf{r}$ for some L is

$$\int \left(\frac{2\pi}{3} Ll\right)^{-3/2} \exp\left(-\frac{3r^2}{2Ll}\right) dL = \left(\frac{3}{2\pi l}\right)\frac{1}{r}.$$

If there were a very strong self-repulsion, the polymer would shoot out in a straight line and the average would be taken over the orientation of this straight line, i.e., would give $(4\pi r^2)^{-1}$. These give upper and lower bounds on the form of the mean polymer density so that one expects the χ integration to be centered about a steepest descent function χ having a dependence lying between $\frac{1}{r}$ and $\frac{1}{r^2}$ and in fact it will turn out to go like $\frac{1}{r^{4/3}}$.

It is convenient to Fourier transform G with respect to L

$$\left(iE - \frac{l}{6}\nabla^2 + i\chi\right) G(E, \mathbf{r}, [\chi]) = \delta(r) \tag{3.1}$$

and to seek a solution in the form

$$G = e^{\phi}/r. \tag{3.2}$$

Then

$$i(E+\chi) - \frac{l}{6} r^2 \mathscr{L}(\phi) - \frac{l}{6}\frac{d^2\phi}{dr^2} - \frac{l}{6}\left(\frac{d\phi}{dr}\right)^2 = 0 \tag{3.3}$$

where $\mathscr{L}(\phi)$ contains the angular derivatives. It will turn out that the steepest descent function is spherically symmetric, so the angular terms will be ignored for the present and ϕ treated as if it were $\phi(r, E)$ and $\chi(\mathbf{r})$ also as if it were $\chi(r)$. The JWKB argument is now that the $(d\phi/dr)^2$ term dominates over the $d^2\phi/dr^2$ term (which can be confirmed subsequently) so that

$$\phi \cong \left(\frac{6i}{l}\right)^{1/2} \int_0^r (E+\chi(s))^{1/2} ds \tag{3.4}$$

and one is left with

$$p = \mathscr{N} \int \delta\chi dE \exp\left[\int_0^r \left(\frac{6}{l}\right)^{1/2} i^{1/2}(E+\chi)^{1/2} ds - iEL - \frac{l^2}{2v}\int \chi^2 d^3 s\right]. \tag{3.5}$$

(One must watch for complications at the branch point $E+\chi=0$; note also that one integral is ds, the other d^3s). To evaluate, one looks for the $\bar{E}$, $\bar{\chi}$ which make the exponent stationary: differentiating with respect to E

$$iL = \frac{1}{2}\left(\frac{6i}{l}\right)^{1/2} \int_0^r (\bar{E}+\bar{\chi})^{-1/2} ds \tag{3.6}$$

and functionally with respect to χ

$$\frac{l^2}{v}\bar{\chi}(s) = \left(\frac{1}{4\pi s^2}\right)\frac{1}{2}\left(\frac{3i}{l}\right)^{1/2} (\bar{E}+\bar{\chi})^{-1/2} \quad \begin{matrix} s < r \\ s > r \end{matrix} \tag{3.7}$$

$$= 0\}.$$

Therefore one may write also

$$iL = \frac{l^2}{v}\int_0^r \bar{\chi}(s) ds. \tag{3.8}$$

Clearly

$$\bar{\chi} = \bar{\chi}(s, \bar{E}) \tag{3.9}$$

and

$$\bar{E} = \bar{E}(r, L). \tag{3.10}$$

Make these equations clearer by introducing

$$\zeta = \frac{5}{3}\left(\frac{L}{r^{5/3}}\right)\frac{\pi^{1/6}}{2}\left(\frac{v}{6l}\right)^{1/3}$$

$$\bar{\chi} = \left(\frac{1}{8\pi}\right)^{2/3}\left(\frac{6}{l}\right)^{1/2}\left(\frac{v}{l^2}\right)^{2/3} S^{-4/3}\vartheta \tag{3.11}$$

$$\bar{E}=\left(\frac{1}{8\pi}\right)^{2/3}\left(\frac{6}{l}\right)^{1/2}\left(\frac{v}{l^2}\right)^{2/3} r^{-4/3}\epsilon$$

$$s'=s/r$$

Then one has to determine ϑ, ϵ in terms of ζ where

$$\zeta=\frac{5}{3}\int_0^1 \frac{ds's'^{2/3}}{(\vartheta+\epsilon s'^{4/3})^{1/2}} \tag{3.12}$$

$$\vartheta=(\vartheta+\epsilon s'^{4/3})^{-1/2} \tag{3.13}$$

$$\zeta=\frac{5}{3}\int_0^1 ds's'^{2/3}\vartheta(s'). \tag{3.14}$$

The ϵ, ϑ, s' relation is plotted below

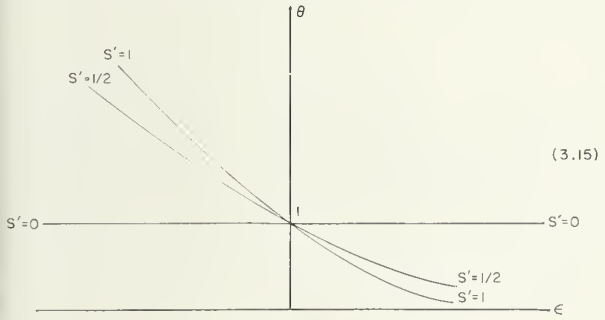

(3.15)

Special cases are $\epsilon=0$, $\vartheta=1$, $(\zeta=1)$; $\epsilon=-\infty$, $\vartheta=\epsilon^{-1/2}s'^{-2/3}$; $\epsilon=-\infty$, $\vartheta=-\epsilon s'^{4/3}$. This, physically sensible, solution has ϑ positive and leads to a relation like

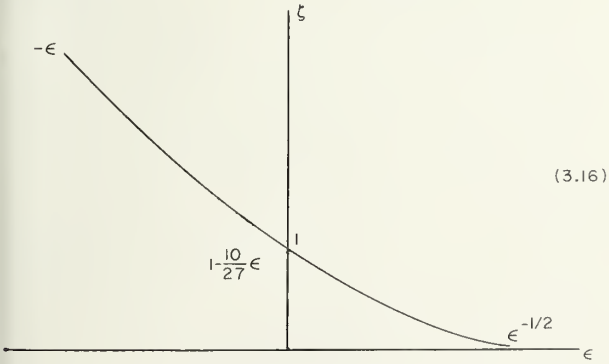

(3.16)

One may now see that neglecting fluctuations for the moment

$$p(\mathbf{r}, L)=\mathcal{N}(L)\exp\left[\int_0^r\left(\frac{6i}{l}\right)^{1/2}(\bar{E}+\bar{\chi})^{1/2}ds - i\bar{E}L-\frac{l^2}{2v}\int\bar{\chi}^2d^3s\right] \tag{3.17}$$

$$p(\mathbf{r}\ \ L)=\mathcal{N}(L)\exp\left[-r^{1/3}F(\zeta,\vartheta,\epsilon)\right] \tag{3.18}$$

$$=\mathcal{N}(L)\exp\left[-r^{1/3}F(Lr^{-5/3})\right] \tag{3.19}$$

$$=\mathcal{N}(L)\exp\left[-Z(r, L)\right]. \tag{3.20}$$

say.

The function e^{-Z} is sketched in the introduction. Its maximum comes at $\partial Z/\partial r=0$, i.e.,

$$0=\frac{\partial Z}{\partial\bar{E}}\frac{\partial\bar{E}}{\partial r}+\int\frac{\delta Z}{\delta\bar{\chi}(s)}\frac{\partial\bar{\chi}(s)}{\partial r}d^3s + \left[-\frac{4\pi l^2}{v}r^2\bar{\chi}^2(r)+\left(\frac{6i}{l}\right)^{1/2}(\bar{E}+\bar{\chi})^{1/2}\right] \tag{3.21}$$

Since Z is stationary with respect to E and $\bar{\chi}$ this gives

$$\frac{4\pi l^2}{v}\bar{\chi}^2(r_m)r_m^2=\left(\frac{6i}{l}\right)^{1/2}(\bar{E}+\bar{\chi}(r_m)^{1/2} \tag{3.22}$$

i.e.,

$$\bar{\chi}(r=r_m)=\left(\frac{6}{l}\right)^{1/3}\left(\frac{v}{4\pi l^2}\right)^{2/3}\frac{1}{r_m^{4/3}}. \tag{3.23}$$

Near the peak the

$$\zeta=\zeta_m \text{ i.e., } L=\left(\frac{l}{v}\right)^{1/3} r_m^{5/3}\times\text{constant}. \tag{3.24}$$

And the distribution looks like

$$\mathcal{N}(L)\exp\left(-f\left(L-gr^{5/3}\left(\frac{l}{v}\right)^{1/3}\right)^2 r^{-3}l^{-2}v\right) \tag{3.25}$$

where f and g are constants derived from (3.23), (3.13), and (3.14). For the right ζ is small, ϵ large so that $\zeta\propto\epsilon^{-1/2}$.

$$F\propto\frac{1}{\zeta}. \tag{3.26}$$

This implies a distribution $b\mathcal{N}\exp(-cr^2/2L)$ where b and c are constants. Towards the origin p becomes very small, and one is in the well-known trouble of trying to fit a tail of a function by working away from its maximum. This will be considered in detail in section 4.

The fluctuations i.e., the remaining quadratic integrals over $E-\bar{E}$ and $\chi-\bar{\chi}$ have not yet been

considered. Unlike steepest descent methods in a single variable, these are of great consequence and indeed are the substance of conventional field theory. To go straight ahead expanding ϕ to order χ^2 is inadequate as can be seen physically. Consider what one expects the addition of one more molecule to the polymer to involve. Say for the moment one confined oneself to steps on a close packed lattice. There would be at most eleven sites to go on to i.e., 12, less the one it is at. But it must have wandered around the neighborhood before it arrived at the present site, so one expects a further reduction bringing the number of available sites to $\mu < 11$. In addition the long range effect reduces it further to $\mu(1+f(n))$ (where $f(n)$ will turn out to be $(\log n)/5n$). If one were not using the steepest descent method by normal field theory one would argue, after Dyson, that by studying the perturbation series, that (using $\langle G\rangle$ for (2.16) unnormalized)

$$\left(iE-\frac{l}{6}k^2+\Sigma(k,\,E)\right)\langle G(k,\,E)\rangle=1 \tag{3.27}$$

where in the first approximation

$$\Sigma(k,\,E)=\int\frac{|V(\mathbf{k}-\mathbf{j})|^2}{iE-\frac{l}{6}\mathbf{j}^2}\,d^3j \tag{3.28}$$

but it is difficult to get in general. If $\langle G\rangle$ is considered to have a pole i.e., $\left(iE-l'\frac{k^2}{6}+\Sigma_0\right)\langle G\rangle\cong 1$ and Σ is expanded around it

$$\Sigma=\Sigma_0-\Sigma_1k^2+\Sigma_2\left(iE-\frac{l'}{6}k^2\right)+\ldots \tag{3.29}$$

$$\left(iE-\frac{(1+\Sigma_1)}{(1+\Sigma_2)}\frac{l}{6}k^2+\frac{\Sigma_0}{1+\Sigma_2}\right)\langle G\rangle=\frac{1}{1+\Sigma_2}. \tag{3.30}$$

Here $\frac{1+\Sigma_1}{1+\Sigma_2}\,l=l'$ is a "renormalized" step length, and the $\Sigma_0/(1+\Sigma_2)$ factor represents the changed number of available sites as expected. (Since it gives a $e^{-\Sigma_0 L}$ factor in $\langle G\rangle$ it will not appear in p). The conventional field theory fails completely to describe the long range effects and it is these which determine the $\overline{\mathbf{r}^2}$: L relation. As has been shown the present theory suggests that these long range effects are simulated by a potential centered at the origin. The local effects should be adequately handled by the conventional methods and they really will involve the fine structure of V, and if one attempts to use the pseudo potential one gets divergences. To avoid these one must write

$$p(r,\,E,\,[\chi])=\frac{1}{r}\,e^{\{A+\int B(\chi-\overline{\chi})+\int C(\chi-\overline{\chi})^2+iEL+iE(L-\overline{L})+D(E-\overline{E})\}} \tag{3.31}$$

where

$$(\nabla^2+\nabla A\nabla)A(r)=-\overline{\chi}(r)$$

$$(\nabla^2+2\nabla A\nabla)B(r,\,r')=\delta(r-r')$$

$$(\nabla^2+2\nabla A\nabla)C(r,\,r_2,\,r_3)=\nabla B(r,\,r_2)\nabla B(r,\,r_3)$$

$$\frac{l^2}{v}\,V^{-1}\chi=\frac{1}{4\pi r^2}\,\nabla B.$$

and so on. The interference between $\overline{\chi}$ and the fluctuations is analogous to the Lamb shift and a proof is needed that this does not interfere with the functional forms discovered so far. Though this appears to be so by explicit calculation, I am trying to obtain a general proof on the lines of the Dyson treatment of electrodynamics.

4. The Inner Region

One can see why the inner region has been so far inaccessible. The solution has a peak near $L\sim r^{3/5}$ and almost all the probability lies in the peak. This means that though the chance of the polymer getting back close to the origin is small, it is much larger than that suggested by the solution (3.5). That solution suggests that in order to be still near $r\sim 0$ as $L\to\infty$ one must have stayed all the time near $r\sim 0$. Clearly what will happen is that one will go out into the high probability region and then walk back to the inner region. Since under the parametric integral sign one has a Markov process one may always break up G

$$G(\mathbf{r},\,L,\,[\chi])=\int G(\mathbf{r}-\mathbf{s},\,L-M,\,[\chi])G(\mathbf{s},\,M,\,[\chi])\,d^3s \tag{4.1}$$

Note there is no integral over M and the left-hand side should be independent of M. To modify (4.1) to be M independent one can average along the

whole length to give

$$p=\frac{1}{L}\int_0^L dM\int d^3s$$

$$\int \delta\chi G(\mathbf{r}-\mathbf{s},\ L-M[\chi])G(\mathbf{s},\ M,\ [\chi])W. \qquad (4.2)$$

Now average using the JWKB for the G

$$p=\frac{1}{L}\int_0^L dM\int d^3s\int \delta\chi|\mathbf{r}-\mathbf{s}|^{-1}|\mathbf{s}|^{-1}\int dE_1\int dE_2$$

$$\exp\left\{-\frac{l^2}{2r}\int\chi^2 d^3a+\left(\frac{6i}{l}\right)^{1/2}\int_0^s\frac{d^3a}{a^2}\,(E_2+\chi)^{1/2}\right.$$

$$\left.+\left(\frac{6i}{l}\right)^{1/2}\int_s^r\frac{d^3a}{|a-s|^2}\,(E_1+\chi)^{1/2}-iE_1(L-M)-iE_2M\right\}\cdot \qquad (4.3)$$

$$\bar{\chi}(a)=\frac{v}{l^2}\frac{\Theta(|a|<|\mathbf{s}|)}{a^2}(E_2+\chi)^{-1/2}\left(\frac{6i}{l}\right)$$

$$+\frac{v}{l^2}\frac{\Theta(|\mathbf{a}-\mathbf{s}|<|\mathbf{r}-s|)}{|a-s|^2(E_1+\chi)^{1/2}} \qquad (4.4)$$

$$i(L-M)=\left(\frac{6i}{l}\right)^{1/2}\int_{|\mathbf{a}-\mathbf{s}|<|\mathbf{r}-\mathbf{s}|}\frac{d^3a}{|s-a|^2}(E_1+\chi)^{-1/2} \qquad (4.5)$$

$$vM=\left(\frac{6i}{l}\right)^{1/2}\int_{|\mathbf{a}|<|\mathbf{s}|}\frac{d^3a}{a^2}(E_2+\chi)^{-1/2}. \qquad (4.6)$$

In particular to get back to $\mathbf{r}=0$ one has

$$\bar{\chi}=\left(\frac{6i}{l}\right)^{1/2}\left\{\frac{\Theta(|\mathbf{a}|<|\mathbf{s}|)}{a^2}(E_2+\chi)^{-1/2}\right.$$

$$\left.+\frac{\Theta(|\mathbf{a}-\mathbf{s}|<|\mathbf{s}|)}{|a-s|^2}(E_1+\chi)^{-1/2}\right\} \qquad (4.7)$$

$$iL=\left(\frac{6i}{l}\right)^{1/2}\int d^3a\left(\frac{\Theta(|\mathbf{a}|<|\mathbf{s}|)}{a^2}(E_2+\chi)^{-1/2}\right.$$

$$\left.+\frac{\Theta(|\mathbf{a}-\mathbf{s}|<|\mathbf{s}|)}{|\mathbf{a}-\mathbf{s}|^2}(E_1+\chi)^{-1/2}\right)\cdot \qquad (4.8)$$

I won't write out the details from here on for the answer is defined dimensionally and must be

$$p(\mathbf{0},\ L)\propto L^{-9/5}\ \text{i.e.,}\ n^{-9/5}. \qquad (4.9)$$

The details of the integration serve to fix the constant. Presumably one could break up G at more than one point and get a better value for this constant, but the $n^{-9/5}$ would still come the same.[1]

Having sketched out the entire function one can now normalize and get the height of the peak $L^{-17/10}$ which clearly dominates the rest of the function. By evaluating $\bar{r}^2$ one finds a series, the expansion parameter being $(L^{-1/10}v^{-1/3}l^{7/10})$ which must be small for the above analysis to be valid.

Finally, the number of walks can be remarked upon since it is an interesting combinatorial point even if it has little bearing on polymers. As has been noted, the dominant feature will be the local effect of the effective phase space available per molecule. The long range effect will come from the unnormalized Green function which is

$$\frac{\mu^{L/l}}{r}\frac{1}{r^{3/2}}\exp\left(-\int(L-gr^{5/3})^2/r^3\right)\cdot \qquad (4.10)$$

Integrating over r one gets the leading term to be $\sim\mu^n n^{1/5}$.

5. The Collapse of Polymers

What happens when the virial coefficient changes sign?[2] Instead of the repulsion pushing the polymer out faster than the random configurations, it will now be pulled in. For v large and attractive the polymer will condense into a solid ball, a state easily obtained experimentally even for a single chain. But for v near zero a new semicondensed state appears possible, and passage through the Flory temperature (i.e., $v=0$) will produce a phase change for a very long chain [3]. The physical picture will be of the polymer repeatedly passing through the same region of space so that again a polymer density is set up which now traps the polymer. Consider this problem from the point of view of I i.e., study the probability that, after a chain length $L'(0<L'<L)$, the polymer will be at $\mathbf{r}$, $q(r, L', [L])$. As in I (where the present q is called p) one can argue that the polymer field can be represented by approximating

[1] This value has been conjectured by Fisher, Faraday Society Discussion **25**, p. 200.

[2] Dr. J. Mazur has pointed out to me that $v=0$ may be much more complicated than is generally supposed. The discussion of this point due to Flory assumes that chains with $v=0$ are Gaussian, but a single chain is a distinctly nonuniform entity having a high "polymer density" at its center of gravity, tending to a low value at the end points. So one could have a '$v(L)$' effect from the middle to the ends. The following discussion may need modifying in the light of this comment.

$$\int_0^L \int_0^L V(\mathbf{R}(L')-\mathbf{R}(L''))dL'dL''$$

$$\cong \int_0^L V(\mathbf{R}(L')-\mathbf{s})q(\mathbf{s}, L'')dL'dL''. \qquad (3.32)$$

But $q(r, L')$ can now be argued to be independent of L' since the self trapped polymer will repeatedly go through every point of its density; it will, of course, still be a function of L. Since V is short range one may now approximate by writing

$$\int_0^L \int_0^L V(\mathbf{R}(L')-\mathbf{S})q(\mathbf{S}, L'')dL'dL''$$

$$\cong \frac{w}{L}\int_0^L \int_0^L q(R(L'), L'')dL'dL'' \qquad (5.1)$$

$$= w\int_0^L \tilde{q}(R(L'))dL'$$

where w is Lvl^{-2}. This now gives a functional integral in the Markov form so that one can break the functional integral up to L at an intermediate L' and define

$$q(r', L') = \mathcal{N}(L')\int \exp\left[-\frac{3l}{2}\int_0^{L'}\left(\frac{\partial \mathbf{R}}{\partial L''}\right)^2 dL''\right.$$

$$\left. - w\int_0^{L'} \tilde{q}(R(L''))\right]\delta R \qquad (5.2)$$

which satisfies

$$\left(\frac{\partial}{\partial L'} - \frac{l}{6}\nabla^2 + w\tilde{q}(r) - C(L')\right)q = \delta(r). \qquad (5.3)$$

Ignoring C for the moment, the resulting differential equation will have eigenfunctions E_n,

$$\left(\frac{\partial}{\partial L'} - \frac{l}{6}\nabla^2 + w\tilde{q}(r)\right)q_n e^{E_n L'} = 0 \qquad (5.4)$$

$$\left(\frac{\partial}{\partial L'} - \frac{l}{6}\nabla^2 + w\tilde{q}(r)\right)g(r, L) = \delta(r)\delta(L')$$

$$g(r, L) = \sum q_n(r)q_n^+(0)e^{E_n L'}\Theta(L'). \qquad (5.5)$$

There will be positive and negative eigenvalues. As $L' \to \infty$ only the positive ones survive and unless the largest positive eigenvalue tends also to zero the whole expression will diverge i.e., this eigenvalue is brought to zero by the normalization. Thus one is led to the eq (5.6) in which C' now takes the role usually taken by the eigenvalue, and since q will not depend on L', $\tilde{q}$ can be identified with it:

$$\left(\frac{l}{6}\nabla^2 + w(q(r)-q^2)\right)q(r) = 0$$

$$\int q(r)d^3r = 1$$

$$\overline{q^2} = \int q^2(r)d^3r. \qquad (5.6)$$

By redefining $r = r'w/l$ one brings the equation into the final form

$$-\frac{1}{3}\left(\frac{d^2}{dr'^2} + \frac{2}{r'}\frac{d}{dr'}\right)q + \left(\frac{w}{l}\right)^3(q-\overline{q^2})q = 0 \qquad (5.4)$$

rather like the Schrödinger equation with an attractive potential and eigenvalue $\overline{q^2}$. The solution has to be obtained numerically and clearly will have the form

$$q = Q(rl^3/vL)\left(\frac{l^3}{vL}\right)^3, \qquad (5.5)$$

where Q is a dimensionless function. Clearly in this case

$$\overline{r^2} \propto v^2L^2l^{-6} \qquad (5.6)$$

which is quite different both from the $L^{6/5}$ and the Einstein Law, $\overline{r^2} \propto Ll$. The distribution changes abruptly as

$$v > 0 \to v = 0 \to v < 0.$$

I have been greatly helped by discussions with Professor G. Gee, Professor C. Domb, Professor M. E. Fisher and Dr. J. Mazur.

6. References

[1] Reference to the latest numerical work is contained in Domb, C., Gillis, J., and Wilmers, G., Proc. Phys. Soc. **85**, 625 (1965); and in a paper by J. Mazur to be published. The relation to this problem as a run-in to the Ising model is discussed in Professor Domb's contribution to the conference.

[2] Edwards, S. F., Proc. Phys. Soc. **85**, 613 (1965).

[3] The standard text particularly with reference to $v-0$ is Flory, P. J., Principles of Polymer Chemistry, Cornell University (1953).

Some Comments on Techniques of Modern Low-Temperature Calorimetry

I. M. Firth

University of St. Andrews, St. Andrews, Scotland

Introduction

Precision calorimetry at low temperatures started in 1929 when a sensitive phosphor-bronze thermometer was made by Keesom and Van Den Ende [1]. This led shortly to the discovery of the heat capacity connected with the superconductive phase transition [2] and also the electronic heat capacity in metals [3] was discovered and found to be in reasonable agreement with the theoretical predictions. Recently with the use of carbon resistance thermometers [4] and a-c bridge lock-in amplifier methods of measurement [5], a new era of precision has been entered. This has allowed the more exciting phase transitions at low temperatures to be checked. This era has come opportunely for at a recent meeting in Washington on "Phenomena in the Neighborhood of Critical Points" [6] it was emphasized that to obtain agreement with theoretical predictions very great care and precision must be taken in experimental measurements, not only of heat capacities, but of all properties related to such critical phenomena: e.g., magnetization, thermal conductivity, optical and neutron diffraction.

In considering the present situation in calorimetry, it is useful to review the way in which the main requirements of low temperature calorimetry were introduced. Although Gaede [7] used a metal calorimeter isolated somewhat from its surroundings it was Nernst [8] who recognized a few years later in 1909, that on account of surroundings there was usually a temperature gradient inside a calorimeter which would prevent making accurate, or often meaningful, measurements. To obviate this he placed the calorimeter in a vacuum realizing that, radiation being small at low temperatures, it was possible to obtain excellent thermal isolation and reduce the above error to a minimum.

Of course, it was necessary to change the temperature of the calorimeter and to do this he used an exchange gas, noting in the course of his work the drawback of remnant gas on the thermal isolation and, absorbed gas on the calorimeter on the heat capacity measured. Temperature was measured by a platinum resistance thermometer the wire of which also acted as the electrical heating element for the calorimeter. Measurements with this arrangement were uncertain even with the most careful calibration of the resistance, because of irregular changes in the resistance of the platinum wire heating the calorimeter. Nernst avoided this disadvantage and at the same time made his method more simple, by measuring the variations of temperature resulting from electrical heating by using a thermocouple [9]. One junction was fixed to the calorimeter and the other lay on a lead block also in the vacuum chamber, figure 1. The heat capacity of lead being large, the temperature of the block remained nearly constant and any small drift took place slowly and uniformily so that the temperature of that junction could be corrected. A copper shield that enclosed the calorimeter was soldered to the lead block and this refinement was a great improvement on the open calorimeter. Nernst could measure temperature to 0.1 °K and specific heat to ~2 percent.

It is easy to see from this arrangement how adiabatic methods developed. The thermal insulation of this device can never be perfect so long as there

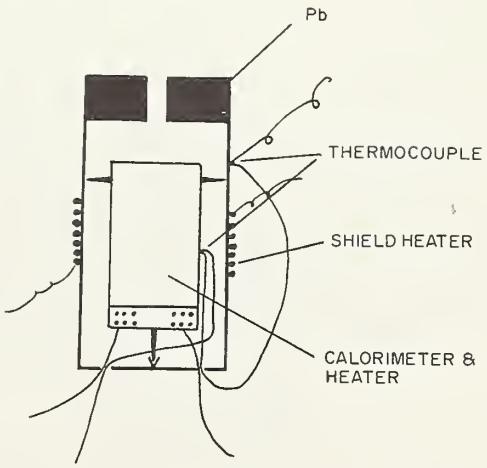

FIGURE 1. *Calorimeter of Nernst showing the lead block, copper shield, heaters, and measuring thermocouple.*

is a temperature difference between the calorimeter and the shield. But, by heating the shield so that the temperature difference is zero at all times, i.e., there is no voltage across the thermocouple, there will be no heat input to the calorimeter by radiation or by conduction along its supporting threads. All heat that is applied to the calorimeter through the heater then goes completely towards raising its temperature and no corrections have to be made for heat losses: a correction has to be added because of the joule heating in the heater leads but it has been shown rigorously that half the heat generated in the leads goes into the calorimeter [10]. In adiabatic schemes a second thermometer is required to measure the temperature of the calorimeter.

Methods

Nernst used a constant heat input to his calorimeter but since then intermittent heating has often been used in adiabatic calorimetry. However, recently in accurate work on some phase transitions e.g., Buckingham and Fairbank [11] on the superfluid transition in He^4, Schiffman et al. [12], on superconducting transitions, a preference has been shown again for constant heating methods. There are two reasons for this preference. In measuring the input of heat during a pulse where the pulse may be only a few seconds in duration, the current through, and the voltage across, the heater are difficult to measure accurately. The power is often of the order of a few ergs per second which means that currents of a few microamps and voltages of a few millivolts have to be measured with devices that have a short response time. Secondly, after the pulse, the recorded temperature will not settle down for some time, and in any case the temperature immediately after the pulse is difficult to ascertain. It is important to know what this temperature is after the pulse and how it is drifting with time so that meaningful extrapolations can be made to the middle of the heating pulses to measure the temperature increment caused by the pulse. Schiffman [13] has observed that in the same temperature range, from pulse to pulse, the calculated heat capacities of the calorimeter may not be consistent. Where measurements on solids are carried out, "overheating" may easily occur (as Parkinson and Quarrington [14] have described) because of the small thermal conduction of the solid. This gives more uncertainty about the temperature of the sample for it will always be less than that measured for the calorimeter. Corrections for overheating can be applied but extrapolation of the temperature drift curves on both sides of the heat pulse are more uncertain. It should be stated, however, that where the extraneous heat input to the calorimeter is large only the pulse method may be useful.

It is usual to measure temperatures in the range 0.3 to 5 °K with an a-c bridge, using a high gain lock-in amplifier as detector, and a carbon resistor as the temperature sensitive arm of the bridge [4, 5]. Commercial carbon radio resistors, especially made to be temperature insensitive at room temperature were found some years ago to be most usefully sensitive at low temperature. Bridges of this type can detect changes of 10^{-7} °K, that is 0.02Ω in 46 kΩ when the resistor is chosen with care.

In the advanced scheme of Schiffman et al. [12], during continuous heating the bridge is repeatedly unbalanced by very small steps in a sense that the bridge returns to balance as the heating progresses. The time taken between successive balances is measured by electronic counters. The temperature jump between balances is small and so the heat capacity is related linearly to the power input and the time intervals. There is no doubt about extrapolating the heating curve as there is in the pulse method, for this is an inherent feature of this method.

The same method can be used to evaluate the extraneous heat input to the calorimeter. Heating is stopped and the temperature drift observed in the same way. It is a simple matter to examine the stray heat input at different temperatures in the range under study. More consistent data on the heat leak is also obtained by repeating measurements with varying electrical heat inputs knowing that the heat capacity remains constant, so obtaining the heat leak from a difference equation, figure 2.

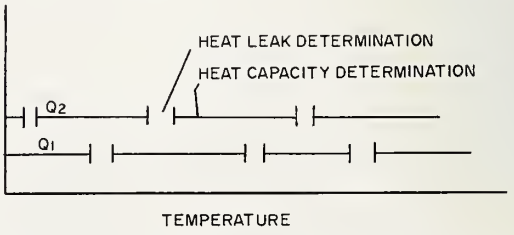

FIGURE 2. *Heat capacity and leak determined at two different heat inputs.*

With careful attention to the points that follow in this discussion, leaks as low as 1–10 erg per minute, a temperature sensitivity of 10^{-6} to 10^{-7} °K and an accuracy in measuring the heat capacity of 0.05 percent can be obtained.

An interesting experimental feature of the continuous heating method can be noted here. If the continuous record of the output of the bridge is simultaneously differentiated, a direct recording is obtained that is, to first approximation, proportional to the heat capacity. This is so because over small increments of temperature both the temperature response of the carbon resistance thermometer and the response of the off-balance voltage of the bridge, with respect to the resistance thermometer arm, are practically linear. Directly monitoring the heat capacity in this way is often useful in observing a singularity in the temperature dependence of the heat capacity that characterizes so many critical point phenomena.

The best possible radiation shield is one that encloses the calorimeter within the vacuum space. The temperature of the shield must be monitored, compared to that of the calorimeter and adjusted to it by a controlled heater in adiabatic schemes. For temperatures above 20 °K the comparison is conveniently done by two thermocouples. Below this temperature comparison by temperature sensitive resistors is difficult because it would be most difficult to make a matched pair: in the case of commercial carbon resistors, choosing a matched pair would be almost impossible. In this temperature range, therefore, the shield very often is held at some mean temperature close to that being investigated. This is a perfectly satisfactory technique when the range of measurement is small, so often the case in studies on critical phenomena. In fact, where the bath temperature can be adjusted, and adequately controlled, the shield may be disposed of completely, the walls of the vacuum chamber acting as the "adiabatic" shield. This omission restricts the versatility of the apparatus for it is difficult to adjust liquid helium to above 4.2 °K, because the vapor pressure is higher than 1 atm, or to just above 2.2 °K where boiling takes place vigorously.

Hence for greatest versatility an independent shield should be used. Germanium thermometers [15] are very useful in measuring the temperature of the shield for they can be calibrated under repeated cycling to room temperature to 0.05 percent and they respond to changes in temperature in 50 msec. The temperature controlling system must be smooth and accurate in operation, or as Nernst emphasized [9], the heat leak will fluctuate randomly. In certain applications a temperature guard ring from which the calorimeter is suspended may be sufficient to reduce heat leaks: all electrical leads and other connections to the calorimeter are, of course locked to it.

RF Effects

It was not realized until the report of Ambler and Plumb [16] that there is often considerable eddy current heating in calorimeters caused by commercial radio transmitters, particularly those in the television bands. Although the situation in the U.K. is not quite as serious as that in the U.S., because of the greater restriction on the number of T.V. channels, there will be very few laboratories now that are not within 50 miles of some transmitter. Television transmitters have a very small vertical beam angle and generally have some horizontal directivity. Consequently they have a high aerial gain so that the effective radiated power may be as much as 500 kW. At a distance of 10 miles the rf radiation density would be, therefore, about 10^4 erg $sec^{-1}m^2$, and at 50 miles, as much as $4\ 10^2$ erg $sec^{-1}m^{-2}$. In a poorly screened system, with many earth loops, if only a small part of this is picked up by the equipment connected to the calorimeter there would be an overwhelming contribution to the otherwise small extraneous heat input to the calorimeter.

It would be possible to enclose the whole apparatus in an rf shielded cage but this is inconvenient and expensive. In preference, other precautions should be taken: as much equipment as possible should be operated from battery supplies; leads should be screened with a solid, continuous conductor—normal braided screening is effective in keeping rf fields in, but is quite useless in excluding them; necessary removable joints in the leads should be made by connectors that give complete screening and force the connector pins together with great pressure.

Vibrations

This is only one of the extraneous heat inputs that can be avoided with careful experimental planning. Others arise from vibrations of the whole ap-

paratus or of the calorimeter on its suspension system. Good isolation of the cryostat from the laboratory can be achieved by using a massive frame mounted on supports whose period of oscillation is very low. Coil springs with a dampening cushion of crimped knitted stainless steel mesh is good but an air or water hydraulic suspension will give a very long period, the pressure of the fluid being adjusted accordingly. Where the cryostat bath is pumped to reduce its temperature, the periodic fluctuation in gas pressure in the pumping line caused by the periodic pumping action of rotary pumps, can be eliminated by using a large baffle volume or a system of plumbing that causes destructive interference of the periodic pressure fluctuations at the cryostat head. Vibration along the pipes must be removed before the cryostat suspension by massive clamping or ingenious bellows systems. Isolation not only reduces the acoustical heat input but removes the experimenter's dependence on the random noisy doings of his colleagues!

It is customary now to use mechanical heat switches instead of low pressure exchange gas to cool the calorimeter and to make adjustments of its temperature. To achieve good thermal contact over the switch at low temperatures the pressure between calorimeter and bath has to be large even though the contact surfaces are coated with indium, which remains somewhat plastic even at low temperatures. Raising the calorimeter by the supporting threads does not generally produce sufficient contact force and upon release gives rise to wild pendulum oscillations of the calorimeter. For an average calorimeter swinging over 1° these oscillations add 10^2 ergs to the calorimeter and equilibrium may not be established for many minutes. The use of a metal bellows piston to lift the calorimeter on to the heat switch enables a large contact force to be exerted and allows controlled slow release on to the suspension threads without causing oscillations.

Heating

As only a few ergs per second are required in heating the calorimeter during heat capacity measurements, a mercury battery is a very convenient source of stable heater current. The current and voltage to the heater can be monitored, or if the heater resistance can be reliably calibrated in the working temperature range, only the current need be recorded. Often constantan wire is used as the heater element but in the range 1 to 5 °K this wire shows a large variation in resistance. The external heater current control circuitry can be chosen so that the power input is least sensitive to this change in resistance.

Accuracy

To obtain the highest long term accuracy, the important parts of the measuring equipment must be placed in a thermostatically controlled, room temperature bath. The a-c bridge for temperature measurement and the heater supply and control circuit are the most important. Remembering that a change of 1 part in 10^6 in the calorimeter thermometer is to be measured, the other arms of the a-c bridge must be stable to this amount. Considering the temperature coefficient of standard resistances to be 0.001 percent per °C, a local change in laboratory temperature of 0.1 °C will be sufficient to reduce the required accuracy. The accuracy is also hampered by the seeming impossibility of finding a switch for the other arms of the bridge that does have a reproducible contact resistance on repeated cycling.

The accuracy of the whole experiment depends largely on the accuracy of calibration of the thermometer. There have been many suggestions as to how the original equation of Clement and Quinell [4], representing the temperature response of carbon resistors, can be improved. The more notable of these have been by Hoare [17] and Moody and Rhodes [18] who introduced an expression involving a large number of adjustable parameters in the form $\frac{1}{T}=\sum_n a_n(\ln R)^n$, $n=0, 1, 2, \ldots$. This expression allows easy recalculation to high accuracy of all the parameters after each calibration, and removes the necessity to use correction graphs. Having an exact description of the temperature response facilities subsequent conversion of resistance to temperature in calculations to determine the heat capacity.

In this expression the best values for the coefficients are determined by minimizing $\sum_{i=1}^{N}\left[\left(\frac{1}{T_i}-\frac{1}{T_{Ri}}\right)T_i^2\right]^2$, where T_i is the absolute temperature obtained from accurate vapor pressure measurements. T_{Ri} the temperature given by the above expression from measurements of resistance

and N the number of pairs of T and R used in the calibration. Minimizing this quantity leads to the linear simultaneous equations for a_n and does not give undue emphasis to any region in the temperature range. Moody and Rhodes found it unnecessary to go beyond $n=3$ because more terms than this did not reduce significantly the rms deviation between experimental and calculated values of temperature.

An important part of this calibration proceedure is that a computer was programmed to perform the calculations. The rms deviation was calculated and calibration points that were above a preset value, for a given value of u, were rejected: the response parameters were then recalibrated until the allowed deviation was not exceeded.

Automatic Evaluation of Heat Capacity

There can be few workers now who calculate manually the heat capacity from experimental data: the repetitive calculation involved can be better done, in less time, by computer. With a well designed method of undertaking the experiment, data can be recorded automatically so reducing the overall time to perform the calculations, and the errors in recording large amounts of data.

In the continuous or intermittent techniques the methods of recording data automatically are different, intermittent method being more difficult. Here, for each heating period the duration, and voltages to the heater are recorded to give the energy input and so must be the values of pairs of temperature and time during the drift periods before and after the heating pulse. Care must be taken however, not to record any overheating for only those parts of the drift curve that are linear will allow a computer to be programmed to extrapolate to the middle of the heating pulse. It is clear from the discussion of Parkinson and Quarrington [14] that this purposeful neglect of important data cannot lead to results of great accuracy. However, automatic schemes using intermittent methods have been devised [19].

From what has been said already about the techniques of Schiffman et al. [12], automatic methods could be used here to obtain meaningful records: the energy input can be monitored by repeatedly recording the current to the calorimeter heater: the time between known small temperature jumps is easily available. The temperature drift, caused by extraneous heat input, can be recorded similarly, as can the thermometer calibration information, except here the bath temperature would be recorded against a definite balance condition of the a-c bridge.

The computer programme could be in three parts. Firstly, the calibration calculation of the carbon resistance thermometer; secondly, the heater input, extraneous heat input and temperatures of the calorimeter would be found: and thirdly, the specific heat would be computed. After taking experimental results for some 12 hr, the final results should be obtained in about 30 min of computer time. This is to be compared with 30 to 40 hr by manual calculations.

To take full advantage of this modification of calorimetric practice both techniques and data recording proceedings have to be carefully considered. Precautions must be taken to ensure that necessary information is not thrown away in the process of recording and that sufficient checks are included in the whole process, from apparatus to final results, so that meaningful results are obtained.

References

[1] W. H. Keesom and J. N. Van Den Ende, Leiden Comm. No. 203C (1929).
[2] W. H. Keesom and P. H. Van Laer, Physica **5**, 193 (1938).
[3] J. A. Kok and W. H. Keesom, Physica **1**, 175 (1934).
[4] J. R. Clement and E. H. Quinell, Phys. Rev. **92**, 258 (1953).
[5] C. F. Kellers The specific heat of liquid helium near the lambda point, PhD Thesis, Duke University (1960).
[6] Phenomena in the Neighborhood of Critical Points, NBS Misc. Publ. 273.
[7] W. Gaede, Physik. Zeitscher. **4**, 105 (1902).
[8] A. Eucken, Physik. Zeitscher. **10**, 586 (1910); W. Nernst, Ann. d Physik **36**, 395 (1911).
[9] W. Nernst, Zeitscher. f. Elektrochein. **20**, 357 (1914).
[10] W. Mercouroff, Cryogenics **3**, 171 (1963).
[11] M. J. Buckingham and W. M. Fairbank, Prog. Low Temp. Phys. **3**, 80 (1961).
[12] C. A. Schiffman, J. F. Cochran, M. Garber and G. Pearsall, Rev. Mod. Phys. **36**, 127 (1961).
[13] C. A. Schiffman, private communication.
[14] D. H. Parkinson and J. E. Quarrington, Proc. Phys. Soc. A **67**, 569 (1964).
[15] F. J. Low, Advan. Cryog. Eng. **7**, 514 (1961).
[16] E. A. Ambler and H. Plumb, Rev. Sci. Instr. **31**, 656 (1962).
[17] F. E. Hoare, Proc. Phys. Soc. B, **68**, 388 (1955).
[18] D. E. Moody and P. Rhodes, Cryogenics **3**, 77 (1963).
[19] H. J. Blythe, T. J. Harvey, F. E. Hoare, and D. E. Moody, Cryogenics **4**, 28 (1964).

List of Participants

Alperin, H. A.
Brookhaven National Laboratory
Upton, N.Y.

Alpert, S. S.
Columbia Radiation Laboratory
Columbia University
New York, N.Y.

Als-Nielsen, J.
Atomic Energy Commission
Research Establishment Risö
Roskilde, Denmark.

Anderson, P. W.
Bell Telephone Laboratories
Murray Hill, N.J.

Andrews, D.
University of Missouri
Columbia, Mo.

Arrott, A.
Ford Motor Scientific Laboratory
Dearborn, Mich.

Baer, S.
Yeshiva University
New York, N.Y.

Barieau, R. E.
U.S. Bureau of Mines
Amarillo, Tex.

Barry, J. H.
Ohio University
Athens, Ohio.

Bashaw, J.
Cornell University
Ithaca, N.Y.

Baur, M. E.
University of California
Los Angeles, Calif.

Beckett, C. W.
National Bureau of Standards
Washington, D.C.

Beenakker, J. J. M.
Kamerlingh Onnes Laboratory
Leiden, The Netherlands.

Benedek, G. B.
Massachusetts Institute of Technology
Cambridge, Mass.

Betts, D. D.
University of Toronto
Toronto, Ont., Canada.

Bienenstock, A.
Harvard University
Cambridge, Mass.

Bloom, M.
University of British Columbia
Vancouver, B.C., Canada.

Blume, M.
Brookhaven National Laboratory
Upton , N.Y.

Boyd, M. E.
National Bureau of Standards
Washington, D.C.

Brumberger, H.
Syracuse University
Syracuse, N.Y.

Buckingham, M. J.
University of Western Australia
Nedlands W. A., Australia.

Buff, F. P.
University of Rochester
Rochester, N.Y.

Callen, E.
Naval Ordnance Laboratory
White Oaks, Md.

Callen, H. B.
University of Pennsylvania
Philadelphia, Pa.

Carr, H. Y.
Rutgers University
New Brunswick, N.J.

Caulfield, D. F.
Catholic University
Washington, D.C.

Chase, C. E.
National Magnetic Laboratory
Massachusetts Institute of Technology
Cambridge, Mass.

Chestnut, D.
Shell Development Company
Houston, Tex.

Chu, B.
University of Kansas
Lawrence, Kans.

Cohen, E. G. D.
Rockefeller Institute
New York, N.Y.

Cooper, Martin J.
Brandeis University
Waltham, Mass.

Cooper, Martyn J.
Brookhaven National Laboratory
Upton, N.Y.

Craig, P. P.
Brookhaven National Laboratory
Upton, N.Y.

Davis, B. W.
University of North Carolina
Chapel Hill, N.C.

Debye, P.
Cornell University
Ithaca, N.Y.

Dietrich, O. W.
Atomic Energy Commission
Research Establishment Risö
Roskilde, Denmark.

Domb, C.
University of London King's College
London, England.

De Dominicis, C.
Commissariat á l'Energie Atomique
Centre d'Etudes Nucléaires de Saclay
Saclay, France.

Dorfman, J. R.
University of Maryland
College Park, Md.

Douglass, D. H., Jr.
University of Chicago
Chicago, Ill.

Edwards, M. H.
Royal Military College
Kingston, Ontario
Canada

Edwards, S. F.
University of Manchester
Manchester, England

Emery, V. J.
Brookhaven National Laboratory
Upton, N.Y.

Fairbank, W. M.
Stanford University
Stanford, Calif.

Farrell, R.
Catholic University
Washington, D.C.

Felderhof, B. U.
Instituut voor Theoretische Fysica der Rijksuniversiteit
Utrecht, The Netherlands.

Firth, I. M.
University of St. Andrews
St. Andrews, Scotland.

Fisher, M. E.
University of London King's College
London, England

Fixman, M.
Yale University
New Haven, Conn.
Ford, N. C.
University of Massachusetts
Amherst, Mass.
Friedberg, S. A.
Carnegie Institute of Technology
Pittsburgh, Pa.
Gammel, J. L.
Texas A and M College
College Station, Tex.
Gammon, R.
Johns Hopkins University
Baltimore, Md.
Garcia-Colin, L. S.
Dirección del Reactor Nŭclear
Comision Nacional de Energía Nuclear
Insurgentes Sur 1079, 1er piso
México 18, D. F., México.
Garland, C. W.
Massachusetts Institute of Technology
Cambridge, Mass.
Gilmer, G. H.
Washington and Lee University
Lexington, Va.
Green, M. S.
National Bureau of Standards
Washington, D.C.
Grindlay, J.
National Research Council
Ottawa, Ont., Canada.
Guth, E.
Oak Ridge National Laboratory
Oak Ridge, Tenn.
Guttman, L.
Argonne National Laboratory
Argonne, Ill.
Hammel, E. F.
Los Alamos Scientific Laboratory
Los Alamos, N. Mex.
Heims, S. P.
Brandeis University
Waltham, Mass.
Helfand, E.
Bell Telephone Laboratories
Murray Hill, N.J.
Heller, P.
Brandeis University
Waltham, Mass.
Herzfeld, K. F.
Catholic University
Washington, D.C.
Hill, R. M.
Lockheed Research Laboratories
Palo Alto, Calif.
Hilsenrath, J.
National Bureau of Standards
Washington, D.C.
Hiroike, K.
University of Chicago
Chicago, Ill.
Hohenberg, P. C.
Bell Telephone Laboratories
Murray Hill, N.J.
Horwitz, G.
Yeshiva University
New York, N.Y.
Hudson, R. P.
National Bureau of Standards
Washington, D.C.
Hugenholtz, N.
Instituut voor Theoretische Fysica der Rijksuniversiteit
Groningen, The Netherlands.
Hynne, F.
University of Copenhagen
Copenhagen, Denmark.
Ikenberry, L. D.
University of North Carolina
Chapel Hill, N.C.
Isihara, A.
State University of New York
Buffalo, N.Y.
Jackel, R.
Office of Naval Research
Washington, D.C.
Jackson, J. L.
Howard University
Washington, D.C.
Jacrot, B.
Commissariat á l'Energie Atomique
Centre d'Etudes Nucléaires de Saclay
Saclay, France.
Jalickee, J.
Catholic University
Washington, D.C.
Katsura, S.
Tohoku University
Sendai, Japan.
Kasteleyn, P. W.
Instituut-Lorentz der Rijksuniversiteit
Leiden, The Netherlands.
Kawasaki, K.
Massachusetts Institute of Technology
Cambridge, Mass.
Kawatra, M. P.
Courant Institute of Mathematical Sciences
New York, N.Y.
Keating, D. T.
Brookhaven National Laboratory
Upton, N.Y.
Keen, B. E.
Yale University
New Haven, Conn.
Kellers, C. F., Jr.
Wells College
Aurora, N.Y.
Kerr, E.
Los Alamos Scientific Laboratory
Los Alamos, N. Mex.
Kestin, J.
Brown University
Providence, R.I.
Kierstead, H. A.
Argonne National Laboratory
Argonne, Ill.
Kikuchi, R.
Hughes Research Laboratory
Malibu, Calif.
Klein, M.
National Bureau of Standards
Washington, D.C.
Klein, M. J.
Case Institute of Technology
Cleveland, Ohio
Knobler, C. M.
University of California
Los Angeles, Calif.
Kouvel, J. S.
General Electric Research Laboratory
Schenectady, N.Y.
Langer, J. S.
Carnegie Institute of Technology
Pittsburgh, Pa.
Larsen, S. Y.
National Bureau of Standards
Washington, D.C.
Leff, H. S.
Case Institute of Technology
Cleveland, Ohio
Levitt, L. C.
Georgetown University
Washington, D.C.

Lieb, E.
Yeshiva University
New York, N.Y.
Lipsicas, M.
Brookhaven National Laboratory
Upton, N.Y.
Livesay, B. R.
Georgia Institute of Technology
Atlanta, Ga.
Lorentzen, H. L.
Universitetets Kemiske Institutt
Blindern-Oslo, Norway.
Manchester, F. D.
University of Toronto
Toronto, Ont., Canada.
Marcus, P. M.
International Business Machines Corporation
Watson Research Center
Yorktown Heights, N.Y.
Marshall, W.
Atomic Energy Research Establishment
Theoretical Physics Division
Harwell, England.
Martin, P. C.
Harvard University
Cambridge, Mass.
Marvin, R. S.
National Bureau of Standards
Washington, D.C.
Matsubara, T.
Kyoto University
Kyoto, Japan.
McIntyre, D.
National Bureau of Standards
Washington, D.C.
Melrose, J. C.
Socony Mobil Oil Co.
Field Research Laboratory
Dallas, Tex.
Michels, A. M. J. F.
Van der Waals Laboratorium
Universiteit van Amsterdam
Amsterdam-C, The Netherlands.
Misawa, S.
Massachusetts Institute of Technology
Cambridge, Mass.
Moldover, M. R.
Stanford University
Stanford, Calif.
Montroll, E. W.
Institute for Defense Analysis
Washington, D.C.
Moorjani, K.
Catholic University
Washington, D.C.
Morita, T.
Catholic University
Washington, D.C.
Moruzzi, V. L.
International Business Machines Incorporated
Watson Research Center
Yorktown Heights, N.Y.
Mountain, R. D.
National Bureau of Standards
Washington, D.C.
Muenster, A.
University of Frankfurt
Frankfurt, Germany.
Nagel, J. F.
Yale University
New Haven, Conn.
Naiditch, S.
Unified Science Associates, Inc.
Pasadena, Calif.
Nathans, R.
Brookhaven National Laboratory
Upton, N.Y.
Neighbours, J. R.
U.S. Naval Postgraduate School
Monterey, Calif.
Nielsen, P.
University of Copenhagen
Copenhagen, Denmark.
Nishimura, H.
Catholic University
Washington, D.C.
Oppenheim, I.
Massachusetts Institute of Technology
Cambridge, Mass.
Papoular, M.
University of California
Los Angeles, Calif.
Parette, G.
Commissariat á l'Energie Atomique
Centre d'Etudes Nucléaires de Saclay
Saclay, France.
Parks, R. D.
University of Rochester
Rochester, N.Y.
Passell, L.
Brookhaven National Laboratory
Upton, N.Y.
Piccirelli, R. A.
National Bureau of Standards
Washington, D.C.
Pings, C. J.
California Institute of Technology
Pasadena, Calif.
Potter, R. L.
American Cyanamid Company
Stamford Research Laboratory
Stamford, Conn.
Rao, N. G.
Catholic University
Washington, D.C.
Renard, R.
Massachusetts Institute of Technology
Cambridge, Mass.
Ricci, P.
Universita di Roma
Rome, Italy.
Rice, O. K.
University of North Carolina
Chapel Hill, N.C.
Roder, H. M.
National Bureau of Standards
Boulder, Colo.
Ross, J.
Brown University
Providence, R. I.
Rowlinson, J. S.
Imperial College
London, England.
Rubin, R. J.
National Bureau of Standards
Washington, D.C.
Rudnick, I.
University of California
Los Angeles, Calif.
Ruelle, D.
Institut des Hautes Etudes Scientifiques
Bures-Sur-Yvette (S. et O.), France.
Rushbrooke, G. S.
University of New Castle
New-Castle-on-the-Tyne, England.
Schmidt, E. H. W.
Technische Hochschule München
Munich, Germany.
Schmidt, P.
University of Missouri
Columbia, Mo.
Schultz, T. D.
New York University
University Heights, Bronx, N.Y.

Schwartz, L. H.
Northwestern University
Evanston, Ill.

Scott, R. L.
University of California
Los Angeles, Calif.

Sengers, J. M. H. (Mrs.)
National Bureau of Standards
Washington, D.C.

Sengers, J. V.
National Bureau of Standards
Washington, D.C.

Sette, D.
Universita di Roma
Rome, Italy

Sherman, R. H.
Los Alamos Scientific Laboratory
Los Alamos, N. Mex.

Shirane, G.
Brookhaven National Laboratory
Upton, N.Y.

Sikora, P. T.
North Carolina College
Durham, N.C.

Singwi, K. S.
Argonne National Laboratory
Argonne, Ill.

Smart, J. S.
International Business Machines Corporation
Watson Research Center
Yorktown Heights, N.Y.

Stillinger, F. H.
Bell Telephone Laboratories
Murray Hill, N.J.

Storer, R. G.
Courant Institute of Mathematical Sciences
New York, N.Y.

Stout, J. W.
University of Chicago
Chicago, Ill.

Tanaka, T.
Catholic University
Washington, D.C.

Taylor, T. R.
University of Missouri
Columbia, Mo.

Teaney, D. T.
International Business Machines Corporation
Watson Research Center
Yorktown Heights, N.Y.

Temperley, H. N. V.
United Kingdom Atomic Energy Authority
Aldermaston, England.

Tisza, L.
Massachusetts Institute of Technology
Cambridge, Mass.

Trappeniers, N. J.
Van der Waals Laboratorium
Universiteit van Amsterdam
Amsterdam-C, The Netherlands.

Uhlenbeck, G. E.
Rockefeller Institute
New York, N.Y.

Ulrich, D. V.
Bridgewater College
Bridgewater, Va.

van Kampen, N. G.
Instituut voor Theoretische Fysica der Rijksuniversiteit
Utrecht, The Netherlands.

van Leeuwen, J. M. J.
Instituut voor Theoretische Fysica der Katholieke Universitei
Nijmegen, The Netherlands.

Verlet, L.
Université de Paris
Orsay, France

Villain, J.
Commissariat á l'Energie Atomique
Centre d'Etudes Nucléaires de Saclay
Saclay, France

Walker, C. B.
U.S. Army Materials Research Agency
Watertown, Mass.

Walker, J. F., Jr.
New York University
Bronx, N.Y.

Walker, L. R.
Bell Telephone Laboratories
Murray Hill, N.J.

Webb, W. W.
Cornell University
Ithaca, N.Y.

Weber, L. A.
National Bureau of Standards
Boulder, Colo.

Weinstock, J.
National Bureau of Standards
Boulder, Colo.

White, J. A.
University of Maryland
College Park, Md.

Wilkinson, M. K.
Oak Ridge National Laboratory
Oak Ridge, Tenn.

Wims, A. M.
National Bureau of Standards
Washington, D.C.

Wolf, W. P.
Yale University
New Haven, Conn.

Yamamoto, T.
Kyoto University
Kyoto, Japan.

Yang, C. N.
Princeton University
Princeton, N.J.

Yeh, Y.
Columbia Radiation Laboratory
Columbia University
New York, N.Y.

Younglove, B. A.
National Bureau of Standards
Boulder, Colo.

Zuber, N.
General Electric Company
Schenectady, N.Y.

Zwanzig, R. W.
National Bureau of Standards
Washington, D.C.

U.S. GOVERNMENT PRINTING OFFICE : 1966 OL—209-493